

AD-757 183

DYNAMIC LOADS IN UNDERWATER EXPLOSION

B. V. Zamyshlyayev, et al

Naval Intelligence Support Center
Washington, D. C.

2 February 1973

DISTRIBUTED BY:

NTIS

National Technical Information Service
U. S. DEPARTMENT OF COMMERCE
5285 Port Royal Road, Springfield Va. 22151



DEPARTMENT OF THE NAVY
NAVAL INTELLIGENCE SUPPORT CENTER
TRANSLATION DIVISION
4301 SUITLAND ROAD
WASHINGTON, D.C. 20390

AD 757183

CLASSIFICATION:

UNCLASSIFIED

APPROVED FOR PUBLIC RELEASE, DISTRIBUTION UNLIMITED

TITLE:

Dynamic Loads in Underwater Explosion

Dinamicheskiye nagruzki v podvodnom vzryve

AUTHOR(S):

Zamyshlyayev, B. V., and Yakovlev, Yu. S.

PAGES:

463

SOURCE:

Sudostroyeniye, Leningrad, 1967
Complete Translation

Reproduced by
NATIONAL TECHNICAL
INFORMATION SERVICE
U S Department of Commerce
Springfield VA 22151

ORIGINAL LANGUAGE:

Russian

TRANSLATOR:

C

NISC TRANSLATION NO.

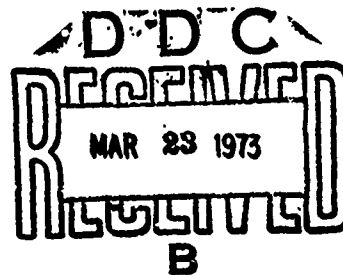
3391

APPROVED

P.T.K.

DATE

2 February 1973



Details of illustrations in
this document may be better
studied on microfiche.

TABLE OF CONTENTS

Foreword	1
----------------	---

CHAPTER I

PRESSURE FIELDS DURING UNDERWATER EXPLOSION IN A FREE FLUID

§1. Second-Order Discontinuity Surfaces. Dynamic Compatibility Conditions	6
§2. Differential Equations of Gas Dynamics. Equations of the Characteristics	18
§3. Some Precise Solutions for One-Dimensional Transient Fluid Motion	25
§4. Laws of Similarity in the Theory of Explosion. Gas Bubble Expansion	32
§5. Approximate Evaluation of Pressure Fields in Underwater Explosion in an Infinite Fluid	48
§6. The Basic Equations of Short-Wave Theory. Asymptotic Presentations of an Underwater Shock-Wave	64
§7. The Effect of a Free Fluid Surface on Pressure Fields in Underwater Explosion	76
§8. Formation and Development of Cavitation in the Reflection of an Underwater Shock-Wave on a Free Surface	103
§9. Reflection of a Shock-Wave on the Bottom of a Basin [Linear Theory]	114
§10. The Influence of Nonlinear Effects on the Parameters of a Wave Reflected on a Basin Bottom. Pressure Fields during Underwater Explosion in Low Water	120

CHAPTER II

DIFFRACTION PROBLEMS OF THE THEORY OF UNDERWATER EXPLOSION

§11. The Concept of Diffraction Problems. General Research Methods	131
§12. Diffraction of a Plane Wave by an Absolutely Rigid Wedge	142
§13. Diffraction of a Unit Wave by a Rigid Plate	167

- §14. Hydrodynamic Forces Induced by the Progressive Motion
of a Rectangular-Shaped Piston Having Rigid Walls..183
- §15. Pressure Field During Progressive Motion of Circular
Shaped Piston. General Concepts on Solving Diffraction
Problems with the aid of the Integral of Radiation....199
- §16. Diffraction of a Spherical Wave by the End-Face of
a Semi-Infinite Rigid Round Cylinder.....208
- §17. Diffraction of a Plane Wave by a Rigid Sphere.....217
- §18. Diffraction of a Plane Wave by a Rigid Round
Cylinder.....237
- §19. Hydrodynamic Forces in the Progressive Motion of
an Absolutely Rigid Body of Arbitrary Shape.....246
- §20. Hydrodynamic Forces Formed When a Plane Wave Falls
onto an Immobile Absolutely-Rigid Obstacle of
Finite Dimensions and Arbitrary Shape.....261

CHAPTER III THE EVALUATION OF EXTERNAL FORCES

- §21. Generalized Hydrodynamic Forces of the First and
Second Category..... 280
- §22. The Interaction of a Shock-Wave with a Free Rigid
Plate..... 283
- §23. Integro-Differential Equation of Piston Motion
Under the Influence of an Underwater Shock Wave...304
- §24. The Motion of a Plate of Finite Dimensions Under
the Influence of a Shock Wave.....319
- §25. Evaluation of Generalized Forces During Incidence
of a Shock-Wave onto an Absolutely Rigid Body
of Arbitrary Shape.....329
- §26. Interaction of a Shock-Wave with an Elastic Plate
of Finite Thickness.....345
- §27. General Concepts on the Interaction of a Shock-Wave
with an Elastic Plate Attached by its Edges.....360
- §28. The Pressure Field and Generalized Hydrodynamic
Force of the Second Category Induced by De-
formation of an Elastic Plate Attached by
its Edges to a Rigid Infinite Wall..... 369

§29. Practical Evaluation of the Parameters of Motion of an Elastic Plate Having Edges Attached to a Rigid Wall Under the Influence of an Under- water Shock-Wave.....	383
§30. Interaction of an Underwater Shock-Wave with a Rectangular Plate Forming Part of a Cover.....	397
§31. The Interaction of an Underwater Shock-Wave with an Elastic Isolated Plate of Finite Dimensions.....	415
§32. Formation and Development of Cavitation During Interaction of a Shock-Wave with a Plate.....	427
§33. Dynamic Calculation of an Infinite Plate on a Solid Elastic Foundation, Allowing for Cavi- tation.....	442
§34. Dynamic Calculation of Plates Attached by their Edges, Allowing for Cavitation Effects.....	453
References.....	462

DYNAMIC LOADS IN UNDERWATER EXPLOSION

by

B. V. Zamyshlyayev and Yu. S. Yakovlev

Foreword

In the total complex of problems in modern shipbuilding, dynamic strength occupies a prominent place. Since theoretical methods for evaluating stresses and deformation under known loads have been thoroughly researched in many studies, there is significant value in the study of external forces.

Dynamic loads in underwater explosion are a separate and essential part of the total problem of external forces. Final solutions in the field of dynamic loads have only recently appeared in the scientific literature. This is explained by difficulties arising in research of similar problems. Indeed, even when evaluating the hydrodynamic field for the simplest case of an undeformed obstacle, we must take into account the effect of a shock wave passing around an obstacle, in addition to the reflection and refraction of waves; this "rounding of waves" is usually called diffraction. The analytic intricacy of wave equation diffraction problems is well known. It is this fact alone which has hindered the development of practical methods for dynamic calculation of structures.

Consequently, it seemed appropriate to present the primary findings in the field of diffraction problems of the theory of underwater explosion within a separate chapter of this monograph (Chapter II). We discuss diffraction of a plane wave around a completely rigid wedge. The first solution of this problem was given by S. L. Sobolyov and V. I. Smirnov [18, 19]. Another simpler method was given by A. A. Kharkevich in his study of the diffraction field at the edge of a semi-infinite plate [21].

The use of the method recommended by Kharkevich, which consisted in using a Laplace equation in place of a wave equation, allowed us to derive simple relationships without difficulty. The use of these relationships enabled us to explain the distinctive features of the diffraction field by an angle and give practical methods for evaluating external forces for the effect of a shock wave on the body of a ship whose outlines can be geometrically reduced to a polygon.

Thus we thought it necessary to explain the possible use of a radiation integral solution, in some cases, in the analysis of diffraction problems and to indicate those cases where its use would not lead to appreciable error.

The study of wave equation boundary-value problems permitted us to form conclusions on the general mathematical features of a description of a single wave being diffracted around an obstacle, the motion of this obstacle at a velocity which changes according to the unit function law, and to establish a connection between wave solutions and solutions based on the classic notion of a noncompressible fluid. We found that after a certain time interval, the load developing during the diffraction of a wave around a body is easy to calculate in terms of apparent mass. The proper approximation of this transient function permits us to analyze the external forces for the entire period of transient motion, with sufficient accuracy for practical application. On this basis, in particular, the diffraction load on a round cylinder and an ellipsoid of revolution can be written in a very simple form.

For these reasons, we can speak of designing an approximate but rather universal method for evaluating hydrodynamic forces, based on the assumption of an obstacle having absolute rigidity (collective forces of the first order).

The appreciable acoustic resistance of water predetermines the

second basic problem in evaluating external forces. The motion of an obstacle during elastic-plastic deformations generates wave disturbances which greatly affect the total hydrodynamic field. The interrelationship between deformation and load necessitates the study of the systems of integral-differential equations of motion. A defined approximation of the kernel permits us to reduce these equations to ordinary differential equations. The representation of motion in its main forms of change enables us to investigate these equations independently of each other, in some cases. In this way, we can find an evaluation of hydrodynamic forces of the second order which takes into account the effect of deformation and displacement on the resulting load.

In the interaction of a direct shock wave resulting from the motion of an obstacle with an expansion wave, negative stresses may be created in a fluid and subsequently, areas of cavitation. This process may no longer be described by classic hydrodynamic equations and requires the development of special research methods. However, we must take account of this process in many cases, since the external load depends greatly on it. This type of problem can be solved by using integrated evaluations based on the universal laws of conservation of energy and momentum.

The entire range of questions is reflected in the contents of Chapter III. Since the nature of interaction of a wave and a structure and the final formulas derived are in many respects defined by the direct shock-wave curve, and since universal theoretical research methods are based on a certain apparatus of gas dynamics, the second and third chapters of this monograph are preceded by an introductory first chapter which briefly states the necessary data for hydrodynamic fields in underwater explosion in a free fluid. Nevertheless, some sections in this introductory chapter do contain new elements. Subsequent development of Kirkwood's ideas in particular, permitted us to derive a clear picture of underwater explosion at great charge depths. Consideration of nonlinear effects with utilization of the Fermat principle made it possible to derive a rather simple method for evaluating the effect of a free surface and the bottom of a basin

in the reflection of a spherical wave.

Very little literature exists on the subject of this monograph, with the exception of information covered in Chapter I. Clarification of questions on acoustic wave diffraction around an obstacle was facilitated by the work of S. L. Sobolyov, V. I. Smirnov, and A. A. Kharkevich. R. Cowle's book ("Underwater Explosions" [10]) and Yu. S. Yakovlev's book ("The Hydrodynamics of Explosion" [26]), as well as a number of articles, mainly by S. A. Khristianovich, were of aid in writing Chapter I and several paragraphs in Chapters II and III; these last articles have been published at various times in the journal "Applied Mathematics and Mechanics".

The main contribution to the solution of this problem was made, in our opinion, by the work of Academicians V. V. Novozhilov, D. A. Aleksandrin, Yu. V. Golyainov, M. N. Lefonova, K. V. Lopukhov, I. L. Mironov, I. G. Novoselov, A. N. Patrashev, A. K. Pertsev, L. I. Slep-yan, Yu. A. Fyodorovich, L. V. Fremke, and to some degree, the authors of this book.

The large number of papers recently published in the field of shell dynamics compels us to view the problem of interaction between a shock wave and a shell as a separate, important, and interesting problem; a brief summary of even the main aspects of this theory would require a separate monograph. In this study, we will only be concerned with certain aspects of this question, mainly from the standpoint of evaluating the diffraction field near an absolutely rigid body.

The manuscript of this book was reviewed by L. I. Slep-yan, V. A. Timofeyev, and P. F. Fomin. Y. I. Kolyzheva designed the layout. To these persons, and to the scientific editor of this book, Acad. V. V. Novozhilov the authors express their sincerest appreciation.

Comments and questions concerning this book should be sent to:
"Sudostroyeniye" Publishers, 8 Gogol Street, Leningrad, D-65, USSR.

CHAPTER I

PRESSURE FIELDS FORMED DURING UNDERWATER EXPLOSION IN A FREE FLUID

§1. Second-Order Discontinuity Surfaces. Dynamic Compatibility Conditions.

In the explosion resulting from the rapid liberation of energy, high pressures and temperatures are formed. These quantities are generally distributed arbitrarily along the boundary surface between the detonation products and the ambient medium. At the same time, the existence of this unique boundary surface of two media is incompatible with the laws of conservation of matter, momentum, and energy. Transient disintegration of the initial surface occurs as three new surfaces are formed. The distinctive feature of each of these surfaces is the abrupt change in hydrodynamic parameters (pressure, density, temperature, and particle velocity). These surfaces are called discontinuity surfaces; if the hydrodynamic parameters themselves change abruptly, we are speaking of second-order discontinuity surfaces; if their first or high derivatives change - of first-order discontinuity surfaces.

In underwater explosion, the surface propagated through the ambient medium is a non-stationary second-order discontinuity surface (shock-wave front). The boundary surface between explosion products and the medium is a stationary second-order discontinuity surface (gas-bubble surface). The third surface propagated through the products of explosion is a first-order discontinuity surface, or the "characteristic".

The main task of the theory of explosion in an infinite medium is the study of transient fluid motion between two boundary surfaces, the shock-wave front and the gas-bubble surface. This motion is characterized by a system of partial differential equations. A statement of the problem entails the recording of this system and the definition

of the previously mentioned boundary conditions.

Using the law of conservation of momentum and the law of conservation of matter, Leonard Euler (1755) first established the equation of motion and the equation of discontinuity for an ideal fluid. These equations, which are universal for all fluids and gases, have the form

$$\rho \frac{d\vec{v}}{dt} + \text{grad } p = 0, \quad (1.1)$$

$$\frac{d\rho}{dt} + \rho \text{div } \vec{v} = 0. \quad (1.2)$$

The two equations of motion include five variables: pressure p^* , density ρ , and three components of the velocity vector v_x , v_y , and v_z . Without adding any other variables, the equation of discontinuity nevertheless completes the system. Sometimes, the assumption is made that the problem can be solved, considering that density is constant (the hypothesis of a noncompressible fluid). Accordingly, the equations of motion and the equation of discontinuity form a closed system and for a one-dimensional case a solution may be derived using quadratic equations. This is precisely what Lamb did at one time (1923), the first person to theoretically derive the pressure field in underwater explosion. To this very day, his solution has not lost its methodological and practical value for the analysis of individual problems.

In a general statement of the problem, however, the use of the hypothesis of fluid noncompressibility is inadmissible, since under the high pressures formed during explosions fluids are highly compressed. Water, for example, is compressed by more than 20% at pressures of 10,000 atm. But this is not the deciding factor. The main objection, with respect to the possible utilization of the hypothesis of noncompressibility, is revealed on investigating the energy balance. As is well known, an assumption on noncompressibility of a

*In studying transient flow resulting from underwater explosion, pressure (p) is understood as being pressure in excess of hydrostatic pressure.

medium does not permit us to take into account the dissipation of energy, thereby totally excluding dissipative processes from analysis. However, in the propagation of a shock wave formed at the beginning of the first pulsation of the gas bubble in an underwater explosion, one cannot ignore that about 60% of the initial energy is dissipated. Ultimately, the hypothesis of noncompressibility excludes from discussion shock waves and their concomitant local areas of heightened pressure and the finite propagation rate of disturbances.

Therefore, we must write additional equations to completely describe the system of (1.1) and (1.2). These equations are the equation of state and the equation of energy. These equations contain another two variables which were not previously mentioned: absolute temperature T and heat flux ϵ . However, the high rate of occurrence of explosive processes almost eliminates heat exchange with the ambient medium. Heat flux is assumed to be equal to zero, and the system of equation is closed. After excluding temperature using an equation of state, we generally derive five equations. For of them are universal for all fluids and gases. The difference in the physical properties of various media is reflected only in the condition of adiabaticity (in terms of the quantity of internal energy, defined by the parameters of state).

Problems of a mathematical nature compel us to reject the initial system of equations from our analysis of the universal case of fluid spatial motion. At the present time, only a few studies have been carried out on motion having plane, axial, and spherical symmetry. It is namely one-dimensional motion, however, which is of practical interest.

The initial system of equations is integrated with respect to boundary conditions assigned at the two boundary surface - the shock-wave front and the gas-bubble surface. We will investigate these conditions in greater detail, bearing in mind that the wave-front is a non-stationary second-order discontinuity surface where the quantities of the fluid hydrodynamic parameters abruptly change.

If we assume that the equation of a second-order discontinuity surface Σ is

$$F(x, y, z, t) = 0,$$

then the area $F > 0$ can be considered relatively positive, the parameters of this area being assigned the index $+$; accordingly, the quantities in the area $F < 0$ will be assigned the index $-$.

A discontinuity or rapid change in function b on surface Σ we shall call the difference in

$$b_+ - b_- = [b]. \quad (1.3)$$

Let us introduce the notion of the rate of travel of surface Σ at any given point. The rate of travel is the limit of the ratio of a point traveling along a normal toward the surface to time

$$N = \lim_{\Delta t \rightarrow 0} \frac{\Delta n}{\Delta t}. \quad (1.4)$$

Velocity N defines the motion of a discontinuity surface with respect to a stationary observer.

Another interesting quantity is the rate of motion of a discontinuity surface with reference to particles of fluid, called the discontinuity-surface propagation-rate and designated by the symbol θ .

By definition

$$\left. \begin{aligned} \theta_+ &= N - v_{n+} \\ \theta_- &= N - v_{n-} \end{aligned} \right\} \quad (1.5)$$

On discontinuity surfaces, as in other areas of fluid motion, the universal laws of conservation of momentum and energy are satisfied.

The mathematical form for writing these laws is called

dynamic compatibility conditions.

N. Ye. Kochin (1926) derived these conditions in the form

$$[\rho\theta] = 0, \quad (1.6)$$

$$\rho\theta [\vec{v}] = [p] \vec{n}, \quad (1.7)$$

$$\rho\theta \left[\frac{v^2}{2} + \frac{1}{A} u \right] = [\rho v_n], \quad (1.8)$$

where we also designate: u - internal energy; A - thermal work equivalent.*

If the rate of propagation $\theta = 0$, the discontinuity surface is not in motion with respect to the particles and is called stationary. Based on (1.7), pressure discontinuity $[p] = 0$ on such a surface. By definition, as well as on the basis of (1.8), density discontinuity $[\rho]$ is relative. The discontinuity of tangential velocity components is also relative. This is easily verified by scalar multiplication of both sides of equality (1.7) by the unit vector $\vec{\tau}$ which is at right angles to \vec{n} . Consequently, a stationary second-order discontinuity surface is often called a tangential discontinuity surface or sometimes, a contact surface.

If the rate of propagation $\theta \neq 0$, a discontinuity surface is called non-stationary. On this surface there is always an abrupt change in the quantity of pressure and the normal components of the particle speed vector: $[p] \neq 0$, $[v_n] \neq 0$. Indeed, if we assume that $[p] = 0$, then based on (1.7) $[v_n] = 0$ and consequently, based on (1.8) $\theta = 0$. According to (1.6) $[\rho] = 0$, i.e., there is no second-order discontinuity.

Let us examine the corollaries derived from dynamic compatibility conditions for non-stationary second-order discontinuity surfaces.

*Assuming that internal energy is expressed in thermal units.

First of all, let us note that the three equations, (1.6)-(1.8) include seven variables: N , ρ_+ , ρ_- , \bar{v}_+ , \bar{v}_- , p_+ , and p_-^* . Thus, if the hydrodynamic parameters of an undisturbed medium are known (ρ_+ , v_+ , p_+), we only have to be given one element on the discontinuity surface so that the remaining parameters are identically defined.

After excluding mass velocity v from (1.6) and (1.7), it is easy to derive expressions for the rate of propagation of the shock-wave front

$$\theta_-^2 = \frac{\rho_+ |\rho|}{\rho_- |\rho|}, \quad (1.9)$$

$$\theta_+^2 = \frac{\rho_- |\rho|}{\rho_+ |\rho|}. \quad (1.10)$$

The physical interpretation of equalities (1.9) and (1.10) will become quite clear if we use specific volume τ ($\tau = 1/\rho$) instead of density ρ . We then find that

$$\theta_-^2 = \tau_-^2 \frac{\rho_- - \rho_+}{\tau_+ - \tau_-}, \quad (1.11)$$

$$\theta_+^2 = \tau_+^2 \frac{\rho_- - \rho_+}{\tau_+ - \tau_-}. \quad (1.12)$$

Let us first examine expression (1.12). For a given initial state, the coefficient τ_+^2 is constant. Consequently, the propagation rate of shock-waves θ_+ , corresponding to various degrees of compression, depends only on the ratio $(\rho_- - \rho_+)/(\tau_+ - \tau_-)$, i.e., it is a function of the tangent of the slope of the corresponding straight lines which connect initial point p_+ , τ_+ with points p_- , τ_- (Fig. 1). The propagation rate of small disturbances at point A is defined by the slope of tangent AD

$$\theta_+^2|_A = -\tau_+^2 \frac{dp}{d\tau} = \frac{dp}{d\rho} = a_+^2$$

* θ and u are not independent variables, since by definition $\theta = N - v_n$, and the quantity of internal energy u is expressed in terms of p and ρ by means of an equation of state.

and is equal to the speed of sound in an undisturbed medium a_+ . We can also see that $\theta_+ \geq a_+$.

Based on identical arguments (see Fig. 1) it follows that $\theta_+ \leq a_-$.*

If we are examining a stationary second-order discontinuity surface where $N = 0$ and consequently, $\theta = -v_n$, then the relationships derived produce an important corollary: a second-order discontinuity can be created only in supersonic fluid flows. In the stationary problems of gas dynamics, this discontinuity is usually called a consolidation discontinuity.

Since passage through the local speed of sound qualitatively changes the nature of motion, the ratio of the speed of particles to the speed of sound, $M = v/a$ is often used as a criterion of similarity. This criterion, called the Mach number, can easily be extended to nonstationary processes. In this connection, we should of course examine reversed motion by studying the motion of particles with respect to the wave-front.

We will then define the two Mach numbers

$$M_+ = \frac{\theta_+}{a_+}, \quad (1.13)$$

$$M_- = \frac{\theta_-}{a_-}, \quad (1.14)$$

where $M_- < 1$ if $M_+ > 1$.

In most cases which are of practical importance, a shock-wave is propagated in an undisturbed medium. In this connection, $v_+ = 0$, $\theta_+ = N$. Consequently, the velocity of shock-wave motion is always greater than the speed of sound ahead of the front ($M_+ = (N/a_+) > 1$).

*As we know, pressure change is $(\partial^2 p)/(\partial t^2) > 0$ for the dynamic adiabatic curve of water, on which we base the universal nature of the conclusions formulated.

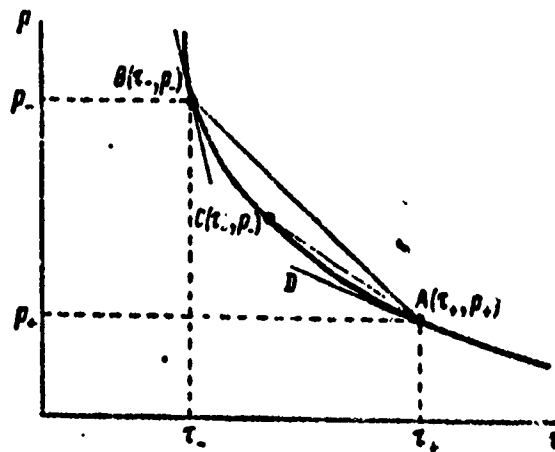


Fig. 1. Schematic Comparison of Shock-Wave Propagation Rate and Local Speed of Sound.

However, the difference in the rates of wave motion and particle motion is always less than the speed of sound behind the front ($M_- = (N - v_n/a_-) < 1$; $N < a_- + v_n$). On this basis, weak disturbances in a fluid which are propagated at the local speed of sound can catch up to the shock-wave front, but cannot outdistance it.

Inequality $M_+ > 1 > M_-$ is often given as evidence that the only second-order discontinuities which are possible, are those in which pressure increases (Cemlen theorem).

Let us return to dynamic compatibility conditions (1.6)-(1.8). After excluding the variables v and θ , we find that

$$u_- - u_+ = \frac{1}{2} (p_+ + p_-) \left[\frac{1}{\rho} \right]. \quad (1.15)$$

Equation (1.15) is the dynamic or shock adiabatic equation.

For an ideal gas, the quantity of internal energy is expressed by a linear function of absolute temperature

$$u = c_v T, \quad (1.16)$$

and the equation of state is the Mendeleyev-Clapeyron equation

$$p = \rho RT. \quad (1.17)$$

Moreover, the product of the gas-constant R times the thermal-work-equivalent is equal to the difference in specific heats at constant pressure and volume

$$AR = c_p - c_v. \quad (1.18)$$

Using these relationships, equation (1.15) can be written in the form

$$(p_+ + p_-) \left[\frac{1}{\rho} \right] + \frac{2}{k-1} \left[\frac{p}{\rho} \right] = 0 \quad (1.19)$$

or, by expanding the signs of the discontinuities and performing simple transformations,

$$\frac{p_-}{p_+} = \frac{(k+1)p_- - (k-1)p_+}{(k+1)p_+ - (k-1)p_-}, \quad (1.20)$$

where $k = c_p/c_v$ - the adiabatic coefficient.

Equality (1.20) is the dynamic adiabatic curve of an ideal gas, or the Hugoniot adiabatic curve. The Hugoniot adiabatic curve intersects the static adiabatic curve (the Poissonian adiabatic curve)

$$\frac{p_-}{p_+} = \left(\frac{\rho_-}{\rho_+} \right)^k \quad (1.21)$$

at point $(p_-/p_+) = 1$, $(\rho_-/\rho_+) = 1$ and has a second-order tangency at this point.

The theoretical distinction between the Hugoniot and the Poissonian adiabatic curves is that the Poissonian adiabatic curve is a single-parameter curve, whereas the Hugoniot curve is a two-parameter curve. To exhaust all possible Poissonian adiabatic curves, one only has to run through a one-dimensional series of entropy (S) values; while to exhaust all possible Hugoniot adiabatic curves, one must

plot "infinity squared" curves to satisfy all possible values of p_+ and ρ_+ . In other words, in contrast to the Poissonian adiabatic curve, where entropy maintains a constant value, every point on a dynamic adiabatic curve is satisfied by a certain value of entropy which is inherent only to that point. Consequently, if an area of variable pressure is formed behind the shock-wave front, there will be a concomitant area of variable entropy.

The function of entropy of an ideal gas is defined by the equality

$$\Delta S = \frac{c_v}{A} \ln \left\{ \frac{p_+}{p_-} \left(\frac{\rho_-}{\rho_+} \right)^k \right\}. \quad (1.22)$$

Using equation (1.20), we can derive an order expansion $\Delta \rho / \rho_+$ of function ΔS near point (ρ_+, p_+) :

$$\Delta S = \frac{c_v}{A} \frac{k^2 - k}{12} \left(\frac{\Delta p}{p_+} \right)^3 \left[1 - \frac{3}{2} \frac{\Delta p}{p_+} + \dots \right]. \quad (1.23)$$

Based on (1.23), at small values of $\Delta \rho / \rho_+$, an increment of entropy in the shock-wave is proportional to the cube of relative consolidation. In weak shock-waves, the increment in entropy is so small that we can view the propagation of such waves as an isentropic process, with no detriment to practical precision.

Assertions made for a dynamic adiabatic curve of an ideal gas, with respect to quality, are also valid for other fluids and gases. For quantitative evaluations, we must know the thermodynamic properties of the medium and, above all, the equation of state. Numerous attempts a theoretical derivation of the equation of state for water have not produced the desired results; for this reason, various empirical and semi-empirical equations of state for water are used to solve practical problems which, as a rule, approximate Bridgman's experimental data in one form or another.

For an area of high pressure ($p > 30 \cdot 10^3$ kG/cm²), we can recom-

mend the following empirical dynamic adiabatic equation for water:

$$p - p_0 = 4250 \left[\left(\frac{p}{p_0} \right)^{0.29} - 1 \right]. \quad (1.24)$$

At pressures less than $30 \cdot 10^3$ kG/cm², the change in entropy may be disregarded and consequently, the static and dynamic adiabatic curves almost coincide and can be expressed by the so-called Tête equation:

$$p - p_0 = B \left[\left(\frac{p}{p_0} \right)^n - 1 \right], \quad (1.25)$$

where $B = \rho_0 a_0^2 / n = 3045$ kG/cm² (where $t = 15^\circ\text{C}$, $a_0 = 1460$ m/s, and $n = 7.15$).

Equations (1.24) or (1.25) in conjunction with equalities (1.6) and (1.7) constitute a system which permits us to identically define any hydrodynamic parameter in a shock-wave front, if we are given one of them in conjunction with the parameters of an undisturbed fluid.

For the sake of convenience, we will write the system of these relationships after assigning the parameters of the front the index " ϕ " and the parameters of the undisturbed medium the index "0".

Based on (1.6) and (1.7) we immediately find that

$$p_\phi - p_0 = \rho_0 (\lambda - v_0) (v_\phi - v_0), \quad (1.26)$$

$$N = \frac{\rho_\phi v_\phi - \rho_0 v_0}{p_\phi - p_0}, \quad (1.27)$$

$$v_\phi = N \frac{p_\phi - p_0}{\rho_\phi} + v_0 \frac{\rho_0}{\rho_\phi}. \quad (1.28)$$

$$(v_\phi - v_0)^2 = (p_\phi - p_0) \left(\frac{1}{\rho_\phi} - \frac{1}{\rho_0} \right). \quad (1.29)$$

If $v_0 \equiv 0$, then

$$p_\phi - p_0 = \rho_0 N v_\phi, \quad (1.30)$$

$$v_\phi = N \frac{p_\phi - p_0}{\rho_\phi} \quad (1.31)$$

$$v_\phi = \sqrt{(p_\phi - p_0) \left(\frac{1}{\rho_0} - \frac{1}{\rho_\phi} \right)} \quad (1.32)$$

Equalities (1.26)-(1.32) are valid for all fluids and gases.
For water, when pressure on the front is in excess of 30,000 kg/cm²

$$p_\phi - p_0 = d \left[\left(\frac{\rho_\phi}{\rho_0} \right)^k - 1 \right] \text{ kg/cm}^2, \quad (1.24a)$$

$$N^2 = \frac{d (\rho_\phi^k - \rho_0^k)}{\rho_0^{k+1} \left(1 - \frac{\rho_0}{\rho_\phi} \right)} \text{ cm}^2/\text{sec}^2, \quad (1.33)$$

$$v^2 = \frac{d (\rho_\phi^k - \rho_0^k)}{\rho_0^{k+1}} \left(1 - \frac{\rho_0}{\rho_\phi} \right) \text{ cm}^2/\text{sec}^2, \quad (1.34)$$

where $d = 4250 \text{ kg/cm}^2$, $k = 6.29$.

For isentropic motion ($p < 30,000 \text{ kg/cm}^2$), according to the Tête equation

$$N^2 = \frac{p_\phi - p_0}{\rho_0 \left(1 - \frac{1}{\sqrt{1 + \frac{p_\phi - p_0}{B}}} \right)} \quad (1.35)$$

$$v_\phi^2 = \frac{1}{\rho_0} (p_\phi - p_0) \left[1 - \frac{1}{\sqrt{1 + \frac{p_\phi - p_0}{B}}} \right] \quad (1.36)$$

$$a_\phi^2 = n \frac{p_\phi - p_0 + B}{\rho_\phi} \quad (1.37)$$

In studying the propagation of an underwater shock-wave having pressure on the front less than 1,000 kg/cm², dynamic compatibility conditions can be linearized.

After performing simple operations, considering that $p_\phi \ll B_n$, we find that

$$v_\phi = a_0 \frac{p_\phi - p_0}{Bn} \quad (1.38)$$

$$a_\phi = a_0 \left[1 + \frac{n-1}{2Bn} (p_\phi - p_0) \right] \quad (1.39)$$

$$N = a_0 \left[1 + \frac{n+1}{4Bn} (p_\phi - p_0) \right] \quad (1.40)$$

$$p_\phi = p_0 \left[1 + \frac{1}{n} \frac{p_\phi - p_0}{B} \right]. \quad (1.41)$$

Let us note that the linearized dynamic compatability conditions for an ideal gas have the form (for $\Delta p_\phi / p_0 \ll 1$)

$$u_\phi = u_0 \frac{1}{k} \frac{\Delta p_\phi}{p_0}, \quad (1.42)$$

$$a_\phi = a_0 \left(1 + \frac{k-1}{2k} \frac{\Delta p_\phi}{p_0} \right), \quad (1.43)$$

$$N = u_0 \left(1 + \frac{k-1}{4k} \frac{\Delta p_\phi}{p_0} \right), \quad (1.44)$$

$$p_\phi = p_0 \left(1 + \frac{1}{k} \frac{\Delta p_\phi}{p_0} \right), \quad (1.45)$$

where Δp_ϕ - excess pressure on the shock-wave front.

In contrasting (1.38)-(1.41) to (1.42)-(1.45), we can see an identity of the systems by replacing the adiabatic exponent with the exponent n and pressure p_0 with the constant B . Let us now give a complete general characterization of the physical-mathematical formulation and an analysis of the problem of propagation of weak shock-waves in an ideal gas or fluid.

§2. Differential Equations of Gas Dynamics. Equations of the Characteristics.

An abrupt change in hydrodynamic parameters of a fluid occurs only on discontinuity surface. In the remaining area, the transient motion induced by the explosion can be described by a system of differential equations from gas dynamics. These equations are the equations of motion, the equation of discontinuity, and the equation of energy. The derivation of these equations has been given in many hydrodynamics courses and thus, there is no need to repeat it here.

The equations of motion on a rectangular system of coordinates have the form

$$\left. \begin{aligned} \frac{\partial v_x}{\partial t} + v_x \frac{\partial v_x}{\partial x} + v_y \frac{\partial v_x}{\partial y} + v_z \frac{\partial v_x}{\partial z} &= -\frac{1}{\rho} \frac{\partial p}{\partial x} \\ \frac{\partial v_y}{\partial t} + v_x \frac{\partial v_y}{\partial x} + v_y \frac{\partial v_y}{\partial y} + v_z \frac{\partial v_y}{\partial z} &= -\frac{1}{\rho} \frac{\partial p}{\partial y} \\ \frac{\partial v_z}{\partial t} + v_x \frac{\partial v_z}{\partial x} + v_y \frac{\partial v_z}{\partial y} + v_z \frac{\partial v_z}{\partial z} &= -\frac{1}{\rho} \frac{\partial p}{\partial z} \end{aligned} \right\} \quad (2.1)$$

or in vectorial form

$$\frac{\partial \vec{v}}{\partial t} + (\vec{v} \cdot \nabla) \vec{v} + \frac{1}{\rho} \nabla p = 0, \quad (2.2)$$

where ∇ designates the so-called Hamiltonian operator:

$$\nabla = i \frac{\partial}{\partial x} + j \frac{\partial}{\partial y} + k \frac{\partial}{\partial z}. \quad (2.3)$$

We often can also use an equation of motion in the Gromeko-Lamb form: *

$$\frac{\partial \vec{v}}{\partial t} + \nabla \frac{v^2}{2} - \vec{v} \times \text{rot } \vec{v} + \frac{1}{\rho} \nabla p = 0. \quad (2.4)$$

The equation of discontinuity expressing the law of conservation of matter has the form:

$$\frac{\partial \rho}{\partial t} + \text{div} (\rho \vec{v}) = 0 \quad (2.5)$$

or if we expand the sign of divergence,

$$\frac{\partial \rho}{\partial t} + \frac{\partial (\rho v_x)}{\partial x} + \frac{\partial (\rho v_y)}{\partial y} + \frac{\partial (\rho v_z)}{\partial z} = 0. \quad (2.6)$$

Finally, the last equation which completely describes the system

* $\text{rot } \vec{v}$ designates a velocity curl - the vectorial product of the Hamiltonian operator ∇ times the velocity vector \vec{v} :

$$\text{rot } \vec{v} = \nabla \times \vec{v} = \begin{vmatrix} i & j & k \\ \frac{\partial}{\partial x} & \frac{\partial}{\partial y} & \frac{\partial}{\partial z} \\ v_x & v_y & v_z \end{vmatrix}$$

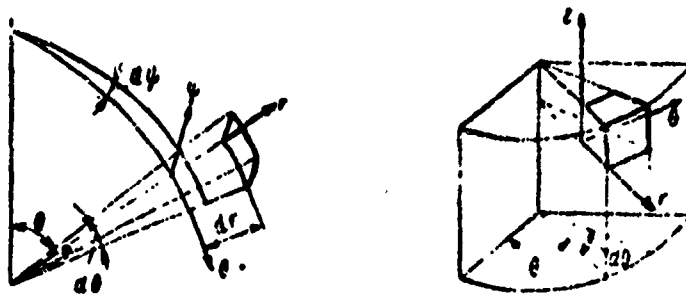


Fig. 2. Spherical and Cylindrical Coordinate Systems.

is the adiabatic curve equation. This equation can be a mathematical expression that entropy of a particle remains constant in the adiabatic process

$$\frac{dS}{dt} = 0 \quad (2.7)$$

or

$$\frac{\partial S}{\partial t} + v_x \frac{\partial S}{\partial x} + v_y \frac{\partial S}{\partial y} + v_z \frac{\partial S}{\partial z} = 0. \quad (2.8)$$

In many problems it is more suitable if we write equations in curvilinear coordinates, and not in Cartesian coordinates. Cylindrical and spherical coordinates are special cases of the former.

The connection between cylindrical and rectangular coordinates is defined by the relationships (Fig. 2)

$$\left. \begin{aligned} x &= r \cos \theta & r &= \sqrt{x^2 + y^2} \\ y &= r \sin \theta & \theta &= \arctg \frac{y}{x} \\ z &= z & z &= z \end{aligned} \right\} \quad (2.9)$$

The spherical coordinates r, θ, ψ (Fig. 2) are connected with Cartesian coordinates by the relationships

$$\left. \begin{aligned} x &= r \sin \theta \cos \psi & r &= \sqrt{x^2 + y^2 + z^2} \\ y &= r \sin \theta \sin \psi & \theta &= \arctg \frac{\sqrt{x^2 + y^2}}{z} \\ z &= r \cos \theta & \psi &= \arctg \frac{y}{x} \end{aligned} \right\} \quad (2.10)$$

The equations of motion and the equation of discontinuity in a

cylindrical system of coordinates have the form

$$\left. \begin{aligned} \frac{\partial v_r}{\partial t} + v_r \frac{\partial v_r}{\partial r} + \frac{v_\theta}{r} \frac{\partial v_r}{\partial \theta} + v_z \frac{\partial v_r}{\partial z} - \frac{v_\theta^2}{r} &= -\frac{1}{\rho} \frac{\partial p}{\partial r}, \\ \frac{\partial v_\theta}{\partial t} + v_r \frac{\partial v_\theta}{\partial r} + \frac{v_\theta}{r} \frac{\partial v_\theta}{\partial \theta} + v_z \frac{\partial v_\theta}{\partial z} + \frac{v_r v_\theta}{r} &= -\frac{1}{\rho r} \frac{\partial p}{\partial \theta}, \\ \frac{\partial v_z}{\partial t} + v_r \frac{\partial v_z}{\partial r} + \frac{v_\theta}{r} \frac{\partial v_z}{\partial \theta} + v_z \frac{\partial v_z}{\partial z} &= -\frac{1}{\rho} \frac{\partial p}{\partial z}, \\ \frac{\partial \rho}{\partial t} + \frac{1}{r} \frac{\partial (\rho r v_r)}{\partial r} + \frac{1}{r} \frac{\partial (\rho v_\theta)}{\partial \theta} + \frac{\partial (\rho v_z)}{\partial z} &= 0. \end{aligned} \right\} \quad (2.11)$$

In spherical coordinates, they are written in the following manner:

$$\left. \begin{aligned} \frac{\partial v_r}{\partial t} + v_r \frac{\partial v_r}{\partial r} + \frac{v_\theta}{r} \frac{\partial v_r}{\partial \theta} + \frac{v_\phi}{r \sin \theta} \frac{\partial v_r}{\partial \phi} - \frac{v_\theta^2 + v_\phi^2}{r} &= -\frac{1}{\rho} \frac{\partial p}{\partial r}, \\ \frac{\partial v_\theta}{\partial t} + v_r \frac{\partial v_\theta}{\partial r} + \frac{v_\theta}{r} \frac{\partial v_\theta}{\partial \theta} + \frac{v_\phi}{r \sin \theta} \frac{\partial v_\theta}{\partial \phi} + \frac{v_r v_\theta}{r} - & \\ - \frac{v_\phi^2 \cot \theta}{r} &= -\frac{1}{\rho r} \frac{\partial p}{\partial \theta}, \\ \frac{\partial v_\phi}{\partial t} + v_r \frac{\partial v_\phi}{\partial r} + \frac{v_\theta}{r} \frac{\partial v_\phi}{\partial \theta} + \frac{v_\phi}{r \sin \theta} \frac{\partial v_\phi}{\partial \phi} + \frac{v_r v_\phi}{r} + & \\ + \frac{v_\theta v_\phi \cot \theta}{r} &= -\frac{1}{\rho r \sin \theta} \frac{\partial p}{\partial \phi}, \\ \frac{\partial \rho}{\partial t} + \frac{1}{r^2} \frac{\partial (\rho r^2 v_r)}{\partial r} + \frac{1}{r \sin \theta} \frac{\partial (\rho v_\theta \sin \theta)}{\partial \theta} + \frac{1}{r \sin \theta} \frac{\partial (\rho v_\phi)}{\partial \phi} &= 0. \end{aligned} \right\} \quad (2.12)$$

In view of the difficulty in integrating these systems, we more often examine one-dimensional fluid motion. This is motion which is a function of one spatial coordinate r , and time t . Special cases of one-dimensional motion are motion having plane, cylindrical, and spherical symmetry.

On the basis of (2.1), (2.6), (2.8), (2.11), and (2.12) it is not difficult to derive equations of one-dimensional motion in the form

$$\frac{\partial v}{\partial t} + v \frac{\partial v}{\partial r} + \frac{1}{\rho} \frac{\partial p}{\partial r} = 0, \quad (2.13)$$

$$\frac{\partial \rho}{\partial t} + v \frac{\partial \rho}{\partial r} + \rho \frac{\partial v}{\partial r} + \frac{(v-1)v}{r} = 0, \quad (2.14)$$

$$\frac{\partial S}{\partial t} + v \frac{\partial S}{\partial r} = 0, \quad (2.15)$$

where $v = 1, 2$, and 3 , respectively, for motion having plane, cylindrical, and spherical symmetry.

For isentropic flow, equation (2.15) is replaced by an equation in finite form [for an ideal gas - by the Poissonian adiabatic curve $p/\rho^k = p_0/\rho_0^k$; for water - by the Tête equation (1.25)]. It is suitable, in this case, to use the variables v and α in the system (2.13)-(2.15) in place of the variables v , p , and ρ . As a result of simple transformations we find that*

$$\frac{\partial v}{\partial t} + v \frac{\partial v}{\partial r} + \frac{2\alpha}{n-1} \frac{\partial \alpha}{\partial r} = 0, \quad (2.16)$$

$$\frac{\partial \alpha}{\partial t} + v \frac{\partial \alpha}{\partial r} + \frac{n-1}{2} \alpha \frac{\partial v}{\partial r} + \frac{n-1}{2} \frac{(v-1)\alpha v}{r} = 0. \quad (2.17)$$

In spite of the apparent notational simplicity, no precise solution of system (2.16)-(2.17) has been derived. Consequently, we use various approximate methods. The most widely-used and universal of these is the characteristic method, the essence of which we will explain in brief.

Let us assume that in the plane r, t we are given curve L whose equation is $r = r(t)$. The functions v_L, α_L on this curve are known. The problem consists in defining the integrals of the system of equations (2.16), (2.17) which could be converted into the given values in curve L . In other words, we must find the integral surface which satisfies equations (2.16), (2.17) and passes through curve L . The task of defining a solution with respect to these conditions is usually called a Cauchy problem.

Let us consider that the functions v and α are the analytic functions of r and t . The following equalities are plotted on curve L

*The corresponding system for an ideal gas differs from (2.16)-(2.17) only in that it will have the adiabatic coefficient k in place of the quantity n .

$$\left. \begin{aligned} \frac{dv_L}{dt} &= \frac{\partial v_L}{\partial t} + r' \frac{\partial v_L}{\partial r} \\ \frac{da_L}{dt} &= \frac{\partial a_L}{\partial t} + r' \frac{\partial a_L}{\partial r} \end{aligned} \right\} \quad (2.18)$$

Moreover, the equations of hydrodynamics, (2.16) and (2.17), must be satisfied on the same curve.

Let us explain which constraints are imposed on the basic system of equations because the solution of this system must satisfy the given values of hydrodynamic parameters on curve L. For this purpose, let us find the magnitudes of the partial derivatives $\partial v_L / \partial t$ and $\partial a_L / \partial t$ on the basis of (2.18), and substitute them in equations (2.16) and (2.17). We will then find that:

$$\left. \begin{aligned} (v - r') \frac{\partial v}{\partial r} + \frac{2a}{n-1} \frac{\partial a}{\partial r} &= - \frac{dv_L}{dt} \\ \frac{n-1}{2} a \frac{\partial v}{\partial r} + (v - r') \frac{\partial a}{\partial r} &= - \frac{da_L}{dt} - \frac{n-1}{2} \frac{(v-1)av}{r} \end{aligned} \right\} \quad (2.19)$$

System (2.19), generally speaking, permits us to find the partial derivatives $\partial v / \partial r$ and $\partial a / \partial r$, except where the determinants are equal to zero. Moreover, there is a countless set of values for the derivatives $\partial v / \partial v$ and $\partial a / \partial r$ which satisfy a given system, i.e., a countless set of integral surface may pass through curve L. This curve is called the characteristic curve (eigenvalues).

In the universal theory of differential equations it has been proven that:

the solution of characteristic equations is equivalent to the solution of an initial system of equations;

the characteristics are invariant during substitution of variables which establishes an equivalent transformation of the points in one space to the points of another space.

Characteristic equations are not difficult to write after equalizing the determinants of the initial system to zero:*

* The second determinant of the system is not written out, since no additional conditions are imposed on the hydrodynamic parameters.

$$\Delta = \begin{vmatrix} v - r' & \frac{2a}{n-1} \\ \frac{n-1}{2} a & v - r' \end{vmatrix} = 0, \quad (2.20)$$

$$\Delta_1 = \begin{vmatrix} -\frac{dv_L}{dt} & \frac{2a}{n-1} \\ -\frac{da_L}{dt} - \frac{n-1}{2} \frac{(v-1)}{r} & va(v-r') \end{vmatrix} = 0. \quad (2.21)$$

The determinant of (2.20) becomes zero, if

$$\left. \begin{aligned} v - r' + a &= 0 & \frac{dr}{dt} &= v + a, \\ v - r' - a &= 0 & \frac{dr}{dt} &= v - a. \end{aligned} \right\} \quad (2.22)$$

Based on the equations in (2.22), the characteristics are propagated at the speed of sound.

According to (2.21)

$$\Delta_1 = -(v - r') \frac{dv_L}{dt} + \frac{2a}{n-1} \frac{da_L}{dt} + a^2 v \frac{(v-1)}{r} = 0.$$

Where $v - r' = \pm a$

$$\pm \frac{av_L}{dt} + \frac{2}{n-1} \frac{da_L}{dt} + av \frac{v-1}{r} = 0. \quad (2.23)$$

The first-class characteristic value is

$$\frac{dr}{dt} = v + a. \quad (2.24)$$

In this characteristic, according to (2.23)

$$\frac{dv}{dt} + \frac{2}{n-1} \frac{da}{dt} = -av \frac{v-1}{r}. \quad (2.25)$$

The second-class characteristic value is

$$\frac{dr}{dt} = v - a. \quad (2.26)$$

* After defining the characteristics we will henceforth omit the index L.

The following relationship must be satisfied in (2.26):

$$\frac{dv}{dt} - \frac{2}{n-1} \frac{da}{dt} = av \frac{\gamma-1}{r}. \quad (2.27)$$

First and second-class characteristic equation systems cannot be solved independently of each other, since each of them represents two equations having four variables. Nevertheless, it is much simpler to integrate these equations than to integrate the initial system of partial differential equations. This also constitutes the basic merit of the characteristics method. System (2.24)-(2.27) generally has no integrable combinations. However, for motion having plane symmetry, the equations of the characteristics have first integrals.

It is now possible to find precise solutions. Let us now move to a familiarization with these solutions.

§3. Some Precise Solutions for One-Dimensional Transient Fluid Motion

For one-dimensional isentropic motion having plane symmetry ($\nu = 1$), equations (2.25) and (2.27) are integrated and system (2.24)-(2.27) assumes the form

$$\left. \begin{aligned} \frac{dr}{dt} &= v + a, \\ v + \frac{2}{n-1} a &= \text{const} = 2\xi; \end{aligned} \right\} \quad (3.1)$$

$$\left. \begin{aligned} \frac{dr}{dt} &= v - a, \\ v - \frac{2}{n-1} a &= \text{const} = 2\eta. \end{aligned} \right\} \quad (3.2)$$

Let us view r and t as functions of the characteristic integers ξ and η :

$$\left. \begin{aligned} r &= r(\xi, \eta), \\ t &= t(\xi, \eta). \end{aligned} \right\} \quad (3.3)$$

Since the quantity ξ is constant in the first-class characteristic, r and t in this characteristic will be functions only of η

$$dr = \frac{\partial r}{\partial \eta} d\eta, \quad dt = \frac{\partial t}{\partial \eta} d\eta.$$

On this basis, the first equation in (3.1) can be written in the form

$$\frac{\partial r}{\partial \eta} = (v + a) \frac{\partial t}{\partial \eta}. \quad (3.4)$$

By analogy, in the second-class characteristic

$$\frac{\partial r}{\partial \xi} = (v - a) \frac{\partial t}{\partial \xi}. \quad (3.5)$$

Moreover, based on the second equations in (3.1) and (3.2)

$$\left. \begin{aligned} v &= \xi + \eta, \\ a &= \frac{n-1}{2} (\xi - \eta). \end{aligned} \right\} \quad (3.6)$$

After substituting this result in (3.4) and (3.5), we will find that

$$\left. \begin{aligned} \frac{\partial r}{\partial \eta} &= \left(\frac{n+1}{2} \xi + \frac{3-n}{2} \eta \right) \frac{\partial t}{\partial \eta}, \\ \frac{\partial r}{\partial \xi} &= \left(\frac{3-n}{2} \xi + \frac{n+1}{2} \eta \right) \frac{\partial t}{\partial \xi}. \end{aligned} \right\} \quad (3.7)$$

System (3.7) is called a canonical system of gas dynamics equations for motion having constant entropy. In contrast to the quasilinear system (2.16)-(2.17), system (3.7) is linear and can be reduced to an even simpler form. For this purpose, we only have to differentiate the first equation in (3.7) with respect to ξ , the second with respect to η , and subtract one from the other.

Consequently, we find that

$$[(n-1)\xi - (n-1)\eta] \frac{\partial^2 t}{\partial \xi \partial \eta} + \frac{n+1}{2} \left(\frac{\partial t}{\partial \xi} - \frac{\partial t}{\partial \eta} \right) = 0$$

or

$$\frac{\partial^2 t}{\partial \xi \partial \eta} = \frac{n+1}{2(n-1)(\xi - \eta)} \left(\frac{\partial t}{\partial \xi} - \frac{\partial t}{\partial \eta} \right). \quad (3.8)$$

If $\frac{1}{2} \frac{n+1}{n-1} = m$, where m is an integer, then equation (3.8) is called a Darboux equation and is integrated in finite form. For air in particular, assuming that $n = k = 1.4$, we will find that $m = 3$. For water, $n \approx 7$ and the quantity $\frac{1}{2} \frac{n+1}{n-1}$ is a fractional number. In this case, however, as is shown in paper [26], after choosing the appropriate form of approximation for the condition of isentropy the system of equations of plane motion can be reduced to a Darboux equation.*

Let us touch upon yet another case of isentropic motion of a fluid having plane symmetry which permits integration of gas dynamics equations in finite form. Let us assume that the quantities of particle velocity v and the speed of sound are constant values along one of the first-series characteristics in plane r, t . according to the first equality in (3.1), this characteristic will be a straight line, since it has $dr/dt = \text{constant}$. The second-class characteristics L_1, L_2, \dots, L_i intersect this straight line at points M_1, M_2, \dots, M_i .

For the points indicated, the following equalities are valid:

$$v_{M_1} - \frac{2}{n-1} a_{M_1} = 2\eta_1,$$

$$v_{M_2} - \frac{2}{n-1} a_{M_2} = 2\eta_2,$$

$$\dots \dots \dots$$

$$v_{M_i} - \frac{2}{n-1} a_{M_i} = 2\eta_i,$$

and since the quantities v and a are constant at points M_1, M_2, \dots, M_i , the characteristic integers $\eta_1, \eta_2, \dots, \eta_i$ become equal.

* At pressure up to $2,000 \text{ kg/cm}^2$, one possible form of this approximation is

$$\frac{p+B}{p_0+B} = \left[1.67 \left(\frac{p}{p_0} \right)^3 - 2.78 \left(\frac{p}{p_0} \right) + 1.54 \right] \frac{0.149}{\left[1 - 0.65 \frac{p}{p_0} \right]^3}.$$

In this connection, the quantity m in the Darboux equation equals one.

Thus, the relationship is

$$v - \frac{2}{n-1} a = 2\gamma_0 \quad (3.9)$$

will be satisfied not only along the given characteristic, but in its entire plane.

If we now express the quantity α in terms of v and substitute it in the equation of motion (2.16), we will arrive at a partial differential linear equation of the first order

$$\frac{\partial v}{\partial t} + \left[\frac{n+1}{2} v - (n-1) \gamma_0 \right] \frac{\partial v}{\partial r} = 0, \quad (3.10)$$

which is equivalent to a system of ordinary differential equations

$$\frac{dt}{1} = \frac{dr}{\frac{n+1}{2} v - (n-1) \gamma_0} = \frac{dv}{0}. \quad (3.11)$$

The common integral of (3.11) is

$$r = \left[\frac{n+1}{2} v - (n-1) \gamma_0 \right] t + \varphi(v). \quad (3.12)$$

This result was first obtained by Riemann in 1860. The solution of (3.12) and (3.9) is called a Riemannian trend or a unidirectional direct wave. If we assume, by analogy, that the quantities of particle velocity and the speed of sound are second-class characteristic constants, we get:

$$r = \left[\frac{n+1}{2} v - (n-1) \gamma_0 \right] t + \varphi_1(v), \quad (3.13)$$

$$v + \frac{2}{n-1} a = 2\gamma_0. \quad (3.14)$$

The solution of (3.13) and (3.14) is called a unidirectional backward wave.

Unidirectional direct and backward waves, which depend only on one arbitrary function, are not special cases of the general solution

of initial system (2.16), (2.17). They are particular solutions of this system which describe completely fixed physical processes. The chief feature of these solutions is that motion characterized by a unidirectional direct or backward wave can be associated with an area of rest or, generally, with an area of stationary medium motion.

If the function $\phi(v)$ or $\phi_1(v)$ in (3.12) or (3.13) is exactly equal to zero, then motion is only a function of the ratio of r/t . The distribution of hydrodynamic parameters at various points in time will be similar to each other, only differing in scale. This type of motion is called self-similar. The natural extension of self-similar motion is the dependence of hydrodynamic parameters on the parameter t^α/r^β , where α and β are constants. For self-similar motion, integration of a system of partial differential equations can always be reduced to integration of ordinary differential equations.

Let us touch briefly upon yet another class of precise solutions for transient motion of a fluid which is valid for studying disturbances of infinitely low amplitude. These solutions are often called the acoustic approximation.

Let us cite the hydrodynamic equations which are required for further statement in acoustic approximation, restricting ourselves to an examination of one-dimensional motion.

Let us assume that

$$\left. \begin{aligned} p &= p_0 + p', \\ \rho &= \rho_0 + \rho'. \end{aligned} \right\} \quad (3.15)$$

The ratios ρ'/ρ_0 and v/a_0 will be considered small, of the first order. Then, according to (2.13), (2.14), and (3.15), for one-dimensional motion we will find that

$$\frac{\partial v}{\partial t} + v \frac{\partial v}{\partial r} + \frac{1}{\rho_0 + \rho'} \frac{\partial p'}{\partial r} = 0, \quad (3.16)$$

$$\frac{\partial p'}{\partial t} + v \frac{\partial p'}{\partial r} + (\rho_0 + \rho') \frac{\partial v}{\partial r} + \frac{(v-1)(\rho_0 + \rho')}{r} v = 0. \quad (3.17)$$

Disregarding numerically-small second-order values in equations (3.16) and (3.17) and bearing in mind that

$$\frac{\partial \rho}{\partial t} = \frac{d\rho}{dp} \frac{\partial p}{\partial t} = \frac{1}{a_0^2} \frac{\partial p}{\partial t},$$

we will have

$$\left. \begin{aligned} \rho_0 \frac{\partial v}{\partial t} + \frac{\partial p'}{\partial r} &= 0, \\ \frac{1}{a_0^2} \frac{\partial p'}{\partial t} + \rho_0 \frac{\partial v}{\partial r} + \frac{(v-1)\rho_0 v}{r} &= 0. \end{aligned} \right\} \quad (3.18)$$

Differentiating the first equation in (3.18) with respect to r , the second with respect to t , and subtracting the second from the first, we find that

$$\frac{\partial^2 p'}{\partial r^2} - \frac{1}{a_0^2} \frac{\partial^2 p'}{\partial t^2} - \frac{(v-1)}{r} \rho_0 \frac{\partial v}{\partial t} = 0. \quad (3.19)$$

After substituting $\rho_0 \frac{\partial v}{\partial t} = - \frac{\partial p'}{\partial r}$, we will find that

$$\frac{\partial^2 p'}{\partial r^2} - \frac{1}{a_0^2} \frac{\partial^2 p'}{\partial t^2} + \frac{(v-1)}{r} \frac{\partial p'}{\partial r} = 0. \quad (3.20)$$

Equation (3.20) is called a wave equation. It is easy to prove that this type of equation will be satisfied by ρ' and v for the assumptions formulated.

For motion having plane symmetry ($v = 1$), the solution of the wave equation is

$$\rho' = f_1\left(t - \frac{r}{a_0}\right) + f_2\left(t + \frac{r}{a_0}\right). \quad (3.21)$$

Based on the structure of (3.21), this equation represents the sum of two traveling waves; any disturbance formed at some point r travels at the speed of sound a_0 , remaining unchanged in form.

For the case of motion having spherical symmetry, the physical sense of the wave equation solution remains the same, the difference being that disturbance amplitudes will change in inverse proportion to the distance

$$p' = \frac{f_1\left(t - \frac{r}{a_0}\right) + f_2\left(t + \frac{r}{a_0}\right)}{r} \quad (3.22)$$

The solution of (3.20) for motion having axial symmetry has a slightly more complex form:

$$p' = \int \frac{f_1\left(t - \frac{r}{a_0}\right)}{\sqrt{r^2 - R^2}} dr + \int \frac{f_2\left(t + \frac{r}{a_0}\right)}{\sqrt{r^2 - R^2}} dr,$$

where we designate the distance from a point having pressure p' to the origin of the coordinates, in terms of r , as before; and the distance from the same point to the axis of symmetry in terms of R .

In all these cases, the functions f_1 and f_2 have been set on the basis of the problem's boundary conditions.

In conclusion, let us formulate recommendations for the practical application of the acoustic approximation. For this purpose, let us evaluate the order of magnitude in the initial equation of motion, (3.16). Let us note that according to dynamic compatibility condition,

$$v \sim \frac{p'}{\rho_0 a_0}.$$

The spatial and temporal characteristics are associated by the scale of the speed of sound

$$r \sim a_0 t.$$

Consequently, the term $v \frac{\partial v}{\partial r}$, which was rejected in acoustics equations will be of the order of magnitude $p'/\rho_0 a_0^2$ in comparison to $\frac{v}{t}$ and $\frac{1}{\rho_0} \frac{\partial p'}{\partial r}$

Let us assume that an error of $\approx 5\%$ is possible. In other words, let

$$\frac{\Delta p_\phi}{p_0 a_0^2} \leq 0.05.$$

Substituting the appropriate density and speed of sound* values into this equation, we come to the conclusion that the use of the acoustic approximation for water is possible with the error indicated where pressure on the front is $\leq 1100 \text{ kg/cm}^2$; and in the air where $\Delta p_\phi \leq 0.07 \text{ kg/cm}^2$.

In our arguments we have been based on dynamic compatibility conditions and therefore, the conclusion that we formulate, strictly speaking, is only valid for the proximity of a shock-wave front.

§4. Laws of Similarity in the Theory of Explosion. Gas Bubble Expansion.

Generally, in motion of a compressible, ponderable, viscous fluid, the conditions of similarity require the equality of four dimensionless criteria at similar points in flow:

homochronicity number, or Strouhal number

$$Sh = \frac{w}{l}, \quad (4.1)$$

Froude number

$$Fr = \frac{w^2}{gl}, \quad (4.2)$$

Euler number

$$Eu = \frac{p}{\rho w^2}. \quad (4.3)$$

* For water, $\rho_0 = 102 \text{ kg}\cdot\text{sec}^2/\text{m}^4$, $a_0 = 1500 \text{ m/sec.}$; for air, $\rho_0 = 0.125 \text{ kg}\cdot\text{sec}^2/\text{m}^4$, $c_0 = 340 \text{ m/sec.}$

Reynolds number

$$Re = \frac{vl}{\nu}, \quad (4.4)$$

where g - the acceleration of gravity; ν - the kinematic coefficient of viscosity.

In most problems in the theory of explosion we can utilize the notions of an ideal fluid from gas dynamics. Consequently, we only have to consider two of the four criteria of similarity - the homochronicity number and the Euler number. Nonfulfillment of similarity for the Froude and Reynolds numbers does not entail a scaling effect.

Let us assume that natural and test explosion are being produced in the same medium ($\rho_0 = \rho_0$). On the basis of dynamic compatibility conditions, irrespective of the cause of shock-wave formation, there is an equivalent interrelationship between hydrodynamic parameters on the front. Consequently, if we established that pressure quantities on the wave-front are identical at certain distances from the explosion centers of two charges, then the Euler numbers would be identically equal

$$\frac{p_M}{\rho_M v_M^2} = \frac{p_m}{\rho_m v_m^2}. \quad (4.5)$$

Based on the condition of homochronicity, (4.1), it follows that

$$\frac{t_M}{l_M} = \frac{t_m}{l_m}. \quad (4.6)$$

Thus, in simulating fluid motion induced by an explosion, the scale of linear dimensions must be identical with the time scale.

The typical linear dimensions defining the scale of effects in explosion in an infinite medium are the charge dimensions. The following law of similarity for explosion of identical explosives is based on this: the parameters of transient motion induced by an explosion do not change if the scales of length and time, by which these

parameters are measured, are increased or reduced by the same number of times as are the charge dimensions.

The formulation of the laws of similarity is slightly complicated when contrasting the hydrodynamic fields in a fluid which are formed during the explosion of different explosives. As experience shows us, our similarity can be based on the energy principle. Of course, owing to differences in boundary conditions in direct proximity to a charge, no similarity in the fields will be observed. However, since the energy dissipation process occurs at a high rate for strong shock waves, the time inevitably comes when the pressure values will be identical at certain distances from the centers of two different charges; and consequently, because of dynamic compatibility conditions, the quantities of density and particle speed will be identical.

Compatible points may be characterized by an equation of the ratios

$$\frac{t_1}{\sqrt[3]{E_1}} = \frac{t_2}{\sqrt[3]{E_2}} \quad (4.7)$$

where E_1 and E_2 - energy liberated during the explosion of two different charges.

Compatible time periods will be found in the same relationship

$$\frac{t_1}{t_2} = \frac{\sqrt[3]{E_1}}{\sqrt[3]{E_2}} \quad (4.8)$$

The energy of an explosion is proportional to the weight of the charge, G . The latter, in turn, equivalently defines the quantity of the radius of a spherical equivalent charge, because

$$G = \frac{4}{3} \pi R_0^3 \gamma \quad (4.9)$$

where γ - the density of the explosive.

Given that $\gamma = 1.6 \text{ g/cm}^3$ for trinitrotoluene, we will find that

$$R_0 = 0.053 \sqrt[3]{G}. \quad (4.10)$$

where R_0 - the charge radius, m.; G - weight, kg.

These notions will be used many times henceforth.

In addition to the shock-wave front, the gas-bubble surface is a limiting surface of transient fluid motion during an explosion.

Let us first discuss, after Lamb [36], the expansion of a gas bubble in an infinite noncompressible medium.

Considering the motion has spherical symmetry, we will write the equation of discontinuity in the form

$$\frac{\partial \rho}{\partial t} + v \frac{\partial \rho}{\partial r} + \rho \frac{\partial v}{\partial r} + \frac{2v\rho}{r} = 0. \quad (2.14)$$

Given that $\rho = \rho_0 = \text{constant}$, we will find that

$$\frac{\partial v}{\partial r} + \frac{2v}{r} = 0. \quad (4.11)$$

Integrating (4.11), we find that

$$v = \frac{f(t)}{r^2}, \quad (4.12)$$

where $f(t)$ - an arbitrary function of time.

Let us use the equation of motion

$$\frac{\partial v}{\partial t} + v \frac{\partial v}{\partial r} + \frac{1}{\rho} \frac{\partial p}{\partial r} = 0. \quad (2.13a)$$

After substituting the quantity v in it according to (4.12), we will have

$$\frac{\partial p}{\partial r} = -\frac{\rho_0}{r^3} f'(t) + \frac{2\rho_0}{r^3} |f(t)|^2. \quad (4.13)$$

Integrating equality (4.13) with respect to r , we find

$$p = \frac{p_0}{r} f'(t) - \frac{p_0}{2r^2} |f(t)|^2 + F(t), \quad (4.14)$$

where $F(t)$ - another arbitrary function of time.

The value of $F(t)$ is found based on the condition that $r \rightarrow \infty$ $p \rightarrow p_0$, where p_0 - hydrostatic pressure deep in the explosion center:

$$p_0 = p_a + \gamma H, \quad (4.15)$$

p_a - atmospheric pressure; γ - gravimetric density of water; H - explosion depth.

Since $f(t)$ and $f'(t)$ are finite, we will find that from equation (4.14) $F(t) \equiv p_0$ and consequently,

$$p = p_0 + \frac{p_0}{r} f'(t) - \frac{p_0}{2r^2} |f(t)|^2. \quad (4.16)$$

The function $f(t)$ can easily be evaluated on the basis of dynamic compatibility conditions at the boundary of the gas bubble. Since this boundary is a stationary second-order discontinuity surface, the following equalities must be satisfied in it, according to (1.6) and (1.7)

$$\left. \begin{aligned} [v] &= 0, \\ [\rho] &= 0. \end{aligned} \right\} \quad (4.17)$$

Let the radius of the gas bubble be characterized by the coordinate R . Then, according to (4.12) and the first equation in (4.17)

$$\frac{dR}{dt} = \frac{f(t)}{R^2}, \quad (4.18)$$

whence

$$\left. \begin{aligned} f(t) &= R^2 \frac{dR}{dt}, \\ f'(t) &= R^2 \frac{d^2 R}{dt^2} + 2R \left(\frac{dR}{dt} \right)^2. \end{aligned} \right\} \quad (4.19)$$

If we also designate pressure on the gas-bubble surface in terms of p_r , on the basis of (4.16) and (4.19) we can write for this surface

$$p_r - p_0 = \frac{\rho_0}{R} \left[R^3 \frac{d^2 R}{dt^2} + 2R \left(\frac{dR}{dt} \right)^2 \right] - \frac{p_0}{2R^0} R^0 \left(\frac{dR}{dt} \right)^2$$

or by solving with respect to $d^2 R/dt^2$,

$$\frac{d^2 R}{dt^2} = \frac{p_r - p_0}{\rho_0 R} - \frac{3}{2} \frac{1}{R} \left(\frac{dR}{dt} \right)^2. \quad (4.20)$$

An ordinary differential equation, (4.20), permits us to define the motion of the gas-bubble surface $R(t)$, if we are given the pressure change within it $p_r(R)$.

The adiabatic expansion of TNT denonation products was studied by Jones. The Jones adiabatic curve is shown in Fig. 3 which has been borrowed from Cowle's book [10]. It can be approximated by the relationship

$$p_r = \frac{A}{(\bar{R})^x}, \quad (4.21)$$

where $\bar{R} = R/R_0$ - the relative radius of the gas-bubble; A, x - coefficients which are constant for a fixed range of variation in \bar{R} (Table 1).

Assuming that density and pressure within the gas-bubble are uniformly distributed (the so-called notion of "ordinary" explosion), we integrate (4.20) using (4.21):

introducing another variable

$$\xi = \frac{1}{2} \left(\frac{dR}{dt} \right)^2, \quad \left. \begin{aligned} \frac{d\xi}{dR} &= \frac{d\xi}{dt} \frac{dt}{dR} = \frac{dR}{dt} \frac{d^2 R}{dt^2} \frac{dt}{dR} = \frac{d^2 R}{dt^2} \end{aligned} \right\} \quad (4.22)$$

we derive a linear differential equation with respect to ξ :

$$\frac{d\xi}{dR} + \frac{3\xi}{R} = \frac{1}{\rho_0 R} \left[\frac{A}{R^{3x}} - \nu_0 \right]. \quad (4.23)$$

Table 1

Coefficients	$1.0 < \bar{R} < 1.5$	$1.5 < \bar{R} < 1.7$	$1.7 < \bar{R} < 2.5$	$\bar{R} < 2.5$
$A, \text{ g/cm}^3$	100 000	27 200	16 900	8600
n	2.39	1.77	1.47	1.25

$p, \text{ kg/cm}^2$

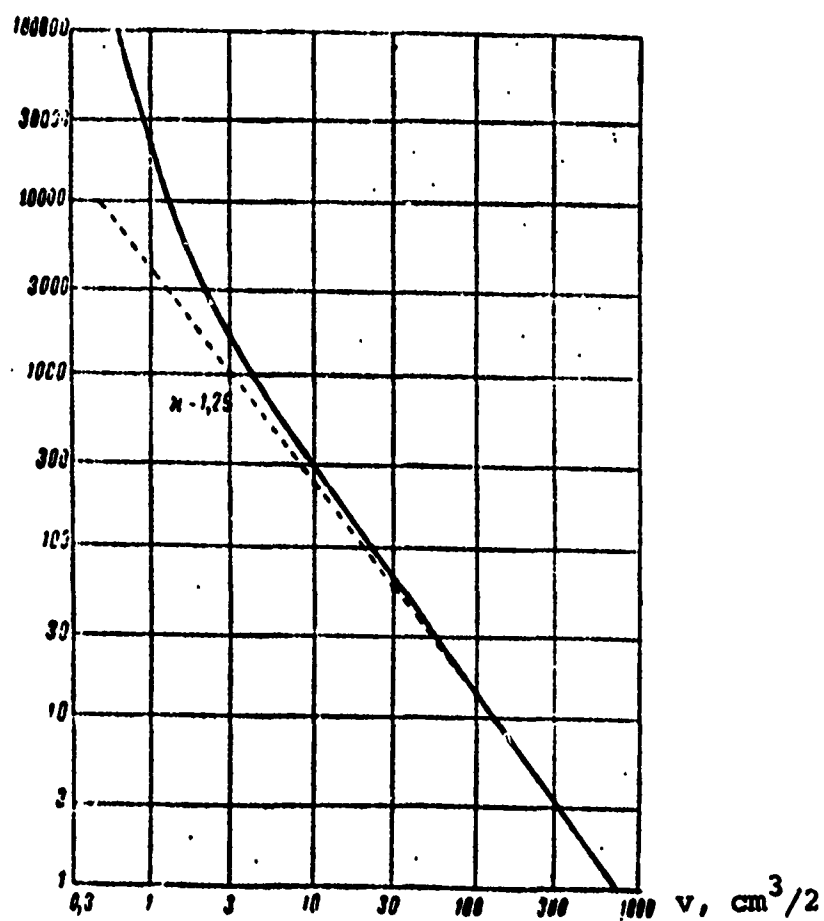


Fig. 3. Adiabatic Curve for Products of TNT
(according to Jones).

The solution of equation(4.23) has the form

$$C = \frac{C}{R^3} - \frac{p_0}{3\rho_0} \left(\frac{1}{x-1} \frac{A}{\rho_0 R^{3x}} + 1 \right). \quad (4.24)$$

Since at the point of maximum gas-bubble expansion its surface speed is equal to zero, when $\bar{R} = \bar{R}_{\max}$, $dR/dt = 0$ and $\xi = 0$, whence

$$C = \frac{\rho_0 \bar{R}_{\max}^3}{3\rho_0} \left(\frac{1}{x-1} \frac{A}{\rho_0 \bar{R}_{\max}^{3x}} + 1 \right).$$

Substituting this value in (4.24) and returning to the variable \bar{R} , we find that:

$$\frac{dR}{dt} = \sqrt{\frac{2}{3} \frac{p_0}{\rho_0 R^3} \left[\frac{1}{x-1} \frac{A}{\rho_0} \left(\frac{1}{\bar{R}_{\max}^{3(x-1)}} - \frac{1}{\bar{R}^{3(x-1)}} \right) + \bar{R}_{\max}^3 - R^3 \right]}. \quad (4.25)$$

A numerical integration of (4.25) permits us to find the relationship of the gas-bubble radius as a function of time. Having this relationship, we can easily calculate particle speed at any point in the medium:

$$\left. \begin{aligned} f(t) &= R^2 \frac{dR}{dt}, \\ v &= \frac{f(t)}{r^2} = \frac{R^2}{r^2} \frac{dR}{dt}. \end{aligned} \right\} \quad (4.26)$$

On the basis of (4.26) and (4.16) the quantities of pressure are defined. A final solution is derived for the problem. However, in view of previously-state concepts (cf. §1), this solution cannot even be utilized for the approximate evaluation of pressure fields in an underwater explosion. At the same time, it does permit us to derive a simple relationship for calculating the first pulsation period of a gas-bubble.

Let us return to equation (4.25) for this purpose. If we exclude the initial expansion section from our examination, then starting with some $\bar{R} > 1$, we can disregard the first term in brackets in the radicand of (4.25). Instead of (4.25) we will then find that

$$\frac{d\bar{R}}{dt} = \sqrt{\frac{2}{3} \frac{p_0}{\rho_0 R_0^3} \left[\left(\frac{\bar{R}_{\max}}{\bar{R}} \right)^3 - 1 \right]}. \quad (4.25a)$$

based on which the gas-bubble expansion time to its maximum radius will be defined by the relationship

$$t_{\max} = R_0 \sqrt{\frac{3}{2} \frac{p_0}{\rho_0}} \int_1^{\bar{R}_{\max}} \frac{d\bar{R}}{\sqrt{\left(\frac{\bar{R}_{\max}}{\bar{R}}\right)^3 - 1}}. \quad (4.27)$$

Introducing another variable $x = \left(\frac{\bar{R}}{\bar{R}_{\max}}\right)^3$ and considering that $x_0 = \frac{1}{\bar{R}_{\max}^3} \approx 0$, we will write formula (4.27) in the form

$$t_{\max} = \sqrt{\frac{1}{6} \frac{p_0}{\rho_0}} R_0 \bar{R}_{\max} \int_0^1 x^{r-1} (1-x)^{q-1} dx, \quad (4.28)$$

where $r = 5/6$ and $q = 1/2$.

As we know*, the integral in (4.28) is a total β -function (a primitive Euler integral):

$$B_1(r, q) = \int_0^1 x^{r-1} (1-x)^{q-1} dx.$$

It can easily be calculated in terms of Γ -functions:

$$B_1(r, q) = \frac{\Gamma(r) \Gamma(q)}{\Gamma(r+q)};$$

specifically,

$$B_1\left(\frac{5}{6}, \frac{1}{2}\right) = \frac{\Gamma\left(\frac{5}{6}\right) \Gamma\left(\frac{1}{2}\right)}{\Gamma\left(\frac{4}{3}\right)} = 2.24.$$

Substituting this result in (4.28), we can write

$$t_{\max} = \frac{0.915 p_0^{1/2} R_0 \bar{R}_{\max}}{\rho_0^{1/2}}. \quad (4.29)$$

The first pulsation period is

* Cf. E. T. Whittaker, J. N. Watson, A Course in Modern Analysis, Part II, GIRML (1963).

$$T = 2t_{\max} = \frac{1.83 p_0^{1/2} R_0 \bar{R}_{\max}}{p_0^{1/2}} \quad (4.30)$$

or in a dimensionless form,

$$\bar{T} = \frac{2t_{\max} a_0}{R_0} = \frac{1.83 p_0^{1/2} \bar{R}_{\max}}{p_0^{1/2}}. \quad (4.31)$$

Let us return to equation (4.27) which will now be written in the form of an integral having a variable upper limit and new variables $y = R/R_{\max}$, $\tau = t/T$.

We have

$$\tau = 0.67 \int_{y_0}^y \frac{dy}{\left[\left(\frac{1}{y}\right)^3 - 1\right]^{1/2}}. \quad (4.32)$$

When $y \gg 1$, the integral of (4.32) is calculated by parts:

$$\tau = 0.268 (y^{2.5} - y_0^{2.5}) \quad (4.33)$$

or similarly,

$$\bar{R} = (1 + \tau \bar{t})^{0.4}, \quad (4.34)$$

where

$$\tau_i = 3.73 \frac{\bar{R}_{\max}^{2.5}}{\bar{t}}. \quad (4.35)$$

Relationships (4.34) and (4.35) permit us to approximately calculate gas-bubble motion for any initial hydrostatic pressure values. In this connection, the only parameter which must be given is the first pulsation period (or maximum radius).

Evaluations made on this scheme do not produce considerable error for small p_0 , until it becomes necessary to calculate the internal energy of the detonation products ($\bar{R} < 0.4 \bar{R}_{\max}$).

Henceforth, we will need more complete and precise information on gas-bubble motion. This information forms the basis of the theory developed by Herring [10].

Let us give a brief account of Herring's solution, supplementing it somewhat. Let us return to Euler's equation for motion having spherical symmetry

$$\frac{\partial v}{\partial t} + v \frac{\partial v}{\partial r} = -\frac{1}{\rho} \frac{dp}{dr}. \quad (2.13)$$

Integrating this equation from the gas-bubble surface to infinity, we find that:

$$\int_R^\infty \frac{\partial v}{\partial t} dr + \int_R^\infty v \frac{\partial v}{\partial r} dr = - \int_R^\infty \frac{dp}{\rho}. \quad (4.36)$$

We will introduce spherical divergence of velocity as a new variable

$$\lambda = \frac{1}{r^2} \frac{\partial}{\partial r} (r^2 v) = \frac{\partial v}{\partial r} + \frac{2}{r} v.$$

Let us integrate the first term in (4.36) by parts, using this expression:

$$\int_R^\infty \frac{\partial v}{\partial t} dr = - \int_R^\infty \frac{\partial}{\partial t} (r^2 v) d\left(\frac{1}{r}\right) = -r \frac{\partial v}{\partial t} \Big|_R^\infty + \int_R^\infty r \frac{\partial \lambda}{\partial t} dr.$$

but

$$\frac{\partial v}{\partial t} \Big|_{r=R} = \frac{d}{dt} \Big|_R - v \frac{\partial v}{\partial r} \Big|_{r=R} = \frac{d^2 R}{dt^2} - \frac{dR}{dt} \lambda(R) + \frac{2}{R} \left(\frac{dR}{dt} \right)^2.$$

Thus,

$$\int_R^\infty \frac{\partial v}{\partial t} dr = R \frac{d^2 R}{dt^2} - R \frac{dR}{dt} \lambda(R) + 2 \left(\frac{dR}{dt} \right)^2 + \int_R^\infty r \frac{\partial \lambda}{\partial t} dr.$$

The second integral of (4.36) is taken by parts:

$$\int_R^\infty v \frac{\partial v}{\partial r} dr = \frac{v^2}{2} \Big|_R^\infty = -\frac{1}{2} \left(\frac{dR}{dt} \right)^2.$$

Equation (4.36) can be written in the form

$$R \frac{d^2 R}{dt^2} + \frac{3}{2} \left(\frac{dR}{dt} \right)^2 - R \frac{dR}{dt} \lambda(R) + \int_R^{\infty} r \frac{\partial \lambda}{\partial t} dr = - \int_R^{\infty} \frac{dp}{r}. \quad (4.37)$$

If we are examining a range of pressures which are not in excess of 1000 kg/cm², we can use the acoustic approximation to define the integral consisting of the left side of equation (4.37). Function λ will then be the solution of a wave equation of the type (3.20):

$$\lambda = \frac{1}{r} f \left(t - \frac{r}{a_0} \right).$$

Considering this, we can write

$$\int_R^{\infty} r \frac{\partial \lambda}{\partial t} dr = -a_0 \int_R^{\infty} \frac{\partial}{\partial r} (r \lambda) dr = -a_0 r \lambda \Big|_R^{\infty} = a_0 R \lambda(R),$$

and equation (4.37) is reduced to the form

$$R \frac{d^2 R}{dt^2} + \frac{3}{2} \left(\frac{dR}{dt} \right)^2 + a_0 R \lambda(R) \left(1 - \frac{1}{a_0} \frac{dR}{dt} \right) = - \int_R^{\infty} \frac{dp}{r}. \quad (4.38)$$

Let us note, furthermore, that according to the equation of discontinuity, (2.14),

$$\lambda(R) = - \frac{1}{r} \frac{dp}{dt} \Big|_{r=R} = - \frac{1}{a_0^2 r} \frac{dp}{dt} \Big|_{r=R}.$$

Therefore,

$$R \frac{d^2 R}{dt^2} + \frac{3}{2} \left(\frac{dR}{dt} \right)^2 = \frac{a_0 R}{a_0^2 r} \frac{dp}{dt} \Big|_{r=R} \left(1 - \frac{1}{a_0} \frac{dR}{dt} \right) - \int_R^{\infty} \frac{dp}{r}.$$

Within the range of pressures assumed, we can state roughly that $a \approx a_0$, $\rho \approx \rho_0$. Consequently,

$$R \frac{d^2 R}{dt^2} + \frac{3}{2} \left(\frac{dR}{dt} \right)^2 = \frac{R}{r a_0} \frac{dp}{dt} \Big|_{r=R} \left(1 - \frac{1}{a_0} \frac{dR}{dt} \right) + \frac{p_r - p_0}{\rho_0}. \quad (4.39)$$

Equation (4.39) differs from (4.20) only in the first term on the right side which takes into account compressibility of water. The left side of (4.39) is a derivative in terms of R of the function

$(1/2)R^3(dR/dt)^2$ divided by R^2 . Considering this fact, and choosing a value of R^* as the lower limit of integration where the assumptions are valid to a certain precision, let us integrate (4.39). Consequently, we will find that

$$\begin{aligned} & R^2 \left(\frac{dR}{dt} \right)^2 - R^{*2} \left(\frac{dR}{dt} \right)^2 \Big|_{R=R^*} = \\ & = \int_{R^*}^R \left[\frac{p_r - p_0}{\rho_0} + \frac{R}{\rho_0 a_0} \frac{dp}{dt} \Big|_{r=R} \left(1 - \frac{1}{a_0} \frac{dR}{dt} \right) \right] 2R^2 dR. \end{aligned} \quad (4.40)$$

Multiplying both sides of the equation by $2\pi\rho_0$, let us rewrite equation (4.40) in the form

$$\begin{aligned} & \frac{1}{2} (4\pi\rho_0 R^3) \left(\frac{dR}{dt} \right)^2 - \frac{1}{2} (4\pi\rho_0 R^{*3}) \left(\frac{dR}{dt} \right)^2 \Big|_{R=R^*} = \\ & = \int_{R^*}^R p_r (4\pi R^2) dR - \frac{4}{3} \pi (R^3 - R^{*3}) p_0 - \\ & - \frac{4\pi}{a_0} \int_{R^*}^R \left(- \frac{dp}{dt} \right) \Big|_{r=R} \left(1 - \frac{1}{a_0} \frac{dR}{dt} \right) R^2 dR. \end{aligned} \quad (4.41)$$

It is not difficult to give a physical picture of the relationship derived. The left side of equation (4.41) characterizes the increment in kinetic energy of a radial flow of fluid. The first term on the right side defines the work performed by detonation products during expansion of the gas-bubble from R^* to R :

$$\begin{aligned} \int_{R^*}^R p_r (4\pi R^2) dR &= \int_{R^*}^R p_r (4\pi R^2) dR - \int_{R^*}^R p_r (4\pi R^2) dR = \\ &= E_{\text{in}}(R^*) - E_{\text{in}}(R). \end{aligned} \quad (4.42)$$

The second term on the right side is equal to the work performed in overcoming hydrostatic pressure during expansion of the gas-bubble; the third term on the right side defines the energy expended in the radiation of pressure (shock-wave) during expansion of the gas-bubble from initial radius R^* to the flowing radius R . Let us combine the terms containing the initial radius R^* as a parameter, and designate

that

$$E^* = \frac{1}{2} (4\pi\rho_0 R^{*3}) \left(\frac{dR}{dt} \right)^2 \Big|_{R=R^*} + E_{\text{en}}(R^*) + \frac{4}{3} \pi R^{*3} \rho_0. \quad (4.43)$$

Then, (4.42) can be written in the form

$$\frac{1}{2} (4\pi\rho_0 R^3) \left(\frac{dR}{dt} \right)^2 + E_{\text{en}}(R) + \frac{4}{3} \pi R^3 \rho_0 = E^* - E_{\text{en},s}(R), \quad (4.44)$$

where

$$\begin{aligned} E_{\text{en},s}(R) &= \frac{4\pi}{a_0} \int_{R^*}^R \left(-\frac{dp}{dt} \right) \Big|_{r=R} \left(1 - \frac{1}{a_0} \frac{dR}{dt} \right) R^3 dR = \\ &= \frac{4\pi}{a_0} \int_{R^*}^R \left(-\frac{dp}{dR} \right) \Big|_{r=R} \frac{dR}{dt} \left(1 - \frac{1}{a_0} \frac{dR}{dt} \right) R^3 dR. \end{aligned} \quad (4.45)$$

Using concepts from the theory of similarity, let us reduce (4.45) to a dimensionless form. Assuming that

$$\begin{aligned} \bar{R} &= \frac{R}{R_0}, \\ \bar{t} &= \frac{a_0 t}{R_0}. \end{aligned}$$

where R_0 - initial charge radius calculated according to (4.10), we will find that

$$\frac{3}{2} \rho_0 R_0^3 \bar{R}^3 \left(\frac{d\bar{R}}{d\bar{t}} \right)^2 + e_{\text{en}}(\bar{R}) + \bar{R}^3 \rho_0 = e^* - e_{\text{en},s}(\bar{R}), \quad (4.46)$$

where

$$e_{\text{en}}(\bar{R}) = \frac{E_{\text{en}}}{\frac{4}{3} \pi R_0^3} = 3 \int_{\bar{R}^*}^{\bar{R}} \rho_0 \bar{R}^3 d\bar{R}, \quad (4.47)$$

$$e^* = \frac{3}{2} \rho_0 R_0^3 \bar{R}^{*3} \left(\frac{d\bar{R}}{d\bar{t}} \right)^2 \Big|_{\bar{R}=\bar{R}^*} + e_{\text{en}}(\bar{R}^*) + \bar{R}^{*3} \rho_0. \quad (4.48)$$

$$e_{\text{en},s} = 3 \int_{\bar{R}^*}^{\bar{R}} \left(-\frac{dp}{d\bar{R}} \right) \Big|_{\bar{r}=\bar{R}} \left(\frac{d\bar{R}}{d\bar{t}} \right) \left(1 - \frac{d\bar{R}}{d\bar{t}} \right) \bar{R}^3 d\bar{R}. \quad (4.49)$$

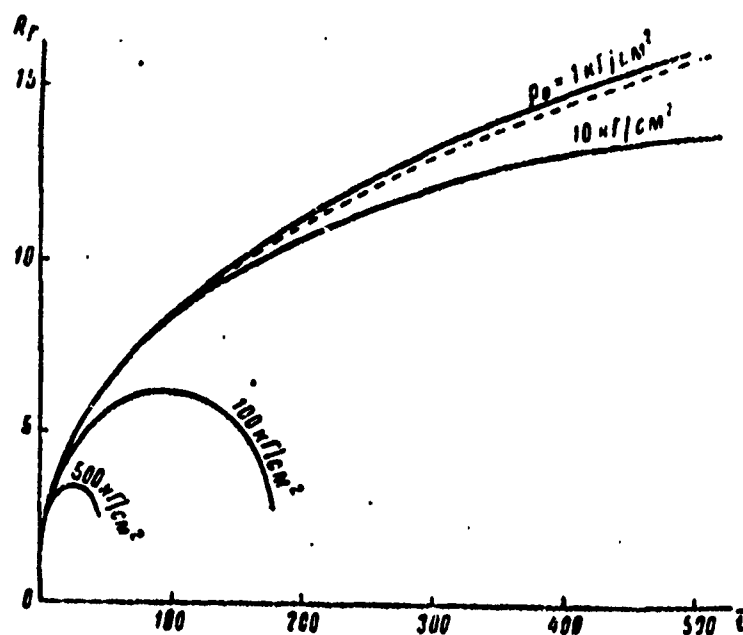


Fig. 4. Time Rate of Change in Gas-Bubble Radius.

Equation (4.46) is an integro-differential equation* with respect to \bar{R}^1 . It can be numerically integrated without difficulty. It is advisable, in this connection, to calculate from \bar{R}_{\max} to $\bar{R}^* \approx 2$. **

In the interval $\bar{R} < 2$, the process of gas-bubble expansion is only slightly affected by hydrostatic pressure and therefore, this range can be calculated once and for all by the characteristics method (see §5).

Subsequently, calculations for various p_0 are carried out from \bar{R} to \bar{R}_{\max} .

Omitting details of calculation, let us only cite the final results, with a brief explanation of their physical nature. Let us first note that energy expended in the formation of an underwater shock-wave is as great as hydrostatic pressure p_0 is small.

*If we reject $\epsilon_{\text{взл}}$, (4.46) becomes an ordinary differential equation of the 1st order.

**Based on data of study [10], it was assumed that $p_0 = 2.55 \text{ kg/cm}^2$, $\bar{R}_{\max} = 22.3$. Also, $\bar{R}^* = 2$, $t = 1.17$, & $\epsilon^* = 38,300 \text{ kg}\cdot\text{cm/cm}^3$.

A rough approximation of the corresponding calculations results in the expression

$$\frac{\gamma_n}{\epsilon_n} = \frac{\epsilon_n - \epsilon^*}{\epsilon_n} \cdot \frac{\epsilon_{n+1}(\bar{R}_{n+1})}{\epsilon_n} = 0,56 - 1,06 \cdot 10^{-3} (\bar{\rho}_n^{0,01} - 1). \quad (4.50)$$

where ε_n - total explosive energy; \bar{p}_0 - initial hydrostatic pressure, adjusted to 1 atm.

The nature of gas-bubble motion in time is shown in Figs. 4 & 5.

For the range $1 < \bar{p}_0 < 100$,

$$\bar{R} = \begin{cases} (1 + 2\bar{t})^{0.4} & 2 < \bar{R} < 0.6\bar{R}_{\max} \\ \bar{R}_{\max} \left(\sin \frac{\pi \bar{t}}{\bar{T}} \right)^{0.5} & \bar{R} \geq 0.6\bar{R}_{\max} \end{cases} \quad (4.51)$$

According to (4.46) and (4.50), the maximum radius of the gas-bubble can be derived from the equation

$$\frac{34.400}{R^{0.75}} + R_{m31}^2 \bar{p}_0 = 31.700 + 76.3 (\bar{p}_0^{0.61} - 1). \quad (4.52)$$

whose solution results may be accurately approximated by the relationship

$$\bar{R}_{max} = \frac{30,7}{p_0^{0,38}}. \quad (4.53)$$

The first pulsation period is roughly equal to

$$T = \frac{8710}{\rho_0^{0.83}} \cdot \frac{R_0}{a_0} = 0.307 \frac{G^{1/2}}{\rho_0^{0.83}}. \quad (4.54)$$

Relationship (4.54) almost coincides with the semi-empirical formula whose structure was derived from Lamb's solution [10].

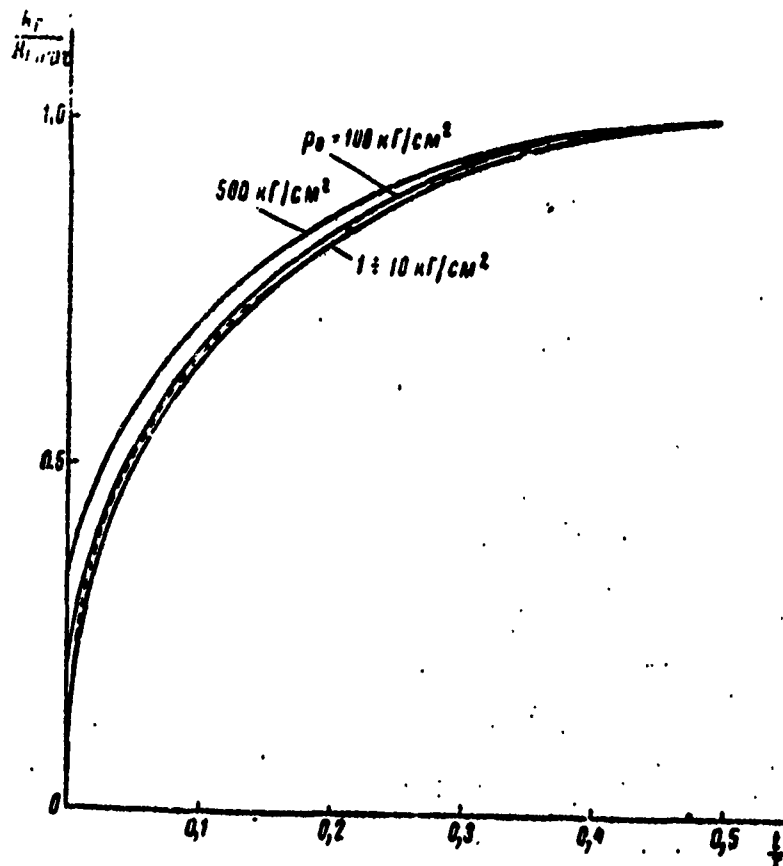


Fig. 5. Relative Size of Gas-Bubble as a Function of Relative Time in Underwater Explosions in an Infinite Medium Having Different Initial Hydrostatic Pressure.

§5. Approximate Evaluation of Pressure Field in Underwater Explosion in an Infinite Fluid.

The limiting conditions on a shock-wave front and gas-bubble surface previously examined permit us to move on to the integration of hydrodynamics equations for evaluating transient fluid motion induced by an explosion.

From the many currently-known approximation integration methods, let us touch upon only the one proposed by Kirkwood and Bethe [10], who examined isentropic one-dimensional motion having spherical symmetry. They found it convenient to introduce another variable - enthalpy - which is associated with internal energy, pressure, and density by the expression

$$w = E + \frac{p}{\rho}, \quad (5.1)$$

whence

$$dw = dE + \frac{dp}{\rho} + p d\left(\frac{1}{\rho}\right). \quad (5.2)$$

According to the laws of thermodynamics,

$$dQ = TdS = dE + p d\left(\frac{1}{\rho}\right). \quad (5.3)$$

Since entropy S is considered a constant, on the basis of (5.2) and (5.3),

$$dw = \frac{dp}{\rho}. \quad (5.4)$$

The equation of motion and the equation of discontinuity were previously written in the form

$$\frac{\partial \bar{v}}{\partial t} + (\bar{v} \nabla) \bar{v} + \frac{1}{\rho} \nabla p = 0. \quad (2.2)$$

$$\frac{dp}{dt} + p \operatorname{div} \bar{v} = \frac{\partial p}{\partial t} + \operatorname{div} (p \bar{v}) = 0. \quad (2.5)$$

Let us introduce, following Kirkwood and Bethe, so-called kinetic enthalpy, defining it by the equation

$$\Omega = w + \frac{1}{2} v^2. \quad (5.5)$$

Then,

$$\nabla \Omega = \nabla w + (\bar{v} \nabla) \bar{v}. \quad (5.6)$$

In view of (5.4) and (5.6), the equation of motion (2.2) can be written thus:

$$\left. \begin{aligned} \frac{d\bar{v}}{dt} &= -\nabla w, \\ \frac{d\bar{v}}{dt} &= -\nabla \Omega. \end{aligned} \right\} \quad (5.7)$$

Let us furthermore note that

$$\frac{dp}{dt} = \frac{dp}{dp} \frac{dp}{dt} = \frac{1}{a^3} \frac{dp}{dt} = \frac{p}{a^2} \frac{da}{dt}. \quad (5.8)$$

Using this equation and relationship (5.5), let us transform the equation of discontinuity (2.5):

$$\begin{aligned} \operatorname{div} \bar{v} &= \frac{1}{a^2} \frac{da}{dt} = \frac{1}{a^3} \left(\frac{d\Omega}{dt} - \frac{1}{2} \frac{dv^2}{dt} \right) = \frac{1}{a^3} \left(\frac{\partial \Omega}{\partial t} + \bar{v} \nabla \Omega - \frac{1}{2} \frac{dv^2}{dt} \right) = \\ &= \frac{1}{a^3} \left(\frac{\partial \Omega}{\partial t} - \bar{v} \frac{\partial \bar{v}}{\partial t} - \frac{1}{2} \frac{dv^2}{dt} \right) = \frac{1}{a^3} \frac{\partial \Omega}{\partial t} + \frac{1}{a^3} \left[\frac{1}{2} (\bar{v} \nabla) v^2 - \frac{dv^2}{dt} \right] = \\ &= \frac{1}{a^3} \frac{\partial \Omega}{\partial t} - \frac{1}{a^3} \left[\frac{1}{2} (\bar{v} \nabla) v^2 + \frac{\partial v^2}{\partial t} \right]. \end{aligned} \quad (5.9)$$

Let us introduce velocity potential ϕ

$$\bar{v} = -\nabla \phi, \quad (5.10)$$

then, the equation of motion is written in the form

$$\Omega = \frac{\partial \phi}{\partial t}; \quad (5.11)$$

the equation of discontinuity

$$\Delta^2 \phi = \frac{1}{a^2} \frac{\partial^2 \phi}{\partial t^2} + \frac{1}{a^3} \left[\frac{1}{2} (\bar{v} \nabla) v^2 - \frac{\partial v^2}{\partial t} \right] = \frac{1}{a^3} \frac{\partial^2 \phi}{\partial t^2} - \frac{1}{a^3} \left[\frac{1}{2} (\bar{v} \nabla) v^2 + \frac{\partial v^2}{\partial t} \right]. \quad (5.12)$$

The Laplace operator for one-dimensional motion having spherical symmetry is

$$\Delta^2 \phi = \frac{\partial^2 \phi}{\partial r^2} + \frac{2}{r} \frac{\partial \phi}{\partial r}.$$

Allowing for this, (5.12) can be written in the following way:

$$\frac{\partial^2 \phi}{\partial r^2} + \frac{2}{r} \frac{\partial \phi}{\partial r} - \frac{1}{a^3} \frac{\partial^2 \phi}{\partial t^2} = -\frac{1}{a^3} \left(\frac{v}{2} \frac{\partial v^2}{\partial r} + \frac{\partial v^2}{\partial t} \right). \quad (5.13)$$

If we seek a solution in the form $\phi = \psi/r$, then in place of (5.11) and (5.13) we will have:

$$r\Omega = \frac{\partial \Phi}{\partial t}, \quad (5.14)$$

$$\frac{\partial^2 \Phi}{\partial r^2} - \frac{1}{a^2} \frac{\partial^2 \Phi}{\partial t^2} = -\frac{r}{a^2} \left(\frac{v}{2} \frac{\partial v^2}{\partial r} + \frac{\partial v^2}{\partial t} \right). \quad (5.15)$$

The derived equations, generally speaking, are no simpler than the initial equations. However, they present a clear physical picture and permit us to examine the two limiting cases without difficulty - an incompressible fluid and the acoustic approximation - which in turn enables us to project simpler schemes for writing approximate solutions.

Indeed, when $\alpha \rightarrow \infty$ (incompressibility hypothesis) & $\Phi = \Phi(t)$, $\phi = \frac{\Phi(t)}{r}$ and we arrive at the expression for velocity v as given by Lamb [see (4.12)]. When $\alpha \rightarrow \alpha_0$, particle velocity is small and the right side of (5.15) can be assumed to equal zero. In this case,

$$\phi = \frac{\Phi\left(t - \frac{r}{a_0}\right)}{r} \quad (5.16)$$

The function of $G = r\Omega$, according to (5.16) and (5.14), is equal to

$$G = r\Omega = \Phi'\left(t - \frac{r}{a_0}\right). \quad (5.17)$$

$$v = -\frac{\partial \phi}{\partial r} = \frac{\Phi'\left(t - \frac{r}{a_0}\right)}{a_0} + \frac{\Phi\left(t - \frac{r}{a_0}\right)}{r^2}. \quad (5.18)$$

Considering that in this case

$$\Omega = \frac{\partial p}{\partial r} + \frac{1}{2} v^2,$$

and introducing a new function

$$F\left(t - \frac{r}{a_0}\right) = \rho_0 \Phi\left(t - \frac{r}{a_0}\right),$$

we can derive the Gilmore solution [33] from (5.17) and (5.18):

$$\Delta p + \frac{1}{2} \rho_0 v^2 = \frac{F' \left(t - \frac{r}{a_0} \right)}{r}, \quad (5.19)$$

$$v = \frac{F' \left(t - \frac{r}{a_0} \right)}{\rho_0 a_0 r} + \frac{F \left(t - \frac{r}{a_0} \right)}{\rho_0 r^2}. \quad (5.20)$$

This solution differs from the acoustic solution [cf. (3.22)] only in that the quantity $r\Delta p$ is not propagated at a rate α_0 , but at $G = r\Omega$. However, this difference is often considerable. Thus, in the proximity of the gas-bubble some time after the explosion, the speed of sound is close to α_0 and the ratio of v/α_0 is small. At the same time, the quantity $(1/2)\rho_0 v^2$ is not only not less than Δp , but much exceeds it.

In spite of this, the Gilmore solution does not guarantee sufficient precision of evaluations both in the proximity of the shock-wave front and at the origin of its tail section. Kirkwood and Bethe suggested examining the permutation of function G with some variable velocity c for waves of finite amplitude:

$$c = \left(\frac{\partial r}{\partial t} \right)_{G=\text{const}}. \quad (5.21)$$

The function $r(G, t)$ can be plotted in the form of a series of curves in plane r, t for various values of G . If the parameters of gas-bubble motion are given, it is easy to define the function G at its boundary at a given moment in time t_r . The propagation rate of quantity $G(t_r)$ is a function of the parameter t_r and the coordinate of point $r(G, t)$:

$$c = c(t_r, r).$$

The time interval in terms of which quantity G becomes equal to $G(t_r)$ at point r is

$$\tau = t - t_r = \int_r^{t_r} \frac{dr}{c(t_r, r)}. \quad (5.22)$$

Time τ is often called the "lag time".

By definition of function G , kinetic enthalpy $\Omega(r, t)$ is

$$\Omega(r, t) = \frac{G(t, r)}{r} = \frac{G(t_r)}{r} = \frac{R}{r} \Omega(t_r), \quad (5.23)$$

where $\Omega(t_r)$ is defined at the boundary of the gas-bubble R at time t_r .

Therefore, in order to evaluate pressure fields, we only have to calculate the kinetic enthalpy on the gas-bubble surface and find the lag time τ . The first problem is easily solved using relationships established in the preceeding section. We must know the function of $c = c(t_r, r)$ to define the lag time. Kirkwood and Bethe carried out these calculations only for the shock-wave front proximity. For this area, they were able to assume that

$$c = a \cdot \sigma, \quad (5.24)$$

where σ - the Riemannian function:

$$\sigma = \int_{p_0}^p a \frac{dp}{p}, \quad (5.25)$$

and moreover, to roughly assume that

$$v \approx 1. \quad (5.26)$$

Since each of the quantities α , ρ , σ , and ω near the front is a function of Δp , the lag time τ can be easily calculated and this problem is brought to final solution. However, Kirkwood and Bethe's scheme is untenable for calculating pressure on the wave tail, because mass velocity v at that point is considerably greater than σ and equation (5.24) is invalid.

To define the function $c = c(t_r, r)$, more general considerations are required. Let us return to equation (5.15) for this purpose. Let us seek its solution in the form

$$\Phi = \Phi\left(1 - \frac{r - r^0}{c}\right), \quad (5.27)$$

where r - the running coordinate; r^* - the distance from explosion center to a certain fixed observation point; $c = c(r^*)$ - the propagation rate of function $G(t_r)$ at point r^* .

Let us express mass velocity v and its partial derivatives in terms of function Φ

$$\begin{aligned} v &= -\frac{\partial \psi}{\partial r} = \frac{\Phi}{r^2} - \frac{1}{r} \frac{\partial \Phi}{\partial r}, \\ \frac{\partial v}{\partial r} &= -\frac{2\Phi}{r^3} + \frac{2}{r^2} \frac{\partial \Phi}{\partial r} - \frac{1}{r} \frac{\partial^2 \Phi}{\partial r^2} = -\frac{2v}{r} - \frac{1}{r} \frac{\partial^2 \Phi}{\partial r^2}, \\ \frac{\partial v}{\partial t} &= \frac{1}{r^2} \frac{\partial \Phi}{\partial t} - \frac{1}{r} \frac{\partial^2 \Phi}{\partial r \partial t}. \end{aligned}$$

Substituting the relationships derived in (5.15), we will find that

$$\frac{\partial^2 \Phi}{\partial r^2} - \frac{1}{a^2} \frac{\partial^2 \Phi}{\partial t^2} = \frac{1}{a^2} \left(2v^2 + v^2 \frac{\partial^2 \Phi}{\partial r^2} - \frac{2v}{r} \frac{\partial \Phi}{\partial t} + 2v \frac{\partial^2 \Phi}{\partial r \partial t} \right)$$

or, in view of (5.17),

$$\frac{\partial^2 \Phi}{\partial r^2} = \frac{1}{a^2 - v^2} \left(\frac{\partial^2 \Phi}{\partial t^2} + 2v \frac{\partial^2 \Phi}{\partial r \partial t} + 2v^2 - 2v\Omega \right). \quad (5.28)$$

Allowing for (5.27), equation (5.28) will be written in the form

$$\frac{\Phi''}{c^2} = \frac{1}{a^2 - v^2} \left(\Phi'' - \frac{2v}{c} \Phi'' + 2v^2 - 2v\Omega \right) \quad (5.29)$$

or

$$\left[1 - \frac{(c-v)^2}{a^2} \right] \Phi'' = -2v \frac{c'}{a^2} (\Omega - v^2). \quad (5.30)$$

Let us assume that

$$c = a + v - \delta. \quad (5.31)$$

Then, we can assume that $\delta \ll a$ for pressures which are not too high; and that $c^2/a^2 = 1$ to a precision within small quantities of the

first order.

Therefore, instead of (5.30), we will derive

$$\frac{\delta}{a} \Phi'' = -v(2 - v^2)$$

or, since

$$\begin{aligned} \Phi'' &= \frac{\partial}{\partial t} \Phi' = \frac{\partial}{\partial t} (r\Omega) = r \frac{\partial \Omega}{\partial t}, \\ \delta &= -v \frac{(\Omega - v^2) a}{r \frac{\partial \Omega}{\partial t}} \approx -v \frac{(\Omega - v^2) a_0}{r \frac{\partial \Omega}{\partial t}}. \end{aligned} \quad (5.32)$$

The local speed of sound α and mass velocity v enter into (5.32) in addition to δ . The speed of sound can easily be calculated according to the given excess pressure Δp , if the equation of state is given. The mass velocity of particles is associated with the functions Φ and Ω by the equation

$$v(t, r) = -\frac{\partial \Phi}{\partial r} = \frac{\Phi}{r^2} - \frac{1}{r} \frac{\partial \Phi}{\partial r} = \frac{\Phi}{r^2} + \frac{1}{rc} \frac{\partial \Phi}{\partial t} = \frac{\Phi}{r^2} + \frac{\Omega}{c}. \quad (5.33)$$

Relationship (5.33) is valid for the entire area of transient fluid motion, including the boundary of the gas-bubble R . Since the quantities v and Ω can easily be calculated at this boundary, we have for the function of potential Φ from (5.33)

$$\Phi(t_r) = R^2 v^*, \quad (5.34)$$

where

$$v^* = v_r - \frac{u_r}{c(t_r, R)}. \quad (5.35)$$

Considering the small function of the second term in (5.35) and the small difference between c and α_0 , in equations (5.34), (5.35), we can assume that $c(t_r, R) = \alpha_0$. Then, using (5.33)-(5.35), let us derive an expression for defining mass velocity in terms of the known parameters of gas-bubble motion

$$v(t, r) = \frac{R^2 v^*}{r^2} + \frac{R u_r}{r a_n}, \quad (5.36)$$

where

$$v^* = v_r - \frac{u_r}{a_0}. \quad (5.37)$$

For practical calculation of pressure fields, we only have to represent the quantities ω and α as functions of pressure.

Let us use the condition of isentropy in the form of a Tête equation for this purpose:

$$\Delta p = B \left[\left(\frac{p}{p_0} \right)^{\frac{1}{n}} - 1 \right]. \quad (1.25)$$

For $\Delta p < B$ let us derive:

$$\begin{aligned} a &= \sqrt{\frac{dp}{d\rho}} = a_0 \left(1 + \frac{\Delta p}{B} \right)^{\frac{n-1}{2n}} = \\ &= a_0 \left[1 + \frac{n-1}{2nB} \Delta p \left(1 - \frac{n+1}{4nB} \Delta p + \dots \right) \right]. \end{aligned} \quad (5.38)$$

$$\begin{aligned} \omega &= \int_0^t \frac{dp}{\rho} = \frac{a_0^2}{n-1} \left[\left(1 + \frac{\Delta p}{B} \right)^{\frac{n-1}{n}} - 1 \right] = \\ &= \frac{\Delta p}{p_0} \left(1 - \frac{\Delta p}{2nB} + \dots \right). \end{aligned} \quad (5.39)$$

For $\Delta p < 1000 \text{ kg/cm}^2$, we will derive from (5.5) and (5.39) with great precision that

$$\alpha = \frac{\Delta p}{p_0} + \frac{1}{2} v^2. \quad (5.40)$$

According to (5.24), (5.36), and (5.40), excess pressure on the shock-wave, expressed in terms of gas-bubble parameters is

$$\Delta p(r, t) = \frac{p_0 u_r R}{r} - \frac{1}{2} p_0 \frac{R^2}{r^2} \left(\frac{R v^*}{r} + \frac{u_r}{a_0} \right)^2, \quad (5.41)$$

where

$$p_0^{\Omega} = \Delta p_r + \frac{1}{2} \rho_0 v_r^2 \quad (5.42)$$

or, using dimensionless parameters,

$$\left. \begin{aligned} \bar{t} &= \frac{a_0 t}{R_0} \\ \bar{R} &= \frac{R}{R_0} \\ \bar{r} &= \frac{r}{R_0} \\ \bar{v} &= \frac{v}{a_0} \end{aligned} \right\} \quad (5.43)$$

$$\Delta p(\bar{r}, \bar{t}) = \frac{\rho_0 a_0 \bar{R}}{\bar{r}} - \frac{1}{2} n B \frac{\bar{R}^2}{\bar{r}^2} \left(\frac{\bar{R} \bar{v}}{\bar{r}} + \frac{\rho_0 a_0}{n B} \right)^2 \quad (5.44)$$

where

$$p_0^{\Omega} = \Delta p_r + \frac{1}{2} n B v_r^2 \quad (5.45)$$

$$\left. \begin{aligned} \bar{t} &= \bar{t}_r + \tau, \\ n B &= \rho_0 a_0^2 \end{aligned} \right\} \quad (5.46)$$

Let us return to the definition of lag time τ . Formula (5.32) was previously derived, into which enter the quantities v , Ω , and $\partial \Omega / \partial t$. The first two quantities have already been calculated [cf. (5.36), (5.40), and (5.41)]; to evaluate the derivative $\partial \Omega / \partial t$ we can roughly assume that

$$\frac{\partial \Omega}{\partial t} \approx \frac{1}{r} \frac{\partial Q}{\partial t} \quad (5.47)$$

The relationships derived, in conjunction with the more refined data on gas-bubble expansion (cf. 54) and widely-known empirical formulas for evaluating pressures on a shock-wave front were used as the basis for calculating pressure fields in underwater explosion at various depths. Omitting the details of calculation, let us cite only the final results.

Pressure on a shock-wave front is defined by the relationships*
 *The second part of (5.48) taken from Cowle [10].

$$p_m = \begin{cases} 450 \cdot \left(\frac{G}{r}\right)^{1.3} = \frac{17000}{r^{1.3}} & \text{where } 6 < \bar{r} < 12 \\ 533 \cdot \left(\frac{G}{r}\right)^{1.13} = \frac{14700}{r^{1.13}} & \text{where } 12 < \bar{r} < 240. \end{cases} \quad (5.48)$$

The arrival time \bar{t}_ϕ of a wave-front at a given point \bar{r} is characterized in the data of Table 2.

Table 2

\bar{r}	5	6	7	8	10	12
\bar{t}_ϕ	2.3	3.1	3.9	4.6	6.4	8.2

For $\bar{r} > 12$, the following approximation is valid:

$$\left. \begin{aligned} \bar{t}_\phi &= \bar{r} - m, \\ m &= 11.4 - \frac{10.6}{\bar{r}^{0.13}} + \frac{1.51}{\bar{r}^{1.3}}. \end{aligned} \right\} \quad (5.49)$$

When the charge is not too deep ($p_0 < 10 \text{ kg/cm}^2$), pressure in the proximity of the shock-wave front can be described by the expressions:

$$p(t) = p_m \begin{cases} e^{-\frac{t}{\theta}} & \text{where } t < 0 \\ \frac{0.368}{\frac{t}{\theta}} & \text{where } 0 < t < (5 + 10)\theta, \end{cases} \quad (5.50)$$

where θ - the exponential damping constant depending on distance

$$\frac{a_0 \theta}{R_0} = \bar{\theta} \approx 3.5 \left[\lg \bar{r} - 0.9 \right] \quad \text{where } 30 < \bar{r} < 240. \quad (5.51)$$

In accordance with (5.50), the pressure surge quantity is

$$[\dots] = \int_0^t p dt = p_m \theta \begin{cases} 1 - e^{-\frac{t}{\theta}} & \text{where } t < 0 \\ 0.632 + 0.368 \ln \frac{t}{\theta} & \text{where } 0 < t < (5 + 10)\theta. \end{cases} \quad (5.52)$$

An important feature of fluid motion during explosion is the energy flux density. It is customary to call this the [...] integral*

[Translator's note: two items on this page designated [...] indicate words and symbols missing in original text].

* Δ here also designates an increment in the quantity enclosed in brackets in equation (5.53). Therefore, integral (5.53) expresses excess energy transmitted by a shock-wave through a unit of surface.

$$E = \int_0^t \rho_0 \Delta \left(u + \frac{1}{2} v^2 + \frac{p}{\rho} \right) dt. \quad (5.53)$$

At pressures less than 1000 kg/cm^2 , we can disregard the first two terms in equation (5.53).

Since the rate of particle motion near the shock-wave front can also be calculated in the acoustic approximation

$$v = \frac{1}{a_0} (p - p_0) + \frac{1}{a_0} \int_0^t (p - p_0) dt, \quad (5.54)$$

we will derive an expression for energy flux density in the form

$$E = \frac{1}{a_0} \int_0^t \Delta p^2 dt + \frac{1}{2a_0} \int_0^t \Delta p \left| \int_0^t \Delta p dt' \right| dt. \quad (5.55)$$

In proportion to the increase in distance r , the second term, which represents the influence of the so-called "speed of the retarding flux" would become negligibly small in comparison to the first.

Using (5.50), we will derive

$$E = \frac{p_m^2}{2a_0} (C + D \frac{a_0}{r}). \quad (5.56)$$

$$C = \begin{cases} 1 - e^{-\frac{t}{\theta}} & \text{where } t < \theta \\ 1.135 - \frac{0.27}{\frac{t}{\theta}} & \text{where } \theta < t < (5 - 10)\theta, \end{cases}$$

$$D = \begin{cases} 1 - e^{-\frac{t}{\theta}} \left(2 - e^{-\frac{t}{\theta}} \right) & \text{where } t < \theta \\ 0.10 - 0.135 \ln \frac{2t}{\theta} & \text{where } \theta < t < (5 - 10)\theta. \end{cases}$$

Let us remember that relationships (5.50)-(5.56) are valid for $[...] < 10 \text{ kg/cm}^2$ and $t < 10 \theta$.

The calculated findings of pressure change for a wide range of charge depths and for the entire effect-time of the compression and reflection phases are shown in Figs. 6 & 7. We can see that as hydrostatic pressure p_0 increases, excess pressure drops considerably

solely in the tail section of the shock-wave. For $p_0 < 100 \text{ kg/cm}^2$, pressure hardly changes when $t < 0$.

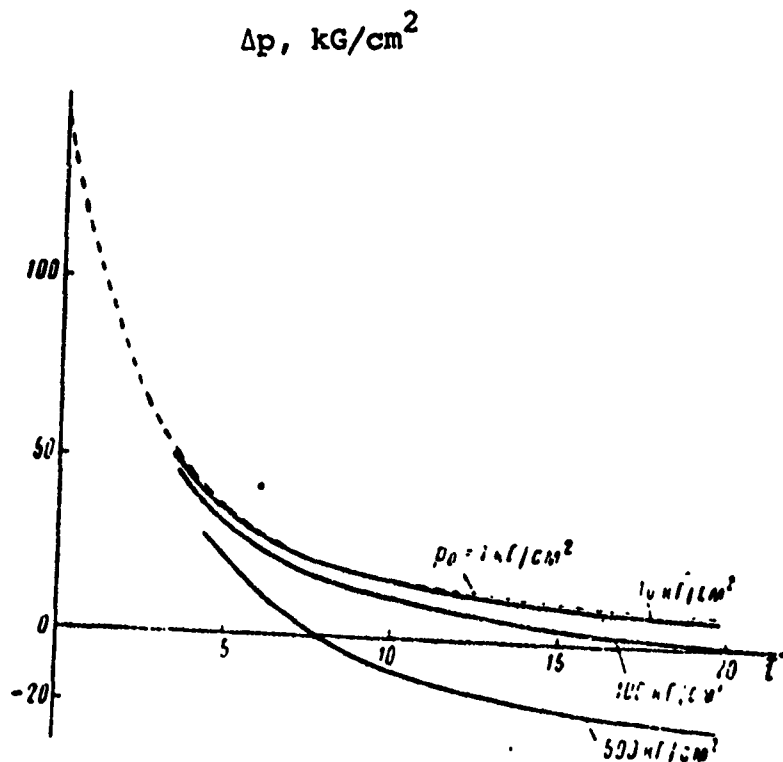


Fig. 6. Change in Excess Pressure Behind Shock-Wave Front for $\bar{r} = 60$ at Initial Period in Time.

————— theoretically calculated
 ----- calculated by empirical formula

The entire range for $\bar{r} > 10$ and $p_0 \leq 100$ can be approximated by the relationships:

$$\Delta p(i, \bar{r}, p_0) = \begin{cases} \Delta p^* \left[1 - \left(\frac{\bar{t}}{\bar{t}^*} \right)^{1.5} \right] - \frac{1}{\bar{r}^2} (5750 \bar{t}^{-0.51} - 0.115 \bar{p}_0^{1.15} \bar{t}^2) & \text{where } \bar{t} < \bar{t}^* \\ \frac{1}{\bar{r}^2} \left(\frac{0.7 \bar{p}_0^{0.96}}{\bar{t}} + 6.1 \bar{p}_0^{0.65} \bar{t} - 30.7 \bar{p}_0^{0.65} \bar{t}^{0.36} \right) - \frac{1}{\bar{r}^2} \left[\frac{1.7 \cdot 10^4}{\bar{p}_0^{0.43}} (1 - \bar{t}^{0.1}) \right] & \text{where } \bar{t} > \bar{t}^*. \end{cases} \quad (5.57)$$

where p^* is defined prior to some point in time \bar{t}_1 by equation (5.50); and in the interval $\bar{t}_1 < \bar{t} < \bar{t}^*$ according to the formula:

$$\Delta p^* = \frac{1}{\bar{r}} \frac{7320}{(\bar{t} + 5.2 - m)^{0.87}}; \quad (5.58)$$

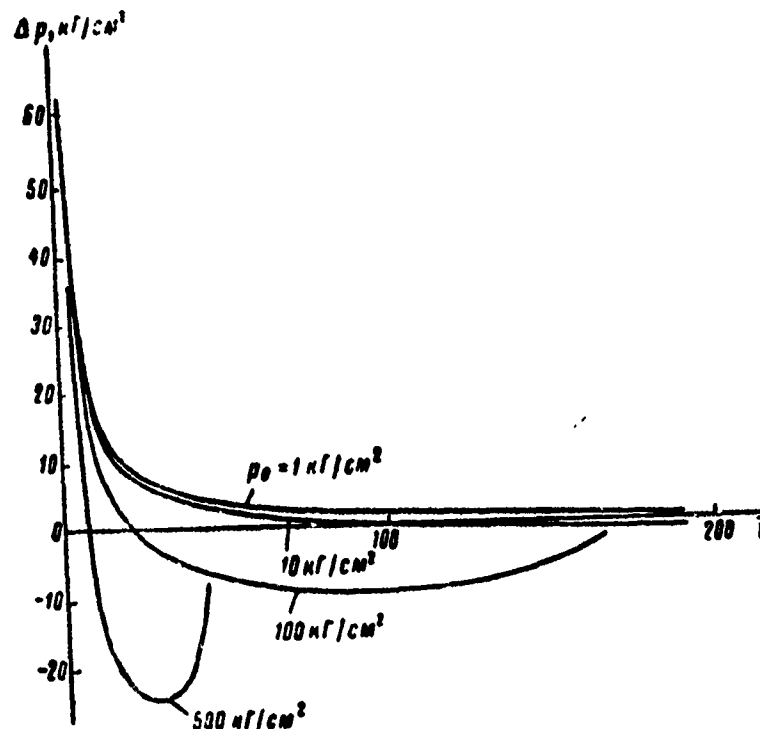


Fig. 7. Time Rate of Change in Excess Pressure for $\bar{r} = 60$ in Underwater Explosion in Infinite Medium.

$$\xi = \sin \frac{\pi \bar{t}}{2\bar{t}_m}; \quad (5.59)$$

$$\bar{t}^* = \frac{850}{\bar{p}_0^{0.81}} - \frac{20}{\bar{p}_0^{1.15}} + m; \quad (5.60)$$

$$\bar{t}_* = \frac{\bar{r}}{2} - \bar{R}_{max} + m = \frac{4350}{\bar{p}_0^{0.83}} - \frac{30.7}{\bar{p}_0^{0.35}} + m; \quad (5.61)$$

\bar{p}_0 - hydrostatic pressure, adjusted to 1 atm.

Time \bar{t}_1 is derived from the equation

$$\frac{i_1}{(\bar{t}_1 + 5.2 - m)^{0.87}} = 5 \cdot 10^{-4} \Delta p_m \bar{r}; \quad (5.62)$$

quantity $m = \bar{r} - \bar{t}_\phi$, according to formula (5.49); and time \bar{t} is counted from the moment that the shock-wave approaches the observation point.

Since the second terms in the formulas of (5.57) change in pro-

portion to $1/\bar{r}^*$, they can be rejected when $r > 60$. For this purpose, the range of distances is

$$\Delta p(\bar{r}, \bar{r}_0, \bar{p}_0) = \begin{cases} \Delta p^* \left[1 - \left(\frac{\bar{r}}{\bar{r}^*} \right)^{1.5} \right] & \text{where } \bar{r} < \bar{r}^* \\ \frac{1}{\bar{r}} \left(\frac{0.7\bar{p}_0^{0.96}}{\bar{r}} + 6.1\bar{p}_0^{0.42} \frac{1-\bar{r}}{\bar{r}^{0.92}} - 30.7\bar{p}_0^{0.65} \frac{1}{\bar{r}} \right) & \text{where } \bar{r} > \bar{r}^* \end{cases} \quad (5.63)$$

The physically-dimensionless time \bar{t}^* characterizes the positive phase of the kinetic enthalpy quantity $\Omega(t)$ and in formula (5.63) it coincides with the positive excess pressure effect time ($\bar{t}^* = \bar{t}_+$). The relationship $\bar{t}_+ = \bar{t}_+(r)$ where $\bar{p}_0 = 1$ is shown in Fig. 8.

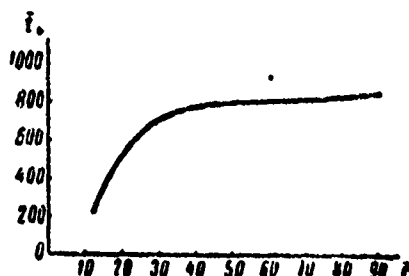


Fig. 8. Duration of Excess Pressure Compression Phase of Underwater Shock-Wave as a Function of Distance in Underwater Explosion in an Infinite Medium, for $p_0 = 1 \text{ kg/cm}^2$.

The shortest compression phase occurs at distances equal to the gas-bubble radius, when the pressure inside it becomes equal to p_0 :

$$\bar{t}_{+ \min} = \frac{200}{\bar{p}_0^{0.67}} \quad (5.64)$$

The change in the duration of the compression phase as a function of hydrostatic pressure, where $\bar{r} > 60$, can be judged on the basis of (5.60). We can easily calculate minimum pressure in the reflection phase from (5.57), if we assume that* $\bar{t} = \bar{t}_m$ ($\xi = 1$):

$$\Delta p_{\min} = \frac{1}{\bar{r}} (0.7\bar{p}_0^{0.96} - 30.7\bar{p}_0^{0.65}) \approx - \frac{30\bar{p}_0^{0.65}}{\bar{r}} \quad (5.65)$$

*It is also apparent that $\Delta p_{\min} = R_{\max}/\bar{r}$, where Δp_r - pressure in the gas-bubble corresponding to \bar{R}_{\max} .

The results of calculations made according to these formulas permit us to form a total judgment about the effect of initial hydrostatic pressure on shock-wave parameters. For small values of p_0 , the initial time interval of abrupt pressure change ($\bar{t} = \bar{\theta}$) is considerably less than the duration of the entire compression phase (e.g., where $p_0 = 1 \text{ kG/cm}^2$ and $r = 60$, $\bar{t}_+/\bar{\theta} \approx 230$). As p_0 increases, the duration of the compression phase is shortened, and where $p_0 = 100 \text{ kG/cm}^2$ it exceeds θ by only 6 times.

To an even greater extent, the duration of the reflection phase is shortened as p_0 increases. The reflection phase exceeds t_+ by about 8.5 times where $p_0 = 1 \text{ kG/cm}^2$ and by only 4.5 times where $p_0 = 500 \text{ kG/cm}^2$.

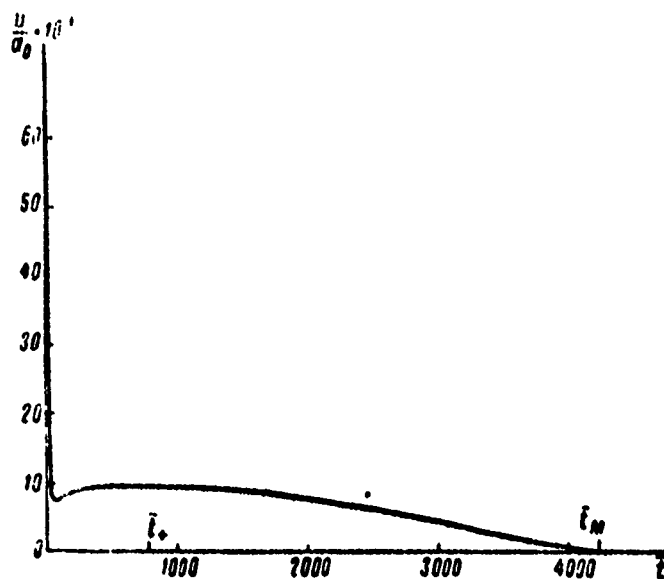


Fig. 9. Change in Mass Velocity of Particles in Shock-Wave Where $\bar{r} = 60$ in Underwater Explosion in an Infinite Medium having Initial Hydrostatic Pressure $p_0 = 1 \text{ kG/cm}^2$.

The derived results also permit us to calculate the quantity of the total momentum in both the compression and reflection phases. Specifically, the positive phase momentum for $\bar{r} > 60$ can be described by the relationship

$$\bar{J} = \frac{u_0 J}{R_0} = \frac{78.0 \text{ (kN)}}{r p_0^{0.2}} \quad [\text{kG/cm}^2]. \quad (5.66)$$

We can use equation (5.54) to evaluate the momentum of particles where $\bar{r} > 60$. Where $\bar{r} < 60$, we should use the more precise relationship (5.36). The nature of variation in momentum for $\bar{r} = 60$ and $p_0 = 1$ is shown in Fig. 9.

The maximum migration of particles during the passage of a shock-wave is roughly equal to

$$S_{\max} = \begin{cases} \bar{r} \left[\sqrt{1 - \left(\frac{30.7}{\bar{r} p_0^{0.35}} \right)^2} - 1 \right], & \text{where } \bar{r} < 2R_{\max} \\ \frac{3.55}{\bar{r} p_0^{0.2}} + \frac{9650}{\bar{r}^2 p_0^{1.04}}, & \text{where } \bar{r} > 2R_{\max}. \end{cases} \quad (5.67)$$

One should note that the relationships cited, which characterize the effect of initial hydrostatic pressure of the parameters of the hydrodynamic field during underwater explosion, have been derived by approximate theoretical calculations and have not been experimentally verified.

§6. The Basic Equations of Short-Wave Theory. Asymptotic Presentations of an Underwater Shock-Wave.

As we move away from the center of explosion, the motion of the gas-bubble has a decreasing effect on the parameters of the underwater shock-wave. It becomes feasible to study the propagation of shock-waves as a physical process, independent of the conditions of its formation. Despite the fact that we are assuming considerable distances from the center of explosion, the acoustic approximation cannot always provide qualitatively-correct descriptions of this process on account of the specific properties of shock waves and the factor of nonlinearity which is part of their nature. The study of shock-waves requires a fundamentally different theory. A theory

which is suitable for this purpose is the short-wave theory which has been developed in recent years by S. A. Khristianovich, A. A. Grib, and O. S. Ryzhov [2].

Let us state the principles of this theory in brief form.

Let us examine isentropic axial-symmetric fluid motion. Using the variables v_r , v_θ , and a in system (2.12), let us write the equations of motion and the equation of discontinuity in the form

$$\frac{\partial v_r}{\partial t} + v_r \frac{\partial v_r}{\partial r} + \frac{v_\theta}{r} \frac{\partial v_r}{\partial \theta} - \frac{v_\theta^2}{r} + \frac{2}{n-1} a \frac{\partial a}{\partial r} = 0, \quad (6.1)$$

$$\frac{\partial v_\theta}{\partial t} + v_r \frac{\partial v_\theta}{\partial r} + \frac{v_\theta}{r} \frac{\partial v_\theta}{\partial \theta} + \frac{v_r v_\theta}{r} + \frac{2}{n-1} \frac{a}{r} \frac{\partial a}{\partial \theta} = 0, \quad (6.2)$$

$$\begin{aligned} \frac{\partial a}{\partial t} + v_r \frac{\partial a}{\partial r} + \frac{v_\theta}{r} \frac{\partial a}{\partial \theta} + \frac{n-1}{2} \frac{a}{r} \left(r \frac{\partial v_r}{\partial r} + \right. \\ \left. + \frac{\partial v_\theta}{\partial \theta} + 2v_r + v_\theta \operatorname{ctg} \theta \right) = 0. \end{aligned} \quad (6.3)$$

It becomes convenient to replace independent variables, defining their association with earlier proofs by the equations

$$\left. \begin{aligned} \beta &= \frac{r}{l}, \\ \tau &= \ln t. \end{aligned} \right\} \quad (6.4)$$

Performing the appropriate transformations, we will find that

$$\frac{\partial v_r}{\partial \tau} - \beta \frac{\partial v_r}{\partial \beta} + v_r \frac{\partial v_r}{\partial \beta} + \frac{v_\theta}{\beta} \frac{\partial v_r}{\partial \theta} - \frac{v_\theta^2}{\beta} + \frac{2}{n-1} a \frac{\partial a}{\partial \beta} = 0, \quad (6.5)$$

$$\frac{\partial v_\theta}{\partial \tau} - \beta \frac{\partial v_\theta}{\partial \beta} + v_r \frac{\partial v_\theta}{\partial \beta} + \frac{v_\theta}{\beta} \frac{\partial v_\theta}{\partial \theta} + \frac{v_r v_\theta}{\beta} + \frac{2}{n-1} \frac{a}{\beta} \frac{\partial a}{\partial \theta} = 0, \quad (6.6)$$

$$\begin{aligned} \frac{\partial a}{\partial \tau} - \beta \frac{\partial a}{\partial \beta} + v_r \frac{\partial a}{\partial \beta} + \frac{v_\theta}{\beta} \frac{\partial a}{\partial \theta} + \frac{n-1}{2} \frac{a}{\beta} \times \\ \times \left(\beta \frac{\partial v_r}{\partial \beta} + \frac{\partial v_\theta}{\partial \theta} + 2v_r + v_\theta \operatorname{ctg} \theta \right) = 0. \end{aligned} \quad (6.7)$$

The reduction of the basic system of gas dynamics equations to the form (6.5)-(6.7) is of a preparatory nature.

The chief prerequisites of short-wave theory amount to an

assertion that we may present the variables which enter into these equations in the form

$$\left. \begin{aligned} v &= a_0 M^* \mu, \\ v_0 &= a_0 V^* \sqrt{\frac{n+1}{2}} \nu, \\ \theta &= \theta^* \sqrt{\frac{n+1}{2}} \gamma, \\ r &= a_0 t \left(1 + \frac{n+1}{2} M^* \delta \right), \\ \beta &= a_0 \left(1 + \frac{n+1}{2} M^* \delta \right), \\ a &= a_0 \left(1 + \frac{n-1}{2} M^* \alpha \right), \end{aligned} \right\} \quad (6.8)$$

where M^* , V^* , θ^* - small quantities of the first or higher order;
 μ , ν , γ , δ , α - quantities on the order of one.

In other words, this assumes we are studying motion characterized by change in hydrodynamic parameters in a relatively small area adjoining the shock-front. The ratio of the length of this area to the distance from the center of explosion is on the order of M^* . Consequently, an assumption that M^* is a small quantity is an assumption that the wave is short.

Using new variables, system (6.5)-(6.7) can be reduced to the form

$$\alpha = \mu, \quad (6.9)$$

$$\frac{\partial \mu}{\partial \gamma} - \frac{\partial \nu}{\partial \delta} = 0, \quad (6.10)$$

$$\left. \begin{aligned} \frac{\partial \mu}{\partial \tau} + (\mu - \delta) \frac{\partial \mu}{\partial \gamma} + \frac{1}{2} \frac{\partial \nu}{\partial \gamma} + \mu + \frac{\nu}{2\gamma} &= 0, \\ \frac{\partial \mu}{\partial \tau} + (\mu - \delta) \frac{\partial \mu}{\partial \gamma} + \frac{1}{2} \frac{\partial \nu}{\partial \gamma} + \mu &= 0. \end{aligned} \right\} \quad (6.11)^*$$

* The first equation in (6.11) relates to the case of motion in the proximity of the axis $\theta = 0$ and the second, in the proximity of a finite angle θ .

The derived equations are much simpler than the initial equations. They permit us to find solutions in finite form for a series of important practical problems. Specifically, Khristianovich examined the propagation of an underwater shock-wave at considerable distances from the point of explosion from the standpoint of short wave theory [22]. Let us mention the basic premises of this study. Equation (6.11) becomes an ordinary differential equation and adopts the form

$$(\mu - \delta) \frac{d\delta}{d\mu} + \mu = 0$$

or likewise,

$$\frac{d\delta}{d\mu} - \frac{\delta}{\mu} + 1 = 0. \quad (6.12)$$

The common integral of (6.12) is

$$\delta = C\mu - \mu \ln \mu \quad (6.13)$$

or, using the variables v , r , and t and using equations

$$v = a_0 M^* \mu, \quad (6.14)$$

$$r = a_0 t \left(1 + \frac{n+1}{2} M^* \delta \right), \quad (6.15)$$

we will derive

$$\frac{2}{n+1} \frac{1}{M^*} \left(\frac{r}{a_0 t} - 1 \right) = \frac{v}{a_0 M^*} \left(C - \ln \frac{v}{M^* a_0} \right). \quad (6.16)$$

Relationship (6.16), in conjunction with dynamic compatibility conditions (1.38) and (1.40), permits us to establish the laws of motion of an underwater shock-wave front. Using expression (1.38), equation (6.16) can be written in the form

$$\frac{r}{t a_0} = a_0 \left(1 + C \frac{n+1}{2} \frac{p_0}{B n} - \frac{n+1}{2} \frac{p_0}{B n} \ln \frac{p_0}{B n M^*} \right). \quad (6.17)$$

It is convenient to replace the arbitrary constant C with another arbitrary constant, assuming that

$$C = \ln \frac{p^0}{BnM^0}.$$

Then,

$$r_\phi = a_0 \left(1 + \frac{n+1}{2} \frac{p_\phi}{Bn} \ln \frac{p^0}{p_\phi} \right) t_\phi. \quad (6.18)$$

Differentiating, we find that:

$$dr_\phi = a_0 \left(1 + \frac{n+1}{2} \frac{p_\phi}{Bn} \ln \frac{p^0}{p_\phi} \right) dt_\phi + a_0 t_\phi \frac{n+1}{2Bn} \times \\ \times \left(\ln \frac{p^0}{p_\phi} - 1 \right) dp_\phi. \quad (6.19)$$

On the other hand, according to (1.40)

$$N = a_0 \left(1 + \frac{n+1}{4} \frac{p_\phi}{Bn} \right)$$

or, likewise,

$$dr_\phi = a_0 \left(1 + \frac{n+1}{4} \frac{p_\phi}{Bn} \right) dt_\phi. \quad (6.20)$$

Excluding dr_ϕ from (6.19) and (6.20) and performing elementary transformations, we get:

$$\frac{dt_\phi}{t_\phi} = - \left[1 - \frac{1}{2 \left(\ln \frac{p^0}{p_\phi} - \frac{1}{2} \right)} \right] d \ln p_\phi.$$

Integrating, we derive

$$t_\phi = \frac{C_1}{p_\phi \sqrt{\ln \frac{p^0}{p_\phi} - \frac{1}{2}}}. \quad (6.21)$$

It is known from the theory of similarity that equal quantities of pressure on the front are satisfied by equal compatible distances and times, the modulus of similarity being the radius of the charge. For this reason, it is appropriate to introduce another constant, A , in place of the integration constant C_1 :

$$A = \frac{C_1 a_0}{R_0}.$$

Thus,

$$\frac{t_{\phi} a_0}{R_0} = \frac{A}{p_{\phi} \sqrt{\ln \frac{p^*}{p_{\phi}} - \frac{1}{2}}}. \quad (6.22)$$

Taking account of (6.22), relationship (6.18) can be written in the form

$$\frac{r_{\phi}}{R_0} = \frac{A}{p_{\phi}} \frac{1 + \frac{1}{2}(n+1) \frac{p_{\phi}}{Bn} \ln \frac{p^*}{p_{\phi}}}{\sqrt{\ln \frac{p^*}{p_{\phi}} - 0.5}}. \quad (6.23)$$

Equations (6.22) and (6.23) express the asymptotic laws of change in pressure on the front of an underwater shock-wave as a function of distance and time. The constants A and p^* which enter into these equations have been used on the basis of analyzing experimental data.

Let us find the spatial extension of a section of a shock-wave from the front to a point having a given amplitude of pressure p. According to (6.15)

$$r_{\phi} - r = a_0 t_{\phi} \frac{n+1}{2} M^* (\delta_{\phi} - \delta), \quad (6.24)$$

according to (6.13), however,

$$\delta = p(C - \ln p) = \frac{v}{a_0 M^*} \left(C - \ln \frac{v}{a_0 M^*} \right).$$

In the proximity of the front, we can consider that

$$v = a_0 \frac{p}{Bn}.$$

Therefore,

$$\delta = \frac{p}{Bn M^*} \left(C - \ln \frac{p}{Bn M^*} \right).$$

or, since

$$C = \ln \frac{p^*}{BnM^*},$$

$$\delta = \frac{p}{BnM^*} \ln \frac{p^*}{p}. \quad (6.25)$$

Substituting (6.25) in (6.24), we will have

$$r_\phi - r = a_\phi t_\phi \frac{n+1}{2Bn} \left(p_\phi \ln \frac{p^*}{p_\phi} - p \ln \frac{p^*}{p} \right)$$

or, according to (6.22)

$$\frac{r_\phi - r}{R_0} = \frac{A}{Bn} \frac{n+1}{2} \frac{\ln \frac{p^*}{p_\phi} - \frac{p}{p_\phi} \ln \frac{p^*}{p}}{\sqrt{\ln \frac{p^*}{p_\phi} - 0.5}}. \quad (6.26)$$

The effect-time of pressure as amplitude changes from p_ϕ to p is

$$\Delta t = \frac{r_\phi - r}{a_\phi}. \quad (6.27)$$

Specifically, assuming that $p = p_\phi/e$, we can derive the time interval during which pressure drops e -fold from (6.26)-(6.27):

$$\Delta \bar{t}_e = \frac{\Delta t a_\phi}{R_0} = \frac{n+1}{2} \frac{A}{Bn} \frac{(e-1) \ln \frac{p^*}{p_\phi} - 1}{e \sqrt{\ln \frac{p^*}{p_\phi} - 0.5}}. \quad (6.28)$$

In order to use fixed relationships in quantitative evaluations, Khristianovich suggested the use of the arbitrary constants entering into (6.22)-(6.28) based on an experimental pressure-time contour recorded at the relative distance of $\bar{r} = 90$. The quantities A and p^* which were calculated on the basis of conditions of equality of pressure on the wave-front and at point $\Delta \bar{t}_e = 0$, in this connection, were equal to $p^* = 17,000 \text{ kg/cm}^2$ and $A = 16,200 \text{ kg/cm}^2$.

This choice of constants A and p^* introduced some error into the theoretical formulas which can be reduced. Indeed, the wave contour naturally affects the asymptotic law of pressure damping on the front. The assumption of self-similar motion leads to a wave form similar to triangular. At the same time, the actual law of change in the pressure-time curve differs considerably from triangular (Fig. 10). The self-similar solution rather precisely describes the drop in pressure behind the front for a time interval which is considerably less than θ . Consequently, the best convergence of theoretical relationships with experimental data can be attained if we require equality in the slope of pressure contours in the proximity of the front, in addition to equality of pressures on the front, as our approximation conditions.

Since the initial drop in the actual pressure contour can be well described by the exponent

$$p = p_0 e^{-\frac{dt}{\theta}}, \quad (6.29)$$

then, differentiating we will derive

$$\left. \frac{dt}{dp} \right|_{p=p_0} = -\frac{\theta}{p_0}. \quad (6.30)$$

Considering (6.26), these conditions may be presented in the form

$$\theta = \frac{n+1}{2nB} \frac{A^* \left(\ln \frac{p^*}{p_0} - 1 \right)}{\sqrt{\ln \frac{p^*}{p_0} - 0.5}}. \quad (6.31)$$

Equations (6.31) and (6.23) can be utilized with greater precision than (6.28) and (6.23) for defining the constants A^* and p^* .

Let us note that this is not the only means of studying the asymptotic laws of shock-wave propagation. Other research means have been developed, at one time, in the studies of Kryussar [5],

L. D. Landau [11], Osborne and Taylor [39], Kirkwood and Bethe [10], L. Ya. Gutin and P. F. Korotkov [9]. All of them proceeded from several assumptions on wave-form and the nature of energy dissipation on the front.

Following the common ideas of these studies, we can easily derive more refined asymptotic relationships for an underwater shock-wave front. For this purpose, our first initial premise will be that in the area of a low-amplitude spherical wave-front, the quantity $p\bar{r} = \text{constant} = k$ is traveling at a velocity

$$a + v = a_0 \left(1 + \frac{n+1}{2nB} p \right). \quad (6.32)$$

The validity of this assertion was explained rather thoroughly in the preceding section : to be specific, it follows from the Kirkwood-Bethe theory. Our second initial premise will be the dynamic compatibility conditions.

Let there be on some spherical surface \bar{R} a change in pressure in time. To evaluate the time of passage of the quantity k and its corresponding pressure $p = k/\bar{r}$ through an arbitrary point k , we can then write

$$\begin{aligned} \bar{t} &= \bar{t}_0 + \int_{\bar{k}}^{\bar{r}} \frac{d\bar{r}}{\frac{a}{a_0} v} = \bar{t}_0 + \int_{\bar{k}}^{\bar{r}} \frac{d\bar{r}}{1 + \frac{n+1}{2nB} \frac{k}{\bar{r}}} \\ &= \bar{t}_0 + \bar{r} - \bar{R} - \frac{n+1}{2nB} p \bar{r} \ln \frac{\bar{r}}{\bar{R}}, \end{aligned} \quad (6.33)$$

where \bar{t}_0 - passage time of quantity $k = p\bar{r}$ through initial observation point.

Equation (6.33) is the approximate solution for hydrodynamics equations describing the head of a spherical shock-wave at great distances from the explosion (for an underwater shock-wave at distances of more than $60 R_0$). Specifically, for pressure on a wave

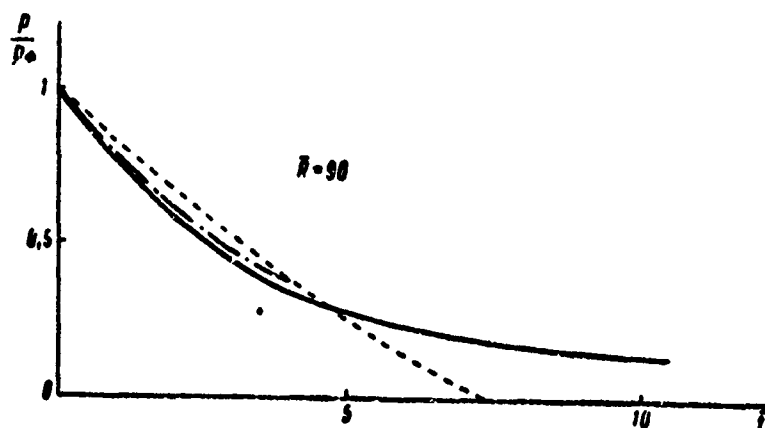


Fig. 10. Comparison of Pressure Contour Used in Khristianovich's Self-Similar Solution with Experimental Contour.

———— experimental curve;
 ----- used in Khristianovich's solution;
 -.-.-.- initial curve according to Cowle's data.

front according to (6.33),

$$t_0 = \bar{t}_0 + \bar{r}_0 - \bar{R} - \frac{n+1}{2nB} p_0 \bar{r}_0 \ln \frac{\bar{r}_0}{\bar{R}}; \quad (6.34)$$

moreover, dynamic compatibility conditions are satisfied in the wave-front:

$$dr_0 = N dt_0 = a_0 \left(1 + \frac{n+1}{4nB} p_0 \right) dt_0. \quad (6.35)$$

In the proximity of a wave-front (where $t_0 < 0$), according to (5.50),

$$p_0(t) = p_m e^{-\frac{t}{\bar{t}_0}}, \quad (6.36)$$

where \bar{t}_0 - time, counted from the time the wave-front arrives at the initial observation point \bar{R} .

Based on (6.36),

$$t_0 = 0 \ln \frac{p_m}{p_0} = \bar{t}_0 \ln \frac{p_m \bar{R}}{p_0 \bar{R}} = \bar{t}_0 \ln \frac{p_m \bar{R}}{p_0 \bar{R}}.$$

Substituting this result in (6.34) and differentiating, we find that

$$d\bar{t}_\phi = \left[1 - \frac{n+1}{2nB} p_\phi \left(1 + \ln \frac{\bar{r}_\phi}{R} \right) - \frac{\bar{\theta}_0}{\bar{r}_\phi} \right] d\bar{r}_\phi - \left(\frac{n+1}{2nB} \bar{r}_\phi \ln \frac{\bar{r}_\phi}{R} + \frac{\bar{\theta}_0}{p_\phi} \right) dp_\phi. \quad (6.37)$$

Excluding $d\bar{t}_\phi$ from (6.35) and (6.37), we derive:

$$\begin{aligned} & \left[\frac{n+1}{4nB} p_\phi \left(1 + 2 \ln \frac{\bar{r}_\phi}{R} \right) + \frac{\bar{\theta}_0}{\bar{r}_\phi} \right] d\bar{r}_\phi = \\ & = - \left(\frac{n+1}{2nB} \bar{r}_\phi \ln \frac{\bar{r}_\phi}{R} + \frac{\bar{\theta}_0}{p_\phi} \right) dp_\phi \end{aligned}$$

or

$$\frac{dp_\phi}{p_\phi} = - \frac{d\bar{r}_\phi}{\bar{r}_\phi} - \frac{1}{2} \frac{1}{\frac{2nB}{n+1} \frac{\bar{\theta}_0}{p_\phi \bar{r}_\phi} + \ln \frac{\bar{r}_\phi}{R}} \frac{d\bar{r}_\phi}{\bar{r}_\phi}. \quad (6.38)$$

The approximate solution for ordinary differential equation (6.38) for a shock-wave having an exponential profile has the form*

$$p_\phi = \frac{p_m \bar{R}}{\bar{r}} \frac{1}{\sqrt{1 + \frac{n+1}{2nB} \frac{p_m \bar{R}}{2\bar{\theta}_0} \ln \frac{\bar{r}}{R}}}, \quad (6.39)$$

where p_m and $\bar{\theta}_0$ - pressure on the front and the constant of exponential damping on initial surface \bar{R} .

After defining pressure on the front p_ϕ , we can easily find a relationship for p , \bar{r} , and $\Delta \bar{t}$ by using equations (6.33), (6.34), and (5.50). Consequently, let us derive

$$\begin{aligned} \Delta \bar{t} = & \frac{n+1}{2nB} p_\phi \bar{r} \left(1 - \frac{p}{p_\phi} \right) \ln \frac{\bar{r}}{R} + \\ & + \begin{cases} \bar{\theta}_0 \ln \frac{p_\phi}{p} & \text{при } p > \frac{p_m \bar{R}}{\bar{r}} \\ \bar{\theta}_0 \left(0.368 \frac{p_\phi}{p} b - \ln b \right) & \text{при } p < \frac{p_m \bar{R}}{\bar{r}}. \end{cases} \end{aligned} \quad (6.40)$$

*If we assume that $\bar{\theta}_0/p_\phi \bar{r}_\phi = \bar{\tau}_0/p_m \bar{R} = \text{constant}$ at the initial point (where $\bar{\tau}_0 = \alpha_0 \tau_0/R_0$, τ_0 - effect-time of positive pressure phase), a precise solution can be derived for differential equation (6.38) which will correspond to the asymptotic behavior of a shock-wave having a linear profile.

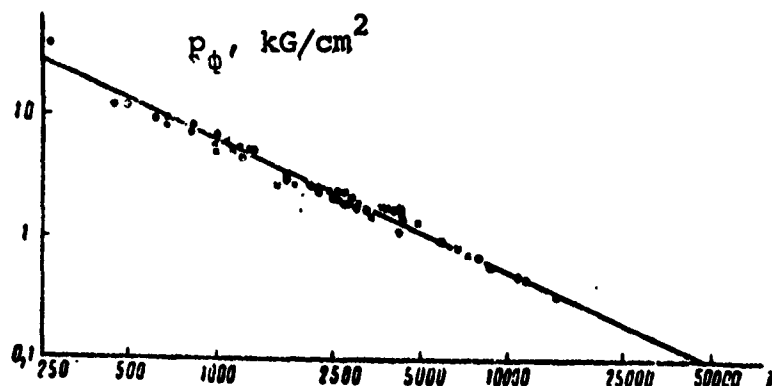


Fig. 11. Comparison of Asymptotic Solution for p_ϕ with Arons' Experimental Data.

• - explosion of charge, $G = 11.3$ kg;

× - explosion of charge, $G = 25$ kg.

where

$$b = \frac{p_m \bar{R}}{p_\phi r},$$

Δt is the time interval, counted from the wave-front arrival at point \bar{r} .

Hence, we immediately find the characteristic time θ , corresponding to an "e"-fold drop in pressure:

$$\theta = \bar{\theta}_n (b - \ln b) + 0.632 \frac{n+1}{2nB} p_\phi \bar{r} \ln \frac{\bar{r}}{R}. \quad (6.41)$$

Using the surface $\bar{R} = 240$ as the initial surface and using the semi-empirical formulas of the preceding paragraph, we can find a simpler expression to characterize asymptotic change in pressure on the front of an underwater shock-wave, after calculating instead of (6.39)

$$p_\phi = \frac{10000}{\bar{r} \sqrt{\lg \bar{r} - 0.4}}. \quad (6.42)$$

A similarly-derived formula for the constant of exponential damping does not differ greatly from (5.51) and has the form

$$\bar{\theta} = 3.7 \sqrt{\lg \bar{r} - 1}. \quad (6.43)$$

The theoretical findings from formula (6.42) are compared with Arons' experimental data [27] in Fig. 11. A good convergence of theory and experiment permits us to recommend final fixed relationships for practical evaluations.

As additional research has shown, the pressure contour of an underwater shock-wave does not change much as the distance from the explosion increases; even at a distance of 100,000 radii from the charge, the approximate relationships of the preceding section [formulas (5.50)-(5.67) in §5] are valid.

§7. The Effect of a Free Fluid Surface on Pressure Fields in Underwater Explosion.

In underwater explosion at relatively small depths, a free fluid surface exerts a considerable effect on the parameters of the hydrodynamic field. The moment a shock-wave encounters a free surface, a refracted compression wave is formed in the air and a reflected expansion wave is formed in the water. Owing to a significant difference in the quantities of acoustic resistance of the media, the rate of particle motion on the free surface is almost double that of particles behind the wave-front in an infinite medium.

The motion of fluid at elevated velocities leads to a reduction in fluid density in a specific layer; this, in turn, entails a drop in pressure. Propagating at the local speed of sound, this disturbance creates a combination of elementary waves having reduced pressure and different amplitudes (characteristics).

If we are examining an explosion at great depths, and measurements are made at relatively small distances from the epicenter, the difference in the propagation rates of the characteristics is negligible. We can then solve problems using the acoustic (linear) approximation. In this case, the limiting conditions are satisfied by applying two fields of different signs. The simplest method for

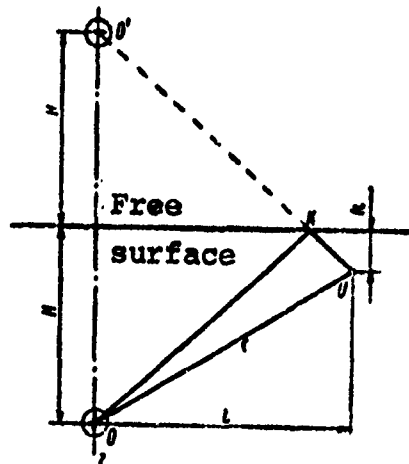


Fig. 12. Diagram of Mirror Reflection of Source and Runoff.

calculating the effect of a free surface is the method of mirror reflection of the source and runoff, the main point of which is illustrated in Fig. 12. A direct wave is viewed as a disturbance originating from the source in the lower-half-plane; a reflected wave is an imaginary runoff in the upper half-plane.

Since the pressure field in the acoustic approximation of a direct wave can be expressed by the relationship

$$p_{up}(t, r) = p_m(r) f\left(t - \frac{r}{a_0}\right) z_0\left(t - \frac{r}{a_0}\right), \quad (7.1)$$

where

$$r = \sqrt{L^2 + (H - h)^2}$$

$$z_0\left(t - \frac{r}{a_0}\right) = \begin{cases} 0 & \text{where } t < r/a_0, \\ 1 & \text{where } t \geq r/a_0, \end{cases}$$

the net pressure field is

$$p = p_m(r) f\left(t - \frac{r}{a_0}\right) z_0\left(t - \frac{r}{a_0}\right) - p_m(r') f\left(t - \frac{r'}{a_0}\right) z_0\left(t - \frac{r'}{a_0}\right), \quad (7.2)$$

where

$$r' = \sqrt{L^2 + (H + h)^2}.$$

A formal corollary of (7.2) is the possible formation of negative stresses in the fluid.

The question arises as to whether water is capable of withstanding these stresses. Individual experiments have shown that, under certain conditions, water which is free of mechanical impurities can withstand negative pressures of up to 280 kg/cm^2 (cf., for example, [28]).

In practical application, however, we most often observe the rapid development of cavitation phenomena and a drop in pressure to the state of vacuum.

The reflection of shock-waves on a free surface has been well recorded by experimental methods. We can show the moment that a reflected wave approaches a point by shearing the pressure curve in an explosion oscillogram. Several oscillograms are shown in Fig. 13 to illustrate this point. The solid lines in Fig. 13 indicate pressure oscillograms obtained by experimentation; the dotted lines indicate pressure oscillograms calculated according to formula (7.2).^{*} As we can see, there is total coincidence of theoretical and experimental data, prior to the moment when the expansion wave converges. The theoretical curves indicate the possible existence of an area of negative stresses which was not recorded in the experiment.

The effect-time of the positive pressure phase is apparently

^{*}A form of the functions $p_m(r)$ and $f(t - r/\alpha_0)$ is used according to data of §5.

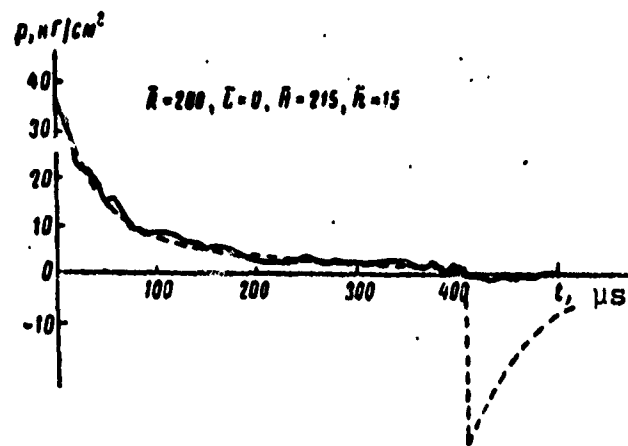
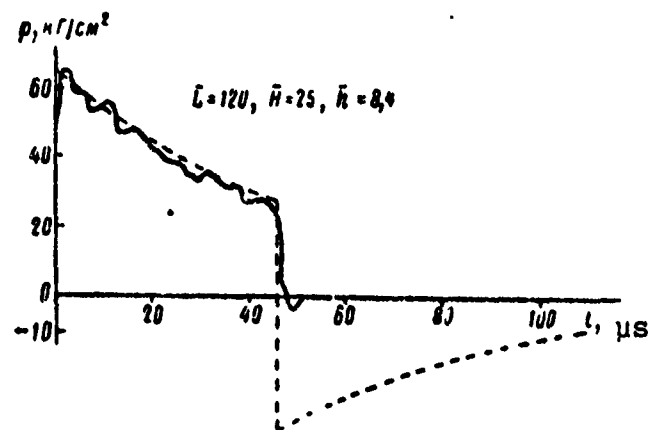
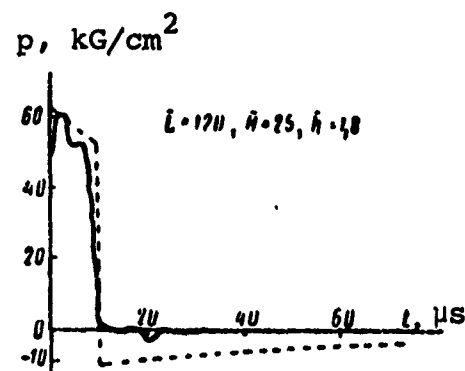


Fig. 13. Typical Pressure Oscillograms, allowing for the effect of free surface (where $G = 53 \text{ g}$).

defined by the difference in the arrival times of a direct wave and a wave reflected on a free surface at a given point.* Since the distance traveled by a direct wave is equal to $\sqrt{L^2 + (H - h)^2}$ and the distance traveled by the reflected wave is equal to $\sqrt{L^2 + (H + h)^2}$ then

$$t_{ak} = \frac{1}{a_0} \left| \sqrt{L^2 + (H + h)^2} - \sqrt{L^2 + (H - h)^2} \right| = \frac{r}{a_0} \left(\sqrt{1 + \frac{4Hh}{r^2}} - 1 \right). \quad (7.3)$$

For small quantities H and h , it is roughly equal to

$$t_{ak} \approx \begin{cases} \frac{2Hh}{a_0 r} & \text{where } \frac{1}{r} \sqrt{Hh} < 0.1 \\ \frac{2Hh}{a_0 L} & \text{where } \frac{H+h}{L} < 0.2. \end{cases} \quad (7.4)$$

Hence, it follows that the effect-time of the positive pressure phase, allowing for the free surface in the acoustic approximation, is defined by purely geometric features and does not depend on the weight of the charge (except for previously-specified cases).

A reduction in the duration of the positive phase of a shock-wave brings about a change in its integral characteristics.

Based on an exponential pressure-to-time curve for total momentum where $t_{ak} < \theta$, we will derive

$$J_{ak} = \int_0^{t_{ak}} p_m e^{-\frac{t}{\theta}} dt = p_m \theta \left(1 - e^{-\frac{t_{ak}}{\theta}} \right). \quad (7.5)$$

For values of the ratio t_{ak}/θ that are not too great,

$$J_{ak} = \begin{cases} p_m t_{ak} \left(1 - \frac{t_{ak}}{2\theta} \right) & \text{where } \frac{t_{ak}}{\theta} < 0.35 \\ p_m t_{ak} & \text{where } \frac{t_{ak}}{\theta} < 0.04. \end{cases} \quad (7.6)$$

*This is valid if the arrival time is shorter than the duration of the excess-pressure positive phase, which always occurs in shallow explosions.

Where $t_{ak} < 0$ [cf. (5.53)-(5.56)], energy flux density is

$$E = \frac{p_m^2 \theta}{2\rho_0 a_0} \left\{ \left(1 - e^{-\frac{2t_{ak}}{\theta}} \right) + \frac{a_0 \theta}{r} \left[1 - e^{-\frac{t_{ak}}{\theta}} \left(2 - e^{-\frac{t_{ak}}{\theta}} \right) \right] \right\}. \quad (7.7)$$

For distances $\bar{r} > 20$ (with error not exceeding 5%),

$$E = \frac{p_m^2 \theta}{2\rho_0 a_0} \left(1 - e^{-\frac{2t_{ak}}{\theta}} \right). \quad (7.8)$$

We have discussed a scheme for calculating the effect of free surface of a fluid in the acoustic approximation which is clear and simple, but has a limited field of application. If we examine pressure fields near a free surface at a distance from the epicenter which considerably exceeds the depth of explosion, then we must take into account the nonlinearity of the reflection process: nonlinearity is associated with the difference in the rates of propagation of elementary pressure-reduction waves. Low-amplitude characteristic waves, propagating at the local speed of sound, can sometimes overtake the shock-wave front and weaken it. In contrast, some characteristics, having considerable negative amplitude and propagating at the speed of sound in an undisturbed medium, will recede from the front. Therefore, the nonlinear effect of free surface may be revealed both in a reduction of direct-wave amplitude and in a distortion of the entire pressure-time contour, as the total duration of the positive phase increases.

A number of researchers undertook the study of these phenomena. The primary findings were achieved by S. A. Khristianovich, A. A. Grib, A. G. Ryabinin, Ya. F. Sharov, B. V. Zamyshlyayev, and B. I. Zaslavskiy, who devised a nonlinear theory for the interaction of an underwater shock-wave with a free fluid surface, and suggested approximate formulas for evaluating pressure fields.

Let us first examine regular reflection of a plane wave having one-valued amplitude on a free surface (Fig. 14).

or, considering that angles δ_{np} and δ_{xap} are similar and rejecting numerically-small second-order values,

$$N_{xap} \approx a + v_\phi \cos 2\delta_{np} - a_0 \frac{p_{\phi.p}}{nB}.$$

Substituting the values of the speed of sound and the velocity of particles according to (1.38) and (1.39) in this expression, we find that:

$$N_{xap} = a_0 \left\{ 1 + \frac{n+1}{2nB} (p_\phi - p_{\phi.p}) - \frac{p_\phi}{nB} (1 - \cos 2\delta_{np}) \right\}. \quad (7.10)$$

Solving (7.10) and (7.9) simultaneously, we will derive:

$$\begin{aligned} \cos \delta_{xap} = \cos \delta_{np} \left[1 + \frac{n+1}{2nB} (p_\phi - p_{\phi.p}) - \right. \\ \left. - \left(\frac{n+5}{4} - \cos 2\delta_{np} \right) \frac{p_\phi}{nB} \right]. \end{aligned} \quad (7.11)$$

For small angles of incidence ($\cos \delta_{np} \approx 1 - \frac{1}{2}\delta_{np}^2$), equation (7.11) becomes the relationship

$$\cos \delta_{xap} \approx \frac{1 + \frac{n+1}{2nB} (p_\phi - p_{\phi.p})}{1 + \frac{n+1}{4nB} p_\phi + \frac{1}{2} \delta_{np}^2}, \quad (7.12)$$

which was first established by Khristianovich [3].

Equation (7.11) permits us to plot the pressure curve at a given point. Let the depth of this point be equal to h . As a direct wave front approaches this point ($t = 0$), pressure abruptly increases to p_ϕ and remains constant until a zero amplitude characteristic approaches ($p_{\phi.p} = 0$).

On the basis of simple geometric plots (Fig. 14), this time interval is

$$t_0 = \frac{h (t_{\delta_{np}} + t_{\delta_{xap}})}{\frac{N_\phi}{\cos \delta_{np}}}. \quad (7.13)$$

Convergence time of a characteristic having arbitrary amplitude at this point is

$$t = \frac{h \cos \vartheta_{np}}{N_{\phi}} (\operatorname{tg} \vartheta_{np} + \operatorname{tg} \vartheta_{xap}). \quad (7.14)$$

Substituting the value of ϑ_{xap} according to (7.11) in (7.14) and performing transformations, we find that

$$t = \frac{2h}{a_0} \sin \vartheta_{np} \left\{ 1 - \frac{n+1}{4nB} p_{\phi} + \frac{1}{\sin^2 \vartheta_{np}} \left[\left(\frac{n+5}{4} - \cos 2\vartheta_{np} \right) \times \right. \right. \\ \left. \left. \times \frac{p_{\phi}}{2nB} - \frac{n+1}{4nB} (p_{\phi} - p_{a.p.}) \right] \right\}. \quad (7.15)$$

This same result can be derived on the basis of the Fermat principle, according to which any disturbance in space propagates along the path having the minimum mean-free-path time.

Our initial time reading will be the moment the wave-front arrives at a point $x = 0, z = 0$ (Fig. 15). Then, the travel time of a point common to the direct-wave front and the expansion wave, at distance x , is

$$t = \frac{x \cos \vartheta_{np}}{N_{\phi}}. \quad (7.16)$$

The mean free path of the characteristic from point K to point U will equal $\sqrt{h^2 + (L-x)^2}$.

The slope of the characteristic, with respect to the free surface, is

$$\vartheta_{xap} = \operatorname{arctg} \frac{h}{L-x} = \arccos \frac{L-x}{\sqrt{h^2 + (L-x)^2}}, \quad (7.17)$$

and consequently, the arrival time of a given characteristic at point U is

$$t_{xap} = \frac{x \cos \vartheta_{np}}{N_{\phi}} + \frac{\sqrt{h^2 + (L-x)^2}}{N_{xap}}. \quad (7.18)$$

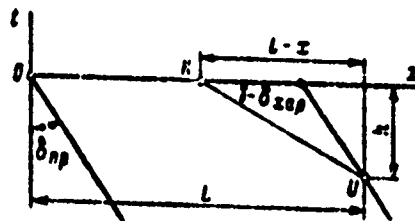


Fig. 15. Diagram of the Reflection of a Plane Shock-Wave on a Free Surface.

Using the Fermat principle, let us find the position of point K from the condition that

$$\frac{dt_{xap}}{dx} = 0.$$

We have

$$x = L - h \frac{\frac{N_{xap} \cos \delta_{np}}{N_{\phi}}}{\sqrt{1 - \left(\frac{N_{xap} \cos \delta_{np}}{N_{\phi}} \right)^2}}. \quad (7.19)$$

The quantity $(N_{xap} \cos \delta_{np}) / (N_{\phi}) = \cos \delta_{xap}$, which enters into equation (7.19) is easily calculated using (7.11), if we are given the pressure of the expansion wave $p_{B.p}$.

Therefore, according to (7.18) and (7.19), the arrival time of the characteristic of given amplitude at point U is

$$t(p_{B.p}) = \frac{L - h \frac{\cos \delta_{xap}}{1 - \cos^2 \delta_{xap}}}{N_{\phi} \cos \delta_{np}} + \frac{h}{N_{xap} \sqrt{1 - \cos^2 \delta_{xap}}}. \quad (7.20)$$

The shock-wave front arrives at this point at the point in time (cf. Fig. 15)

$$t_{\phi} = \frac{L - h \operatorname{tg} \delta_{np} \cos \delta_{np}}{N_{\phi}}. \quad (7.21)$$

Starting the time-count as a shock-wave front converges with a point, and taking (7.11) into account, after several simple transformations instead of (7.20) we derive

$$t = \frac{2h}{a_n} \sin \delta_{np} \left\{ 1 - \frac{n+1}{4nB} p_{\phi} + \right.$$

$$+ \frac{1}{\sin^2 \delta_{np}} \left[\left(\frac{n+5}{4} - \cos 2\delta_{np} \right) \frac{p_\phi}{4nB} - \frac{n+1}{4nB} (p_\phi - p_{s.p.}) \right] \Bigg\}.$$

which totally coincides with (7.15). Specifically, the zero amplitude characteristic ($p_{s.p.} = 0$) converges with a given point some time after the shock-wave front arrives:

$$t_0 = \frac{2h}{a_0} \sin \delta_{np} \left\{ 1 - \left[\frac{n+1}{4} + \frac{1}{2 \sin^2 \delta_{np}} \left(\frac{n-3}{4} + \cos 2\delta_{np} \right) \right] \frac{p_\phi}{nB} \right\}. \quad (7.22)$$

For the maximum amplitude characteristic, we will derive

$$t_1 = \frac{2h}{a_0} \sin \delta_{np} \left\{ 1 - \left[\frac{n+1}{4} - \frac{1}{2 \sin^2 \delta_{np}} \left(\frac{n+5}{4} - \cos 2\delta_{np} \right) \right] \frac{p_\phi}{nB} \right\}. \quad (7.23)$$

These equations permit us to refine our earlier conclusion concerning the use of linear approximation formulas to calculate the effect of free surface. Indeed, let us assume that we may replace the gradual drop in pressure over time $t \leq 0.2t_+$ by an instantaneous drop in pressure, i.e., $t_+ - t_0/t_+ \leq 0.2$. Then, after substituting the corresponding values of t_+ and t_0 , we will derive

$$\frac{n+1}{4nB} \frac{p_\phi}{\sin^2 \delta_{np}} \leq 0.2,$$

$$\delta_{np} > \arcsin \sqrt{5 \frac{n+1}{4nB} p_\phi}. \quad (7.24)$$

These considerations are not valid for the entire possible range of direct-wave slope change. Starting from an angle, which will henceforth be called the critical angle (δ^*), expansion waves will overtake the direct-wave front, distort its shape, and alter its amplitude. Irregular reflection will occur.

Let us find the quantity of the critical angle δ^* by comparing the rates of travel of the expansion-wave front (zero amplitude characteristic) and the direct-wave front.

The zero amplitude characteristic travels toward the free surface at a velocity of

$$a + v_\phi \cos \delta_{np} = a_0 \left(1 + \frac{n-1}{2nB} p_\phi + \frac{p_\phi}{nB} \cos \delta_{np} \right). \quad (7.25)$$

The rate of travel of the wave front in the same direction is

$$\frac{N_\phi}{\cos \delta_{np}} = \frac{a_0}{\cos \delta_{np}} \left(1 + \frac{n+1}{4nB} p_\phi \right). \quad (7.26)$$

The critical angle is defined by the equation

$$1 + \frac{n-1}{2nB} p_\phi + \frac{p_\phi}{nB} \cos \delta_{np}^* = \frac{1}{\cos \delta_{np}^*} \left(1 + \frac{n+1}{4nB} p_\phi \right). \quad (7.27)$$

Considering that angle δ^* is small, and therefore assuming that $\delta^* = 1 - (1/2) \delta^{*2}$, we derive

$$1 + \frac{n+1}{2nB} p_\phi = 1 + \frac{n+1}{4nB} p_\phi + \frac{1}{2} \delta^{*2},$$

whence

$$\delta^* = \sqrt{\frac{n+1}{2nB} p_\phi}. \quad (7.28)$$

If the slope is $\delta_{np} > \delta^*$, pressure-reduction waves do not overtake the shock-wave front. Regular reflection occurs. Where $\delta_{np} < \delta^*$, reflection becomes irregular. The point of intersection of the expansion-wave front and the shock-wave front is displaced downward away from the free surface. The portion of the shock-wave front adjoining the free surface curves. Pressure in this portion of the front are less than in an infinite fluid.

Let us examine irregular reflection for a case which is most important with respect to practical applications: spherical-wave propagation.

For the sake of simplicity, we will consider the slope of the wave to be small ($\cos \delta_{np} \approx 1$). Then, according to (7.10), the rate

of travel of a characteristic if given amplitude is

$$N_{xap} = a_0 \left[1 + \frac{n+1}{2Bn} (p_\phi - p_{s.p}) \right] = a_0 \left(1 + \frac{n+1}{2Bn} p_\phi \eta \right). \quad (7.29)$$

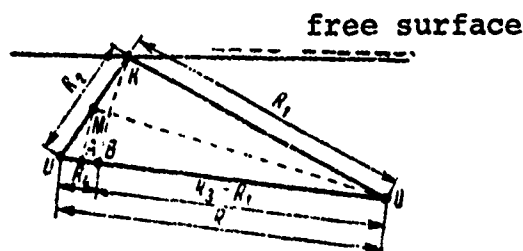


Fig. 16. Diagram of Propagation of the Direct and Reflected Wave.

where

$$\eta = \frac{p_\phi - p_{s.p}}{p_\phi}. \quad (7.30)$$

A diagram of reflection is shown in Fig. 16. The underwater shock-wave front arrives at an arbitrary point in the fluid U from the center of explosion O at some point in time. Elementary pressure-reduction waves (the characteristics) arrive at the same point from various points on the free surface at different times.

Depending on the relative juxtaposition of the explosion center O and the measurement point U , the following primary cases can occur:

1. The zero amplitude characteristic will arrive at point U after the shock-wave front. Pressure at this point will be the same as in an infinite fluid.
2. The zero amplitude characteristic will arrive at point U at the same time as the direct-wave front. Pressure on the front will be the same as in an infinite fluid. The nonlinear influence of free surface will be revealed in distortion of the shape of the shock-wave.
3. Some elementary pressure-reduction waves will arrive at point O at the same time as the front arrives. Pressure on the front

will be less than in an infinite fluid.

Let us explain the circumstances where a direct shock-wave front and the zero amplitude characteristic will arrive at a given point simultaneously.

For the zero amplitude characteristic, $p_{B,p} = 0$, $\eta = 1$, and consequently, according to (7.29)

$$N_{\text{asp}}^0 = u_0 \left(1 + \frac{n+1}{2Bn} p_\phi \right). \quad (7.31)$$

Using the Fermat principle, let us find the position of point K on the free surface, from which the zero amplitude characteristic first arrives at point U. According to this principle, the time required for the wave to travel along dotted line OKU must be the minimum.

The simultaneous arrival and the direct wave and the zero amplitude characteristic at point U can be written in the form (Fig. 16)

$$t_2 = t_4, \quad (7.32)$$

where t_2 - travel time of the zero amplitude characteristic from point K to point U; t_4 - travel time of the direct-wave front from point B to point U.

To evaluate the time interval t_2 , we have (Fig. 16)

$$\frac{t_2}{R_0} = \int_0^{\bar{R}_1} \frac{d\bar{R}}{u_0 \left(1 + \frac{n+1}{2Bn} p_\phi \right)} \approx \frac{\bar{R}_1}{u_0} - \frac{n+1}{2Bn} \frac{1}{u_0} \int_0^{\bar{R}_1} p_\phi d\bar{R}. \quad (7.33)$$

since pressure on the front p_ϕ can be represented as a function of dimensionless distance, the integral of (7.33) is easily calculated. However, simpler relationships can be derived, if we utilize the mean rate of travel in the appropriate portions for evaluating

the time intervals t_2 and t_4 .

In this case,

$$\frac{t_2}{R_0} = \frac{\bar{R}_2}{N_{\text{exp. cp}}^0} = \frac{\bar{R}_2}{a_0 \left(1 + \frac{n+1}{2Bn} p_M\right)} = \frac{\bar{R}_2}{a_0} \left(1 - \frac{n+1}{2Bn} p_M\right), \quad (7.34)$$

where p_M - pressure on the front of a shock-wave at point M or A

$$p_M = \frac{14700}{R_M^{1.13}}.$$

or a wave-front

$$\frac{t_4}{R_0} = \frac{R_4}{N_{\text{cp. } \Phi}} = \frac{\bar{R}_4}{a_0 \left(1 + \frac{n+1}{4Bn} p_M\right)} = \frac{\bar{R}_4}{a_0} \left(1 - \frac{n+1}{4Bn} p_M\right). \quad (7.35)$$

Let us designate that

$$\xi = \frac{x}{L}, \quad (7.36)$$

where x - horizontal distance between points K and U; L - horizontal distance between points O and U.

Then, for distances entering into expressions (7.34) and (7.35), we find that (Fig. 16)

$$\begin{aligned} \bar{R}_1 &= \frac{R_1}{R_0} = \frac{1}{R_0} \sqrt{(L-x)^2 + H^2} \simeq L(1-\xi) \times \\ &\times \left[1 + \frac{1}{2} \frac{H^2}{L^2 (1-\xi)^2}\right], \\ \bar{R}_2 &= \frac{1}{R_0} \sqrt{x^2 + h^2} \simeq L\xi \left(1 + \frac{1}{2} \frac{h^2}{L^2 \xi^2}\right), \\ \bar{R}_U &= \frac{1}{R_0} \sqrt{L^2 + (H-h)^2} \simeq L \left[1 + \frac{1}{2} \frac{(H-h)^2}{L^2}\right], \\ \bar{R}_4 &= \bar{R}_U - \bar{R}_1 = L \left[\xi + \frac{(1-\xi)(H-h)^2 - H^2}{2L^2(1-\xi)}\right], \\ \bar{R}_N &= \bar{R}_A = \frac{1}{2} (\bar{R}_U + \bar{R}_1) = \\ &= \frac{1}{2} L \left[2 - \xi + \frac{(H-h)^2(1-\xi) + H^2}{2L^2(1-\xi)}\right] \simeq L \left(1 - \frac{1}{2} \xi\right). \end{aligned} \quad (7.37)$$

According to (7.32), (7.34), and (7.35)

$$\frac{\bar{R}_2}{a_0} \left(1 - \frac{n+1}{2Bn} p_M \right) = \frac{\bar{R}_4}{a_0} \left(1 - \frac{n+1}{4Bn} p_M \right). \quad (7.38)$$

Moreover,

$$\frac{n+1}{4Bn} p_M = \frac{8.15}{4 \cdot 30.15 \cdot 7.15} \frac{14700}{L^{1.13} \left(1 - \frac{1}{2} \xi \right)^{1.13}} = \frac{1.375}{L^{1.13} (1 - 0.5\xi)^{1.13}}. \quad (7.39)$$

Substituting the expressions for \bar{R}_2 , \bar{R}_4 , and $(n+1)/(4Bn)p_M$ into (7.38), according to (7.37) and (7.39) we will find that

$$\begin{aligned} & \bar{L} \xi \left(1 + \frac{1}{2} \frac{\bar{h}^2}{L^2 \xi^2} \right) \left[1 - \frac{2.75}{L^{1.13} (1 - 0.5\xi)^{1.13}} \right] = \\ & = \bar{L} \left[\xi + \frac{(1-\xi)(\bar{H} - \bar{h})^2 - \bar{H}^2}{2 \bar{L} (1-\xi)} \right] \left[1 - \frac{1.375}{L^{1.13} (1 - 0.5\xi)^{1.13}} \right] \end{aligned}$$

or, performing a transformation and rejecting numerically-small values of higher order,

$$\frac{(\bar{H} - \bar{h})^2 (1 - \xi) - \bar{H}^2}{2 \bar{L} \xi (1 - \xi)} = \frac{\bar{h}^2}{2 L^2 \xi^2} - \frac{1.375}{L^{1.13} (1 - 0.5\xi)^{1.13}},$$

whence

$$\bar{L} = \left\{ \frac{(\bar{h} + \xi (\bar{H} - \bar{h}))^2 (1 - 0.5\xi)^{1.13}}{2.75 \xi^2 (1 - \xi)} \right\}^{1.13}. \quad (7.40)$$

The relative distance \bar{L} defined by (7.40) will be called the critical distance (\bar{L}_{kp}). When $\bar{L} \geq \bar{L}_{kp}$, the shock-wave front overtakes the expansion wave. According to the Fermat principle, the parameter ξ must be chosen so that the quantity \bar{L}_{kp} is the minimum.*

After calculating $\partial \bar{L} / \partial \xi$, equating the derived expression to zero, and performing simple transformations, we find that

*We can easily verify that this requirement is tantamount to satisfying the wave brachistochrone conditions along dotted line OKU (Fig. 16).

$$\xi(1-\xi) \left[\frac{2(\bar{H}-\bar{h})}{\bar{h}+\xi(\bar{H}-\bar{h})} - \frac{0.565}{1-0.5\xi} \right] = 2-3\xi. \quad (7.41)$$

Equation (7.41) can be solved easily in two particular cases:

where $\bar{h} = 0$

$$\xi = 0,$$

where $\bar{h} = \bar{H}$

$$\xi = 0.72^*$$

Substituting this result into (7.40), we can derive

where $\bar{h} = 0$

$$\bar{L}_{\text{HP}} = 0.31\bar{H}^{2.3}, \quad (7.42)$$

where $\bar{h} = \bar{H}$

$$\bar{L}_{\text{HP}} = 1.61\bar{H}^{2.3}. \quad (7.43)$$

On the basis of (7.42) and (7.43), formula (7.40) may be estimated by the approximate expression

$$\bar{L}_{\text{HP}} = \bar{H}^{1.3} (0.31\bar{H} + 1.3\bar{h}). \quad (7.44)$$

An inference on the precision of the approximation can be made on the basis of Fig. 17 which shows the results of the corresponding calculations.

Similar arguments enable us not only to evaluate the distance

* To be more precise, when $\bar{h} = \bar{H}$, this equation becomes a quadratic equation, whose root is within the range 0-1 and is equal to 0.72.

L_{kp} , but also the plot the pressure contour in the zone where $L \leq L_{kp}$. Indeed, the arrival time of a characteristic wave of arbitrary amplitude η at some point, counted from the moment of arrival at the same point by the shock-wave front, is (Fig. 16)

$$t(\eta) = t_2(\eta) - t_4, \quad (7.32a)$$

where

$$\frac{t_2(\eta)}{R_0} = \frac{R_2}{a_0} \left(1 - \frac{n+1}{2Bn} p_M \eta \right),$$

and t_4 is subtracted according to formula (7.35).

Performing transformations with the aid of (7.37) and (7.39), equation (7.32a) will be written in the form

$$\bar{t}(\eta) = \frac{a_0 t(\eta)}{R_0} = \frac{|\bar{h} + \xi(\bar{H} - \bar{h})|^2}{2\bar{L}\xi(1-\xi)} - \frac{1.375(2\eta-1)\xi}{\bar{L}^{0.13}(1-0.5\xi)^{1.13}}. \quad (7.45)$$

Based on (7.45) specifically, the time interval between the arrival of the wave-front and the zero amplitude characteristic ($\eta = 1$) wave at some point constitutes

$$t_c = \frac{|\bar{h} + \xi(\bar{H} - \bar{h})|^2}{2\bar{L}\xi(1-\xi)} - \frac{1.375\xi}{\bar{L}^{0.13}(1-0.5\xi)^{1.13}}. \quad (7.46)$$

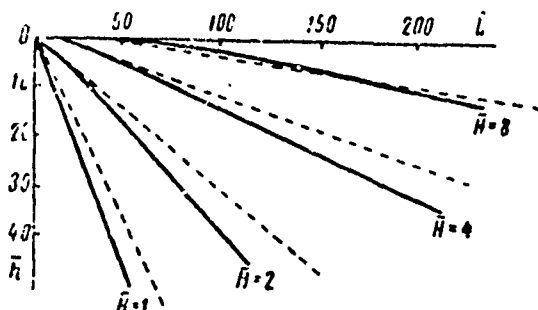


Fig. 17. Zone Boundaries of the Effect of a Free Surface on a Direct-Wave Front at Different Charge Depths.

————— theoretically calculated;
 ----- by approximation.

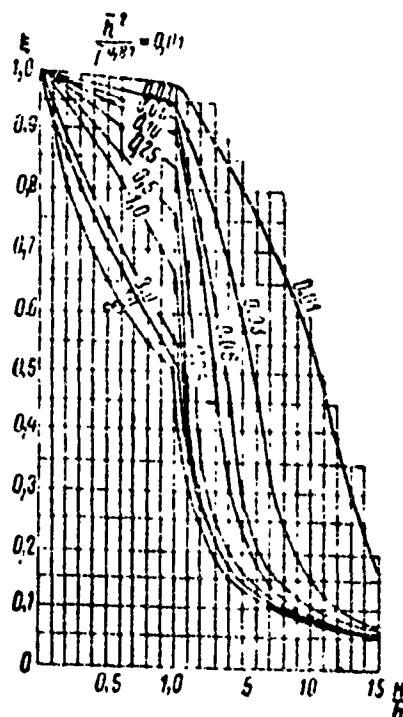


Fig. 18. ξ for \bar{t}_0 as a function of H/h and $\bar{h}^2 / \bar{L}^{0.87}$.

For a maximum amplitude characteristic wave,

$$\bar{t}_+ = \frac{(h + \xi(\bar{H} - \bar{h}))^2}{2\bar{L}\xi(1 - \xi)} + \frac{1.375\xi}{\bar{L}^{0.17}(1 - 0.5\xi)^{1.17}}. \quad (7.47)$$

On the basis of the Fermat principle, the parameter ξ in formulas (7.45)-(7.47) is defined from the equality $\partial t / \partial \xi = 0$.

Fig. 18. shows a combination of the numerical solution of this equation and (7.46). The theoretical results of ξ for \bar{t}_0 can be approximated by the relation

$$\xi = \frac{\bar{h}}{H + \bar{h}} \left(1 - e^{-\frac{\bar{H} + \bar{h}}{\bar{L}^{0.5}}} \right).$$

Formulas (7.46) and (7.47) permit us to define the limit of possible application of the acoustic solution. Assuming, as previously, [cf. (7.24)] that the pressure-drop time interval comprises no more than 20% of the total duration, we get

$$\frac{t_+ - t_0}{t_+} \leq 0.2.$$

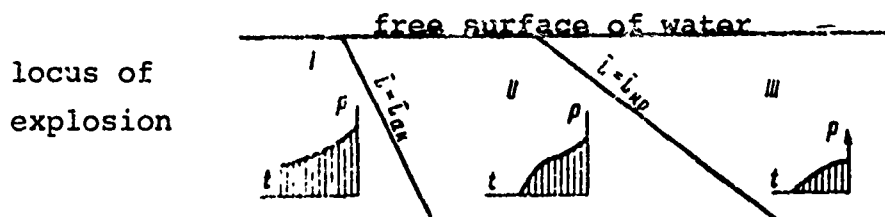


Fig. 19. Zones of Nonlinear Effect of Free Surface on Shock-Wave Parameters.

Using this inequality in conjunction with (7.46) and (7.47), and approximating the theoretical results by an expression similar in structure to (7.44), we find that

$$L_{\text{non}} \approx 0.1 H^{2.3} \left(1 + 0.5 \frac{h}{H} \right). \quad (7.48)$$

Therefore, equations (7.44) and (7.48) delimit the entire observation area into three zones (Fig. 19).

In zone I, where $\bar{L} < \bar{L}_{\text{ak}}$, acoustic approximation formulas may be accurately used to evaluate the parameters of an underwater shock-wave. In zone II, there is substantial distortion in the tail section of the pressure contour and the parameters of the front are not a function of the free surface. In zone III, the effect of the free surface embraces the entire pressure contour, including the parameters at the front.

In zone II, when given the parameters ξ and η , the wave contour is graphed directly with the aid of relation (7.45).

Despite its simplicity, this method is rather unwieldy and therefore, for practical purposes it is convenient to use a simpler approximation, which can be realized if we impose the following premises:

- at the moment of convergence of a zero amplitude characteristic wave $t = 0$, pressure in the wave is the same as in an infinite fluid ($p = p_{\infty}$);

- the characteristic wave $\eta = 0.5$ has the same rate of travel as the shock-wave front and consequently, $t = t_{0.5}$, corresponding to a pressure $p = 0.5 p_{\infty}$;

- the maximum amplitude characteristic wave $\eta = 0$ arrives at a point in time $t = t_+$; the resultant pressure at this time is equal to zero.

Thus, for a constant amplitude wave, using the parabolic law of pressure variation in the interval $t_0 - t_+$, we find that

$$p = p_{\infty} \left\{ \left[\sigma_0(t) - \sigma_0(t - t_0) \right] + \left[1 - \left(\frac{t - t_0}{t_+ - t_0} \right)^n \right] \left[\sigma_0(t - t_0) - \sigma_0(t - t_+) \right] \right\}. \quad (7.49)$$

If we calculate approximately that in an infinite medium, pressure changes with respect to the exponential law

$$p = p_{\infty} e^{-\frac{t}{t_0}},$$

then, instead of (7.49) we can write

$$p = p_{\infty} \left\{ e^{-\frac{t}{t_0}} \left[\sigma_0(t) - \sigma_0(t - t_0) \right] + \left[1 - \left(\frac{t - t_0}{t_+ - t_0} \right)^n \right] \times \left[\sigma_0(t - t_0) - \sigma_0(t - t_+) \right] \right\}. \quad (7.50)$$

In equations (7.49) and (7.50), the exponent n is found from the apparent relation

$$n = \frac{\lg 0.5}{\lg \left(\frac{t_{0.5} - t_0}{t_+ - t_0} \right)}. \quad (7.51)$$

The moment t_0^* is found as the point of intersection of the exponent and an n -th degree parabola

$$e^{-\frac{t}{t_0}} = 1 - \left(\frac{t - t_0}{t_+ - t_0} \right)^n. \quad (7.52)$$

Fig. 20 shows a pressure contour which exemplifies the cited arguments.

is the ratio of critical distance to distance from the point of observation [cf. (7.44)]:

$$k = \frac{L_{cr}}{L} = \frac{0.31 H^{2.1}}{L} \left(1 + 4.2 \frac{h}{H} \right). \quad (7.56)$$

We naturally assume that maximum pressure in the wave is mainly defined by the parameter k :

$$p_m = p \cdot f(k). \quad (7.57)$$

The form of function f can be derived by analyzing magnitudes of pressure at points situated in the free surface of the fluid.

We previously wrote for the critical angle

$$\delta^* = \sqrt{\frac{H+1}{2nB}} p_\phi. \quad (7.28)$$

or, taking (5.48) into account

$$\delta^* = \frac{1.66}{L^{0.435}}. \quad (7.58)$$

The slope of an undistorted direct-wave is

$$\delta_{np} \approx \frac{\bar{H}}{L}.$$

According to the solution for a plane wave [3], pressure at a point in a free surface in a region of irregular reflection is defined by the relation

$$\begin{aligned} p_m &= p \cdot \frac{1}{4} \left(1 + \frac{\delta_{np}}{\delta^*} \right)^2 = p \cdot \frac{1}{4} \left(1 + \frac{\bar{H}}{1.66 L^{0.435}} \right)^2 = \\ &= p \cdot \frac{1}{4} (1 + k^{0.435})^2. \end{aligned} \quad (7.59)$$

As calculations show, in the range $0.05 < k < 1$

$$\frac{1}{4} (1 + k^{0.435})^2 \approx \sqrt{k}.$$

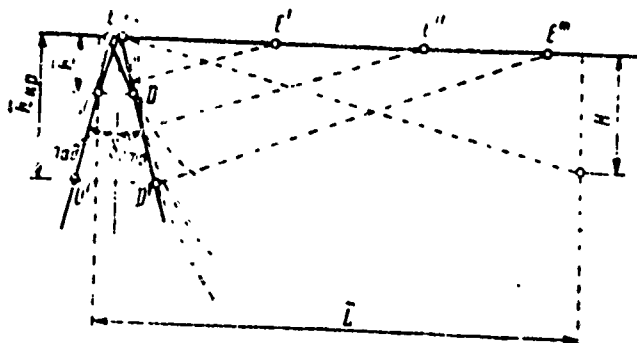


Fig. 22. Diagram of Irregular Reflection of Direct Wave on Free Surface.

The slope of the direct wave and the angle of reflection of the given characteristic wave are associated by the common nature of point E:

$$\frac{a_p}{\cos \delta_{up}} = \frac{N_\phi}{\cos \delta_{np}}.$$

In view of relation (1.44) for N_ϕ , as well as the fact that for small angles $\cos \delta \approx 1 - (1/2)\delta^2$, we will find:

$$\delta_{up} = \delta_{np} \sqrt{1 + \frac{n+1}{2nB} \frac{\rho_m}{v_{np}^2}}. \quad (7.62)$$

Considering that in an area of regular reflection the free surface has no effect on the parameters of the front, and that the relationship

$$\delta_{np} \approx \frac{H}{L},$$

$$\rho_m = \frac{14700}{L^{1.13}}, \quad (5.48)$$

occurs, according to expression (7.61)

$$t = \frac{2hH}{a_1 L} \beta = \beta t_{ak}, \quad (7.63)$$

where

$$\beta = \frac{1}{2} \left[1 + \sqrt{1 + \left(\frac{1.66 L^{0.435}}{H} \right)^2} \right]. \quad (7.64)$$

In an area of irregular reflection, pressure on the front decreases and the front curves. Moreover, as the point approaches the free surface from critical depth h_{np} , pressure will drop even more; consequently, there will be a reduction in the rate of propagation of the front and its curvature will increase (Fig. 22).

If pressure on the shock-wave front is equal to p_m , taking into account weakening by the characteristics of the expansion wave, the rate of propagation of the characteristic wave (which by then has overtaken the front) according to (7.10) will be

$$N_{\phi} = a_0 \left(1 + \frac{n-1}{2nB} p_m \right).$$

Then, the slope of the shock-wave front with the free surface can be defined from the condition of equality of the horizontal components of travel of the front and the characteristic wave

$$\frac{N_{\phi}}{\cos \delta_{np}} = N_{\phi np},$$

i.e.,

$$\frac{1}{\cos \delta_{np}} \left(1 + \frac{n-1}{4nB} p_m \right) = 1 + \frac{n-1}{2nB} p_m.$$

Hence, considering that $\cos \delta_{np} \approx 1 - (1/2) \delta_{np}^2$, we can derive

$$\delta_{np} = \sqrt{\frac{n-1}{2nB} p_m} \quad (7.65)$$

and according to expression (7.62),

$$\delta_{orp} = \sqrt{2} \delta_{np} = \sqrt{2} \sqrt{\frac{n-1}{2nB} p_m}. \quad (7.66)$$

Consequently, according to (7.61) and (7.66), the effect-time of the positive pressure phase near the free surface in an area of irregular reflection is

$$t_+ = 2.4 \frac{h}{a_0} \sqrt{\frac{n-1}{2nB} p_m}. \quad (7.67)$$

Considering that p_m is defined according to formula (7.59) for points situated near the free surface, we finally derive

$$t_* = \beta t_{sk}, \quad (7.68)$$

where

$$\beta = 0.6 \left(1 + \frac{1.66 \bar{L}^{0.435}}{H} \right). \quad (7.69)$$

Since the theoretical calculations of the coefficient β , according to formulas (7.64) and (7.69) do not differ from each other by more than 17% during the variation of $k_h = 0$ from 1 to 0.001, equation (7.47) can be utilized for practical evaluations. It can be approximated more simply by the expression

$$t_* = t_{sk} \beta, \quad (7.70)$$

where

$$t_{sk} = \frac{2Hh}{a_0 L}, \quad (7.4)$$

$$\beta = 0.7 + \frac{0.83 \bar{L}^{0.435} - 0.1 \bar{h}}{H}. \quad (7.71)$$

The pressure contour is close to parabolic

$$p(t) = p_m \left[1 - \left(\frac{t}{t_*} \right)^n \right] [\gamma_0(t) - c_0(t - t_*)]. \quad (7.72)$$

The average value of the exponent n is roughly equal to 1.15, which corresponds to the coefficient of completeness

$$\gamma = \frac{n}{n+1} = 0.6.$$

The quantity of total momentum, according to (7.72), is

$$J = \frac{n}{n+1} p_m t_*. \quad (7.73)$$

According to (5.55) and (7.72), energy flux density is defined by the expression

$$E = \frac{2n^2}{(n+1)(2n+1)} \cdot \frac{p_m^2 t_+}{\rho_0 a_0} \quad (7.74)$$

§8. Formation and Development of Cavitation in the Reflection of an Underwater Shock-Wave on a Free Surface.

As is well known, cavitation is the process of forming discontinuities in a fluid due to local pressure reduction. Cavitation effects are closely associated with the strength characteristics of a fluid in the formation of tensile stresses. In the studies of Ya. I. Frenkel' [20], Ya. B. Zel'dovich [6], J. C. Fischer [31], it is asserted that the upper limit of volumetric strength of water is defined by a quantity of the order 1500-3000 atm. Briggs proved experimentally [28] that distilled water which is free of mechanical impurities and air bubbles can withstand stresses of about 280 atm., its strength being chiefly a function of temperature. It has also been proven that the presence of solid particles, gas bubbles, and other similar deposits in a fluid sharply reduces its capacity to withstand tensile stresses. In view of this, cavitation discontinuities usually form when pressure is slightly less than the pressure of saturated steam.

In examining cavitation under actual basin conditions, we will refer to this last assertion. For the cavitation effect to occur, tensile forces must overcome the forces of hydrostatic pressure and induce underpressure equal to the quantity p_H .

Consequently,

$$p_{\text{pes}} = -(\rho_k + \rho_0) \quad (8.1)$$

where p_{pes} - net excess pressure, inducing cavitation of a fluid;
 p_0 - hydrostatic pressure at a given depth h :

$$p_0 = p_{atm} + \rho_0 g h. \quad (8.2)$$

Let us examine the gradient of an exponential plane wave along the normal toward the free surface in the acoustic approximation

$$p = p_m e^{-\frac{t - \frac{z}{a_0}}{\tau_0}} \tau_0 \left(t - \frac{z}{a_0} \right). \quad (8.3)$$

If water could withstand great tensile stresses, the net pressure at point $z = -h$ could be defined by the relation

$$p_{pc,1}(t, h) = p_m \left[e^{-\frac{t + \frac{h}{a_0}}{\tau_0}} \tau_0 \left(t + \frac{h}{a_0} \right) - e^{-\frac{t - \frac{h}{a_0}}{\tau_0}} \tau_0 \left(t - \frac{h}{a_0} \right) \right], \quad (8.4)$$

where t - time, counted from the moment of convergence of the wave front with the free surface.

At the moment of convergence of a reflected-wave front with a point ($t = h/\alpha_0$), pressure will be, according to (8.4),

$$p_m \left(e^{-\frac{2h}{a_0 \tau_0}} - 1 \right).$$

If this quantity is equated to the pressure inducing cavitation in the fluid, we will derive a relation which easily yields the thickness of the cavitation layer h_1 (Fig. 23)

$$p_m \left(e^{-\frac{2h_1}{a_0 \tau_0}} - 1 \right) = -(\rho_k + p_{atm} + \rho_0 g h_1) \quad (8.5)$$

$$h_1 = -\frac{a_0 \tau_0}{2} \ln \left(1 - \frac{\rho_k + p_{atm} + \rho_0 g h_1}{p_m} \right). \quad (8.6)$$

A layer of water h_1 thick, moving upward at a fixed velocity, separates from the main fluid mass, forming a region where pressure will be on the order of the pressure of saturated steam, i.e., it will be close to zero.

For the tail section of a direct wave, the first cavitation

discontinuity functions like a new free surface, except that pressure on the free surface is equal to atmospheric pressure, while it is close to zero at the cavitation discontinuity boundary. Consequently, there will be a reflection of the tail section of the wave on the first cavitation discontinuity surface. A new cavitation discontinuity may occur during the propagation process of the nascent expansion wave.

The depth h_2 of the second cavitation discontinuity surface can be found from the equation (Fig. 23)

$$\rho_m e^{-\frac{2h_1}{a_0 h}} - \left(\rho_m e^{-\frac{2h_1}{a_0 h}} + p_{ATM} + g' h_1 \right) = - (p_K + p_{ATM} + g' h_2); \quad (8.7)$$

according to (8.5), however,

$$\rho_m e^{-\frac{2h_1}{a_0 h}} + p_{ATM} + g' h_1 = p_m - p_K.$$

Therefore,

$$e^{-\frac{2h_2}{a_0 h}} = 1 - \frac{2p_K - p_{ATM} - g' h_2}{\rho_m}$$

or

$$h_2 = -\frac{a_0 h}{2} \ln \left(1 - \frac{2p_K - p_{ATM} - g' h_2}{\rho_m} \right). \quad (8.8)$$

The process of cavitation layer formation will continue as long as negative stresses in excess of p_K are formed in the water.

The depth of the i -th cavitation discontinuity is

$$h_i = -\frac{a_0 h}{2} \ln \left\{ 1 - \frac{2p_K - p_{ATM} - g' h_i}{\rho_m} \right\}, \quad (8.9)$$

while the thickness of the i -th cavitation layer is

$$\Delta h_i = h_i - h_{i-1}. \quad (8.10)$$

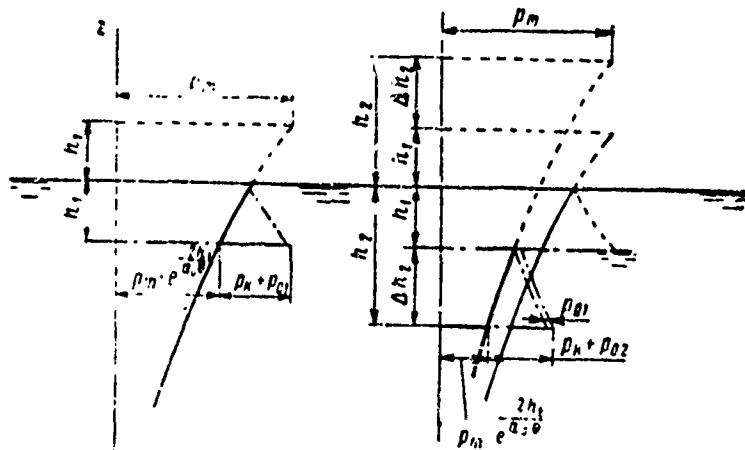


Fig. 23. Diagram of Cavitation Discontinuity Formation.

Similar arguments permit us to find the depth and thickness of the i -th cavitation layer for the oblique gradient of a plane wave onto a free surface. The difference is that pressure on the direct wave, if axes x and z are situated in the mean free path of the wave, will not be a function of $t - z/\alpha$, but of $t - (z/\alpha_0)\cos\beta - (z/\alpha_0)\sin\beta$, i.e., in place of (8.3) we will have

$$p = p_m e^{-\frac{t - \frac{x}{a_0} \cos \beta - \frac{z}{a_1} \sin \beta}{\theta}} \cdot \rho_m \left(t - \frac{x}{a_0} \cos \beta - \frac{z}{a_1} \sin \beta \right). \quad (8.11)$$

The net pressure at the moment of convergence of a reflected wave is

$$p_{1m} = p_m \left(e^{-\frac{2h}{a_1 \theta} \sin \beta} - 1 \right). \quad (8.12)$$

The depth of the i -th cavitation discontinuity will be found by solving the transcendental equation

$$h_i = -\frac{a_1 \theta}{2 \sin \beta} \ln \left(1 - \frac{\rho_m \cdot p_{1m} \cdot R_{12} \cdot h_i}{p_m} \right). \quad (8.13)$$

The derived relations permit us to form the following conclusions:

the thickness of separated cavitation layers increases with depth;

an increase in pressure on the front p_m , or a decrease in pressure of cavitation p_H induces a reduction in the thickness of cavitation layers and an increase in their number.

The change in hydrostatic pressure with depth has a considerable effect on the thickness of cavitation layers and the propagation depth of cavitation only for high values of θ , corresponding to the explosion of very large charges.

The concept of formation and development of cavitation during reflection of a shock-wave on a free surface provides only an outline of this phenomenon. Actually, cavitation discontinuity does not occur instantaneously and along the entire plane, but gradually and in the form of individual bubbles. The concentration of bubbles is at its maximum in the region of theoretical depths of cavitation discontinuity formation. As the experiments of Yu. Popov have shown, discontinuity surfaces are sometimes observed very clearly (Fig. 24).

Experiments attest that cavitation effects are absent where pressure on the wave-front is $p_m < 2.5 \text{ kg/cm}^2$. Where $p_m > 5 \text{ kg/cm}^2$, a continuous layer of cavitation bubbles is formed in the water. In this case, after the reflected-wave front arrives net pressure is close to total vacuum, subsequently rising to a magnitude which slightly exceeds initial hydrostatic pressure. This was first noted by I. B. Sinani in 1953. We can assume that the motion of the cavitation layers induces the secondary rise in pressure. Traveling at various speeds, incipient cavitation layers collide with each other. New shock-wave systems are formed as a result of collision; their propagation in the fluid brings about repeated rises in pressure.

An approximate idea of the nature of cavitation layer motion can be obtained on the basis of the law of conservation of momentum and the law of conservation of energy.

Since the initial momentum of a system of i layers is acquired

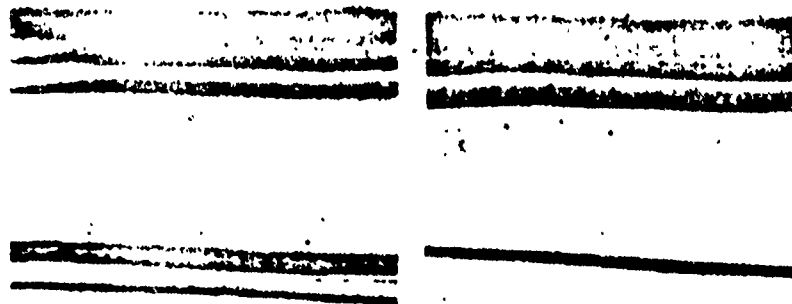


Fig. 24. Formation of Cavitation Layers in Reflection of a Shock-Wave on a Free Surface.

under the influence of direct and reflected-wave pressure which does not extend beyond the scope of these layers, it is equal to the momentum translated by the direct wave through the i -th cavitation discontinuity surface prior to the time of its formation, i.e.,

$$Q_i = \int_{-t_i}^{t_i} p \left(t + \frac{h_i}{a_0} \sin \beta \right) dt = \int_0^{2t_i} p(t) dt = J(2t_i). \quad (8.14)$$

From the moment of formation of the i -th cavitation discontinuity, only the forces of atmospheric counterpressure and gravity act upon the system of i layers.

A change in momentum is equal to the momentum of these forces:

$$Q_i - Q_i(t) = (p_{atm} + g\rho_0 h_i)(t - t_i); \quad (8.15)$$

the mean speed of layer motion is

$$u_i(t) = \frac{Q_i(t)}{\rho_0 h_i} = \frac{J(2t_i) - (p_{atm} + g\rho_0 h_i)(t - t_i)}{\rho_0 h_i}; \quad (8.16)$$

the kinetic energy of their motion is

$$T_i(t) = \frac{\rho_0 h_i}{2} [u_i(t)]^2. \quad (8.17)$$

From the law of conservation of energy it follows that this quantity must be equal to the energy of the shock-wave, the forces of counterpressure and gravity excluded. Since a wave propagates at an angle β to the free surface, the initial value of energy will be $E(2t_i)\sin\beta$. The energy of the forces of counterpressure and gravity is

$$A = (p_{\text{ср}} + g_0 h_i) [W_i(t) - W_i(t_i)], \quad (8.18)$$

where

$$W_i(t_i) = \frac{J(2t_i)}{\rho_0 u_0} \sin \beta. \quad (8.19)$$

Thus,

$$E(2t_i) \sin \beta - (p_{\text{ср}} + g_0 h_i) [W_i(t) - W_i(t_i)] = T_i(t). \quad (8.20)$$

(On the basis of (8.17)-(8.20), the following association has been established between the net travel of layers on one hand, and the momentum and shock-wave energy on the other:

$$W_i(t) = W_i(t_i) + \frac{E(2t_i) \sin \beta - \frac{1}{2} \rho_0 h_i u_i^2}{p_{\text{ср}} + g_0 h_i}. \quad (8.21)$$

Let us mention that the magnitudes of pressure momentum and energy in the shock-wave are defined using its parameters in the following manner:

$$J(2t_i) = \rho_m \theta \left(1 - e^{-\frac{2t_i}{\theta}}\right), \quad (8.22)$$

$$E(2t_i) = \frac{\rho_m^2 \theta}{2\rho_0 a_0} \left(1 - e^{-\frac{4t_i}{\theta}}\right). \quad (8.23)$$

Formulas (8.16) and (8.21) are valid for the time interval beginning with the moment of adjunction of the i -th layer to the first layer and ending with the moment of overtake of these layers by the i -th + 1 layer.

The moment in time t_1^* when the i -th + 1 layer overtakes the upper layers can be defined from the condition of equality of permutations

$$W_i(t_i^*) = W_{i+1}(t_i^*), \quad (8.24)$$

where

$$W_{i+1}(t_i^*) = W_{i+1}(t_{i+1}) + u_{0,i+1}(t_i^* - t_{i+1}) - \frac{g}{2}(t_i^* - t_{i+1})^2, \\ u_{0,i+1} = \frac{\sin \beta}{\rho_0 a_0} \left(2\rho_m e^{-\frac{2t_{i+1}}{\theta}} + \rho_k + \rho_{\text{atm}} + g\rho_0 h_{i+1} \right).$$

Condition (8.24) is transformed to a quadratic equation with respect to t_1^* , which can be solved without difficulty.

Using the established equalities, let us find the greatest displacement of points in the free surface of a fluid. Given that upon acquiring maximum permutation W_{max} , k upper layers combine. Then, in view of the fact that with W_{max} the velocity is $u_1(t) = 0$, we will find from (8.16) that

$$t_m = t_k + \frac{J(2t_k)}{\rho_{\text{atm}} + g\rho_0 h_k}. \quad (8.25)$$

According to (8.19) and (8.20), maximum displacement is

$$W_{\text{max}} = \sin \beta \left[\frac{J(2t_k)}{\rho_0 a_0} + \frac{F(2t_k)}{\rho_{\text{atm}} + g\rho_0 h_k} \right]. \quad (8.26)$$

For quantitative evaluations, we must evaluate time t_H . This can be done with the aid of the preceding relationships, if we use the condition of equality of permutations toward moment t_m of free surface points and of cavitation layer points.

Omitting the operations, let us cite only the final equation, with whose aid the quantity t_H is defined*

*Equation (8.27) has been established under the assumption that $p_m \gg p_H$

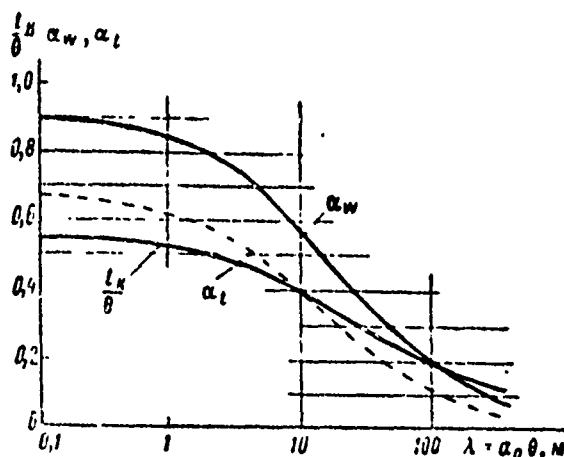


Fig. 25. t_H/θ , α_W , α_t as a function of λ .

$$\exp\left(-\frac{2t_H}{\theta}\right) - \frac{g\rho_0 a_0 \theta \left(1 - e^{-\frac{2t_H}{\theta}}\right)}{\sin^2 \beta \cdot \rho_{\text{сгн}} + g\rho_0 a_0 t_H} = 1. \quad (8.27)$$

Calculated values of t_H/θ for the case of a normal gradient ($\beta = \pi/2$) are shown in Fig. 25. The coefficients α_W and α_t are shown in the same graph as functions of $\lambda = \alpha_0 \theta$. For a normal wave gradient where $p_m \gg p_H$, these coefficients permit us to represent the solution of equations (8.25) and (8.26) in the form

$$W_{\text{max}} = \frac{p_m^2 \theta}{2\rho_0 a_0} \alpha_W(\lambda) = E_{\text{нотн}} x_W(\lambda). \quad (8.28)$$

$$t_m = p_m \theta x_t(\lambda) = J_{\text{нотн}} x_t(\lambda). \quad (8.29)$$

The magnitude of the greatest displacement of points of the free surface, neglecting cavitation effects, is

$$W'_{\text{max}} = \frac{2J_{\text{нотн}}}{\rho_1 a_0} \sin \beta. \quad (8.30)$$

We can see by comparing (8.26), (8.28), and (8.30), that considerable changes in the final relationships can introduce consideration of cavitation effects.

In conclusion, let us note that after the upper layers acquire maximum travel, they begin to move downward. This motion is described by the same formulas that describe upward motion; and it

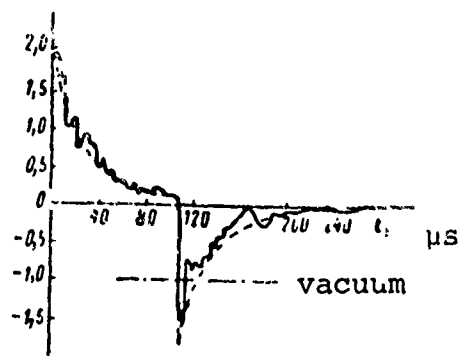


Fig. 26. Pressure Oscillogram for Reflection of Shock-Wave on Free Surface with the Absence of Cavitation.

— experiment;
 - - - - calculated, neglecting cavitation
 -.-.-.- calculated, allowing for cavitation.

continues until the upper layers encounter the surface of a great bulk of water.

The moment of collision (t_{coyA}) can be defined from the condition of equality of free surface and bulk-water-boundary permutation. With this collision, secondary compression waves are formed, propagating in opposite directions from the collision surface. The amplitude of these waves can be easily found from the condition of equality of normal components of velocities

$$u_1(t_{\text{coyA}}) + \frac{p_{\text{coyA}}}{\rho_0 u_0} \sin \beta = u_{\text{noA}}(t_{\text{coyA}}) - \frac{p_{\text{coyA}}}{\rho_0 u_0} \sin \beta,$$

whence

$$p_{\text{coyA}} = \frac{\rho_0 a_0}{2 \sin \beta} [u_{\text{noA}}(t_{\text{coyA}}) - u_1(t_{\text{coyA}})]. \quad (8.31)$$

The calculations performed show that when $p_m \gg p_H$, the highest amplitudes of compression waves formed during collision of cavitation layers with the great bulk of fluid are roughly equal to half the pressure on the wave-front

$$p_{\text{coyA}} \approx \frac{1}{2} p_m. \quad (8.32)$$

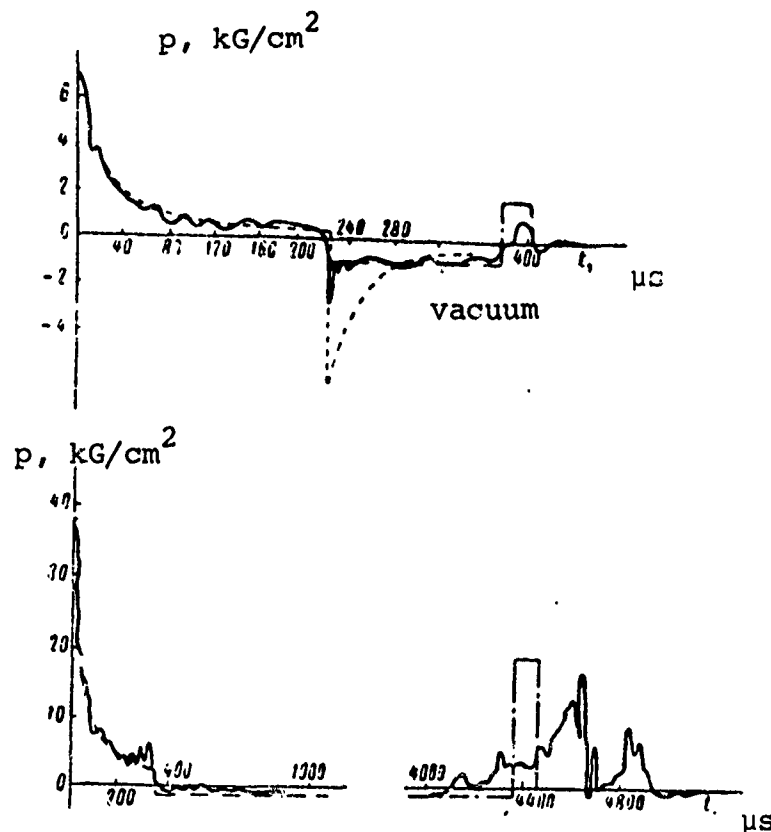


Fig. 27. Cavitation Zone Pressure Oscillogram.
(designations as in Fig. 26).

The moment of collision is

$$t_{\text{coll}} \approx \frac{1.8 p_m \theta}{p_{\text{atm}}} \quad (8.33)$$

In spite of the considerable schematization of actual processes, calculations performed with respect to the formulas cited are in satisfactory agreement with test data. This is attested by the oscillograms shown in figs. 26, 27.

A similar problem was considered by A. N. Patrashev in a slightly different formulation.

§9. Reflection of a Shock-Wave on the Bottom of a Basin
[Linear Theory].

The study of the effect of a basin bottom on pressure fields in underwater explosion is associated with theoretical difficulties. To begin with, a knowledge of the mechanical properties of the ground is required. Information of this sort is extremely limited, but it attests to the extremely wide range of acoustic resistance of ground (from 0.1 to 4.8 of water's acoustic resistance). This predetermines the varied nature of reflection.* In some cases, we must take the non-uniformity of the ground and its layered structure into consideration. The topography of the basin bottom is important, especially if it does not yield to mathematical evaluation.

Consequently, it is now more feasible to consider the qualitative than the quantitative aspect of the phenomenon.

For approximate analysis, let us make the following assumptions. The surface of the bottom will be considered a plane interface of two media. The ground will be considered an isotropic elastic half-space.

As is well known, two types of elastic waves can propagate in unbounded isotropic solid bodies: longitudinal waves formed as a result of volumetric deformation, and transverse waves determined by shear deformations. These waves are sometimes called expansion waves and distortion waves, respectively. The rate of propagation of longitudinal c and transverse b waves is expressed by the relations

$$c = \sqrt{\frac{\lambda + \frac{2}{3}\mu}{\rho}}, \quad (9.1)$$

$$b = \sqrt{\frac{\mu}{\rho}}, \quad (9.2)$$

where λ and μ - elastic constants, often called Lamé constants, which

* This range of acoustic ground resistances is satisfied by values of the reflection factor for the straight wave gradient from -0.8 to +0.7.

fully define the properties of an isotropic body.*

In addition to these two wave systems, another type of wave can be formed as a result of their interaction with the interface of two media - the so-called Rayleigh surface wave. The amplitude of Rayleigh waves attenuates with depth with respect to an exponential law. Consequently, Rayleigh waves seem to propagate in sizes and therefore, attenuate more slowly with distance. The buildup of compression in seismic waves does not occur abruptly, but gradually, in contrast to shock-waves. This is attributed to the fact that compressibility increases as pressure increases over a wide range of pressures in elastic-plastic media.

The following qualitative description may be given for the wave picture in a fluid during single reflection on the bottom of a basin. Given that an explosion occurs at some point O ($z = -H_1$) in the system of coordinates given in Fig. 28. At some moment in time, a direct wave reaches the bottom of the basin.

Its gradient is

$$\beta = \arccos \frac{L}{\sqrt{L^2 + H_1^2}}. \quad (9.3)$$

The rate of wave travel along the bottom surface is

$$N_A = \frac{a_0}{\cos \beta}. \quad (9.4)$$

At large β , the rate N_A at first exceeds the propagation rate of longitudinal c and transverse b waves on the ground. Disturbances in the fluid will be characterized by direct and reflected waves. Reflection will be regular. At some value of the angle $\beta = \beta_0$, the speed of N_A and c will be identical, i.e., the following relation

* The Lamé constant μ is equal to the shear modulus G . The association between the modulus of longitudinal elasticity E , the constant λ , and the Poisson bracket ν is expressed by the relation

$$\lambda = \frac{E\nu}{(1 + \nu)(1 - 2\nu)}$$

are the spherical surface envelopes of elementary disturbances which accordingly determine the head and lateral waves (Fig. 28).

A Rayleigh wave propagates along the ground-water interface. The disturbance it generates is customarily called a ground wave. Moreover, in irregular reflection zones near the bottom, a region of raised pressure is formed ahead of the shock-wave front. This region is formed as a result of superposition of wave disturbances induced by forward-emergent longitudinal and transverse waves. This region is usually called the "forewave".

Thus, another head, lateral, ground, and forewave is formed (in addition to the reflected wave) when the shock-wave drops to the bottom of a basin. Since these systems are induced by the propagation of wave disturbances on the ground, they are often called waves of seismic origin.

A model oscillogram of seismic-origin waves is shown in Fig. 29. The head, lateral, direct, and forewaves are clearly visible. Depending on the distance to the explosion epicenter, the head and lateral waves are either separated from each other by a fixed time interval, or they arrive at some point as some net wave disturbance.

A comparison of direct and reflected-wave amplitudes with seismic-origin wave amplitudes permits us to conclude that waves of seismic origin cannot be considered in practical calculations. The only exception is the forewave - a region of smooth pressure change ahead of the front. The highest pressures are formed in the forewave in the case of a mean-velocity bottom ($c > \alpha_0 > b$): the primary energy of wave disturbances on the ground is concentrated at the direct-wave front. In other cases, forewave amplitudes are small and can be disregarded.

From the standpoint of practical application, the reflected wave offers the greatest interest. In some cases, solving the problem in a linear formulation is sufficient to describe it. Let us

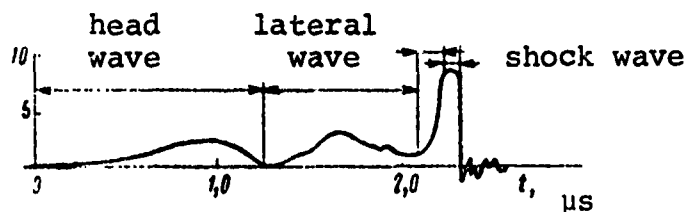


Fig. 29. Typical Oscillogram of Wave of Seismic Origin.

state the problem in brief.

In the upper half-space (ideal fluid) on a spherical surface having a radius R_0 , we are given a change in pressure

$$p = p_0 e^{-\frac{t}{\theta}}. \quad (9.9)$$

The association between pressure and the velocity of particles in this half-space is expressed with the aid of the potential function ϕ :

$$p = -\rho_0 \frac{\partial \phi}{\partial t}, \quad (9.10)$$

$$\bar{u} = \text{grad } \phi. \quad (9.11)$$

The field of deformations and stresses in the lower half-space (elastic medium) is defined by the system of equations of the theory of elasticity

$$\bar{u} = \text{grad } \phi^* + \text{rot } \bar{\psi}, \quad (9.12)$$

$$\frac{\partial^2 \phi^*}{\partial t^2} = \left(\frac{\lambda + 2\mu}{\rho} \right) \Delta \phi^*, \quad (9.13)$$

$$\frac{\partial^2 \bar{\psi}}{\partial t^2} = \frac{\mu}{\rho} \Delta \bar{\psi}, \quad (9.14)$$

where \bar{u} - the velocity vector of elastic medium deformation;
 ϕ^* , $\bar{\psi}$ - scalar and vectorial displacement potentials.

On the plane interface of an ideal fluid and an elastic medium the condition of rigid contact is satisfied (the equality of normal components of particle velocities and pressure magnitudes).

An analysis of this system of equations was performed by Ye. I. Shemyakin [24] using the method of incomplete separation of variables. Without stopping to state Shemyakin's solution, let us cite only the final results which he obtained.

If we represent pressure in the direct wave in the form

$$p = \frac{14700}{r_{np}^{1.13}} e^{-\frac{t-t_{np}}{\theta}}, \quad (9.15)$$

where

$$\bar{r}_{np} = \frac{1}{R_0} \sqrt{L^2 + (H_1 - h_1)^2}, \quad (9.16)$$

$$t_{np} = \frac{1}{a_0} \sqrt{L^2 + (H_1 - h_1)^2}. \quad (9.17)$$

H_1 and h_1 - distance from the bottom to the charge center and measurement point, respectively, then for pressure in the reflected wave we will derive

$$p_{orp} = k_{orp}(\beta) \frac{11700}{r_{orp}^{1.13}} e^{-\frac{t-t_{orp}}{\theta}}. \quad (9.18)$$

Here

$$\bar{r}_{orp} = \frac{1}{R_0} \sqrt{L^2 + (H_1 + h_1)^2}, \quad (9.19)$$

$$t_{orp} = \frac{1}{a_0} \sqrt{L^2 + (H_1 + h_1)^2}, \quad (9.20)$$

$$\beta = \text{arctg} \frac{H_1 + h_1}{L}. \quad (9.21)$$

The coefficient $k_{orp}(\beta)$ is only a function of the acoustic properties of the ground and the gradient. For the most typical grounds, this permits us to once and for all plot angle diagrams of $k_{orp}(\beta)$

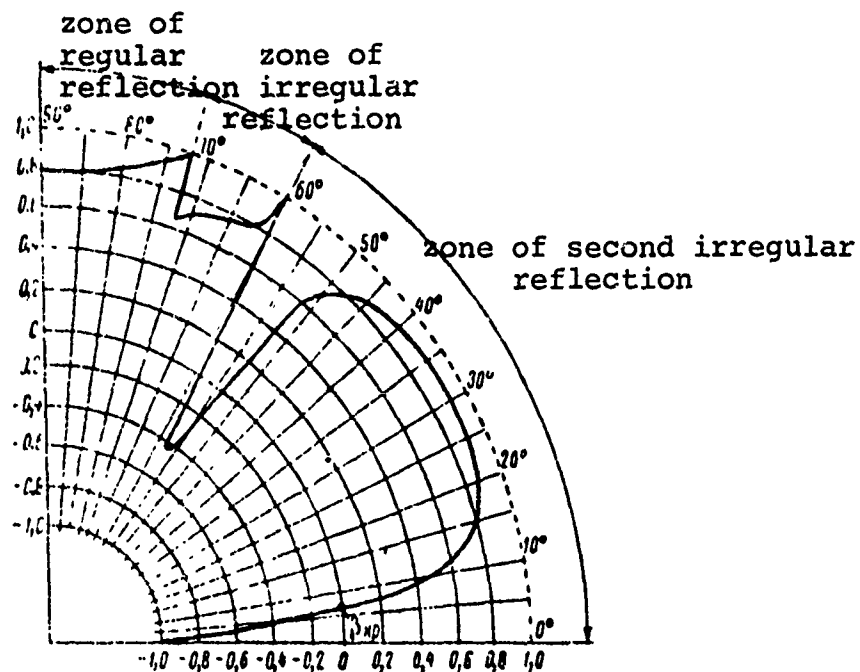


Fig. 30. Angle Diagram for Rocky Ground.

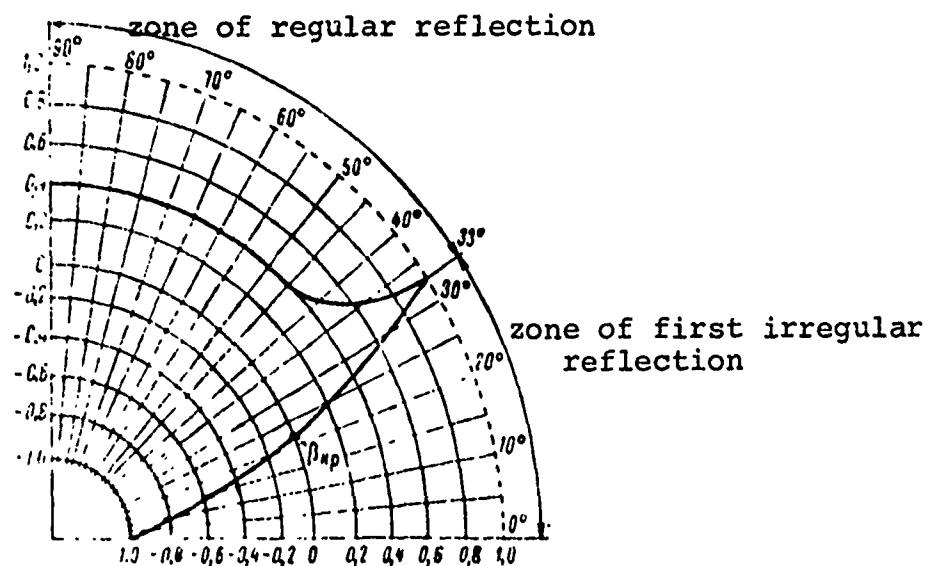


Fig. 31. Angle Diagram for Sandy Ground.

which are suited to practical calculations. Angle diagrams for rocky and sandy bottoms are shown in Figs. 30 and 31.

Formulas (9.15)-(9.21) rather accurately describe the pressure field only at large gradients. At small angles, deviations in the velocities of the direct and reflected waves from the speed of sound become substantial. In some cases, a confluence of wave fronts is possible as the Mach wave is formed.

On the basis of linear theory (cf. Figs. 30, 31), starting at fixed gradients $\beta < \beta_{kp}$ the coefficient of reflection becomes negative, and with reflection on the bottom expansion waves are formed. This is attributed to the fact that in this range of gradients ($0 < \beta < \beta_{kp}$), excess pressure in the direct wave induces motion in the ground downward away from the interface, at velocities exceeding the normal (for this boundary) components of particle velocity in the direct wave. Experimental study of the negative reflection region has shown that expansion waves formed during reflection on the bottom have lower amplitude and duration in comparison to expansion waves during reflection on a free surface. A secondary rise in pressure occurs following them. Because of this effect, the effect-time of the positive phase and the integral characteristics of an underwater shock-wave barely change under the influence of an expansion wave from the basin bottom (in the absence of free surface effect). The expansion wave only must be taken into account when evaluating pressure on a wave-front and in its close proximity. This problem, of course, cannot be considered within the framework of linear theory.

§10. The Influence of Nonlinear Effects on the Parameters of A Wave Reflected on a Basin Bottom. Pressure Fields during Underwater Explosion in Low Water.

From the standpoint of practical application, of all the nonlinear effects accompanying the reflection of an underwater shock-wave on the bottom of a basin, the evaluation of expansion wave influence

is of the greatest interest. The study of expansion waves during explosions in low water is particularly essential: because of the proximity of the charge to the bottom, the zone of positive reflections will only occupy a small vicinity around the epicenter. The influence of the free surface substantially limits positive pressure phase effect-time through the entire depth of the fluid layer. Therefore, in a shallow water area at some distance from the epicenter, there will be no secondary pressure rises associated with the effect of the basin bottom. In these cases, we only have to consider the weakening effect of both boundary surfaces.

The problem of interaction between the direct wave and an expansion wave reflected on the basin bottom has much in common with the previously considered problems of wave reflection on a free surface (see §7). The difference is that during the reflection of an elementary pressure-reduction wave on the bottom (expansion wave characteristics), interfaces are not formed at every point during the convergence of a direct-wave front, but only at a fixed distance which is a function of the angle of incidence. Moreover, the maximum amplitude of the expansion wave in this case is a function of the coefficient of reflection and consequently, it cannot amount to the amplitude in the direct-wave front.

The time of arrival of the characteristic of given amplitude at a point, with respect to the set of conditions mentioned above, increases in comparison with the case of reflection on a free surface. Let us find the boundary of the region where the direct-wave front and zero amplitude characteristic wave simultaneously arrive.

By analogy with (7.40), this boundary apparently will be defined by the equation

$$L_{kp} = \left\{ \frac{h_1 \xi_1 (H_1 - h_1)^2 (1 - 0.5\xi_1)^{1.13}}{2.75\xi_1^2 (1 - \xi_1)} \right\}^{1.15}, \quad (10.1)$$

where

$$\xi_1 = \frac{x}{L}. \quad (10.2)$$

x - horizontal distance from the point of observation to a point on the bottom whence the zero amplitude characteristic wave first arrives.

If expansion waves are formed with the drop of a direct wave at any angle, the quantity ξ_1 would be defined by an equation which is identical to (7.41) (based on the Fermat principle)

$$\xi_1(1-\xi_1)\left(\frac{2}{h_1} - \frac{0.565}{1-0.5\xi_1}\right) = 2-3\xi_1. \quad (10.3)$$

However, expansion waves are formed during the reflection of the direct wave on the bottom only at angles of incidence of $\beta < \beta_{kp}$. Consequently, the parameter ξ_1 cannot exceed the quantity ξ_0 :

$$\xi_0 = \frac{\bar{x}_0}{L} = \frac{L - \frac{\bar{H}_1}{\lg \beta_{kp}}}{L} = 1 - \frac{\bar{H}_1}{L \lg \beta_{kp}}. \quad (10.4)$$

If the inequality $\xi_1 < \xi_0$ is satisfied, formulas (10.1) and (10.3) will be valid. If however, $\xi_1 > \xi_0$, we ought to assume that $\xi_1 = \xi_0$ in formula (10.1), since the zero amplitude characteristic will reach the direct-wave front namely from point ξ_0 . According to (10.1) and (10.4),

$$\bar{L}_{kp} = \left[\frac{\bar{h}_1 \left(1 - \frac{H_1}{L \lg \beta_{kp}}\right) (\bar{H}_1 - \bar{h}_1)^2 \left(0.5 + \frac{\bar{H}_1}{2L \lg \beta_{kp}}\right)^{1.13}}{2.75 \left(1 - \frac{H_1}{L \lg \beta_{kp}}\right)^2 \frac{\bar{H}_1}{L \lg \beta_{kp}}} \right]^{1.13} \quad (10.5)$$

or solving for \bar{h}_1 ,

$$\bar{h}_{1kp} = \frac{1-\zeta}{\zeta} \left[\sqrt{\frac{6.02\bar{L}^{0.87}}{(1+\zeta)^{1.13}}} - H_1 \right]. \quad (10.6)$$

where

$$\zeta = \frac{\bar{H}_1}{L \lg \beta_{kp}}. \quad (10.7)$$

For measurement points situated on the bottom of a basin, the influence of expansion wave characteristics only occurs for distances

$$\bar{L} > \frac{\bar{H}_1}{\operatorname{tg} \beta_{\text{kp}}}.$$

On the other hand, this distance cannot be less than critical distance

$$\bar{L} \geq \bar{L}_{\text{kp}, \bar{h}_1=0},$$

but as has been shown [cf. (7.42)], where $\bar{h}_1 = 0$

$$\bar{L}_{\text{kp}} = 0.31 \bar{H}_1^{2.3}. \quad (10.8)$$

Thus, if

$$\frac{\bar{H}_1}{\operatorname{tg} \beta_{\text{kp}}} < 0.31 \bar{H}_1^{2.3}$$

or

$$\bar{H}_1 > \left(\frac{3.23}{\operatorname{tg} \beta_{\text{kp}}} \right)^{0.77}. \quad (10.9)$$

then the critical distance for points situated on the bottom is defined by formulas derived for the free surface.

If

$$\frac{\bar{H}_1}{\operatorname{tg} \beta_{\text{kp}}} > 0.31 \bar{H}_1^{2.3}, \quad \bar{H}_1 < \left(\frac{3.23}{\operatorname{tg} \beta_{\text{kp}}} \right)^{0.77}. \quad (10.10)$$

then the critical distance is defined by the position of the point of zero reflection. In the first case, we can use a formula analogous to (7.44) in place of (10.1)

$$\bar{L}_{\text{kp}} = \bar{H}_1^{1.3} (0.31 \bar{H}_1 + 1.3 \bar{h}_1); \quad (10.11)$$

but in the second case [when $\bar{H}_1 < \left(\frac{3.23}{\text{tg} \beta_{\text{np}}}\right)^{0.77}$], we use the relation

$$L_{\text{np}} = \frac{\bar{H}_1}{\text{tg} \beta_{\text{np}}} \left[1 + \frac{\bar{h}_1}{2.06 \left(\frac{\bar{H}_1}{\text{tg} \beta_{\text{np}}} \right)^{0.435} - \bar{H}_1} \right], \quad (10.12)$$

which is a rough approximation of (10.5)

Moving now to an evaluation of pressure on the front of the direct wave, let us use the method developed in §7.

If characteristic waves of any amplitude are formed in a region of negative reflection, maximum pressure is determined by relation (7.60). Since the amplitude of an expansion wave cannot be greater than $p_m k_{\text{отр}}(\beta)^*$, pressure on the front cannot be less than $p_m(1 + k_{\text{отр}})$.

Thus, for points situated near the basin bottom ($h_1 = 0$), the degree of weakening in maximum pressure on the front is defined by the larger of the equations [cf. (7.59)]

$$\alpha_1^0 = \left\{ \frac{1}{4} \left(1 + \frac{\bar{H}_1}{1.66 L^{0.435}} \right)^2 \right. \\ \left. 1 + k_{\text{отр}}(\beta_{\text{np}}) \right\} \quad (10.13)$$

where β_{np} - angle of incidence of direct wave.

For the range $0 \leq \bar{h}_1 \leq \bar{h}_{\text{np}}$, the approximate relation can be used

$$\alpha_1 = \alpha_1^0 \sqrt[3]{1 + \left[\left(\frac{1}{\alpha_1^0} \right)^3 - 1 \right] \frac{\bar{h}_1}{\bar{h}_{\text{np}}}}, \quad (10.14)$$

which satisfies both the conditions at the basin bottom (where $\bar{h}_1 = 0$, $\alpha_1 = \alpha_1^0$) and at the boundary of the zone of influence (where $\bar{h}_1 = \bar{h}_{\text{np}}$, $\alpha_1 = 1$) and the previously-formulated relation of p_m as a

function of \bar{h} [cf. formula (7.60)].

Thus, in the zone where the basin bottom weakens the parameters of the front, maximum pressure can be defined by the formula

$$p_m = \alpha_1 p_0, \quad (10.15)$$

where the coefficient α_1 is calculated according to (10.14) and (10.13).

Let us now consider the combined effect of a free fluid surface and the basin bottom on the pressure fields during underwater explosion. This problem is of particular importance in evaluating the explosive effect in low water. Let us note, above all, that in the presence of two boundary surfaces the repeated reflection of wave systems occurs; consequently, the quantity of wave disturbances of different physical nature increases in geometric progression. The nonlinear interaction of these systems, in a general statement of the problem, causes insurmountable difficulties. However, as experience shows, it is sufficient for practical applications if we limit ourselves to the study of the first reflections.

If we neglect waves of seismic origin, we can point out five typical zones during the reflection of a shock-wave on a high-velocity bottom ($c > b > \alpha_0$) and on a free surface where $\bar{H}_1 < \left(\frac{3.23}{\text{tg} \beta_{\text{HP}}}\right)^{0.77}$ (Fig. 32). The boundaries of these zones can be roughly defined by relations (7.48), (7.44), and (10.11) or (10.12). Zones I and II correspond to the region of positive reflection on the bottom. Zones IV and V - correspond to regions of negative reflection. In zone I, the influence of reflected waves can be evaluated in the acoustic (linear) approximation. In zone II, the influence of nonlinear reflection effects on both boundary surfaces is revealed in distortion of the tail section of the pressure contour. In zones III, IV, and V, the weakening effect of the free surface, basin bottom, and both boundary surfaces, respectively, encompasses the entire pressure contour, including the shock-wave front. Pressure on the direct-wave front in zones I and II is evaluated as in an infinite medium [acc-

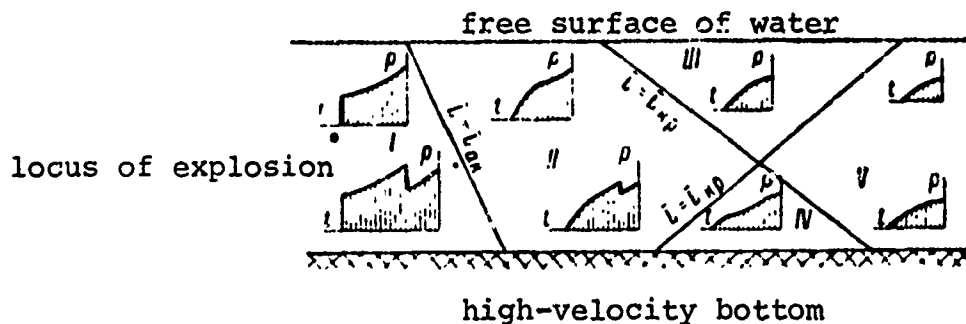


Fig. 32. Zones of Nonlinear Influence of Free Surface and High-Velocity Bottom on the Parameters of a Shock-wave.

ording to formula (5.48)]. In zones III and IV, pressure is defined by relations (7.60) and (10.15), respectively. In zone V, the wave front is weakened by the expansion waves of both boundary surfaces. Considering (7.60) and (10.15), pressure on the front is

$$p_m \approx p_0 \frac{1}{2} k \alpha_1, \quad (10.16)$$

where k is found according to (7.56) and α_1 - with the aid of (10.14).

It is somewhat more complicated to plot pressure contours and define the effect-time of the positive phase. Evaluations at this point become even more approximate in nature. We can, nevertheless, formulate several recommendations.

In zones I, II, and III, the free surface effect predominates. Consequently, we can use the corresponding relations [formulas (7.61)-(7.64)] for approximate evaluations of the positive phase effect-time. In zones IV and V, effect-time is defined by the influence of the expansion wave not only on the free surface, but also on the basin bottom. However, the absence of high amplitudes in the expansion wave formed during reflection on the bottom renders them incapable of totally reducing the pressure in the direct wave. Therefore, the positive phase effect-time in these zones will be mainly defined by the free surface effect. A reduction in pressure due to basin bottom influence naturally reduces the positive pressure phase effect-time of the shock-wave in comparison to the magnitude which

would be assumed if the influence of only free surface was taken into account.

This effect may be partially defined if we consider that the positive phase effect-time is reduced roughly in proportion to $\sqrt{\alpha_1}$.*

$$t_1 = t_{ak} \beta \sqrt{\alpha_1} \quad (10.17)$$

where t_{ak} is defined according to formula (7.4), β - according to formula (7.64), and α_1 - according to formula (10.14).

The shape of the pressure-time contour, in the event of combined influence of a free surface and the basin bottom, differs slightly from the similar curve derived as a result of only the free surface effect. Therefore, pressure as a function of time can be calculated with the aid of a relation similar to (7.72):

$$p(t) = p_{ak} \sqrt[3]{k_2} \left[1 - \left(\frac{t}{t_{ak} \beta \sqrt{\alpha_1}} \right)^n \right] \quad (10.18)$$

where the exponent n can be approximately assumed to be equal to $n = 1.5$.

The integral characteristics of a wave are evaluated according to formulas which are similar to (7.73) and (7.74).

This scheme did not take cavitation regions in a fluid into account and, as calculations have shown, is valid if the depth of the water area is not too small (no less than 4 charge radii). With shallow depths, the quasi-linear evaluation method used for hydrodynamic fields becomes unacceptable. The rather intense head wave near the epicenter, reflecting on the free surface, creates a cavitation region over the entire fluid layer. This region is impermeable to the remaining wave systems. At the same time, as the depth of the water area increases, the effect-time at the basin bottom will increase. It becomes necessary to take secondary pressure rise, which follows from the bottom after the expansion phase, into consid-

*cf. footnote p. 128

eration.

Where $\bar{H}_1 > \left(\frac{3.23}{\text{tg}\beta_{\text{HP}}}\right)^{0.77}$, the negative reflection zone does not coincide with zones IV and V and will encompass part of zone II and III. Consequently, other additional typical zones will be formed.

Thus, the considered case of underwater explosion in low water is a widespread, but partial case, even with a high-velocity bottom.

A medium-velocity ground-surface ($c > a_0 > b$) has several specific distinctive features. A substantial rise in pressure is observed in a fixed range of distances because of forewave of considerable amplitude. At present, it is difficult to produce any kind of quantitative evaluations.

The physical picture of reflection changes if we change our reference to low-velocity ground-surfaces. We can consider the bottom as the second free fluid surface. In this case, the problem of exploding a charge at half-depth of the water area is equivalent to exploding a charge of half the weight on an absolutely rigid bottom in a basin which is half as deep.

A solution of this problem, in a rather rigorous formulation, was obtained by A. G. Ryabinin and B. A. Lugovtsev using short-wave theory methods [12]. The utilization of their findings for practical purposes, however, is difficult. The approximate solution of the same problem obtained by Ryabinin produces more suitable results.

Following the previously-assumed scheme, let us note that we

*Change in duration of the positive pressure phase in proportion to $\sqrt{a_1}$ can be clearly demonstrated for point lying only on the free surface. More precise calculation leads to considerable decreases in effect-time at points of observation situated near the basin bottom.

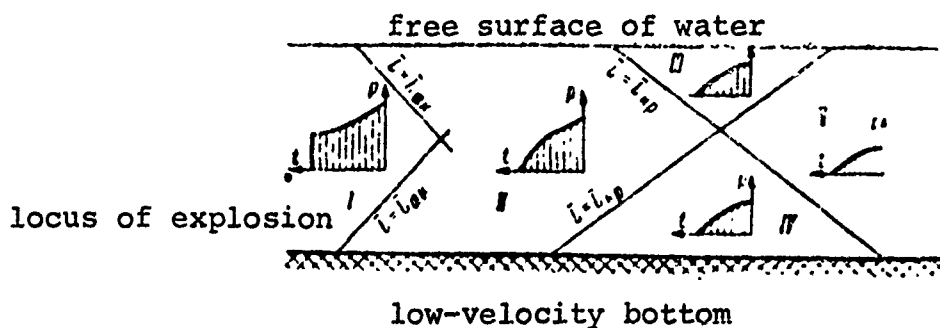


Fig. 33. Zones of Nonlinear Influence of Free Surface and Low-Velocity Bottom on the Parameters of a Shock-wave.

can point out five typical zones of reflection for the case of a low-velocity bottom (Fig. 33). The boundaries of these zones can be roughly defined by the relations (7.48) and (7.44):

$$L_{\text{sk}} = \begin{cases} 0,1 \bar{H}^{2,3} \left(1 + 0,5 \frac{h}{H}\right) \\ 0,1 \bar{H}_1^{2,3} \left(1 + 0,5 \frac{h_1}{H_1}\right), \end{cases} \quad (10.19)$$

$$L_{\text{sp}} = \begin{cases} 0,31 \bar{H}^{2,3} \left(1 + 4,2 \frac{h}{H}\right) \\ 0,31 \bar{H}_1^{2,3} \left(1 + 4,2 \frac{h_1}{H_1}\right). \end{cases} \quad (10.20)$$

Regular reflection of the shock-wave on the free surface and basin bottom occurs in zones I and II. In zones III, IV, and V, the reflection is irregular. Pressure on the front in zones I and II is the same as in an infinite medium. In zones III and IV, pressure is defined with allowance for weakening by one of the boundary surfaces.

$$p_m = \begin{cases} \int_1^3 k p_0, \\ \int_1^3 k_1 p_0, \end{cases} \quad (10.21)$$

where k is found according to formula (7.56), k_1 - likewise according to (7.56), but replacing \bar{h} and \bar{H} by \bar{h}_1 and \bar{H}_1 .

In zone V, maximum pressure is defined by the relation

$$p_m = \int_1^3 k k_1 p_0. \quad (10.22)$$

The positive pressure phase effect-time is equal to the smallest value calculated according to the formulas

$$t = \begin{cases} t_{\text{ca n}} \\ t_{\text{zho}} \end{cases} \quad (10.23)$$

where

$$t_{\text{ca n}} = \begin{cases} t_{\text{ca n}} \\ \beta_1 t_{\text{ca n}} \\ \beta_1 \sqrt{k} t_{\text{ca n}} \end{cases} \quad \begin{array}{l} \text{where } \bar{L} < \bar{L}_{\text{ca n}} \\ \text{where } \bar{L}_{\text{ca n}} < \bar{L} < \bar{L}_{\text{kp}} \\ \text{where } \bar{L} > \bar{L}_{\text{kp}} \end{array} \quad (10.24)$$

$$t_{\text{zho}} = \begin{cases} t_{\text{zho}} \\ \beta_1 t_{\text{zho}} \\ \beta_1 \sqrt{k} t_{\text{zho}} \end{cases} \quad \begin{array}{l} \text{where } \bar{L} < \bar{L}_{\text{zho}} \\ \text{where } \bar{L}_{\text{zho}} < \bar{L} < \bar{L}_{\text{kp}} \\ \text{where } \bar{L} > \bar{L}_{\text{kp}} \end{array} \quad (10.25)$$

$$t_{\text{ca n}} = \frac{1}{a_0} \left| \sqrt{L^2 + (H + h)^2} - \sqrt{L^2 + (H - h)^2} \right|, \quad (10.26)$$

$$t_{\text{zho}} = \frac{1}{a_0} \left| \sqrt{L^2 + (H_1 + h_1)^2} - \sqrt{L^2 + (H_1 - h_1)^2} \right|, \quad (10.27)$$

β - defined according to formula (7.64); β_1 - likewise according to (7.64), but substituting \bar{h}_1 and \bar{H}_1 for \bar{h} and \bar{H} .

The calculation of effect-time according to formulas (10.24) and (10.25) in zones II, III, IV, and V produces some exaggeration of this quantity for observation points situated in the middle of the basin, since it does not take into full consideration the nonlinear nature of the reciprocal influence of the characteristics of both expansion waves. The remaining evaluations can be given approximately with the aid of the corresponding relations in §7, allowing for the cited relationships.

* * * * *

CHAPTER II

DIFFRACTION PROBLEMS OF THE THEORY OF UNDERWATER EXPLOSION

§11. The Concept of Diffraction Problems. General Research Methods.

The simple boundary problems of the theory of underwater explosion which were considered in the preceding chapter assumed the infinity of interfaces of two media. This assumption cannot, of course, be considered valid when a shock-wave encounters an obstacle of finite dimensions. In this case, an obstacle is enveloped by a shock-wave in addition to the reflection and refraction of waves. This process is called diffraction.

The study of diffraction phenomena is of great practical value, since we cannot discuss the load formed on the obstacle upon the impact of a shock wave, the pressure fields in the fluid near obstacles, the dynamic calculation of structural strength, etc., without evaluating the effect of diffraction.

The diffraction field is a function of both the direct wave parameters and the dimensions and shape of the obstacle. The diffraction field is nonstationary, even when the wave is stationary. The wave at first encompasses only a part of the body surface. In proportion to the flow of the wave, the disturbance propagates into greater and greater volumes, interacting with the direct and reflected waves.

If this interaction is nonlinear and the direct wave is nonstationary, incipient mathematical problems become insurmountable. As a rule, however, a practical necessity for evaluating external forces during underwater explosion arises at distances which are typified by a range of pressures on the order of hundreds of atmospheres or less. We can utilize the acoustic approximation in this connection. Moreover, in many cases the curvature of a wave-front surface can

likewise be disregarded. The solution of the problem of external forces amounts to the study of the linear interaction of a plane wave with obstacles of various shapes. But the problem remains extremely complicated, even in this simplified formulation; especially for diffraction around elastic bodies. In this last case, a system of refracted longitudinal and transverse waves is formed, in addition to the reflected and diffracted waves. When each of these wave systems reaches the boundary surfaces, it creates new reflected and refracted waves whose number increases in a geometric progression. Thus, the only means accessible to research is the evaluation of diffraction fields, neglecting the wave nature of disturbance propagation in the obstacle material. The loads derived under this assumption are customarily called first-class hydrodynamic forces. The effect of obstacle compliance, as well as several additional considerations on the admissibility of formulated hypotheses will be examined subsequently.

Turning now to a qualitative description of the diffraction process, let us employ the Huygens principle: every point on a wave or surface with which a wave interacts can be considered an elementary source of wave disturbances. By using this concept we can easily graph the fronts of reflected and diffracted waves, and sometimes, even contemplate general means for solving the problem.

Given that a spherical wave is propagating from a point source O (Fig. 34), encountering some obstacle D in its path which is assumed to be absolutely rigid. If the direct-wave front has already traveled some distance from the initial surface of encounter with the obstacle, the position of reflected and diffracted wave fronts (line CC) can be found easily with the aid of the Huygens principle. It follows from the law of conservation of matter that the change in fluid density in a space limited by a spherical front BB, in the absence of an obstacle, will be equal to the change in density in the same space, minus the portion occupied by the obstacle (dotted line in the figure). In the acoustic approximation, the change in density is proportional to the change in pressure. Hence it follows that with the introduction of an obstacle, the decrease in the

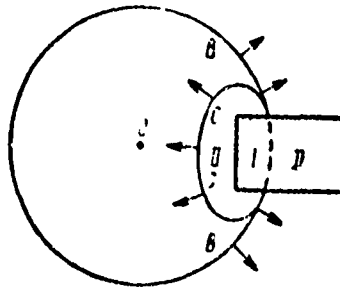


Fig. 34. Diffraction of a Spherical Wave Around a Solid Body.

volume of the field is neutralized by a rise in pressure in the same portion of the field where the reflected and diffracted waves are formed.

On this basis we can generally assert that if a zone having heightened pressure (as compared to pressure in a freely propagating wave) is formed in a field, the formation of a reduced-pressure zone is certain.

This fact can be expressed mathematically by the relation

$$\int_{V_1} \Delta p_1 dV_1 = \int_{V_2} \Delta p_2 dV_2, \quad (11.1)$$

where Δp_1 and Δp_2 - pressure increments in regions V_1 and V_2 in comparison to pressure in a freely propagating wave.

In some cases, the regions V_1 and V_2 and the distribution of pressure within them are symmetrical. Equation (11.1) may then be applied to any pair of symmetrically-arranged volume parameters, for which

$$\Delta p_1 = \Delta p_2. \quad (11.2)$$

It is often convenient to interpret symmetrical cases as the result of the isochronous presence of a source and an equally-intense runoff. Let us illustrate. Given a plane wave, propagating parallel to a plane rigid screen having a small opening at point O (Fig. 35).

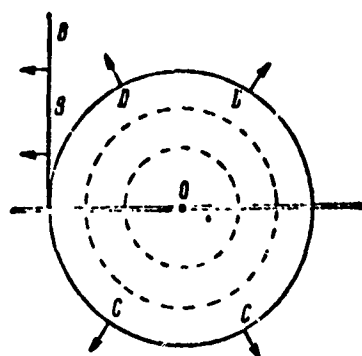


Fig. 35. Diffraction of Plane Wave Near Opening in Rigid Wall.

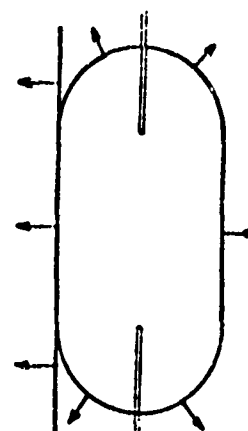


Fig. 36. Diffraction of Plane Wave Near Opening of Arbitrary Shape in Rigid Wall.

Then, a diffraction wave having its center at point O and front CC is formed on the other side of the screen. Pressure drops accordingly on this side of the screen, which can be viewed as the result of a negative source of the same intensity forming at point O . Thus, the opening O is a source for the lower half-space and a runoff for the upper half-space. The distribution of pressure in regions DDO and CCO will be symmetrical at some arbitrary moment in time.

This is valid for the more general case. Given a plane wave propagating from left to right which encounters a plane rigid screen having an opening of arbitrary shape and arbitrary dimensions (Fig. 36). To the right of the screen is formed a "transient" diffraction wave, while to the left, a plane front of a reflected wave and a reflected diffraction wave are formed, which are symmetrical to the "transient" wave. It is easily verified that the symmetry of the transient, reflected, and diffraction waves is maintained with the limiting passage to right up to total elimination of the screen.

The usefulness of utilizing the Huygens principle can be illustrated as well by an example of a plane wave dropping at an angle θ onto an infinite immobile rigid wedge having an apex angle of 2α (Fig. 37). As soon as the direct wave touches the rib (point O), it appears to be sliced by it. One portion of the wave moves ahead (direct wave

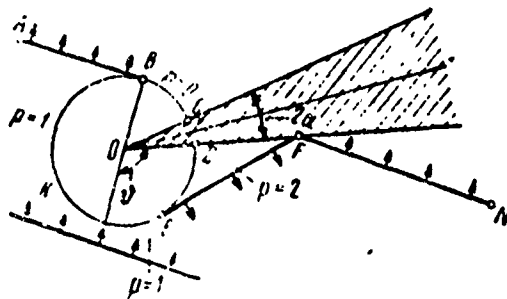


Fig. 37. Diffraction of Plane Wave Around Rigid Wedge.

AB) and the other portion of the wave is reflected on the edge (reflected wave EF). A region of diffraction is formed. Point O becomes a source of new disturbances associated with the flow of the direct wave into the shadow zone of the obstacle. The front of these disturbances is easily plotted according to the Huygens principle, and is a circle with its center at point O. This picture, while not changing in quality over the course of time, increases the scale. The diffraction wave propagating through the region of the direct and reflected waves alters the hydrodynamic field.

The chief method of quantitative evaluations of diffraction phenomena under the assumptions formulated above is the method of linear superposition of wave fields. This method, naturally, assumes the reverse effect, too - the expansion of any wave disturbance into its basic components, the choice of which is defined only by research convenience. The most widespread expansion is that where sine curves and cosine curves, or one-valued discontinuity functions form the basic components (Heaviside function, Dirac δ -function).

In the first case, expansion is realized with the aid of the Fourier integral. For a direct wave, for example, the time rate of pressure change can be represented in the form

$$p(t) = \frac{1}{2\pi} \int_{-\infty}^{\infty} s(\omega) e^{i\omega t} d\omega, \quad (11.3)$$

$$s(\omega) = \int_{-\infty}^{\infty} p(t) e^{-i\omega t} dt. \quad (11.4)$$

The Fourier integral is given here in complex form and is a nonperiodic function in the form of the sum of an infinite number of variations which are similar in frequency and infinitely-small in amplitude [the interval between components is $d\omega$ and the amplitude of each component is $s(\omega) d\omega$].

Expansion into unit functions is realized with the aid of the Duhamel integral.* Let us note that the unit function $\sigma_0(t - \tau_H)$ is, by definition, characterized by the equation

$$\sigma_0(t - \tau) = \begin{cases} 0 & \text{where } t < \tau \\ 1 & \text{where } t > \tau \end{cases} \quad (11.5)$$

This definition yields a method for expanding the given function into unit functions; this expansion is shown in Fig. 38.

The analytic expression for the broken line which corresponds to the given curve has the form

$$\begin{aligned} f(t) &= f(0) \sigma_0(t) + [f(\Delta t) - f(0)] \sigma_0(t - \Delta t) + \\ &+ [f(2\Delta t) - f(\Delta t)] \sigma_0(t - 2\Delta t) + \dots = \\ &= \sum_{k\Delta t=0}^{k\Delta t=t} [f(k\Delta t) - f((k-1)\Delta t)] \sigma_0(t - k\Delta t). \end{aligned} \quad (11.6)$$

Expression (11.6) assumes a limiting process where $\Delta t \rightarrow 0$. Then, an increment in function f will be replaced by its differential, the summation goes over into the integral, the summation variable $k\Delta t$ can be replaced by the integration variable τ , and the broken line $f(k\Delta t)$ will coincide with the given function $f(t)$. Consequently we find that

$$f(t) = \int_0^t \sigma_0(t - \tau) df(\tau). \quad (11.7)$$

*This material, and all the basic ideas and concepts of this section are taken from A. A. Kharkevich [21].

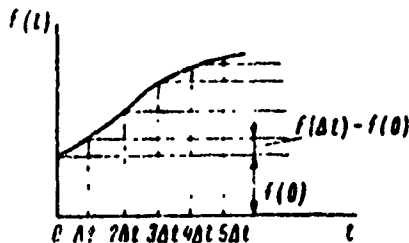


Fig. Diagram of the Function with the aid of the Duhamel Integral.

Integral (11.7) must be understood in the Stieltjes sense, i.e., it is applicable where function $f(t)$ has discontinuities. If $f(t)$ is continuous, then (11.7) takes the form

$$f(t) = \int_0^t \sigma_0(t - \tau) f'(\tau) d\tau. \quad (11.8)$$

If finite discontinuities exist, we must add the sum of the products of jump-discontinuity magnitudes times $\sigma_0(t - \tau_k)$, where τ_k - the abscissas of discontinuity points. Thus, if function $f(t)$ is equal to zero where $t < 0$, and where $t = 0$ jumps to the value $f(0)$ (Fig. 38), using a derivative to express the generalized differential in (11.7) we can write

$$f(t) = f(0) \sigma_0(t) + \int_0^t \sigma_0(t - \tau) f'(\tau) d\tau. \quad (11.9)$$

Employing (11.7)-(11.9), we can reduce any diffraction problem to a problem of diffraction of a single wave. Given, for example, some hydrodynamic characteristic of the process $F_0(t)$, found by solving the single wave diffraction problem $\sigma_0(t)$. Then, this characteristic for the same problem, but with a wave of arbitrary profile $p(t)$ can be derived according to the formula

$$F(t) = \int_0^t F_0(t - \tau) dp(\tau). \quad (11.10)$$

This happens to be the Duhamel integral in a Stieltjes form. The function $F_0(t)$ is called a transient function. Substitution

of variables and integration by parts yields several equivalent forms from (11.10), one of which will be the most suitable:

$$\begin{aligned}
 F(t) &= p(0)F_0(t) + \int_0^t F_0(t-\tau)p'(\tau)d\tau = \\
 &= p(0)F_0(t) + \int_0^t F_0(\tau)p'(t-\tau)d\tau = F_0(0)p(t) + \\
 &+ \int_0^t F_0'(t-\tau)p(\tau)d\tau = F_0(0)p(t) + \int_0^t F_0'(\tau)p(t-\tau)d\tau.
 \end{aligned}
 \tag{11.11}$$

Consequently, we can see that the Fourier integral and the Duhamel integral are equivalent from a methodological standpoint. In problems dealing with the physical processes of propagation and diffraction of shock-waves, the Duhamel integral reduces to a considerably smaller number of calculations.

Alongside the zero-order unit discontinuity function $\sigma_0(t)$, there has been wide use in mathematical physics of a first-order unit discontinuity function $\sigma_1(t)$ in recent years. This function is often called a Dirac δ -function. The Dirac delta-function $\delta(t)$ is equal to zero for all values of $t \neq 0$; where $t = 0$, it jumps to the value $+\infty$. At the same time, however, the integral of this function which is taken with respect to the interval including the point of discontinuity, retains a finite value equal to one:

$$\delta(t-\tau) = \begin{cases} \infty & \text{where } t = \tau \\ 0 & \text{where } t \neq \tau \end{cases} \tag{11.12}$$

$$\int_{-\infty}^{\infty} \delta(t-\tau)dt = 1, \tag{11.13}$$

$$\int_a^b \delta(t-\tau)dt = \begin{cases} 1 & \text{where } b > \tau > a \\ 0 & \text{where } \tau > b \quad \text{or} \quad \tau < a. \end{cases} \tag{11.14}$$

Based on the definition of the delta-function, it follows that it can aid in representing any function as an integral of itself

$$f(t) = \int_{-\infty}^{\infty} f(\tau) \delta(t - \tau) d\tau, \quad (11.15)$$

and where $t \geq 0$,

$$f(t) \varepsilon_0(t) = \int_0^{\infty} f(\tau) \delta(t - \tau) d\tau. \quad (11.16)$$

If the problem is solved for a delta-function-type wave, we can effect a change to a wave having the profile $p(t)$ with the aid of the Duhamel integral

$$F(t) = \int_0^t F_0(t - \tau) p(\tau) d\tau. \quad (11.17)$$

where $F_0(t)$ - solution of the problem for a delta-function-type wave.

Because the delta-function can be graphed with the aid of the the most diverse auxiliary functions, satisfying conditions (11.12)-(11.14) to the limit, its use in solving problems in some cases is simpler than in any other presentations.

The mathematical analysis of diffraction problems was first carried out by Kirchhoff. For a homogeneous wave equation in three-dimensional space he derived a very general relation, defining the potential at any point in space in terms of values of this potential; and in terms of its derivatives on an arbitrary closed surface, encompassing the region in which the chosen point is situated.

The Kirchhoff formula has the form

$$\begin{aligned} \varphi(\xi, \eta, \zeta, t) = \frac{1}{4\pi} \int_S \left\{ -\varphi\left(x, y, z, t - \frac{r}{u_0}\right) \frac{\partial}{\partial n} \frac{1}{r} + \right. \\ \left. + \frac{1}{r} \left[\frac{\partial \varphi\left(x, y, z, t - \frac{r}{u_0}\right)}{\partial n} \right] + \frac{1}{u_0} \frac{\partial}{\partial n} \frac{\partial \varphi\left(x, y, z, t - \frac{r}{u_0}\right)}{\partial t} \right\} dS, \end{aligned} \quad (11.18)$$

where $\phi(\xi, \eta, \zeta, t)$ - the potential at point A (ξ, η, ζ), encompassed by an arbitrary surface S; n - exterior normal to the surface; r - distance from element dS to point A(ξ, η, ζ).

Despite the completeness of the mathematical solution, analysis of diffraction problems with the aid of the Kirchhoff formula encounters theoretical difficulties. Indeed, although the surface on which we must be given the values of potential and its normal derivative can be arbitrarily selected, in most physical problems there are no reliable data on these quantities on the selected surface until the problem is solved. Hence, there is a need for additional assumptions on the distribution of the potential and its derivatives on the boundary surface. At best, this leads to the method of successive approximations. It should be added that even for the simplest cases, surface integrals entering into (11.18) cannot be taken in finite form.

Consequently, for approximate analysis the Kirchhoff formula is not as a rule applied, but the so-called integral of emission which is a mathematical form of writing the Huygens principle:

$$\varphi_A = \frac{1}{2\pi} \int_S \frac{v_n \left(1 - \frac{r}{a_n}\right)}{r} dS, \quad (11.19)$$

where v_n - the normal component of velocity of the surface element dS ; r - distance from dS to point A.

The application of (11.19), as with the Kirchhoff formula (11.18), can only be made when the point where the potential is evaluated is in "direct view" with respect to the arbitrary surface element. Let us indicate the sequence of operations associated with the application of the emission integral in diffraction problems. Given that we must find the pressure field in a fluid, allowing for the effect of an absolutely rigid plane obstacle of given configuration. In this case, we first calculate the normal components of particle velocity at points in the fluid directly in contact with the obstacle surface.

This is done based on the assumption that the obstacle itself is not present. After changing the sign, the derived quantities are substituted into the integral of radiation.

The sum of the direct wave potential and the potential found in this manner defines the unknown pressure field. The boundary condition

$$\left. \frac{\partial \varphi}{\partial n} \right|_s = 0.$$

is apparently satisfied on the obstacle surface.

At all remaining points on the surface of closure, the potential is considered to be the same as in a free fluid. This introduces a certain error into hydrodynamic field evaluation.

The number of problems which can be precisely solved using the integral of radiation is quite limited. In spite of the apparent simplicity of the mathematical formulation, the solutions are found to be, as a rule, complicated and unwieldy. The need arises to seek other mathematical methods for analyzing diffraction problems.

Among these methods, we should note the method of functional-invariant solutions of the wave equation, developed by V. I. Smirnov and S. L. Sobolyov [18], [19]. The method of incomplete separation of variables, developed by G. I. Petrashen and his group [14], [15] has become very popular. V. V. Novozhilov first considered the problem of interaction of an underwater shock-wave with an elastic round cylinder using the Laplace transform.

A. A. Kharkevich pointed out extremely general principles for solving diffraction problems [21]. Specifically, he developed the method of using the Laplace equation in place of the wave equation. Kharkevich's ideas are in wide use in this chapter of the book. We can obtain new findings on the basis of his ideas which, though not claiming completeness, nonetheless give us a clear picture of

diffraction of an underwater shock-wave by an obstacle.

§12. Diffraction of a Plane Wave By an Absolutely Rigid Wedge.

Let us consider the interaction of a unit-amplitude plane wave with an absolutely rigid and immobile wedge. The apex angle of the wedge is arbitrary. The angle of incidence of the wave is also arbitrary. The amplitude of the wave admits the possibility of utilizing the acoustic approximation.

S. L. Sobolyov and V. I. Smirnov (1934) first obtained a precise solution of this problem using the method of functional-invariant wave equation solutions [19]. This same problem was considered abroad by Keller and Blank in 1951 [35]. Irvin Kay [34] derived a solution for the case of a wave of arbitrary shape. A review of foreign studies in this field of research may be found in Lu Ting's article [38].

We will show that the problem can be solved most simply by using the method developed by Kharkevich in his study of wave diffraction at the edge of a semi-infinite plate. Let us begin with two particular cases: gliding of a wave along one of the edges of a wedge, and normal incidence of a wave onto the wedge.

Gliding of a Wave Parallel to One Edge of a Wedge

A diagram of this process is shown in Fig. 39. The wave front CD propagates from left to right. The diffraction field evolves in a cylinder $r = a_0 t$ having a directrix OKDBO. The system of coordinates is cylindrical. The z axis coincides with the edge of the wedge; the angle α is measured from the plane of the upper edge of the wedge clockwise. Time count begins when the wave front arrives at point O.

According to the definition of a unit-wave, pressure behind its front is equal to one, and ahead of the front - to zero. Thus, to

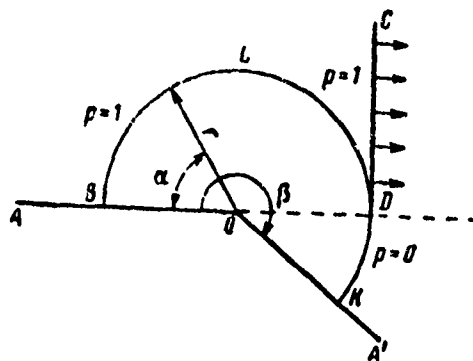


Fig. 39. Diffraction of a Plane Wave in the presence of Gliding along the Edge of a Wedge.

the right of CD in the upper half-space and outside of diffraction circle DK in the lower half-space, pressure is equal to zero. Behind the front CD outside the diffraction circle DLB, pressure is equal to one. The problem consists in evaluating pressure in the diffraction region. By virtue of the assumption of absolute obstacle rigidity, the boundary condition

$$v_n = \frac{\partial \varphi}{\partial n} = 0, \quad (12.1)$$

must be satisfied on the obstacle surface; where v_1 - normal component of particle velocity; ϕ - potential of velocity.

It is convenient to utilize conditions (12.1) in a different form. Since

$$p = -\rho_0 \frac{\partial \varphi}{\partial t}, \quad (12.2)$$

then

$$\frac{\partial p}{\partial n} = -\rho_0 \frac{\partial}{\partial n} \frac{\partial \varphi}{\partial t} = -\rho_0 \frac{\partial}{\partial t} \frac{\partial \varphi}{\partial n}. \quad (12.3)$$

It follows from a comparison of (12.1) and (12.3) that on the surface of an absolutely rigid obstacle we must find that

$$\left. \frac{\partial p}{\partial n} \right|_s = 0. \quad (12.4)$$

Pressure in the fluid satisfies an axially-symmetric wave equation

$$\frac{\partial^2 p}{\partial r^2} + \frac{1}{r} \frac{\partial p}{\partial r} + \frac{1}{r^2} \frac{\partial^2 p}{\partial \alpha^2} - \frac{1}{a_0^2} \frac{\partial^2 p}{\partial t^2} = 0. \quad (12.5)$$

Thus, the problem is reduced to solving wave equation (12.5) for the magnitude of pressure $p(\frac{r}{a_0 t}, \alpha)$ in the diffraction circle having a radius $a_0 t$, with boundary conditions on the obstacle surface being

$$\left. \frac{\partial p}{\partial n} \right|_S = 0,$$

and on the diffraction circle surface

$$p(1, \alpha) = \begin{cases} 1 & 0 \leq \alpha \leq \pi \\ 0 & \pi \leq \alpha \leq \beta. \end{cases} \quad (12.6)$$

Conditions (12.6) are based on the fact that a diffraction wave does not have a pressure jump on the front. This can easily be verified by using geometric acoustics methods and examining the energy balance transmitted by the direct wave front.*

Following Kharkevich, let us substitute the variables in equation (12.5)**

$$\left. \begin{aligned} z &= \text{Arch } \frac{a_0 t}{r}, \\ \frac{a_0 t}{r} &= \text{ch } z. \end{aligned} \right\} \quad (12.7)$$

The partial derivatives entering into (12.5) will take the form

* Cf., for example, G. F. Ludloff, Aerodynamics of Explosive Waves, Collection of articles, "Problems in Mechanics", IL: 1955.

**This same procedures was used by I. G. Novoselov in his study of a diffraction wave at a right angle.

$$\begin{aligned}\frac{\partial p}{\partial r} &= \frac{\partial p}{\partial z} z' \left(-\frac{a_0 f}{r^2} \right), \\ \frac{\partial^2 p}{\partial r^2} &= \frac{\partial^2 p}{\partial z^2} z'^2 \frac{a_0^2 f^2}{r^4} + \frac{\partial p}{\partial z} \left(z'' \frac{a_0^2 f^2}{r^4} + 2z' \frac{a_0 f}{r^2} \right), \\ \frac{\partial^2 p}{\partial t^2} &= \frac{\partial^2 p}{\partial z^2} z'^2 \frac{a_0^2}{r^4} + \frac{\partial p}{\partial z} z'' \frac{a_0^2}{r^2}.\end{aligned}$$

Substituting these quantities into (12.5) and keeping (12.7), we perform some simple transformations and find that

$$\frac{\partial^2 p}{\partial z'^2} + \frac{\partial^2 p}{\partial z^2} = 0. \quad (12.8)$$

Equation (12.8) is a Laplace equation in canonical form.

Using new variables, the boundary conditions (12.4) and (12.6) will be written: on the obstacle surface

$$\left. \frac{\partial p}{\partial n} \right|_s = \begin{cases} p'_s(z, 0) = 0 \\ p'_s(z, \beta) = 0, \end{cases} \quad \begin{aligned} (12.9a) \\ (12.9b) \end{aligned}$$

on the diffraction circle surface

$$p(0, z) = \begin{cases} 1 & 0 \leq \alpha \leq \pi \\ 0 & \pi < \alpha < 2\pi. \end{cases} \quad \begin{aligned} (12.10a) \\ (12.10b) \end{aligned}$$

The solution of equation (12.8) will be sought using the Fourier method.

Let us assume

$$p(z, z) = Z(z) A(z). \quad (12.11)$$

Then, substituting (12.11) into (12.8), we will find that

$$\frac{Z''(z)}{Z(z)} = -\frac{A''(z)}{A(z)}. \quad (12.12)$$

Equation (12.2) can occur only when the right and left sides are equal to the same constant, i.e.,

$$\left. \begin{aligned} Z''(z) - \lambda^2 Z(z) &= 0, \\ A''(z) + \lambda^2 A(z) &= 0. \end{aligned} \right\} \quad (12.13)$$

The general solutions of the first and second equations in (12.13) have the form

$$\left. \begin{aligned} Z(z) &= C_1 e^{i\lambda z} + C_2 e^{-i\lambda z}, \\ A(z) &= C_3 \cos \lambda z + C_4 \sin \lambda z. \end{aligned} \right\} \quad (12.14)$$

Because function $p(z, \alpha)$ is limited, $C_1 \equiv 0$. From condition (12.9a) it follows that $C_4 \equiv 0$, and from condition (12.9b) that $= (\pi m)/(\beta)$, where $m = 0; 1; 2 \dots$.

Thus,

$$p(z, \alpha) = \sum_{m=0}^{\infty} C_m e^{-\frac{\pi}{\beta} m z} \cos \frac{\pi m}{\beta} \alpha. \quad (12.15)$$

Where $z = 0$, (12.15) yields

$$p(0, \alpha) = \sum_{m=0}^{\infty} C_m \cos \frac{\pi m}{\beta} \alpha. \quad (12.16)$$

On the other hand, function $p(0, \alpha)$ is given by boundary condition (12.10).

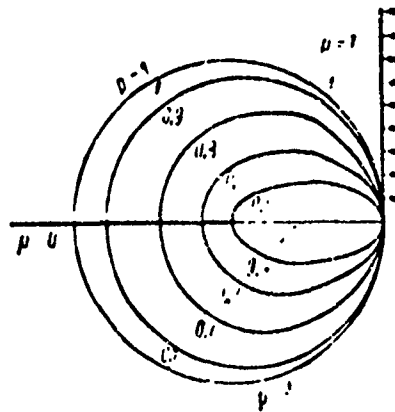


Fig. 40. Surface of Equal Pressures During Diffraction of Wave At Edge of a Plate.

After writing the function in the form of a Fourier series, we will find that

$$p(0, z) = \frac{a_0}{2} + \sum_{k=1}^{\infty} a_k \cos \frac{\pi k}{\beta} z, \quad (12.17)$$

where

$$a_k = \frac{2}{\beta} \int_0^{\beta} p(0, z) \cos \frac{k\pi z}{\beta} dz = \frac{2}{\beta} \int_0^{\beta} \cos \frac{k\pi z}{\beta} dz = \frac{2}{\pi k} \sin \frac{\pi k}{\beta}.$$

After comparing (12.16) and (12.17), we can replace (12.15) with

$$p(z, \alpha) = \frac{\pi}{\beta} + \frac{2}{\pi} \sum_{k=1}^{\infty} \frac{1}{k} \sin \frac{\pi k}{\beta} \cos \frac{\pi k}{\beta} z e^{-\frac{\pi k}{\beta} \alpha}. \quad (12.18)$$

Returning to our initial argument for evaluating pressure in a diffraction region, we find that

$$p\left(\frac{r}{a_0}, \alpha\right) = \frac{\pi}{\beta} + \frac{2}{\pi} \sum_{k=1}^{\infty} \frac{1}{k} \sin \frac{\pi k}{\beta} \cos \frac{\pi k}{\beta} \alpha e^{-\frac{\pi k}{\beta} \text{Arch} \frac{a_0}{r}}. \quad (12.19)$$

In the particular case of a rigid plate ($\beta = 2\pi$), we have

$$p\left(\frac{r}{a_0}, \alpha\right) = \frac{1}{2} \left(1 + \frac{4}{\pi} \sum_{k=1}^{\infty} \frac{1}{k} \sin \frac{\pi k}{2} \cos \frac{\pi k}{2} \alpha e^{-\frac{k}{2} \text{Arch} \frac{a_0}{r}} \right) =$$

$$= \frac{1}{2} \left[1 + \frac{4}{\pi} \sum_{n=1}^{\infty} \frac{\cos(2n-1) \frac{\alpha}{2} e^{-\frac{2n-1}{2} \text{Arch} \frac{a_0}{r}}}{(-1)^{n-1} (2n-1)} \right]. \quad (12.20)$$

Expression (12.20) totally coincides with Kharkevich's solution and, as he showed, may be written in finite form

$$p\left(\frac{r}{a_0 f}, \alpha\right) = \frac{1}{2} \left[1 \pm \frac{2}{\pi} \operatorname{arctg} \sqrt{\frac{1 + \cos \alpha}{\frac{a_0 f}{r} - 1}} \right], \quad (12.21)$$

where the signs + and - relate, respectively, to the upper and lower semicircle. The lines of equal pressure, plotted on the basis of calculations according to (12.21), are shown in Fig. 40 [21].

In the range of angles $0 < \alpha < \pi$, a solution of (12.19) can easily be found in finite form. Let us rewrite it in the following manner:

$$p(z, \alpha) = -\frac{\pi}{\beta} + \frac{1}{\pi} \sum_{k=1}^{\infty} \frac{1}{k} \sin \frac{\pi}{\beta} (\pi + \alpha) k e^{-\frac{\pi k}{\beta} z} + \\ + \frac{1}{\pi} \sum_{k=1}^{\infty} \frac{1}{k} \sin \frac{\pi}{\beta} (\pi - \alpha) k e^{-\frac{\pi k}{\beta} z}. \quad (12.22)$$

Let us employ the identity [1]

$$\sum_{k=1}^{\infty} \frac{q^k \sin x k}{k} = \operatorname{arctg} \frac{q \sin x}{1 - q \cos x} \quad \text{where} \quad q^2 < 1, \quad 0 < x < 2\pi. \quad (12.23)$$

Then the first summation of (12.22) can be written in the form

$$\frac{1}{\pi} \sum_{k=1}^{\infty} \frac{1}{k} \sin \frac{\pi}{\beta} (\pi + \alpha) k e^{-\frac{\pi k}{\beta} z} = \frac{1}{\pi} \operatorname{arctg} \frac{\sin \frac{\pi}{\beta} (\pi + \alpha)}{e^{\frac{\pi}{\beta} z} - \cos \frac{\pi}{\beta} (\pi - \alpha)},$$

and the second - in the form

$$\frac{1}{\pi} \sum_{k=1}^{\infty} \frac{1}{k} \sin \frac{\pi}{\beta} (\pi - \alpha) k e^{-\frac{\pi k}{\beta} z} = \frac{1}{\pi} \operatorname{arctg} \frac{\sin \frac{\pi}{\beta} (\pi - \alpha)}{e^{\frac{\pi}{\beta} z} - \cos \frac{\pi}{\beta} (\pi - \alpha)}.$$

Consequently, in the interval $0 < \alpha < \pi$

$$p\left(\frac{r}{a_0 t}, \alpha\right) = \frac{\pi}{\beta} + \frac{1}{\pi} \operatorname{arctg} \frac{\sin \frac{\pi}{\beta} (\pi + \alpha)}{e^{\frac{\pi}{\beta} \operatorname{Arch} \frac{a_0 t}{r}} - \cos \frac{\pi}{\beta} (\pi + \alpha)} + \\ + \frac{1}{\pi} \operatorname{arctg} \frac{\sin \frac{\pi}{\beta} (\pi - \alpha)}{e^{\frac{\pi}{\beta} \operatorname{Arch} \frac{a_0 t}{r}} - \cos \frac{\pi}{\beta} (\pi - \alpha)} \quad (12.24)$$

Pressure $p\left(\frac{r}{a_0 t}, \alpha\right)$, where $0 < \pi$ (in the upper half-space) may be considered as the result of applying two waves - the direct and the diffraction. Consequently, when we must evaluate pressure only in a diffraction wave p_d , it suffices to deduct pressure in the direct wave (equal to one) from $p\left(\frac{r}{a_0 t}, \alpha\right)$ [the latter is defined by expression (12.24)].

For example, on the upper edge of the wedge ($\alpha = 0$), we will find

$$p_d = - \left(1 - \frac{\pi}{\beta} - \frac{2}{\pi} \operatorname{arctg} \frac{\sin \frac{\pi}{\beta}}{e^{\frac{\pi}{\beta} \operatorname{Arch} \frac{a_0 t}{r}} - \cos \frac{\pi}{\beta}} \right) \quad (12.25)$$

From (12.25), specifically, it follows that: for diffraction of a wave by a right angle ($\beta = \frac{3}{2}\pi$)

$$p_d = - \left(\frac{1}{3} - \frac{2}{\pi} \operatorname{arctg} \frac{\sqrt{3}}{2e^{\frac{1}{3} \operatorname{Arch} \frac{a_0 t}{r}} - 1} \right) = \\ = - \left\{ \frac{1}{3} - \frac{2}{\pi} \operatorname{arctg} \frac{\sqrt{3}}{2 \left[\frac{a_0 t}{r} + \sqrt{\left(\frac{a_0 t}{r} \right)^2 - 1} \right]^{1/3} - 1} \right\} \quad (12.26)$$

For diffraction of a wave by a semi-infinite plate ($\beta = 2\pi$)

$$p_2 = - \left[\frac{1}{2} - \frac{2}{\pi} \operatorname{arctg} \frac{1}{\sqrt{\frac{a_0 t}{r}} \cdot \sqrt{\left(\frac{a_0 t}{r}\right)^2 - 1}} \right] =$$

$$= - \left(\frac{1}{2} - \frac{1}{\pi} \operatorname{arctg} \frac{\sqrt{2}}{\sqrt{\frac{a_0 t}{r} - 1}} \right). \quad (12.27)$$

Diffraction of a Wave Falling Along the Normal to One Corner of a Wedge

A general picture of this effect is shown in Fig. 41. A unit-amplitude direct-wave front has attained position EN; the fronts of the reflected waves are indicated by straight lines CD and EF. Diffraction develops in the cylinder having the directrix OBDKFO. Ahead of the front EN and outside the arc EK (where $\beta > \frac{3}{2}\pi$, Fig. 41b), pressure is equal to zero. Behind the front EN and outside of line EFDC, pressure is equal to one. In the region EKF and ABDC, behind the reflected-wave fronts and outside the diffraction circle, pressure is equal to two.

The problem consists in evaluating pressure $p(\frac{r}{a_0 t}, \alpha)$ in a diffraction circle having a radius $a_0 t$. In other words, we must find a solution for wave equation (12.5) with the following boundary conditions:

on the surface of a rigid wedge

$$\left. \frac{\partial p}{\partial n} \right|_s = 0, \quad (12.28)$$

on the boundary of a diffraction circle where $\beta < \frac{3}{2}\pi$

$$p(1, \alpha) = \begin{cases} 2 & 0 < \alpha < \frac{\pi}{2} \\ 1 & \frac{\pi}{2} < \alpha < 2\beta - \frac{3}{2}\pi \\ 2 & 2\beta - \frac{3}{2}\pi < \alpha < \beta. \end{cases} \quad (12.29)$$

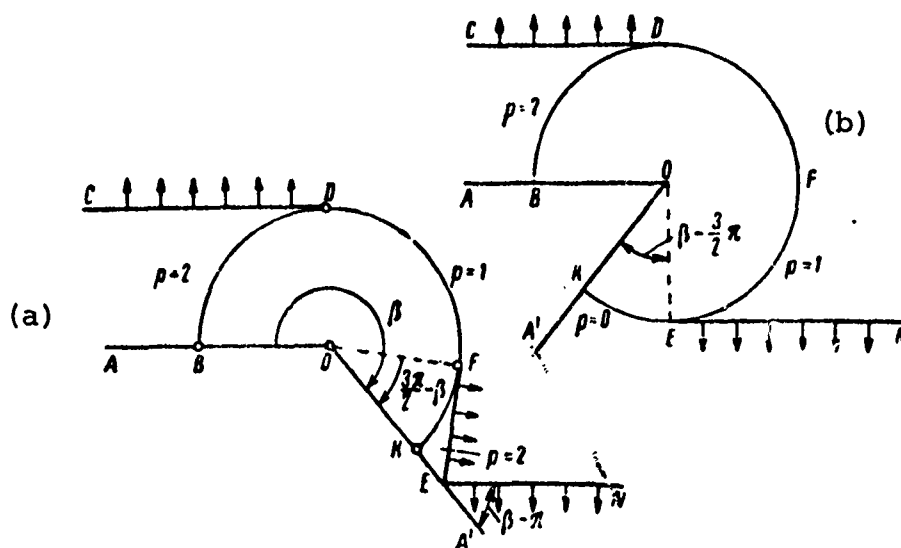


Fig. 41. Diagram of Diffraction of a Plane Wave During Normal Incidence onto One Wedge Edge: (a) $\beta < \frac{3}{2}\pi$
 $\beta > \frac{3}{2}\pi$.

where $\beta > \frac{3}{2}\pi$

$$p(1, \alpha) = \begin{cases} 2 & 0 \leq \alpha < \frac{\pi}{2} \\ 1 & \frac{\pi}{2} \leq \alpha \leq \frac{3}{2}\pi \\ 0 & \frac{3}{2}\pi \leq \alpha \leq \beta. \end{cases} \quad (12.30)$$

Using (12.7) to substitute the variables as before, we arrive at the Laplace equation (12.8) with a boundary condition on the surface of a wedge (12.9). The only difference between this and the preceding problem is in the writing of conditions on the diffraction circle.

By analogy with (12.15), a solution can be sought in the form

$$p(z, \alpha) = \sum_{m=0}^{\infty} C_m e^{-\frac{z}{\beta} m \alpha} \cos \frac{\pi m}{\beta} \alpha. \quad (12.31)$$

Where $z = 0$

$$p(0, \alpha) = \sum_{m=0}^{\infty} C_m \cos \frac{\pi m}{\beta} \alpha. \quad (12.32)$$

The coefficients C_m are found by expanding the function $p(0, \alpha)$ given by equations (12.29) and (12.30) into a Fourier series.

We have

$$\rho(0, z) = \frac{a_0}{2} + \sum_{k=1}^{\infty} a_k \cos \frac{\pi k}{\beta} z, \quad (12.33)$$

where

$$a_k = \frac{2}{\beta} \int_0^{\beta} \rho(0, z) \cos \frac{k\pi z}{\beta} dz. \quad (12.34)$$

According to (12.29)

$$\begin{aligned} a_k &= \frac{2}{\beta} \int_0^{\frac{\pi}{2}} 2 \cos \frac{k\pi z}{\beta} dz + \frac{2}{\beta} \int_{\frac{\pi}{2}}^{2\beta - \frac{3}{2}\pi} \cos \frac{k\pi z}{\beta} dz + \\ &+ \frac{2}{\beta} \int_{2\beta - \frac{3}{2}\pi}^{\beta} 2 \cos \frac{k\pi z}{\beta} dz = \frac{2}{k\pi} \sin \frac{k\pi^2}{2\beta} + \frac{2}{k\pi} \sin \frac{3}{2} \frac{k\pi^2}{\beta}. \end{aligned}$$

The very same result occurs for boundary conditions (12.30).

Thus, in place of (12.32) we can write:

$$\begin{aligned} \rho(z, a) &= \frac{2\pi}{\beta} + \frac{2}{\pi} \sum_{k=1}^{\infty} \frac{1}{k} \left(\sin \frac{\pi^2}{2\beta} k + \sin \frac{3\pi^2}{2\beta} k \right) \times \\ &\times \cos \left(\frac{\pi}{\beta} ak \right) e^{-\frac{\pi^2}{\beta} k}, \end{aligned} \quad (12.35)$$

or, returning to our previous variables,

$$\begin{aligned} \rho \left(\frac{t}{a_0 t}, z \right) &= \frac{2\pi}{\beta} + \frac{2}{\pi} \sum_{k=1}^{\infty} \frac{1}{k} \left(\sin \frac{\pi^2}{2\beta} k + \sin \frac{3\pi^2}{2\beta} k \right) \times \\ &\times \cos \left(\frac{\pi}{\beta} ak \right) e^{-\frac{\pi^2}{\beta} k \operatorname{Arctg} \frac{a_0 t}{r}}. \end{aligned} \quad (12.36)$$

In the particular case of an absolutely rigid plate ($\beta = 2\pi$)

$$\rho \left(\frac{t}{a_0 t}, a \right) = 1 + \frac{2}{\pi} \sum_{k=1}^{\infty} \frac{1}{k} \left(\sin \frac{k\pi}{4} + \sin \frac{3k\pi}{4} \right) \times$$

$$\times \cos\left(\frac{\pi}{2} k\right) e^{-\frac{k}{2} \operatorname{Arch} \frac{a, t}{r}} = 1 + \frac{2\sqrt{2}}{\pi} \sum_{n=1}^{\infty} \zeta_n \frac{\cos(2n-1) \frac{\alpha}{2}}{2n-1} \times \\ \times e^{-\frac{2n-1}{2} \operatorname{Arch} \frac{a, t}{r}},$$

where

$$\zeta_n = 1; 1; -1; -1; 1 \dots \quad (12.37)$$

This expression coincides with Kharkevich's solution [21]. In finite form it is written thus:

$$\rho\left(\frac{r}{a, t}, \alpha\right) = 1 \pm \frac{1}{\pi} \operatorname{arctg} \frac{2 \cos \frac{\alpha}{2} \sqrt{\frac{a, t}{r} - 1}}{\frac{a, t}{r} - 1 - \cos \alpha}, \quad (12.38)$$

where the signs + and - relate to the upper and lower semicircles, respectively.

We will use relation (12.23) to derive expression (12.36) in finite form.

Where $0 < \alpha < \frac{\pi}{2}$, we have:

$$\rho(z, \alpha) = \frac{2\pi}{3} + \frac{1}{\pi} \sum_{k=1}^{\infty} \frac{1}{k} \sin \frac{\pi}{3} \left(\frac{\pi}{2} + \alpha \right) k e^{-\frac{\pi z}{3}} + \\ + \frac{1}{\pi} \sum_{k=1}^{\infty} \frac{1}{k} \sin \frac{\pi}{3} \left(\frac{\pi}{2} - \alpha \right) k e^{-\frac{\pi z}{3}} + \\ + \frac{1}{\pi} \sum_{k=1}^{\infty} \frac{1}{k} \sin \frac{\pi}{3} \left(\frac{3\pi}{2} + \alpha \right) k e^{-\frac{\pi z}{3}} + \\ + \frac{1}{\pi} \sum_{k=1}^{\infty} \frac{1}{k} \sin \frac{\pi}{3} \left(\frac{3\pi}{2} - \alpha \right) k e^{-\frac{\pi z}{3}} \dots$$

$$\begin{aligned}
&= \frac{2\pi}{3} + \frac{1}{\pi} \left[\operatorname{arctg} \frac{\sin \frac{\pi}{3} \left(\frac{\pi}{2} - \alpha \right)}{e^{\frac{\pi}{3} z} - \cos \frac{\pi}{3} \left(\frac{\pi}{2} - \alpha \right)} + \right. \\
&+ \operatorname{arctg} \frac{\sin \frac{\pi}{3} \left(\frac{\pi}{2} - \alpha \right)}{e^{\frac{\pi}{3} z} - \cos \frac{\pi}{3} \left(\frac{\pi}{2} - \alpha \right)} + \operatorname{arctg} \frac{\sin \frac{\pi}{3} \left(\frac{3\pi}{2} - \alpha \right)}{e^{\frac{\pi}{3} z} - \cos \frac{\pi}{3} \left(\frac{3\pi}{2} - \alpha \right)} + \\
&\left. + \operatorname{arctg} \frac{\sin \frac{\pi}{3} \left(\frac{3\pi}{2} - \alpha \right)}{e^{\frac{\pi}{3} z} - \cos \frac{\pi}{3} \left(\frac{3\pi}{2} - \alpha \right)} \right] \quad (12.39)
\end{aligned}$$

or

$$p\left(\frac{r}{a_0 t}, \alpha\right) = \frac{2\pi}{3} + \frac{1}{\pi} \sum_{i=1}^4 \operatorname{arctg} \frac{\sin \frac{\pi}{3} \gamma_i}{e^{\frac{\pi}{3} \operatorname{Arch} \frac{a_0 t}{r}} - \cos \frac{\pi}{3} \gamma_i} \quad (12.40)$$

where

$$\gamma_{1,2} = \frac{\pi}{2} \pm \alpha; \quad \gamma_{3,4} = \frac{3\pi}{2} \pm \alpha.$$

Net pressure $p\left(\frac{r}{a_0 t}, \alpha\right)$ over the upper wedge edge ($\alpha < \frac{\pi}{2}$) is composed of pressure from the direct, reflected, and diffraction waves.

Thus, in order to determine the pressure of the diffraction wave only p_d , we must subtract 2 from the quantity $p\left(\frac{r}{a_0 t}, \alpha\right)$. Consequently, on the upper wedge edge ($\alpha = 0$), we will find that

$$\begin{aligned}
p_d = -2 + \frac{2\pi}{3} + \frac{2}{\pi} \left(\operatorname{arctg} \frac{\sin \frac{\pi^2}{23}}{e^{\frac{\pi}{3} \operatorname{Arch} \frac{a_0 t}{r}} - \cos \frac{\pi^2}{23}} + \right. \\
\left. + \operatorname{arctg} \frac{\sin \frac{3\pi^2}{23}}{e^{\frac{\pi}{3} \operatorname{Arch} \frac{a_0 t}{r}} - \cos \frac{3\pi^2}{23}} \right) \quad (12.41)
\end{aligned}$$

Diffraction of a Unit Wave During Arbitrary Incidence onto Rigid Wedge

In relation to the angle at which a wave encounters an obstacle, two types of wave reflection are possible: on one wedge corner (Fig. 42a) or by both corners (Fig. 42b).

We can easily find the position of the fronts using the Huygens principle. In the first case (where the angle of incidence of the wave is $\gamma < \beta - \pi$, Fig. 42a), the angle characterizing the point of tangency of the direct-wave front to the diffraction circle is $\alpha_E = \pi + \gamma$. The angle characterizing the point of tangency of the reflected wave to the diffraction circle differs from angle α_E by 2γ and is equal to $\alpha_D = \pi - \gamma$. In the second case, the wave picture becomes complicated. After convergence of the direct wave with the edge of the wedge, where $\gamma > \beta - \pi$, two reflected waves are formed. The points of tangency of these waves to the diffraction circle are characterized by the angles (Fig. 52b)

$$\alpha_1 = \pi - \gamma$$

and

$$\alpha_2 = \beta - \angle KOF = \beta - |\gamma - (\beta - \pi)| = 2\beta - \pi - \gamma.$$

As we can see, this problem differs from those considered earlier only by the boundary conditions on the diffraction circle.

In this case, on the boundary of the diffraction region where $\gamma < \beta - \pi$

$$\rho(0, \alpha) = \begin{cases} 2 & 0 < \alpha < \pi - \gamma \\ 1 & \pi - \gamma < \alpha < \pi + \gamma \\ 0 & \pi + \gamma < \alpha < \beta \end{cases} \quad (12.42)$$

while where $\gamma > \beta - \pi$

$$p(0, \alpha) = \begin{cases} 2 & 0 < \alpha < \pi - \gamma \\ 1 & \pi - \gamma < \alpha < 2\pi - \pi - \gamma \\ 2 & 2\pi - \pi - \gamma < \alpha < 3\pi \end{cases} \quad (12.43)$$

Expanding the function $p(0, \alpha)$ into a Fourier series, we yield an expression common to (12.42) and (12.43)

$$p(0, \alpha) = \frac{2\pi}{\beta} + \frac{2}{\pi} \sum_{k=1}^{\infty} \frac{1}{k} \left[\sin \frac{\pi}{\beta} (\pi - \gamma) k + \sin \frac{\pi}{\beta} (\pi + \gamma) k \right] \cos \frac{\pi}{\beta} \alpha k. \quad (12.44)$$

Consequently, pressure in the region of diffraction is

$$p\left(\frac{r}{a_0 l}, \alpha\right) = \frac{2\pi}{\beta} + \frac{2}{\pi} \sum_{k=1}^{\infty} \frac{1}{k} \left[\sin \frac{\pi}{\beta} (\pi - \gamma) k + \sin \frac{\pi}{\beta} (\pi + \gamma) k \right] \cos \frac{\pi}{\beta} \alpha k \cdot e^{-\frac{rk}{\beta} \text{Arch} \frac{a_0 l}{r}}. \quad (12.45)$$

In the particular case $\gamma = \frac{\pi}{2}$, we will derive an earlier-fixed formula (12.36) for normal wave incidence. However, for $\gamma = 0$ the solution of (12.45) exceeds the result of (12.18) by an even factor of 2, which is the result of a well-known acoustic paradox that does not admit a limiting process.*

*Under actual conditions, all obstacles have finite dimensions. In this case, the zone of doubled amplitude begins with the latter angle and is reduced when the angle of incidence γ is reduced. At the same time, the life of doubled pressure is reduced (cf. Fig. 48, 48). When $\gamma \rightarrow 0$, the zone of the acoustic paradox will formally exist only on the wall, and the "paradox" life tends toward zero (at the moment that the front arrives). Moreover, at angles of incidence which are close to a shear angle, regular reflection of finite-amplitude waves cannot occur. It is replaced by irregular reflection having the formation of Mach waves.

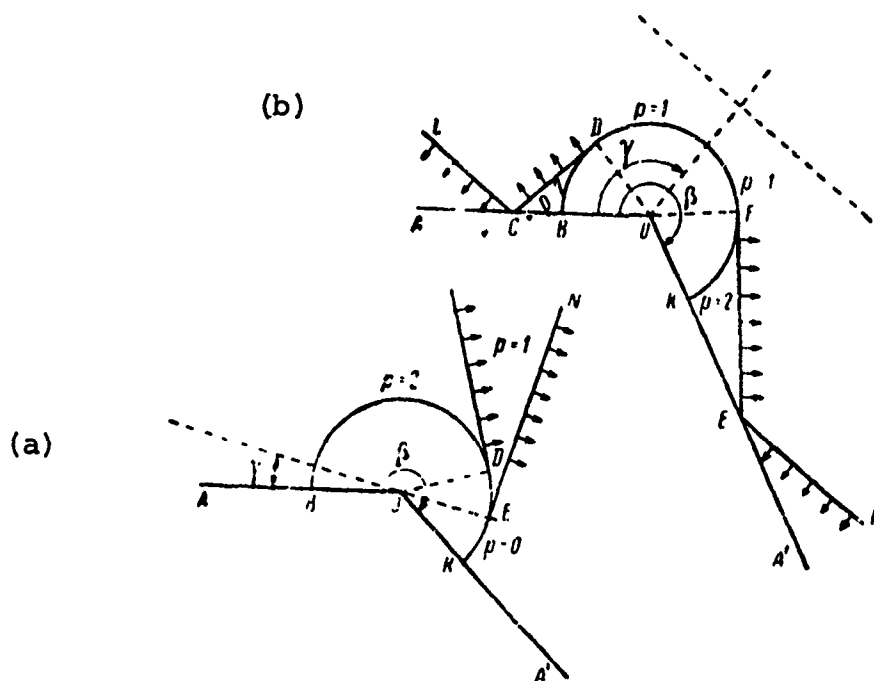


Fig. 42. Diagram of Diffraction of Plane Wave at Arbitrary Angle of Encounter with Rigid Wedge: (a) $\gamma < \beta - \pi$; (b) $\gamma > \beta - \pi$.

For $0 < \alpha < \pi - \gamma$ and $\frac{x}{a_0 t} \leq 1$, using (12.23) as before, equation (12.45) can be written in finite form

$$p\left(\frac{x}{a_0 t}, z\right) = \frac{2\pi}{\beta} + \frac{1}{\pi} \sum_{l=1}^{\infty} \operatorname{arctg} \frac{\sin \frac{\pi}{\beta} \gamma_l}{\gamma_l - \cos \frac{\pi}{\beta} \gamma_l}, \quad (12.46)$$

where

$$\begin{aligned} \gamma_l &= e^{\sqrt{1 - \left(\frac{a_0 t}{r}\right)^2}} = \frac{a_0 t}{r} + \sqrt{\left(\frac{a_0 t}{r}\right)^2 - 1}, \\ \gamma_{1,2} &= (\pi - \gamma) \pm \alpha, \\ \gamma_{3,4} &= (\pi + \gamma) \pm \alpha. \end{aligned}$$

Into (12.46), we take the values of arctg in the first quadrant having the sign of the argument.

Sobolyov [19] was the first to consider solving this problem in another way. For the entire range of change in angle α ($0 \leq \alpha \leq \beta$),

his results can be written in the form:

for the case where a shady area exists ($\gamma < \beta - \pi$)

$$p\left(\frac{r}{a_0 l}, \alpha\right) = \frac{1}{\pi} \sum_{i=1}^4 \operatorname{arctg} \left(\frac{1 + \zeta^{\frac{\pi}{2\beta}}}{1 - \zeta^{\frac{\pi}{2\beta}}} \operatorname{tg} \frac{\pi}{2\beta} \chi_i \right), \quad (12.47)$$

where

$$\begin{aligned} \zeta &= \frac{a_0 l}{r} - \sqrt{\left(\frac{a_0 l}{r}\right)^2 - 1}, \\ \chi_{1,2} &= (\pi - \gamma) \pm \alpha, \\ \chi_{3,4} &= (\pi + \gamma) \pm \alpha; \end{aligned}$$

for the case where no shady area exists ($\gamma > \beta - \pi$)

$$p\left(\frac{r}{a_0 l}, \alpha\right) = 2 + \frac{1}{\pi} \sum_{i=1}^4 \operatorname{arctg} \left(\frac{1 + \zeta^{\frac{\pi}{2\beta}}}{1 - \zeta^{\frac{\pi}{2\beta}}} \operatorname{tg} \frac{\pi}{2\beta} \chi_i^* \right), \quad (12.48)$$

where

$$\begin{aligned} \chi_{1,2}^* &= (\pi - \gamma) \pm \alpha, \\ \chi_{3,4}^* &= (\pi + \gamma - 2\beta) \pm \alpha. \end{aligned}$$

In formulas (12.47) and (12.48), we take the values of arctg having the same sign and in the same quadrant (first or second) where the argument (angle $\frac{\pi}{2\beta} \chi^*$) is found. These formulas define net pressure at the point and can be utilized for the time interval following convergence of the diffraction wave.

Evaluation of pressure on the obstacle surface is of the greatest interest from a practical standpoint. Using (12.46) and (12.47), we have:

on the "exposed" side of the wedge ($\alpha = 0$)

$$p\left(\frac{r}{a_0 t}, 0\right) = \frac{2\pi}{\beta} + \frac{2}{\pi} \left[\operatorname{arctg} \frac{\sin \frac{\pi}{\beta} (\pi - \gamma)}{\frac{r}{a_0 t} - \cos \frac{\pi}{\beta} (\pi - \gamma)} + \operatorname{arctg} \frac{\sin \frac{\pi}{\beta} (\pi + \gamma)}{\frac{r}{a_0 t} - \cos \frac{\pi}{\beta} (\pi + \gamma)} \right] \quad (12.49)$$

on the "lee" side of the wedge ($\alpha = \beta$)

$$p\left(\frac{r}{a_0 t}, \beta\right) = 2 - \frac{2}{\pi} \left[\operatorname{arctg} \frac{1 + \frac{r}{a_0 t}}{1 - \frac{r}{a_0 t}} \operatorname{ctg} \frac{\pi}{2\beta} (\pi - \gamma) + \operatorname{arctg} \frac{1 + \frac{r}{a_0 t}}{1 - \frac{r}{a_0 t}} \operatorname{ctg} \frac{\pi}{2\beta} (\pi + \gamma) \right] \quad (12.50)$$

Pressure on the "exposed" side of the wedge, where $\alpha < \pi - \gamma$, can be considered the result of applying three waves: direct, reflected, and diffraction. To determine pressure in the diffraction wave, it suffices to subtract the pressure of the direct and reflected waves (equal to 2) from p . If $\gamma < \pi - \beta$, then where $\alpha > \pi + \gamma$, pressure in the "lee" region is defined only by the diffraction wave. Therefore, $p_d = p$.

Diffraction of a Wave of Triangular Profile by a Rigid Wedge

The problems considered above assumed the unlimited duration of a wave and the infinity of diffraction effects associated with it. Actually, the pressure on a shock-wave changes with respect to a fixed law. The positive pressure phase and the wave length are finite. The region of formation of diffraction processes, which is a function of wave length, is likewise finite.

Let us illustrate these facts with the simple example of diffract-

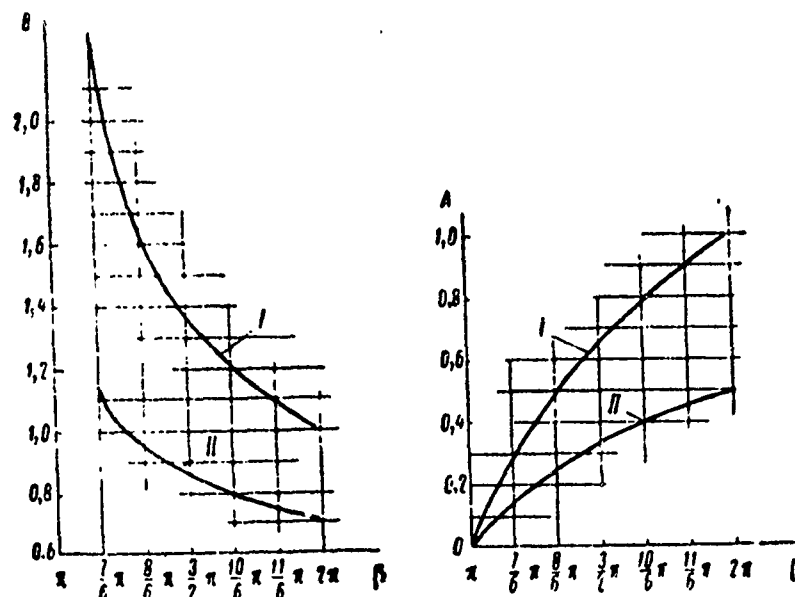


Fig. 43. The coefficients A and B as Functions of β . (I) normal incidence; (II) shear incidence.

ion of a wave of triangular profile by a rigid wedge. This problem is of considerable interest, in terms of practical application, because the time rate of pressure change is almost linear in the proximity of a free surface (cf. §7).

Therefore,

$$p(t) = p_{\phi} f(t), \quad (12.51)$$

where

$$f(t) = \left(1 - \frac{t}{t_1}\right) [z_0(t) - z_0(t - t_1)], \quad (12.52)$$

p_{ϕ} - pressure on the front; t - time, counted after the wave arrives at a given point; t_1 - duration of positive pressure phase.

For a wave of arbitrary profile, the solution of the diffraction problem can be derived using the Duhamel integral, if it is given for a unit wave. Therefore, there is no need to begin our study from the very beginning. We can utilize previously-derived results and calculated only the appropriate integrals. However, in spite of the



simplicity of the derived solutions and the selection of function $f(t)$, the calculation of the Duhamel integral is of considerable difficulty.

Consequently, it is extremely important to simplify the relations which characterize the diffraction field of pressure. This problem was considered by K. V. Lopukhov, who suggested the following approximation

$$p_1\left(\frac{u_0 t}{r}, \gamma, \beta, \alpha\right) = A \frac{2}{\pi} \operatorname{arctg} B \sqrt{\frac{u_0 t}{r} - 1} z_0\left(t - \frac{r}{u_0}\right), \quad (12.53)$$

where A - the greatest magnitude of pressure in a diffraction wave;
 B - the diffraction coefficient.

The coefficients A and B are functions of the angles α , β , and γ . The numerical value of these coefficients for points situated on the "face" side of the wedge ($\alpha = 0$) are shown in Fig. 43 for the normal & shear incidence of a unit wave. Error of approximation can be seen from Fig. 44, where the corresponding comparisons are given.

Let us write a wave of triangular profile (12.52) as the sum of three waves

$$p(t) = p_{\psi} z_0(t) - \frac{p_{\psi}}{t} z_0(t) + \frac{p_{\psi}}{t} (t - t_+) z_0(t - t_+). \quad (12.54)$$

We can see from the structure of (12.54) that with a given wave profile (in addition to solving the problem of unit-amplitude wave diffraction*) we must also derive a solution of the same problem for a wave of the form

$$\sigma_{-1}(t) = \int_0^t \sigma_0(\tau) d\tau = t z_0(t). \quad (12.55)$$

This last equation can easily be derived by utilizing the Duhamel integral in its initial form (11.11), assuming that $[\sigma_{-1}(t)]' =$

*The transient function appropriate to this solution is designated as in §11, using $F_0(t)$.

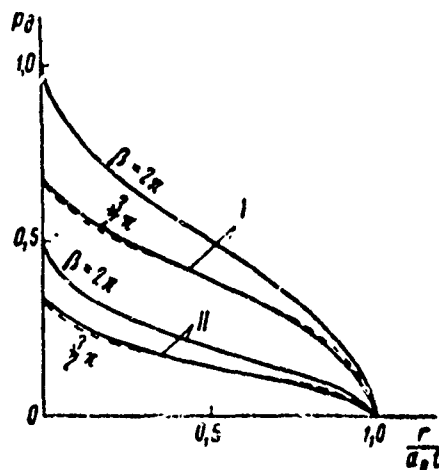


Fig. 44. Comparison of Approximation and Precise Calculation for Pressure in Diffraction Waves.

(I) normal incidence; (II) shear incidence.

————— precise calculation;
 ----- approximation.

$$= \sigma_0(t).$$

The unknown solution will be designated using $H(t)$:

$$H(t) = \int_0^t F_1(t-\tau) z_0(\tau) d\tau = z_0(t) \int_0^t F_1(\tau) d\tau. \quad (12.56)$$

By complete analogy for a wave of the form

$$\left. \begin{aligned} (t-t_+) z_0(t-t_+) &= z_{-1}(t-t_+), \\ H_1(t) &= \int_0^t F_1(t-\tau) z_0(\tau-t_+) d\tau. \end{aligned} \right\} \quad (12.57)$$

Because where $\tau < t_+$ $\sigma_0(\tau - t_+) = 0$, then

$$H_1(t) = z_0(t-t_+) \int_0^{t-t_+} F_1(\tau) d\tau = H(t-t_+). \quad (12.58)$$

Thus, the solution for a wave of triangular profile has the form

$$F(t) = p_0 F_1(t) - \frac{p_0}{t_-} H(t) + \frac{p_0}{t_+} H(t-t_+). \quad (12.59)$$

In the given case, the transient function $F_{\sigma}(t)$ is the approximation of (12.53)

$$F_{\sigma}(t) = A \frac{2}{\pi} \operatorname{arctg} B \sqrt{\frac{a_0 t}{r} - 1} \varphi_0\left(t - \frac{r}{a_0}\right)$$

and consequently, according to (12.56)

$$\begin{aligned} H(t) &= \int_0^t F_{\sigma}(t-\tau) \varphi_0(\tau) d\tau = \varphi_0(t) \int_0^t F_{\sigma}(\tau) d\tau = \\ &= \varphi_0\left(t - \frac{r}{a_0}\right) A \frac{2}{\pi} \int_{\frac{r}{a_0}}^t \operatorname{arctg} B \sqrt{\frac{a_0 \tau}{r} - 1} d\tau = \\ &= A \frac{2}{\pi} \left\{ \left(t - \frac{r}{a_0} + \frac{r}{a_0 B^2}\right) \operatorname{arctg} B \sqrt{\frac{a_0 t}{r} - 1} - \right. \\ &\quad \left. - \frac{r}{B a_0} \sqrt{\frac{a_0 t}{r} - 1} \right\} \varphi_0\left(t - \frac{r}{a_0}\right). \end{aligned} \quad (12.60)$$

Let us note that the simplicity of defining function $H(t)$ for some transient function $F_{\sigma}(t)$ permits us to derive a solution for a wave of arbitrary profile, if we write it in the form

$$p(t) = p_m \varphi_0(t) + \sum_{k=1}^n \frac{p_m}{\pm T_k} (t - t_k) \varphi_0(t - t_k), \quad (12.61)$$

where t_k - moment of appearance of k -th wave; p_m - maximum pressure on wave front; T_k - typical time interval whose meaning is illustrated in Fig. 45.

The solution of the diffraction problem for wave (12.61) will be

$$F(t) = p_m F_{\sigma}(t) + \sum_{k=1}^n \frac{p_m}{\pm T_k} H(t - t_k). \quad (12.62)$$

Let us introduce dimensional quantities

$$\bar{t} = \frac{t}{t_r}; \quad \bar{t} = \frac{t}{a_0 t_r} = \frac{t}{\lambda}, \quad (12.63)$$

where λ - the wave length.

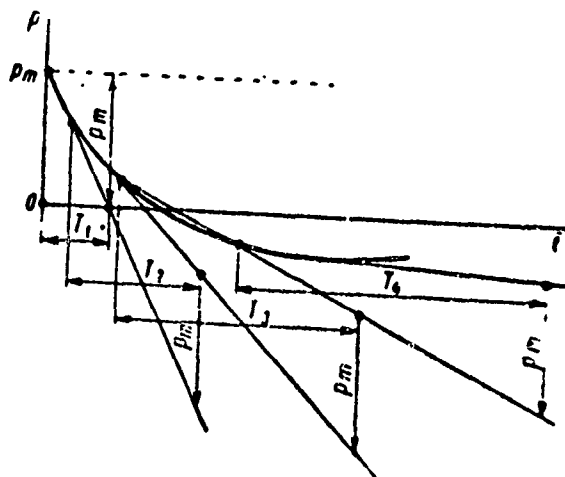


Fig. 45. Diagram of Approximation of Arbitrary Contour by Linear Relations.

Then, according to (12.59)-(12.60), the diffraction field of a wave of triangular profile will be derived in the form

$$\begin{aligned}
 p_2(t, z) = & p_0 A \frac{2}{\pi} \left\{ \left[\operatorname{arctg} B \sqrt{\frac{\bar{t}}{\xi} - 1} - \right. \right. \\
 & - \left(t + \xi \frac{1-B^2}{B^2} \right) \operatorname{arctg} B \sqrt{\frac{\bar{t}}{\xi} - 1} + \frac{\xi}{B} \sqrt{\frac{\bar{t}}{\xi} - 1} \left. \right] \mathcal{J}_0(\bar{t} - \xi) + \\
 & + \left[\left(t - 1 + \xi \frac{1-B^2}{B^2} \right) \operatorname{arctg} B \sqrt{\frac{1}{\xi} (\bar{t} - 1) - 1} - \right. \\
 & \left. \left. - \frac{\xi}{B} \sqrt{\frac{1}{\xi} (\bar{t} - 1) - 1} \right] \mathcal{J}_0(\bar{t} - 1 - \xi) \right\}.
 \end{aligned}
 \tag{12.64}$$

Let us explain the physical picture of diffraction in somewhat greater detail, using as our example the normal incidence of a wave on a wedge $\beta = \frac{3}{2}\pi$. A diagram of this effect is shown in Fig. 46. Because pressure in a direct wave acts for a limited time t_+ , at some points in space the diffraction wave will arrive after direct-wave pressure at these points has dropped to zero. Consequently, the diffraction wave distorts the field of the direct wave only in a certain region whose boundary can be defined by the equation

$$\frac{r}{a_0} = t + \frac{x}{a_0},$$

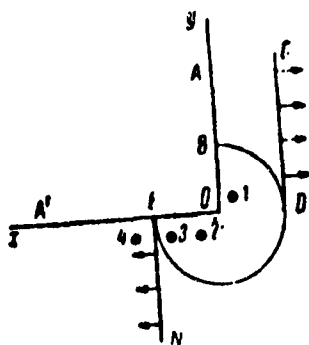


Fig. 46. Diagram of Situation of Points in Region of Diffraction of Wave By Right Angle.

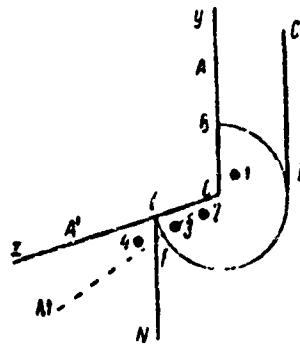


Fig. 48. Diagram of Situation of Points in Region of Diffraction.

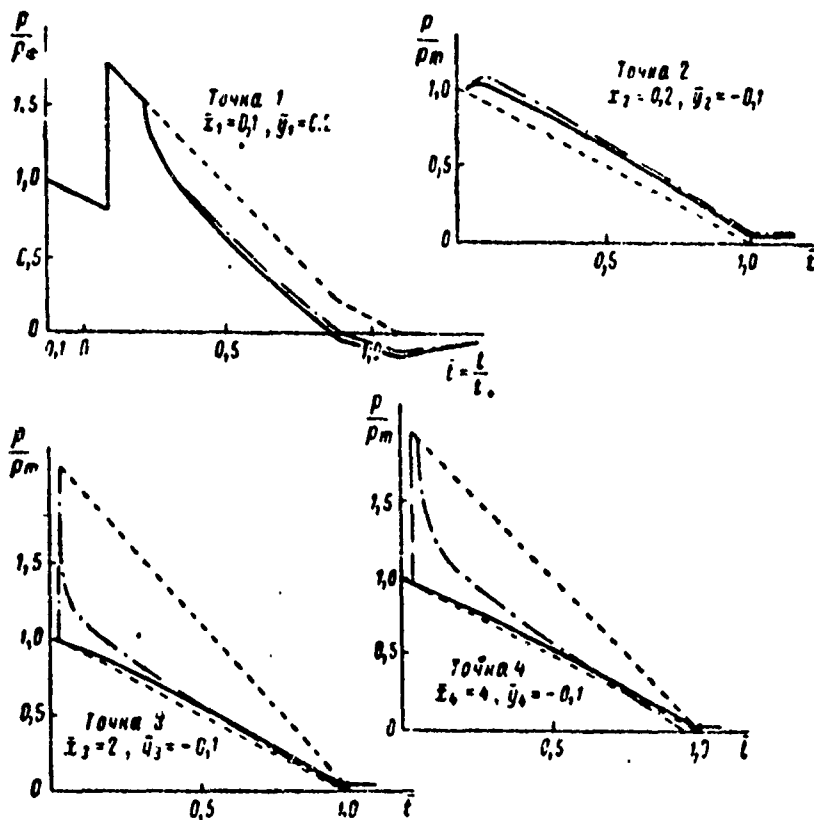


Fig. 47. Pressure Contours at Various Points in Diffraction Region by Right Angle.

or, likewise,

$$\bar{x} = \frac{x}{a_0 t_+} = \frac{x}{l}; \quad \xi = \frac{r}{a_0 t_+}. \quad (12.65)$$

where

$$\xi = 1 + \bar{x}.$$

From (12.65) specifically, it follows that in the plane of the leading edge of a wedge ($x = 0$), distortion of the direct-wave contour by a diffraction wave is possible at distances equal to the wave length $\lambda = a_0 t_+$, and to the right of the edge - at distances not exceeding $\lambda/2$.

The nature of pressure change, allowing for diffraction, is given in Fig. 47 for several points (solid lines). Pressure is plotted with a dotted line, without allowance for diffraction effects. We can see that at distances $\xi > 0.2$ (greater than 0.2λ), the effect of diffraction is negligible.

The picture changes slightly if the angle of incidence of a wave onto a rectangular wedge is greater than $\frac{\pi}{2}$ ($\gamma > \frac{\pi}{2}$), or if the wedge angle is $\beta < \frac{3}{2}\pi$ (Fig. 48). In this case, reflection will occur on both wedge corners. A second pressure peak will be formed and the pulse will increase (dotted-hatched line in Fig. 47).

The case of shear propagation of a triangular-profile wave along one side of a right angle is also of interest. The nature of pressure change for several points is given in Fig. 49. As before, for the corner of a wedge along which the wave propagates, the diffraction effect is considerable where $\xi < 0.2$ ($r < 0.2\lambda$). The diffraction wave of the "lee" region is characterized by low amplitude in comparison to the amplitude of the direct wave, the smooth increment in pressure, and the increased duration of the positive phase.

We can consequently conclude that when a wave hits an obstacle, whose dimensions considerably exceed the wave length, diffraction processes at angle points may be considered independently of each other.

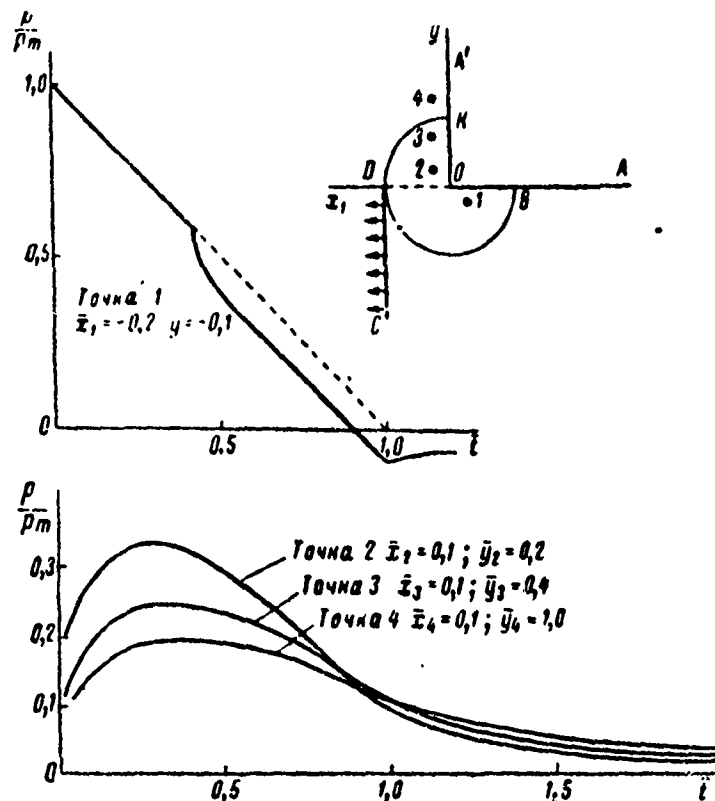


Fig. 49. Pressure Contours at Various Points in the Diffraction Region.

§13. Diffraction of a Unit Wave By a Rigid Plate.

In this section we will consider diffraction of a unit wave by a plate which is partially submerged in water and by a plate of finite width.

Diffraction of a Unit Wave of Limited Duration By a Rigid Plate Partially Submerged in Water*

Given that in a fluid T deep an absolutely rigid infinitely-long plate is submerged. The lower edge of this plate is parallel to the free surface (Fig. 50). At an angle θ , a unit-amplitude plane wave of duration τ hits this plate. We must find the pressure field by

*The results stated in this section are from K. V. Lopukhov.

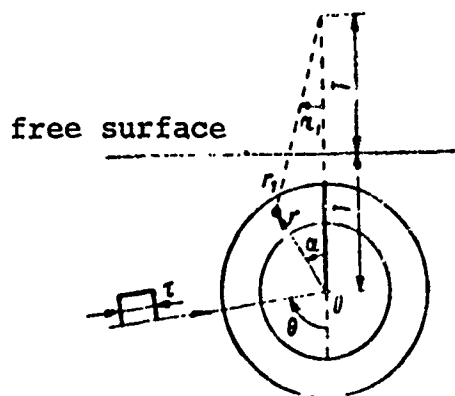


Fig. 50. Diagram of Diffraction of Underwater Shock-Wave By the Edge of a Plate Submerged in Water.

this plate.

In order to solve this problem, let us employ an earlier-derived expression for pressure in the region of diffraction during incidence of a unit-amplitude wave on a rigid wedge surface.

Assuming that $\beta = 2\pi$ in (12.45), we will find that*

$$\begin{aligned}
 p\left(\frac{r}{a}, \alpha\right) &= 1 + \frac{2}{\pi} \sum_{k=1}^{\infty} \frac{1}{k} \left[\sin\left(\frac{\pi}{2} - \frac{\gamma}{2}\right) k + \right. \\
 &\quad \left. + \sin\left(\frac{\pi}{2} + \frac{\gamma}{2}\right) k \right] \cos \frac{\alpha}{2} k e^{-\frac{k}{2} \text{Arch} \frac{a}{r}} = \\
 &= 1 + \frac{4}{\pi} \sum_{n=1}^{\infty} (-1)^{n-1} \frac{\cos \frac{2n-1}{2} \gamma \cos \frac{2n-1}{2} \alpha - \frac{2n-1}{2} \text{Arch} \frac{a}{r}}{2n-1} e^{-\frac{k}{2} \text{Arch} \frac{a}{r}}. \quad (13.1)
 \end{aligned}$$

*The result (13.1) coincides with Kharkevich's solution. In his study [21], he likewise indicates using an expression in finite form in place of (13.1).

Using Euler's formula and assuming that $\theta = \pi - \gamma$, we will write this result in the form

$$p(z, \gamma) = 1 + \frac{2}{\pi} \operatorname{Re} \sum_{n=1}^{\infty} i \frac{e^{\frac{2n-1}{2}(-z-i(\theta+\gamma))}}{2n-1} + \\ + \frac{2}{\pi} \operatorname{Re} \sum_{n=1}^{\infty} i \frac{e^{\frac{2n-1}{2}(-z-i(\theta-\gamma))}}{2n-1}, \quad (13.2)$$

where

$$z = \operatorname{Arch} \frac{a_0 l}{r}.$$

Let us designate that

$$-z - i(\theta + \gamma) = 2x, \\ -z - i(\theta - \gamma) = 2y.$$

Considering that $\operatorname{arch} e^x = \frac{1}{i} \operatorname{arctg} i e^x$, expression (13.2) can be rewritten in the form

$$p(z, \gamma) = 1 + \frac{2}{\pi} \operatorname{Re} (\operatorname{arctg} i e^x + \operatorname{arctg} i e^y). \quad (13.3)$$

After dividing the real part into (13.3) and performing simple transformations, we derive

$$p\left(\frac{a_0 l}{r}, \gamma\right) = 1 \pm \frac{1}{\pi} \operatorname{arctg} \frac{2 \sqrt{\frac{a_0 l}{r} - 1} \sin \frac{\theta}{2} \cos \frac{\alpha'}{2}}{\frac{a_0 l}{r} - 1 \pm \cos \theta - \cos \alpha'}, \quad (13.4)$$

where α' - the angle measured for points ahead of the obstacle in a counter-clockwise direction ($\alpha' = \alpha$) and for points behind the obstacle in a clockwise direction ($\alpha' = 2\pi - \alpha$); the minus corresponds to points beyond the obstacle; the plus - to points ahead of the obstacle.

Let us designate that

$$\chi(\theta, x', r, t) = \frac{1}{\pi} \arctg \frac{2 \sqrt{\frac{a_0 t}{r} - 1} \sin \frac{\theta}{2} \cos \frac{x'}{2}}{\frac{a_0 t}{r} - 1 + \cos \theta - \cos x'} \quad (13.5)$$

Then, pressure at points behind the obstacle, according to Fig. 50, will be

$$p_I = \left[z_0 \left(t - \frac{r}{a_0} \cos(x' - \theta) \right) - z_0 \left(t - \frac{r}{a_0} \right) \right] z_0(x' - \theta) + \\ + [1 - \chi(\theta, x', r, t)] z_0 \left(t - \frac{r}{a_0} \right) [z_0(x') - z_0(x' - \pi)], \quad (13.6)$$

where the first term defines pressure at a point prior to the arrival of the diffraction wave, and the second term - after its arrival.

Pressure at points ahead of the obstacle plane can be found from the equation

$$p_{II} = z_0 \left[t - \frac{r}{a_0} \cos(x' + \theta) \right] - z_0 \left(t - \frac{r}{a_0} \right) + \\ + \left[z_0 \left[t - \frac{r}{a_0} \cos(x' - \theta) \right] - z_0 \left(t - \frac{r}{a_0} \right) \right] [z_0(x') - z_0(x' - \theta)] + \\ + [1 + \chi(\theta, x', r, t)] z_0 \left(t - \frac{r}{a_0} \right) [z_0(x') - z_0(x' - \pi)]. \quad (13.7)$$

The first term of this formula defines the action of the direct wave; the second - the reflected wave; the third - pressure after convergence of the diffraction wave at the point.

Combining the expressions for p_I and p_{II} , we can derive the formula for an arbitrary point by a screen during propagation of a unit-amplitude wave having unlimited effect-time

$$p_I(t) = [1 + \chi(\theta, x, r, t)] z_0 \left(t - \frac{r}{a_0} \right) + \left[z_0 \left[t - \frac{r}{a_0} \cos(x - \theta) \right] - \right. \\ \left. - z_0 \left(t - \frac{r}{a_0} \right) \right] [z_0(x) - z_0(x - 2\pi + \theta)] + \\ + \left[z_0 \left[t - \frac{r}{a_0} \cos(x - \theta) \right] - z_0 \left(t - \frac{r}{a_0} \right) \right] [z_0(x) - z_0(x - \theta)]. \quad (13.8)$$

Let us designate this expression using $F(\theta, \alpha, r, t)$:

$$p_1(t) = F(\theta, \alpha, r, t). \quad (13.9)$$

We apparently can calculate wave effect-time by adding the solution of the unit-expansion-wave diffraction problem to (13.8). This solution can be written in the form

$$p_2(t) = -F(\theta, \alpha, r, t - \tau). \quad (13.10)$$

Thus, for a unit-wave τ in duration,

$$p(t) = p_1(t) + p_2(t) = F(\theta, \alpha, r, t) - F(\theta, \alpha, r, t - \tau). \quad (13.11)$$

The effect of the free surface can easily be evaluated by using the method of mirror reflection of sources and runoffs. Situating an imaginary source at point O (Fig. 50), for a wave reflected on a free surface we will find that

$$p_3(t) = -F(\theta, \alpha_1, r_1, t) + F(\theta, \alpha_1, r_1, t - \tau). \quad (13.12)$$

Thus, we will derive a solution of the problem formulated in the form

$$p(t) = F(\theta, \alpha, r, t) - F(\theta, \alpha, r, t - \tau) - F(\theta, \alpha_1, r_1, t) + F(\theta, \alpha_1, r_1, t - \tau). \quad (13.13)$$

An analysis of these relationships permits us to conclude that:

1. The diffraction field reduces pressure at points behind an obstacle in the "exposed" region in comparison to pressure on the direct wave. This pressure decrease becomes more significant as the angle α' is reduced.

2. At points in the "lee" region defined by the angles $\alpha' < \theta$, the pressure jump vanishes and is replaced by a gradual increment in

pressure. With an increase in the angle α' from zero to θ , the increment in pressure becomes steeper and where $\alpha' = \theta$ a pressure jump appears which remains during further increase in angle α' .

3. Pressure effect-time at points behind the obstacle may be greater than on the direct wave. This is attributed to screening by the obstacle of the direct effect of the free surface.

Diffraction of a Unit-Wave By a Rigid Plate of Finite Width

Diffraction of a unit-wave by a plate $2a$ wide was first considered by Fox [32]. He derived a precise solution in the form of an infinite series using the Kirchhoff integral and the Laplace transform. Pressure on the back side of the plate as a function of dimensionless time $\bar{t} = (a_0 t)/(2a)$ and the dimensionless coordinate $\xi = x/(2a)$ (measured from the upper edge) Fox expressed with the equation

$$\begin{aligned} p(\xi, \bar{t}) = & \sum_{n=0}^{\infty} (-1)^n [p_n(\xi, \bar{t} - \xi - n) + \\ & + p_n(1 - \xi, \bar{t} - \xi - n)], \end{aligned} \quad (13.14)$$

where

$$\begin{aligned} p_0(\xi, \gamma_0) &= \frac{2}{\pi} \operatorname{arctg} \sqrt{\frac{\gamma_0}{\xi}} \sigma_0(\gamma_0), \\ p_n(\xi, \gamma_n) &= \frac{1}{\pi} \int_0^{\gamma_n} \frac{p_{n-1}(1 - \tau, \gamma_n - 2\tau)}{\xi + \tau} \sqrt{\frac{\xi}{\tau}} d\tau, \\ \gamma_n &= \bar{t} - \xi - n. \end{aligned} \quad (13.15)$$

Based on the ideas of V. I. Smirnov, S. L. Sobolyov, and A. A. Kharkevich, this same problem was later studied by K. V. Lopukhov and V. I. Kirsanov. We will state it, following Lopukhov and Kirsanov.

Given a plane unit wave falling along the normal onto a rigid

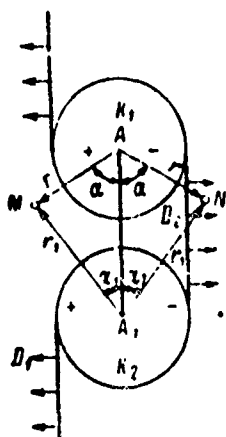


Fig. 51. Diagram of Beginning Diffraction of Shock-Wave By Plate of Finite Width.

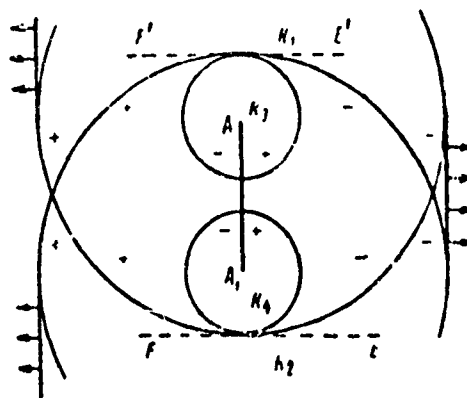


Fig. 52. Diagram of Formation of Second Pair of Diffraction Waves at Edges of Plate of Finite Width.

plate $2a$ in width. By virtue of symmetry, this is equivalent to a wave falling onto an obstacle a in height, which is fixed in a horizontal plane. At the start of this process, we will observe the wave picture shown in Fig. 51. In region D_1 , the medium is at rest. In region D_2 , two waves propagate: the direct and the reflected wave. Diffraction effects evolve in circles K_1 and K_2 (which have a radius $a_0 t$). The diffraction waves in the "lee" quadrants of circles K_1 and K_2 are compression waves; in quadrants which are symmetrical with respect to the plate's plane, they are expansion waves. The wave picture henceforth becomes complicated. The diffraction waves K_1 and K_2 , upon reaching the opposite edges of the plate are diffracted, forming waves K_3 and K_4 , etc. (Fig. 52). The left semicircles of waves K_3 and K_4 are diffracted expansion waves, and the right semicircles are compression waves; the signs of subsequent diffraction waves be alternate in pairs.

Let us consider point M , which is situated near the plate in a leeward zone and point N which is symmetrical to it (Fig. 51). Let us characterize the position of point M by the coordinates r , α and r_1 , α_1 . The association between these coordinates can be expressed by the apparent relations

$$r_1 = \sqrt{(2a)^2 + r^2 - 4a \arccos \alpha}, \quad (13.16)$$

$$\alpha_1 = \arcsin\left(\frac{r}{r_1} \sin \alpha\right). \quad (13.17)$$

The first two diffraction waves arriving at point M are also compression waves, and precisely coincide with the diffraction waves formed during normal incidence of a unit-wave onto a half-plane (onto a wedge having an angle $\beta = 2\pi$, cf. 12).

They can be evaluated with the aid of (12.38):

$$p_1(r, \alpha, t) = \left(1 - \frac{1}{\pi} \operatorname{arctg} \frac{2 \cos \frac{\alpha}{2} \sqrt{\frac{a_0 t}{r} - 1}}{\frac{a_0 t}{r} - 1 - \cos \alpha}\right) j_0\left(t - \frac{r}{a_0}\right) \quad (13.18)$$

or introducing dimensionless coordinates suggested by Fox, $\bar{t} = \frac{a_0 t}{2a}$, $\xi = \frac{r}{2a}$, with the aid of the expression

$$p_1(\xi, \alpha, \bar{t}) = \left(1 - \frac{1}{\pi} \operatorname{arctg} \frac{2 \cos \frac{\alpha}{2} \sqrt{\frac{\bar{t}}{\xi} - 1}}{\frac{\bar{t}}{\xi} - 1 - \cos \alpha}\right) j_0(\bar{t} - \xi).$$

Apparently, pressure in a diffracted compression wave arriving at point M from the edge of plate A_1 will be defined by the same formula, replacing r and α by r_1 and α_1 .

At point N we will observe diffracted expansion waves of the same magnitude as at M, but of opposite sign. Pressure in the next pair of diffracted waves can be defined without difficulty if we consider that the wave fronts K_1 and K_2 at points A_1 and A_2 are plane. The wave contours at these points, apparently, can be derived from (13.19) if we assume that $\xi = \xi_1 = 1$ ($r = r_1 = 2a$) and $\alpha = \alpha_1 = 0$, i.e.,

$$\begin{aligned} p_1(1, 0, \bar{t}_1) &= \left(1 - \frac{1}{\pi} \operatorname{arctg} \frac{2\sqrt{\bar{t}_1}}{\bar{t}_1 - 1}\right) j_0(\bar{t}_1) = \\ &= \frac{2}{\pi} \operatorname{arctg} \sqrt{\bar{t}_1} j_0(\bar{t}_1), \end{aligned} \quad (13.20)$$

where

$$\bar{t}_1 = \bar{t} - 1 = \frac{a_0 t}{2a} - 1. \quad (13.21)$$

The diffraction processes evolving at both edges of the plate are identical and therefore, it suffices to consider one of them. Because waves which are identical in amplitude but opposite in sign pass on both sides of each edge of the plate, it suffices to consider diffraction by the edge of a wave having an amplitude $2p_1$.

For diffraction of a unit-wave we formerly had [cf. (12.21)]:

$$p_1 = -\left(\frac{1}{2} - \frac{1}{\pi} \operatorname{arctg} \sqrt{\frac{1 + \cos \alpha}{\frac{a_0 t_1}{r} - 1}}\right) \sigma_0\left(t_1 - \frac{r}{a_0}\right), \quad (13.22)$$

or if we use the variables \bar{t}_1 and ξ ,

$$\begin{aligned} p_{1_0} &= -\frac{1}{\pi} \left(\frac{\pi}{2} - \operatorname{arctg} \sqrt{\frac{1 + \cos \alpha}{\frac{\bar{t}_1}{\xi} - 1}} \right) \sigma_0(\bar{t}_1 - \xi) = \\ &= -\frac{1}{\pi} \operatorname{arctg} \sqrt{\frac{1 + \cos \alpha}{\frac{\bar{t}_1}{\xi} - 1}} \sigma_0(\bar{t}_1 - \xi) = \\ &= -\frac{1}{\pi} \operatorname{arctg} B_0 \sqrt{\frac{\bar{t}_1}{\xi} - 1} \sigma_0(\bar{t}_1 - \xi), \end{aligned}$$

where

$$B_0 = \frac{1}{1 + \cos \alpha}. \quad (13.23)$$

Expression (13.23) is a transient function for deriving the diffraction field caused by the propagation of a wave $2p_1$ (with the aid of the Duhamel integral). According to (11.11),

$$p_1(\xi, \alpha, \bar{t}_1) = \int_0^{\bar{t}_1} 2p_1(1, 0, t_1) p_1(\xi, \alpha, \bar{t}_1 - t_1) dt_1 =$$

$$= \frac{2}{\pi} \left[\operatorname{arctg} \sqrt{\bar{t}_1 + \left(\frac{1}{B_0^2} - 1 \right)} + \right. \\ \left. + \operatorname{arctg} B_0 \sqrt{\frac{1}{\bar{t}} (\bar{t}_1 + 1) - 1 - \frac{\pi}{2}} \right] \alpha_0(\bar{t}_1 - \bar{t}). \quad (13.24)$$

The signs of diffracted waves alternate in pairs. Following the third and fourth expansion waves, the fifth and sixth diffracted compression waves arrive at point M from edges A and A₁ (the third pair of diffracted waves). Pressure calculation of these waves is carried out by analogy to that already completed.

Integrating the diffraction fields for a point situated behind the plate, it is possible to write (the indexes "n" and "τ" will henceforth designate the face and lee sides of the plate):

$$p_\tau(\bar{t}, \alpha, \bar{t}) = \sum_{n=1}^{\infty} (-1)^{n-1} \left[p_n(\bar{t}, \alpha, \bar{t}_{n-1}) \alpha_0(\bar{t}_{n-1} - \bar{t}) + \right. \\ \left. + p_n(\bar{t}, \alpha, \bar{t}_{n-1}) \alpha_0(\bar{t}_{n-1} - \bar{t}_1) \right]. \quad (13.25)$$

Net pressure at points ahead of the plate is composed of pressure on the direct and reflected waves, and likewise on the diffracted wave p_τ, but taken with the opposite sign from that used in (13.25):

$$p_n = \alpha_0(t - \bar{t} \sin \alpha) + \alpha_0(\bar{t} - \bar{t} \sin \alpha) - p_\tau(\bar{t}, \alpha, \bar{t}). \quad (13.26)$$

The difference in pressure at symmetrical points on the plate surface will be

$$p_n - p_\tau = 2 [\alpha_0(\bar{t}) - p_\tau]. \quad (13.27)$$

Fig. 53 shows the change in pressure for several points on the lee surface of the plate. We can easily see that the effect of the third pair of diffracted waves is small. Consequently, Lopukhov and Kirsanov suggested a limitation on consideration of pressure change in the time interval $\bar{t} < 2.5$.

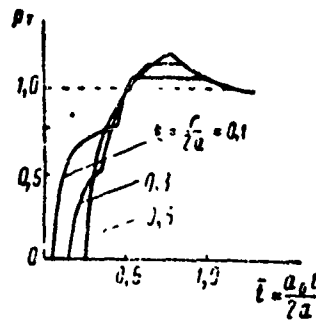


Fig. 53. Net Pressure at Various Points on Lee Side of Plate.

In problems of a practical nature, the mean load on the plate, adjusted to a unit of surface, is often of the greatest interest. We can derive its value for $\bar{t} < 2.5$ by integrating (13.25) with respect to ξ from 0 to 1 and subsequent utilization of relations (13.26) and (13.27).

Calculated findings may be approximated by the relationship

$$F_{r, cp} = \bar{t} z_0(\bar{t}) - 1.27 \left[(0.914\bar{t} - 1) \operatorname{arctg} \sqrt{\bar{t} - 1} + 0.086 \sqrt{\bar{t} - 1} \right] z_0(\bar{t} - 1). \quad (13.28)$$

Calculated thus, the mean specific pulse of the net load can be defined by the approximation

$$J_{pec, cp} = \frac{2a}{a_0} 2 \left\{ \left(\bar{t} - \frac{1}{2} \bar{t}^2 \right) z_0(\bar{t}) + 1.27 \left[(0.457\bar{t}^2 - \bar{t}) \operatorname{arctg} \sqrt{\bar{t} - 1} - (0.095\bar{t} - 0.638) \sqrt{\bar{t} - 1} \right] z_0(\bar{t} - 1) \right\}. \quad (13.29)$$

Where $\bar{t} > 2.5$, these quantities are close to their limiting values

$$\left. \begin{aligned} F_{r, cp} &= F_{n, cp} = 1, \\ F_{pec, cp} &= 0, \\ J_{pec, cp} &= \frac{\pi}{4} \frac{2a}{a_0}. \end{aligned} \right\} \quad (13.30)$$

$t < \frac{2a}{a_0}$, the picture is no different than in diffraction of a wave by a wedge [cf. (12.40)].

Pressure on a diffraction wave is

$$p_1(r, \alpha, t) = -2 + \frac{2\pi}{\beta} + \frac{1}{\pi} \sum_{i=1}^1 \operatorname{arctg} \frac{\sin \frac{\pi}{\beta} \chi_i}{e^{\frac{\pi}{\beta} \operatorname{Arch} \frac{a_0 t}{r}} - \cos \frac{\pi}{\beta} \chi_i}, \quad (13.31)$$

where

$$\chi_{1,2} = \frac{\pi}{2} \pm \alpha,$$

$$\chi_{3,4} = \frac{3\pi}{2} \pm \alpha.$$

The wave picture henceforth becomes complicated. Waves K and K', upon reaching angles A and A₁, are diffracted and form a new pair of waves; in turn, these waves will generate new diffraction disturbances after time interval $\Delta t = (2a)/(a_0)$.

As before, we can derive a solution by considering the diffraction picture during shearing of a plane wave by one of the wedge corners (§12). However, because the use of the Duhamel integral for expressions of the type (12.24) is associated with considerable mathematical difficulties, a simpler approximation is of greater advantage. The expression (12.53) which was given before can be such an approximation

$$\begin{aligned} p_1 &= -A \frac{2}{\pi} \operatorname{arctg} B \left[\sqrt{\frac{a_0 t}{r} - 1} J_0 \left(t - \frac{r}{a_0} \right) = \right. \\ &= -A \frac{2}{\pi} \operatorname{arctg} B \left[\sqrt{\frac{t}{\xi} - 1} J_0(t - \xi), \right. \end{aligned} \quad (13.32)$$

where $\bar{t} = \frac{a_0 t}{2a}$, $\xi = \frac{r}{2a}$,

$A = A(\beta)$ - the limiting value of pressure on a diffracted wave;

$B = B(\beta, \alpha)$ - the diffraction coefficient.

For the particular case of a shearing and normal incidence of

a wave, the quantities A and B are cited in Fig. 43. If we designate these coefficients A_N, B_1 (for normal incidence) and A_T, B_0 (for shearing incidence), then pressure on the opposite edge of the end-face ($\xi = 1, \alpha = 0$) for the n-th diffraction wave can be approximated by the relation

$$p_n(\xi = 1, \alpha = 0, \bar{t}_n) = (-1)^n A_N A_T^{n-1} \frac{2}{\pi} \arctg B_n \sqrt{\bar{t}_n} z_0(\bar{t}_n), \quad (13.33)$$

where

$$\bar{t}_n = t - n.$$

By analogy with (13.24), for pressure on the (n-th + 1) diffraction wave with the aid of the Duhamel integral, we will find that

$$p_{n+1}(\xi, \alpha, t_n) = (-1)^{n+1} A_N A_T^n \frac{2}{\pi} \left[\arctg B_n \sqrt{\bar{t}_n + \left(\frac{1}{B_0^2} - 1 \right) \xi} + \right. \\ \left. + \arctg B_0 \sqrt{\frac{1}{\xi} \left(\bar{t}_n + \frac{1}{B_n^2} \right) - 1 - \frac{\pi}{2}} \right]. \quad (13.34)$$

The value of coefficient B_n is found successively from the best approximation of pressure on the n-th diffraction wave by relationship (13.33) (where $\xi = 1, \alpha = 0$).

Summing waves from both edges and likewise, taking the direct and reflected waves into account, we will yield an expression for the net pressure at points situated in front of the end-face.

$$p_2(\xi, \alpha, t) = z_0(t + \xi \sin \alpha) + z_0(t - \xi \sin \alpha) + \\ + \sum_{n=1}^{\infty} \left[p_n(\xi, \alpha, t_{n-1}) z_0(t_{n-1} - \xi) + \right. \\ \left. + p_n(\xi, \alpha, \bar{t}_{n-1}) z_0(\bar{t}_{n-1} - \xi) \right]. \quad (13.35)$$

where

$$\begin{aligned} \sigma_0(\bar{t} + \xi \sin \alpha) & - \text{pressure on the direct wave;} \\ \sigma_0(\bar{t} - \xi \sin \alpha) & - \text{pressure on the reflected wave.} \end{aligned}$$

Fig. 57 shows the pressure curves at the center of the end-face ($\xi = 0.5$, $\alpha = 0$) for the three slope angles of the lateral walls.*

If we know the limiting values of pressure on each diffraction wave, we can easily find the limiting value of net pressure. Actually, if $t \rightarrow \infty$, the first pair of diffraction waves will reduce the pressure by $2A_N$, the second will increase it by $2A_N A_T$, the third will reduce it by $2A_N A_T^2$, and so forth, i.e.,

$$\begin{aligned} \lim_{t \rightarrow \infty} p_t &= 2 - 2A_N + 2A_N A_T - 2A_N A_T^2 + \dots = \\ &= \lim_{t \rightarrow \infty} 2 \left[1 - \frac{A_N}{1 + A_T} (1 - A_T^2) \right] = 2 \left(1 - \frac{A_N}{1 + A_T} \right). \end{aligned} \quad (13.36)$$

Hence, for some given values of the slope of the lateral walls, we have

where

$$\beta = \pi \quad (A_N = A_T = 0) \quad \lim p_t = 2;$$

$$\beta = \frac{7}{6} \pi \quad (A_N = 2A_T = 0.29) \quad \lim p_t = 1.50;$$

$$\beta = \frac{3}{2} \pi \quad \left(A_N = \frac{2}{3}; A_T = \frac{1}{3}; B_0 = 0.85; B_1 = 1.35; B_2 = 0.40; \right.$$

$$B_3 = 0.14; B_4 = 0.05);$$

$$\beta = \frac{8}{6} \pi \quad (A_N = 0.50; A_T = 0.25; B_0 = 0.95; B_1 = 1.65; B_2 = 0.50;$$

$$B_3 = 0.23; B_4 = 0.09);$$

$$\beta = \frac{7}{6} \pi \quad (A_N = 0.29; A_T = 0.145; B_0 = 1.10; B_1 = 2.25; B_2 = 0.65;$$

$$B_3 = 0.25; B_4 = 0.10).$$

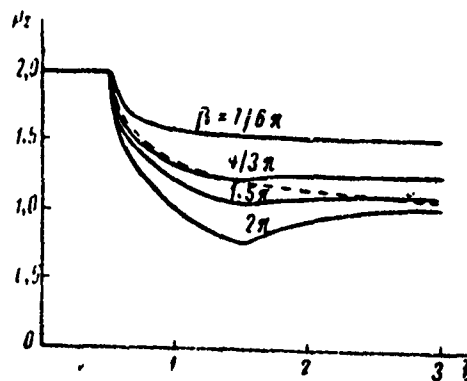


Fig. 57. Net Pressure on Mean Point on Surface of End-Face.

----- solution with aid of the integral of radiation.

$$\beta = \frac{8}{6} \pi \quad (A_N = 2A_s = 0.50) \quad \lim p_z = 1.20;$$

$$\beta = \frac{3}{2} \pi \quad (A_N = 2A_s = \frac{2}{3}) \quad \lim p_z = 1.$$

These findings attest that diffraction effects reduce initial pressure to a greater degree as the slope of the lateral walls increases. However, in contrast to an obstacle of finite dimensions, pressure is reduced to a magnitude which exceeds the pressure on a direct wave; only where $\beta = (3/2)\pi$ does it tend toward this value. We can see from (13.36) what, for practical purposes, the calculation of the first two-four pairs of diffraction waves is sufficient. It is sometimes important to evaluate the mean specific net load on the end-face. This can be done by integrating net pressures from $\xi = 0$ to $\xi = 1$.

The specific load variation curves for several values of angle β are shown in Fig. 58. We can easily see that the nature of variation in the specific load on the end-face of trapezoidal shape differs considerably from that for a plate of the same width. This distinction is of qualitative nature and is chiefly defined by the fact that at the end-face, the specific load does not drop to zero during a finite interval of time.

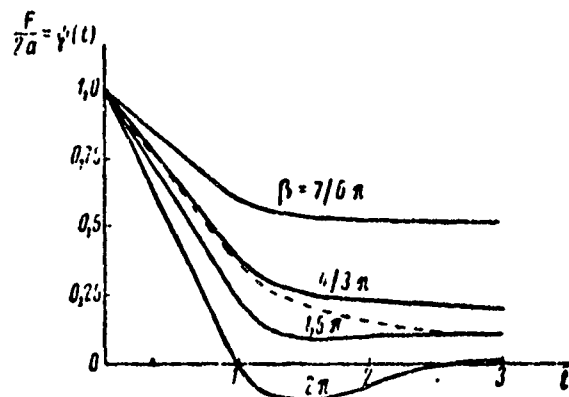


Fig. 58. Net Specific Load on End-Face.
 ----- solution with the aid of the
 integral of radiation.

§14. Hydrodynamic Forces Induced by the Progressive Motion of a Rectangular-Shaped Piston Having Rigid Walls.

The diffraction problems considered above assumed a moving wave and an immobile obstacle. The physical essence of this effect is theoretically no difference if we study a moving obstacle and the wave disturbances generated in a medium as the result of this motion. Actually, in both the first and second case we must solve a wave equation for similar boundary conditions; this is done by the same mathematical methods. This comprises the common nature between diffraction problems and problems of radiation.

The simplest case of radiation - the motion at a given velocity $v(t)$ of a plane infinite screen.

In this case, the solution of the wave equation for pressure on a plane wave will take the form:

$$p(z, t) = \rho_0 v \left(t - \frac{z}{a_0} \right) \chi_0 \left(t - \frac{z}{a_0} \right), \quad (14.1)$$

where z - motion of observation point away from the screen and time t is counted at the moment motion begins.

If the obstacle dimensions are finite, diffraction processes are formed. Where a screen is moving at a velocity which varies with respect to the unit function law, a solution of the problem of radiation totally coincides with the evaluation of the diffraction field by that same immobile obstacle with the incidence of a unit wave. This fact was clearly formulated in the works of Kharkevich and was utilized by him in his study of the radiation of a rigid screen of semi-infinite dimensions having a rectilinear edge [21].

We will begin with an examination of the problem of motion with respect to the unit function law of an infinitely-long piston (2a wide), having a plane immobile infinite wall. In this case, the use of the integral of radiation is the simplest method. The solution derived will be precise to the extent that we may consider the emergence of the piston from the wall plane to be negligible.

Because the velocity of the piston is defined by the unit function law

$$v = v_0(t), \quad (14.2)$$

the intensity of primary sources, uniformly distributed along its surface, must conform to this law.

Thus, according to (11.19), the potential at an arbitrary point in the fluid is

$$\varphi_A = \frac{1}{2\pi} \iint_S \frac{v_0(t-\tau)}{R} ds. \quad (14.3)$$

The magnitude of pressure is associated with the function of the potential by the equation

$$p = -\rho_0 \frac{\partial \varphi}{\partial t}. \quad (14.4)$$

and consequently, in our case

$$p_A = \frac{\rho_0}{2\pi} \iint_S \frac{v_0(t-\tau)}{R} dS. \quad (14.5)$$

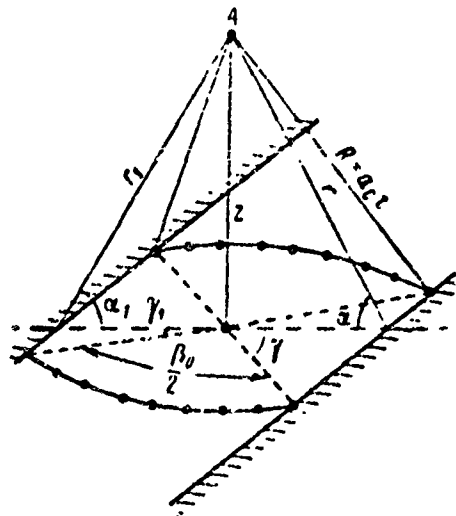


Fig. 59. Diagram of Radiation During Motion of Plane Piston.

The surface element dS can be written in the form (Fig. 59)

$$dS = R dR d\beta. \quad (14.6)$$

The quantities R and τ are associated by the relationship

$$R = a_0 \tau. \quad (14.7)$$

Thus,

$$\begin{aligned} p_A &= \frac{a_0}{2\pi} \int_0^{2\pi} \int_0^{\beta_0} z_1(t - \tau) d\beta_0 d\tau = \frac{a_0 a_0}{2\pi} \int_b^b \beta_0(\tau) z_1(t - \tau) d\tau = \\ &= \epsilon_0 a_0 \frac{\beta_0(t)}{2\pi} z_0\left(t - \frac{b}{a_0}\right), \end{aligned} \quad (14.8)$$

where b - the least distance from point A to the piston (as a function of the arrangement of point $b = z$ or $b = r$);

$\beta_0(t)$ - the sectoral angle of arrangement of primary sources in circle having the radius $R = a_0 t$;

z - distance point A is removed from the piston plane;

r - shortest distance between point A and the piston edge.

We can see from (14.8) that the problem reduces to an evaluation

of $\beta_0(t)$ or likewise, $\beta_0(R)$. Let us first discuss the case where the observation point A is situated in front of the piston (Fig. 59). It is apparent that where $\frac{z}{a_0} < t < \frac{r}{a_0}$ ($\gamma < r_1$), disturbances will arrive at the point of observation simultaneously from all sources situated in a circle having the radius $\sqrt{(a_0 t)^2 - z^2}$. The angle is $\beta_0 = 2\pi$. Consequently, where $t < \frac{r}{a_0}$

$$p = \rho_0 a_0^2 \left(t - \frac{z}{a_0} \right). \quad (14.9)$$

This finding corresponds to the case of motion of an infinite piston. Point A still "has not sensed" the finite dimensions of the piston.

Where $t > \frac{r}{a_0}$ (but $t < \frac{r_1}{a_0}$), the sector of distribution of radiation points will be less than 2π by the angle γ (Fig. 59) and will be equal to

$$\gamma = 2 \arccos \frac{r \cos \alpha}{\sqrt{(a_0 t)^2 - (r \sin \alpha)^2}}, \quad (14.10)$$

i.e.,

$$\beta_0 = 2\pi - 2 \arccos \frac{\cos \alpha}{\sqrt{\left(\frac{a_0 t}{r}\right)^2 - \sin^2 \alpha}}, \quad (14.11)$$

where

$$\alpha = \arcsin \frac{z}{r}. \quad (14.12)$$

Thus, where $\frac{r_1}{a_0} > t > \frac{r}{a_0}$

$$p = \rho_0 a_0^2 \left[1 - \frac{1}{\pi} \arccos \frac{\cos \alpha}{\sqrt{\left(\frac{a_0 t}{r}\right)^2 - \sin^2 \alpha}} \right] a_0 \left(t - \frac{r}{a_0} \right). \quad (14.13)$$

Where $t > \frac{r_1}{a_0}$, the sector is further reduced by the angle γ_1

(Fig. 59)

$$\left. \begin{aligned} \gamma_1 &= 2 \arccos \frac{\cos \alpha_1}{\sqrt{\left(\frac{a_0 t}{r_1}\right)^2 - \sin^2 \alpha_1}} \\ \alpha_1 &= \arcsin \frac{z}{r_1} \end{aligned} \right\} \quad (14.14)$$

Combining the derived evaluations for pressure at a point situated in front of a moving piston, we will find that

$$\begin{aligned} \frac{1}{\rho_0 u_0} p(r, \alpha, t) = & \\ = \sigma_0 \left(t - \frac{z}{a_0} \right) - \frac{1}{\pi} \arccos \frac{\cos \alpha}{\sqrt{\left(\frac{a_0 t}{r}\right)^2 - \sin^2 \alpha}} \sigma_0 \left(t - \frac{r}{a_0} \right) - & \\ - \frac{1}{\pi} \arccos \frac{\cos \alpha_1}{\sqrt{\left(\frac{a_0 t}{r_1}\right)^2 - \sin^2 \alpha_1}} \sigma_0 \left(t - \frac{r_1}{a_0} \right). & \end{aligned} \quad (14.15)$$

The first term of (14.15) is the pressure of radiation for motion of an infinite plane screen; the second and third terms characterize the diffraction waves formed at its edges.

On the piston surface ($z = 0, \alpha = \alpha_1 = 0$)

$$\begin{aligned} \frac{1}{\rho_0 u_0} p(r, 0, t) = \sigma_0(t) - \frac{1}{\pi} \arccos \frac{r}{a_0 t} \sigma_0 \left(t - \frac{r}{a_0} \right) - & \\ - \frac{1}{\pi} \arccos \frac{2a - r}{a_0 t} \sigma_0 \left(t - \frac{2a - r}{a_0} \right). & \end{aligned} \quad (14.16)$$

With the aid of (14.16), we can easily calculate the net specific load acting on the piston:

$$\frac{F}{2a} = \rho_0 a_0 \psi(t) = \frac{1}{2a} \int_0^{2a} p(r, 0, t) dr =$$

$$= \rho_0 a_0 \left[\sigma_0(t) - \frac{2}{2a\pi} \int_0^{2a} \arccos \frac{r}{a_0 t} \sigma_0 \left(t - \frac{r}{a_0} \right) dr \right]. \quad (14.17)$$

The value of the integral

$$J_1 = \int_0^{2a} \arccos \frac{r}{a_0 t} \sigma_0 \left(t - \frac{r}{a_0} \right) dr$$

is

easy to find if bear in mind the properties of the unit function $\sigma_0 \left(t - \frac{r}{a_0} \right)$; and namely, where $t < \frac{2a}{a_0}$

$$J_1 = \int_0^{a_0 t} \arccos \frac{r}{a_0 t} dr = a_0 t; \quad (14.18)$$

where $t > \frac{2a}{a_0}$

$$J_1 = \int_0^{2a} \arccos \frac{r}{a_0 t} dr = a_0 t + 2a \arccos \frac{2a}{a_0 t} - \sqrt{(a_0 t)^2 - 4a^2}. \quad (14.19)$$

If we utilize the previous designation for dimensionless time $\bar{t} = \frac{a_0 t}{2a}$, then combining the results of (14.17)-(14.19) will yield

$$\psi(\bar{t}) = \begin{cases} 1 - \frac{2}{\pi} \bar{t} & \text{where } \bar{t} < 1 \\ 1 - \frac{2}{\pi} \left(\bar{t} + \arccos \frac{1}{\bar{t}} - \sqrt{\bar{t}^2 - 1} \right) & \text{where } \bar{t} > 1. \end{cases} \quad (14.20)$$

The result of (14.20) coincides with solutions derived by other methods by Kh. A. Rakhmatulin, D. A. Aleksandrin, I. L. Mironov, I. G. Novoselov, and D. V. Zamyshlyayev. In the given case, the use of the integral of radiation more rapidly and more simply leads to the goal.

Let us now study the more complex case of motion of a rectangular piston of finite dimensions. In order to explain the basic physical features of this process, let us first consider a semi-infinite screen

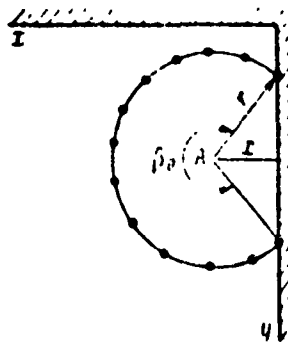


Fig. 60. Diagram of Radiation in Region of Angle during Motion of a Plane Piston.

having two mutually-perpendicular rigid side walls (Fig. 60). As before, let us consider that the screen moves according to the unit discontinuity function law

$$v = \sigma_0(t). \quad (14.21)$$

For points situated on the surface of the screen, according to (14.8), we will have

$$p = \frac{\rho_0 a_0}{2\pi} \beta_0(t) \sigma_0(t). \quad (14.22)$$

While $r = a_0 t$ is less than the distances between point A and the wall edge ($r < x$, $r < y$, Fig. 60), the angle $\beta_0 = 2\pi$. When $x < r < y$, the angle β_0 is reduced by the quantity

$$\gamma_1 = 2 \arccos \frac{x}{r} = 2 \arccos \frac{x}{a_0 t},$$

and where $y < r < \sqrt{x^2 + y^2}$ further reduced by the quantity

$$\gamma_2 = 2 \arccos \frac{y}{r} = 2 \arccos \frac{y}{a_0 t}.$$

Pressure at point A, where $r < \sqrt{x^2 + y^2}$ is

$$\frac{p}{\rho_0 a_0} = 1 - \frac{1}{\pi} \arccos \frac{x}{a_0 t} \sigma_0 \left(t - \frac{x}{a_0} \right) - \frac{1}{\pi} \arccos \frac{y}{a_0 t} \sigma_0 \left(t - \frac{y}{a_0} \right). \quad (14.23)$$

As soon as the quantity r becomes greater than the distance between the point of observation and the angle ($r > \sqrt{x^2 + y^2}$), the angle β_0 becomes equal to

$$\beta_0 = \frac{3}{2} \pi - \arccos \frac{x}{r} - \arccos \frac{y}{r}.$$

For this range,

$$\frac{1}{\rho_0 a_0} p = \left(\frac{3}{4} - \frac{1}{2\pi} \arccos \frac{x}{a_0 t} - \frac{1}{2\pi} \arccos \frac{y}{a_0 t} \right) a_0 \left(t - \frac{\sqrt{x^2 + y^2}}{a_0} \right). \quad (14.24)$$

The solution of (14.23) and (14.24) can be written as the sum of the unit-amplitude direct wave and the diffraction waves formed at the edges; therefore, to determine pressure on diffraction waves, we only have to subtract one from (14.23) and (14.24). Then,

where $t < \frac{\sqrt{x^2 + y^2}}{a_0}$

$$\begin{aligned} \frac{1}{\rho_0 a_0} p_1 = & -\frac{1}{\pi} \left[\arccos \frac{x}{a_0 t} a_0 \left(t - \frac{x}{a_0} \right) + \right. \\ & \left. + \arccos \frac{y}{a_0 t} a_0 \left(t - \frac{y}{a_0} \right) \right], \end{aligned} \quad (14.25)$$

where $t > \frac{\sqrt{x^2 + y^2}}{a_0}$

$$\begin{aligned} \frac{1}{\rho_0 a_0} p_2 = & -\frac{1}{2\pi} \left(\arccos \frac{x}{a_0 t} + \right. \\ & \left. + \arccos \frac{y}{a_0 t} + \frac{\pi}{2} \right) a_0 \left(t - \frac{\sqrt{x^2 + y^2}}{a_0} \right). \end{aligned} \quad (14.26)$$

It is convenient to separate the pressure component from the last equation: this component takes the effect of screen-edge finiteness into account. We only have to subtract (14.25) from (14.26) for this purpose.

Thus,

$$\begin{aligned} \frac{1}{c_0 a_0} p_3 = \frac{1}{2\pi} \left(\arccos \frac{x}{a_0 t} + \right. \\ \left. + \arccos \frac{y}{a_0 t} - \frac{\pi}{2} \right) \sigma_0 \left(t - \frac{\sqrt{x^2 + y^2}}{a_0} \right). \end{aligned} \quad (14.27)$$

The derived relationships permit us to evaluate the pressure fields during the motion of a rectangular piston of finite dimensions having sides $2a$ and $2b$. In this case, the net pressure can be written as the sum of the waves generated by the motion of an infinite plate; and the diffraction waves formed at each edge and at each angle:

$$\begin{aligned} \frac{1}{c_0 a_0} p(x, y, t) = 1 - p_1(x, t) - p_1(2a - x, t) - p_2(y, t) - \\ - p_2(2b - y, t) + p_3(x, y, t) + p_3(2a - x, y, t) + \\ + p_3(x, 2b - y, t) + p_3(2a - x, 2b - y, t), \end{aligned} \quad (14.28)$$

where

$$p_1(x, t) = \frac{1}{\pi} \arccos \frac{x}{a_0 t} \sigma_0 \left(t - \frac{x}{a_0} \right), \quad (14.29)$$

$$p_2(y, t) = \frac{1}{\pi} \arccos \frac{y}{a_0 t} \sigma_0 \left(t - \frac{y}{a_0} \right), \quad (14.30)$$

$$\begin{aligned} p_3(x, y, t) = \frac{1}{2\pi} \left(\arccos \frac{x}{a_0 t} + \right. \\ \left. + \arccos \frac{y}{a_0 t} - \frac{\pi}{2} \right) \sigma_0 \left(t - \frac{\sqrt{x^2 + y^2}}{a_0} \right). \end{aligned} \quad (14.31)$$

It follows from (14.28)-(14.31) that as soon as all the diffraction waves arrive at a point, the pressure on the point vanishes.

Let us find the net load acting upon the piston. For this purpose, let us integrate (14.28) with respect to the piston surface.

In view of the problem's symmetry, we can write

$$\begin{aligned}
 F(t) &= S_{\rho_0} \rho_0 \psi(t) = F_0 \psi(t), \\
 \psi(t) &= \frac{1}{S} \int_0^{2a} \int_0^{2b} [1 - 2\rho_1(x, t) - 2\rho_2(y, t) + 4\rho_3(x, y, t)] dx dy = \\
 &= 1 - \frac{2}{\pi} \frac{1}{2a} J_1 - \frac{2}{\pi} \frac{1}{2b} J_2 + \frac{2}{\pi} \frac{1}{2a2b} J_3 - \frac{1}{2a2b} J_4,
 \end{aligned} \tag{14.32}$$

where

$$J_1 = \int_0^{2a} \arccos \frac{x}{a_0 t} \sigma_0 \left(t - \frac{x}{a_0} \right) dx, \tag{14.33}$$

$$J_2 = \int_0^{2b} \arccos \frac{y}{a_0 t} \sigma_0 \left(t - \frac{y}{a_0} \right) dy, \tag{14.34}$$

$$J_3 = \int_0^{2a} \int_0^{2b} \left(\arccos \frac{x}{a_0 t} + \arccos \frac{y}{a_0 t} \right) \sigma_0 \left(t - \frac{\sqrt{x^2 + y^2}}{a_0} \right) dx dy, \tag{14.35}$$

$$J_4 = \int_0^{2a} \int_0^{2b} \sigma_0 \left(t - \frac{\sqrt{x^2 + y^2}}{a_0} \right) dx dy. \tag{14.36}$$

Calculation of integrals (14.33)-(14.36) is not difficult. Let us perform a replacement of the variables $z = \frac{x}{a_0 t} = \frac{\lambda}{2a\bar{t}}$.

Where $t < \frac{2a}{a_0}$, ($\bar{t} < 1$)

$$J_1 = \int_0^{a_0 t} \arccos \frac{x}{a_0 t} dx = 2a\bar{t} \int_0^1 \arccos z dz = 2a\bar{t}; \tag{14.37}$$

Where $t > \frac{2a}{a_0}$ ($\bar{t} > 1$)

$$\begin{aligned}
 J_1 &= \int_0^{2a} \arccos \frac{x}{a_0 t} dx = 2a\bar{t} \int_{\frac{1}{\bar{t}}}^1 \arccos z dz = \\
 &= 2a \left(\bar{t} + \arccos \frac{1}{\bar{t}} - \sqrt{\bar{t}^2 - 1} \right).
 \end{aligned} \tag{14.38}$$

By total analogy,

where $t < \frac{2b}{a_0} \left(\bar{t} < \frac{1}{n} \right) *$

$$J_2 = 2a\bar{t}, \quad (14.39)$$

where $t > \frac{2b}{a_0} \left(\bar{t} > \frac{1}{n} \right)$

$$J_2 = \frac{2a}{n} \left[n\bar{t} + \arccos \frac{1}{n\bar{t}} - \sqrt{(n\bar{t})^2 - 1} \right]. \quad (14.40)$$

For the integral J_3 where $\bar{t} < 1$

$$\begin{aligned} J_3 &= \int_0^{a_0 t} \arccos \frac{x}{a_0 t} dx \int_0^{\sqrt{(a_0 t)^2 - x^2}} dy + \int_0^{a_0 t} \arccos \frac{y}{a_0 t} dy \int_0^{\sqrt{(a_0 t)^2 - y^2}} dx = \\ &= 2(2a\bar{t})^2 \int_0^1 \sqrt{1-z^2} \arccos z dz = \frac{1}{2} (2a\bar{t})^2 \left(1 + \frac{\pi^2}{3} \right)^{**}; \end{aligned} \quad (14.41)$$

where $1 < \bar{t} < \frac{1}{n}$

$$\begin{aligned} J_3 &= \int_0^{2a} \arccos \frac{x}{a_0 t} dx \int_0^{\sqrt{(a_0 t)^2 - x^2}} dy + \int_0^{2a} \arccos \frac{y}{a_0 t} dy \int_0^{\sqrt{(a_0 t)^2 - 2a^2}} dx + \\ &+ \int_{\sqrt{(a_0 t)^2 - 2a^2}}^{a_0 t} \arccos \frac{y}{a_0 t} dy \int_0^{\sqrt{(a_0 t)^2 - y^2}} dx = \end{aligned}$$

*For the convenience of transcription, here and henceforth the ratio of sides a/b will be designated using n .

$$\begin{aligned} &^{**} \int \sqrt{1-z^2} \arccos z dz = \frac{1}{2} (z \sqrt{1-z^2} + \arcsin z) \arccos z + \\ &+ \frac{1}{2} \int \frac{z \sqrt{1-z^2} + \arcsin z}{1-z^2} dz = \frac{1}{2} z \sqrt{1-z^2} + \frac{1}{2} \arccos z \arcsin z + \\ &+ \frac{1}{4} z^2 + \frac{1}{2} \int \arcsin z d \arcsin z = \frac{1}{2} \left[z \sqrt{1-z^2} \arccos z + \right. \\ &\left. + \arcsin z \arccos z + \frac{1}{2} (\arcsin z)^2 + \frac{1}{2} z^2 \right]. \end{aligned}$$

$$\begin{aligned}
&= (2a\bar{i})^2 \int_0^{\frac{1}{\bar{i}}} \sqrt{1-z^2} \arccos z dz + (2a)^2 \bar{i} \int_0^{\sqrt{1-\frac{1}{\bar{i}^2}}} \arccos z dz + \\
&\quad + (2a\bar{i})^2 \int_{\sqrt{1-\frac{1}{\bar{i}^2}}}^1 \sqrt{1-z^2} \cdot \arccos z dz = \\
&= (2a)^2 \left[\frac{\pi}{4} \sqrt{\bar{i}^2-1} - \frac{1}{2} + \bar{i} + \frac{\pi}{4} \bar{i}^2 \arcsin \frac{1}{\bar{i}} \right]; \quad (14.42)
\end{aligned}$$

where $\frac{1}{n} < \bar{i} < \sqrt{1 + \frac{1}{n^2}}$

$$\begin{aligned}
J_3 &= \int_0^{\sqrt{(a,t)^2 - (2a)^2}} \arccos \frac{x}{a,t} dx \int_0^{2a} dy + \int_{\sqrt{(a,t)^2 - (2a)^2}}^{2a} \arccos \frac{x}{a,t} dx \int_0^{\sqrt{(a,t)^2 - x^2}} dy + \\
&\quad + \int_0^{\sqrt{(a,t)^2 - (2a)^2}} \arccos \frac{y}{a,t} dy \int_0^{2a} dx + \int_{\sqrt{(a,t)^2 - (2a)^2}}^{2a} \arccos \frac{y}{a,t} dy \int_0^{\sqrt{(a,t)^2 - y^2}} dx = \\
&= (2a)^2 \frac{\bar{i}}{n} \int_0^{\sqrt{1 - \left(\frac{1}{n\bar{i}}\right)^2}} \arccos z dz + (2a)^2 \bar{i}^2 \int_{\sqrt{1 - \left(\frac{1}{n\bar{i}}\right)^2}}^{\frac{1}{\bar{i}}} \sqrt{1-z^2} \arccos z dz + \\
&\quad + (2a)^2 \bar{i} \int_0^{\sqrt{1 - \frac{1}{\bar{i}^2}}} \arccos z dz + (2a)^2 \bar{i}^3 \int_{\sqrt{1 - \frac{1}{\bar{i}^2}}}^{\frac{1}{n\bar{i}}} \sqrt{1-z^2} \arccos z dz = \\
&= (2a)^2 \left\{ \frac{\pi}{4} \left[\sqrt{\bar{i}^2-1} + \frac{1}{n\bar{i}} \sqrt{(n\bar{i})^2-1} + \bar{i}^2 \arcsin \frac{1}{\bar{i}} + \right. \right. \\
&\quad \left. \left. + \bar{i}^2 \arcsin \frac{1}{n\bar{i}} \right] + \bar{i} + \frac{\bar{i}}{n} - \frac{1}{2} \left(1 + \frac{1}{n^2} + \bar{i}^2 + \bar{i}^2 \frac{\pi^2}{4} \right) \right\}. \quad (14.43)
\end{aligned}$$

For the integral of J_4 where $\bar{t} < 1$

$$J_4 = \int_0^{\frac{a}{t}} dx \int_0^{\sqrt{(a/t)^2 - x^2}} dy = \int_0^{\frac{a}{t}} \sqrt{(a/t)^2 - x^2} dx = \\ = \frac{1}{2} (a/t)^2 \arcsin 1 = \frac{\pi}{4} (2a)^2 \bar{t}^2; \quad (14.44)$$

where $1 < \bar{t} < \frac{1}{n}$

$$J_4 = \int_0^{\frac{a}{t}} dx \int_0^{\sqrt{(a/t)^2 - x^2}} dy = (2a)^2 \frac{1}{2} \left(\sqrt{\bar{t}^2 - 1} + \bar{t}^2 \arcsin \frac{1}{\bar{t}} \right); \quad (14.45)$$

where $\frac{1}{n} < \bar{t} < \sqrt{1 + \frac{1}{n^2}}$

$$J_4 = \int_0^{\sqrt{(a/t)^2 - (2b)^2}} 2b dx + \int_{\sqrt{(a/t)^2 - (2b)^2}}^{\frac{2a}{t}} \sqrt{(a/t)^2 - x^2} dx = \\ = (2a)^2 \frac{1}{2} \left[\sqrt{\bar{t}^2 - 1} + \bar{t}^2 \arcsin \frac{1}{\bar{t}} + \frac{1}{n^2} \sqrt{(n\bar{t})^2 - 1} - \bar{t}^2 \arcsin \sqrt{1 - \frac{1}{(n\bar{t})^2}} \right]. \quad (14.46)$$

Collecting the derived evaluations and performing transformations, we will find that:*

$$\psi(\bar{t}) = \begin{cases} 1 - \frac{2}{\pi} (1+n) \bar{t} + \frac{n}{\pi} \bar{t}^2 & \text{where } \bar{t} < 1 \\ 1 - \frac{n}{\pi} - \frac{2}{\pi} \bar{t} - \frac{2}{\pi} \arccos \frac{1}{\bar{t}} + \frac{2}{\pi} \sqrt{\bar{t}^2 - 1} & \text{where } 1 < \bar{t} < \frac{1}{n} \\ 1 - \frac{1}{\pi} \left(n + \frac{1}{n} \right) - \frac{2}{\pi} \left(\arccos \frac{1}{\bar{t}} + \arccos \frac{1}{n\bar{t}} \right) + \\ + \frac{2}{\pi} \left[\sqrt{\bar{t}^2 - 1} + \sqrt{(n\bar{t})^2 - 1} \right] - \frac{n}{\pi} \bar{t}^2 & \text{where } \frac{1}{n} < \bar{t} < \sqrt{1 + \frac{1}{n^2}}. \end{cases} \quad (14.47)$$

*I. L. Mironov obtained a similar result using a Fourier-Bessel integral.

The varied form of transcribing the function $\psi(t)$ on a piston of finite dimensions for diverse time intervals is easily attributed to physical concepts. Where $\bar{t} < 1$, diffraction waves do not yet encompass the entire piston surface. In the interval $1 < \bar{t} < \frac{1}{n}$ diffraction waves succeeded in running along the short side of the piston, but did not succeed in running the entire length. At moment $t = \sqrt{1 + (1/n^2)}$, diffraction processes terminate. Pressure at an arbitrary point on the piston vanishes. In the particular case $n = 0$ ($b \rightarrow \infty$), from (14.47) we find the previously fixed relationship (14.20) for an infinitely-long piston.

There is, however, a theoretical difference between (14.20) and (14.47). In the motion of an infinitely-long piston, the net load approaches zero only where $\bar{t} \rightarrow \infty$, whereas for a piston of finite dimensions $\psi(\bar{t}) \equiv 0$ where $\bar{t} \geq \sqrt{1 + (1/n^2)}$.

We can easily expand the derived solution to motion of a piston according to an arbitrary law. In this case, using the Duhamel integral, we find that:

$$p(t) = p_0(t) W(0) + \int_0^t W(t-\tau) p_0(\tau) d\tau, \quad (14.48)$$

$$\left. \begin{aligned} F(t) &= F_0(t) W(0) + \int_0^t W(t-\tau) F_0(\tau) d\tau, \\ F_0 &= F_0(t), \end{aligned} \right\} \quad (14.49)$$

where $p_0(t)$, $F_0(t)$ - transient functions [solution of problem for motion according to the law $\sigma_0(t)$];

$W(t)$, $\dot{W}(t)$, and $\ddot{W}(t)$ - piston motion, velocity, and acceleration.

Let us study expression (14.49) in greater detail. Assuming $W(0) = \dot{W}(0) = 0$, we derive

$$F(t) = F_0 \int_0^t W(t-\tau) \dot{\psi}(\tau) d\tau, \quad (14.50)$$

or, integrating by parts twice,

$$F(t) = F_0 W(t) \psi(0) + F_0 \dot{W}(t) \psi'(0) + F_0 \int_0^t \ddot{W}(t-\tau) \psi''(\tau) d\tau. \quad (14.51)$$

Expression (14.51) can be calculated quite simply for the time interval in which function $\psi(t)$ is linear. Thus, for an infinitely long piston, according to (14.20), where $\bar{t} < 1$, $\psi(\bar{t}) = 1 - \frac{2}{\pi} \bar{t}$. In this case

$$\begin{aligned} \psi(0) &= 1, \\ \psi'_t &= -\frac{2}{\pi} \frac{a_0}{2a} = -\frac{a_0}{\pi a}, \\ \psi''_t &= 0, \end{aligned}$$

and for the net load we will find that

$$F(t) = 2a_0 a_0 \ddot{W}(t) - \frac{2a_0^2}{\pi} \dot{W}(t). \quad (14.52)$$

As we mentioned earlier, for a piston of finite dimensions, the function $\psi(t) \equiv 0$ if $t > t^*$, where

$$t^* = \frac{\sqrt{4a^2 + 4b^2}}{a_0} = \frac{2a}{a_0} \sqrt{1 + \frac{1}{n^2}}.$$

Consequently,

$$F(t) = \begin{cases} F_0 \int_0^t \ddot{W}(t-\tau) \psi(\tau) d\tau & t < t^* \\ F_0 \int_0^{t^*} \ddot{W}(t-\tau) \psi(\tau) d\tau & t > t^*. \end{cases} \quad (14.53)$$

If in some interval of time Δt acceleration of the piston undergoes little change, then for it

$$F_1(t) = \ddot{W}(t) F_0 \int_0^{t^*} \psi(\tau) d\tau. \quad (14.54)$$

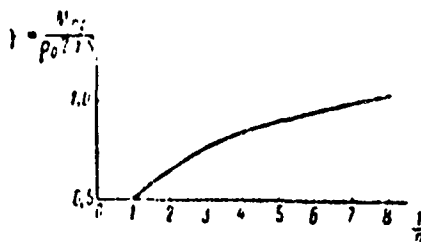


Fig. 61. The Coefficient of Apparent Mass, for Motion of a Rectangular Piston, As A Function of the Relationship of the Sides $n = a/b$.

The same expression can be derived for an arbitrary moment in time if we consider the liquid to be incompressible. Actually, where $a_0 \rightarrow \infty$, $t^* \rightarrow 0$; as a result of a limiting process in (14.53), we again get (14.54).

The coefficient, where the magnitude of acceleration is $W(t)$,

$$F_0 \int_0^t \psi(\tau) d\tau = M_{app}$$

is known in hydrodynamics as apparent mass.

Thus, for the present a result has been derived for the particular example. It is of interest from three points of view. Most of all, it becomes clear that the wave nature of diffraction processes accompanying the motion of bodies in a compressible fluid must be taken into account for only a fixed time interval; after that interval elapses, it suffices to consider the non-steady state with the aid of apparent mass. Hence, it turns out that if we solve the problem of evaluating net load acting upon a body during its motion in a fluid according to the unit function law, we likewise solve the problem of determining apparent mass. This method sometimes is simpler than the classical method. For the considered problem, the relation of the coefficient of apparent mass as a function of the ratio of sides of a rectangle is shown in Fig. 61. If, on the other hand, we know the apparent mass of a body, we can make some judgment on its initial period of motion where the diffraction processes are considerable. All these ideas will be developed subsequently.

§15. Pressure Field During Progressive Motion of Circular-Shaped Piston. General Concepts on Solving Diffraction Problems with the Aid of the Integral of Radiation.

The problem of motion of a circular-shaped piston was first studied by Kharkevich. It was later studied in various formulations by I. L. Mironov, D. A. Aleksandrin, as well as by the authors of this book.

Let us first consider a piston having absolutely rigid walls, moving at a velocity

$$v = v_0(t). \quad (15.1)$$

Using the integral of radiation and reiterating the arguments of the preceding section, we derive pressure at an arbitrary point in the form

$$p_A = \frac{2a_0}{2\pi} \beta_0(t) v_0\left(t - \frac{b}{a_0}\right), \quad (15.2)$$

where b - the shortest distance between point A and the piston.

If the projection of point A falls on the piston (Fig. 62), then during the time interval $z/a_0 < t < R_1/a_0$, the angle $\beta_0 = 2\pi$ and consequently, $p = \rho_0 a_0$. At the moment in time $t = R_2/a_0$, disturbances from the most distant elementary sources will reach the point of observation and pressure will vanish.

Thus,

$$p_A = \rho_0 a_0 \left\{ v_0\left(t - \frac{z}{a_0}\right) - v_0\left(t - \frac{R_1}{a_0}\right) + \frac{1}{2\pi} \beta_0(t) \left[v_0\left(t - \frac{R_1}{a_0}\right) - v_0\left(t - \frac{R_2}{a_0}\right) \right] \right\}. \quad (15.3)$$

In order to determine $\beta_0(t)^*$, let us consider a triangle whose

*Since $R = a_0 t$, a determination of $\beta(t)$ is equivalent to determining $\beta(R)$.

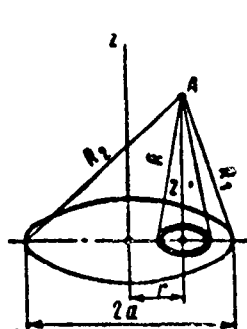


Fig. 62. On Evaluating Pressure at a Point Projected onto a Moving Round Piston.

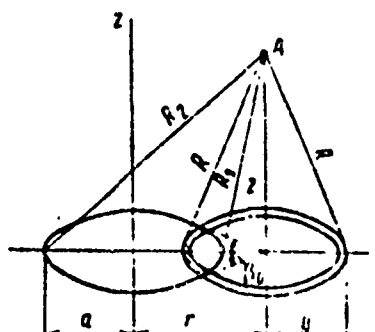


Fig. 63. On Evaluating Pressure at a Point Not Projected onto a Round Piston.

angles are the center of a piston, the projection of point A, and the point of intersection of the circle having a radius $\sqrt{R^2 - z^2}$ with the edge of the piston (Fig. 63).

We have

$$a^2 = r^2 + (\sqrt{R^2 - z^2})^2 - 2r\sqrt{R^2 - z^2} \cdot \cos \frac{1}{2} \varphi_0,$$

where r and z - coordinates of the point of observation, whence

$$\varphi_0(R) = 2 \arccos \frac{r^2 - a^2 + R^2 - z^2}{2r\sqrt{R^2 - z^2}} \quad (15.4)$$

or, taking into consideration that $R = a_0 t$, and using dimensionless coordinates,

$$\begin{aligned} \bar{r} &= \frac{r}{a}; \quad \bar{z} = \frac{z}{a}; \quad \bar{t} = \frac{a_0 t}{a}, \\ \varphi_0(\bar{t}) &= 2 \arccos \frac{\bar{r}^2 - \bar{z}^2 - 1 + \bar{t}^2}{2\bar{r}\sqrt{\bar{t}^2 - \bar{z}^2}}. \end{aligned} \quad (15.5)$$

We can easily prove that relationship (15.5) remains valid for the case where point A is not projected onto the piston surface. In this case, pressure can be found according to the formula

$$p_A = \rho_0 a_0 \frac{1}{2\pi} \varphi_0(\bar{t}) [z_0(\bar{t} - \bar{R}_1) - \sigma_0(\bar{t} - \bar{R}_2)], \quad (15.6)$$

where

$$\left. \begin{aligned} \bar{R}_1 &= \frac{R_1}{a} = \sqrt{z^2 + (\bar{r}-1)^2} \\ \bar{R}_2 &= \frac{R_2}{a} = \sqrt{z^2 + (\bar{r}+1)^2} \end{aligned} \right\} \quad (15.7)$$

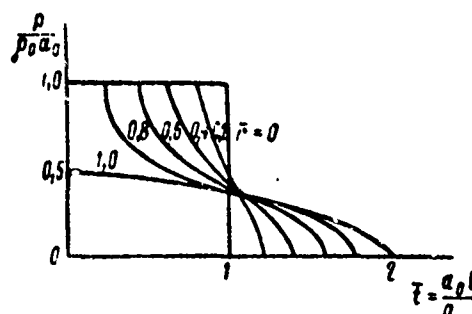


Fig. 64. Net Pressure at Various Points on Surface of Round Piston.

At points on a piston ($z = 0$, $r \leq 1$), according to (15.3), (15.5), and (15.6), pressure is

$$\begin{aligned} p(\bar{r}, \bar{t}) &= \rho_0 a_0 \left\{ \sigma_0(\bar{t}) - \sigma_0(\bar{t} + \bar{r} - 1) + \right. \\ &\quad \left. + \frac{1}{\pi} \arccos \frac{\bar{t}^2 + \bar{r}^2 - 1}{2\bar{r}\bar{t}} [\sigma_0(\bar{t} + \bar{r} - 1) - \sigma_0(\bar{t} - \bar{r} - 1)] \right\}. \end{aligned} \quad (15.8)$$

Pressure variation for several points is shown in Fig. 64, taken from [21].

Let us find the net load acting upon the piston. For this purpose, let us integrate (15.8) with respect to the piston area

$$F(\bar{t}) = \int_S p(\bar{r}, \bar{t}) dS. \quad (15.9)$$

Because $dS = 2\pi r dr$, then

$$F(\bar{t}) = 2\pi \int_0^1 p(\bar{r}, \bar{t}) r dr. \quad (15.10)$$

Let us introduce the function $\psi(\bar{t})$, which is associated with function $F(\bar{t})$ by the equation

$$F(\bar{t}) = \pi a^2 \rho_0 a_0 \psi(\bar{t}). \quad (15.11)$$

We then derive

$$\psi(\bar{t}) = \frac{2}{a^2 \rho_0 a_0} \int_0^a p(\bar{r}, \bar{t}) r dr. \quad (15.12)$$

Using the dimensionless variable $\bar{r} = r/a$, and in view of (15.8), the integral of (15.12) will be rewritten in the form

$$\begin{aligned} \psi(\bar{t}) = 2 \left[\sigma_0(\bar{t}) \int_0^1 \bar{r} d\bar{r} - \int_0^1 \sigma_0(\bar{t} + \bar{r} - 1) \bar{r} d\bar{r} + \right. \\ \left. + \frac{1}{\pi} \int_0^1 \arccos \frac{\bar{t}^2 + \bar{r}^2 - 1}{2\bar{r}\bar{t}} \sigma_0(\bar{t} + \bar{r} - 1) \bar{r} d\bar{r} - \right. \\ \left. - \frac{1}{\pi} \int_0^1 \arccos \frac{\bar{t}^2 - \bar{r}^2 - 1}{2\bar{r}\bar{t}} \sigma_0(\bar{t} - \bar{r} - 1) \bar{r} d\bar{r} \right]. \end{aligned} \quad (15.13)$$

Taking the properties of the discontinuity function of zero order into account, we have

$$\begin{aligned} \psi(\bar{t}) = \frac{(\bar{t}-1)^2}{2} [\sigma_0(\bar{t}) - \sigma_0(\bar{t}-1)] + \frac{1}{\pi} [\sigma_0(\bar{t}) - \sigma_0(\bar{t}-1)] \times \\ \times \int_{\bar{t}-1}^1 \arccos \frac{\bar{t}^2 + \bar{r}^2 - 1}{2\bar{r}\bar{t}} \bar{r} d\bar{r} + \frac{1}{\pi} [\sigma_0(\bar{t}-1) - \sigma_0(\bar{t}-2)] \times \\ \times \int_{\bar{t}-1}^1 \arccos \frac{\bar{t}^2 + \bar{r}^2 - 1}{2\bar{r}\bar{t}} \bar{r} d\bar{r}. \end{aligned} \quad (15.14)$$

The indefinite integral

$$J_1 = \int \arccos \frac{\bar{t}^2 + \bar{r}^2 - 1}{2\bar{r}\bar{t}} \bar{r} d\bar{r}$$

is taken by parts:

$$\begin{aligned}
J_1 &= \frac{\bar{r}^2}{2} \arccos \frac{\bar{r}^2 + \bar{r}^2 - 1}{2\bar{r}\bar{i}} - \frac{1}{2} \int \frac{|\bar{r} - \bar{i}(\bar{r} - 1)| d\bar{r}}{\sqrt{-(\bar{r} - 1)^2 + 2\bar{r}^2(\bar{r} + 1) - \bar{r}^4}} \\
&= \frac{1}{2} \bar{r}^2 \arccos \frac{\bar{r}^2 + \bar{r}^2 - 1}{2\bar{r}\bar{i}} + \frac{1}{2} \arcsin \frac{\bar{r}^2 - 1 - \bar{r}^2}{2\bar{i}} - \\
&\quad - \frac{1}{4} \sqrt{-(\bar{r} - 1)^2 + 2\bar{r}^2(\bar{r} + 1) - \bar{r}^4}.
\end{aligned} \tag{15.15}$$

Hence,

$$\begin{aligned}
J_1(\bar{r} = 1) &= \frac{1}{2} \arccos \frac{\bar{i}}{2} + \frac{1}{2} \arcsin \left(-\frac{\bar{i}}{2} \right) - \\
&\quad - \frac{\bar{i}}{2} \sqrt{1 - \left(\frac{\bar{i}}{2} \right)^2} = \arccos \frac{\bar{i}}{2} - \frac{\pi}{4} - \frac{\bar{i}}{2} \sqrt{1 - \left(\frac{\bar{i}}{2} \right)^2}, \\
J_1(\bar{r} = 1 - \bar{i}) &= \frac{\pi}{2} (1 - \bar{i})^2 - \frac{\pi}{4}, \\
J_1(\bar{r} = \bar{i} - 1) &= -\frac{\pi}{4}.
\end{aligned}$$

Combining the derived results, we will find that

$$\psi(\bar{i}) = \frac{2}{\pi} \left[\arccos \frac{\bar{i}}{2} - \frac{\bar{i}}{2} \sqrt{1 - \left(\frac{\bar{i}}{2} \right)^2} \right] [\alpha_0(\bar{i}) - \alpha_0(\bar{i} - 2)]. \tag{15.16}$$

The nature of variation of function $\psi(\bar{i})$ is shown in Fig. 65. As in the previously considered problem on a rectangular piston, the greatest net load is observed at the initial moment of time. It subsequently falls abruptly and is equal to zero after the run time of a wave having the same diameter as the piston. After this period of time has elapsed, the motion of a piston having constant velocity encounters no resistance from the medium.

The result obtained with the aid of the Duhamel integral can be expanded to motion of a piston according to an arbitrary law. By analogy with (14.50) for zero initial data [$W(0) = \dot{W}(0) = 0$], we can write

$$F(t) = F_0 \int_0^t W(t - \tau) \psi(\tau) d\tau, \tag{15.17}$$

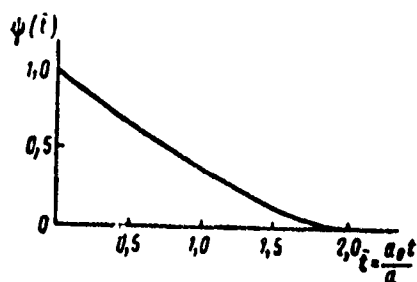


Fig.65. Change in Net Load Acting on a Round Piston During Motion According to the Unit Function Law.

or integrating twice by parts,

$$F(t) = F_0 W(t) + F_0 \psi'(0) W(t) + F_0 \int_0^t W(t-\tau) \psi''(\tau) d\tau. \quad (15.18)$$

However,

$$\begin{aligned} \psi'_t(\bar{t}) &= -\frac{2}{\pi} \sqrt{1 - \frac{\bar{t}^2}{4}} \cdot \frac{a_0}{a} [\sigma_0(\bar{t}) - \sigma_0(\bar{t} - 2)] = \\ &= -\frac{2a_0}{\pi a} \sqrt{1 - \left(\frac{a_0 \bar{t}}{2a}\right)^2} \left[\sigma_0(t) - \sigma_0\left(t - \frac{2a}{a_0}\right) \right], \end{aligned} \quad (15.19)$$

$$\psi''_t(t) = \frac{a_0^3}{2\pi a^3} \cdot \frac{t}{\sqrt{1 - \left(\frac{a_0 t}{2a}\right)^2}} \left[\sigma_0(t) - \sigma_0\left(t - \frac{2a}{a_0}\right) \right]. \quad (15.20)$$

Thus, for the net load we will have:

where $t < \frac{2a}{a_0}$

$$F(t) = \pi a^2 \rho_0 a_0 \dot{W}(t) - 2\rho_0 a_0^2 a W(t) + \frac{\rho_0 a_0^4}{2a} \int_0^t \frac{W'(t-\tau) \tau d\tau}{\sqrt{1 - \left(\frac{a_0 \tau}{2a}\right)^2}}; \quad (15.21)$$

where $t > \frac{2a}{a_0}$

$$F(t) = \pi a^2 \rho_0 a_0 \dot{W}(t) - 2\rho_0 a_0^2 a W(t) + \frac{\rho_0 a_0^4}{2a} \int_0^{\frac{2a}{a_0}} \frac{W'(t-\tau) \tau d\tau}{\sqrt{1 - \left(\frac{a_0 \tau}{2a}\right)^2}}. \quad (15.22)$$

In study [26], function $F(t)$ was derived in the form

$$F = 2a^2 a_0 \rho_0 \left[\frac{\pi}{2} \dot{W}(t) - \frac{a_0}{a} W(t) + \right. \\ \left. + \frac{a_0}{a} \int_0^{\frac{\pi}{2}} W\left(t - \frac{2a}{a_0} \sin \varphi\right) a_0 \left(t - \frac{2a}{a_0} \sin \varphi\right) \sin \varphi d\varphi \right]. \quad (15.23)$$

We can easily show that the replacement of the variables $\tau = (2a)/(a_0) \sin \phi$ reduces formula (15.23) to (15.22) and the results coincide.

We mentioned earlier that the integral of the function $F_0 \psi(t)$, within limits from zero to $t^* = (2a)/(a_0)$, produces the value of apparent mass. In view of (15.11) and (15.16), we find that:

$$M_{ap} = \pi a^2 \rho_0 a_0 \frac{a}{a_0} \int_0^{\frac{2}{\pi}} \left[\arccos \frac{\tau}{2} - \frac{\tau}{2} \sqrt{1 - \left(\frac{\tau}{2}\right)^2} \right] d\tau = \frac{8}{3} \rho_0 a^3.$$

As we well know, apparent mass during progressive motion of a disc is equal to precisely this quantity. However, in the case of motion of a thin disc, this quantity characterizes the total load on both sides of the disc; while in the case of motion of a round piston, only the load on its front side.

The problems considered permit us to make some general remarks on the possibility of utilizing the integral of radiation in the study of diffraction effects. The chief requirement is for "direct visibility" from the point of observation to the elementary source of radiation. Consequently, the plane must be the radiating surface. We must have defined premises on the distribution of sources on the surface of closure. These premises are always hypothetical because boundary conditions permit us to establish the intensity of sources only on the surface of the body. With the aid of the integral of radiation we can derive a precise solution only for the half-space in front of a plane moving piston or screen having a rigid immobile

wall of finite dimensions. Not one of the actually encountered diffraction problems can be reduced to this formulation.

As we mentioned earlier, when utilizing the integral of radiation, the intensity of sources distributed on the surface of a body is selected so that the normal velocity component of the net field on this surface is equal to zero. The surface of closure has special features: it is "transparent" for the direct wave, but at the same time does not pass disturbance propagation radiated by the sources situated on the facial surface of the obstacle.

Inasmuch as no actual surfaces have these features, a fixed error occurs. Moreover, the use of the integral of radiation often permits us to most simply derive a final result. For this reason, the evaluation of diffraction problem solution error with the aid of the integral of radiation becomes important.

Let us make an evaluation for several particular cases. In §12 we considered the incidence of a unit-amplitude wave along the normal to one corner of a wedge. The solution of a basically similar problem was derived in §14 with the aid of the integral of radiation [cf. (14.13)].

The pressure diffraction-component was equal to

$$p_1\left(\frac{r}{a_0 t}, \alpha\right) = -\frac{1}{\pi} \arccos \frac{\cos \alpha}{\sqrt{\left(\frac{a_0 t}{r}\right)^2 - \sin^2 \alpha}} \cdot \tau_0\left(t - \frac{r}{a_0}\right). \quad (15.24)$$

For points situated on the surface of the obstacle ($\alpha = 0$),

$$p_1\left(\frac{r}{a_0 t}, 0\right) = -\frac{1}{\pi} \arccos \frac{r}{a_0 t} \cdot \tau_0\left(t - \frac{r}{a_0}\right). \quad (15.25)$$

Fig. 66. shows the results of comparing this solution with the precise solution for various wedge angles. We can see that a satisfactory convergence of findings only occurs where $\beta = (4/3)\pi$. An

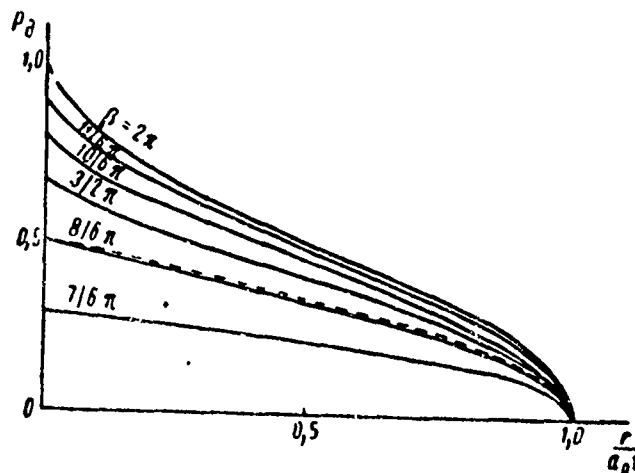


Fig. 66. Pressure Change in Diffraction Waves Formed on the Edge of an Angle During Normal Incidence of a Unit-Wave on One of the Edges of that Angle.

————— precise solution,
 ----- solution with the aid of the integral
 of radiation.

assumption on the motion of a piston having a semi-infinite wall was equivalent to normal incidence of a wave onto a wedge having an internal angle of $(4/3)\pi$.

As our second example, let us take the case of incidence of a unit-wave along the normal onto a rigid end-face of trapezoidal shape (§13). The analog to this is motion of an infinitely-long piston having a rigid wall (§14).

The calculated results of specific load and pressure on the central point of a piston [cf. formulas (14.15) and (14.20)] as compared with the corresponding data of §13 are cited in Fig. 67. As can be seen from the drawing, for the initial period of motion ($\bar{t} < 1.5$), a solution with the aid of the integral of radiation almost coincides with the calculation for $\beta = (4/3)\pi$, and subsequently tends toward $\beta = (3/2)\pi$.

Thus, we can conclude that in analyzing diffraction problems, the use of the integral of radiation leads to correct qualitative conclusions. Quantitative evaluations, however, can be very approximate.

The best convergence of results occurs in the study of diffraction by the flat end-faces of elongated bodies having lateral walls which are perpendicular to the end-faces. The greatest error occurs in calculations for plates.

§16. Diffraction of a Spherical Wave by the End-Face of a Semi-Infinite Rigid Round Cylinder.

The conversion from diffraction of plane waves by an obstacle to diffraction of a spherical wave is associated with mathematical difficulties. Therefore, the primary features of this process will be explained using the simplest example of the flow-around of the end-face of a semi-infinite rigid round cylinder by a spherical wave. To evaluate the hydrodynamic fields, let us employ the integral of radiation. As we mentioned, this method is the simplest method, because it eliminates repeated diffraction waves from consideration. Moreover, in view of the assertions of the preceding section, this method should not produce appreciable error in quantitative evaluations.

As we know, the potential characterizing the propagation of a direct wave during spherically-symmetric motion can be written in the form

$$\varphi = -\frac{f(\bar{i} - \bar{R})}{\bar{R}} z_0(\bar{i} - \bar{R}), \quad (16.1)$$

where, for convenience, we introduce the dimensionless coordinates $\bar{R} = R/a$, $\bar{i} = \frac{a_0 t}{a}$ (a - the radius of the end-face).

The magnitude of the normal component in the plane of the obstacle is

$$\begin{aligned} \frac{v_n}{a_n} = \bar{v}_n &= \frac{\partial \bar{i}}{\partial n} = \frac{\partial \bar{i}}{\partial \bar{R}} \frac{\partial \bar{R}}{\partial n} = \\ &= \frac{z_n}{a \bar{R}} \left\{ \frac{f(\bar{i} - \bar{R}) z_0(\bar{i} - \bar{R})}{\bar{R}^2} - \frac{\frac{d}{d\bar{R}} [f(\bar{i} - \bar{R}) z_0(\bar{i} - \bar{R})]}{\bar{R}} \right\}. \end{aligned} \quad (16.2)$$

The boundary value condition will be satisfied if hydrodynamic sources are arranged at points on the surface of the end-face so that the additional velocity of fluid particles induced by these sources is equal in magnitude, but opposite in the sign of velocity; velocity is defined by the relationship (16.2). We can achieve similar results with the aid of the integral of radiation, which in this case is conveniently written in the form

$$\bar{v}_A = -\frac{1}{2\pi} \int_0^{\bar{z}} \int_0^{\bar{r}} \frac{v_n(\bar{r} - \bar{R}^*)}{\bar{R}^*} \bar{r} d\bar{r} d\bar{z}, \quad (16.3)$$

where \bar{R} - the distance between an arbitrary point on the surface of the end-face and point A.

Considering a case of axial symmetry, we find on the basis of (16.2) that

$$\begin{aligned} \bar{v}_A = & -\bar{z}_0 \int_0^1 \frac{f(\bar{r} - \bar{R} - \bar{R}^*)}{\bar{R}^* \bar{R}^*} \bar{z}_0 (\bar{r} - \bar{R} - \bar{R}^*) \bar{r} d\bar{r} + \\ & + \bar{z}_0 \int_0^1 \frac{d}{d(\bar{R} + \bar{R}^*)} \frac{|f(\bar{r} - \bar{R} - \bar{R}^*) \bar{z}_0 (\bar{r} - \bar{R} - \bar{R}^*)|}{\bar{R}^* \bar{R}^*} \bar{r} d\bar{r}. \end{aligned} \quad (16.4)$$

Let us introduce the substitution

$$\begin{aligned} \bar{R} + \bar{R}^* &= x, \\ \bar{R} &= \sqrt{\bar{r}^2 + \bar{z}_0^2}, \quad \bar{R}_0 = \sqrt{1 + \bar{z}_0^2}; \\ \bar{R}^* &= \sqrt{\bar{r}^2 + \bar{z}^2}, \quad \bar{R}_0^* = \sqrt{1 + \bar{z}^2}. \end{aligned}$$

Then,

$$\begin{aligned} \left(\frac{\bar{r}}{\bar{R}} + \frac{\bar{r}}{\bar{R}^*} \right) d\bar{r} &= \frac{\bar{r} x d\bar{r}}{\bar{R} \bar{R}^*} = dx, \\ \frac{\bar{r} d\bar{r}}{\bar{R} \bar{R}^*} &= \frac{1}{x} dx; \quad \frac{1}{x} = \frac{1}{\bar{R} + \bar{R}^*} = \frac{\bar{R} - \bar{R}^*}{\bar{z}_0^2 - \bar{z}^2}, \\ \bar{r} d\bar{r} &= \bar{R} \bar{R}^* \frac{\bar{R} - \bar{R}^*}{\bar{z}_0^2 - \bar{z}^2} dx, \end{aligned}$$

$$\begin{aligned}
\frac{\bar{z}_0^2 - \bar{z}^2}{x} &= \bar{R} - \bar{R}^*; \quad \frac{\bar{z}_0^2 - \bar{z}^2}{x} + x = 2\bar{R}, \\
\bar{z}_0^2 - \bar{z}^2 + x^2 &= 2\bar{R}x, \quad (\bar{z}_0^2 - \bar{z}^2 + x^2)^2 = 4\bar{R}^2 x^2; \\
\bar{R}^2 &= \frac{(\bar{z}_0^2 - \bar{z}^2 + x^2)^2}{4x^2}, \\
J_0 &= \int_0^1 \frac{f(\bar{i} - \bar{R} - \bar{R}^*)}{\bar{R}^2 \bar{R}^*} \sigma_0(\bar{i} - \bar{R} - \bar{R}^*) \bar{r} d\bar{r} = \\
&= \int_{\bar{z}_0 + \bar{z}^*}^{\bar{R}_0 + \bar{R}_0^*} \frac{f(\bar{i} - x)}{\bar{R}^2 \bar{R}^*} \sigma_0(\bar{i} - x) \bar{R} \bar{R}^* \frac{dx}{x} = \int_{\bar{z}_0 + \bar{z}^*}^{\bar{R}_0 + \bar{R}_0^*} \frac{f(\bar{i} - x)}{\bar{R}^2} \sigma_0(\bar{i} - x) \frac{dx}{x} = \\
&= 4 \int_{\bar{z}_0 + \bar{z}^*}^{\bar{R}_0 + \bar{R}_0^*} \frac{f(\bar{i} - x) \sigma_0(\bar{i} - x)}{(\bar{z}_0^2 - \bar{z}^2 + x^2)^2} x dx. \tag{16.5}
\end{aligned}$$

By complete analogy,

$$\begin{aligned}
J_1 &= \int_0^1 \frac{d}{d(R^* : R)} \frac{[f(\bar{i} - \bar{R} - \bar{R}^*) \sigma_0(\bar{i} - \bar{R} - \bar{R}^*)]}{\bar{R}^2 \bar{R}^*} \bar{r} d\bar{r} = \\
&= 2 \int_{\bar{z}_0 + \bar{z}^*}^{\bar{R}_0 + \bar{R}_0^*} \frac{\frac{d}{dx} [f(\bar{i} - x) \sigma_0(\bar{i} - x)]}{\bar{z}_0^2 - \bar{z}^2 + x^2} dx. \tag{16.6}
\end{aligned}$$

Thus, the potential at point A is

$$\begin{aligned}
\varphi_A &= -4\bar{z}_0 \int_{\bar{z}_0 + \bar{z}^*}^{\bar{R}_0 + \bar{R}_0^*} \frac{f(\bar{i} - x) \sigma_0(\bar{i} - x)}{(\bar{z}_0^2 - \bar{z}^2 + x^2)^2} x dx + \\
&+ 2\bar{z}_0 \int_{\bar{z}_0 + \bar{z}^*}^{\bar{R}_0 + \bar{R}_0^*} \frac{\frac{d}{dx} [f(\bar{i} - x) \sigma_0(\bar{i} - x)]}{\bar{z}_0^2 - \bar{z}^2 + x^2} dx. \tag{16.7}
\end{aligned}$$

Integration by parts yields

$$\varphi_A = 2\bar{z}_0 \frac{f(\bar{i} - x) \sigma_0(\bar{i} - x)}{\bar{z}_0^2 - \bar{z}^2 + x^2} \Big|_{\bar{z}_0 + \bar{z}^*}^{\bar{R}_0 + \bar{R}_0^*}$$

or, using previous designations,

$$\varphi_A = -2\bar{z}_0 \left[\frac{f(\bar{t} - \bar{z}_0 - \bar{z}^*) \varphi_0(\bar{t} - \bar{z}_0 - \bar{z}^*)}{2\bar{z}_0(\bar{z}_0 + \bar{z}^*)} - \right. \\ \left. - \frac{f(\bar{t} - \sqrt{1 + \bar{z}_0^2} - \sqrt{1 + \bar{z}^{*2}})}{2\sqrt{1 + \bar{z}_0^2}(\sqrt{1 + \bar{z}_0^2} + \sqrt{1 + \bar{z}^{*2}})} \times \right. \\ \left. \times \varphi_0(\bar{t} - \sqrt{1 + \bar{z}_0^2} - \sqrt{1 + \bar{z}^{*2}}) \right]. \quad (16.8)$$

If we add direct-wave potential to the potential of (16.8) and use a certain relationship $p = -\rho_0 \frac{\partial \phi}{\partial t}$, we derive the magnitude of pressure at points lying on the axis of symmetry:

$$\rho(0, z^*, \bar{t}) = \frac{\rho_0 \omega_0}{a} \left\{ \frac{1}{\bar{z}_0 - \bar{z}^*} \frac{\partial}{\partial t} [f(\bar{t} - \bar{z}_0 - \bar{z}^*) \varphi_0(\bar{t} - \bar{z}_0 - \bar{z}^*)] + \right. \\ \left. + \frac{1}{\bar{z}_0 + \bar{z}^*} \frac{\partial}{\partial t} [f(\bar{t} - \bar{z}_0 - \bar{z}^*) \varphi_0(\bar{t} - \bar{z}_0 - \bar{z}^*)] - \right. \\ \left. - \frac{\bar{z}_0}{\sqrt{1 + \bar{z}_0^2}(\sqrt{1 + \bar{z}_0^2} + \sqrt{1 + \bar{z}^{*2}})} \frac{\partial}{\partial t} \times \right. \\ \left. \times [f(\bar{t} - \sqrt{1 + \bar{z}_0^2} - \sqrt{1 + \bar{z}^{*2}}) \times \right. \\ \left. \times \varphi_0(\bar{t} - \sqrt{1 + \bar{z}_0^2} - \sqrt{1 + \bar{z}^{*2}})] \right\}. \quad (16.9)$$

The first two terms of equation (16.9) correspond to the case of an infinite obstacle. They define the direct and reflected waves. The third term describes the expansion wave formed by the edge of the obstacle. The diffraction wave picture is shown in Fig. 67.

The solution of this same problem under the assumption of the incompressibility of a medium is of interest. Final formulas can be derived in this case both as a result of the limiting process in relations (16.8), (16.9) toward an infinitely-great speed of sound, and by means of direct consideration of the potential

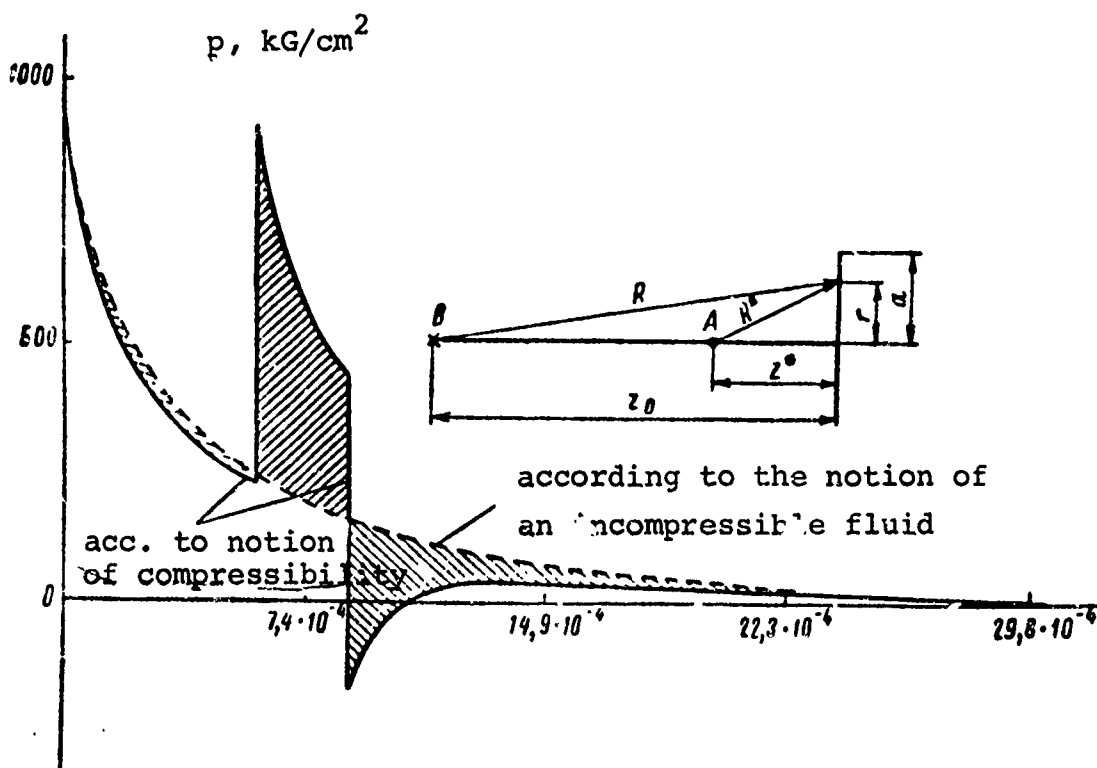


Fig. 67. Nature of Variation in Pressure During Explosion, Allowing for a Rigid End-Face, According to the Notions of an Incompressible and Compressible Fluid.

$$\varphi_A = -\frac{f(\bar{r})}{R}. \quad (16.10)$$

The integral of radiation (16.3) is consequently written in the form

$$\varphi_A = -\frac{1}{2\pi} \int_0^{2\pi} \int_0^1 \frac{\bar{z}_0 f(\bar{r})}{\bar{R}^3 \bar{R}^*} \bar{r} d\bar{r} d\bar{\varphi}. \quad (16.11)$$

This integral is taken in finite form if point A lies on the z axis. After simple transformations we will find that

$$\varphi(0, \bar{z}^*) = -f(\bar{r}) \frac{\bar{z}^* \sqrt{1 + \bar{z}_0^2} - \bar{z}_0 \sqrt{1 + \bar{z}^{*2}}}{(\bar{z}^{*2} - \bar{z}_0^2) \sqrt{1 + \bar{z}_0^2}}. \quad (16.12)$$

Because $p = -\rho_0 \frac{\partial \phi}{\partial t}$, we come to the conclusion that the presence of an obstacle of finite dimensions in a fluid causes a proportional

change in the magnitude of pressure at a given point. The coefficient of proportionality is a function only of the geometric characteristics of the problem.

Fig. 67 shows the results of comparing pressure according to the notion of fluid incompressibility and compressibility. We can easily see that the net pulse is identical in both cases. The assumption of incompressibility of a medium is in full agreement with the physical essence of the hypothesis, and produces only a slight redistribution in pressures. This fact permits us to apply, in individual cases (where the net pulse is a deciding factor), a simpler notion of fluid incompressibility for approximate calculations.

The evaluation of pressure magnitudes at an arbitrary point in space runs into deeper problems. This problem can be solved, for the present, only for a plane wave (cf. §15).

For direct comparison, it suffices to multiply the solution of (15.3) by the constant quantity $1/(\rho_0 a_0)$ and add direct-wave pressure. Then we will find that

$$\begin{aligned} p(\bar{r}, \bar{z}', \bar{t}) = & z_0(\bar{t} + \bar{z}') + z_0(\bar{t} - \bar{z}') - z_0(\bar{t} - \bar{R}_1) + \\ & + \frac{1}{2\pi} \oint_0(\bar{t}) [z_0(\bar{t} - \bar{R}_1) - z_0(\bar{t} - \bar{R}_2)] \end{aligned} \quad (16.13)$$

where, as before,

$$\oint_0(\bar{t}) = 2 \arccos \frac{\bar{r}^2 - \bar{z}'^2 - 1 + \bar{t}^2}{2\bar{r} \sqrt{\bar{r}^2 - \bar{z}'^2}}, \quad (15.5)$$

$$\begin{aligned} \bar{R}_1 &= \sqrt{\bar{z}'^2 + (\bar{r} - 1)^2} && - \text{distance to nearest edge of end-face;} \\ \bar{R}_2 &= \sqrt{\bar{z}'^2 + (\bar{r} + 1)^2} && - \text{distance to most distant edge of the} \\ &&& \text{end-face.} \end{aligned}$$

Because (16.8) and (16.9) are valid for a wave of arbitrary shape, and we are most interested in an exponential wave, let us

write the pressure in the case of incidence of a wave along the normal (an exponentially-profiled wave), transforming (16.13) with the aid of the Duhamel integral: where $\bar{r} < 1$

$$\begin{aligned}
 p(\bar{r}, \bar{z}^*, \bar{t}) = & p_m e^{-\frac{1}{\theta}(\bar{t} + \bar{z}^*)} \sigma_0(\bar{t} + \bar{z}^*) + p_m e^{-\frac{1}{\theta}(\bar{t} - \bar{z}^*)} \sigma_0(\bar{t} - \bar{z}^*) - \\
 & - p_m e^{-\frac{1}{\theta}(\bar{t} - \bar{R}_1)} \sigma_0(\bar{t} - \bar{R}_1) + p_m \frac{\beta_0(\bar{t})}{2\pi} [\sigma_0(\bar{t} - \bar{R}_1) - \sigma_0(\bar{t} - \bar{R}_2)] - \\
 & - \frac{p_m}{2\pi\theta} e^{-\frac{\bar{t}}{\theta}} \int_{\bar{R}_1}^{\bar{R}_2} e^{-\frac{\bar{\tau}}{\theta}} \beta_0(\bar{\tau}) \sigma_0(\bar{t} - \bar{\tau})' d\bar{\tau},
 \end{aligned}
 \tag{16.14}$$

where p_m - maximum pressure on the direct-wave front; $\theta = \frac{a_0 \theta}{a}$ - the dimensionless exponential damping constant.

As in formula (16.9), the first term of (16.14) expresses a direct wave and the second - a reflected wave. The three latter terms define an expansion wave propagating from the edge of the end-face. This wave arrives at point A at time $\bar{t} = \bar{R}_1$ (point E in Fig. 68). In the interval $\bar{R}_1 < \bar{t} < \bar{R}_2$, elementary expansion waves converge upon point A first with greater, then with lesser, and then with greater intensity (section of contour EF in Fig. 68). Where $\bar{t} > \bar{R}_2$, the unsteady flow continues a while longer, being nonuniformly determined by damping disturbances proceeding from the edges of the obstacles. In proportion to the approach of point \bar{r} to the center, slope EF approaches the vertical. Ultimately, where $\bar{r} = 0$ ($\bar{R}_1 = \bar{R}_2$) formula (16.14) acquires the form

$$\begin{aligned}
 p(0, \bar{z}^*, \bar{t}) = & p_m \left[e^{-\frac{\bar{t} + \bar{z}^*}{\theta}} \sigma_0(\bar{t} + \bar{z}^*) + e^{-\frac{\bar{t} - \bar{z}^*}{\theta}} \sigma_0(\bar{t} - \bar{z}^*) - \right. \\
 & \left. - e^{-\frac{\bar{t} - \bar{R}_0}{\theta}} \sigma_0(\bar{t} - \bar{R}_0) \right].
 \end{aligned}
 \tag{16.15}$$

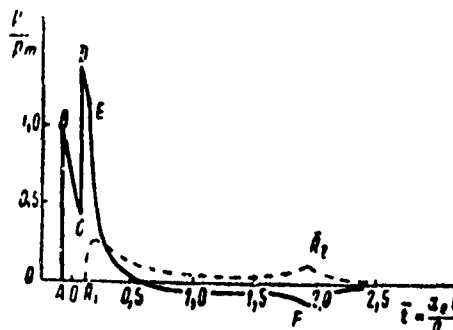


Fig. 68. Net Pressure at Points Situated Symmetrically In Front of and Behind a Disc $\bar{z} = 0.08$, $\bar{r} = 0.92$, during Normal Incidence of an Exponentially-Shaped Wave $\bar{\theta} = 0.02$ onto Said Disc.

—— in front of disc;
 ----- behind disc.

Also important is the case of a wave falling at an arbitrary angle. However, the study of this problem is considerably more complex than for normal incidence, because the disturbance arrival-time at a given point will be a function of the formation time of elementary sources on the surface of the obstacle (in addition to geometric parameters).

This problem was first considered by Lopukhov. Omitting the operations and reasoning, let us cite several of his findings.

Fig. 69 shows a comparison of pressure contours at a given point for normal and oblique incidence of a plane wave. We can easily see that the nature of the contour is retained. The reflected wave front arrives from a point which is displaced with respect to the geometric center. Pressure variation resulting from diffraction occurs more smoothly.

In the case of diffraction of a wave by a disc, as we said earlier, the precision of theoretical evaluations is reduced. However, it would be useful to give some data for a qualitative description. Thus, with the aid of the integral of radiation we can easily calculate pressure at points behind the disc. According to the prin-

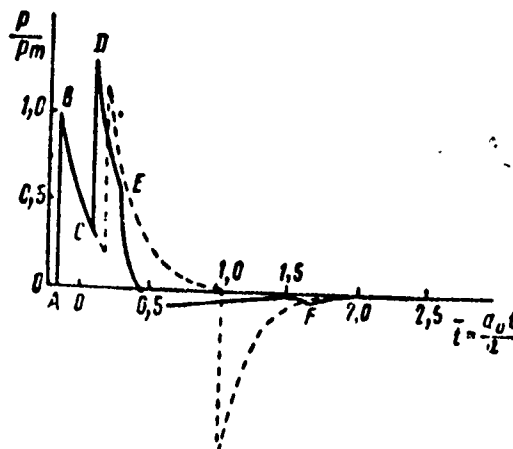


Fig. 69. Net Pressure at Points Situated in Front of a Disc $\bar{z} = 0.17$, $\bar{r} = 0$, during Incidence of Exponential-shaped Wave $\bar{\theta} = 0.2$.
 ——— 45° gradient;
 ----- normal incidence.

ciple of symmetry, pressure will be determined by the three last terms in (16.14), taken with opposite signs

$$\begin{aligned}
 p(\bar{r}, -\bar{z}^*, \bar{t}) = & p_m e^{-\frac{1-\bar{R}_1}{\bar{\theta}}} \alpha_0(t - \bar{R}_1) - \\
 & - \frac{p_m}{2\pi} \beta_0(\bar{t}) [\alpha_0(\bar{t} - \bar{R}_1) - \alpha_0(\bar{t} - \bar{R}_2)] + \\
 & + \frac{p_m}{2\pi} \frac{1}{\bar{\theta}} e^{-\frac{\bar{t}}{\bar{\theta}}} \int_{\bar{R}_1}^{\bar{R}_2} e^{-\frac{\bar{t}}{\bar{\theta}}} \beta_0(\bar{\tau}) \alpha_0(\bar{t} - \bar{\tau}) d\bar{\tau}.
 \end{aligned}
 \tag{16.16}$$

The pressure curve shows a sharp increment at its inception ($\bar{t} = \bar{R}_1$) and in the proximity of $\bar{t} = \bar{R}_2$ (Fig. 70). If point A is located on the axis of symmetry, pressure on it will change as on a direct wave.

Consequently, we can make the following conclusions:

1. When a shock-wave flows past an obstacle, an expansion wave is formed which propagates from the edges and distorts the direct wave contour.

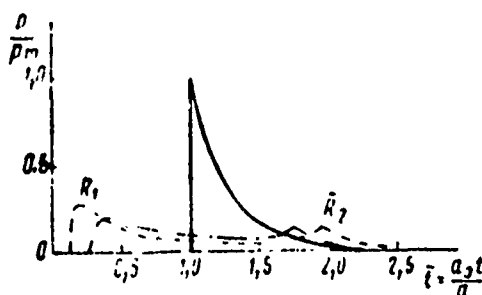


Fig. 70. Net Pressure at Points Situated Behind a Disc During Normal Incidence Onto Said Disc of an Exponential-Shaped Wave $\bar{\theta} = 0.2$, $\bar{z} = 0.08$.

— $\bar{r} = 0$;
 - - - $\bar{r} = 0.75$;
 - . - . - $\bar{r} = 0.92$.

2. At points situated in front of the disc (end-face) and projected onto it, the section of the pressure contour containing the direct and reflected-wave fronts remains the same as in the case of an infinite obstacle.

3. When a direct wave flows behind a disc, the increment in pressure on the front becomes gradual, and maximum pressure at points behind the disc are abruptly reduced, except for points lying on the axis of symmetry.

4. Pressure at points which are not projected onto the disc, are distorted by positive and negative waves emerging from the surface of the disc and its edge.

5. Similar phenomena should occur in diffraction of a direct shock-wave by plane obstacles of other shapes.

§17. Diffraction of a Plane Wave By a Rigid Sphere

The diffraction of a plane wave by a rigid sphere was first examined by Kharkevich [21] and later, applying other methods, by M. N. Lefonova and O. K. Fyodorov.

We will state this problem slightly differently, using the findings of study [21]. Let us use a spherical system of coordinates having its inception at the center of a sphere. The angle θ will be measured from the half-line emanating from the center of the sphere laterally in opposite direction to the propagation of the wave. The wave processes in this system of coordinates have axial symmetry and are not a function of the angle ψ . They are characterized by the wave equation

$$\frac{\partial^2 \phi}{\partial r^2} + \frac{2}{r} \frac{\partial \phi}{\partial r} + \frac{1}{r^2 \sin \theta} \frac{\partial}{\partial \theta} \left(\sin \theta \frac{\partial \phi}{\partial \theta} \right) - \frac{1}{a_0^2} \frac{\partial^2 \phi}{\partial t^2} = 0, \quad (17.1)$$

where ϕ - the potential of the additional pressure field induced by the presence of a sphere.

The association of pressure and the potential function is defined by the equation

$$p_A = -\rho_0 \frac{\partial \phi}{\partial t}. \quad (17.2)$$

The field of radial velocities is expressed by the relation

$$v_{rA} = \frac{\partial \phi}{\partial r}. \quad (17.3)$$

The boundary conditions when integrating (17.1) are:

equality of the normal velocity components to zero on the surface of the sphere

$$\left. \frac{\partial \phi}{\partial r} \right|_{r=a} = -v_{rnp} \big|_{r=a}, \quad (17.4)$$

where v_{rnp} - the radial velocity component of particles in the direct wave;

equality to zero of potential function of disturbed fluid motion at an infinitely-great distance from the sphere

$$\text{where } \left. \begin{array}{l} \dots \\ \varphi = 0 \end{array} \right\} \quad (17.5)$$

We know from general courses on mathematical physics that the solution of (17.1) can be written in the form of a Legendre polynomial series*

$$\varphi = \sum \varphi_n(r, t) P_n(\cos \theta), \quad (17.6)$$

where $P_n(\cos \theta)$ - the Legendre polynomial to the n th power.

Upon substituting (17.6) into (17.1), we derive an equation for defining the functions $\varphi_n(r, t)$

$$P_n \left(\frac{\partial^2 \varphi_n}{\partial r^2} + \frac{2}{r} \frac{\partial \varphi_n}{\partial r} \right) + \frac{1}{r^2} [(1 - \cos^2 \theta) P_n' - 2 \cos \theta P_n'] \varphi_n - \frac{1}{a_0^2} \frac{\partial^2 \varphi_n}{\partial t^2} P_n = 0$$

or, because the functions of P_n satisfy the Legendre differential equation,

$$\begin{aligned} (1 - z^2) \frac{d^2 u}{dz^2} - 2z \frac{du}{dz} + n(n+1)u &= 0, \\ \frac{\partial^2 \varphi_n}{\partial r^2} + \frac{2}{r} \frac{\partial \varphi_n}{\partial r} - \frac{n(n+1)}{r^2} \varphi_n - \frac{1}{a_0^2} \frac{\partial^2 \varphi_n}{\partial t^2} &= 0. \end{aligned} \quad (17.7)$$

To solve (17.7), let us employ the Laplace transform

$$\bar{\varphi}_n = \int_0^\infty \varphi_n e^{-vt} dt, \quad (17.8)$$

where v - some complex integer having a positive real part.

*Cf., for example, N. S. Koshlyakov, E. B. Gliner, M. M. Smirnov, Basic Differential Equations of Mathematical Physics, GIFML, Moscow, (1962).

After multiplying (17.7) by e^{-vt} and integrating with respect to t from 0 to infinity with zero initial data, we get an ordinary differential equation to depict $\bar{\varphi}_n(r, \theta, v)$:

$$\frac{d^2 \bar{\varphi}_n}{dr^2} + \frac{2}{r} \frac{d \bar{\varphi}_n}{dr} - \left[\frac{v^2}{a_0^2} + \frac{n(n+1)}{r^2} \right] \bar{\varphi}_n = 0. \quad (17.9)$$

Substituting the variables $\bar{\varphi}_n = \frac{\theta}{\sqrt{x}}$, $x = \frac{vr}{a_0}$, this equation reduces to a Bessel equation

$$x^2 y'' + xy' - \left[x^2 + \left(n + \frac{1}{2} \right)^2 \right] y = 0. \quad (17.10)$$

The general solution of (17.10) is*

$$y = C_1 I_{n+\frac{1}{2}}(x) + C_2 K_{n+\frac{1}{2}}(x), \quad (17.11)$$

where $I_{n+\frac{1}{2}}(x)$ and $K_{n+\frac{1}{2}}(x)$ - first and second-series modified Bessel functions** of the $n + 1/2$ order:

$$I_{n+\frac{1}{2}}(x) = i^{-(n+\frac{1}{2})} J_{n+\frac{1}{2}}(ix);$$

$$J_{n+\frac{1}{2}}(ix) \quad - \text{a first-series Bessel function;}$$

$$K_{n+\frac{1}{2}}(x) = \frac{\pi}{2 \sin\left(n + \frac{1}{2}\right)\pi} \left[I_{-(n+\frac{1}{2})}(x) - I_{n+\frac{1}{2}}(x) \right].$$

Because where $x \rightarrow \infty$, $I_{n+\frac{1}{2}}(x) \rightarrow \infty$ (considering the second boundary condition of the problem), we should assume that $C_1 \equiv 0$.

*Cf., for example, E. T. Whittaker, J. N. Watson, Course on Modern Analysis, T. I. GIFML, (1963).

**Modified second-series Bessel functions are often called Macdonald functions.

Thus,

$$y = C_0 K_{n+\frac{1}{2}}(x).$$

or using our previous variables,

$$\bar{\varphi}_n = \frac{C_n}{V_i} K_{n+\frac{1}{2}}\left(\frac{vr}{a_0}\right). \quad (17.12)$$

In mathematical physics, the so-called Stokes function* is often employed $f_n(x)$, $F_n(x)$. The association of these functions with first-series Bessel functions can be expressed by the relation

$$f_n(ix) = i^{-(n+1)} e^{ix} \sqrt{\frac{\pi x}{2}} \left[J_{n+\frac{1}{2}}(x) + (-1)^n J_{-n-\frac{1}{2}}(x) \right], \quad (17.13)$$

$$F_n(ix) = ix(2n+1)^{-1} [nf_{n-1}(ix) + (n+1)f_{n+1}(ix)]. \quad (17.14)$$

Employing the Stokes function, Kharkevich derived a solution of (17.9) in the form**

$$\bar{\varphi}_n = B_n \frac{e^{-\frac{vr}{a_0}}}{r} f_n\left(\frac{vr}{a_0}\right). \quad (17.15)$$

*The Stokes function is often called the Bessel Spherical function.

**For the first items, the functions $f_n(z)$ and $F_n(z)$ have the form (we will henceforth require the function $F_n(z)$):

$f_0(z) = 1$	$F_0(z) = z + 1$
$f_1(z) = 1 + \frac{1}{z}$	$F_1(z) = z + 2 + \frac{2}{z}$
$f_2(z) = 1 + \frac{3}{z} + \frac{3}{z^2}$	$F_2(z) = z + 4 + \frac{9}{z} + \frac{9}{z^2}$
$f_3(z) = 1 + \frac{6}{z} + \frac{15}{z^2} + \frac{15}{z^3}$	$F_3(z) = z + 7 + \frac{27}{z} + \frac{60}{z^2} + \frac{60}{z^3}$
$f_4(z) = 1 + \frac{10}{z} + \frac{45}{z^2} + \frac{105}{z^3} + \frac{105}{z^4}$	$F_4(z) = z + 11 + \frac{65}{z} + \frac{260}{z^2} + \frac{525}{z^3} + \frac{525}{z^4}$
$f_5(z) = 1 + \frac{15}{z} + \frac{105}{z^2} + \frac{420}{z^3} + \frac{945}{z^4} + \frac{945}{z^5}$	$F_5(z) = z + 16 + \frac{135}{z} + \frac{735}{z^2} + \frac{2625}{z^3} + \frac{5570}{z^4} + \frac{5570}{z^5}$

In equations (17.12) and (17.15), the coefficients C_n and B_n are taken from the boundary value conditions of the problem.

Using a transform on the left side of (17.4) instead of the original, let us designate that

$$\left. \frac{\partial \tilde{v}_n}{\partial r} \right|_{r=a} = -\tilde{b}_n, \quad (17.16)$$

\tilde{b}_n - a transform of the n th expansion coefficient with respect to the Legendre functions of the normal velocity component of particles behind the front of a unit wave

$$v_{np} = \sum_{n=0}^{\infty} b_n P_n(\cos \theta), \quad (17.17)$$

$$\tilde{b}_n = \int_0^{\infty} b_n e^{-\lambda t} dt. \quad (17.18)$$

In view of the fact that $(1+z)f_n(z) - zf_n'(z) = F_n(z)$ and integrating (17.15), we find that

$$\frac{\partial \tilde{v}_n}{\partial r} = -B_n \frac{e^{-\frac{r}{a_0}}}{r^2} F_n\left(\frac{r}{a_0}\right), \quad (17.19)$$

$$\tilde{b}_n = \frac{a^2 \tilde{b}_n \left(\frac{va}{a_0}\right)}{e^{-\frac{va}{a_0}} F_n\left(\frac{va}{a_0}\right)}. \quad (17.20)$$

After substituting the calculated coefficient values into (17.15), we find the solution in transforms of the basic equation (17.1)

$$\tilde{v}_n = \tilde{b}_n \left(\frac{va}{a_0}\right) \frac{a^2}{r} e^{-\frac{r-a}{a_0}} \frac{f_n\left(\frac{vr}{a_0}\right)}{F_n\left(\frac{va}{a_0}\right)}. \quad (17.21)$$

The quantities b_n entering into (17.21) are expansion coefficients with respect to the Legendre functions of the normal velocity component of particles behind the front of a unit wave.

Let us calculate these coefficients. In the selected system of coordinates, the position of the unit-wave front will be defined by the equation

$$t = \frac{a}{a_0} - \frac{r \cos \theta}{a_0}; \quad (17.22)$$

the velocity of particles behind the front is

$$v_{np} = \frac{1}{\rho_0 a_0} a_0 \left(t - \frac{a}{a_0} + \frac{r \cos \theta}{a_0} \right); \quad (17.23)$$

the maximum component of this velocity toward the surface of the sphere is

$$v_{rnp} = v_{np} \cos \theta = \frac{1}{\rho_0 a_0} \cos \theta \left(t - \frac{a}{a_0} + \frac{a \cos \theta}{a_0} \right); \quad (17.24)$$

that same velocity component in transforms is

$$\bar{v}_{rnp} = - \frac{1}{\rho_0 a_0} \cos \theta \frac{e^{-\frac{a}{a_0} (1 - \cos \theta)}}{v}. \quad (17.25)$$

Let us write \bar{v}_{rnp} as a Legendre polynomial series

$$\bar{v}_{rnp} = \sum_{n=0}^{\infty} \bar{b}_n P_n(\cos \theta).$$

To define the coefficients of \bar{b}_n , let us employ a familiar equation

$$\begin{aligned} \bar{b}_n &= - \frac{2n+1}{2} \frac{1}{\rho_0 a_0} \frac{e^{-\frac{a}{a_0}}}{v} \int_0^\pi e^{\frac{va}{a_0} \cos \theta} \cos \theta P_n(\cos \theta) \sin \theta d\theta = \\ &= \frac{2n+1}{2} \frac{1}{\rho_0 a_0} \frac{e^{-\frac{a}{a_0}}}{v} \int_{-1}^1 e^{\frac{va}{a_0} x} P_n(x) x dx. \end{aligned} \quad (17.26)$$

The integral (f (17.26) for any $P_n(x)$ can be easily calculated.* For the first two coefficients specifically,

$$\begin{aligned} \bar{b}_0 &= -\frac{1}{2} \frac{a}{\rho_0 a_0^2} \frac{e^{-\bar{v}}}{\bar{v}} \frac{e^{\bar{v}}(\bar{v}-1) + e^{-\bar{v}}(\bar{v}+1)}{\bar{v}^2} = \\ &= \frac{a}{\rho_0 a_0^2} \frac{e^{-\bar{v}}}{\bar{v}} \left(\frac{\text{ch } \bar{v}}{\bar{v}} - \frac{\text{sh } \bar{v}}{\bar{v}^2} \right), \end{aligned} \quad (17.27)$$

where

$$\bar{v} = \frac{va}{a_0},$$

$$\begin{aligned} \bar{b}_1 &= -\frac{3}{2} \frac{a}{\rho_0 a_0^2} \frac{e^{-\bar{v}}}{\bar{v}^3} \left[e^{\bar{v}}(\bar{v}^2 - 2\bar{v} + 2) - e^{-\bar{v}}(\bar{v}^2 + 2\bar{v} + 2) \right] = \\ &= 3 \frac{a}{\rho_0 a_0^2} \frac{e^{-\bar{v}}}{\bar{v}} \left(-\frac{\text{sh } \bar{v}}{\bar{v}} + 2 \frac{\text{ch } \bar{v}}{\bar{v}^3} - 2 \frac{\text{sh } \bar{v}}{\bar{v}^3} \right). \end{aligned} \quad (17.28)$$

For an arbitrary value of n , with the aid of the Stokes polynomials the formula for \bar{b}_n can be written in the form:

$$b_n = \frac{2n+1}{2} \frac{a}{\rho_0 a_0^2} \frac{e^{-\bar{v}}}{\bar{v}^3} \left[F_n(-\bar{v}) e^{\bar{v}} - (-1)^n F_n(\bar{v}) e^{-\bar{v}} \right]. \quad (17.29)$$

After the coefficients of \bar{b}_n have been calculated, it is easy to define the pressure fields. For this purpose let us employ the relation

$$p = -\rho_0 \frac{\partial \varphi}{\partial t}. \quad (17.30)$$

*Let us note that

$$\begin{aligned} P_0(x) &= 1, \quad P_1(x) = x, \\ P_2(x) &= \frac{1}{2} (3x^2 - 1), \quad P_3(x) = \frac{1}{2} (5x^3 - 3x), \\ P_4(x) &= \frac{1}{8} (35x^4 - 30x^2 + 3), \quad P_5(x) = \frac{1}{8} (63x^5 - 70x^3 + 15x). \end{aligned}$$

Here and until the end of this section, $x = \cos \theta$.

which in transforms may be written in the form

$$\bar{p} = -\rho_0 \bar{\psi}. \quad (17.31)$$

According to (17.6) and (17.15), we have

$$\bar{p}_2 = -\rho_0 a_0 \frac{a^2}{r} e^{-\frac{r-a}{a}} \sum_{n=0}^{\infty} \bar{b}_n(\bar{v}) \frac{f_n\left(\frac{vr}{a_0}\right)}{F_n\left(\frac{v_2}{a_0}\right)} P_n(\cos \theta). \quad (17.32)$$

For points situated on the surface of the sphere ($r = a$),

$$\bar{p}_2 = -\rho_0 a_0 v \sum_{n=0}^{\infty} \bar{b}_n(\bar{v}) \bar{\psi}_n(v) P_n(\cos \theta), \quad (17.33)$$

where

$$\bar{\psi}_n(\bar{v}) = \frac{a}{a_0} \frac{f_n(\bar{v})}{F_n(\bar{v})}. \quad (17.34)$$

The conversion in (17.33) from transform to original can be effected with the aid of the Mellin integral

$$p_2 = -\rho_0 a_0 \sum_{n=0}^{\infty} \left[\frac{1}{2\pi i} \int_{(L)} v \bar{b}_n(\bar{v}) \bar{\psi}_n(\bar{v}) e^{v'} dv \right] P_n(\cos \theta), \quad (17.35)$$

where the contour (L) passes from point $\chi_0 - i_{\infty}$ to point $\chi_0 + i_{\infty}$ in the right half-plane of the complex variable $v = \chi + i\eta$ in such a way that all the characteristics of the subintegral function lie to the left of this contour.

We can simplify calculations considerably by using the generalized Borel theorem.

According to this theorem

$$f_1(\cdot) f_2(\cdot) = \int_0^1 f_1(t + \tau) f_2(\tau) d\tau \quad (17.36)$$

where

$$\bar{f}_1(v) \doteq f_1(t) = \frac{1}{2\pi i} \int_{(L)} \bar{f}_1(v) e^{vt} dv, \quad (17.37)$$

$$\bar{f}_2(v) \doteq f_2(t) = \frac{1}{2\pi i} \int_{(L)} \bar{f}_2(v) e^{vt} dv. \quad (17.38)$$

Consequently,

$$\begin{aligned} \rho_A &= -\rho_0 a_0 \sum_{n=0}^{\infty} \left[\int_0^t \frac{d}{dt} b_n \left(\frac{a_0 t}{a} - \frac{a_n \tau}{a} \right) \psi_n \left(\frac{a_0 \tau}{a} \right) d\tau \right] P_n(\cos \theta) = \\ &= -\rho_0 a_0 \sum_{n=0}^{\infty} \left[\int_0^{\bar{t}} \dot{b}_n (\bar{t} - \bar{\tau}) \psi_n(\bar{\tau}) d\bar{\tau} \right] P_n(\cos \theta). \end{aligned} \quad (17.39)$$

Integrating by parts and considering that

$$\psi_n(0) = 1^*, \quad a \sum b_n(t) P_n(\cos \theta) = v_{r,sp},$$

we derive

$$\begin{aligned} \rho_A &= -\rho_0 a_0 v_{r,sp} - \rho_0 a_0 \sum_{n=0}^{\infty} \left[\int_0^{\bar{t}} b_n(\bar{\tau}) \frac{d}{d\bar{\tau}} \psi_n(\bar{t} - \bar{\tau}) d\bar{\tau} \right] P_n(\cos \theta) = \\ &= \cos \theta z_0 (\bar{t} - 1 + \cos \theta) - \rho_0 a_0 \sum_{n=0}^{\infty} \left[\int_0^{\bar{t}} b_n(\bar{\tau}) \frac{d}{d\bar{\tau}} \psi_n(\bar{t} - \bar{\tau}) d\bar{\tau} \right] P_n(\cos \theta), \end{aligned} \quad (17.40)$$

where

$$\psi_n(\bar{t}) = \frac{1}{2\pi i} \int_{(L)} \bar{\psi}_n(\bar{v}) e^{v\bar{t}} d\bar{v} = \frac{1}{2\pi i} \int_{(L)} \frac{f_n(\bar{v})}{F_n(\bar{v})} e^{v\bar{t}} d\bar{v}. \quad (17.41)$$

In this form, we can easily find the originals of functions $\psi_n(\bar{t})$. Actually, using the theorem on residues, and in view of the fact that the function $\psi_n(\bar{t})$ is meromorphic**,

*From (17.34) we can see that where $v \rightarrow \infty$, $\bar{\psi}_n(v) \rightarrow \frac{1}{v}$.

**A meromorphic function is a one-valued analytic function $f(z)$ in a complex plane which has only a pole as its special points differing from $z = \infty$.

$$\frac{1}{2\pi i} \int_{(L)} \frac{f_n(\bar{v})}{F_n(\bar{v})} e^{\bar{v}i} d\bar{v} = \sum_{k=1,2} \text{Res}_{\bar{v}_k} \left[\frac{f_n(\bar{v})}{F_n(\bar{v})} e^{\bar{v}i} \right]. \quad (17.42)$$

where $\text{Res}_{\bar{v}_k}$ - residues of functions at points \bar{v}_k ;
 \bar{v}_k - roots of the equation $F_n(\bar{v}) = 0$.

The roots of the Stokes polynomials $F_n(\bar{v})$ are given in Kharkevich's study [21]. Also given there is an expression for the originals of function $\psi_n(\bar{t})$ in the form

$$\psi_n(\bar{t}) = \sum_{k=1}^{n+1} \frac{\bar{v}_k^n f_n(\bar{v}_k)}{\Phi'(\bar{v}_k)} e^{\bar{v}_k \bar{t}}, \quad (17.43)$$

where

$$\Phi(\bar{v}) = \bar{v}^n F_n(\bar{v}),$$

$$\Phi'(\bar{v}) = \frac{d}{d\bar{v}} \Phi(\bar{v}).$$

Because where $n = 0$, $\bar{v}_1 = -1.00$ and where $n = 1$, $\bar{v}_1 = -1.0 + i$ and $\bar{v}_2 = -1.0$, then

$$\psi_0(\bar{t}) = \frac{f_0(-1)}{\Phi_0(-1)} e^{-\bar{t}} = e^{-\bar{t}}, \quad (17.44)$$

$$\begin{aligned} \psi_1(\bar{t}) &= \frac{(-1-i)f_1(-1-i)}{\Phi_1(-1-i)} e^{(-1+i)\bar{t}} + \\ &+ \frac{(-1-i)f_1(-1-i)}{\Phi_1(-1-i)} e^{(-1-i)\bar{t}} = e^{-\bar{t}} \cos \bar{t}. \end{aligned} \quad (17.45)$$

The originals of the coefficients of b_n can be found directly from formula

$$\begin{aligned} b_n &= \frac{2n+1}{2} \int_0^\pi v_{np} P_n(\cos \theta) \sin \theta d\theta = \\ &= -\frac{2n+1}{2} \int_1^{-1} v_{np} P_n(x) dx, \end{aligned} \quad (17.46)$$

where, according to (17.24)

$$v_{np} = -\frac{1}{\rho_0 a_0} x \sigma_0 (\bar{t} - 1 + x). \quad (17.47)$$

Considering that $\sigma_0(\bar{t} - 1 + x) \equiv 0$ where $x < 1 - \bar{t}$, for $\bar{t} < 2$ we find that

$$b_n = \frac{2n+1}{2} \frac{1}{\rho_0 a_0} \int_0^{1-\bar{t}} x P_n(x) dx, \quad (17.48)$$

where $\bar{t} > 2$

$$b_n = \frac{2n+1}{2} \frac{1}{\rho_0 a_0} \int_0^1 x P_n(x) dx. \quad (17.49)$$

The integrals of (17.48) and (17.49) are taken in finite form for any n . Specifically, where $\bar{t} < 2$

$$\begin{aligned} b_0 &= -\frac{1}{\rho_0 a_0} \frac{\bar{t}}{4} (2 - \bar{t}), \\ b_1 &= -\frac{1}{\rho_0 a_0} \frac{\bar{t}}{2} (3 - 3\bar{t} + \bar{t}^2), \\ b_2 &= -\frac{1}{\rho_0 a_0} \frac{5}{8} \left\{ \frac{3}{2} [1 - (1 - \bar{t})^4] - 2\bar{t} + \bar{t}^2 \right\}, \end{aligned} \quad (17.50)$$

while where $\bar{t} > 2$

$$\left. \begin{aligned} b_0 &= b_2 = \dots = b_n = 0, \\ b_1 &= -\frac{1}{\rho_0 a_0}. \end{aligned} \right\} \quad (17.51)$$

Thus, the solution of this problem is derived using infinite series. Employing this solution, we can calculate the pressure at any point in a fluid. Calculated pressure results in terms of the first four terms of the series, for three points on the surface of a sphere, are shown in Fig. 71 (calculation performed by O. K. Fyodorov).

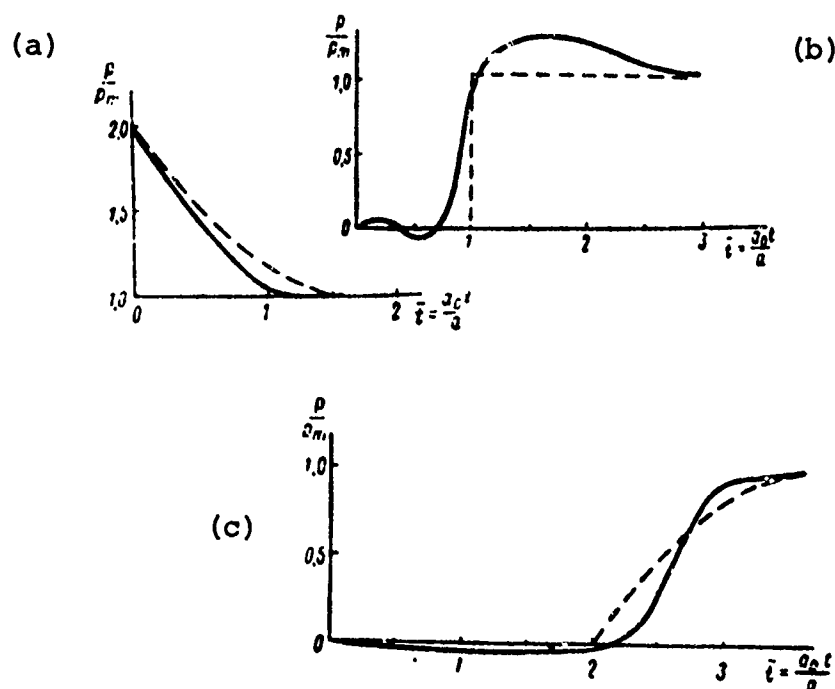


Fig. 71. Net Pressure at Points on a Sphere During Incidence onto it of a Unit Shock Wave: a - $\theta = 0^\circ$; b - $\theta = 90^\circ$; c - $\theta = \pi$.

———— solution allowing for four terms of the series;

----- approximate solution according to formulas (17.81) and (17.82)

We can see from the figure that the pressure on the surface of the sphere rather quickly becomes equal to the pressure on a direct wave. At points situated on the facial side, pressure changes in jumps; on the lee side, it changes gradually. Pressure equalization time is roughly equal to the running time of a wave along the radius of the sphere.

This problem is similar to the problem on progressive motion of a sphere. The difference is that in the latter case, the normal component of particle velocity on the surface of the sphere is

$$v_r = v_0(t) \cos \theta, \quad (17.52)$$

i.e., it is not determined by summation from zero to $n \rightarrow \infty$, but only by one of the Legendre polynomials $[P_1(x)]$. Moreover,

$$\left. \begin{aligned} b_1 &= -\sigma_0(t), \\ \bar{b}_1 &= -\frac{1}{v}. \end{aligned} \right\} \quad (17.53)$$

Thus, this solution is a particular case of the solution previously derived. According to (17.33), on the surface of a sphere

$$\bar{p}_{n..} = \rho_0 a_0 \bar{\psi}_1(\bar{v}) \cos \theta, \quad (17.54)$$

where, according to (17.34)

$$\bar{\psi}_1(v) = \frac{a}{a_0} \frac{f_1(\bar{v})}{F_1(v)}. \quad (17.55)$$

Using the original and considering (17.45), we will get

$$p_{n..}(a, \theta, t) = \rho_0 a_0 \bar{\psi}_1(\bar{v}) \cos \theta = \rho_0 a e^{-t} \cos \bar{v} \cos \theta. \quad (17.56)$$

It follows from this expression that at the initial moment in time, pressure on the surface of the sphere jumps from zero to $\rho_0 a_0 \cos \theta$; pressure subsequently has the common nature of a time rate of variation independent of the point coordinates.

Let us find the net load acting upon a sphere both in the case of progressive motion and in the case of its diffraction of a unit amplitude plane wave. For this purpose we must integrate the quantities of the elementary loads with respect to the sphere surface. The projection of of these loads on the z axis is equal to:

$$dF_z = p dS \cos \theta = p 2\pi a^2 \sin \theta \cos \theta d\theta = -p 2\pi a^2 x dx. \quad (17.57)$$

In view of (17.56), the projection of the net force onto the z axis during progressive motion of a sphere will be derived in the form

$$F_z = -2\pi a^2 \rho_0 a_0 e^{-t} \cos \bar{v} \int_0^1 x dx = -\frac{4}{3} \pi a^3 \rho_0 a_0 \bar{\psi}_1(\bar{v}). \quad (17.58)$$

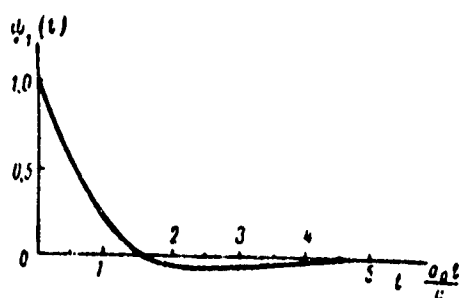


Fig. 72. The Function $\psi_1(\bar{t})$ for Progressive Motion of a Sphere according to the Unit Function Law.

where

$$\psi_1(\bar{t}) = e^{-\bar{t}} \cos \bar{t}.$$

We can easily see that the law of variation in net load is exactly the same as for an arbitrary point on a sphere (Fig. 72). If there were no diffraction (the hypothesis of plane reflection), then function $\psi_1(\bar{t})$ would be identically equal to its greatest value $\psi_1(0) \equiv 1$.

In diffraction of a plane unit wave by a sphere, pressure at an arbitrary point will be composed of pressure on the direct wave and pressure caused by flow-around of the sphere

$$p_z = p_{np} + p_a. \quad (17.59)$$

Let us calculate separately the net pressure of these components. According to (17.23) and (17.57)

$$F_{np}(t) = 2\pi a^2 \int_{-1}^1 \sigma_0(t-1+x) x dx. \quad (17.60)$$

However, where $x < 1 - \bar{t}$, $\sigma_0(t-1+x) \equiv 0$ and consequently, for $\bar{t} < 2$

$$F_{np}(\bar{t}) = 2\pi a^2 \int_{1-\bar{t}}^1 x dx = \pi a^2 (2\bar{t} - \bar{t}^2); \quad (17.61)$$

where $\bar{t} > 2$

$$F_{np}(\bar{t}) = 0. \quad (17.62)$$

For the second load component, let us first find the transform. According to (17.33)

$$\bar{F}_n = -2\pi\epsilon_0 a^2 \sum_{n=0}^{\infty} \sqrt{b_n(\bar{v})} \bar{\psi}_n(\bar{v}) \int_{-1}^{+1} P_n(x) x dx. \quad (17.63)$$

Because of the orthogonality of the Legendre polynomials, all the terms of (17.63) except the first-order term are equal to zero [$x = P_1(x)$]. Consequently,

$$F_n = -\frac{4}{3} \pi a^2 \epsilon_0 a_0 b_1(\bar{v}) \bar{\psi}_1(\bar{v}). \quad (17.64)$$

Employing, as we did before, the generalized Borel theorem and changing from transform to original, we will find that:

$$F_n(\bar{t}) = -\frac{4}{3} \pi a^2 \epsilon_0 a_0 \int_0^{\bar{t}} b_1'(\bar{t} - \bar{\tau}) \psi_1(\bar{\tau}) d\bar{\tau}. \quad (17.65)$$

Differentiation with respect to \bar{t} of the second equation in (17.50) (where $\bar{t} < 2$) yields

$$b_1'(\bar{t}) = -\frac{3}{2} \frac{1}{\epsilon_0 a_0} (1 - \bar{t})^2 \sigma_0(\bar{t}), \quad (17.66)$$

where $\bar{t} > 2$

$$b_1'(\bar{t}) = 0.$$

Substituting these expressions into (17.65) and considering (17.45), we find that:

where $\bar{t} < 2$

$$\begin{aligned} F_n(\bar{t}) &= 2\pi a^2 \int_0^{\bar{t}} [1 - (\bar{t} - \bar{\tau})]^2 e^{-\bar{\tau}} \cos \bar{\tau} d\bar{\tau} = \\ &= 2\pi a^2 \left(2e^{-\bar{t}} \sin \bar{t} - \bar{t} + \frac{\bar{t}^2}{2} \right). \end{aligned} \quad (17.67)$$

where $\bar{t} > 2$

$$F_1(\bar{t}) = 2\pi a^2 \int_{\bar{t}-2}^{\bar{t}} [1 - (\bar{t} - \bar{\tau})]^2 e^{-\bar{\tau}} \cos \bar{\tau} d\bar{\tau} = 4\pi a^2 e^{-\bar{t}} \sin \bar{t}. \quad (17.68)$$

Combining the results of (17.61), (17.62), (17.67), and (17.68) the summary load from the action of the direct and diffraction wave will be written in the form (Fig. 73)

$$F_2(\bar{t}) = 4\pi a^2 e^{-\bar{t}} \sin \bar{t}. \quad (17.69)$$

Expression (17.69) was derived by Kharkevich [21] in a slightly different manner.

It is easy to notice that the force acting on the sphere rather quickly vanishes, which is associated with the equalization of pressure at all points on the sphere surface.

With the aid of the Duhamel integral, we can easily expand the formulas established to a wave of arbitrary profile. Specifically, the net force during diffraction of an exponential-shaped wave by a sphere is defined by the relation

$$F_1(\bar{t}) = 4\pi a^2 \rho_m \frac{1}{\frac{1}{6} - 2\frac{1}{6} + 2} \left\{ -\frac{1}{6} e^{-\frac{\bar{t}}{6}} + e^{-\bar{t}} \times \right. \\ \left. \times \left[\left(2 - \frac{1}{6} \right) \sin \bar{t} + \frac{1}{6} \cos \bar{t} \right] \right\}. \quad (17.70)$$

Integrating (17.70) with respect to time from zero to infinity, we can see that the total pulse of load F_2 will be equal to zero. We will derive the same result during incidence of a finite-duration arbitrary-shaped wave onto a sphere.

The extreme simplicity of formulas (17.67)-(17.69) attracts our attention. At first glance it even seems somewhat unexpected, since the solution would seem less complicated than the problem - determin-

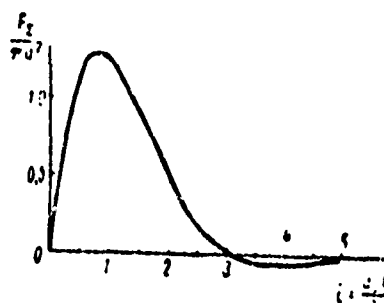


Fig. 73. Net Force Acting On Immobile Sphere During Incidence on It of Unit Shock-Wave.

ation of pressure on an arbitrary point on the surface of a sphere - and was derived using an infinite series. Moreover, similar effects often occur and can be attributed to the properties of orthogonal polynomials. This often makes integral evaluations very simple.

This fact causes us to consider the question of whether we can employ the method of determining net load \bar{F}_A for the approximate evaluation of pressure on a given point.

To illustrate this, let us return to expression (17.65), which we will write in the form*

$$F_A(\bar{t}) = \int_0^{\bar{t}} \frac{d}{d\bar{t}} Q(\bar{t} - \bar{\tau}) \psi_1(\bar{\tau}) d\bar{\tau}, \quad (17.71)$$

where

$$Q(\bar{t}) = -\frac{4}{3} \pi a^2 \rho_0 a_0 b_1(\bar{t}), \quad (17.72)$$

$$b_1(\bar{t}) = -\frac{1}{\rho_0 a_0} \frac{\bar{t}}{2} (3 - 3\bar{t} + \bar{t}^2). \quad (17.50b)$$

The function $Q(\bar{t})$ corresponds to $F_A(\bar{t})$ where $\psi_1 \equiv 1$ and is thus the second component of net load, obtained under the assumption of the hypothesis of plane reflection. In this connection, $\psi_1(\bar{t})$ characterizes the change in load owing to diffraction, while $Q(\bar{t})$ - owing to

*Expression (17.71) corresponds to the Duhamel integral for $Q(0) = 0$.

the sphere being drawn into the wave. If $Q(\bar{t})$ were a unit function, the load would be defined by the function $\psi_1(\bar{t})$, as occurred in the motion of a sphere according to the law of unit function [cf. 17.58)]. The symmetry of functions $Q(\bar{t})$ and $\psi_1(\bar{t})$ formulated in this sense permits us to consider the problem of determining pressure on an arbitrary point on a sphere according to the following pattern:

pressure is determined under the assumption of the hypothesis of plane reflection $p_a^*(a, \theta, \bar{t}_1)$;

employing the structure of the Duhamel integral, we introduce a function which takes diffraction $\psi_1(t_1)$ into consideration:

$$\begin{aligned} p_a(a, \theta, t_1) &= p_a^*(a, \theta, 0) \psi_1(\bar{t}_1) + \int_0^{\bar{t}_1} \frac{d}{d\bar{t}_1} p_a^*(\bar{t}_1 - \bar{\tau}) \psi_1(\bar{\tau}) d\bar{\tau} = \\ &= p_a^*(a, \theta, \bar{t}_1) + \int_0^{\bar{t}_1} p_a^*(\bar{\tau}) \frac{d}{d\bar{t}_1} \psi_1(\bar{t}_1 - \bar{\tau}) d\bar{\tau}. \end{aligned} \quad (17.73)$$

For a sphere

$$p_a^*(a, \theta, \bar{t}_1) = p_{np}(\bar{t}_1) \cos \theta, \quad (17.74)$$

where \bar{t}_1 - dimensionless time, counted from the moment the wave front converges with the point of observation.

In the case of unit wave incidence

$$p_a^*(a, \theta, \bar{t}_1) = a_0(\bar{t}_1) \cos \theta, \quad (17.75)$$

and (17.73) acquires a simple form

$$p_a(a, \theta, \bar{t}_1) = a_0(\bar{t}_1) \cos \theta \psi_1(\bar{t}_1), \quad (17.76)$$

where

$$t_1 = \bar{t} - 1 + \cos \theta.$$

Formula (17.76) coincides with the precise expression (17.40), if we consider that $\psi_n = \psi_1$ in the latter. We can easily be convinced of this fact in view of the fact that

$$v_{r,ap} = -\frac{1}{\rho_0 a_n} \dot{p}_2, \quad (17.77)$$

$$\sum_{n=1}^{\infty} b_n(\bar{t}) P_n(\cos \theta) = v_{r,p} = -\frac{\dot{p}_1}{\rho_0 a_n}. \quad (17.78)$$

Substituting (17.77) and (17.78) into (17.40), we derive (17.76).

The equality between all the functions ψ_n is accurately realised for the initial moment in time. This is easily shown by employing asymptotic representations of the Stokes polynomials in the range of transforms

$$P_n(\cos \theta) \sim \frac{1}{2} \left(1 - \frac{1}{2} + \dots \right), \quad (17.79)$$

whence

$$\lim_{\bar{t} \rightarrow 0} \psi_n(\bar{t}) = (1 - \bar{t}) \psi_0(\bar{t}). \quad (17.80)$$

Based on the preceding arguments, according to (17.76), we can write the approximate expression for net pressure on an arbitrary point on a sphere in the following form

$$p_k(a, \theta, \bar{t}_1) = [1 + \psi_1(\bar{t}_1) \cos \theta] \psi_0(\bar{t}_1). \quad (17.81)$$

where

$$\psi_1(\bar{t}_1) = e^{-\bar{t}_1} \cos \bar{t}_1. \quad (17.82)$$

Calculated results according to (17.81) are shown in comparison to the "precise" solution in Fig. 71. "Precise" solution implies, in this case, calculations according to formula (17.40) having four series terms.

The good agreement between these solutions attests to the feasibility of using the substantially simpler approximate relationships of (17.73) to describe the pressure diffraction field.

§18. Diffraction of a Plane Wave By a Rigid Round Cylinder

A number of researchers have studied the diffraction of a plane wave by a round cylinder. The most important results were obtained by V. V. Novozhilov, R. Skalak and M. Freedman, V. L. Prisekin, Yu. A. Fyodorovich, Yu. V. Goryainov, A. K. Pertsev, and others.

The formulation of this problem has much in common with the problem considered earlier. Onto an infinitely-long rigid round cylinder falls a plane wave of unit amplitude, whose front is parallel to the cylinder axis. We must find the pressure diffraction field and calculate the net force acting on the cylinder.

The additional pressure field induced by the presence of a cylinder in the fluid is characterized by the potential function, which is defined by the wave equation

$$\frac{\partial^2 \varphi}{\partial r^2} + \frac{1}{r} \frac{\partial \varphi}{\partial r} - \frac{1}{r^2} \frac{\partial^2 \varphi}{\partial \theta^2} - \frac{1}{a_0^2} \frac{\partial^2 \varphi}{\partial t^2} = 0. \quad (18.1)$$

The association of pressure and particle velocity with the potential function is expressed by the relations

$$\left. \begin{aligned} p &= -\rho_0 \frac{\partial \varphi}{\partial t} \\ v_r &= \frac{\partial \varphi}{\partial r} \end{aligned} \right\} \quad (18.2)$$

While considering a similar problem in the preceding section, we established a close association between unit wave diffraction problems and the problem of radiation in the motion of a body at a velocity which changes according to the unit function law. Thus, let us first consider the progressive motion of a cylinder at a velocity which can be described by the unit function law. Then, the limiting

conditions can be written thus:

on the surface of a cylinder

$$\frac{\partial \varphi}{\partial r} = \cos \theta_0(t), \quad (18.3)$$

where θ - the angle measured from a half-line perpendicular to the cylinder axis and coinciding with the direction of its motion.

At great distances from the cylinder, where $r \rightarrow \infty$

$$\varphi \rightarrow 0. \quad (18.4)$$

The solution of equation (18.1) will be sought in the form

$$\varphi(r, \theta, t) = \sum_{n=0}^{\infty} \varphi_n(r, t) \cos n\theta. \quad (18.5)$$

To define functions $\varphi_n(r, t)$ from (18.1), we find that

$$\frac{\partial^2 \varphi_n}{\partial r^2} + \frac{1}{r} \frac{\partial \varphi_n}{\partial r} - \frac{n^2}{r^2} \varphi_n - \frac{1}{a_0^2} \frac{\partial^2 \varphi_n}{\partial t^2} = 0. \quad (18.6)$$

Let us apply the Laplace transform to equation (18.6)

$$\bar{\varphi}_n = \int_0^{\infty} \varphi_n e^{-\nu t} dt, \quad (18.7)$$

where ν - a complex number having a positive real part.

Consequently, we find

$$\frac{d^2 \bar{\varphi}_n}{dr^2} + \frac{1}{r} \frac{d \bar{\varphi}_n}{dr} - \left(\frac{n^2}{r^2} + \frac{\nu^2}{a_0^2} \right) \bar{\varphi}_n = 0. \quad (18.8)$$

Equation (18.8) is the Bessel equation. Its general solution is

$$\bar{\varphi}_n = B_n I_n \left(\frac{\nu r}{a_0} \right) + C_n K_n \left(\frac{\nu r}{a_0} \right), \quad (18.9)$$

where $I_n(x)$ - modified Bessel functions of the first type; $K_n(x)$ -

modified Bessel functions of the second type (Macdonald functions).

On the basis of the second limiting condition, we should assume that $B_n \equiv 0$ (where $r \rightarrow \infty$, $I_n \rightarrow \infty$). Therefore,

$$\varphi_n = C_n K_n \left(\frac{\sqrt{r}}{a_0} \right). \quad (18.10)$$

To define the coefficients of C_n , let us employ the first limiting condition of the problem. We can see from its form that in this case there will only be one series term in the expansion of the function $\partial \bar{\varphi} / \partial r$ with respect to cosines. Because the transform of the unit function $\sigma_0(t)$ is $1/v$, according to (18.3)

$$\left. \frac{\partial \bar{\varphi}_1}{\partial r} \right|_{r=a} = C_1 \frac{v}{a_0} K_1' \left(\frac{\sqrt{a}}{a_0} \right) = \frac{1}{v},$$

whence

$$C_1 = \frac{a_0}{v^2} \frac{1}{K_1' \left(\frac{\sqrt{a}}{a_0} \right)}. \quad (18.11)$$

Consequently, according to (18.10) and (18.5)

$$\bar{\varphi} = \frac{a_0}{v^2} \frac{K_1 \left(\frac{\sqrt{r}}{a_0} \right)}{K_1' \left(\frac{\sqrt{a}}{a_0} \right)} \cos \theta. \quad (18.12)$$

Using the original instead of the transform, and employing the generalized Borel theorem, we will find that

$$\bar{\varphi} \rightarrow \varphi = a_0 \int_0^t \sigma_0(t-\tau) \left[\frac{1}{2\pi i} \int_{(L)} \frac{K_1 \left(\frac{\sqrt{r}}{a_0} \right)}{v \cdot K_1' \left(\frac{\sqrt{a}}{a_0} \right)} e^{v\tau} dv \right] d\tau \cos \theta. \quad (18.13)$$

Differentiating with respect to t , and in view of the properties of the Dirac delta function, we find that the magnitude of pressure on the cylinder surface is

$$p(a, \theta, t) = p_0 \psi_1(t) \cos \theta, \quad (18.14)$$

where

$$\left. \begin{aligned} \psi_1\left(\frac{a_0 \bar{t}}{a}\right) &= -\frac{1}{2\pi i} \int_{(L)} \frac{K_1(\bar{v})}{\bar{v} K_1'(\bar{v})} e^{\bar{v} \bar{t}} d\bar{v}, \\ \bar{v} &= \frac{va}{a_0}, \\ \bar{t} &= \frac{a_0 t}{a}. \end{aligned} \right\} \quad (18.15)$$

The values of the denominator roots of the subintegral function of (18.15) are

$$\bar{v}_{1,2} = -0,644 \pm i0,501.$$

Goryainov suggested the approximation of the function ψ_1 in the form

$$(t) \approx (1,216 \cos 0,5\bar{t} + 0,189 \sin 0,5\bar{t}) e^{-0,644\bar{t}} - 0,216 e^{-0,75\bar{t}}. \quad (18.16)$$

The net load per unit length of the cylinder is determined by the expression

$$F_z = \int_0^{2\pi} p \cos \theta a d\theta = \rho_0 a_0 a \psi_1(t) \int_0^{2\pi} \cos^2 \theta d\theta = \pi \rho_0 a_0 a \psi_1(t). \quad (18.17)$$

This finding is totally similar to the one derived earlier in the study of sphere motion. The nature of variation in net force and motion at an arbitrary point on a surface is defined by a general function of time. A graph of $\psi_1(\bar{t})$ is shown in Fig. 74. The appearance of the curve is similar to one for the motion of a sphere (cf. Fig. 72). It differs only by its slower drop in pressure which is easily attributed to the geometry of the process (plane flow-around instead of spatial).

Diffraction of a unit wave by a cylinder is similar in formulation to the problem already considered. The difference is in the formulation of the first boundary condition. As before [cf. formulas (17.22)-(17.25)], the normal component of particle velocity behind the front is

$$v_{np} = -\frac{1}{\rho_0 a_0} \cos \theta_{30} \left(t - \frac{a}{a_0} + \frac{a \cos \theta}{a_0} \right), \quad (18.18)$$

where it is customary to begin counting time from the moment the wave front arrives at the surface of the cylinder.

To determine the coefficients of C_n , we should expand expression (18.18) into a series in terms of cosines

$$v_{np} = -\frac{1}{\varepsilon_0 u_0} \sum_{n=0}^{\infty} C_n \cos n\theta. \quad (18.19)$$

According to the laws for defining the coefficients of the Fourier series

$$\left. \begin{aligned} C_0 &= -a_0 u_0 \frac{1}{2\pi} \int_0^{2\pi} v_{np} d\theta, \\ C_n &= -a_n u_0 \frac{1}{\pi} \int_0^{2\pi} v_{np} \cos n\theta d\theta, \end{aligned} \right\} \quad (18.20)$$

whence, after substituting (18.19) into (18.20) and performing simple calculations,

where $\bar{\varepsilon} < 2$

$$\left. \begin{aligned} C_0 &= \frac{1}{\pi} \sin \beta, \\ C_1 &= \frac{1}{\pi} \left(\beta + \frac{1}{2} \sin 2\beta \right), \\ &\dots \dots \dots \\ C_n &= \frac{1}{\pi} \left[\frac{\sin (n-1)\beta}{n-1} + \frac{\sin (n+1)\beta}{n+1} \right], \end{aligned} \right\} \quad (18.21)$$

where

$$\beta = \arccos(1 - \bar{\varepsilon}). \quad (18.22)$$

Where $\bar{\varepsilon} > 2$

$$\left. \begin{aligned} C_0 &= C_2 = \dots = C_n = 0, \\ C_1 &= 1. \end{aligned} \right\} \quad (18.23)$$

Using the same arguments as in the preceding section [cf. (17.39), (17.40)], we will find the addition pressure at points situated on the surface of the cylinder in the form

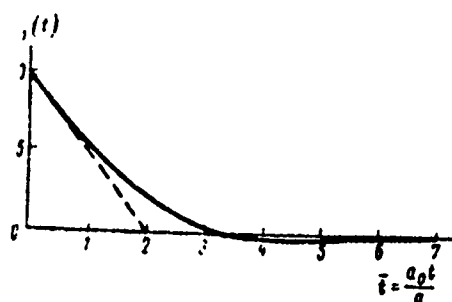


Fig. 74. Function $\psi_1(\bar{t})$ for Progressive Motion of a Round Cylinder according to the Unit Function Law.

————— calculated;
 ----- approximated.

$$p_n(a, \theta, \bar{t}) = \cos \theta z_0 (\bar{t} - 1 + \cos \theta) + \sum_{n=0}^{\infty} \left[\int_0^{\bar{t}} C_n(\bar{\tau}) \frac{d\psi_n(\bar{t} - \bar{\tau})}{d\bar{\tau}} d\bar{\tau} \right] \cos n\theta, \quad (18.24)$$

(where

$$\psi_n(\bar{t}) = -\frac{1}{2\pi i} \int_{(L)} \frac{K_n(\bar{v})}{\bar{v} K_n(\bar{v})} e^{\bar{v} \bar{t}} d\bar{v}. \quad (18.25)$$

Calculation of the function $\psi_n(\bar{t})$ is associated with mathematical difficulties. Its precise value was first derived by Goryainov in conjunction with I. L. Mironov, A. K. Pertsev, and A. Ya. Rukolaine.

It is defined by the expression

$$\psi_n(\bar{t}) = (-1)^n \int_0^{\bar{t}} \frac{e^{-x\bar{t}} dx}{[nK_n(x) + xK_{n-1}(x)]^2 + x^2 [nI_n(x) - xI_{n-1}(x)]^2} - \sum_{i=1}^N \frac{\bar{v}_i}{\bar{v}_i^2 + n^2} e^{\bar{v}_i \bar{t}}, \quad (18.26)$$

where $I_n(x)$, $K_n(x)$ - modified Bessel functions of the n -th order of the first and second type; \bar{v}_i - complex conjugate roots of the equation*

*The number of roots is determined by the closest even number to the expression $n + 1/2$.

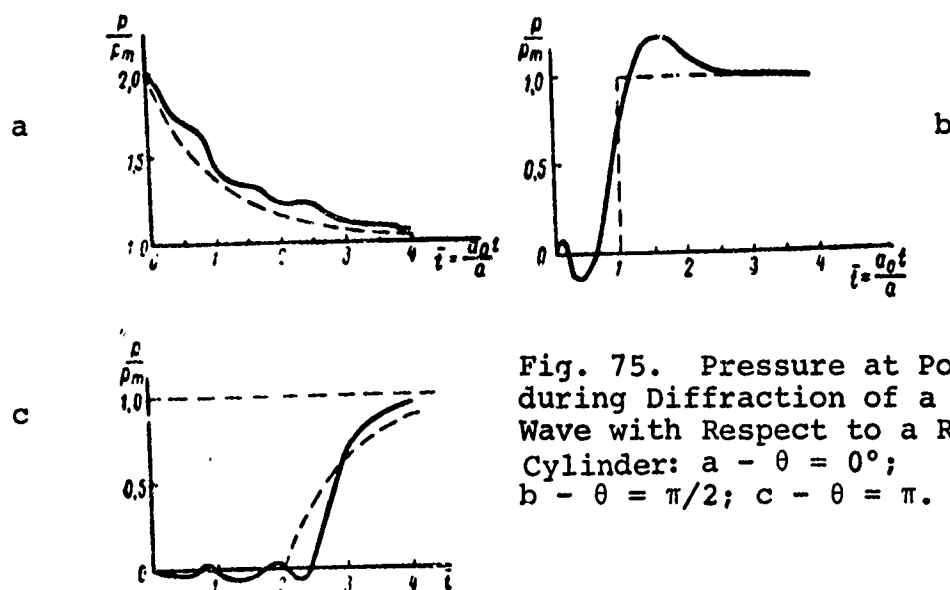


Fig. 75. Pressure at Points during Diffraction of a Unit Wave with Respect to a Round Cylinder: a - $\theta = 0^\circ$; b - $\theta = \pi/2$; c - $\theta = \pi$.

————— calculated, allowing for eight terms of the series
 ----- approximated, using the rough approximation $\psi(t)$

$$\bar{v}K'_n(\bar{v}) = -nK_n(\bar{v}) - \bar{v}K'_{n-1}(\bar{v}) = 0. \quad (18.27)$$

For $n = 1, 2, 3$, Skalak and Freeman cite the values of the roots in their study.

The calculated pressure in terms of the first eight terms of the series for several points on the surface of a cylinder is shown in Fig. 75 (calculated by Goryainov). Comparing these data with Fig. 71 we can conclude that the nature of variation in pressure on the surface of a cylinder is the same as on the surface of a sphere, except for a somewhat retarded drop in amplitude.

As before, pressure may be approximated roughly in the form

$$p_2(a, \theta, t) = \cos \theta \psi_1(\bar{t} - 1 + \cos \theta) \psi_0(\bar{t} - 1 + \cos \theta). \quad (18.28)$$

The net pressure (allowing for the direct wave) is

$$p(a, \theta, t) = [1 + \cos \theta \psi_1(\bar{t} - 1 + \cos \theta)] \psi_0(\bar{t} - 1 + \cos \theta). \quad (18.29)$$

or, by counting time from the moment the direct-wave front converges with the point of observation

$$\begin{aligned}\bar{t}_1 &= \bar{t} - 1 + \cos \theta \\ p(a, \theta, \bar{t}_1) &= [1 + \psi_1(\bar{t}_1) \cos \theta] \sigma_0(\bar{t}_1).\end{aligned}\quad (18.30)$$

The function $\psi_1(\bar{t}_1)$ can be approximated with roughly the same precision by a linear or exponential relation (the linear approximation is shown in Fig. 74). Thus,

$$\psi_1(\bar{t}_1) = \begin{cases} e^{-\bar{t}_1} \\ 1 - \frac{\bar{t}_1}{2} \end{cases} \quad (18.31)$$

Allowing for (18.31), formulas (18.29) and (18.30) may be rewritten in a form which is quite suitable for practical calculations

$$p(a, \theta, \bar{t}_1) \simeq (1 + e^{-\bar{t}_1} \cos \theta) \sigma_0(\bar{t}_1), \quad * (18.32)$$

$$p(a, \theta, \bar{t}_1) \simeq \sigma_0(\bar{t}_1) + \left(1 - \frac{\bar{t}_1}{2}\right) \cos \theta [\sigma_0(\bar{t}_1) - \sigma_0(\bar{t}_1 - 2)]. \quad (18.33)$$

Let us now calculate the cumulative load acting on a unit length of the cylinder when a plane wave falls onto it. Let us individually evaluate the two components of this load. For the direct wave $p_{np} = \sigma_0(\bar{t} - 1 + \cos \theta)$, we find that

$$F_{np}(\bar{t}) = \int_0^{2\pi} \sigma_0(\bar{t} - 1 + \cos \theta) a \cos \theta d\theta. \quad (18.34)$$

Considering that $\sigma_0(\bar{t} - 1 + \cos \theta) = 0$ where $\cos \theta < 1 - \bar{t}$ (i.e., where $\theta > \arccos(1 - \bar{t})$ and $2\pi - \theta > \arccos(1 - \bar{t})$), for $\bar{t} < 2$ we will find that

$$F_{np}(\bar{t}) = 2a \int_0^{\arccos(1-\bar{t})} \cos \theta d\theta = 2a \sqrt{2\bar{t} - \bar{t}^2}. \quad (18.35)$$

*Formula (18.32) was suggested by Yu. A. Fyodorovich.

Where $\bar{t} > 2$

$$F_{np}(\bar{t}) \approx 0.$$

The second component of the cumulative load will be calculated by employing the previously derived expression (18.24) for the quantity of additional pressure:

$$\begin{aligned} F_A(\bar{t}) = & a \int_0^{2\pi} p_A(a, \theta, \bar{t}) \cos \theta d\theta = a \int_0^{2\pi} \sigma_0(\bar{t} - 1 + \cos \theta) \cos^2 \theta d\theta + \\ & + a \sum_{n=0}^{\infty} \left[\int_0^{\bar{t}} C_n(\bar{\tau}) \frac{d}{d\bar{t}} \psi_n(\bar{t} - \bar{\tau}) d\bar{\tau} \right] \int_0^{2\pi} \cos \theta \cos n\theta d\theta. \end{aligned} \quad (18.36)$$

Due to the orthogonality of the function $\cos n\theta$, all the terms of the series in (18.36), except one ($n = 1$) vanish. Consequently,

$$\begin{aligned} F_A(\bar{t}) = & a \int_0^{2\pi} \sigma_0(\bar{t} - 1 + \\ & + \cos \theta) \cos^2 \theta d\theta + \\ & + a\pi \int_0^{\bar{t}} C_1(\bar{\tau}) \frac{d}{d\bar{t}} \psi_1(\bar{t} - \bar{\tau}) d\bar{\tau}. \end{aligned} \quad (18.37)$$

In view of the property of the unit function, and likewise (18.21) and (18.22), we will find that:

where $\bar{t} < 2$

$$\begin{aligned} F_A(\bar{t}) = & 2a \int_0^{\arccos(1-\bar{t})} \cos^2 \theta d\theta + a \int_0^{\bar{t}} \left[\arccos(1 - \bar{\tau}) + \right. \\ & \left. + \sqrt{2\bar{\tau} - \bar{\tau}^2} \cdot (1 - \bar{\tau}) \right] \frac{d}{d\bar{t}} \psi_1(\bar{t} - \bar{\tau}) d\bar{\tau} = \\ = & a \left\{ \arccos(1 - \bar{t}) + \sqrt{2\bar{t} - \bar{t}^2} (1 - \bar{t}) + \int_0^{\bar{t}} \left[\arccos(1 - \bar{\tau}) + \right. \right. \\ & \left. \left. + \sqrt{2\bar{\tau} - \bar{\tau}^2} (1 - \bar{\tau}) \right] \cdot \frac{d}{d\bar{t}} \psi_1(\bar{t} - \bar{\tau}) d\bar{\tau} \right\}; \end{aligned} \quad (18.38)$$

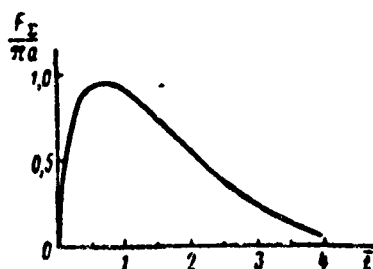


Fig. 76. Net Force Acting on Immobile Round Cylinder Where Unit Shock-Wave Falls onto It.

where $\bar{t} > 2$

$$\begin{aligned}
 F_x(\bar{t}) &= \pi a + a \int_0^2 \left[\arccos(1 - \bar{\tau}) + \sqrt{2\bar{\tau} - \bar{\tau}^2}(1 - \bar{\tau}) \right] \times \\
 &\quad \times \frac{d}{d\bar{t}} \psi_1(\bar{t} - \bar{\tau}) d\bar{\tau} + \pi a \int_2^{\bar{t}} \frac{d}{d\bar{t}} \psi_1(\bar{t} - \bar{\tau}) d\bar{\tau} = \\
 &= a \int_0^2 \left[\arccos(1 - \bar{\tau}) + \sqrt{2\bar{\tau} - \bar{\tau}^2}(1 - \bar{\tau}) \right] \times \\
 &\quad \times \frac{d}{d\bar{t}} \psi_1(\bar{t} - \bar{\tau}) d\bar{\tau} + \pi a \psi_1(\bar{t} - 2).
 \end{aligned}
 \tag{18.39}$$

The calculated cumulative loads according to the formulas cited by Goryainov are shown in Fig. 76.

§19. Hydrodynamic Forces in the Progressive Motion of an Absolutely Rigid Body of Arbitrary Shape

The general method for solving the problem, developed in the preceding section can be also used in evaluating hydrodynamic forces formed in progressive motion of arbitrarily-shaped bodies.* In this case, the net load is defined by the relation

*Strictly speaking, this is valid for free bodies if the shape is symmetric with respect to the direction of motion.

$$F_z = - \iint_S p(x, y, z, t) \cos \hat{n} z dS = \rho_0 \iint_S \frac{\partial \varphi}{\partial t} \cos n z dS \quad (19.1)$$

where $p(x, y, z, t)$ - pressure on the surface of a body;
 n - the direction of the external normal at point
 x, y, z .

The motion of a body occurs in the direction of the z axis at
a velocity of $z = \sigma_0(t)$.

The velocity potential of the disturbed fluid motion is characterized by the wave equation

$$\frac{\partial^2 \varphi}{\partial x^2} + \frac{\partial^2 \varphi}{\partial y^2} + \frac{\partial^2 \varphi}{\partial z^2} = \frac{1}{a_0^2} \frac{\partial^2 \varphi}{\partial t^2} \quad (19.2)$$

under the following boundary conditions:

on the surface of the body

$$\frac{\partial \varphi}{\partial n} = \dot{z} \cos \hat{n} z, \quad (19.3)$$

at a distance from it

$$\varphi \rightarrow 0 \text{ при } r = \sqrt{x^2 + y^2 + z^2} \rightarrow \infty. \quad (19.4)$$

As before, let us apply a unilateral Laplace transform to equation (19.2)

$$\bar{\varphi} = \int_0^\infty \varphi(x, y, z, t) e^{-vt} dt \quad (19.5)$$

where $\text{Re}(v) > 0$.

Then, in transforms (19.2) will be written as

$$\frac{\partial^2 \bar{\varphi}}{\partial x^2} + \frac{\partial^2 \bar{\varphi}}{\partial y^2} + \frac{\partial^2 \bar{\varphi}}{\partial z^2} = \frac{v^2}{a_0^2} \bar{\varphi}. \quad (19.6)$$

The first limiting condition where $z = \sigma_0(t)$ will be

$$\frac{\partial \bar{\varphi}}{\partial n} = -\frac{1}{v} \cos \hat{n}z. \quad (19.7)$$

Drag force in transforms is

$$\bar{F}_*(v) = \rho_0 v \iint_S \bar{\varphi} \cos \hat{n}z dS. \quad (19.8)$$

Because we have been interested in integral evaluations from the very start, let us stipulate that the function of the potential $\bar{\varphi}$ be measured at points in the medium which are situated on some surfaces S^* which are equidistant to the surface of the body. The physical meaning of S^* surface is that wave disturbances propagating at the same time from all points on the body will have envelope curves lying on these surfaces. The generalized coordinate r for these surfaces will be understood as the shortest distance from the origin of the coordinates to points on these equidistant surfaces along the normal to the surface of the body. We are furthermore given that the corresponding distance from the origin of the coordinates to the surface of the body is equal to a . Then, apparently, the relative coordinate $\bar{r} = r/a = 1$ will be satisfied by the surface of the body S .

Accordingly, it is convenient to additionally designate that

$$\left. \begin{aligned} \bar{\varphi}_*(r, v) &= \iint_{S^*} \bar{\varphi} \cos \hat{n}z dS, \\ \varphi_*(r, t) &= \iint_{S^*} \varphi \cos \hat{n}z dS. \end{aligned} \right\} \quad (19.9)$$

Employing the previously-developed general method, the function $\bar{\varphi}_*(r, v)$ will be written in the form

$$\bar{\varphi}_*(\bar{r}, v) = C(v) \zeta(\bar{r}, v).$$

According to (19.7) and (19.9)

$$\left. \frac{\partial \bar{\varphi}_*}{\partial n} \right|_{\bar{r}=1} = \left. \frac{\partial \bar{\varphi}_*}{\partial r} \right|_{\bar{r}=1} = \frac{1}{v} \iint_S \cos^2 \hat{n}z dS = \frac{A}{v}. \quad (19.10)$$

where

$$A = \int_S \cos^2 \theta \, n_z dS. \quad (19.11)$$

Hence, to define $C(v)$, we have

$$\left. \frac{\partial \bar{\varphi}_*}{\partial r} \right|_{\bar{r}=1} = C(v) \left. \frac{\partial \zeta(\bar{r}, v)}{\partial r} \right|_{\bar{r}=1} = \frac{A}{v},$$

and consequently,

$$\bar{\varphi}_*(\bar{r}, v) = A \frac{\zeta(\bar{r}, v)}{v \left. \frac{\partial \zeta(\bar{r}, v)}{\partial r} \right|_{\bar{r}=1}} = A \frac{\zeta(\bar{r}, v)}{v \xi(v)}, \quad (19.12)$$

where

$$\xi(v) = \left. \frac{\partial \zeta(\bar{r}, v)}{\partial r} \right|_{\bar{r}=1}.$$

According to (19.8) and (19.12), drag is

$$F_*(v) = \rho_0 A \frac{\zeta(v)}{\xi(v)}, \quad (19.13)$$

or, using the original,

$$F_*(t) = \frac{1}{2\pi i} \int_{l-i\infty}^{l+i\infty} \bar{F}_*(v) e^{vt} dv. \quad (19.14)$$

If we are given function $F_*(t)$, then with an arbitrary law of variation in velocity $\dot{z} = \dot{z}(t)$, drag can be derived with the aid of the Duhamel integral

$$F(t) = F_*(t) \dot{z}(0) + \int_0^t \ddot{z}(t-\tau) F_*(\tau) d\tau, \quad (19.15)$$

or with zero initial data [$\dot{z}(0) = 0$]

$$F(t) = \int_0^t \ddot{z}(t-\tau) F_*(\tau) d\tau. \quad (19.16)$$

Let us designate that

$$F_*(t) = -F_0 \dot{\psi}(t), \quad (19.17)$$

where

$$F_0 = -F_*(0) = \rho_0 a_0 A = \rho_0 a_0 \int \int \cos^2 \hat{n} z dS. \quad (19.18)$$

$$\psi(t) = -\frac{1}{2\pi i} \int_L \frac{\xi(v)}{a_0 \dot{\xi}(v)} e^{v t} dv. \quad (19.19)$$

Then

$$F(t) = -F_0 \int_0^t \ddot{z}(t-\tau) \psi(\tau) d\tau. \quad (19.20)$$

Here, F_0 corresponds to drag when calculating in terms of the hypothesis of plane reflection ($\psi \equiv 1$), while function $\psi(t)$ characterizes variation in this force owing to diffraction. The main problem is namely in evaluating the function $\psi(t)$. At the present time, this evaluation can only be done for the simplest cases (an infinite cylinder, sphere, piston, plate). The question arises as to how we should proceed in other, less important cases (with respect to practical applications).

Let us try to plan a means for approximation of a solution. We have noted many times before that the function $\psi(\bar{t})$ depends on one dimensionless parameter, differs greatly from zero only at the initial period in time, and is equal to the running time of the wave between the most distant points on the surface of the body. In this interval, the nature of variation in the function is close to linear. Moreover, as was shown in §14 and 15, the total integral with respect to time from function $\psi(t)$ is proportional to the quantity of apparent mass. Actually, where a_0 approaches infinity, we have from (19.20)

$$F(t) = -\ddot{z}(t) F_0 \int_0^{\bar{t}} \psi(\tau) d\tau. \quad (19.21)$$

Because F_0 is proportional to a_0 and $\psi(\bar{t})$ is a function only of one dimensionless parameter $\bar{t} = a_0 \tau / a$, where $\ddot{z}(t)$ the coefficient known as apparent mass is not a function of the speed of sound and is equal to

$$M_{app} = F_0 \int_0^{\bar{t}} \psi(\tau) d\tau = F_0 \frac{a}{a_0} \int_0^{\bar{t}} \psi(\bar{\tau}) d\bar{\tau}. \quad (19.22)$$

We can arrive at formula (19.22) directly from general physical concepts [17]. Actually, the integral with respect to time of drag of a body in a fluid is equal to the momentum translated to the medium. When the rate of travel changes according to the unit function law, this quantity is different, like apparent mass.

Consequently, the following rough approximation can be suggested for the function $\psi(\bar{t})$

$$\psi_*(\bar{t}) = \left(1 - \frac{\bar{t}}{\bar{t}_*}\right) [\psi_0(\bar{t}) - \psi_0(\bar{t} - \bar{t}_*)]. \quad (19.23)$$

Time \bar{t}_* is defined from the condition of equality of the areas bounded by the curves $\psi_*(\bar{t})$ and $\psi(\bar{t})$:

$$\int_0^{\bar{t}_*} \psi_*(\bar{t}) d\bar{t} = \int_0^{\bar{t}_*} \psi(\bar{t}) d\bar{t} = \frac{M_{np}}{F_0} \frac{a}{a_0},$$

whence

$$\left. \begin{aligned} \bar{t}_* &= \frac{2M_{np}}{F_0} \frac{a}{a_0} \\ \text{or} \quad \bar{t}_* &= \frac{2M_{np}}{F_0} \end{aligned} \right\} \quad (19.24)$$

Thus, the problem of evaluating hydrodynamic force during progressive motion of a body obtains an approximate solution if we are given the quantity of apparent mass.

As an example, let us consider the motion of a prolate ellipsoid of revolution in the direction of the axis of symmetry.

Let us first find the value of F_0 . After expanding the coordinates at the center of the ellipsoid, let us write the equation of its surface

$$\frac{x^2}{a^2} + \frac{y^2}{a^2} + \frac{z^2}{b^2} = 1, \quad (19.25)$$

where a and b are the dimensions of the semiaxes of the ellipsoid

(b > a).

According to (19.18)

$$F_0 = \rho_0 \int_S \cos^2 \hat{n} z dS,$$

or, using a contour integral instead of the surface integral,

$$F_0 = 2\rho_0 a_0 2\pi \int_0^b y \cos^2 \hat{n} z dl = 4\pi \rho_0 a_0 \int_0^b y \sqrt{1 + \left(\frac{dy}{dz}\right)^2} \cos^2 \hat{n} z dz, \quad (19.26)$$

but

$$\begin{aligned} y &= a \sqrt{1 - \left(\frac{z}{b}\right)^2} \\ \frac{dy}{dz} &= -\frac{az}{b \sqrt{b^2 - z^2}}, \\ \cos \hat{n} z &= \frac{1}{\sqrt{1 + \left(\frac{dz}{dy}\right)^2}}. \end{aligned}$$

Substituting these quantities and performing simple transformations, we find that

$$F_0 = 4\pi \rho_0 a_0 \frac{a^2}{\sqrt{k^2 - 1}} \int_0^1 \frac{\bar{z}^2 d\bar{z}}{\sqrt{\frac{k^2 - 1}{k^2} - \bar{z}^2}},$$

where $k = \frac{b}{a}$ $\bar{z} = \frac{z}{b}$.

Integration yields

$$F_0 = 2\pi \rho_0 a_0 \frac{a^2}{k^2 - 1} \left\{ \frac{k^2}{k^2 - 1} \arcsin \sqrt{\frac{k^2 - 1}{k^2}} - \sqrt{\frac{1}{k^2 - 1}} \right\}. \quad (19.27)$$

As we know, the quantity of apparent mass, for the motion of an ellipsoid of revolution in the direction of the larger axis [16], is

$$M_{np} = \rho_0 \frac{4}{3} \pi a^3 k \frac{A}{2B}, \quad (19.28)$$

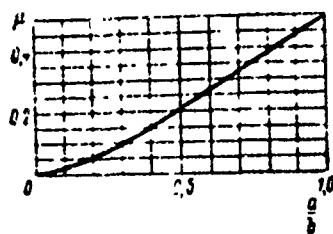


Fig. 77. The Coefficient of Apparent Mass for a Prolate Ellipsoid of Revolution.

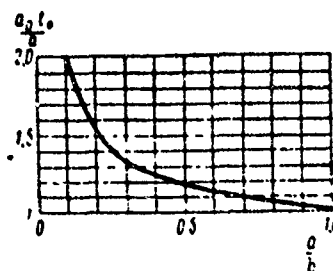


Fig. 78. The Relation of \bar{t}_* as a function of a/b for a prolate ellipsoid of revolution.

where

$$\left. \begin{aligned} A &= \frac{2k}{\sqrt{k^2-1}} \frac{1}{k^2-1} \left[\ln \left(\sqrt{k^2-1} + k \right) - \frac{\sqrt{k^2-1}}{k} \right], \\ B &= \frac{k^2}{k^2-1} \left[1 - \frac{1}{k\sqrt{k^2-1}} \ln \left(\sqrt{k^2-1} + k \right) \right]. \end{aligned} \right\} \quad (19.29)$$

Therefore,

$$\left. \begin{aligned} t_* &= \frac{2M_{np}}{F_0} = \frac{4}{3} \frac{a}{a_0} k \sqrt{k^2-1} \frac{A}{2BC}, \\ \bar{t}_* &= \frac{a_0 t_0}{a} = \frac{4}{3} k \sqrt{k^2-1} \frac{\mu}{C}. \end{aligned} \right\} \quad (19.30)$$

where

$$\mu = \frac{A}{2B}. \quad (19.31)$$

$$C = \frac{k^3}{k^2-1} \arcsin \sqrt{\frac{k^2-1}{k^2}} - \sqrt{\frac{1}{k^2-1}}. \quad (19.32)$$

The relationships of $\mu = \frac{A}{2B}$ and \bar{t}_* as functions of $\frac{1}{k} = \frac{a}{b}$ are shown in Figs. 77-78. For large k , we have

$$\mu \simeq \frac{\ln 2k-1}{k^2},$$

$$C \simeq \frac{\pi}{2},$$

and consequently,

$$\bar{t}_* = \frac{8}{3\pi} (\ln 2k - 1).$$

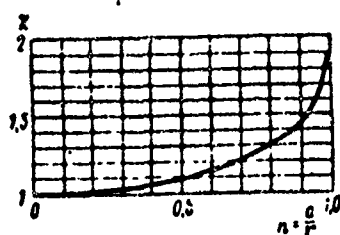


Fig. 79. Coefficient χ for an Infinitely-Long Small Arc of a Circle.

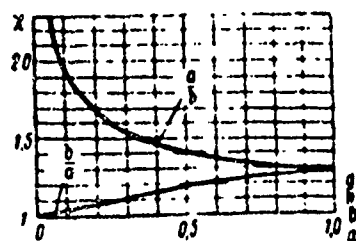


Fig. 80. Coefficient χ for an Infinitely-Long Elliptical Cylinder.

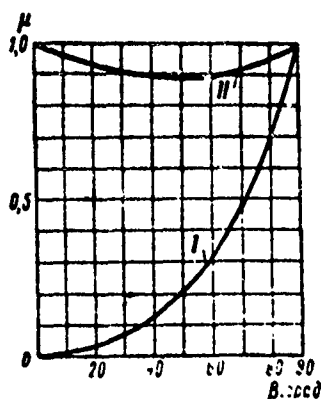


Fig. 81. Coefficient of apparent mass for an infinitely-long cylinder having a lune-shaped cross section.

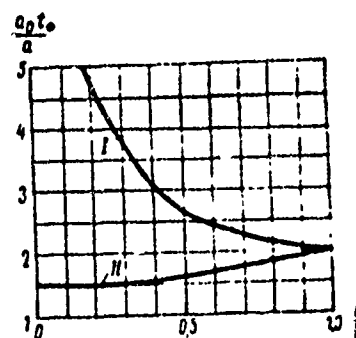


Fig. 82. Relationship of \bar{t}_* as a function of a/b for an infinitely-long cylinder having a lune-shaped cross section.

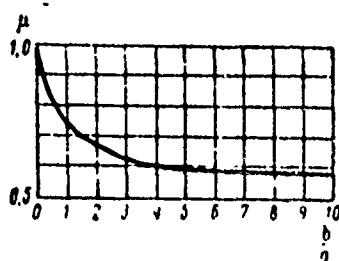


Fig. 83. Coefficient of apparent mass for an infinitely-long rhombic cylinder.

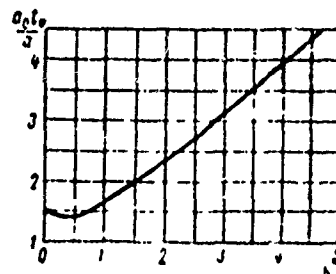


Fig. 84. Relationship of \bar{t}_* as a function of b/a for an infinitely-long rhombic cylinder.

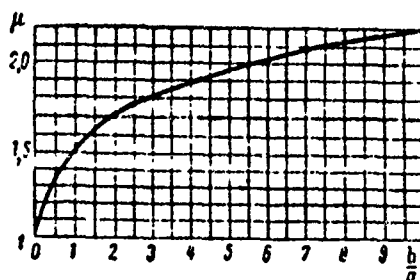


Fig. 85. Coefficient of apparent mass for an infinitely-long rectangular cylinder.

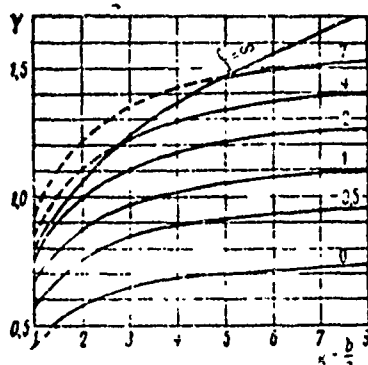


Fig. 86. Coefficient of apparent mass for a parallelepiped.

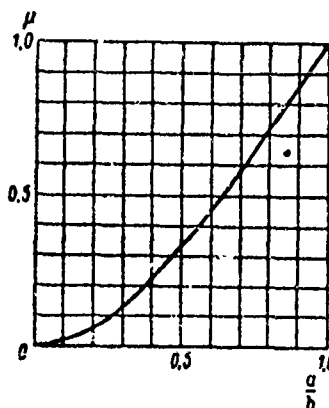


Fig. 87. Coefficient of apparent mass for an elliptical plate.

The quantities F_0 and \bar{E}_* are calculated by analogy for bodies of different shape. Calculated findings for plates of diverse configurations and several geometric bodies are shown in Tables 3 & 4 and in Figs. 79-87.

Table 3

Geometric Bodies	Apparent Mass (M_{np})	$\frac{1}{\rho_0 a_0} F_0$	$\bar{r}_0 \frac{a_0 l_0}{a}$	Note
Plane infinitely-long plate	$\pi \rho_0 a^2$	$4a$	$\frac{\pi}{2}$	
infinitely-long circle arc	$\frac{\pi}{2} \rho_0 a^2 \left(1 + \frac{1}{\cos^2 \alpha} \right)$	$2a \left(\sqrt{1-n^2} + \frac{\arcsin n}{n} \right)$ rad $n = \frac{a}{r} = \sin 2\alpha$	$\frac{\pi}{2} \gamma \frac{r_{de}}{2} \frac{1}{1 - \frac{1}{1-n^2} \frac{\arcsin n}{n}}$	Value of χ shown in Fig. 79
infinitely-long elliptical cylinder	$\pi \rho_0 a^2$	$\frac{4a}{\gamma}$	$\frac{\pi}{2} \gamma$	Values of χ shown in Fig. 80
infinitely-long round cylinder	$\pi \rho_0 a^2$	πa	π	

Table 3 (cont'd)

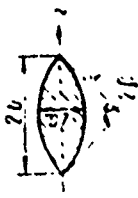
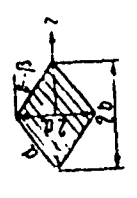
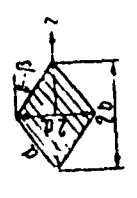
Geometric Bodies	Apparent Mass (M _{ap})	$\frac{I}{I_0} \cdot \frac{r_0}{a}$	$I_0 \cdot \frac{a^3}{a^3}$	Note
infinitely-long cylinder having lune-shaped cross section	 $\mu = \frac{\pi \rho_0 a^2 \sin^2 \beta}{3 - 1 - \frac{2}{\pi} + 2 \left(\frac{\beta}{\pi} \right)^2}$ $I_0 = \frac{\pi \rho_0 a^2 \sin^2 \beta}{3 \left(1 - \frac{2}{\pi} \right)^2}$	$2r \left(\frac{3}{2} - \frac{1}{2} \sin 2\beta \right)$	$\frac{\pi \cdot \sin^2 \beta}{(1 - \cos \beta) \left(\frac{3}{2} - \frac{1}{2} \sin 2\beta \right)}$	values of μ and t_* shown in Figs. 81 & 82 respectively (curves I)
rhombic cylinder	 $\mu = \frac{\pi \rho_0 a^2 \sin^2 \beta}{3 - 1 - \frac{2}{\pi} + 2 \left(\frac{\beta}{\pi} \right)^2}$ $I_0 = \frac{\pi \rho_0 a^2 \sin^2 \beta}{3 \left(1 - \frac{2}{\pi} \right)^2}$	$2r \left(\frac{3}{2} - \frac{1}{2} \sin 2\beta \right)$	$\frac{\pi \cdot \sin^2 \beta}{3 \left(1 - \frac{2}{\pi} \right)^2 \sin 2\beta}$	values of μ and t_* are shown in Figs. 81 & 82 respectively (curves II)
	 $\mu = \frac{\pi \rho_0 a^2 \sin^2 \beta}{3 - 1 - \frac{2}{\pi} + 2 \left(\frac{\beta}{\pi} \right)^2}$ $I_0 = \frac{\pi \rho_0 a^2 \sin^2 \beta}{3 \left(1 - \frac{2}{\pi} \right)^2}$	$4a \sin \beta$	$\frac{\pi \cdot \mu}{2} \sqrt{1 - \left(\frac{b}{a} \right)^2}$	values of μ and t_* shown in Figs. 83 & 84 respectively; $\Gamma(x)$ - gamma function



Table 3 (cont'd)

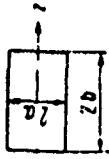
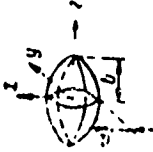


Geometric Bodies	Apparent Mass (M_{np})	$\frac{1}{F_0 d_n} F_0$	$\bar{t}_c = \frac{u_0 t_c}{u}$	Note
infinitely-long rectangular cylinder		$4a$	$\frac{\pi^2}{2}$	values of μ given in Fig. 85
ellipsoid of revolution (prolate)	 $\frac{4}{3} \pi a^3 k, \quad r_{1c} = \frac{b}{k} - \frac{a}{a}$	$\frac{2\pi a^2 C}{ k^2 - 1 }$	$\frac{1}{3} \cdot k k^2 - 1 \frac{\pi}{C}$	values of C - acc. to (19.32) Values of μ and t_* given in Figs. 77 & 78.
sphere		$\frac{4}{3} \pi a^2$	1	
parallelepiped		$8ab$	2γ	Values of γ given in Fig. 86

Table 4

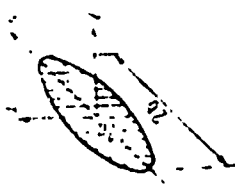
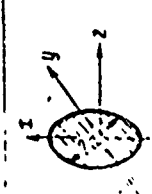
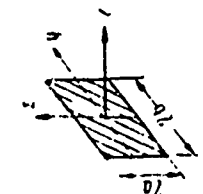

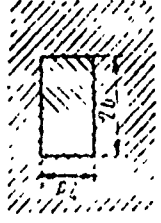
Plates	Apparent Mass (M_{np})	$\frac{1}{2} F_n$	$t_n = \frac{a_n}{a} t_0$	Note
Elliptical plate 	$\frac{8}{3} \rho g a^3$	$2\pi ab$	$\frac{8}{3} \frac{a}{b}$	values of μ given in Fig. 87
Disc 	$\frac{8}{3} \rho g a^3$	$2\pi a^2$	$\frac{8}{3}$	
Finite Rectangular plate 	$\frac{\pi}{4} \frac{k}{\sqrt{1+k^2}} \left(1 - 0.425 \frac{k}{1+k^2} \right)$ where $k = \frac{b}{a}$	$8ab$	2γ	

Table 4 (cont'd)

Plates	Apparent Mass (M_{app})	$\frac{1}{\rho_0} \rho_0$	$\frac{1}{\rho_0} \rho_0$	$\frac{1}{\rho_0} \rho_0$	Note
Round rigid-wall piston 	$\frac{8}{3} \rho_0 a^3$	πa^2	$\frac{16}{3\pi}$		
Rectangular rigid-wall piston 	$8 \rho_0 a^2 b$	$4ab$	4γ	values of γ given in Fig. 61	

§20. Hydrodynamic Forces Formed When Plane Wave Falls onto an Immobile Absolutely-Rigid Obstacle of Finite Dimensions and Arbitrary Shape

As we showed earlier, the problem of evaluating net load for the incidence of a plane wave onto an absolutely-rigid body can be reduced to determining drag for motion at a velocity which changes according to the unit function law. The unit function, in turn, reduces to the calculation of the function $\psi(t)$, which can always be calculated approximately if we are given the body's apparent mass.

Based on these ideas, let us show the way to practical evaluation of the net hydrodynamic force for the incidence of a plane wave onto a body of arbitrary shape.

After having selected the same system of coordinates as in the preceding section, and expanding the z axis in the direction of wave run, pressure on the direct wave and the rate of particle motion will be written in the form

$$p_{np}(z, t) = p_m f\left(t - \frac{z}{a_0}\right) \sigma_0\left(t - \frac{z}{a_0}\right), \quad (20.1)$$

$$v_{np}(z, t) = \frac{p_m}{\rho_0 a_0} f\left(t - \frac{z}{a_0}\right) \tau_0\left(t - \frac{z}{a_0}\right). \quad (20.2)$$

The net load will be written as the sum of two components

$$F(t) = F_{np}(t) + F_d(t), \quad (20.3)$$

where $F_{np}(t)$ - the load from the effect of direct-wave pressure on the surface of the body;

$F_d(t)$ - the load from the effect of additional pressure of the reflected and diffraction waves on the surface of the body.

By definition, the first component of load is

$$F_{np}(t) = - \int_{S_1} p_{np} \cos n z dS = - \rho_m \int_{S_1} f\left(t - \frac{z}{a_0}\right) \times \\ \times \cos\left(t - \frac{z}{a_0}\right) \cos n z dS = - \rho_m \int_{S_1} f\left(t - \frac{z}{a_0}\right) \cos n z dS, \quad (20.4)$$

where S_1 - the portion of the body surface situated in region $z \leq a_0 t$.

The second component is defined by the relation

$$F_n(t) = - \int_{S_1} p_n(x, y, z, t) \cos n z dS = \rho_0 \int_{S_1} \frac{\partial \varphi}{\partial t} \cos n z dS, \quad (20.5)$$

where φ - velocity potential satisfying the wave equation

$$\frac{\partial^2 \varphi}{\partial x^2} + \frac{\partial^2 \varphi}{\partial y^2} + \frac{\partial^2 \varphi}{\partial z^2} = \frac{1}{a_0^2} \frac{\partial^2 \varphi}{\partial t^2}. \quad (20.6)$$

The boundary conditions of the problem are:

on the surface of the body

$$\frac{\partial \varphi}{\partial n} + v_{np} \cos n z = 0 \quad (20.7)$$

or

$$\frac{\partial \varphi}{\partial n} = - \frac{1}{\rho_0 a_0} \rho_m f\left(t - \frac{z}{a_0}\right) \cos\left(t - \frac{z}{a_0}\right) \cos n z; \quad (20.8)$$

at a distance from the body

$$\varphi \rightarrow 0 \text{ при } r = \sqrt{x^2 + y^2 + z^2} \rightarrow \infty.$$

After applying, as before, the unilateral Laplace transform

$$\bar{\varphi} = \int_0^\infty \varphi(x, y, z, t) e^{-\nu t} dt \quad (\operatorname{Re} \nu > 0). \quad (20.9)$$

in transforms we find

$$\frac{\partial^2 \bar{\varphi}}{\partial x^2} + \frac{\partial^2 \bar{\varphi}}{\partial y^2} + \frac{\partial^2 \bar{\varphi}}{\partial z^2} = \frac{v^2}{a_0^2} \bar{\varphi}, \quad (20.10)$$

$$\frac{\partial \bar{\varphi}}{\partial n} = -\bar{v}_{np}(z, v) \cos \hat{n}z \Big|_{z=a_0}. \quad (20.11)$$

Let us designate that*

$$\bar{\varphi}^*(\bar{r}, v) = \int_{S_0} \bar{\varphi} \cos \hat{n}z dS, \quad (20.12)$$

$$\varphi^*(\bar{r}, t) = \int_{S_0} \varphi \cos \hat{n}z dS. \quad (20.13)$$

As in §19, let us write the function $\bar{\varphi}^*(\bar{r}, v)$ in the form

$$\bar{\varphi}^*(\bar{r}, v) = C(v) \bar{\varphi}(\bar{r}, v). \quad (20.14)$$

The boundary condition of (20.11) for $\bar{\varphi}^*(\bar{r}, v)$ can be written thus:

$$\frac{\partial \bar{\varphi}^*}{\partial \bar{r}} \Big|_{\bar{r}=1} = -\bar{Q}(v) \frac{1}{\rho_0 a_0}. \quad (20.15)$$

where $\bar{Q}(v)$ - the transform of the function:

$$Q(t) = \rho_0 a_0 \int_{S_0} \bar{v}_{np} \cos^2 \hat{n}z dS = \rho_m \int_{S_0} f\left(t - \frac{z}{a_0}\right) \times \\ \times a_0 \left(t - \frac{z}{a_0}\right) \cos^2 \hat{n}z dS. \quad (20.16)$$

We can easily illustrate the physical meaning of the function $Q(t)$. The form of its writing shows it to be nothing else than the load formed on the surface of a body under the influence of reflected wave pressure according to the hypothesis of plane reflection.

*As in §19, $\bar{r} = r/a$, where a is the distance from the origin of the coordinates to the surface of the body.

Consequently, according to (20.14) and (20.15)

$$\left. \frac{\partial \bar{\psi}^*}{\partial \bar{r}} \right|_{\bar{r}=1} = C(\nu) \left. \frac{\partial \bar{\psi}(\bar{r}, \nu)}{\partial \bar{r}} \right|_{\bar{r}=1} = -\bar{Q}(\nu)/\rho_0 a_0. \quad (20.17)$$

and consequently,

$$\bar{\psi}^*(\bar{r}, \nu) = -\frac{1}{\rho_0 a_0} \bar{Q}(\nu) \frac{\bar{\psi}(\bar{r}, \nu)}{\xi(\nu)}, \quad (20.18)$$

where

$$\xi(\nu) = \left. \frac{\partial \bar{\psi}(\bar{r}, \nu)}{\partial \bar{r}} \right|_{\bar{r}=1}.$$

Let us write the second component of net load in transforms. According to (20.5), (20.12), and (20.18), we have

$$\begin{aligned} \bar{F}_A &= \rho_0 \nu \int_S \bar{\varphi} \cos n\bar{z} dS = \rho_0 \nu \bar{\psi}^*(\bar{r}, \nu) \Big|_{\bar{r}=1} = \\ &= -\frac{1}{a_0} \nu \bar{Q}(\nu) \frac{\bar{\psi}(\bar{r}, \nu)}{\xi(\nu)} \Big|_{\bar{r}=1}, \end{aligned} \quad (20.19)$$

but [cf., for example, (19.19)]

$$-\frac{1}{a_0} \frac{\bar{\psi}(\bar{r}, \nu)}{\xi(\nu)} \Big|_{\bar{r}=1} = \bar{\psi}(\nu), \quad (20.20)$$

consequently,

$$\bar{F}_A = \nu \bar{Q}(\nu) \bar{\psi}(\nu). \quad (20.21)$$

Based on the Borel theorem for the original, we find that

$$F_A(t) = Q(0) \bar{\psi}(t) + \int_0^t \dot{Q}(t-\tau) \bar{\psi}(\tau) d\tau, \quad (20.22)$$

or, likewise,

$$F_A(t) = Q(t) + \int_0^t Q(t-\tau) \dot{\bar{\psi}}(\tau) d\tau. \quad (20.23)$$

The derived solution is approximate, because it satisfies boundary condition (20.17) in the integral sense of (20.15) and not at each and every point. It will be precise only for bodies having a surface motion which is orthogonal $\cos \hat{n}z$ in form, causing pressure which is distributed along the surface likewise according to the orthogonal law $\cos \hat{n}z$ (e.g., for a sphere and a round cylinder).

For arbitrarily-shaped bodies, precise relationships which establish the association between the diffraction load and drag were derived by L. I. Slepyan [17] by expanding body surface point displacements into a series in terms of a total system of vector functions.

Although relations (20.22) and (20.23) are generally approximate, by satisfying the boundary condition in the integral sense of (20.15), they permit us to precisely reduce the determination of diffraction load for an arbitrary rigid body of finite dimensions to the evaluation of drag of this same body in an ideal fluid. Moreover, the derived solution can easily be expanded to include the case of a shock-wave having a curvilinear front (e.g., spherical). Instead of the boundary condition (20.7), we will have:

$$-\frac{\partial \hat{z}}{\partial n} + v_{np} \cos \hat{n}v_{np} = 0, \quad (20.7a)$$

where $\hat{n}v_{np}$ - the angle between the direction of the external normal to the surface of a body and the direction of the vector of particle velocity in the direct wave.

A corollary of (20.7a) will only be a change in expression (20.16) for $Q(t)$:

$$Q(t) = \rho_0 a_0 \int_S v_{np} \cos \hat{n}v_{np} \cos \hat{n}z dS \quad (20.16a)$$

while retaining the final relations (20.22)-(20.23).

We earlier showed the feasibility of the linear approximation of

the function $\psi(t)$ [cf., for example, (19.23)]. In this case, where $t < t_*$

$$F_A(t) = Q(t) - \frac{1}{t_*} \int_0^t Q(\tau) d\tau, \quad (20.24)$$

where $t > t_*$

$$F_A(t) = Q(t) - \frac{1}{t_*} \int_0^{t_*} Q(t - \tau) d\tau = Q(t) - \frac{1}{t_*} \int_{t-t_*}^t Q(\tau) d\tau. \quad (20.25)$$

Let us designate the function $Q(t)$ for the effect of a unit amplitude wave using $Q_*(t)$. The function $Q_*(t)$ is variable until the wave encompasses the entire body. Henceforth, it becomes constant

$$Q_*(t) \Big|_{t=t_*} = F_0 \frac{1}{t_* a_0} = Q_0, \quad (20.26)$$

where $t_* = \frac{L}{a_0}$,

L - the length of the body in the direction of front propagation.

It follows that $F_A(t)$ is identically equal to zero where $t > t_* + t_*$. Methods of evaluating the functions $\psi(t)$ and $Q_*(t)$ have been illustrated many times above. Therefore, the theoretical portion of the problem can be considered as having been explained.

Let us illustrate these ideas with several examples.

Let us find the hydrodynamic force formed during the incidence of a plane wave onto a sphere. The value of the first load component was previously derived [cf. (17.61) and (17.62)]

$$F_{np} = \begin{cases} \pi a^2 (2\bar{l} - \bar{l}^2) & \text{where } \bar{l} < 2 \\ 0 & \bar{l} > 2. \end{cases} \quad (20.27)$$

According to (20.16), the quantity Q_* is

$$Q_*(t) = \iint_S \cos^2 \theta_{z_0} (\bar{l} + 1 - \cos \theta) dS =$$

$$= \begin{cases} \frac{2}{3} \pi a^2 [1 + (\bar{i} - 1)^2] & \text{where } \bar{i} < 2 \\ \frac{4}{3} \pi a^2 & \bar{i} \geq 2. \end{cases} \quad (20.28)$$

According to Table 3,

$$t_* = \frac{2M_{np}}{F_*} = \frac{a}{a_0}; \quad \bar{i}_* = 1. \quad (20.29)$$

Substituting (20.29) and (20.28) into (20.24) and (20.25), we find that

$$F_*(\bar{i}) = \frac{2}{3} \pi a^2 \begin{cases} \frac{5}{4} + (\bar{i} - 1)^2 - \bar{i} - \frac{1}{4}(\bar{i} - 1)^4 & \text{where } \bar{i} < \bar{i}_* = 1 \\ (\bar{i} - 1)^2 - \frac{(\bar{i} - 1)^4}{4} - \frac{(\bar{i} - 2)^4}{4} & \text{where } 1 < \bar{i} < 2 \\ -\bar{i} + 3 - \frac{1}{4} + \frac{(\bar{i} - 2)^4}{4} & \text{where } 2 < \bar{i} < 3 \\ 0 & \text{where } \bar{i} \geq 3. \end{cases} \quad (20.30)$$

A comparison of (17.67) and (17.68) with (20.30) shows that in the given (but perhaps the only) case, the approximate solution is somewhat more complicated than the precise solution. The convergence of results is satisfactory, as attested in Fig. 88a.

The advantage of the approximate method, from the point of view of simplicity in deriving a solution, becomes apparent when determining the load formed on a round cylinder. In this case [cf. (18.35)],

$$F_{np}(\bar{i}) = \begin{cases} 2a \sqrt{2\bar{i} - \bar{i}^2} & \text{where } \bar{i} < 2 \\ 0 & \bar{i} \geq 2. \end{cases} \quad (20.31)$$

$$Q_*(\bar{i}) = \begin{cases} a \left[\arccos(1 - \bar{i}) + (1 - \bar{i}) \sqrt{2\bar{i} - \bar{i}^2} \right] & \text{where } \bar{i} < 2 \\ a\pi & \text{where } \bar{i} \geq 2. \end{cases} \quad (20.32)$$

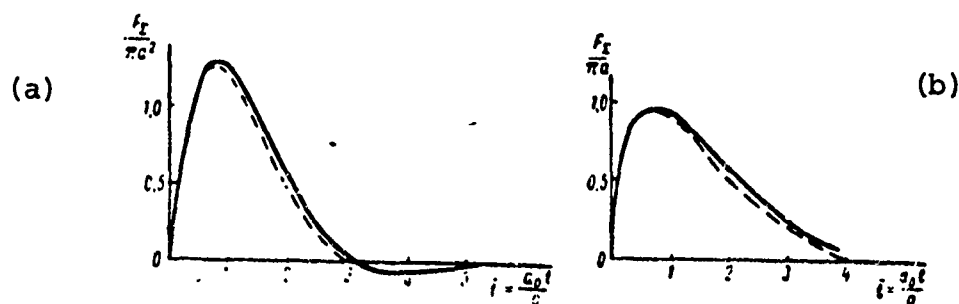


Fig. 88. Net Force Acting Upon an Immobile Rigid Sphere (a) and Round Cylinder (b) During Incidence of a Unit Shock Wave.

————— precise solution; ----- approximated.

while according to Table 3,

$$t_* = \frac{2M_{np}}{F_0} = \frac{2a}{a} \quad \bar{t}_* = 2,$$

$$F_A(\bar{t}) = \pi a \begin{cases} \frac{1}{2\pi} (3 - \bar{t}) \arccos(1 - \bar{t}) + \frac{1}{6\pi} (3 - 8\bar{t} + \bar{t}^2) \sqrt{2\bar{t} - \bar{t}^2} & \text{where } \bar{t} < 2 \\ \frac{3}{2} - \frac{\bar{t}}{2} - \frac{3 - \bar{t}}{2\pi} \arccos(3 - \bar{t}) + \frac{1}{\pi} \left(\frac{1}{2} + \frac{5\bar{t} - 8 - \bar{t}^2}{6} \right) \times & \\ \times \sqrt{6\bar{t} - 8 - \bar{t}^2} & \text{where } 2 < \bar{t} < 4 \\ 0 & \text{where } \bar{t} > 4 \end{cases} \quad (20.33)$$

Results calculated according to the precise (§18) and approximate solutions are shown in Fig. 88b. As we can see from the figure, the convergence is rather good here. The bulk of precise solution calculations cannot be compared with that shown above.

As one example, let us consider the net load acting on an ellipsoid of revolution during incidence of a plane wave. In this case,

$$F_{np}(\bar{t}) = \begin{cases} \pi a^2 (2\bar{t} - \bar{t}^2) & \text{where } \bar{t} < 2 \\ 0 & \text{where } \bar{t} \geq 2, \end{cases} \quad (20.34)$$

$$\text{where } \bar{t} = \frac{a_0 t}{b},$$

b - the large semiaxis of the ellipsoid in whose direction the wave propagates.

The quantity Q_* is calculated exactly as was shown in §19 when evaluating F_0 [cf. (19.26), (19.27)].

We have

$$Q_*(\bar{i}) = \begin{cases} \frac{\pi a^2}{\sqrt{k^2-1}} \left[\frac{k^2 \arcsin \frac{\sqrt{k^2-1}}{k}}{k^2-1} - \frac{1}{\sqrt{k^2-1}} - \frac{k^2 \arcsin \frac{\sqrt{k^2-1}}{k} (1-\bar{i})}{k^2-1} + (1-\bar{i}) \sqrt{\frac{k^2}{k^2-1} - (1-\bar{i})^2} \right] & \text{where } \bar{i} < 2 \\ \frac{2\pi a^2}{\sqrt{k^2-1}} \left(\frac{k^2 \arcsin \sqrt{\frac{k^2-1}{k^2}}}{k^2-1} - \frac{1}{\sqrt{k^2-1}} \right) & \text{where } \bar{i} > 2. \end{cases} \quad (20.35)$$

$$\text{where } k = \frac{b}{a}.$$

According to data of §19 and Table 3,

$$\bar{i}_* = \frac{a^2 f_0}{b} = \frac{4}{\pi} \sqrt{k^2-1} \cdot \frac{\mu}{C}, \quad (20.36)$$

where μ and C are defined by formulas (19.31) and (19.32).

Employing the relations (20.24) and (20.25) and integrating, we find that

$$F_A = \frac{\pi a^2}{\sqrt{k^2-1}} \begin{cases} A_1 \frac{1}{\bar{i}_*} - A_2 + B + C + D & \text{where } \bar{i} < \bar{i}_* \\ -A_2 + A_3 + C - E & \text{where } \bar{i}_* < \bar{i} < 2 \\ A_1 \frac{1-\bar{i}+\bar{i}_*}{\bar{i}_*} + A_3 - E - M & \text{where } 2 < \bar{i} < 2+\bar{i}_* \\ 0 & \text{where } \bar{i} > 2+\bar{i}_*. \end{cases} \quad (20.37)$$

where

$$\begin{aligned}
 A_1 &= -\frac{k^2 \arcsin \frac{\sqrt{k^2-1}}{k}}{k^2-1}, \\
 A_2 &= \left[\frac{k^2 \arcsin \frac{\sqrt{k^2-1}}{k} (1-\bar{i})}{k^2-1} \right] \left(\frac{1-\bar{i}}{\bar{i}_0} \right), \\
 A_3 &= \left[\frac{k^2 \arcsin \frac{\sqrt{k^2-1}}{k} (1-\bar{i} + \bar{i}_0)}{k^2-1} \right] \left(\frac{1-\bar{i} + \bar{i}_0}{\bar{i}_0} \right), \\
 B &= \left(A_1 - \frac{1}{\sqrt{k^2-1}} \right) \left(1 - \frac{\bar{i}}{\bar{i}_0} \right), \\
 C &= \left[\frac{k^2}{k^2-1} - (1-\bar{i})^2 \right] \left(1-\bar{i} \right) \left(1 - \frac{1-\bar{i}}{3\bar{i}_0} \right) - \\
 &\quad - \frac{4k^2}{3\bar{i}_0(k^2-1)}, \\
 D &= \frac{3k^2+1}{\bar{i}_0 \sqrt{k^2-1} 3(k^2-1)}, \\
 E &= \sqrt{\frac{k^2}{k^2-1} - (1-\bar{i} + \bar{i}_0)^2} \left[\frac{(1-\bar{i} + \bar{i}_0)^2}{3\bar{i}_0} - \frac{4k^2}{3\bar{i}_0(k^2-1)} \right], \\
 M &= \frac{1}{\bar{i}_0 \sqrt{k^2-1}} \left[\frac{3k^2+1}{3(k^2-1)} + 2 - \bar{i} + \bar{i}_0 \right].
 \end{aligned} \tag{20.38}$$

The results of calculating hydrodynamic forces F_{np} and F_d for the values of $k = b/a = 1, 2, 5, 10$, and 20 are shown in Fig. 89. This graph permits the visual picture of the diffraction component of load for different relative elongations of the ellipsoid. As k increases, the effect of diffraction is reduced and when $k = b/a > 10$ it may be ignored. This fact is very important in practical evaluations.

The net load $F = F_{np} + F_d$ formed on an ellipsoid as a function of $\bar{t}_1 = (a_0 t)/a$ (a - small semiaxis) is shown in Fig. 90. Aside from the conclusions already made, the graph permits us to consider the change in hydrodynamic force as a function of the relative elongation of the ellipsoid where the transverse cross section is the same.

In conclusion, let us find the load formed during incidence of a plane unit wave onto a parallelepiped having the dimensions $2a \times$

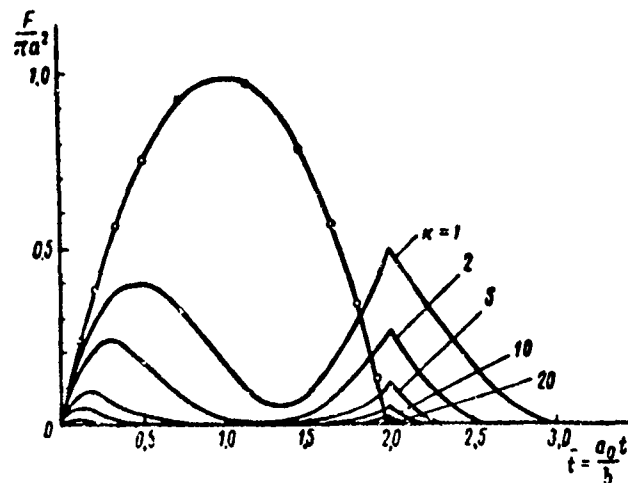


Fig. 89. Net Load Diffraction Component And Component from Direct Wave for Influence of Unit Shock Wave on a Prolate Ellipsoid of Revolution.

————— diffraction component F_d ,
 ----- component from direct wave F_{np}

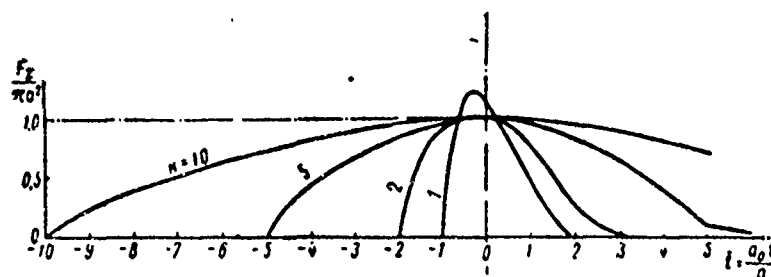


Fig. 90. Net Load for Influence of Unit Shock Wave on Prolate Ellipsoid of Revolution (time count begins when shock-wave front arrives at middle section).

X 2b X 2c. The wave propagates in the direction of edge 2c. In this case,

$$F_{np} = S |z_0(t) - z_0(t - t_1)|, \quad (20.39)$$

$$Q_* = S |z_0(t) + z_0(t - t_1)|, \quad (20.40)$$

where*

$$\left. \begin{aligned} S &= 4ab, \\ t_1 &= \frac{2c}{a_0}, \\ t_* &= \frac{2M_{np}}{F_0} = \frac{2a}{a_0} \gamma. \end{aligned} \right\} \quad (20.41)$$

$$F_A(t) = S \left\{ \left(1 - \frac{t}{t_*}\right) |z_0(t) - z_0(t - t_*)| + \left(1 - \frac{t - t_1}{t_*}\right) \times \right. \\ \left. \times |z_0(t - t_1) - z_0(t - t_1 - t_*)| \right\}. \quad (20.42)$$

The net load is

$$\frac{F(t)}{S} = \frac{F_{np}}{S} \frac{F_A}{F_0} = 2 - \bar{\rho}_1(t) - \bar{\rho}_1(t - t_1), \quad (20.43)$$

where

$$\bar{\rho}_1 = \frac{t}{t_*} z_0(t) - \frac{t - t_*}{t_*} z_0(t - t_*). \quad (20.44)$$

In a limiting case $c \rightarrow 0$, we derive the force formed on a rectangular plate

$$\frac{F(t)}{S} = \frac{F_A}{S} = 2 \left(1 - \frac{t}{t_*}\right) |z_0(t) - z_0(t - t_*)| \quad (20.45)$$

The values of the parameter $t_* = \frac{2a}{a_0} \gamma$ are given in Fig. 86.

*Cf. Tables 3, 4, and Fig. 86.

Let us find the pulse quantity of the net load. Integrating (20.43) for a parallelepiped, we find that

$$J = J_{np} + J_s = S(t_1 + t_s) = \frac{2Sc}{u_1} + \frac{M_{np}}{\rho_0 u_0}, \quad (20.46)$$

for a plate

$$J = J_s = St_1 = \frac{M_{np}}{\rho_0 u_0}. \quad (20.47)$$

The need often arises to define not the overall load acting on a body, but its individual components formed on sections of the surface; these components are in one way or another oriented with respect to the direction of wave propagation. Let us consider this problem using the example of a parallelepiped. Let us start with some general remarks.

We earlier showed that the second load component is defined by a relation similar to the Duhamel integral [cf. (20.22), (20.23)]. The function $\psi(t)$ characterizes change in force due to diffraction, while the function $Q(t)$ characterizes change in force due to the body being drawn into the wave's sphere of effect. Where $\psi(t) \equiv 1$ (the hypothesis of plane reflection), load is defined by the function $Q(t)$. If $Q(t)$ is a unit function, load would be defined by the function $\psi(t)$. Consequently, as we said in §17, there is total analogy between the functions $Q(t)$, $\psi(t)$, and the possible formalization of the solution of this problem. Specifically, the integral evaluations (20.22) and (20.23), at first approximation, can be expanded to an arbitrary portion of the body surface S_1

$$F_A(t)|_{S=S_1} = Q_{S_1}(0)\dot{\psi}(t) + \int_0^t Q_{S_1}(t-\tau)\dot{\psi}(\tau)d\tau, \quad (20.48)$$

or

$$F_A(t)|_{S=S_1} = Q_{S_1}(t) + \int_0^t Q_{S_1}(t-\tau)\dot{\psi}(\tau)d\tau. \quad (20.49)$$

Equations (20.48) and (20.49) would be precise if the additional pressure on an arbitrary point on the body were defined by a general function of time

$$p_A(t) = \cos n\alpha \dot{\psi}(t_1) z_0(t_1), \quad (20.50)$$

where t_1 - time, counted from the moment of the wave front's arrival at a given point.

We earlier noted that in the motion of a sphere and an infinitely-long round cylinder according to the unit function law, the relation (20.50) is satisfied. This generally does not occur, however. Therefore, formulas (20.48) and (20.49) can only be used to perform approximate practical evaluations.

Let us employ these ideas for a separate definition of loads acting on the frontal and lee surfaces of a plate and a parallelepiped. In the first case, in the incidence of a unit wave

$$Q_{\phi} = S z_0(t), \quad (20.51)$$

$$Q_{\tau} = S z_0(t). \quad (20.52)$$

and consequently, according to (20.48)

$$F_{\phi} = F_{A\phi} = S \dot{\psi}(t) z_0(t). \quad (20.53)$$

Adding the load from the direct wave pressure to this, we find

$$F_{\phi} = S(1 + \dot{\psi}(t)) z_0(t). \quad (20.54)$$

$$F_{\tau} = -S(1 - \dot{\psi}(t)) z_0(t), \quad (20.55)$$

or likewise,

$$\frac{F_{\phi}}{S} = 2 + \frac{F_{\tau}}{S} = 2 - \dot{\psi}, \quad (20.56)$$

$$\frac{F}{S} = 2(1 - \bar{p}_r) = 2\psi(t) \sigma_0(t), \quad (20.57)$$

where \bar{p}_r - the average load acting on the lee side of a plate.

Formulas (20.54)-(20.57) coincide with the relations established previously in section §13, attesting to the effectiveness of this method.

If we assume the linear approximation for $\psi(\bar{t})$, taking (20.44) into account, then

$$\frac{F_\phi}{S} = \left(2 - \frac{t}{t_*}\right) [\sigma_0(t) - \sigma_0(t - t_*)] + \sigma_0(t - t_*), \quad (20.58)$$

$$\frac{F_r}{S} = -\frac{t}{t_*} [\sigma_0(t) - \sigma_0(t - t_*)] - \sigma_*(t - t_*). \quad (20.59)$$

Let us employ formula (20.40) to evaluate load at the edges of a parallelepiped

$$Q = S[\sigma_0(t) + \sigma_0(t - t_*)],$$

whence

$$Q_\phi = S\sigma_0(t), \quad (20.60)$$

$$Q_r = S\sigma_0(t - t_*) \quad (20.61)$$

and consequently, according to (20.48)

$$F_{\phi\psi} = S\psi(t) \sigma_0(t), \quad (20.62)$$

$$F_{Ar} = S\psi(t - t_*) \sigma_0(t - t_*). \quad (20.63)$$

Adding the load from direct-wave pressure, we find that

$$F_\phi = S[1 + \psi(t)] \sigma_0(t). \quad (20.64)$$

$$F_r = -S[1 - \psi(t - t_l)] z_0(t - t_l). \quad (20.65)$$

This finding physically satisfies the assumption that at any point on the frontal surface, the diffraction pressure is exactly the same as at a symmetrically situated point on the lee side, differing only by a shift in time by the quantity $t_\ell = \frac{2c}{a_0}$. Strictly speaking, however, this is not so.

In the incidence of a direct wave onto a parallelepiped, diffraction waves are formed on the lee side after the time interval $t_\ell = \frac{2c}{a_0}$ and reach the edges of the facial surface after $\Delta t = 2t_\ell$, and not $\Delta t = t_\ell$ as occurs in the progressive motion; this effect can be described by the function $\psi(t)$. Consequently, formulas (20.48) and (20.49) somewhat reduce the load on the frontal side of the parallelepiped. Diffraction disturbances on the lee side appear at the edges in conjunction with the direct wave, inducing an additional rise in pressure. The error in evaluating net load vanishes and we arrive anew at precise quantities.

By analogy with (20.58) and (20.59), in the case of the linear approximation of the function $\psi(t)$ for loads at the edges of a parallelepiped, we have

$$\frac{F_\phi}{S} = \left(2 - \frac{t}{t_*}\right) [z_0(t) - z_0(t - t_*)] + z_0(t - t_*). \quad (20.66)$$

$$\frac{F_r}{S} = -\frac{t - t_l}{t_*} [z_0(t - t_l) - z_0(t - t_l - t_*)] - z_0(t - t_l - t_*). \quad (20.67)$$

or

$$\frac{F_\phi}{S} = 2 - \bar{p}_r, \quad (20.68)$$

$$\frac{F_r}{S} = -\bar{p}_r(t - t_l), \quad (20.69)$$

where average pressure \bar{p}_r is defined by (20.44)

The results derived can easily be expanded, with the aid of the Duhamel integral, to an arbitrarily-shaped wave

$$p = p_m f(t).$$

This problem is extremely simple, because the function \bar{p}_T is a linear function of time and consequently, as was shown in §12, the Dirac delta function will act as the subintegral expression.

Therefore, it comes down to calculating the expression

$$D(t) = \frac{p_m}{t_*} \int_0^t f(\tau) d\tau. \quad (20.70)$$

Thus for an exponential-shaped wave

$$p = p_m e^{-\frac{t}{t_*}} \sigma_0(t),$$

$$D_1(t) = \left(\frac{p_m}{t_*} \int_0^t e^{-\frac{\tau}{t_*}} d\tau \right) \sigma_0(t) = \frac{p_m t_*}{t_*} \left(1 - e^{-\frac{t}{t_*}} \right) \sigma_0(t); \quad (20.71)$$

for an exponent of limited duration

$$p = p_m e^{-\frac{t}{t_*}} [\sigma_0(t) - \sigma_0(t - t_*)],$$

$$D_2(t) = \frac{p_m t_*}{t_*} \left\{ \sigma_0(t) - e^{-\frac{t}{t_*}} [\sigma_0(t) - \sigma_0(t - t_*)] - e^{-\frac{t-t_*}{t_*}} \sigma_0(t - t_*) \right\}; \quad (20.72)$$

for a triangular-profile wave

$$p = p_m \left(1 - \frac{t}{t_*} \right) [\sigma_0(t) - \sigma_0(t - t_*)],$$

$$D_3(t) = \frac{p_m}{t_*} \left(t - \frac{t^2}{2t_*} \right) [\sigma_0(t) - \sigma_0(t - t_*)] + \frac{p_m t_*}{2t_*} \sigma_0(t - t_*); \quad (20.73)$$

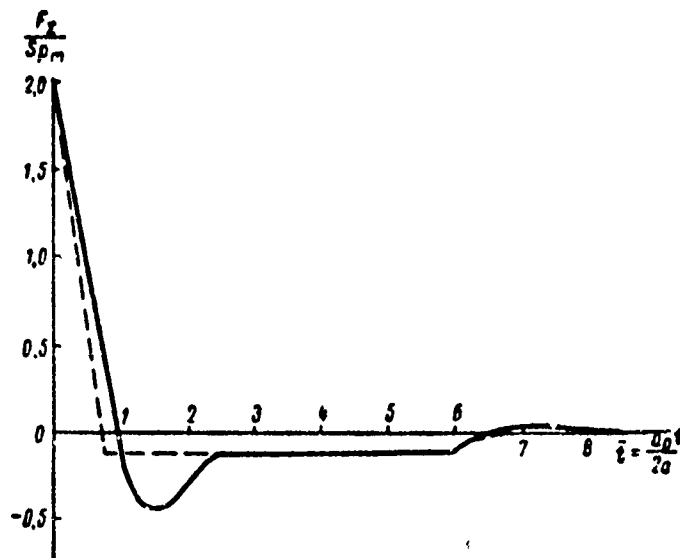


Fig. 91. Net Load on an Infinitely-Long Immobile Rigid Plate $2a$ in Width During Incidence onto it of a Triangular Shock-Wave of the $\tau = 6\frac{2a}{a_0}$ type.

{ for a parabolic-profile wave

$$p = p_m \left[1 - \left(\frac{t}{t_+} \right)^n \right] [z_3(t) - z_0(t)],$$

$$D_4(t) = \frac{p_m t_+}{t_*} \left[\frac{t}{t_+} - \frac{1}{n+1} \left(\frac{t}{t_+} \right)^{n+1} \right] [z_0(t) - z_0(t-t_+)] +$$

$$+ \frac{n}{n+1} \frac{p_m t_*}{t_*} z_0(t-t_+).$$

(20.74)

The load quantities at the edges of a parallelepiped will be

$$\frac{F_\phi}{S} = 2p_m f(t) - D(t) + D(t-t_*), \quad (20.75)$$

$$\frac{F_r}{S} = -[D(t-t_l) - D(t-t_l-t_*)]. \quad (20.76)$$

The net load is

$$\frac{F_\phi + F_r}{S} = 2p_m f(t) - D(t) - D(t-t_l) + D(t-t_*) + D(t-t_l+t_*). \quad (20.77)$$

Apparently, relations (20.75)-(20.77) may also be used for plates. For this purpose, it suffices to assume that $t_\ell \equiv 0$.

To illustrate, plotted in Fig. 91 is the variation curve of the net load acting on an infinitely-long rigid plate $2a$ in width during the normal incidence onto said plate of a triangular-profile plane wave having a duration of $t_+ = 6\frac{2a}{a_0}$. The solid line indicates calculation according to precise relations in section §13; the dotted line indicates calculation according to the formulas of this section. A totally satisfactory convergence of results occurs. This allows us to recommend the use of the simple relations derived here for practical evaluations.

Summing up, we may note that the methods evolved above permit us to reduce the solution of complex diffraction problems for bodies of arbitrary shape to the simplest calculations. It is only necessary to know the quantity of apparent mass of the body under consideration of of a body which is similar to it in contour.

CHAPTER III

THE EVALUATION OF EXTERNAL FORCES

§21. Generalized Hydrodynamic Forces of the First and Second Category

In the study of the interaction of a shock-wave with an obstacle, we ordinarily distinguish between hydrodynamic forces of the first and second category. Hydrodynamic forces of the first category includes forces formed on an obstacle under the assumption of its absolute rigidity. Hydrodynamic forces of the second category account for the effect of structural displacement and deformation.

In the most general case, displacements of a body are characterized by six generalized coordinates: three projections of displacement of center of gravity onto the coordinate axes and three angles of rotation about these axes. The coordinates can be described by the equations of solid body mechanics. We most often employ the Lagrange equation in its second form which, for holonomic systems, has the form

$$\frac{d}{dt} \left(\frac{\partial T}{\partial \dot{q}_i} \right) - \frac{\partial T}{\partial q_i} = F_i, \quad (21.1)$$

where T - kinetic energy of the system; q_i - generalized coordinate; F_i - generalized force.

Structural deformations, as we know, can be described by the corresponding differential equations of the theory of elasticity and plasticity.

The subject of research into the general problem of external forces during underwater explosion consists of the following: analysis of these systems in conjunction with the wave equation, satisfying the condition of equality in the normal velocity components on the surface of a body. The mathematical problems of such a task are

apparent. For purposes of simplification, we are often given the form of elastic-plastic deformation. The motion of several typical points enables us to deduce structural deformation as a whole (the "adduction" method).* In both the strict and simplified formulation, the reciprocal effect of deformation and load are specific for the problem of external forces during underwater explosion. The magnitude and nature of the external load absorbed by the structure is not only a function of the pressure fields during explosion in a free fluid, but also depends to a considerable extent on the characteristics of the structure itself. Structural displacements and deformations induced by the effect of a shockwave in turn lead to a change in the pressure fields. The considerable acoustic resistance of water makes this reciprocal effect extremely substantial.

The reciprocal effect of displacement and load can be illustrated using the simplest of examples. Let us consider the motion of an absolutely rigid body, which is symmetrical with respect to two mutually-perpendicular planes, under the effect of a plane shock-wave propagating along the main axis of symmetry. The motion of the body will be defined by one coordinate:

$$MW = F, \quad (21.2)$$

$$F = - \int_S p_\Sigma \cos nW dS, \quad (21.3)$$

where M - mass of the body; S - its surface; W - displacement; nW - the angle between the direction of motion and the external normal; p_Σ - net pressure on the surfaces of the body formed as a result of interaction with a shock-wave.

The association between net pressure and the potential function can be expressed by the relation

$$p_\Sigma = -\rho_0 \frac{\partial \dot{\varphi}}{\partial t}. \quad (21.4)$$

* The method of "adduction", as applied to dynamic calculation of marine structures, was developed by Yu. A. Shimanskiy [25].

The velocity potential can be defined by the wave equation

$$\frac{\partial^2 \varphi_z}{\partial x^2} + \frac{\partial^2 \varphi_z}{\partial y^2} + \frac{\partial^2 \varphi_z}{\partial z^2} = \frac{1}{a_0^2} \frac{\partial^2 \varphi_z}{\partial t^2}. \quad (21.5)$$

The boundary conditions are: on the surface of the body

$$\left. \frac{\partial \varphi_z}{\partial n} \right|_S = \dot{W} \cos \angle n W. \quad (21.6)$$

at a rather great distance from it

$$\varphi_z|_{r \rightarrow \infty} = \varphi_{np}, \quad (21.7)$$

where φ_{np} - the velocity potential of particles in the direct wave.

Even at its simplest, the solution of this problem led to the need for combined analysis of the wave and integro-differential equation

$$\left. \begin{aligned} M \frac{d^2 W}{dt^2} &= \rho_0 \int_S \frac{\partial \varphi_z}{\partial t} \cos \angle n W dS, \\ \frac{\partial^2 \varphi_z}{\partial x^2} + \frac{\partial^2 \varphi_z}{\partial y^2} + \frac{\partial^2 \varphi_z}{\partial z^2} &= \frac{1}{a_0^2} \frac{\partial^2 \varphi_z}{\partial t^2} \end{aligned} \right\} \quad (21.8)$$

with an extremely "unsuitable" boundary condition (21.6)

The notion of two categories of hydrodynamic forces, in conjunction with the use of the superposition principle, permits us to somewhat simplify the problem. Indeed, if we assume that the external load can be defined by two components F_1 and F_2 , one of which is not a function of structural displacements and deformations, then it is possible to evaluate, in an a priori simple way, the quantity of this component allowing for diffraction phenomena; this was the subject of the preceding chapter. The separate consideration of hydrodynamic forces of the second category permits us, on one hand, to indicate several general approaches with different assumptions on the nature of deformations; and on the other hand, to note in a number of cases relatively simple methods for obtaining final results with a given degree of pre-

cision. This comprises the advantage of the adopted classification of generalized hydrodynamic forces.

In this chapter, primary attention will be focused on the study of hydrodynamic forces of the second category and net loads during the interaction of an underwater shock wave with various types of pliant obstacles.

§22. The Interaction of a Shock-Wave with a Free Rigid Plate

The simplest case of interaction of an underwater shock-wave with a movable obstacle is the normal incidence of a plane wave onto an infinite free rigid plate. There are no diffraction effects present. The field of pressure and particle velocity in the fluid is only a function of one coordinate z . The study of this problem is of both methodological and practical interest, because this method can be used to evaluate the action of a shock wave on a plate where the period of the positive pressure phase is much shorter than the wave running time from the attached contour to the center.

Given that a plate divides two fluid media, each of which is homogeneous, but has its own density and speed of sound. For the positive direction of the z axis, let us use the direction of direct wave run; the origin of time counting - from the moment of arrival of the wave front at the surface of the plate; and the origin of the z axis - on the frontal surface of the plate. Then the pressure field on a direct wave propagating in the first medium will be characterized by the equation

$$p_{np} = p_m f\left(t - \frac{z}{a_1}\right) \varphi_0\left(t - \frac{z}{a_1}\right), \quad (22.1)$$

where p_m - pressure on the front; $f(t)$ - the function describing the change in pressure at the point of observation; a_1 - the speed of sound in the first medium.

The reflected wave can be written as two components: the wave reflected from the immobile obstacle and the wave induced by the motion of the obstacle under the influence of the net load.

The first component is

$$p_{\text{отр}}^I = \rho_m f\left(t + \frac{z}{a_1}\right) \sigma_0\left(t + \frac{z}{a_1}\right). \quad (22.2)$$

To define the second component, let us employ a wave equation for plane-symmetrical motion

$$\frac{\partial^2 \varphi}{\partial z^2} = \frac{1}{a_1^2} \frac{\partial^2 \varphi}{\partial t^2}, \quad (22.3)$$

where φ - the velocity potential of the additional field induced by plate motion.

Solving this equation with zero initial data and boundary conditions

$$\left. \frac{\partial \varphi}{\partial z} \right|_{z=0} = W, \quad (22.4)$$

$$\varphi \rightarrow 0 \text{ при } z \rightarrow \infty \quad (22.5)$$

and using the potential φ to take into account relationships for particle velocity and pressure, for the second component of the pressure field on the reflected wave we will find that

$$p_{\text{отр}}^{II} = -\rho_1 a_1 W' \left(t + \frac{z}{a_1}\right) \sigma_0 \left(t + \frac{z}{a_1}\right), \quad (22.6)$$

where $W(t)$ - displacement of the obstacle; ρ_1 - density of the first medium.

Therefore, the net pressure field in the fluid in front of the obstacle is

$$\begin{aligned} p_{\text{отр}}(z, t) = p_{\text{отр}}^I + p_{\text{отр}}^{II} = & \rho_m f\left(t - \frac{z}{a_1}\right) \sigma_0\left(t - \frac{z}{a_1}\right) + \\ & + \rho_m f\left(t + \frac{z}{a_1}\right) \sigma_0\left(t + \frac{z}{a_1}\right) - \rho_1 a_1 W' \left(t + \frac{z}{a_1}\right) \sigma_0\left(t + \frac{z}{a_1}\right). \end{aligned} \quad (22.7)$$

Because the direction of particle motion in the direct wave coincides with the positive direction of the z axis and in the reflected wave runs counter to it, the net particle velocity in front of the plate is

$$v_{pe}(z, t) = v_{np} - v_{orp} = \frac{p_{np} - p_{orp}}{\rho_1 a_1}. \quad (22.8)$$

We can easily see that for final evaluation of the pressure and velocity fields, we must know the still unknown function $\dot{W}(t)$. Let us use Newton's law to define it

$$m\ddot{W}(t) = F_1(t) + F_2(t), \quad (22.9)$$

where $m = \rho_2 \delta$ - the mass of the plate, adjusted to a unit of area (ρ_2 - the density of the plate material; δ - its thickness);

$F_1(t)$, $F_2(t)$ - generalized hydrodynamic forces of the first and second category, likewise adjusted to a unit of plate area.

By definition, $F_1(t)$ is equal to the net pressure on the immobile obstacle according to (22.7):

$$F_1(t) = 2p_{np}(0, t) = 2\rho_m f(t) z_0(t). \quad (22.10)$$

The generalized force of the second category F_2 is defined by the pressure induced by the motion of the plate. One of the components of this force was previously derived and can be described by formula (22.6).

If the fluid behind the obstacle has a density ρ_3 and a speed of sound a_3 , the radiation pressure in the second medium is

$$p_{rad} = \rho_3 a_3 \dot{W} \left(t - \frac{z - z_0}{a_3} \right) z_0 \left(t - \frac{z - \delta}{a_3} \right). \quad (22.11)$$

Considering that plate displacement occurs due to the difference in pressure on both of its sides, for the generalized force of the

second category we find that

$$F_2(t) = p_{0rp}|_{z=0} - p_{03n}|_{z=-l,0} = -[\rho_1 a_1 \dot{W}(t) + \rho_2 a_2 \dot{W}(t)] z_0(t). \quad (22.12)$$

As follows from (22.12), the net load $F = F_1 + F_2$ is a function of the parameters of obstacle motion; these in turn are defined by the effect of this load. The evaluation of external forces in underwater explosion is impossible in isolation from the study of the structural deformations (displacements) induced by them. This circumstance defines the primary difficulties in the external force problem.

At its simplest, the load F_2 is a linear function of the plate's rate of motion and the derivation of final results offers no problem.

Combining (22.9), (22.10), and (22.12) yields

$$m \ddot{W} + (\rho_1 a_1 + \rho_2 a_2) \dot{W} = 2p_m f(t) z_0(t). \quad (22.13)$$

The general integral of an ordinary differential equation of second order (22.13) is

$$W(t) = W_0 + \frac{\dot{W}_0}{\beta_*} (1 - e^{-\beta_* t}) + \frac{2p_m}{\rho_1 a_1 + \rho_2 a_2} \int_0^t f(\xi) d\xi - \frac{2p_m}{\rho_1 a_1 + \rho_2 a_2} \int_0^t e^{-\beta_* (t-\xi)} f(\xi) d\xi, \quad (22.14)$$

where

$$\beta_* = \frac{\rho_1 a_1 + \rho_2 a_2}{m}.$$

As a rule, from the practical standpoint the solution of (22.14) with zero initial data (where $t = 0$, $W = \dot{W} = 0$) is of primary interest. Let us consider it in greater detail under that assumption. Above all, let us note that, as follows from (22.9), the plate accelerates only where $F = F_1 + F_2 > 0$. Consequently, the maximum velocity \dot{W} is attained at time $t = t_H$, where $F(t_H) = 0$.

Because pressure behind the obstacle is directly proportional to its rate of motion, the maximum pressure value behind the obstacle corresponds to time t_H .

Because

$$F = F_1 + F_2 = 2\rho_{np}(t) - (\rho_1 a_1 + \rho_3 a_3) \dot{W}(t), \quad (22.15)$$

the magnitude of maximum plate motion can be derived from the equation

$$\dot{W}_{max} = \dot{W}(t_H) = \frac{2}{\rho_1 a_1 + \rho_3 a_3} \rho_{np}(t_H). \quad (22.16)$$

According to (22.11), the pressure behind the plate which corresponds to this magnitude is

$$\rho_3 \dot{W}_{max} = \rho_3 a_3 \dot{W}(t_H) = \frac{2\rho_3 a_3}{\rho_1 a_1 + \rho_3 a_3} \rho_{np}(t_H). \quad (22.17)$$

The time t_H of acquisition of maximum velocity is inversely proportion to acceleration and consequently, proportional to the mass of the plate.

The greatest momentum acquired by the plate due to the shock wave can be easily derived by integrating (22.9) from zero to t_H .

We have

$$m \dot{W}(t_H) = m \dot{W}_{max} = \int_0^{t_H} F(\xi) d\xi = J_+, \quad (22.18)$$

where J_+ - the pulse of the positive phase of net load. Comparing (22.18) and (22.16), we conclude that

$$J_+ = \frac{2m}{\rho_1 a_1 + \rho_3 a_3} \rho_{np}(t_H). \quad (22.19)$$

Time t_H , like the nature of variation in parameters of motion, is a function of the direct-wave pressure contour.

Let us evaluate the most often encountered cases in practical applications.

1. Pressure on the direct shock-wave changes according to the unit discontinuity function law

$$p_{dp}(t) = p_m z_0(t).$$

The solution of the differential equation (22.14) with zero initial data has the form

$$\psi(t) = \frac{2p_m}{\rho_1 a_1 + \rho_3 a_3} \left[t - \frac{1}{\beta_*} (1 - e^{-\beta_* t}) \right], \quad (22.20)$$

$$\dot{\psi}(t) = \frac{2p_m}{\rho_1 a_1 + \rho_3 a_3} (1 - e^{-\beta_* t}), \quad (22.21)$$

where

$$\beta_* = \frac{\rho_1 a_1 + \rho_3 a_3}{m}. \quad (22.22)$$

The rate of plate motion at first increases abruptly, and then asymptotically approaches its limiting value

$$\dot{\psi}(t)|_{t \rightarrow \infty} \rightarrow \dot{\psi}_{\max} = \frac{2p_m}{\rho_1 a_1 + \rho_3 a_3}. \quad (22.23)$$

The maximum velocity is not a function of plate mass and can only be defined by pressure on the front and the acoustic properties of the media.

Pressure in front of the obstacle is reduced from the doubled pressure on the direct-wave front to the quantity

$$p_{1 \min} = p_m \left[2 - \frac{2\rho_1 a_1}{\rho_1 a_1 + \rho_3 a_3} \right] = \frac{2\rho_3 a_3}{\rho_1 a_1 + \rho_3 a_3} p_{1*}, \quad (22.24)$$

Pressure behind the obstacle increases from zero to this same quantity

$$p_{3 \max} = p_{1 \min} = \frac{2\rho_3 a_3}{\rho_1 a_1 + \rho_3 a_3} p_{1*}. \quad (22.25)$$

These limiting pressure values coincide with the amplitude of a refracted wave at the interface of two media having acoustic resistances $\rho_1 a_1$ and $\rho_3 a_3$. The presence of a rigid obstacle only induces inertial retardation of the process of refraction. As the acoustic resistance of the medium behind the obstacle increases, pressure in this medium increases; when acoustic resistance is reduced, the pressure drops. When the acoustic resistances of the media are equal, pressure in front of and behind the obstacle tends to equalize itself with the pressure on the direct wave; the rate of plate motion tends to be equalized with the velocity of particles behind the direct wave front. Where $\rho_3 a_3 \ll \rho_1 a_1$, pressure behind the obstacle becomes negligibly small. Net pressure in the medium in front of the obstacle also approaches this same quantity.

2. Pressure on the direct shock-wave changes according to an exponential law

$$p_{np}(t) = p_m e^{-\frac{t}{\tau} c_0(t)}.$$

The solution of the differential equation (22.14) has the form

$$W(t) = \frac{2\rho_m h^2}{m(\beta_1 + \beta_3)(\beta_1 - \beta_3 - 1)} \left[\beta_1 + \beta_3 - 1 + e^{-\frac{t}{\tau}(\beta_1 + \beta_3)} - (\beta_1 + \beta_3)e^{-\frac{t}{\tau}} \right], \quad (22.26)$$

$$\dot{W}(t) = \frac{2\rho_m h}{m(\beta_1 - \beta_3 - 1)} \left[e^{-\frac{t}{\tau}} - e^{-\frac{t}{\tau}(\beta_1 + \beta_3)} \right], \quad (22.27)$$

where

$$\left. \begin{aligned} \beta_1 &= \frac{\rho_1 a_1 h}{m}, \\ \beta_3 &= \frac{\rho_3 a_3 h}{m}. \end{aligned} \right\} \quad (22.28)$$

According to (22.27) and (22.7), net pressure on the frontal surface of the obstacle is

$$\begin{aligned}
 p_1(t) &= 2p_m \left\{ e^{-\frac{t}{\tau}} - \frac{\beta_1}{\beta_1 + \beta_2 - 1} \left[e^{-\frac{t}{\tau}} - e^{-(\beta_1 + \beta_2)\frac{t}{\tau}} \right] \right\} = \\
 &= \frac{2p_m}{\beta_1 + \beta_2 - 1} \left[\beta_1 e^{-(\beta_1 + \beta_2)\frac{t}{\tau}} - (1 - \beta_2) e^{-\frac{t}{\tau}} \right].
 \end{aligned}
 \tag{22.29}$$

According to (22.27) and (22.11), pressure on the lee surface of the plate is

$$p_2(t) = \frac{2p_m\beta_2}{\beta_1 + \beta_2 - 1} \left[e^{-\frac{t}{\tau}} - e^{-(\beta_1 + \beta_2)\frac{t}{\tau}} \right].
 \tag{22.30}$$

The time of acquisition t_H of maximum pressure behind the obstacle (greatest rate of plate motion) can be found by solving the transcendental equation

$$e^{-\frac{t_H}{\tau}} - (\beta_1 + \beta_2) e^{-(\beta_1 + \beta_2)\frac{t_H}{\tau}} = 0,
 \tag{22.31}$$

whence

$$t_H = \tau \frac{\ln(\beta_1 + \beta_2)}{\beta_1 + \beta_2 - 1}.
 \tag{22.32}$$

Considering that

$$p_{np}(t_H) = p_m e^{-\frac{\ln(\beta_1 + \beta_2)}{\beta_1 + \beta_2 - 1}} = p_m (\beta_1 + \beta_2)^{-\frac{1}{\beta_1 + \beta_2 - 1}},
 \tag{22.33}$$

and in view of (22.17), we will derive maximum pressure behind the obstacle in the form

$$p_{s\max} = \frac{2\rho_2 a_2}{\rho_1 a_1 + \rho_2 a_2} p_m (\beta_1 + \beta_2)^{-\frac{1}{\beta_1 + \beta_2 - 1}}.
 \tag{22.34}$$

From the applied point of view, two cases are of the greatest interest: when water is found in front of and behind the obstacle (the problem of plate protective properties) and when water is in front of the plate and air is behind it (dynamic calculation of plates

and covers forming the body of a ship or other hydrotechnic structures).

In the first case, which was first studied by Novozhilov, Lefonova, and Aleksandrin,

$$\beta_1 = \beta_2 = \beta = \frac{2u_0^2}{m}.$$

According to (22.29) and (22.30), pressure in front of and behind the plate will be

$$p_1(t) = \frac{2p_m}{2\beta - 1} \left[(\beta - 1)e^{-\frac{t}{\beta}} + \beta e^{-2\beta \frac{t}{\beta}} \right], \quad (22.35)$$

$$p_2(t) = \frac{2\beta p_m}{2\beta - 1} \left[e^{-\frac{t}{\beta}} - e^{-2\beta \frac{t}{\beta}} \right]. \quad (22.36)$$

The time that the plate acquires the greatest rate of motion will constitute

$$t_m = 0 \frac{\ln 2\beta}{2\beta - 1}. \quad (22.37)$$

The maximum pressure behind the plate corresponding to this time is

$$p_{2max} = p_m e^{-\frac{t_m}{\beta}} = p_m (2\beta)^{\frac{1}{1-2\beta}}. \quad (22.38)$$

Figs. 9 -93 show graphs of the functions $\frac{p_1(t)}{p_m}$, $\frac{p_2(t)}{p_m}$ for different values of β . The graph indicates that pressure in front of and behind the plate remains positive; pressure behind the plate rapidly increases to maximum magnitude, then changing roughly in accordance with the same law as pressure on the direct wave; where $\beta \geq 5$, the protective properties of obstacles are small. Maximum pressure in this case is reduced by no more than 20%.

There is likewise some interest in evaluating the pulse of pressure and energy flux density translated across the obstacle.

According to (5.52), (5.56), and (22.36), for the indicated quantities we get:

$$J = \int_0^{\infty} p_d dt = \frac{2\beta}{2\beta - 1} p_m \left[\int_0^{\infty} e^{-\frac{t}{\tau}} dt - \int_0^{\infty} e^{-\frac{t}{\tau}} dt \right] = p_m \tau, \quad (22.39)$$

$$E = \frac{1}{\rho_0 a_0} \int_0^{\infty} p_d^2 dt = k E_{np}, \quad (22.40)$$

where $k = (2\beta)/(2\beta + 1)$ - the coefficient describing the loss of wave energy as the obstacle passes;

$$E = \frac{1}{2} \frac{p_m^2}{\rho_0 a_0} \quad - \text{direct-wave energy flux density.}$$

Therefore, the pressure pulse in a passing wave is equal to the pressure pulse of the direct wave.* Pulse maintenance occurs with some drop in amplitude due to the increase in activity duration. Energy flux density behind the plate is proportional to the coefficient β , i.e., the shorter the wave is, the less energy flux density is. Where $\beta > 5$, the decrease in wave energy behind the obstacle is not in excess of 10% of the initial energy.

The maximum travel of the obstacle, according to (22.26) where $t \rightarrow \infty$ attains the value

$$W_{max} = \frac{p_m \tau}{\rho_0 a_0}, \quad (22.41)$$

which is equal to the displacement of fluid particles after the direct wave has passed.

Let us now consider the second case ($\beta_1 = \beta$, $\beta_3 = 0$)** , whose primary features were described by Cowle [10]. These data are quite important from the practical standpoint, since they describe the initial phase of interaction of an underwater shock wave with pliant

*As Slepyan showed, this conclusion is valid under considerably more general assumptions.

**Because the acoustic resistance of air is almost 3500 times less than the acoustic resistance of water: $\beta_3/\beta_1 \approx 0.3 \cdot 1/10^3$, we can assume that $\beta_3 = 0$.

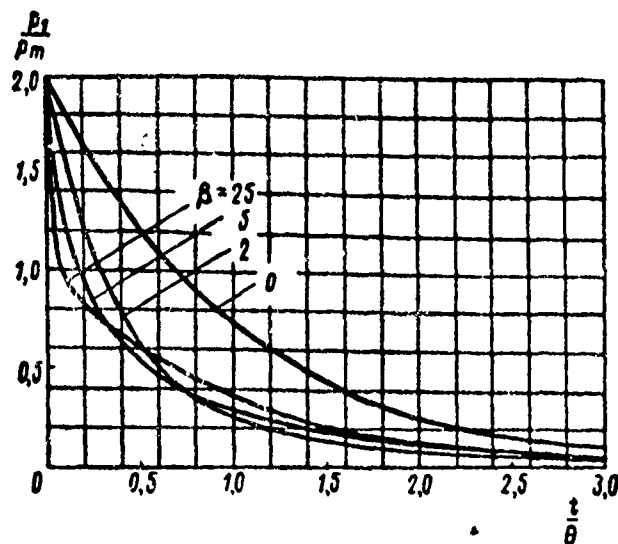


Fig. 92. Net Pressure in Front of a Plate Which is Completely Submerged in Water, for Various Values of $\beta = \frac{0^a 0}{m}$ as a function of Time During the Incidence on Said Plate of an Exponential-shaped Underwater Shock Wave.

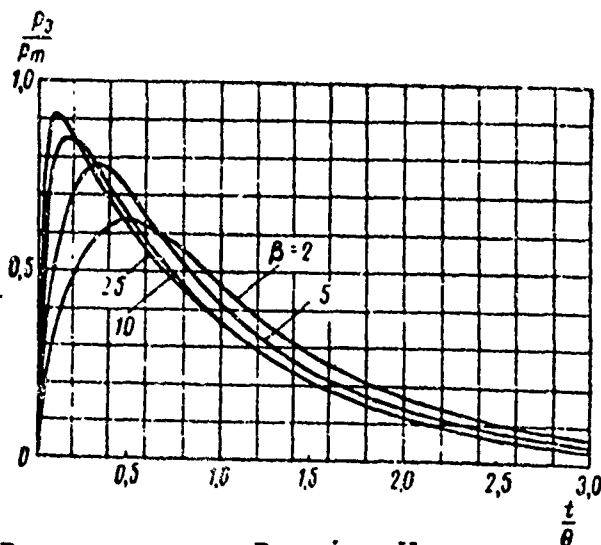


Fig. 93. Pressure on a Passing Wave Behind a Plate which is Completely Submerged in Water, for Various Values of β as a function of Time During the Incidence onto Said Plate of an Exponential-Shaped Underwater Shock Wave.

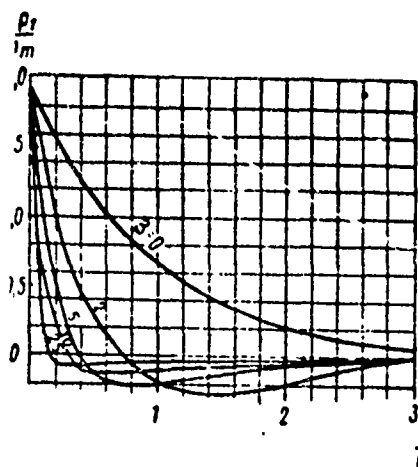


Fig. 94. Net Pressure in front of Plate Separating Two Media (Water and Air) as a Function of Time during Incidence onto said plate of exponential-shaped underwater shock wave.

structures. Employing previously derived results, we get the following relations:

plate travel

$$W(t) = \frac{2\rho_m g}{\rho_0 a_0} \left[1 - \frac{1}{\beta - 1} \left(\beta e^{-\frac{t}{\theta}} - e^{-\frac{\beta t}{\theta}} \right) \right]; \quad (22.42)$$

rate of plate motion

$$\dot{W}(t) = \frac{2\rho_m g}{\rho_0 a_0} \frac{\beta}{\beta - 1} \left(e^{-\frac{t}{\theta}} - e^{-\frac{\beta t}{\theta}} \right), \quad (22.43)$$

pressure on the reflected wave

$$\begin{aligned} p_{orp}(t) &= \rho_m g e^{-\frac{t}{\theta}} - 2\rho_m g \frac{\beta}{\beta - 1} \left(e^{-\frac{t}{\theta}} - e^{-\frac{\beta t}{\theta}} \right) = \\ &= \frac{\rho_m g}{\beta - 1} \left[2e^{-\frac{\beta t}{\theta}} - (1 + \beta)e^{-\frac{t}{\theta}} \right], \end{aligned} \quad (22.44)$$

net pressure

$$p_1(t) = p_m + p_{orp} = \frac{2\rho_m g}{\beta - 1} \left(\beta e^{-\frac{t}{\theta}} - e^{-\frac{\beta t}{\theta}} \right). \quad (22.45)$$

Fig. 94. shows net pressure on a plate plotted against time for various values of the coefficient β . The magnitude $\beta = 0$ is satisfied by an infinitely-large mass (the plate is immobile). In this case, pressure remains positive. For all other values of the coefficient β , there is a rapid drop in pressure as negative stresses are formed in the fluid.

The effect-time of the positive phase of excess net pressure, according to (22.32), is

$$t_n = 6 \frac{\ln 3}{\beta - 1}. \quad (22.46)$$

We can use relation (22.19) to define the pulse of the positive pressure phase. We get

$$J_+ = \frac{2m}{\rho_1 a_1} p_{np}(t_n) = \frac{2p_m \theta}{\beta} e^{-\frac{t_n}{\theta}}. \quad (22.47)$$

Because the total pulse of net pressure is

$$J_1 = \int_0^{\infty} p_1(t) dt = \frac{2p_m \theta}{\beta - 1} \left(e^{-\frac{t}{\theta}} - e^{-\beta \frac{t}{\theta}} \right) \Big|_0^{\infty} = 0, \quad (22.48)$$

the absolute value of the pulse of the negative pressure phase is equal to J_+ .

The net pressure curves have a minimum whose position is defined from the equation

$$-\beta^2 e^{-\beta \frac{t}{\theta}} + e^{-\frac{t}{\theta}} = 0. \quad (22.49)$$

The occurrence time of the minimum is

$$t_{\min} = \theta \frac{2 \ln \beta}{\beta - 1} = 2t_n. \quad (22.50)$$

After substituting (22.50) into (22.45), the quantity of minimum net pressure will be derived in the form

$$p_{\min} = -2p_m a_0^{\frac{1+\beta}{1-\beta}}. \quad (22.51)$$

For the most frequently encountered interval of values $\beta > 5$, the absolute quantity p_{\min} does not exceed $0.18p_m$. At some distance from the obstacle, however, net pressure in the fluid may attain substantially greater negative amplitudes, because at these points the expansion phase of the reflected wave is superimposed on the tail section of the direct wave. According to (22.7) and (22.44), for an arbitrary point in a medium in front of an obstacle

$$p_{\text{res}}(z, t) = p_m \left\{ e^{-\frac{1-z}{a_0}} \gamma_0 \left(t - \frac{z}{a_0} \right) + \right. \\ \left. + \frac{1}{\beta-1} \left[2\gamma_0 e^{-\frac{\beta \left(t + \frac{z}{a_0} \right)}{1-\beta}} - (1+\beta) e^{-\frac{1+\frac{z}{a_0}}{1-\beta}} \right] \gamma_0 \left(t + \frac{z}{a_0} \right) \right\}. \quad (22.52)$$

Calculations according to (22.52) are shown in Fig. 95, which is taken from Cowle [10]. We can see from the figure that zero net pressure is formed to begin with on the plate. Negative stresses of a given amplitude are formed earlier at the corresponding points in the fluid. These stresses propagate in the medium, which is disturbed by the passage of the direct wave of diminishing amplitude. Consequently, in an absolute system of coordinates their rate of travel is slightly greater than the speed of sound. In a fixed range of quantities p_m and β , net negative pressure can be greater than the sum of hydrostatic pressure and the yield stress of the fluid. Cavitation occurs*.

The primary qualitative results during interaction of a plate with a plane wave of other shape remain the same as in this case. Thus, for a direct wave of parabolic and triangular profile, we are restricted only by the writing of the appropriate theoretical relations.

* On the interaction of a shock-wave with a plate, allowing for cavitation, see §32-34.

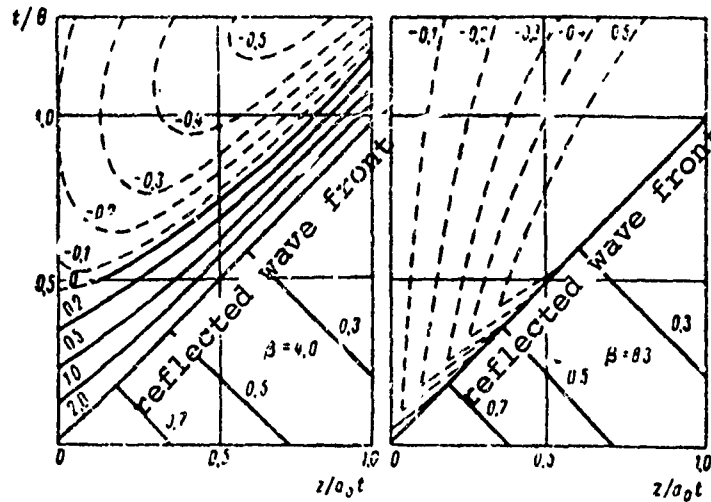


Fig. 95. Net Pressure in Front of a Plate in z and t Axes.

3. Pressure on a direct shock wave is a linear function of time:

$$p_{np}(t) = \left(1 - \frac{t}{t_+}\right) [z_0(t) - z_0(t - t_+)]. \quad (22.53)$$

The solution of differential equation (22.14) will be

$$\begin{aligned} W(t) = & \frac{2p_m}{\rho_1 a_1 + \rho_2 a_2} \left\{ -\frac{t^2}{2t_+} + \left(1 + \frac{1}{\beta_1 + \beta_2}\right) \times \right. \\ & \times \left[t - \frac{t}{\beta_1 + \beta_2} \left(1 - e^{-\frac{-(\beta_1 + \beta_2)t}{t_+}}\right) \right] \Big| z_0(t) - z(t - t_+) \Big| + \\ & + \frac{2p_m t_+}{\rho_1 a_1 + \rho_2 a_2} \left\{ \frac{1}{2} + \frac{1}{\beta_1 + \beta_2} - \frac{1}{\beta_1 + \beta_2} \left(1 + \frac{1}{\beta_1 + \beta_2}\right) \times \right. \\ & \times \left[1 - e^{-\frac{-(\beta_1 + \beta_2)t}{t_+}} \right] + \frac{1}{(\beta_1 + \beta_2)^2} \left[1 - e^{-\frac{-(\beta_1 + \beta_2)(\frac{t}{t_+} - 1)}{t_+}} \right] \Big| z_0(t - t_+) \Big| \right\}. \end{aligned} \quad (22.54)$$

$$\begin{aligned} \dot{W}(t) = & \frac{2p_m}{\rho_1 a_1 + \rho_2 a_2} \left\{ \left[\left(1 - e^{-\frac{-(\beta_1 + \beta_2)t}{t_+}}\right) \left(1 + \frac{1}{\beta_1 + \beta_2}\right) - \frac{t}{t_+} \right] \times \right. \\ & \times [z_0(t) - z_0(t - t_+)] + \left[-e^{-\frac{-(\beta_1 + \beta_2)t}{t_+}} \left(1 + \frac{1}{\beta_1 + \beta_2}\right) + \right. \\ & \left. \left. + \frac{1}{\beta_1 + \beta_2} e^{-\frac{-(\beta_1 + \beta_2)(\frac{t}{t_+} - 1)}{t_+}} \right] z_0(t - t_+) \right\}. \end{aligned} \quad (22.55)$$

where

$$\beta_1 = \frac{\rho_1 a_1 l}{m}, \quad \beta_3 = \frac{\rho_3 a_3 l}{m}. \quad (22.56)$$

With the aid of (22.7), (22.11), and (22.55), we can easily find pressure both at an arbitrary point in the fluid and on the plate.

In the interval $t > t_+$, the rate of plate motion steadily decreases. Its greatest value lies in the interval $0 < t < t_+$ and can be defined by the transcendental equation

$$(1 + \beta_1 + \beta_3) e^{-(\beta_1 + \beta_3) \frac{t_n}{t}} - 1 = 0,$$

whence

$$t_n = t \frac{\ln(1 + \beta_1 + \beta_3)}{\beta_1 + \beta_3} \quad (22.57)$$

According to (22.17) and (22.57), maximum pressure behind the obstacle is

$$\begin{aligned} p_{3 \max} &= \frac{2\rho_3 a_3}{\rho_1 a_1 + \rho_3 a_3} p_m \left(1 - \frac{t_n}{t_+}\right) = \\ &= \frac{2\rho_3 a_3}{\rho_1 a_1 + \rho_3 a_3} p_m \left[1 - \frac{\ln(1 + \beta_1 + \beta_3)}{\beta_1 + \beta_3}\right]. \end{aligned} \quad (22.58)$$

In the event that wave is found in front of and behind the obstacle ($\beta_1 = \beta_3 = 0$; $a_1 = a_3 = a_0$), pressure on the frontal surface is

$$p_1(t) = 2p_m \left(1 - \frac{t}{t_+}\right) |z_0(t) - z_0(t - t_+)| - p_3(t). \quad (22.59)$$

pressure on the lee surface is

$$\begin{aligned} p_2(t) = p_m \left\{ \left[\left(1 - e^{-\beta_1 \frac{t}{t_+}}\right) \left(1 + \frac{1}{2\beta_1}\right) - \frac{t}{t_+} \right] |z_0(t) - z_0(t - t_+)| + \right. \\ \left. + \left[-\left(1 + \frac{1}{2\beta_1}\right) e^{-\beta_1 \frac{t}{t_+}} + \frac{1}{2\beta_1} e^{-\beta_1 \left(\frac{t}{t_+} - 1\right)} \right] z_0(t - t_+) \right\}. \end{aligned} \quad (22.60)$$

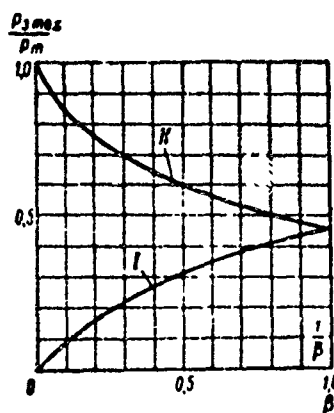


Fig. 96. Relationship of $\frac{p_{3max}}{p_m}$ as a Function of β .

I - along the lower scale of the abscissa axis;
II - along the upper scale of the abscissa axis.

where

$$\beta = \frac{t_0 a_0 t_+}{m}.$$

According to (22.57), the quantity t_H is

$$t_H = \frac{t_+}{2\beta} \ln(1 + 2\beta). \quad (22.61)$$

Pressure behind the obstacle which corresponds to this quantity is

$$p_{3max} = p_m \left[1 - \frac{\ln(1 + 2\beta)}{2\beta} \right]. \quad (22.62)$$

The results of calculating p_{3max}/p_m , describing the degree of "transparency" of the plate for the direct wave, are shown in Fig. 96.

The total pressure pulse on a wave behind the obstacle is equal to the pressure pulse on a direct wave

$$J = \int_0^{t_+} p_3(t) dt = p_m \int_{t_+}^{t_+} \left[\left(1 - e^{-2\beta \frac{t}{t_+}} \right) \left(1 + \frac{1}{2\beta} \right) - \frac{t}{t_+} \right] dt + \int_{t_+}^{t_+} \left[-\frac{1}{2\beta} e^{-2\beta \left(\frac{t}{t_+} - 1 \right)} - \left(1 + \frac{1}{2\beta} \right) e^{-2\beta \frac{t}{t_+}} \right] dt = \frac{p_m t_+}{2}. \quad (22.63)$$

If the plate divides water and air ($\rho_1 = \rho_0$, $\rho_3 \approx 0$; $\beta = \frac{\rho_0 a_0}{m} t_+$)

then in the interval* $t < t_+$ the plate travels

$$W(t) = \frac{2p_m}{\rho_0 a_0} \left\{ -\frac{t^2}{2t_+} + \left(1 + \frac{1}{\beta}\right) \left[t - \frac{t_+}{\beta} \left(1 - e^{-\frac{\beta t}{t_+}}\right) \right] \right\}. \quad (22.64)$$

the rate of motion is

$$\dot{W}(t) = \frac{2p_m}{\rho_0 a_0} \left[\left(1 + \frac{1}{\beta}\right) \left(1 - e^{-\frac{\beta t}{t_+}}\right) - \frac{t}{t_+} \right]. \quad (22.65)$$

pressure on the reflected wave is

$$\begin{aligned} p_{\text{ref}}(t) &= p_m \left(1 - \frac{t}{t_+}\right) - 2p_m \left[\left(1 + \frac{1}{\beta}\right) \left(1 - e^{-\frac{\beta t}{t_+}}\right) - \frac{t}{t_+} \right] = \\ &= p_m \left[1 + \frac{t}{t_+} - 2 \left(1 + \frac{1}{\beta}\right) \left(1 - e^{-\frac{\beta t}{t_+}}\right) \right], \end{aligned} \quad (22.66)$$

net pressure on the plate is

$$p_{\text{net}}(t) = 2p_m \left[1 - \left(1 + \frac{1}{\beta}\right) \left(1 - e^{-\frac{\beta t}{t_+}}\right) \right]. \quad (22.67)$$

the effect-time of the positive phase of net pressure is

$$t_n = \frac{t_+}{\beta} \ln(1 + \beta). \quad (22.68)$$

the positive phase pulse of net pressure is

$$J = \frac{2p_m t_+}{\beta} \left(1 - \frac{t_n}{t_+}\right) \quad (22.69)$$

A graph of net pressure at different values of β is shown in Fig. 97. Their qualitative correspondence can be seen by comparing Figs.

94 and 97.

*In this case, cavitation usually is formed before the effect of pressure in the direct-wave positive phase ends and thus writing a formula for $t > t_+$ makes no sense.

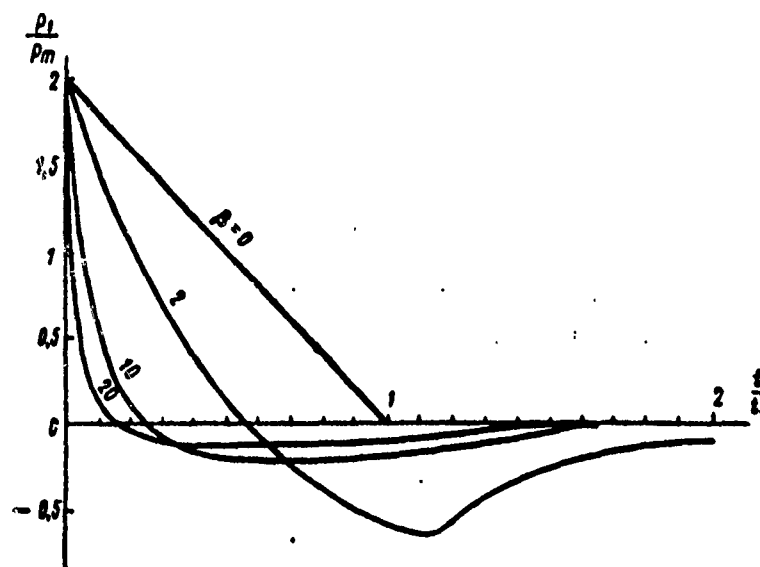


Fig. 97. Relation of $\frac{p_1}{p_m}$ as a function of t for Various Values of $\beta = \frac{\rho_0 a_0 t_+}{m}$ During Incidence of A Direct Wave of Triangular Profile.

4. Pressure on the direct shock wave changes according to a parabolic law:

$$p_{up}(t) = p_m \left[1 - \left(\frac{t}{t_+} \right)^n \right] |z_0(t) - z_0(t - t_+)|. \quad (22.70)$$

The solution of differential equation (22.14) for an arbitrary value of the exponent n in finite form cannot be derived. For whole n 's, these relations may be written; the greater n is, the more unwieldy the theoretical relationships become.

These circumstances make us seek from the very start an approximate solution of the problem. The simplest method is the approximation of the parabola with a linear relation, which permits us to subsequently utilize results which were derived earlier. An equality of pressures on the front and an equality of pulses in the positive phase can serve as the natural conditions of approximation.

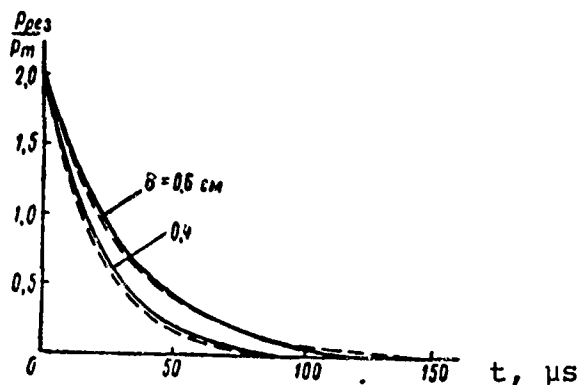


Fig. 98. Net Pressure in Front of a Plate Dividing Two Media: water and Air, During Interaction with Said Plate and Parabolic-shaped Shock Wave ($n = 2$, $t_+ = 600 \mu s$)

————— precise solution,
 ----- approximate solution.

Because for a parabola

$$J = \int_0^{t_+} p_m \left[1 - \left(\frac{t}{t_+} \right)^n \right] dt = \frac{n}{n+1} p_m t_+$$

and for a triangular-shaped wave

$$J = \frac{1}{2} p_m t_+.$$

the association between the true effect-time t_+ and the conditional t_+^* can be expressed by the relation

$$t_+^* = \frac{2n}{n+1} t_+. \quad (22.71)$$

A parabolic-shaped shock wave can be approximated by the relation

$$p(t) = p_m \left(1 - \frac{t}{t_+} \right) [c_0(t) - c_0(t - t_+^*)]. \quad (22.72)$$

The use of this approximation, which is completely admissible for considering the overall interaction picture, leads, however, to considerable error in the initial and most important time period $[0, t_H]$.

Consequently, for the interval $[0, t_+]$ we should use the indicated method to approximate only the initial section of the parabola. Based on this condition, we get

$$t_+^* = \frac{n+1}{2} t_+^{1-n} t_+^n, \quad (22.73)$$

where

$$t_+ = \frac{t_+}{\beta_1 + \beta_2} \times \\ \times \ln \left[1 + (\beta_1 + \beta_2) \frac{t_+^*}{t_+} \right], \quad (22.74)$$

$$\beta_1 = \frac{\rho_1 a_1 t_+}{m} \\ \beta_2 = \frac{\rho_2 a_2 t_+}{m}.$$

We can judge the error of approximation by considering Fig. 98, which gives the theoretical results for a parabolic-shaped direct wave ($n = 2$) according to precise and approximate relations.

Let us note that for $n = 2$, the solution of the differential equation (22.14) has the form

$$W(t) = \frac{2\rho_m t_+}{\rho_1 a_1 + \rho_2 a_2} \left\{ \frac{1}{\beta_1 + \beta_2} \left[1 - \frac{2}{(\beta_1 + \beta_2)^2} \left[e^{-\frac{(\beta_1 + \beta_2)}{t_+} t} - 1 \right] + \right. \right. \\ \left. \left. + \left[1 - \frac{2}{(\beta_1 + \beta_2)^2} \right] \frac{t}{t_+} + \frac{1}{(\beta_1 + \beta_2)} \left(\frac{t}{t_+} \right)^2 - \frac{1}{3} \left(\frac{t}{t_+} \right)^3 \right] \right\}. \quad (22.75)$$

$$W''(t) = \frac{2\rho_m}{\rho_1 a_1 + \rho_2 a_2} \left\{ \left[1 - \frac{2}{(\beta_1 + \beta_2)^2} \right] \left[1 - e^{-\frac{(\beta_1 + \beta_2)}{t_+} t} \right] + \right. \\ \left. + \frac{2}{(\beta_1 + \beta_2)} \frac{t}{t_+} - \left(\frac{t}{t_+} \right)^2 \right\}. \quad (22.76)$$

523. Integro-Differential Equation of Piston Motion Under the Influence of an Underwater Shock Wave

Simple solutions of problems involving the interaction of an underwater shock wave with pliant obstacles (similar to those considered in the preceding section) can be derived for infinite obstacles.

For bodies of finite dimensions, the effects of diffraction lead to rather complex relationships of the generalized hydrodynamic force of the second category as a function of parameters of motion. Let us illustrate the basic aspects of this problem, using as our example progressive motion of a piston with the incidence onto said piston of a plane shock wave.

As was shown earlier, in the motion of a piston according to the unit function law, the magnitude of hydrodynamic load can be defined by the relation [cf. (14.49), (14.47)]:

$$\begin{aligned} F_z &= -F_0 \psi(t), \\ F_0 &= \gamma_0 a_0 S, \end{aligned} \quad (23.1)$$

where $\psi(t)$ - the function describing the diffraction field, changing from one to zero;

S - the area of the piston.

For an arbitrary law of motion, drag can be calculated with the aid of the Duhamel integral

$$F_z = -F_0 \psi(t) \dot{W}(0) - F_0 \int_0^t \dot{W}(t-\tau) \dot{\psi}(\tau) d\tau, \quad (23.2)$$

or with zero initial data [$W(0) = \dot{W}(0) = 0$]

$$F_z = -F_0 \int_0^t \dot{W}(t-\tau) \dot{\psi}(\tau) d\tau. \quad (23.3)$$

Integrating by parts twice, equation (23.3) can be rewritten as

$$F_2 = -F_0 W(t) - F_0 \psi'(0) W(t) - F_0 \int_0^t W(t-\tau) \psi''(\tau) d\tau. \quad (23.4)$$

To calculate the force F_2 , we must know the parameters of motion which are formed as a result of this force and the first category hydrodynamic force acting on this piston. Because the considered system has one degree of freedom,

$$MW = F_1(t) + F_2(t), \quad (23.5)$$

where M - the mass of the piston, or substituting (23.3) or (23.4),

$$MW + F_0 \int_0^t W(t-\tau) \psi(\tau) d\tau = F_1(t), \quad (23.6)$$

$$MW + F_0 W(t) + F_0 \psi'(0) W(t) + F_0 \int_0^t W(t-\tau) \psi''(\tau) d\tau = F_1(t) \quad (23.7)$$

Therefore, the interaction of a shock wave with the piston can be described by an integro-differential equation of the type (23.6) or (23.7). To avoid complicating analysis of these equations with secondary details, let us select the simplest form of function $F_1(t)$. The simplest functional relationship of $F_1(t)$ occurs in the study of generalized forces formed on a plane piston having absolutely-rigid walls along its edges [cf. §14]*. In this case,

$$F_1 = 2Sp_m f(t), \quad (23.8)$$

where S - the area of the piston; $p_m f(t)$ - pressure change on the direct wave.

To solve the integro-differential equations (23.6) and (23.7), we must know the function $\psi(t)$. We became familiarized with the methods of defining this function in §13-14. A typical feature of the function $\psi(t)$ is that it is distinct from zero in the initial period of motion $[0, t_0]$. The duration of this period can be defined by

*We ought not think that this schematization of the problem to all deprives it of meaning. In addition to scientific and methodological interest in the applied respect, it has value for planning and analyzing the measurements of an entire series of instruments and data units (membrane indicators, hydrostatic gauges, stress measurers, etc).

the disturbance propagation-time in the fluid between two most distant points on the surface of the piston. Moreover, as was shown in §10-20, the integral of this function between 0 to t_0 is proportional to the quantity of apparent mass

$$F_0 \int_0^{t_0} \dot{\psi}(t) dt = M_{np}. \quad (23.9)$$

Consequently, if in the interval $[t, t - t_0]$ there is little change in acceleration $\ddot{W}(t)$, then the drag for this time interval can be written as

$$F_2(t) = -F_0 \ddot{W}(t) \int_0^{t_0} \dot{\psi}(\tau) d\tau = -M_{np} \ddot{W}(t). \quad (23.10)$$

In view of the fact that $\psi(t) \equiv 0$ where $t > t_0$, the integro-differential equation (23.7) will be written in the following manner:

where $t < t_0$

$$M\ddot{W} + F_0 \ddot{W} + F_0 \dot{\psi}'(0) \dot{W} + F_0 \int_0^t \ddot{W}(t-\tau) \dot{\psi}''(\tau) d\tau = 2S\rho_m f(t); \quad (23.11)$$

where $t > t_0$

$$M\ddot{W} + F_0 \ddot{W} + F_0 \dot{\psi}'(0) \dot{W} + F_0 \int_0^{t_0} \ddot{W}(t-\tau) \dot{\psi}''(\tau) d\tau = 2S\rho_m f(t). \quad (23.12)$$

The complexity in precisely analyzing an expression of function $\psi(t)$, even for the simplest geometric shapes, causes considerable problems in solving equations (23.11) and (23.12). We therefore usually employ different approximate concepts. The simplest and most popular of these is the previously mentioned "hypothesis of plane reflection". According to this hypothesis, the association between the normal component of fluid particle velocity and pressure on the surface of a body, for the entire period of motion, is assumed to be the same as for a plane acoustic wave. This also assumes that $\psi(t) \equiv 1$. Then, according to (23.3)

$$F_2(t) = -F_0 \ddot{W}(t) = -\rho_0 a_0 S \ddot{W}(t). \quad (23.13)$$

However, we only have to glance at Fig. 65 to be convinced that a similar type assumption is far from the truth. For this reason, the hypothesis of "plane reflection" has a limited field of application and does not preclude the possibility of serious errors.

It is considerably more tempting to select an approximation of the function $\psi(t)$ which on one hand rather well describes the features of a real function and on the other hand, permits us to reduce the integro-differential equation to an ordinary differential equation. Let us show how this can be done. For this purpose, let us integrate (23.6) with respect to t twice. Allowing for zero initial data, we find that

$$MW(t) = \int_0^t \int_0^\tau F_1 d\tau dt - F_0 \int_0^t W(t-\tau) \psi(\tau) d\tau. \quad (23.14)$$

Integration by parts of (23.14) yields

$$M\dot{W}(t) = \int_0^t F_1 d\tau - F_0 W(t) - F_0 \int_0^t W(t-\tau) \psi'(\tau) d\tau. \quad (23.15)$$

$$M\ddot{W}(t) = F_1 - F_0 \dot{W}(t) - F_0 \psi'(0) W(t) - F_0 \int_0^t W(t-\tau) \psi''(\tau) d\tau. \quad (23.16)$$

If we multiply (23.14) by an arbitrary constant C_2 and expression (23.15) by C_1 and combine it with (23.16), we find that:

$$\begin{aligned} M\ddot{W}(t) + (C_1 M + F_0) \dot{W}(t) + [C_2 M + C_1 F_0 + F_0 \psi'(0)] W(t) = \\ = F_1(t) + C_1 \int_0^t F_1(\tau) d\tau + C_2 \int_0^t \int_0^\tau F_1(\xi) d\xi d\tau - \\ - F_0 \int_0^t W(t-\tau) \left(\frac{d^2}{d\tau^2} + C_1 \frac{d}{d\tau} + C_2 \right) \psi(\tau) d\tau. \end{aligned} \quad (23.17)$$

The integro-differential equation (23.17) goes over to a differential if the function $\psi(t)$ will permit us to select values of C_1 & C_2 where the following identity will take place:

$$\frac{d^2 \psi}{dt^2} + C_1 \frac{d\psi}{dt} + C_2 \psi = 0. \quad (23.18)$$

Because where $t > t_0$ $\psi(t) \equiv 0$, the nontrivial solution of (23.18) will only be valid for $t < t_0$. For $t > t_0$, we similarly find that

$$\begin{aligned}
 MW(t) + (C_1 M + F_0)W(t) + [C_2 M + C_1 F_0 + F_0 \psi'(0)]W(t) - \\
 - F_0 \psi'(t_0)W(t - t_0) = F_1(t) + C_1 \int_0^t F_1(\tau) d\tau + \\
 + C_2 \int_0^t \int_0^t F_1(\xi) d\xi d\tau - F_0 \int_0^t W(t - \tau) \left(\frac{d^2}{d\tau^2} + C_1 \frac{d}{d\tau} + C_2 \right) \psi(\tau) d\tau.
 \end{aligned}
 \tag{23.19}$$

Equation (23.19) differs from (23.17) by only one term - $F_0 \psi'(t_0)W(t - t_0)$. Because $W(t) \equiv 0$ where $t \leq 0$, these equations coincide in the interval $0 < t < t_0$.

Therefore, when satisfying (23.18), the problem of integrating the integro-differential equation describing the motion of a piston under the influence of a shock wave can be reduced to the analysis of an ordinary second-order differential equation having constant coefficients and a delayed argument

$$\begin{aligned}
 MW(t) + (C_1 M + F_0)W(t) + [C_2 M + C_1 F_0 + F_0 \psi'(0)]W(t) - \\
 - F_0 \psi'(t_0)W(t - t_0) = F_1(t) + C_1 \int_0^t F_1(\tau) d\tau + \\
 + C_2 \int_0^t \int_0^t F_1(\xi) d\xi d\tau.
 \end{aligned}
 \tag{23.20}$$

Efficient methods for solving similar equations have now been developed. We will not discuss these, however, because in the considered particular problem there still exist further possible simplifications.

Let us return to condition (23.18). It will be satisfied if the function $\psi(t)$ can be approximated by one of the following simple

**THIS
PAGE
IS
MISSING
IN
ORIGINAL
DOCUMENT**

The values of the derivatives of $\psi_*(t)$ at points 0 and t_0 are

$$\left. \begin{aligned} \psi'(0) &= -\frac{q}{t_0}, \\ \psi'(t_0) &= -\frac{\pi}{2} \frac{1}{t_0} e^{-q}. \end{aligned} \right\} \quad (23.23)$$

If we approximate the function $\psi(t)$ with a linear relation

$$\psi_*(t) = \left(1 - \frac{t}{t_*}\right) [\psi_0(t) - \psi_0(t - t_*)], \quad (23.24)$$

where the quantity t_* is found from the condition of equality of areas delimited by the curves of $\psi(t)$ and $\psi_*(t)$ and the coordinate axes

$$t_* = 2 \int_0^{t_0} \psi(t) dt = \frac{2M_{np}}{F_0}, \quad (23.25)$$

then according to the data of Table 5, we should assume that $C_1 = C_2 = 0$. The values of the derivatives are equal to

$$\psi'(0) = \psi'(t_*) = -\frac{1}{t_*} = -\frac{F_0}{2M_{np}}. \quad (23.26)$$

Differential equation (23.20) takes on the form:

where $t < t_*$

$$M\ddot{W}(t) + F_0\dot{W}(t) - \frac{F_0^2}{2M_{np}} W(t) = F_1(t), \quad (23.27)$$

where $t > t_*$

$$M\ddot{W}(t) + F_0\dot{W}(t) - \frac{F_0^2}{2M_{np}} W(t) + \frac{F_0^2}{2M_{np}} W(t - t_*) = F_1(t). \quad (23.28)$$

Ordinary differential equation (23.27) is solved by parts. There is also no difficulty in integrating equation (23.28) with the delayed argument. Some remarks apropos of this will be given later on (§24). Let us now indicate yet another method of approximate solution of the

initial integro-differential equation [26].

The essence of this solution consists in expanding the function $W(t - \tau)$ in the neighborhood t into a Taylor series:

$$W(t - \tau) = W(t) - \frac{\tau}{1!} \dot{W}(t) + \frac{\tau^2}{2!} \ddot{W}(t) - \frac{\tau^3}{3!} \dddot{W}(t) + \dots = \sum_{n=0}^{\infty} \frac{(-1)^n}{n!} \tau^n \frac{d^n W}{dt^n}. \quad (23.29)$$

According to (23.3) and (23.29) for a generalized second category hydrodynamic force F_2 , we find that:

where $t < t_0$

$$F_2 = -F_0 [k_0(t) W(t) + k_1(t) \dot{W}(t) + k_2(t) \ddot{W}(t) + \dots] = -F_0 \sum_{n=0}^{\infty} k_n(t) \frac{d^n W}{dt^n}, \quad (23.30)$$

where

$$\left. \begin{aligned} k_0(t) &= \psi'(t), \\ k_1(t) &= \psi(t) - t\psi'(t), \\ k_2(t) &= \frac{t^2}{2} \psi'(t) - t\psi(t) + \int_0^t \psi(\tau) d\tau, \\ k_n(t) &= \frac{(-1)^n}{n!} \int_0^t \tau^n \psi''(\tau) d\tau = (-1)^n \left[\frac{t^n}{n!} \psi'(t) - \frac{t^{n-1}}{(n-1)!} \psi(t) + \frac{1}{(n-2)!} \int_0^t \tau^{n-2} \psi(\tau) d\tau \right]; \end{aligned} \right\} \quad (23.31)$$

where $t > t_0$

$$F_1 = -F_0 \sum_{n=2}^{\infty} k_n^* \frac{d^n W}{dt^n} = -F_0 [k_2^* \ddot{W}(t) + k_3^* \dddot{W}(t) + \dots], \quad (23.32)$$

where

$$k_n^* = \frac{(-1)^n}{(n-2)!} \int_0^t \tau^{n-2} \psi(\tau) d\tau. \quad (23.33)$$

Specifically, for the motion of a round piston, in view of (15.16), we can easily derive

$$\begin{aligned}
 k_0(t) &= -\frac{a_0}{a} \frac{2}{\pi} \sqrt{1 - \left(\frac{a_0 t}{2a}\right)^2}, \\
 k_1(t) &= 1 - \frac{2}{\pi} \arcsin \frac{a_0 t}{2a} + \frac{1}{\pi} \frac{a_0 t}{a} \sqrt{1 - \left(\frac{a_0 t}{2a}\right)^2}, \\
 k_2(t) &= \frac{a}{a_0} \left[\frac{8}{3\pi} + \frac{1}{3\pi} \left(1 - \frac{a_0^2 t^2}{a^2}\right) \sqrt{1 - \left(\frac{a_0 t}{2a}\right)^2} \right], \\
 &\dots \dots \dots \\
 k_n(t) &= \left(\frac{a}{a_0}\right)^{n-1} (-1)^n \frac{2^{n+1}}{\pi n!} \int_0^{\frac{a_0 t}{2a}} \frac{x^{n+1} dx}{\sqrt{1-x^2}}, \\
 k_n^*(t) &= \left(\frac{a}{a_0}\right)^{n-1} (-1)^n \frac{2^{n+1}}{\pi n!} \int_0^1 \frac{x^{n+1} dx}{\sqrt{1-x^2}},
 \end{aligned} \tag{23.34}$$

where a - the piston radius; a_0 - the speed of sound in water.

The use of a finite number of expansion terms of (23.30) or (23.32) permits us to use an ordinary differential equation instead of an integro-differential equation. In most cases it suffices to restrict ourselves to three series terms. In this case, piston motion will be defined by the second-order differential equations:

where $t < t_0$

$$[M + F_0 k_2(t)] \ddot{W}(t) + F_0 k_1(t) \dot{W}(t) + F_0 k_0(t) W(t) = F_1(t), \tag{23.35}$$

where $t > t_0$

$$(M + F_0 k_2^*) \ddot{W}(t) = F_1. \tag{23.36}$$

Graphs of the coefficients $k_0(t)$, $k_1(t)$ and $k_2(t)$ for a round and a rectangular piston are shown in Figs. 99 and 100. (The ratio of sides of the rectangular piston $b/a = 4$). We can see from the figures that at the initial period of motion, the coefficients $k_0(t)$ and $k_1(t)$, which define the relationship of generalized hydrodynamic

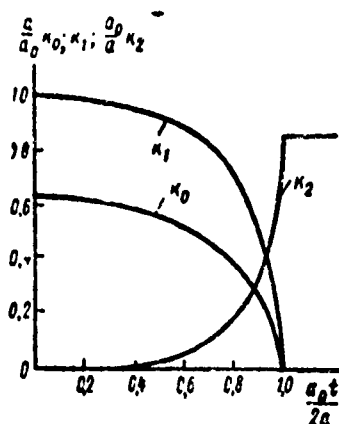


Fig. 99. Relation of Coefficients k for a Round Piston.

force as a function of travel and velocity of the piston, are of primary importance. Around time $t = t_0$, these coefficients vanish. The coefficient $k_2(t)$ reaches its maximum value and becomes a constant proportional to apparent mass. The piston begins moving as in a noncompressible fluid.

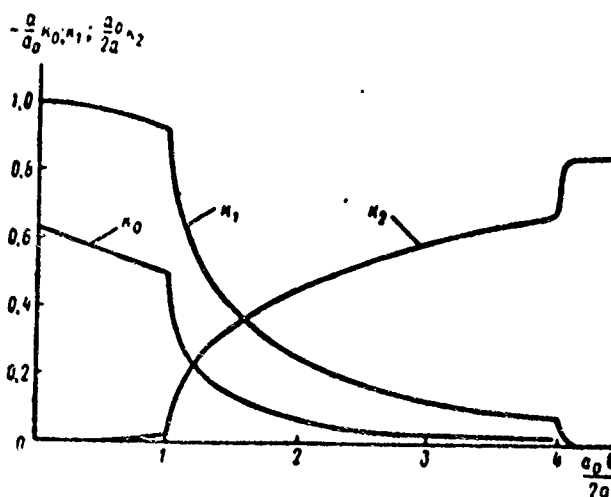


Fig. 100. The Relation of Coefficients k for a Rectangular Piston.

The second-order ordinary differential equation (23.35) in finite form is not integrated, because the variable coefficients entering into it have a rather complex lattice. The use of constant coefficients in this equation is equivalent to approximation of the function $\psi(t)$ with linear relation (23.24).

Considering (23.24) and (23.31) together, we find for $t < t_*$ that

$$\left. \begin{aligned} k_0 &= -\frac{1}{t_*}, \\ k_1 &= 1, \\ k_2 &= 0. \end{aligned} \right\} \quad (23.37)$$

On the basis of (23.24) and (23.33) for $t > t_*$

$$k_2 = \frac{t_*}{2} = \frac{M_{np}}{F_0}. \quad (23.38)$$

Therefore, for the first period of motion ($t < t^*$), we get an equation which is identically coincident with (23.27). For the second period ($t > t^*$), we get an equation of piston motion in a non-compressible fluid

$$(M + M_{np}) \ddot{W}(t) = F_1(t). \quad (23.29)$$

Evaluative precision may be somewhat raised if we adopt the wave run time t_H as our initial period of motion, not in terms of the greatest but in terms of the shortest distance between two opposite points on the piston (for a rectangular piston, along its smaller side). Then, instead of (23.27), we get

$$M \ddot{W}(t) + F_0 \dot{W}(t) - \frac{F_0}{T} W(t) = F_1(t), \quad (23.40)$$

where T - duration of the positive phase of the linear function approximating $\psi(t)$ in the interval $0 < t < t_H$.

The quantity T calculated by Zamyshlyayev and Mironov for a round piston,

$$T = 0,85 \frac{2a}{a_0}, \quad (23.41)$$

for a rectangular piston

$$T = \frac{3\pi}{2(3+2n)} \frac{2a}{a_0}, \quad (23.42)$$

where n - the ratio of sides of the piston ($n = a/b$).

In this case, (23.39) is considered valid for $t > t_H$.

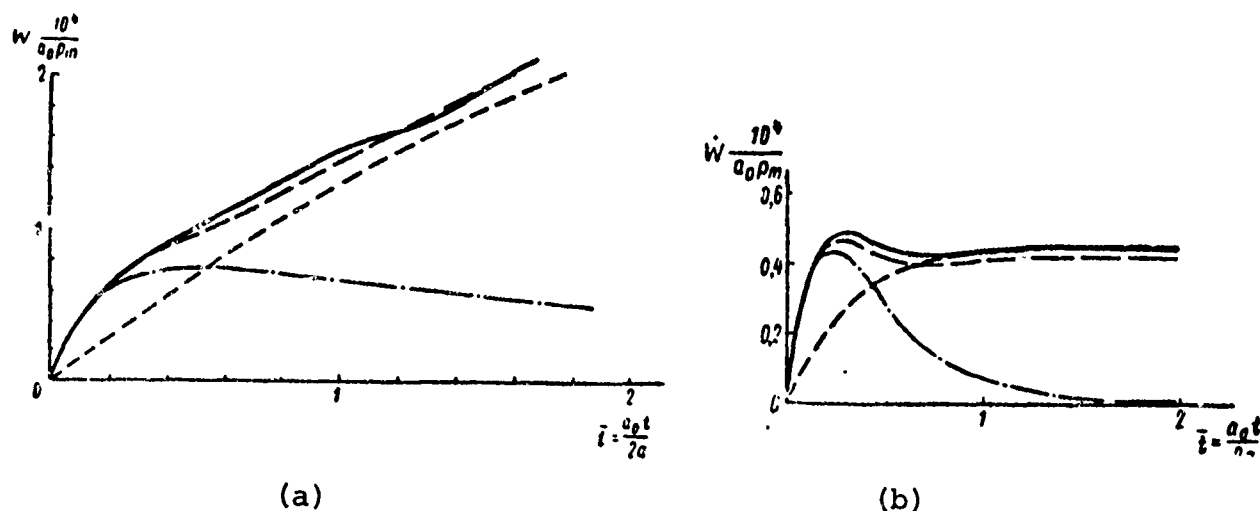


Fig. 101. Rate of Motion of a Round Piston Having Rigid Walls Under the Influence of an Exponential-shaped Shock Wave

($\delta/2a = 0.02$, $(2a\rho_0)/m = 6.4$): (a - $\bar{\theta} = 3$; b - $\bar{\theta} = 0.3$)

- precise solution;
- approximate solution;
- . - . - . - calculated acc. to hypothesis of incompressible fluid;
- . - . - . - calculated acc. to hypothesis of plane reflection.

We can adjudge the degree of precision of the evolved approximate method from Fig. 101, which shows the calculated findings for motion of a round piston according to diverse notions under the influence of an exponential-shaped shock wave. We can see that the precise and approximate solutions almost coincide. The hypothesis of plane reflection is only suited for the very initial interval

and produces an unacceptable divergence in evaluating a finite rate of speed. As time passes, the rate of speed of the piston obtained according to the precise solution approaches the quantity calculated according to the notion of a noncompressible fluid. The qualitative nature of these conclusions is also retained for plane pistons of arbitrary contour.

The possible evaluation of a finite value for the rate of speed according to the notion of a noncompressible fluid can be rigorously proven. Indeed, because we are considering the motion of a body in an ideal medium, then where t approaches infinity,

$$\dot{W}(t) \rightarrow A + Bt. \quad (23.43)$$

On the other hand, integration of (23.6) yields

$$M\dot{W}(t) = \int_0^t \int_0^t F_1(\tau) d\tau d\tau - F_0 \int_0^t \dot{W}(t-\tau) \psi(\tau) d\tau. \quad (23.44)$$

For an exponential-shaped wave $F_1(t) = 2Sp_m e^{-\frac{t}{\theta}}$ and consequently,

$$\int_0^t \int_0^t F_1(\tau) d\tau d\tau = 2Sp_m \left[\theta t + \theta^2 \left(e^{-\frac{t}{\theta}} - 1 \right) \right].$$

Therefore,

$$M\dot{W}(t)|_{t \rightarrow \infty} = -2Sp_m \theta^2 + 2Sp_m \theta t - F_0 \int_0^t \dot{W}(t-\tau) \psi(\tau) d\tau. \quad (23.45)$$

Comparing (23.43) and (23.45) for the coefficient B , we find

$$B = \frac{2Sp_m \theta}{M} - B \frac{F_0}{M} \int_0^t \psi(\tau) d\tau, \quad (23.46)$$

whence

$$\dot{W}(t)|_{t \rightarrow \infty} = B = \frac{2Sp_m \theta}{M + F_0 \int_0^t \psi(\tau) d\tau} = \frac{2Sp_m \theta}{M + M_{np}} = \frac{2SJ}{M + M_{np}}. \quad (23.47)$$

The last expression is something other than the velocity calculated according to the notion of fluid noncompressibility, which also goes to prove the validity of the earlier formulated assertion. If a precise value of the function $\psi(t)$ was a priori unknown, the approximation in the interval $[0, t_1]$ becomes impossible. In this case, we can employ equations (23.27) and (23.39) with a slightly greater error: For formulate these equations, it suffices to know the quantity of apparent mass (cf. Tables 3 and 4).

The solutions of these equations with zero initial data for a shock wave of exponential shape are:

where $t < t_*$

$$\psi(t) = \frac{2p_m S}{M} \left[\frac{e^{-\frac{t}{\theta}}}{\left(\gamma - \frac{1}{\theta}\right)^2 - \omega^2} - \frac{e^{-(\gamma - \omega)t}}{2\omega \left(\gamma - \frac{1}{\theta} - \omega\right)} + \frac{e^{-(\gamma + \omega)t}}{2\omega \left(\gamma - \frac{1}{\theta} + \omega\right)} \right], \quad (23.48)$$

$$\dot{\psi}(t) = \frac{2p_m S}{M} \left[-\frac{\frac{1}{\theta} e^{-\frac{t}{\theta}}}{\left(\gamma - \frac{1}{\theta}\right)^2 - \omega^2} + \frac{(\gamma - \omega) e^{-(\gamma - \omega)t}}{2\omega \left(\gamma - \frac{1}{\theta} - \omega\right)} - \frac{(\gamma + \omega) e^{-(\gamma + \omega)t}}{2\omega \left(\gamma - \frac{1}{\theta} + \omega\right)} \right], \quad (23.49)$$

where

$$2\gamma = \frac{2p_m S}{M}; \quad \omega^2 = \gamma^2 + \frac{F_0^2}{2MM_{np}};$$

where $t > t_*$

$$\begin{aligned} \psi(t) = \psi_* + & \left(\dot{\psi}_* + \frac{2p_m S}{M + M_{np}} e^{-\frac{t_*}{\theta}} \right) (t - t_*) - \\ & - \frac{2p_m S}{M + M_{np}} e^{-\frac{t}{\theta}} \left(1 - e^{-\frac{t - t_*}{\theta}} \right), \end{aligned} \quad (23.50)$$

$$\dot{W}(t) = \dot{W}_* + \frac{2p_m S}{M + M_{np}} e^{-\frac{t-t_*}{t_*}} \left(1 - e^{-\frac{t-t_*}{t_*}} \right), \quad (23.51)$$

where W_* and \dot{W}_* - travel and velocity of the piston at time $t = t_*$.

For a shock wave of triangular profile, when $t_+ > t_*$,

where $t < t_*$

$$\begin{aligned} W(t) = \frac{2p_m S}{M} \left\{ \frac{1}{\omega^2 - \gamma^2} \left[\frac{2\gamma}{(\omega^2 - \gamma^2)t_+} - 1 - \frac{t}{t_+} \right] - \right. \\ \left. - \frac{t_+ (\gamma - \omega) - 1}{2\omega t_+ (\gamma - \omega)^2} e^{-(\gamma - \omega)t} + \frac{t_+ (\gamma + \omega) + 1}{2\omega t_+ (\gamma + \omega)^2} e^{-(\gamma + \omega)t} \right\}, \end{aligned} \quad (23.52)$$

$$\begin{aligned} \dot{W}(t) = \frac{2p_m S}{M} \left[\frac{1}{(\omega^2 - \gamma^2)t_+} + \frac{t_+ (\gamma - \omega) - 1}{2\omega t_+ (\gamma - \omega)} e^{-(\gamma - \omega)t} - \right. \\ \left. - \frac{t_+ (\gamma + \omega) + 1}{2\omega t_+ (\gamma + \omega)} e^{-(\gamma + \omega)t} \right]; \end{aligned} \quad (23.53)$$

where $t > t_*$

$$\begin{aligned} W(t) = W_* + \dot{W}_* (t - t_*) + \frac{p_m S}{M + M_{np}} \times \\ \times \left[(t - t_*)^2 - \frac{(t - t_*)^3}{3t_+} \right], \end{aligned} \quad (23.54)$$

$$\dot{W}(t) = \dot{W}_* + \frac{2p_m S}{M + M_{np}} \left[(t - t_*) - \frac{(t - t_*)^2}{2t_+} \right]. \quad (23.55)$$

§24. The Motion of a Plate of Finite Dimensions Under the Influence of a Shock Wave

The evaluation of generalized forces formed on a free plate under the influence of an underwater shock wave is somewhat more complicated than in the earlier considered case of piston motion. Additional difficulties arise in view of the necessity of taking diffraction effects into account when calculating first category hydrodynamic force. Without the knowledge of this force, it is impossible to define second category force. However, there exists a close association between the diffraction of a wave on an immobile obstacle and the pressure field formed in a fluid with the motion of a body (cf. Chapter II). Specifically, under the normal incidence of a unit wave onto a plate, the hydrodynamic force $F(t)$ can be characterized by the same function of time $\psi(t)$ which plays an important role in evaluating second category hydrodynamic forces. This fact lets us point out a rather simple method for solving the problem.

Let us consider the case of the normal incidence of a unit shock wave onto a free plate.

The equation of motion will be

$$MW(t) = F_1 + F_2. \quad (24.1)$$

According to the results obtained in §20, the magnitude of first category hydrodynamic force is

$$F_1(t) = \rho_m \frac{F_0}{\rho_0 a_0} \psi(t), \quad (24.2)$$

where

$$F_0 = 2\rho_0 a_0 S.$$

According to (23.3), second category hydrodynamic force can be defined by the expression

$$F_2 = -F_0 \int_0^t W(t-\tau) \dot{\psi}(\tau) d\tau. \quad (24.3)$$

Therefore, the equation of motion of a free plate will be the integro-differential equation

$$MW(t) = p_m \frac{F_0}{\rho_0 a_0} \dot{\psi}(t) - F_0 \int_0^t W(t-\tau) \dot{\psi}(\tau) d\tau. \quad (24.4)$$

Equation (24.4) will take on its simplest form if function $\psi(t)$ is possible to approximate with a linear relation. Moreover, in §19 we showed that this approximation is possible with a rather high degree of precision. Allowing for findings derived in the preceding section, these facts permit us to reduce the solution of the integro-differential equation (24.4) to the solution of an ordinary differential equation having a delayed argument:

where $t < t_*$

$$MW(t) + F_0 \dot{W}(t) - \frac{F_0^2}{2M_{np}} W(t) = p_m \frac{F_0}{\rho_0 a_0} \left(1 - \frac{t}{t_*}\right) \times \\ \times [\sigma_0(t) - \sigma_0(t - t_*)]; \quad (24.5)$$

where $t > t_*$

$$MW(t) + F_0 \dot{W}(t) - \frac{F_0^2}{2M_{np}} W(t) + \frac{F_0^2}{2M_{np}} W(t - t_*) = 0, \quad (24.6)$$

where

$$t_* = \frac{2M_{np}}{F_0}.$$

With zero initial data [$\dot{W}(0) = W(0) = 0$], the solution of equation (24.5) has the form

$$\dot{W}(t) = \frac{p_m t_*}{\rho_0 a_0} \left[\bar{t} + \frac{1}{2\omega} (e^{\omega_1 \bar{t}} - e^{\omega_2 \bar{t}}) \right], \quad (24.7)$$

$$W(t) = \frac{p_m}{\rho_0 a_0} \left[1 + \frac{1}{2\omega} (\omega_2 e^{\omega_1 \bar{t}} - \omega_1 e^{\omega_2 \bar{t}}) \right], \quad (24.8)$$

where

$$\left. \begin{aligned} \gamma &= \frac{2\rho_m l_0 S}{M}, \\ \omega &= \sqrt{\gamma^2 + 2\gamma}, \\ a_1 &= -(\gamma - \sqrt{\gamma^2 + 2\gamma}), \\ a_2 &= -(\gamma + \sqrt{\gamma^2 + 2\gamma}), \\ \bar{t} &= \frac{t}{t_0}. \end{aligned} \right\} \quad (24.9)$$

Knowing the solution of (24.5) for the interval $0 < \bar{t} < 1$, it is easy to derive a solution of (24.6) for the interval $1 < \bar{t} < 2$, because for this interval expression (24.7) permits us to evaluate the value of term having the displacement of the argument. After calculating for $1 < \bar{t} < 2$, we find that

$$\begin{aligned} W(t) &= \frac{2\rho_m l_0^2 S}{M} \left\{ \frac{\bar{t}}{2\gamma} + e^{a_1(\bar{t}-1)} \left[C_1 + \frac{\bar{t}-1}{(2\omega)^2} \right] + \right. \\ &\quad \left. + e^{a_2(\bar{t}-1)} \left[C_2 + \frac{\bar{t}-1}{(2\omega)^2} \right] \right\}. \end{aligned} \quad (24.10)$$

$$\begin{aligned} \dot{W}(t) &= \frac{2\rho_m l_0^2 S}{M} \left\{ \frac{1}{2\gamma} + e^{a_1(\bar{t}-1)} \left[C_1 a_1 + \frac{1 + a_1(\bar{t}-1)}{(2\omega)^2} \right] + \right. \\ &\quad \left. + e^{a_2(\bar{t}-1)} \left[C_2 a_2 + \frac{1 + a_2(\bar{t}-1)}{(2\omega)^2} \right] \right\}. \end{aligned} \quad (24.11)$$

where we also designate

$$\left. \begin{aligned} C_1 &= -\frac{1}{2\omega} \left[\gamma_2 x - \frac{a_2}{2\gamma} - \dot{x} + \frac{\gamma+3}{2\omega^2} \right], \\ C_2 &= \frac{1}{2\omega} \left[\gamma_1 x - \frac{a_1}{2\gamma} - \dot{x} + \frac{\gamma+3}{2\omega^2} \right], \\ x &= \frac{W(\bar{t}-1)}{\frac{2\rho_m l_0^2 S}{M}}, \\ \dot{x} &= \frac{\dot{W}(\bar{t}-1)}{\frac{2\rho_m l_0^2 S}{M}}. \end{aligned} \right\} \quad (24.12)$$

Having a solution of (24.6) for the time interval $1 < \bar{t} < 2$, we can derive a solution of this equation for the interval $2 < t < 3$, etc. With such successive solution methods, the limiting values of the functions are of interest where t approaches infinity. Integrating (24.5) and (24.6) for a sufficiently large t , we find that:

$$MW(t) + F_0 W' - \frac{F_0}{t_0} \int_{t-t_0}^t W' dt = \frac{\rho_m F_0}{\rho_0 a_0} \frac{t_0}{2}. \quad (24.13)$$

Where t approaches infinity, $W(t) \rightarrow W_\infty$, $W \rightarrow A + W_\infty t$. Consequently

$$F_0 W - \frac{F_0}{t_0} \int_{t-t_0}^t W dt \rightarrow \frac{F_0 t_0}{2} W_\infty = M_{np} \dot{W}_\infty. \quad (24.14)$$

From a comparison of (24.13) and (24.14) it is clear that the limiting value of the rate of speed of a free plate under the influence of a unit wave is

$$\dot{W}(t) \Big|_{t \rightarrow \infty} = \dot{W}_\infty = \frac{\rho_m F_0}{\rho_0 a_0} \frac{t_0}{2} \frac{1}{M + M_{np}}. \quad (24.15)$$

However, $\frac{\rho_m F_0}{\rho_0 a_0} \frac{t_0}{2} = J_1$ is something other than the total pulse of first category hydrodynamic force F_1 . Consequently, the limiting velocity of a free plate is as if it were moving in a noncompressible fluid under the effect of F_1 .

This quantity differs from the rate of speed of particles behind the wave front by a coefficient of

$$\frac{\dot{W}_\infty}{\frac{\rho_m}{\rho_0 a_0}} = \frac{1}{1 + \frac{M}{M_{np}}} = \frac{1}{1 + \frac{M}{\rho_0 a_0 t_0 S}}. \quad (24.16)$$

Therefore, even when t approaches infinity, a plate of finite dimensions does not acquire the rate of speed equal to the velocity of particles which occurred during the motion of an infinite plate under the influence of a unit wave. The less the width of the plate ($a_0 t_0$) and the greater its mass, the greater the difference in velocities.

Despite the possibility of writing a precise solution of (24.6)

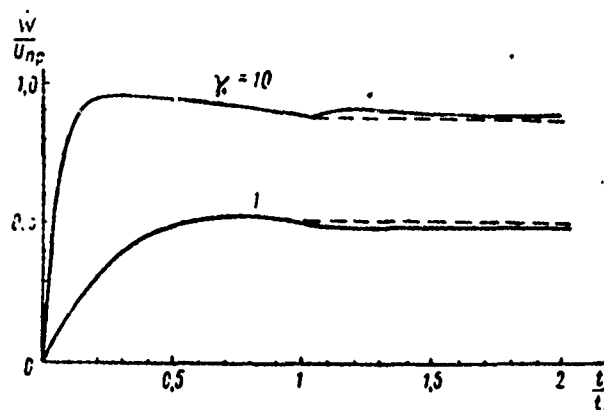


Fig. 102. Change in the Rate of Speed of a Free Plate of Finite Dimensions Under the Influence of a Unit Shock Wave.

————— precise solution;
 ----- simplified solution.

as stated above, the successive calculation of the parameters of motion in proportion to an increase in time is rather tiring. The derived expression for the limiting value of velocity indirectly indicates that where $t > t_*$, the hypothesis of a noncompressible fluid should not produce serious error. Therefore, for approximate evaluations where $t > t_*$, instead of (24.6) we can write

$$(M + M_{up}) \ddot{W}(t) = 0. \quad (24.17)$$

Then, where $t > t_*$

$$W(t) = W_* + \dot{W}_*(t - t_*), \quad (24.18)$$

$$\ddot{W} = \ddot{W}_*, \quad (24.19)$$

where W_* and \dot{W}_* - travel and rate of speed of the plate at time $t = t_*$, as defined by formulas (24.7) and (24.8)

Fig. 102 shows the calculated results of the rate of speed of a free plate according to formulas (24.8) and (24.19), affirming the feasibility of using the simplified arrangement.

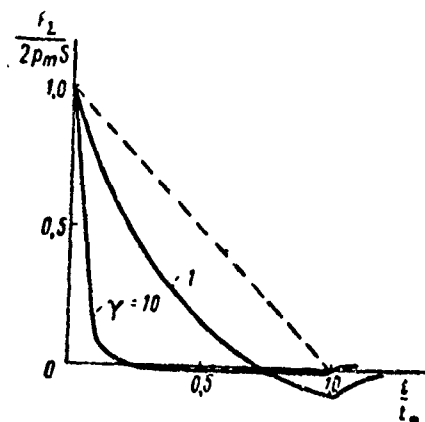


Fig. 103. Change in Net Force Acting on a Free Rigid Plate of Finite Dimensions During Incidence into Said Plate of a Unit Shock Wave ($\gamma = \frac{M_{np}}{M} = \frac{\rho_0 a_0 t_*}{\rho_M \delta}$).

———— total net force;
 ----- generalized first category force for immobile plate.

The nature of change in the net generalized load is shown in Fig. 103. We can see from the figure the extent that the motion of the plate affects the net load. This effect is in proportion to the size of the plate, and is in inverse proportion to its mass.

To determine generalized forces during the incidence of a wave of arbitrary profile onto a free plate, we can employ the Duhamel integral or the solution of differential equations (24.5), (24.6), or (24.17) where F_1 corresponds to a given wave profile. In this last case, the approximation of the function $\psi(t)$ by a linear relationship and the use of the Duhamel integral and (24.2) yields

$$F_1(t) = 2S[p_m f(t) - D(t) + D(t - t_*)], \quad (24.20)$$

where

$$D(t) = \frac{p_m}{t_*} \int_0^t f(\tau) d\tau. \quad (24.21)$$

For some of the forms of shock waves most frequently encountered in practice, we established a relationship of $D(t)$ in §20. Employing these relations, we can obtain final expressions for $F_1(t)$. For an exponential-shape shock-wave, the change in pressure is

$$F_1(t) = 2Sp_m \begin{cases} e^{-\frac{t}{\bar{t}}} - \frac{\bar{\eta}}{\bar{t}_*} \left(1 - e^{-\frac{t}{\bar{t}}}\right), & \text{where } t < t_*, \\ \left(1 + \frac{\bar{\eta}}{\bar{t}_*}\right) e^{-\frac{t}{\bar{t}}} - \frac{\bar{\eta}}{\bar{t}_*} e^{-\frac{t-t_*}{\bar{t}}}, & \text{where } t > t_*. \end{cases} \quad (24.22)$$

If we know the function $F_1(t)$, we can easily integrate (24.5). For $t < t_*$

$$\begin{aligned} W(t) &= \frac{p_m \bar{\eta}}{\rho_0 a_0} \left[1 - e^{-\frac{\bar{t}}{\bar{t}}} - \frac{a_1}{2\omega(1+a_1\bar{\eta})} \left(e^{a_1\bar{t}} - e^{-\frac{\bar{t}}{\bar{t}}} \right) \right] \\ &+ \frac{a_2}{2\omega(1+a_2\bar{\eta})} \left(e^{a_2\bar{t}} - e^{-\frac{\bar{t}}{\bar{t}}} \right) \Bigg] = \frac{p_m \bar{\eta}}{\rho_0 a_0} \left[1 + \frac{2\gamma\bar{\eta}(1+\bar{\eta})}{1-2\gamma\bar{\eta}(1+\bar{\eta})} e^{-\frac{\bar{t}}{\bar{t}}} - \right. \\ &\left. - \frac{a_1}{2\omega(1+a_1\bar{\eta})} e^{a_1\bar{t}} + \frac{a_2}{2\omega(1+a_2\bar{\eta})} e^{a_2\bar{t}} \right]. \end{aligned} \quad (24.23)$$

$$\begin{aligned} W(t) &= \frac{p_m \bar{\eta}}{\rho_0 a_0} \left[-\frac{2\gamma(1+\bar{\eta})}{1-2\gamma\bar{\eta}(1+\bar{\eta})} e^{-\frac{\bar{t}}{\bar{t}}} - \frac{a_1^2}{2\omega(1+a_1\bar{\eta})} e^{a_1\bar{t}} + \right. \\ &\left. + \frac{a_2^2}{2\omega(1+a_2\bar{\eta})} e^{a_2\bar{t}} \right], \end{aligned} \quad (24.24)$$

where $\bar{t} = \frac{t}{t_*}$, $\bar{\eta} = \frac{\eta}{t_*}$.

If we employ the simplified expression for F_2 where $t > t_*$, we must solve the following differential equation to define the parameters of motion:

$$(M + M_{np}) \dot{W} = 2p_m S \left(1 + \frac{\bar{\eta}}{\bar{t}_*} - \frac{\bar{\eta}}{\bar{t}_*} e^{\frac{t_*}{\bar{t}}} \right) e^{-\frac{t}{\bar{t}}} \quad (24.25)$$

with the initial data: at time $t = t_*$, $W = W_*$ and $\dot{W} = \dot{W}_*$.

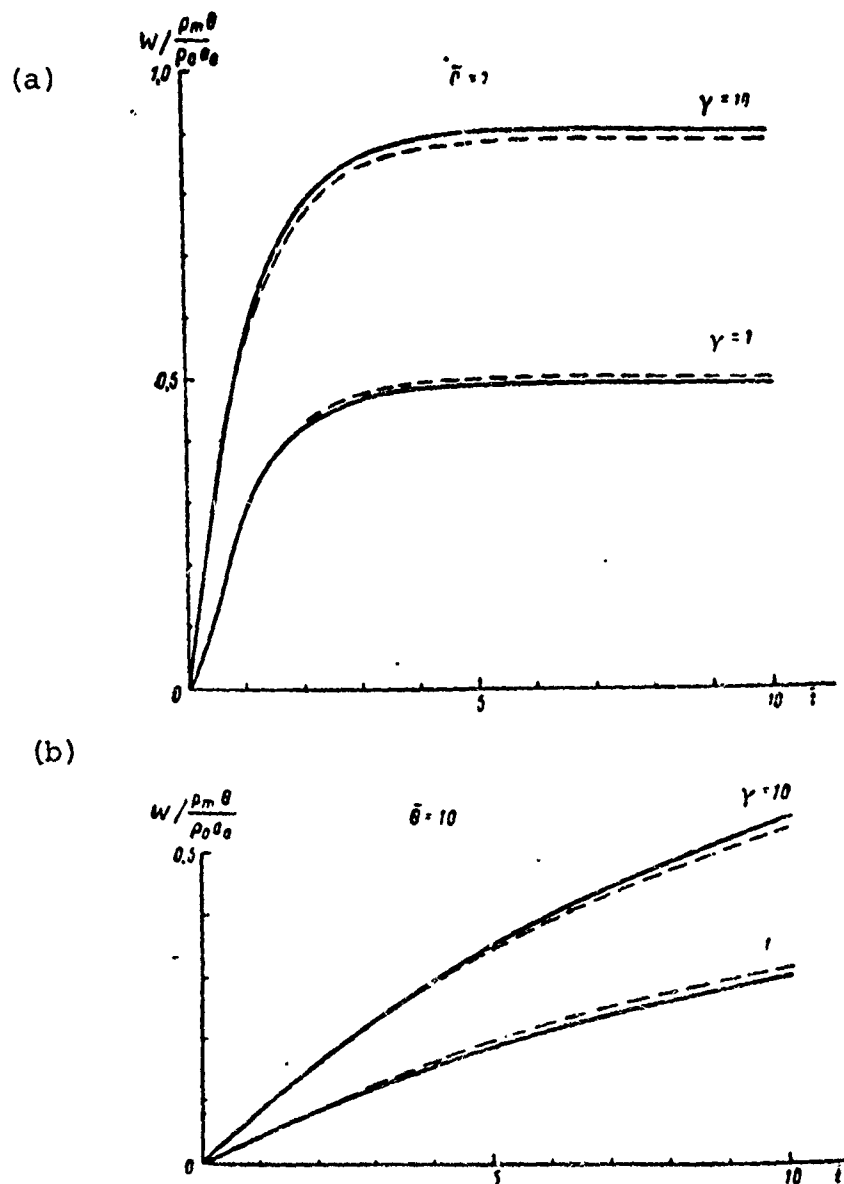


Fig. 104. Travel of Free Plate During Normal Incidence onto Said Plate of Underwater Shock-Wave of Exponential Profile: (a) where $\bar{\theta} = 1$; (b) where $\bar{\theta} = 10$.

————— precise solution;
 ----- approximate solution.

Integration yields

$$W = W_* + \left\{ W_* + \frac{2p_m \theta S}{M(1+\gamma)} \left[\left(1 + \frac{\theta}{t_*}\right) e^{-\frac{t}{t_*}} - \frac{\theta}{t_*} \right] \right\} (t - t_*) + \frac{2p_m \theta S}{M(1+\gamma)} \left[\left(1 + \frac{\theta}{t_*}\right) e^{-\frac{t}{t_*}} - \frac{\theta}{t_*} \right] \left(e^{-\frac{t-t_*}{t_*}} - 1 \right). \quad (24.26)$$

$$\dot{W} = \dot{W}_* - \frac{2p_m \theta S}{M(1+\gamma)} \left[\left(1 + \frac{\theta}{t_*}\right) e^{-\frac{t}{t_*}} - \frac{\theta}{t_*} \right] \left(e^{-\frac{t-t_*}{t_*}} - 1 \right). \quad (24.27)$$

It follows from (24.27) that where t approaches infinity

$$W(t)|_{t \rightarrow \infty} = W_* = \dot{W}_* + \frac{2p_m \theta S}{M(1+\gamma)} \left[\left(1 + \frac{\theta}{t_*}\right) e^{-\frac{t}{t_*}} - \frac{\theta}{t_*} \right] \neq 0.$$

This result does not correspond to the physical picture of the effect and is the result of error in the approximate calculation system used. Indeed, where t approaches infinity, $W_\infty \rightarrow 0$. This can be shown both by using the solution of a precise equation having a delayed argument, as well as by employing integral evaluations. We established earlier [cf. (24.15)] that the limiting value of velocity is proportional to the pulse of first category hydrodynamic force F_1 . But according to (24.20) for any wave having a finite magnitude of pressure, the first category pulse of hydrodynamic force J_1 is equal to zero (cf. §17). We must correct the solutions of (24.26) and (24.27). Apparently, the simplest way is to assume that

$$\dot{W}_* = - \frac{2p_m \theta S}{M(1+\gamma)} \left[\left(1 + \frac{\theta}{t_*}\right) e^{-\frac{t}{t_*}} - \frac{\theta}{t_*} \right]. \quad (24.28)$$

Then, the corrected solution which should be employed instead of (24.26) and (24.27) takes the form

$$W(t) = W_* e^{-\frac{t-t_*}{t_*}}, \quad (24.29)$$

$$W = W_* - \theta W_* \left(e^{-\frac{t-t_*}{t_*}} - 1 \right). \quad (24.30)$$

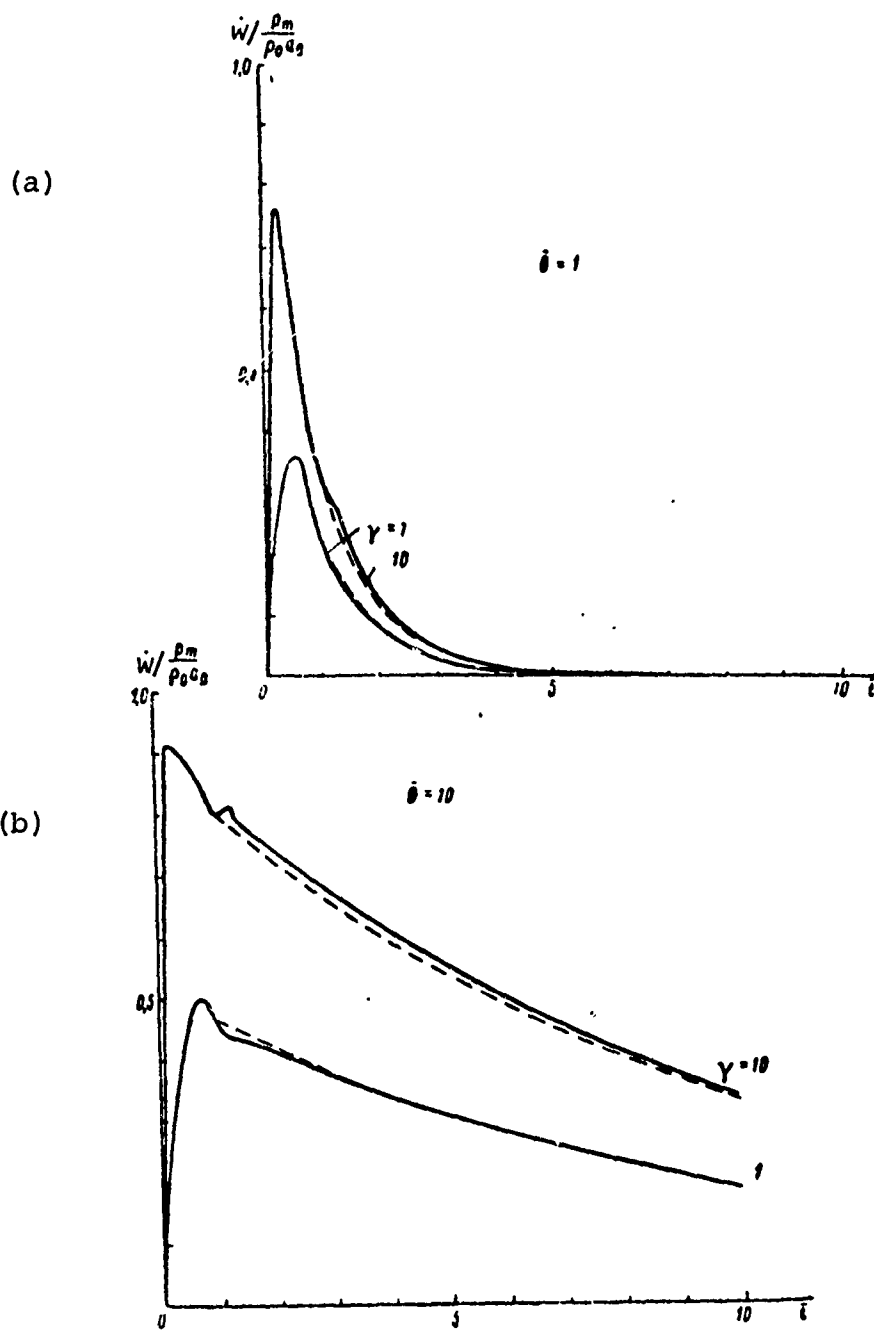


Fig. 105. Rate of Motion of a Free Plate During Normal Incidence onto Said Plate of Underwater Shock Wave of Exponential Profile: (a) where $\theta = 1$; (b) where $\theta = 10$. (Designations the same as in Fig. 104).

Figs. 104-105 show the compared calculated findings of travel and rate of speed of a free plate according to precise and approximate solutions*. We can see that the convergence of data is satisfactory for practical applications.

If we reiterate the arguments given in the derivation of (24.15), we can easily show that under the effect of a wave of limited duration, the coefficient of (24.16) will not longer describe the ratio of velocities, but the ratio of travels of the free plate and particles of the medium during passage of the direct wave

$$\frac{W'}{W_{np}} = \frac{1}{1 + \frac{M}{M_{np}}} \quad (24.31)$$

§25. Evaluation of Generalized Forces During Incidence of a Shock-Wave onto an Absolutely Rigid Body of Arbitrary Shape

For the sake of simplicity, let us restrict ourselves to a discussion of the motion of bodies whose form is symmetric with respect to two mutually-perpendicular planes, during the incidence of a plane wave in the direction of the main axis of symmetry.

The position of the system, in this case, will be characterized by one coordinate. The differential equation of motion will have the form:

$$M \frac{d^2 \psi}{dt^2} = F_1 + F_2 \quad (25.1)$$

The hydrodynamic force of the first category, as was shown in §20, will be expressed using the functions $f(t)$ and $\psi(t)$ [cf. (20.4), (20.23), (20.16)]:

$$F_1 = F_{np} + F_a \quad (25.2)$$

*Computed by N. I. Mordvinova.

$$F_{np} = -p_m \int_{S_1(z, a, t)} \int f\left(t - \frac{z}{a_0}\right) \cos \hat{n} z dS, \quad (25.3)$$

$$F_n = Q(t) + \int_0^t Q(t - \tau) \psi'(\tau) d\tau, \quad (25.4)$$

$$Q(t) = p_m \int_{S_1(z, a, t)} \int f\left(t - \frac{z}{a_0}\right) \cos^2 \hat{n} z dS, \quad (25.5)$$

where S_1 - the portion of the body surface enveloped by the wave (situated in area $z < a_0 t$).

The second category hydrodynamic force according to (23.3) is

$$F_2 = -F_0 \int_0^t \ddot{W}(t - \tau) \psi(\tau) d\tau. \quad (25.6)$$

Therefore, the solution of the problem, as before, is reduced to studying the integro-differential equation

$$\begin{aligned} M\ddot{W} = F_{np}(t) + Q(t) + \int_0^t Q(t - \tau) \psi'(\tau) d\tau - \\ - F_0 \int_0^t \ddot{W}(t - \tau) \psi(\tau) d\tau, \end{aligned} \quad (25.7)$$

$$F_0 = \rho_0 a_0 \int \int \cos^2 \hat{n} z dz. \quad (25.8)$$

This equation will be in its simplest form if $\psi(t)$ is approximated by a linear relation (cf. §19).

Reiterating the arguments of the preceding section, the integro-differential equation (25.7) easily yields an ordinary differential equation of the second order having constant coefficients and a delayed argument. For the time interval $t < t_*$

$$M\ddot{W} + F_0 \dot{W} - \frac{F_0}{t_*} W = F_1. \quad (25.9)$$

Where $t > t_*$, we will get

$$\Delta t W + F_0 W - \frac{F_0}{t_*} [W - W(t - t_*)] = F_1, \quad (25.10)$$

where $t_* = \frac{2M \cdot \psi}{F_0}$.

When we seek an approximate solution, we may replace equation (25.10) by the relation

$$(M + M_{np}) \ddot{W} = F_1. \quad (25.11)$$

The problem of motion of an arbitrarily-shaped body, therefore, under the influence of a shock wave differs from the previously considered problem only by a more complex form of function $F_1(t)$.

In view of the fact that $\psi(\tau) = \left(1 - \frac{\tau}{t_*}\right) [\gamma_0(t) - \gamma_0(t - t_*)]$,

according to (25.2)-(25.4), the function $F_1(t)$ can be written in the form

$$F_1 = F_{np}(t) + Q(t) - \begin{cases} \frac{1}{t_*} \int_0^t Q(\tau) d\tau & \text{where } t < t_* \\ \frac{1}{t_*} \int_{t-t_*}^t Q(\tau) d\tau & \text{where } t > t_* \end{cases} \quad (25.12)$$

The expanded expressions for $F_1(t)$ during incidence of a unit wave onto a sphere, round cylinder, parallelepiped, and ellipsoid of revolution were given in §20. We can adjust these for a wave of arbitrary shape with the aid of the Duhamel integral.

Let us briefly touch upon the study of the motion of the simplest geometric bodies. Let us begin with a rigid parallelepiped. Because this problem differs from the previously considered problem on the motion of a free plate only in the added consideration of the

size of the parallelepiped in the direction of wave run $\delta = 2c$, there is no need to write the solution of equations (25.9)-(25.12): we can limit ourselves to evaluating the limiting characteristics of motion.

As we showed in §20, in the event of incidence onto the facial side of a parallelepiped by a plane unit wave, the first category generalized force can be defined by the equation [cf. (20.58), (20.59)]

$$F_1(t) = \rho_m S [2 - \bar{p}_r(t) - \bar{p}_r(t - t_1)], \quad (25.13)$$

where

$$\begin{aligned} p_1(t) &= \frac{t}{t_*} [z_0(t) - z_0(t - t_*)] + z_0(t_* - t_*) = \\ &= \frac{t}{t_*} z_0(t) - \frac{t - t_*}{t_*} z_0(t - t_*), \end{aligned} \quad (25.14)$$

$$t_1 = \frac{\delta}{a_0} = \frac{2c}{a_0},$$

δ - the size of the parallelepiped in the direction of wave run (the thickness of the plate).

Because the pulse of this force is [cf. (20.46)]

$$J_1 = \rho_m S (t_* + t_1) = \rho_m S t_* \left(1 + \frac{t_1}{t_*}\right) = \rho_m S t_* \left(1 + \frac{\delta}{a_0 t_*}\right) \quad (25.15)$$

and exceeds the pulse for a thin plate by $(1 + \frac{\delta}{a_0 t_*})$ times, then the rate of speed of the parallelepiped, where t approaches infinity, will be higher than the rate of speed of the plate by the same number of times. In other words, according to (25.15) and (24.16)

$$\frac{W_\infty}{\frac{p_m}{\rho_0 a_0}} = \frac{M_{np} \left(1 + \frac{\delta}{a_0 t_*}\right)}{M + M_{np}}, \quad (25.16)$$

however,

$$t_* = \frac{2M_{np}}{F_0} = \frac{M_{np}}{S\rho_0 a_0},$$

while $S\delta = V$, where V - the volume of the parallelepiped.

Therefore, we can rewrite (25.16) in the form

$$\frac{\dot{W}_\infty}{v_{np}} = \frac{M_{np} + V\rho_0}{M_{np} + M}. \quad (25.17)$$

Equation (25.17) shows that if the density of the parallelepiped material is less than the density of water, the limiting value of velocity which it acquires is greater than the rate of speed of particles in the direct wave. If we change the relationship of densities the relationship of velocities also changes. In the event of "zero buoyancy", the rate of speed is the same as the velocity of particles behind the wave front. This deduction may be expanded to bodies of arbitrary shape.*

If the magnitude of the total pressure pulse in the direct wave is limited, the first category hydrodynamic force reduces to the following form with the aid of the Duhamel integral [cf. (20.77)]

$$F_1 = S[2p_m f(t) - D(t) + D(t - t_*) - D(t - t_1) + D(t - t_* - t_1)], \quad (25.18)$$

where

$$D(t) = \frac{\rho_m}{t_*} \int_0^t f(t) dt = \frac{J_{np}(t)}{t_*}. \quad (25.19)$$

Because

$$2p_m \int_0^t d\tau \int_0^\tau f(\xi) d\xi = 2 \int_0^t J_{np}(\tau) d\tau = 2t_* \int_0^t D(\tau) d\tau,$$

while where t approaches infinity

* This, of course, is valid within the framework of the primary problem hypotheses and does not take into account the effect of viscosity of the fluid, the velocity head, etc.

$$\left. \begin{aligned} D(t) &\rightarrow \frac{J_{np}^*}{t_*}, \\ \int_0^t D(\tau) d\tau &\rightarrow \frac{1}{t_*} (A + J_{np}^* t). \end{aligned} \right\} \quad (25.20)$$

then where t approaches infinity

$$\left. \begin{aligned} 2p_m \int_0^t d\tau \int_0^{\tau} f(\xi) d\xi &\rightarrow 2(A + J_{np}^* t), \\ \int_0^t d\tau \int_0^{\tau} D(\xi) d\xi &\rightarrow \frac{1}{t_*} \left(k + At + \frac{J_{np}^*}{2} \cdot t^2 \right), \\ \left[\int_0^t d\tau \int_0^{\tau} D(\xi) d\xi - \int_0^{t_*} d\tau \int_0^{\tau} D(\xi) d\xi \right] &\rightarrow \\ &\rightarrow \left(A + J_{np}^* t - \frac{J_{np}^*}{2} t_* \right), \\ \left[\int_0^{t-t_l} d\tau \int_0^{\tau} D(\xi) d\xi - \int_0^{t_*-t_l} d\tau \int_0^{\tau} D(\xi) d\xi \right] &\rightarrow \\ &\rightarrow \left(A + J_{np}^* (t - t_l) - \frac{J_{np}^*}{2} t_* \right). \end{aligned} \right\}$$

Substituting the derived expressions into (25.13) and integrating, we find that where t approaches infinity

$$\left. \begin{aligned} F_1 &\rightarrow 0, \\ \int_0^t F_1 d\tau &\rightarrow 0, \\ \int_0^t d\tau \int_0^{\tau} F_1(\xi) d\xi &\rightarrow S J_{np}^* (t_* + t_l). \end{aligned} \right\}$$

Because the last quantity exceeds its analogous quantity for a thin plate by $(1 + \frac{t_l}{t_*})$ times, then considering (24.31) and (25.16) for the limiting travel of a parallelepiped, we get the relation

$$W_{\infty} = \frac{J_{np}^*}{\rho_0 a_0} \frac{M_{np}}{M_{np} + M} \frac{V \rho_a}{M}. \quad (25.23)$$

In other words, under the influence of a wave having a limited pressure pulse, the limiting values of displacement are in the same relationship as the limiting relations of velocity during the incidence of a unit wave.

Using (25.12) and reiterating arguments analogous to those given, we can show that this conclusion is valid for bodies of any shape.

The problem of travel of an absolutely solid body under the influence of an acoustic wave was first considered under general assumptions by Novozhilov [13]. He derived relation (25.23) as a result of a limiting process in an integro-differential equation of motion. Slepyan succeeded in showing that the fixed expression for final motion is not just valid for absolutely rigid bodies, but also for elastically-deformable bodies [17]. This conclusion was made by Slepyan not on the basis of studying the corresponding boundary value problems of the wave equation, but from purely physical concepts which were based on his suggested model of a "virtual body".

Equation (25.23) shows that under the influence of a limited pressure pulse, a body having negative buoyancy travels in a fluid at a rate which is less than the rate of displacement of media particles; a body having positive buoyancy travels at a greater rate and ultimately, a body having "zero buoyancy" travels the same distance as do media particles.

Let us now consider the problem of motion of a rigid sphere. It is of interest with respect to methodology, because we can derive a precise solution, permitting the evaluation of error in the approximate methods developed.

We previously had [cf. (17.58)]

$$\psi(t) = e^{-\frac{a \cdot t}{a}} \cos \frac{a \cdot t}{a}. \quad (25.24)$$

This function satisfies condition (23.18) for the coefficients C_1 and C_2 , which are equal to [cf. (23.22)]

$$\left. \begin{aligned} C_1 &= \frac{2a_0}{a}, \\ C_2 &= \frac{2a_0^2}{a^2}. \end{aligned} \right\} \quad (25.25)$$

On substituting these coefficients, the integro-differential equation of motion (23.20) takes on the form

$$\begin{aligned} M\ddot{W}(t) + \left(\frac{2a_0}{a}M + F_0\right)\dot{W}(t) + \frac{a_0}{a}\left(\frac{2a_0}{a}M + F_0\right)W(t) = \\ = F_1(t) + \frac{2a_0}{a}\int_0^t F_1(\tau)d\tau + \frac{2a_0^2}{a^2}\int_0^t\int_0^\tau F_1(\xi)d\xi d\tau. \end{aligned} \quad (25.26)$$

Because the quantity F_0 for a sphere, according to (17.58) is

$$F_0 = \frac{4}{3}\pi a^2 \rho_0 \gamma_0 = \frac{a_0}{a} V \rho_0, \quad (25.27)$$

and its apparent mass is

$$M_{np} = \frac{2}{3}\pi \rho_0 a^3 = \frac{1}{2} \rho_0 V.$$

the ratio a/a_0 can be designated using t_* ($t_* = 2M_{np}/F_0$) with good basis. Moreover, it is convenient to introduce the dimensionless parameter

$$\chi = \frac{\rho_0 V}{M}. \quad (25.28)$$

In its new designations, equation (25.26) is written so:

$$\begin{aligned} M \left[\ddot{W}(t) + \frac{1}{t_*} (2 + \chi) \dot{W}(t) + \frac{1}{t_*^2} (2 + \chi) W(t) \right] = \\ = F_1(t) + \frac{2}{t_*} \int_0^t F_1(\tau) d\tau + \frac{2}{t_*^2} \int_0^t \int_0^\tau F_1(\xi) d\xi d\tau. \end{aligned} \quad (25.29)$$

Let us first consider the case where a unit shock wave having the

amplitude p_m acting on a sphere. A precise expression for the first category generalized hydrodynamic force for this case is derived in the form [cf. (17.69)]

$$F_1(t) = 4\pi a^2 p_m e^{-\frac{a_0 t}{a}} \sin \frac{a_0 t}{a}. \quad (25.30)$$

Because

$$\begin{aligned} \frac{2}{t_*} \int_0^t e^{-\frac{a_0 \tau}{a}} \sin \frac{a_0 \tau}{a} d\tau &= 1 - e^{-\frac{a_0 t}{a}} \left(\sin \frac{a_0 t}{a} + \cos \frac{a_0 t}{a} \right), \\ \frac{2}{t_*^2} \int_0^t \int_0^\tau e^{-\frac{a_0 \xi}{a}} \sin \frac{a_0 \xi}{a} d\xi d\tau &= e^{-\frac{a_0 t}{a}} \cos \frac{a_0 t}{a} + \frac{a_0 t}{a} - 1, \end{aligned}$$

the right side of equation (25.29) will be considerably simplified and will be equal to

$$4\pi a^2 p_m \frac{a_0 t}{a} = 4\pi a^2 p_m \frac{t}{t_*}.$$

Consequently, instead of (25.29) we can write

$$\ddot{W}(t) + \frac{1}{t_*} (2 + \chi) \dot{W}(t) + \frac{1}{t_*^2} (2 + \chi) W(t) = \frac{3p_m t}{\rho_0 a_0 t_*^2}. \quad (25.31)$$

The solution of this equation with zero initial data and where $\chi < 2$ is

$$W(t) = \frac{p_m}{\rho_0 a_0} \frac{3\chi}{2 + \chi} \left[e^{-\omega_1 t} \left(\frac{\chi}{2\omega_2} \sin \omega_2 t + t_* \cos \omega_2 t \right) + t - t_* \right], \quad (25.32)$$

$$\dot{W}(t) = \frac{p_m}{\rho_0 a_0} \frac{3t}{2 + \chi} \left[1 - e^{-\omega_1 t} \left(\sqrt{\frac{2 + \chi}{2 - \chi}} \sin \omega_2 t + \cos \omega_2 t \right) \right], \quad (25.33)$$

where

$$\begin{aligned} \omega_1 &= \frac{2 + \chi}{2t_*}, \\ \omega_2 &= \frac{2 + \chi}{2t_*} \sqrt{\frac{2 - \chi}{2 + \chi}}. \end{aligned}$$

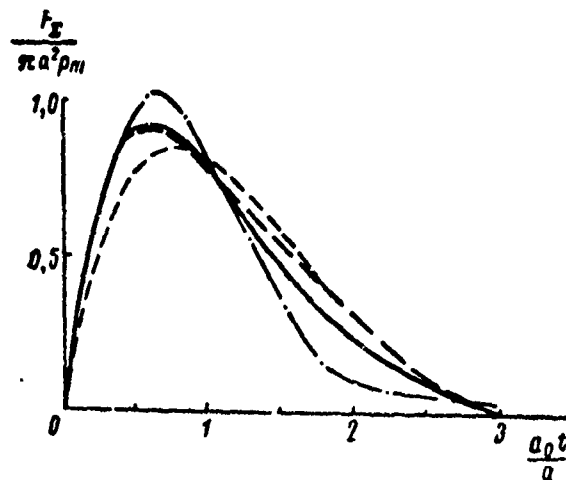


Fig. 106. Net Load on a Rigid Sphere of Zero Buoyancy Under the Influence of a Unit Shock Wave.

————— precise solution,
 - - - - - approximate solution,
 - . - . - . - hypothesis of plane reflection,
 - - - - - notion of fluid noncompressibility.

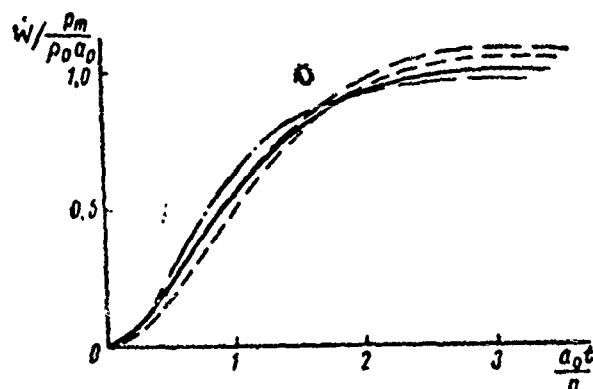


Fig. 107. Rate of Speed of Rigid Sphere of Zero Buoyancy under the Influence of Unit Shock Wave (designations same as in Fig. 106).

Where t approaches infinity, (25.33) goes over into the previously established relation (25.17), common to all bodies

$$\dot{W}(t)|_{t \rightarrow \infty} = \frac{\rho_m}{\rho_0 a_0} \frac{3\gamma}{2 + \gamma} = v_{np} \frac{M_{np} + \rho_0 V}{M_{np} + M}. \quad (25.34)$$

Considering that the net load acting on the sphere is

$$F_z = F_1 + F_2 = M\dot{W},$$

after differentiating (25.33), we find that

$$F_z = 4\pi a^3 \rho_m \frac{2}{\sqrt{4 - \gamma^2}} e^{-\omega_1 t} \sin \omega_2 t \quad (25.35)$$

and according to (25.30),

$$F_z = F_z - F_1 = 4\pi a^3 \rho_m \left\{ \frac{2}{\sqrt{4 - \gamma^2}} e^{-\omega_1 t} \sin \omega_2 t - e^{-\frac{t}{t_0}} \sin \frac{t}{t_0} \right\}. \quad (25.36)$$

In this case, approximate methods have no advantages over the precise method and therefore, they are not cited. Findings calculated by these methods are given in Figs. 106 and 107. We can easily see that there is a good convergence of data. However, this convergence for findings calculated according to the hypothesis of plane reflection is rather random, as shown by Fig. 108, where the quantities of hydrodynamic forces of first and second category are shown separately. As we can see, the "hypothesis of plane reflection" produces considerable errors in signs, which in summation leads to a result which is close to the true result.

There are no theoretical difficulties associated with the use of a wave of arbitrary profile in place of a unit wave in the precise solution derived. Specifically, if we employ the Duhamel integral for an exponential-shape shock wave, we find that

$$\begin{aligned} W(t) = & \frac{\rho_m a_0}{\rho_0 a_0} \frac{3\gamma}{2 + \gamma} \frac{1}{\gamma^2 - (2 + \gamma)(\gamma - 1)} \left\{ \gamma^2 - (2 + \gamma)(\gamma - 1) - \right. \\ & \left. - (\gamma - 2)e^{-\frac{t}{t_0}} - e^{-\omega_1 t} \left[\sqrt{\frac{2 + \gamma}{2 - \gamma}} (\gamma - \gamma_1) \gamma_1 \sin \omega_2 t + \right. \right. \\ & \left. \left. + \gamma_1 (\gamma - 2 - \gamma) \cos \omega_2 t \right] \right\}, \end{aligned} \quad (25.37)$$

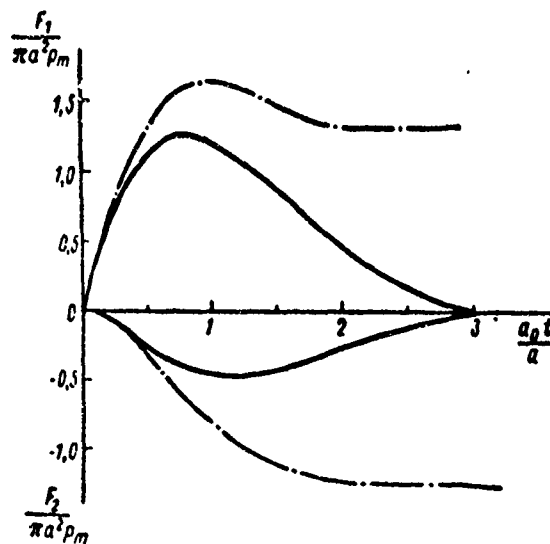


Fig. 108. Generalized Force Components Acting on a Rigid Sphere of Zero Buoyancy during Incidence on Said Sphere of a Unit Shock Wave.

— precise solution,
 - - - - - theoretical solution according to hypothesis of plane reflection.

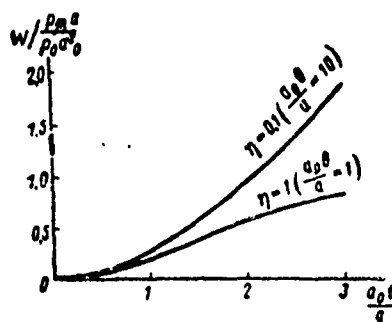


Fig. 109. Travel of Rigid Sphere of Zero Buoyancy Under Influence of Underwater Shock Wave of Exponential Profile.

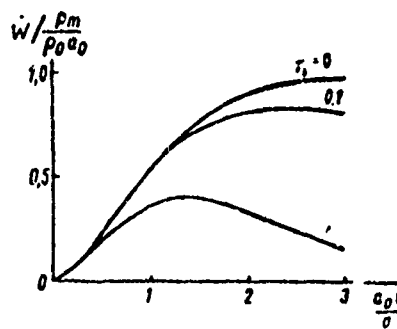


Fig. 110. Rate of Speed of Rigid Sphere of Zero Buoyancy Under Influence of Underwater Shock Wave of Exponential Shape, $\eta = a/a_0\theta$.

$$\begin{aligned} W(t) = & \frac{p_m}{\rho_0 a_0} \frac{3\gamma}{2 + \gamma} \frac{1}{\gamma^2 - (2 + \gamma)(\eta - 1)} \left\{ (\gamma + 2)e^{-\frac{t}{\theta}} - \right. \\ & \left. - e^{-\omega_2 t} \left[\sqrt{\frac{2 + \gamma}{2 - \gamma}} (2 + \gamma - 2\gamma) \sin \omega_2 t + (\gamma + 2) \cos \omega_2 t \right] \right\}. \end{aligned} \quad (25.38)$$

where $\eta = a/a_0 \theta$.

Where $t \rightarrow \infty$, (25.37) goes over into relation (25.23), which is valid for bodies of arbitrary shape

$$W'_{\infty} = W'_{np} \frac{3\gamma}{2 + \gamma} = W'_{np} \frac{M_{np} + V p_0}{M_{np} + M}. \quad (25.39)$$

The nature of variation in velocity and travel of the sphere of "zero buoyancy" under the influence of an exponential-shape shock wave is shown in Figs. 109, 110.

The magnitude of net load is

$$\begin{aligned} F_z = & \frac{4\pi a^2 p_m}{\gamma^2 - 3(\gamma - 1)} \left\{ -\gamma e^{-\frac{t}{\theta}} + e^{-1.5 \frac{a_0 t}{a}} \times \right. \\ & \left. \times \left[\sqrt{3} (2 - \gamma) \sin \frac{1}{2} \sqrt{3} \frac{a_0 t}{a} + \gamma \cos \frac{1}{2} \sqrt{3} \frac{a_0 t}{a} \right] \right\}. \end{aligned} \quad (25.40)$$

In conclusion, let us note that the problem of motion of a sphere under the influence of a shock wave was solved by Lefonova by solving integro-differential equation (25.7) using the operation method.

For bodies of other geometric form, the derivation of precise solutions in finite form is scarcely possible. At this point there is considerable value in the approximate methods developed above. Even they, however, are not always suitable due to the awkwardness of expressions for $F_1(t)$ [cf. §20]. In such cases, a preliminary approximation of $F_1(t)$ by simple functions is always useful.

For well-streamlined bodies, in addition to the recommended solution, we can utilize the simplest solution based on the "hypothesis of plane reflection" with precision sufficient for practical applications. This conclusion follows from both the considered problem of the sphere (Fig. 106, 107) and from analysis of motion of an infinitely-long round cylinder under the influence of a shock wave (Fig. 111).

A precise solution of this problem for a unit wave was numerically derived by Goryainov and Yu. A. Fedorovich. For the net load, Fedorovich suggested the following simple approximation of results for the appropriate calculations:

$$F_z = \pi a \rho_m \left[2.9 \bar{t} e^{-1.8 \bar{t}} + 0.57 (e^{-1.2 \bar{t}} - e^{-18.5 \bar{t}}) \right], \quad (25.41)$$

where $\bar{t} = a_0 t/a$.

Because

$$\ddot{W} = \frac{F_z}{M}, \quad (25.42)$$

expression (25.41) permits us, using a simple integration, to derive the values $W(t)$ and $\dot{W}(t)$ for a wave of unit amplitude; and with the aid of the Duhamel integral for a wave of arbitrary profile.

The approximate evaluation of motion of streamlined bodies can also be made on the basis of the hypothesis of fluid noncompressibility. The effect of second category hydrodynamic forces is taken into account through apparent mass. The equation of motion takes a particularly simple form

$$\ddot{W}(t) = \frac{F_1(t)}{M + M_{np}}. \quad (25.43)$$

If we are considering the case of wave incidence in the direction of the axis of symmetry of a body having a great relative length, the role of diffraction processes becomes negligibly small and the

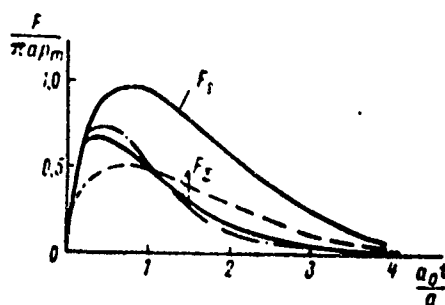


Fig. 111. Net Load on an Infinitely-Long Round Cylinder of Zero Buoyancy During Action on Said Cylinder of Unit Shock Wave.

————— precise solution;
 -.-.-.-.- calculated, hypothesis of plane reflection;
 - - - - - calculated, notion of fluid non-compressibility.

equation of motion becomes even more simplified:

$$M\ddot{W} = F_{np}(t). \quad (25.44)$$

(Specifically, this solution produces good results for prolate ellipsoids of revolution where $b/a > 5$.

Earlier, for a round ellipsoid of revolution during incidence of a unit wave we had [cf. (20.34)]:

$$F_{np}(t) = \begin{cases} \rho_m \frac{\pi a^3 a_0}{b} t \left(2 - \frac{a_0 t}{b}\right) & \text{where } t < \frac{2b}{a_0}, \\ 0 & \text{where } t \geq \frac{2b}{a_0}. \end{cases} \quad (25.45)$$

The solution of equation (25.44) with the right side of (25.45) is:

$$\ddot{W} = \frac{\rho_m}{\rho_0 a_0^2} b \gamma \begin{cases} \frac{1}{4} \bar{t}^3 (1 - \bar{t}) & \text{where } \bar{t} < 2 \\ \bar{t} - 1 & \text{where } \bar{t} > 2, \end{cases} \quad (25.46)$$

$$\ddot{W} = \frac{\rho_m}{\rho_0 a_0^2} \gamma \begin{cases} \frac{3}{4} \bar{t}^2 \left(1 - \frac{1}{3} \bar{t}\right) & \text{where } \bar{t} < 2 \\ 1 & \text{where } \bar{t} > 2, \end{cases} \quad (25.47)$$

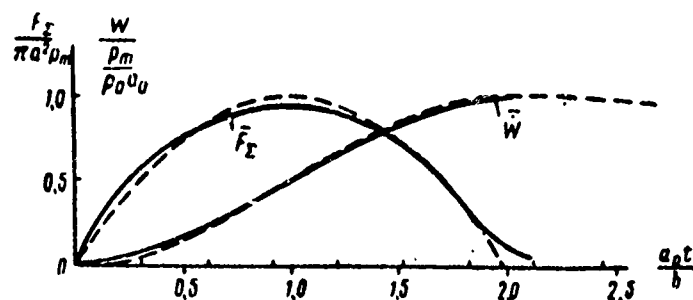


Fig. 112. Net Load and Rate of Speed of Prolate Ellipsoid of Revolution of Zero Buoyancy During Action on Said Ellipsoid of Unit Shock Wave in Direction of Axis.

————— precision solution, function ψ
linearized;
----- approximation solution.

where

$$\bar{t} = \frac{a_0 t}{b},$$

$$\chi = \frac{\rho_b V}{M} = \frac{\frac{4}{3} \pi a^2 b \rho_0}{M}.$$

In the case of an exponential-shape shock wave, employing the Duhamel integral, we find that

$$F_{np} = \pi a^2 \rho_m 2\bar{\theta} \begin{cases} (1 + \bar{\theta}) \left(1 - e^{-\frac{\bar{t}}{\bar{\theta}}} \right) - \bar{t} & \text{where } \bar{t} < 2 \\ \left[(\bar{\theta} - 1) e^{\frac{2}{\bar{\theta}}} - (1 + \bar{\theta}) \right] e^{-\frac{\bar{t}}{\bar{\theta}}} & \text{where } \bar{t} > 2, \end{cases} \quad (25.48)$$

$$W = \frac{\rho_m \bar{\theta}}{\rho_0 a_0} \chi \frac{3}{2} \begin{cases} \bar{\theta}^2 (1 + \bar{\theta}) \left(1 - e^{-\frac{\bar{t}}{\bar{\theta}}} \right) - \\ - \bar{\theta} (1 + \bar{\theta}) \bar{t} + (1 + \bar{\theta}) \bar{t}^2 - \frac{\bar{t}^3}{6} & \text{where } \bar{t} < 2, \\ \frac{2}{3} - \bar{\theta}^2 \left[(1 + \bar{\theta}) + (1 - \bar{\theta}) e^{\frac{2}{\bar{\theta}}} \right] e^{-\frac{\bar{t}}{\bar{\theta}}} & \text{where } \bar{t} > 2, \end{cases} \quad (25.49)$$

$$\dot{\psi} = \frac{p_m}{p_0 a_0} \chi \frac{3}{2} \bar{\theta} \begin{cases} (1 + \bar{\theta}) \bar{t} - \frac{\bar{t}^2}{2} + \bar{\theta} (1 + \bar{\theta}) \left(e^{-\frac{\bar{t}}{\bar{\theta}}} - 1 \right) & \text{where } \bar{t} < 2 \\ \bar{\theta} \left[(1 + \bar{\theta}) + (1 - \bar{\theta}) e^{\frac{\bar{t}}{\bar{\theta}}} \right] e^{-\frac{\bar{t}}{\bar{\theta}}} & \text{where } \bar{t} > 2, \end{cases} \quad (25.50)$$

where

$$\bar{\theta} = \frac{a_0 b}{b}$$

Results calculated according to formulas (25.48)-(25.50) and the formulas of precise solution for the linearized function $\psi(t)$ in the event of a unit wave falling onto an ellipsoid of revolution having $b/a = 5$ are shown in Fig. 112.*

§26. Interaction of a Shock Wave with an Elastic Plate of Finite Thickness

The problems of shock waves interacting with a pliable obstacle which were earlier considered did not take into account the wave nature of disturbance propagation in the material of the obstacle itself, which are induced by its elastic properties. Let us illustrate the effect of this circumstance, using the normal incidence of a plane wave onto an ideally elastic plate of finite thickness as our example. As before, let us use a linear formulation of the problem. The z axis will be directed at right angles to the plane of the plate, to the side of wave propagation. The origin of the coordinates will be situated on the front surface of the plate. Time is counted when the direct wave encounters the front surface. The parameters of the medium will be assigned indexes: 1 - in front of the plate; 2 - the plate; 3 - behind the plate (Fig. 113). The, pressure and the velocity of particles in the i -th medium will be associated with the

*The parameters of motion according to formulas of the precise solution were computed on the "Minsk-1" computer by N. Mordvinova.

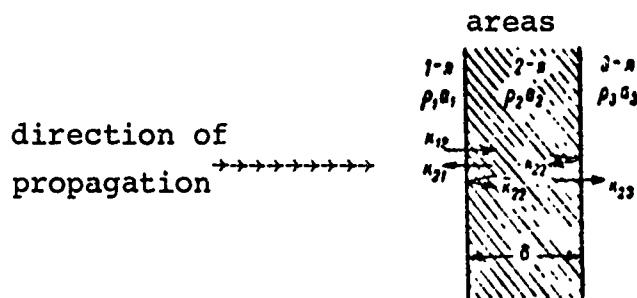


Fig. 113. Diagram of Reflection and Refraction of Shock Wave during Normal Incidence onto Obstacle of Finite Thickness.

potential function by the expressions

$$p_i(z, t) = -\rho_i \frac{\partial \varphi_i(z, t)}{\partial t}, \quad (26.1)$$

$$v_i(z, t) = \frac{\partial \varphi_i(z, t)}{\partial z}. \quad (26.2)$$

The velocity potentials are found from wave equations

$$\frac{\partial^2 \varphi_i(z, t)}{\partial z^2} = \frac{1}{a_i^2} \frac{\partial^2 \varphi_i(z, t)}{\partial t^2}. \quad (26.3)$$

The boundary and initial conditions are:

in area 1

$$\left. \begin{aligned} p_1(z, 0) &= p_{np}(z, 0), \\ v_1(z, 0) &= v_{np}(z, 0), \end{aligned} \right\} \quad (26.4)$$

in area 2 and 3

$$\left. \begin{aligned} p_2(z, 0) &= p_3(z, 0) = 0, \\ v_2(z, 0) &= v_3(z, 0) = 0, \end{aligned} \right\} \quad (26.5)$$

on the interface of media 1-2 and 2-3

$$\left. \begin{aligned} v_1(0, t) &= v_2(0, t); \quad p_1(0, t) = p_2(0, t), \\ v_2(\delta, t) &= v_3(\delta, t); \quad p_2(\delta, t) = p_3(\delta, t), \end{aligned} \right\} \quad (26.6)$$

where $p_{np}(z, 0)$, $v_{np}(z, 0)$ - pressure and rate of speed of particles in the direct wave at initial time;
 δ - thickness of the plate.

G. Lindh solved the problem in its present formulation using the operations method [37]. However, the final results are considerably easier to derive if we immediately employ the known values of the coefficients of reflection (from acoustics) and refraction on an interface of two media [4]. Because we are considering the incidence of a wave along the normal to the surface of the plate, no transverse wave is formed in the obstacle material. The wave processes can be characterized by the propagation of reflected and refracted longitudinal waves. The amplitudes of these waves at the interface of media 1-2 can be defined by the equations

$$\frac{p_{refl}}{p} = \frac{\rho_2 a_2 - \rho_1 a_1}{\rho_2 a_2 + \rho_1 a_1} \quad (26.7)$$

$$\frac{p_{refr}}{p} = \frac{2\rho_2 a_2}{\rho_2 a_2 + \rho_1 a_1} \quad (26.8)$$

Similar relationships occur at the interface of media 2 and 3.

Let us designate that: k_{11} - the coefficient of reflection from the second to the first medium, k_{12} - the coefficient of refraction from the first to the second medium. Then, instead of (26.7) and (26.8), we can write

$$p_{refl}^{1-2} = k_{11} p, \quad (26.9)$$

$$p_{refr}^{1-2} = k_{12} p. \quad (26.10)$$

Until the elastic wave reaches the lee surface of the plate, reflection and refraction of waves will occur just as in the interaction of a wave with the interface of two infinite media.

At the moment the refracted wave propagating in medium 2 toward interface of media 2-3 converges, a new reflected and refracted wave is formed (Fig. 113).

The amplitude of these waves is

$$p_{\text{отр}}^{2-1} = k_{12} p \frac{\rho_1 a_3 - \rho_2 a_2}{\rho_3 a_3 + \rho_2 a_2} = k_{12} k_{22} p, \quad (26.11)$$

$$p_{\text{нпр}}^{2-3} = k_{12} p \frac{2\rho_3 a_3}{\rho_3 a_3 + \rho_2 a_2} = k_{12} k_{23} p, \quad (26.12)$$

where k_{22} - the coefficient of reflection of the wave into the second medium from the third;

k_{23} - the coefficient of wave refraction from the second medium into the third.

The wave reflected on the interface of the second and third media, after reaching the interface of the second and first media, in turn creates a refracted wave; this wave propagates in the first medium and its reflected wave propagates in the second medium.

Pressure on these waves will be

$$p_{\text{нр}}^{2-1} = p_{\text{отр}}^{2-3} \frac{2\rho_1 a_1}{\rho_1 a_1 + \rho_2 a_2} = k_{12} k_{22} k_{21} p, \quad (26.13)$$

$$p_{\text{отр}}^{2-1} = p_{\text{отр}}^{2-3} \frac{\rho_1 a_1 - \rho_2 a_2}{\rho_1 a_1 + \rho_2 a_2} = k_{12} k_{22} \bar{k}_{22} p, \quad (26.14)$$

where k_{21} - the refraction coefficient from the second medium into the first;

k_{22} - the reflection coefficient into the second medium from the first.

Subsequent development of the wave process occurs by analogy to what has already been considered. Pressure on surfaces of the plate will change abruptly over time intervals equalling the duration of wave run-time of a plate twice as thick.

The wave fields in each of the media will be characterized by the equations

$$p_1(z, t) = p \left(t - \frac{z}{a_1} \right) z_0 \left(t - \frac{z}{a_1} \right) + k_{11} p \left(t + \frac{z}{a_1} \right) z_0 \left(t + \frac{z}{a_1} \right) +$$

$$+ k_{12}k_{22}k_{21} \sum_{n=1}^{\infty} \gamma^{n-1} p\left(t - 2nt_1 + \frac{z}{a_1}\right) \sigma_0\left(t - 2nt_1 + \frac{z}{a_1}\right), \quad (26.15)$$

$$\begin{aligned} p_2(z, t) = & k_{12} \sum_{n=1}^{\infty} \gamma^{n-1} p\left(t - [n-1]2t_1 - \frac{z}{a_2}\right) \times \\ & \times \sigma_0\left(t - [n-1]2t_1 - \frac{z}{a_2}\right) + k_{12}k_{22} \sum_{n=1}^{\infty} \gamma^{n-1} p\left(t - 2nt_1 + \frac{z}{a_2}\right) \times \\ & \times \sigma_0\left(t - 2nt_1 + \frac{z}{a_2}\right), \end{aligned} \quad (26.16)$$

$$\begin{aligned} p_3(z, t) = & k_{12}k_{22} \sum_{n=1}^{\infty} \gamma^{n-1} p\left(t - [2n-1]t_1 - \frac{z-b}{a_2}\right) \times \\ & \times \sigma_0\left(t - [2n-1]t_1 - \frac{z-b}{a_2}\right), \end{aligned} \quad (26.17)$$

where $t_1 = \delta/a_2$ - the wave run-time of a plate whose thickness is

$$\gamma = k_{22}\bar{k}_{22}.$$

The geometric interpretation of the solution of (25.15)-(25.17) is given in the form of a wave grid in Fig. 114.

The magnitudes of pressure on the front and lee surface of the plate may be obtained from (26.15) and (26.17) if we assume that $z = 0$ and $z - \delta = 0$, respectively. For a given shape of the direct wave contour, as a rule, we can derive expressions in finite form after summation of the corresponding series.

Because $p = p_m e^{-(t/\theta)}$, $\sigma_0(\tau)$ in the case of an exponential shape wave, pressure on the front surface of the plate can be found from the equation

$$\begin{aligned} p_1(t) = & p_m(1 + k_{11})e^{-t} \cdot \sigma_0(\tau) + \\ & + p_m 2e^{-(t-2\tau_1)} \frac{1 - e^{2\tau_1}}{e^{2\tau_1} - 1} \cdot \sigma_0(\tau - 2\tau_1), \end{aligned} \quad (26.18)$$

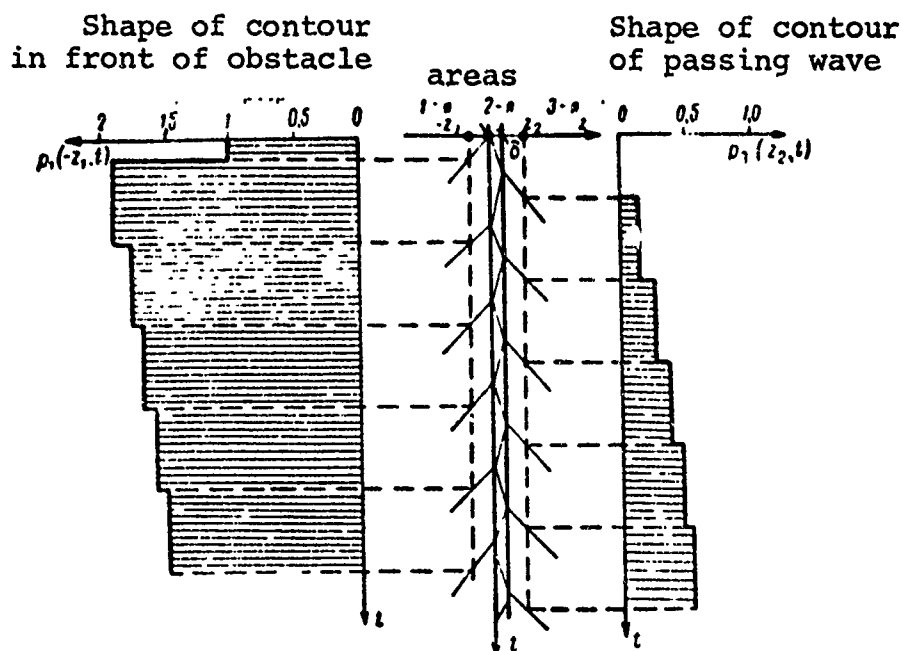


Fig. 114. Wave Grid for Reflection and Refraction of a Unit Shock Wave during Normal Incidence onto Obstacle of Finite Thickness.

where n - an integer satisfying the inequality

$$2n\tau_1 \leq \tau \leq (2n+2)\tau_1, \quad (26.19)$$

$$\left. \begin{aligned} \bar{a} &= k_{12}k_{22}k_{21}, \\ \frac{t}{b} &= \tau, \\ \frac{t_1}{b} &= \tau_1. \end{aligned} \right\} \quad (26.20)$$

Pressure on the lee surface of the plate is

$$p_3(t) = p_0 a e^{-(\tau-\tau_1)} \frac{\gamma^a e^{2n\tau_1} - 1}{\gamma e^{2\tau_1} - 1} a_0 - (\tau - \tau_1), \quad (26.21)$$

where n can be defined from the inequality

$$(2n-1)\tau_1 \leq \tau \leq (2n+1)\tau_1, \quad (26.22)$$

$$a = k_{12}k_{21}, \quad (26.23)$$

In the case of direct wave incidence having a linear contour



$p(t) = p_m(1 - (t/t_+)[\sigma_0(t - t_+)]$, similar expressions have the form:*

$$\begin{aligned} p_1(t) &= p_m(1 - k_{11}) \left(1 - \frac{t}{t_1}\right) [\sigma_0(t) - \sigma_0(t - t_1)] + \\ &+ p_m \bar{\alpha} \left[\left(1 - \frac{t}{t_1}\right) \frac{\gamma^n - 1}{\gamma - 1} + \frac{2t_1}{t_1} \frac{1 - n\gamma^{n-1} - (n+1)\gamma^n}{(\gamma - 1)^2} \right] \sigma_0(t - 2t_1) + \\ &+ p_m \bar{\alpha} \left[\left(\frac{t}{t_1} - 1\right) \frac{\gamma^k - 1}{\gamma - 1} - \frac{2t_1}{t_1} \times \right. \\ &\times \left. \frac{1 - k\gamma^{k-1} - (k+1)\gamma^k}{(\gamma - 1)^2} \right] \sigma_0(t - 2t_1 - t_1), \end{aligned} \quad (26.24)$$

where n and k can be defined from the inequalities

$$2nt_1 \leq t \leq (2n+2)t_1, \quad (26.25)$$

$$2kt_1 + t_1 \leq t < (2k+2)t_1 + t_1, \quad (26.26)$$

$$\begin{aligned} p_3(t) &= p_m \bar{\alpha} \left[\left(1 - \frac{t}{t_1}\right) \frac{\gamma^n - 1}{\gamma - 1} - \right. \\ &- \left. \frac{t_1}{t_1} \frac{1 - (2n-1)\gamma^{n-1} - (2n+1)\gamma^n}{(\gamma - 1)^2} \right] \sigma_0(t - t_1) + \\ &+ p_m \bar{\alpha} \left[\left(\frac{t}{t_1} - 1\right) \frac{\gamma^k - 1}{\gamma - 1} - \right. \\ &- \left. \frac{t_1}{t_1} \frac{1 - (2k-1)\gamma^{k-1} - (2k+1)\gamma^k}{(\gamma - 1)^2} \right] \sigma_0(t - t_1 - t_1), \end{aligned} \quad (26.27)$$

where n and k can be found from the inequalities

$$(2n-1)t_1 \leq t < (2n+1)t_1, \quad (26.28)$$

$$(2k-1)t_1 + t_1 \leq t < (2k+1)t_1 + t_1. \quad (26.29)$$

*Formulas (26.18)-(26.29) were first derived in this form by Zamyshlyayev and Lopukhov.

The first term in (26.18) and (26.24) expresses the total pressure of the direct and reflected waves. Wherever the acoustic resistance of the plate material is greater than the acoustic resistances of the first and third media ($\rho_2 a_2 > \rho_1 a_1$; $\rho_2 a_2 > \rho_3 a_3$), the second terms of (26.18) and (26.24) can describe the pressure of the expansion waves successively passing from the second to the first area.*

According to the solution derived, pressure both in front of and behind the obstacle can be described by a broken line consisting of "steps" which satisfy the emergence toward the surface of a recurrent refracted wave. This broken line is conveniently replaced by a smooth curve. We can either consider the curve passing through the crest of the "steps" (the curve of "peak" pressures) or through the middle of the steps (the curve of "mean" pressures).

From (26.21) for these curves, we can easily derive

$$p_{\text{max}} = p_m^2 \frac{\gamma^{\frac{\tau-\tau_1}{2\tau_1}} e^{2\tau_1} - e^{-(\tau-\tau_1)}}{\gamma e^{2\tau_1} - 1} \varphi_0(\tau - \tau_1), \quad (26.30)$$

$$p_{\text{sep}} = \frac{p_m^2}{2(\gamma e^{2\tau_1} - 1)} \left[\gamma^{\frac{\tau-\tau_1}{2\tau_1}} e^{2\tau_1} - 2e^{-(\tau-\tau_1)} + \gamma^{\frac{\tau-\tau_1}{2\tau_1}} \right] \varphi_0(\tau - \tau_1). \quad (26.31)$$

Similar formulas can be established for a triangular -shape wave.

For practical purposes, it is important to establish the need for considering wave disturbances in the obstacle material. Let us compare the final relations cited in this section with those established in §22 which only consider the material's inertial

*The coefficient $\bar{\alpha}$ has the sign of k_{22} ; $\bar{\alpha} > 0$ if $\rho_3 a_3 > \rho_2 a_2$, $\bar{\alpha} = 0$ if $\rho_3 a_3 = \rho_2 a_2$. The coefficient γ has the sign of the derivation $(\rho_3 a_3 - \rho_2 a_2)(\rho_1 a_1 - \rho_2 a_2)$.

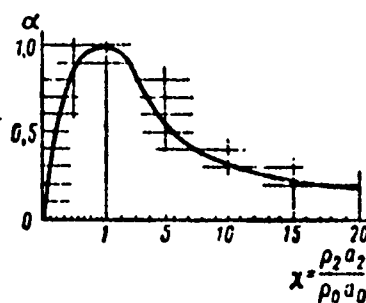


Fig. 115. The Relationship of Degree of Attenuation of Maximum Pressure Behind An Obstacle Having Different Acoustic Resistance.

characteristics. For the sake of simplicity, we will limit ourselves to the question of waves of exponential shape. (Conclusions derived will be of a rather general nature).

Let us compare two important cases, where the first and third medium is water (evaluation of protective characteristics of an obstacle) and where the first medium is water and the third is air (dynamic load on plate which is part of a ship). In the first case, we are interested in pressure behind the obstacle; in the second case, in front of the obstacle.

Assuming that $\rho_1 a_1 = \rho_3 a_3 = \rho_0 a_0$, for the coefficients α and γ entering into (26.21) we get

$$\alpha = k_1 k_{23} = \frac{2\rho_2 a_2}{\rho_2 a_2 + \rho_0 a_0} \frac{2\rho_0 a_0}{\rho_0 a_0 + \rho_2 a_2} = \frac{4\rho_0 a_0 \rho_2 a_2}{(\rho_0 a_0 + \rho_2 a_2)^2}, \quad (26.32)$$

$$\gamma = \left(\frac{\rho_0 a_0 - \rho_2 a_2}{\rho_0 a_0 + \rho_2 a_2} \right)^2, \quad (26.33)$$

consequently,

$$\alpha + \gamma = 1. \quad (26.34)$$

The magnitude of the pulse of the n -th part of the pressure contour behind the obstacle, according to (26.21), is

$$J_n = p_m \theta_2 \frac{\gamma^n e^{2n\tau_1} - 1}{\gamma e^{2\tau_1} - 1} \int_{(2n-1)\tau_1}^{(2n+1)\tau_1} e^{-(\tau-\tau_1)} d\tau =$$

$$= \frac{p_m \theta_2}{\gamma e^{2\tau_1} - 1} (e^{2\tau_1} - 1) [(\gamma^n e^{2n\tau_1} - 1) e^{-2n\tau_1}]. \quad (26.35)$$

The total pulse may be derived by summation of expressions in (26.35) from $n = 1$ to $n = \infty$

$$J = \sum_{n=1}^{\infty} J_n = \frac{p_m \theta_2}{\gamma e^{2\tau_1} - 1} (e^{2\tau_1} - 1) \sum_{n=1}^{\infty} (\gamma^n - e^{-2n\tau_1}) =$$

$$= \frac{p_m \theta_2}{\gamma e^{2\tau_1} - 1} (e^{2\tau_1} - 1) \left[\frac{\gamma}{1-\gamma} - \frac{e^{-2\tau_1}}{1-e^{-2\tau_1}} \right], \quad (26.36)$$

or, by abbreviating and bearing in mind that $\alpha = 1 - \gamma$,

$$J = p_m \theta. \quad (26.37)$$

This is the same result which was established in examining the protective characteristics of absolutely rigid plates [cf. (22.39)].

Therefore, any obstacle does not change the magnitude of the total direct shock-wave pulse. If we consider the wave characteristics of the obstacle material, we must replace the smooth pressure increment curve with a stepped curve. The difference in amplitudes, however, of pressure may be very considerable. Thus from the "wave" equation (26.21) it follows that the lowest maximum pressure behind the obstacle is

$$\min p_{3\max} = p_{m2} = p_m \frac{4f_1}{(1+\gamma)^2}, \quad (26.38)$$

where

$$\gamma = \frac{\rho_2 a_2}{\rho_3 a_3}. \quad (26.39)$$

The relationship $\alpha = \alpha(\gamma)$ is given in Fig. 115.

Because the quantity γ is positive for any χ , the minimum thickness of the obstacle δ_{\min} at which pressure behind it reaches minimum magnitude can be defined from the condition of equality of pressures behind the obstacle when the first and second waves emerge. From (26.21), performing simple transformations, we find that

$$\delta_{\min} = \frac{a_2 \theta}{2} \ln \frac{(1+\gamma)^2}{4\chi}. \quad (26.40)$$

For a shock-wave having a triangular contour, the quantity is

$$\delta_{\min} = \frac{a_2 \theta}{2} \left(\frac{1-\gamma}{1+\gamma} \right)^{\gamma}. \quad (26.41)$$

No such conclusions follow from the "inertial" solution, because where $\delta \rightarrow \infty$, $p_{3\max} \rightarrow 0$. Consequently, the approximate solution for a very thick obstacle may produce considerable error in evaluating pressure amplitudes.

Let us find the boundaries of feasible use of the approximate solution. For this purpose, let us illustrate the increment time of the mean pressure ($\tau_H = t_H/\theta$) defined by the "wave" solution. It can be found from the equation

$$\frac{dp_{3cp}(\tau)}{d\tau} = 0. \quad (26.42)$$

Differentiating (26.31) after transformations, we find that

$$\tau_H = - \frac{1}{1 - \frac{1}{2\gamma_1} \ln \gamma} \ln \left[- \frac{\ln \gamma}{2\gamma_1} \operatorname{ch} \left(\frac{1}{2} \ln \gamma + \tau_1 \right) \right]. \quad (26.43)$$

According to (22.37), the time for this "inertial" solution is

$$\tau_H = \frac{\ln 2\beta}{2\beta - 1} = \frac{\ln 2 \frac{\gamma_1 a_2 \theta}{m}}{2 \frac{\gamma_1 a_2 \theta}{m} - 1}. \quad (26.44)$$

Results calculated according to formulas (26.43) and (26.44) are shown in Fig. 116, where the quantities τ_H are plotted as a function of

$$\beta = \frac{\gamma_1 a_2 \theta}{m} = \frac{1}{\gamma \tau_1}$$

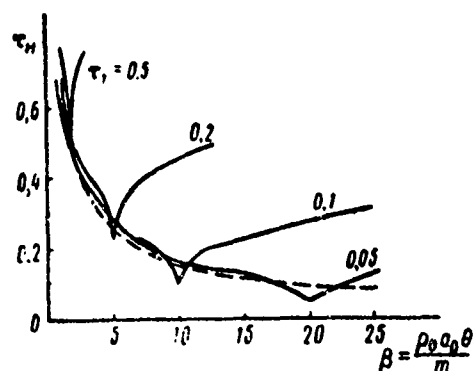


Fig. 116. Relationship of Pressure Increment Time up to Maximum Behind an Obstacle as a Function of β and τ_1

----- inertial solution;
 ————— wave equation.

We can see from the figure that in the area $\chi > 1$ and in some neighborhood $\chi = 1$, the curves are similar. The approximate solution is feasible in this range.

Because the values of pressure behind the obstacle are of prime interest from the standpoint of practical application, let us give a more precise evaluation for the utilization limits of the "inertia" notion. Let us assume that the divergence between the maximum and "mean" values of pressure with respect to a "wave" scheme must not exceed 20%, and the difference in amplitudes of pressure at point τ_H according to the "wave" and "inertia" schemes must not be more than 10%. Then, direct calculation according to formulas (26.30), (26.31), (26.43), and (26.44) yields the structure shown in Fig. 117. The nature of variation of pressure for different ranges of the parameter $\chi = (\rho_2 a_2) / (\rho_0 a_0)$ is illustrated in Fig. 118.

In practice, we most often must deal with steel plates. The theoretical findings for these plates clearly show the effect of thickness δ on pressure change behind the obstacle (shown in Fig. 119).

Let us now define the limits of applicability of the "inertial" solution for evaluating net pressure on a plate which divides air and water. Let us employ the formulas of the "wave" solution (26.18),

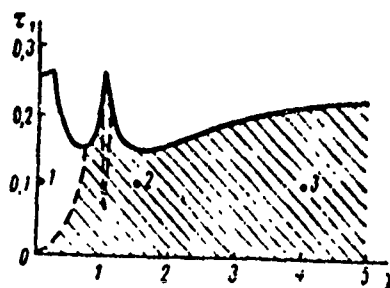


Fig. 117. Field of Application (Dashed Line) of Inertial Solution for Pressure Behind an Obstacle

- limiting curve of the field where the maximum mean pressure is less than the maximum peak by no more than 20%;
- limiting curve of area where inertial solution yields maximum pressure behind obstacle which differs by no more than 10% from max mean pressure from wave solution;
- - the point for which pressure-time curves are calculated acc. to the wave and inertial equations.

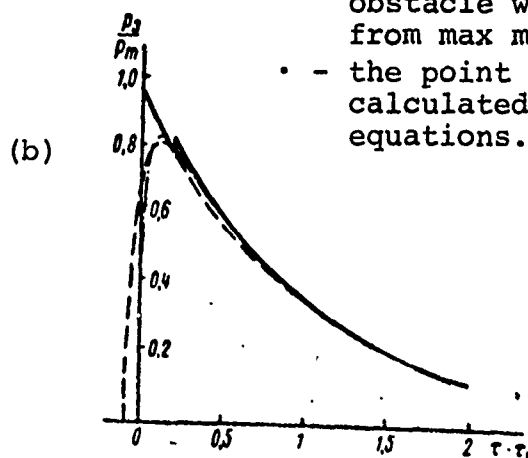
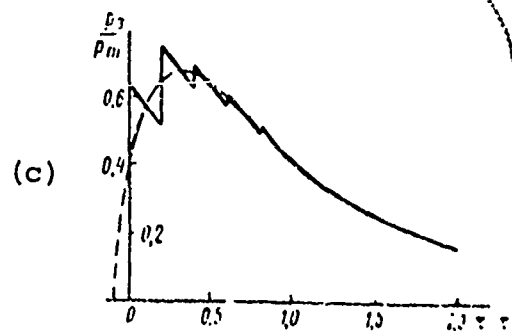
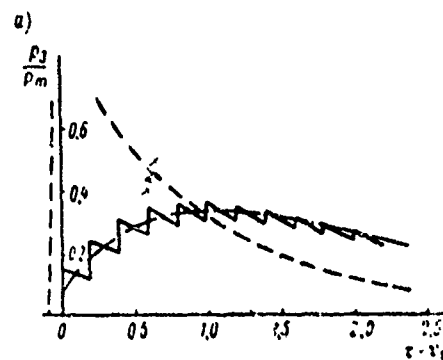


Fig. 118. Change in Pressure Behind an Obstacle where $\tau_1 = 0.1$: (a) for point 1 (Fig. 117) where $\chi = 0.04$; (b) for point 2, where $\chi = 1.5$; (c) for point 3, where $\chi = 4.0$.

- precise wave solution;
- curve of mean pressure acc. to wave solution;
- inertial solution.



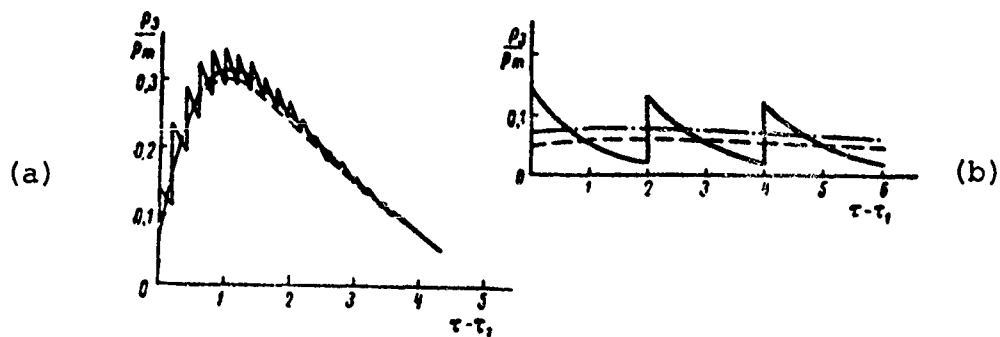


Fig. 119. Pressure Behind a Steel Obstacle Where $\chi = 26.3$; (a) where $\tau_1 = 0.1$; (b) where $\tau_1 = 1.0$. (Designations the same as in Fig. 118).

(26.24) and the formulas of the "inertial" solution (22.35), (22.59) where $\rho_1 a_1 = \rho_0 a_0$; $\rho_3 a_3 \approx 0$. In this case

$$\left. \begin{aligned} k_{11} &= \frac{\chi - 1}{\chi + 1}, \\ \gamma &= \frac{\chi - 1}{\chi + 1} = k_{11}, \\ \bar{a} &= -\frac{4\gamma}{(\gamma + 1)^2}. \end{aligned} \right\} \quad (26.45)$$

Let us calculate the effect time τ_+ and the pulse J_+ of the positive phase of net pressure. For an exponential-shape wave, employing (26.18), we find that

$$\tau_+ = \frac{t}{\theta} = (2n + 2)\tau_1, \quad (26.46)$$

where

$$n = E \left\{ \frac{\ln \left[\frac{1}{2} (1 + \chi) (1 - e^{-2\tau_1}) \right]}{2\tau_1 - \ln 3} \right\},$$

E is the so-called "entier" function (the function denoting the integral part of a number).

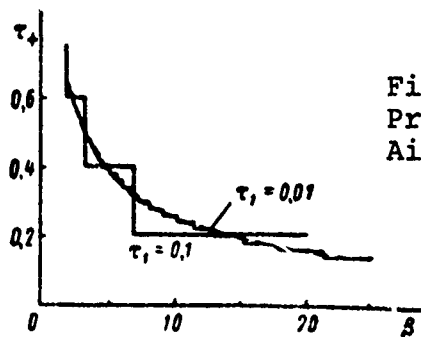


Fig. 120. Effect-Time of Positive Net Pressure on an Obstacle Dividing Air and Water.

— wave solution;
 ----- inertial solution.

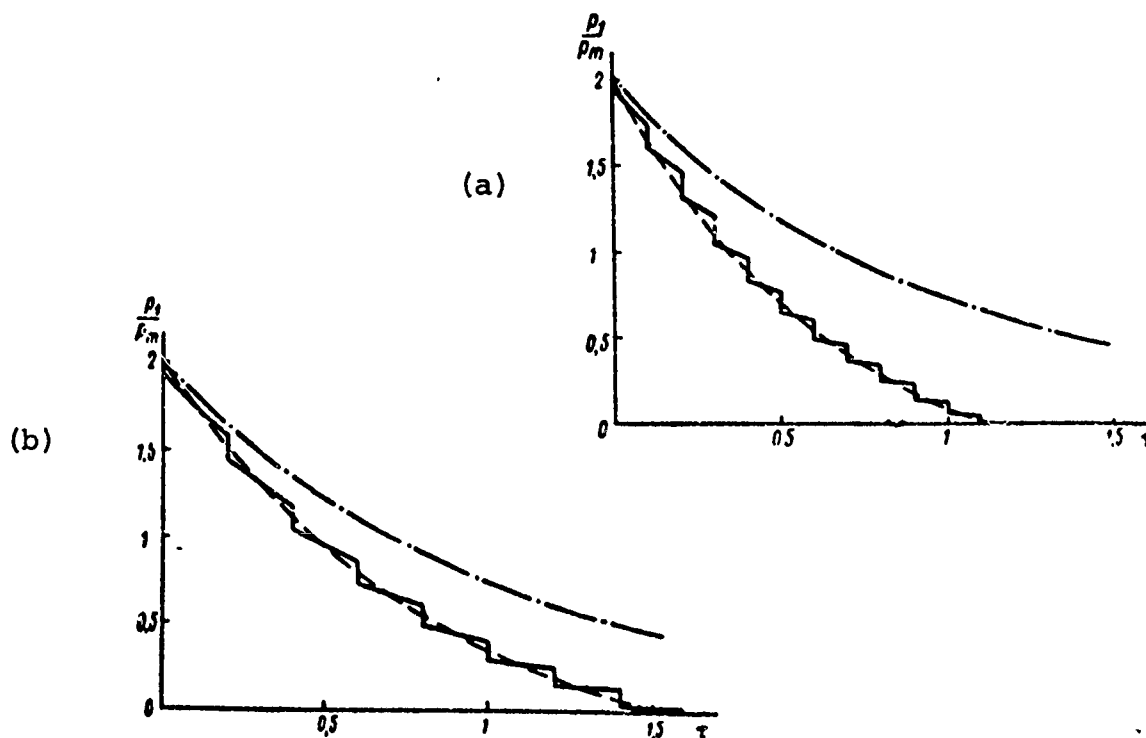


Fig. 121. Net Pressure on a Steel Obstacle ($\chi = 26.3$) Dividing Water and Air During Incidence onto said Obstacle of Exponential Shape Shock Wave: (a) - $\tau_1 = 0.05$; (b) - $\tau_1 = 0.1$.

— wave solution;
 ----- inertial solution;
 - - - - curve of net pressure on absolutely rigid obstacle.

The pulse is

$$J_1 = p_m \theta \left\{ (1 + k_{11}) (1 - e^{-\tau_1}) + \right. \\
\left. + \frac{1}{2} \frac{(e^{2\tau_1} - 1)}{k_{11} e^{2\tau_1} - 1} \left[\frac{k_{11} (k_{11}^2 - 1)}{k_{11} - 1} - \frac{e^{-2\tau_1 \tau_1}}{1 - e^{2\tau_1}} \right] \right\}.$$

(26.47)

Shown in Fig. 120 are the curves of $\tau_+ = \tau_+(\beta)$, where $\beta = \frac{\rho_0 a_0 \theta}{m} = \frac{1}{\chi \tau_1}$. As we can see from the figure, when evaluating the effect-time of the positive phase and consequently, the pulse I_+ , we can utilize the approximate solution for $\tau_1 < 0.1$. In the range of small values of χ , a considerable divergence between the magnitudes of pressure may take place. If we assume a possible error within 20% ($\frac{2}{1 + k_{11}} \leq 1.2$), then χ must be greater than 5. The corresponding theoretical findings according to the precise and approximate solutions for a steel plate are shown in Fig. 121.

The wide range of variation in the parameters χ and τ permits us, in most cases involving practical application, to utilize a simpler "inertial" calculation scheme which does not take into account the wave nature of disturbance propagation in the obstacle material.

(§27. General Concepts on the Interaction of a Shock Wave with an Elastic Plate Attached by Its Edges

In all the previously considered problems, we examined the motion of a system having one degree of freedom. This assumption no longer corresponds to reality when analyzing the interaction of a shock wave with an elastic plate attached by its edges. In this case, we must consider a system having an infinite number of degrees of freedom.*

Problems of this type are usually solved by writing travel in the form of a series in terms of the main (normal) forms of

* In this and subsequent sections, the wave nature of disturbance propagation in the obstacle material is not taken into consideration. We assume that the considered system satisfies the conditions formulated in the preceding section, which permit the use of the approximate "inertial" scheme. This all the more justifies that dynamic calculations belong to the number of problems which have been quite "coarsely" worked out (too many factors remain unaccounted for).

$$W(x, y, z, t) = \sum_{n=0}^{\infty} \omega_n(x, y, z) W_n(t), \quad (27.1)$$

where $\omega_n(x, y, z)$ - are functions defining the main forms of vibration;
 $W_n(t)$ - the main coordinates.

The chief advantage of this presentation is the randomness of one of the main forms of vibration from all the others. Thus, if the main forms of vibration have been defined, motion in terms of any of them can be considered as motion having one degree of freedom.

The difficulties associated with the dynamic calculation of elastic systems include the search for normal functions, and especially the complexity of defining the chief coordinates. The latter task is usually solved with the aid of Lagrange equations of the second type. For this purpose, we must define the kinetic and potential energy of the system.

If we take into consideration only the normal displacement of the plate surface, the kinetic energy of its elastic vibrations can be calculated according to the formula

$$\begin{aligned} T &= \frac{1}{2} \iint_S m W^2 dS = \frac{1}{2} \iint_S m \left(\sum_{n=0}^{\infty} \omega_n \dot{W}_n \right)^2 dS = \\ &= \frac{1}{2} \iint_S m \left(\sum_{n=0}^{\infty} \omega_n^2 \dot{W}_n^2 + 2 \sum_{n=0}^{\infty} \sum_{k=0}^{\infty} \omega_n \omega_k \dot{W}_n \dot{W}_k \right) dS. \end{aligned} \quad (27.2)$$

Due to the orthogonality of the functions of ω_n , however,

$$\iint_S \omega_k \omega_n = 0 \quad \text{при} \quad k \neq n. \quad (27.3)$$

We finally find that:

$$T = \frac{1}{2} \sum_{n=0}^{\infty} \dot{W}_n^2 \iint_S m \omega_n^2 dS = \frac{1}{2} \sum_{n=0}^{\infty} M_n \dot{W}_n^2, \quad (27.4)$$

where m - mass per unit of surface;

$M_n = \iint_S m w_n^2 dS$ - reduced mass of the elastic system, corresponding to the chief coordinate W_n .

By definition, the quantity of reduced mass is equal to the sum of the products of the mass of all points on the body multiplied by the square of travel completed during motion according to the n -th main form of vibration with unit displacement of the main coordinate ($W_n = 1$).

The potential energy of deformation in the elastic range, as we know, is a quadratic form of travel along the main coordinates*

$$V = \frac{1}{2} \sum_{n=0}^{\infty} K_n W_n^2 \quad (27.5)$$

where K_n - the so-called reduced rigidity factor, corresponding to deformation according to the n -th chief form of vibration.

It appears that the reduced rigidity factor is equal to twice the magnitude of potential energy during motion in the n -th form of vibration, which satisfies the displacement of the main coordinate $W_n = 1$.

According to (27.4) and (27.5), Lagrange equations of the second type may be written in the form of an infinite system:

$$\left. \begin{aligned} M_0 \frac{d^2 W_0}{dt^2} + K_0 W_0 &= F_{x_0}, \\ M_1 \frac{d^2 W_1}{dt^2} + K_1 W_1 &= F_{x_1}, \\ &\dots \dots \dots \\ M_n \frac{d^2 W_n}{dt^2} + K_n W_n &= F_{x_n}. \end{aligned} \right\} \quad (27.6)$$

* In the elastic-plastic range this is no longer so. However, additional problems which are associated with the study of plastic deformations introduce no theoretical changes in the physical substance of interaction problems.

where $F_{\Sigma n}$ - generalized force corresponding to the main coordinate W_n .

In order to define F_{Σ} we must write an expression for the work of external forces duringⁿ travel of the n-th main coordinate by the quantity δW_n . Because the migration of points of the obstacle surface in this case is equal to $\omega_n \delta W_n$, the work of the net forces of pressure p_{Σ} can be found according to the formula

$$A = \iint_S p_{\Sigma}(x, y, z, t) \omega_n(x, y, z) \delta W_n(t) dS = \delta W_n \iint_S p_{\Sigma} \omega_n dS. \quad (27.7)$$

The magnitude

$$F_{\Sigma n} = \iint_S p_{\Sigma} \omega_n dS \quad (27.8)$$

is called the generalized force.

The net pressure p_{Σ} can be found by using the function of the wave equation potential which satisfies the boundary condition

$$\left. \frac{\partial \varphi_{\Sigma}}{\partial n} \right|_S = \dot{W}. \quad (27.9)$$

Practical evaluations are convenient to conduct separately for hydrodynamic forces of the first and second category*

$$F_{\Sigma n} = F_{1n} + F_{2n}, \quad (27.10)$$

where

$$F_{1n} = -\rho_0 \iint_S \frac{\partial \varphi_1}{\partial t} \omega_n dS, \quad (27.11)$$

$$F_{2n} = -\rho_0 \iint_S \frac{\partial \varphi_2}{\partial t} \omega_n dS. \quad (27.12)$$

*In this case, hydrodynamic forces of the first category are defined allowing for certain types of buckling; however, as before, they do not depend on the results of obstacle motion and can be calculated independently of the parameters of motion and deformation of the obstacle.

The velocity potential ϕ_1 can be found under the assumption of obstacle immobility with the boundary condition on the surface

$$\frac{\partial \varphi_1}{\partial n} = \frac{\partial \varphi_{np}}{\partial n} + \frac{\partial \varphi_d}{\partial n} = 0, \quad (27.13)$$

where ϕ_{np} and ϕ_d - components of the potential function induced by the direct and diffraction waves.

The potential ϕ_2 on the plate surface is subject to the condition

$$\frac{\partial \varphi_2}{\partial n} = \psi, \quad (27.14)$$

but

$$\psi = \sum_{n=0}^{\infty} \omega_n \psi_n, \quad (27.15)$$

and consequently, the potential of the radiated field ϕ_2 is a function of the parameters of motion in all main forms of vibration. The latter fact indicates the advisability of finding function ϕ_2 in the form of a series

$$\varphi_2 = \sum_{n=0}^{\infty} \omega_n \lambda_n, \quad (27.16)$$

where λ_n on the obstacle surface is a function only of time t .

If this can be achieved in terms of the problem's conditions, then a comparison of (27.14)-(27.16) yields

$$\varphi_n = \omega_n \lambda_n \quad (27.17)$$

which is a function only of one main coordinate W_n .

Employing (27.8), (27.10), (27.12), (27.16), and (27.17) and the feature of orthogonality of the functions of ω_n , we get

$$\begin{aligned}
F_{2n} &= -\rho_0 \iint_S \left[\sum_{k=0}^{\infty} \omega_k \frac{\partial \lambda_k}{\partial t} \right] \omega_n dS = -\rho_0 \sum_{k=0}^{\infty} \frac{\partial \lambda_k}{\partial t} \iint_S \omega_k \omega_n dS = \\
&= -\rho_0 \frac{\partial \lambda_n}{\partial t} \iint_S \omega_n^2 dS.
\end{aligned} \tag{27.18}$$

In this case, the n -th component of the second category hydrodynamic forces is a function only of the n -th main coordinate.

The result obtained permits us to form conclusions on the feasibility of defining any main coordinate from a total of two differential equations

$$M_n \dot{W}_n + K_n W_n = -\rho_0 \iint_S \frac{\partial \varphi_{n1}}{\partial t} \omega_n dS + F_{1n}, \tag{27.19}$$

$$\frac{\partial^2 \varphi_{n1}}{\partial x^2} + \frac{\partial^2 \varphi_{n1}}{\partial y^2} + \frac{\partial^2 \varphi_{n1}}{\partial z^2} = \frac{1}{a_0^2} \frac{\partial^2 \varphi_{n1}}{\partial t^2}. \tag{27.20}$$

The limiting condition for (27.20) is

$$\left. \frac{\partial \varphi_{n1}}{\partial n} \right|_S = \omega_n \dot{W}_n. \tag{27.21}$$

According to (27.16), the net potential of the wave radiation field is

$$\varphi_2 = \sum_{n=0}^{\infty} \varphi_n = \sum_{n=0}^{\infty} \omega_n \lambda_n. \tag{27.22}$$

Strictly speaking, we can only write (27.16) for the simplest cases of shock-wave interaction with an elastic obstacle (problem of plane wave interaction with spherical and round cylindrical envelopes); consequently, in general, any component of second category hydrodynamic forces F_{2n} becomes a function of all the main coordinates and must solve an infinite system of mutually-related differential equations. However, as D. A. Aleksandrin first showed, using the study of the motion of an infinite plate resting on rigid immobile equidistant unilateral supports, for most cases of practical application we can ignore all terms in expressing F_{2n} where $k \neq n$. Consequently, we can roughly define any main coordinate from a total of two differential equations (27.19) and (27.20), which are primarily used to

precisely define W_n .

Later on we will show that the n -th component of second category hydrodynamic force may be written in the form

$$F_{2n} = \begin{cases} -F_{0n} \int_0^t \dot{W}_n(t-\tau) \psi_n(\tau) d\tau & \text{where } t < t_{0n} \\ -F_{0n} \int_0^{t_{0n}} \dot{W}_n(t-\tau) \psi_n(\tau) d\tau & \text{where } t > t_{0n} \end{cases} \quad (27.23)$$

$$-F_{0n} \int_0^{t_{0n}} \dot{W}_n(t-\tau) \psi_n(\tau) d\tau \quad \text{where } t > t_{0n} \quad (27.24)$$

where F_{0n} - a constant, equal to the second category hydrodynamic force component at time $t = 0$ for the motion of the main coordinate according to the unit function law $W_n = \sigma_0(t)$;

t_{0n} - some typical time for which $\psi(t) \equiv 0$ where $t > t_{0n}$;

$\psi_n(t)$ - the kernel, depending on both the shape of the obstacle and its type of deformation (where $t = 0$, $\psi_n(0) = 1$).

Therefore, the problem of a shock-wave interacting with an elastic obstacle reduces to a study of integro-differential equations of the type already considered: where $t < t_{0n}$

$$M_n \ddot{W}_n + K_n W_n = F_{1n} - F_{0n} \int_0^t \dot{W}_n(t-\tau) \psi_n(\tau) d\tau, \quad (27.25)$$

where $t > t_{0n}$

$$M_n \ddot{W}_n + K_n W_n = F_{1n} - F_{0n} \int_0^{t_{0n}} \dot{W}_n(t-\tau) \psi_n(\tau) d\tau. \quad (27.26)$$

The primary difficulties are first of all associated with defining $\psi_n(t)$ from the corresponding boundary value problem of the wave potential and secondly, with deriving a precise solution of integro-differential equations (27.25) and (27.26) themselves. These equations may be reduced to ordinary differential equations for several forms of the function $\psi(t)$.

To prove this assertion, let us employ the method developed in §23. Integrating (27.25) twice with respect to t and dropping out the index n (for the sake of simplicity), allowing for zero initial data we find that

$$\begin{aligned} MW(t) + K \int_0^t \int_0^\tau W(\xi) d\xi d\tau + F_0 \int_0^t W(t-\tau) \psi(\tau) d\tau &= \\ = \int_0^t \int_0^\tau F_1(\xi) d\xi d\tau. \end{aligned} \quad (27.27)$$

Integration by parts and differentiation from (27.27) easily yields

$$\begin{aligned} M\dot{W}(t) + K \int_0^t W(\tau) d\tau + F_0 W(t) + F_0 \int_0^t W(t-\tau) \frac{d}{d\tau} \psi(\tau) d\tau &= \\ = \int_0^t F_1(\tau) d\tau, \end{aligned} \quad (27.28)$$

$$\begin{aligned} M\dot{W}(t) + F_0 \dot{W}(t) + \\ + [K + F_0 \dot{\psi}(0)] W(t) + F_0 \int_0^t W(t-\tau) \frac{d^2}{d\tau^2} \psi(\tau) d\tau = F_1(t). \end{aligned} \quad (27.29)$$

Multiplying (27.27) by C_2 and (27.28) C_1 , and combining these with (27.29), we find that

$$\begin{aligned} M\dot{W}(t) + (F_0 + C_1 M) W(t) + \\ + [K + F_0 \dot{\psi}(0) + C_1 F_0 + C_2 M] W(t) + C_1 K \int_0^t W(\tau) d\tau + \\ + C_2 K \int_0^t \int_0^\tau W(\xi) d\xi d\tau = F_1(t) + C_1 \int_0^t F_1(\tau) d\tau + C_2 \int_0^t \int_0^\tau F_1(\xi) d\xi d\tau - \\ - F_0 \int_0^t W(t-\tau) \left(\frac{d^2}{d\tau^2} + C_3 \frac{d}{d\tau} + C_4 \right) \psi(\tau) d\tau. \end{aligned} \quad (27.30)$$

It follows from (27.30) that if

$$\frac{d^2\psi}{dt^2} + C_1 \frac{d\psi}{dt} + C_2\psi = 0, \quad (27.31)$$

then the initial integro-differential equation goes over into an ordinary differential equation. Forms of the functions $\psi(t)$ which satisfy condition (27.31) were produced earlier (cf. Table 5).

In contrast to an analogous problem of motion of an undeformable obstacle, because of the term containing the reduced rigidity factor, in this case we get an equation of the fourth order having constant coefficients, and not a second-order equation

$$\begin{aligned} M \frac{d^4 W}{dt^4} + (F_0 + C_1 M) \frac{d^3 W}{dt^3} + [K + F_0 \dot{\psi}(0) + C_1 F_0 + C_2 M] \frac{d^2 W}{dt^2} + \\ + C_1 K \frac{dW}{dt} + C_2 K W = \dot{F}_1(t) + C_1 \ddot{F}_1(t) + C_2 \dddot{F}_1(t). \end{aligned} \quad (27.32)$$

Integration of (27.32) should be performed with the following initial data:

$$\left. \begin{aligned} W(0) = \dot{W}(0) = 0, \\ \dot{W}(0) = \frac{F_1(0)}{M}, \\ \ddot{W}(0) = \frac{F_1(0)}{M} - F_0 \frac{F_1(0)}{M}. \end{aligned} \right\} \quad (27.33)$$

The differential equation (27.32) is valid where $t < t_0$. Where $t > t_0$, analogous transformations of (27.26) lead to an ordinary differential equation of the fourth order having constant coefficients and a delayed argument

$$\begin{aligned} M \frac{d^4 W}{dt^4} + (F_0 + C_1 M) \frac{d^3 W}{dt^3} + [F_0 \dot{\psi}(0) + C_1 F_0 + C_2 M] \frac{d^2 W}{dt^2} - \\ - F_0 \dot{\psi}(t_0) \frac{d^2 W(t - t_0)}{dt^2} + C_1 K \frac{dW}{dt} + C_2 K W = \\ = \dot{F}_1(t) + C_1 \ddot{F}_1(t) + C_2 \dddot{F}_1(t) \end{aligned} \quad (27.34)$$

When approximating the function $\psi(t)$ by a linear relation

$$\psi(t) = \left(1 - \frac{t}{t_*}\right) [\psi_0(t) - \psi_0(t - t_*)], \quad (27.35)$$

as we indicated in §23, the coefficients C_1 and C_2 must be assumed to be equal to zero. In this case, we derive a second-order ordinary differential equation from (27.29)

$$M\ddot{W} + F_0\dot{W} + \left(K - \frac{F_0}{t_*}\right)W = F_1 \quad \text{where} \quad t < t_*. \quad (27.36)$$

For $t > t_*$, motion is described by an equation having a delayed argument

$$M\ddot{W} + F_0\dot{W} + \left(K - \frac{F_0}{t_*}\right)W + \frac{F_0}{t_*}W(t - t_*) = F_1. \quad (27.37)$$

These last equations and their methods of solution are practically the same as those examined in §§23-25. The difference consists in considering not just one, but n equations of the type (27.36), (27.37).

As we mentioned, the primary difficulty of the problem lies in defining the functions $\psi_n(t)$ from the corresponding boundary value problem of the wave potential. The following section is devoted to illustrating possible means of finding these functions.

§28. The Pressure Field and Generalized Hydrodynamic Force of the Second Category Induced by Deformation of an Elastic Plate Attached by its Edges to a Rigid Infinite Wall

Let us now consider the motion of an elastic plate attached by its edges to a rigid infinite wall, under the influence of a plane shock-wave. For the sake of determinacy, let us assume that the plate divides water and air.

The presence of a rigid infinite wall greatly simplifies the

evaluation of 2nd category generalized hydrodynamic force: it will be twice the magnitude of pressure of a direct wave.

According to (27.8),

$$F_{1n}(t) = \iint_S 2p(t) \omega_n dS = 2p(t) \alpha_{1n} S, \quad (28.1)$$

where

$$\alpha_{1n} = \frac{\iint_S \omega_n dS}{S}. \quad (28.2)$$

Let us evaluate the possibility of two methods to define second category hydrodynamic force: utilizing the radiation integral (§11, 14, 15) and solving the boundary value problem of the wave equation.

With the aid of the radiation integral for points situated on the surface of a round plate, according to (11.19) and (27.1), we find that

$$p_n(r, t) = \frac{1}{2\pi} \iint_S \frac{W_n\left(t - \frac{|r-r_1|}{a_n}\right) \omega_n(r_1) \alpha_0\left(t - \frac{|r-r_1|}{a_0}\right)}{|r-r_1|} dS, \quad (28.3)$$

where r - the radius-vector of the point of observation; r_1 - the variable radius-vector.

Pressure on any point r on the plate induced by its motion in the form $\omega_n(r)$ at a velocity W_n ,

$$p_{2n}(r, t) = -\frac{\rho_0}{2\pi} \iint_S \frac{W_n\left(t - \frac{|r-r_1|}{a_n}\right) \omega_n(r_1) \alpha_0\left(t - \frac{|r-r_1|}{a_0}\right)}{|r-r_1|} dS. \quad (28.4)$$

We can calculate the integral (28.4) for the center of a plate $r = 0$ rather simply. In this case

$$p_{2n}(0, t) = -\frac{\rho_0}{2\pi} \int_0^{2\pi} \int_0^a \frac{W_n\left(t - \frac{r_1}{a_n}\right) \omega_n(r_1) \alpha_0\left(t - \frac{r_1}{a_0}\right)}{r_1} r_1 dr_1 d\varphi = -\rho_0 \int_0^a W_n\left(t - \frac{r_1}{a_n}\right) \omega_n(r_1) \alpha_0\left(t - \frac{r_1}{a_0}\right) dr_1.$$

where a - the radius of the plate.

Because $\sigma_0(t - \frac{r_1}{a_0}) \equiv 0$ where $r_1 > a_0 t$, then for $t < \frac{a}{a_0}$ we get

$$p_{zn}(0, t) = -\rho_0 \int_0^{a_0 t} W_n\left(t - \frac{r_1}{a_0}\right) \omega_n(r_1) dr_1. \quad (28.5)$$

By replacing the variables $\tau = t - (r_1)/(a_0)$ and integrating by parts, we can easily derive

$$\begin{aligned} p_{zn}(0, t) &= \rho_0 a_0 \int_0^0 W_n(\tau) \omega_n(a_0 t - a_0 \tau) d\tau = \\ &= -\rho_0 a_0 W_n(t) \omega_n(0) - \rho_0 a_0^2 W_n(t) \omega_n'(0) + \\ &+ \rho_0 a_0^3 \int_0^0 W_n(\tau) \omega_n'(a_0 t - a_0 \tau) d\tau. \end{aligned} \quad (28.6)$$

If we consider, as is often done, the motion of a round plate with its edges freely supported as a form of buckling

$$w = 1 - \frac{r^2}{a^2}, \quad (28.7)$$

then $w(0) = 1$; $w(a) = 0$; $w(r) = -\frac{2}{a^2} r^2$.

Substituting these expressions into (28.6), we find that

$$p_z(0, t) = -\rho_0 a_0 W_c(t) + \rho_0 a_0 \frac{2}{a^2} \int_0^t W_c(\tau) d\tau, \quad (28.8)$$

where W_c - migration of the central point on the plate (main coordinate);

$$t_A = \frac{a}{a_0} - \text{wave-run time of the plate radius.}$$

Formula (28.8) was first derived by Kirkwood [10]. Its first term conforms to the solution based on the hypothesis of "plane reflection", the second considering the effect of diffraction waves where $t < t_A$

L. V. Fremke derived a similar relationship for radiation pressure at the center of an infinitely-long plate being deformed into a cylindrical surface $\omega = 1 - (x^2)/(a^2)$

$$p_z(0, t) = -\rho_0 a_0 \ddot{W}_z(t) + \rho_0 a_0 \frac{1}{t^2} \int_0^t W_z(\tau) d\tau. \quad (28.9)$$

It differs from (28.8) by only the coefficient in the second term, indicating the effect of diffraction waves for a round plate is twice as great as for a plate buckling into a cylindrical surface. However, for other points on the plate, we cannot derive such simple results. Consequently, the definition of the second category generalized hydrodynamic force, with the aid of the integral of radiation, becomes very difficult. It is simpler to consider the appropriate boundary value problem of the wave equation.

At this point we will limit ourselves to the study of motion of round and rectangular plates.

For a round plate with the radius a , attached to a rigid infinite wall and buckling in the shape $\omega_n(r)$, the problem of defining the radiation field reduces to defining the potential function ϕ_n which satisfies the wave equation in cylindrical coordinates (henceforth we will cease using the index n):

$$\frac{\partial^2 \phi}{\partial r^2} + \frac{1}{r} \frac{\partial \phi}{\partial r} + \frac{\partial^2 \phi}{\partial z^2} = -\frac{1}{a_0^2} \frac{\partial^2 \phi}{\partial t^2} \quad (28.10)$$

with zero initial data

$$\phi|_{t=0} = \frac{\partial \phi}{\partial t}|_{t=0} = 0 \quad (28.11)$$

and boundary conditions

$$\frac{\partial \phi}{\partial z}|_{z=0} = \begin{cases} 0 & \text{where } r > a \\ -\ddot{W}(t)\omega(r) & \text{where } r < a \end{cases} \quad (28.12)$$

$$\phi|_{r=a} \rightarrow 0 \quad (28.13)$$

We will assume the origin of the coordinates to be at the center of the plate. The z axis is directed toward the interior of the fluid. The positive direction of motion of the plate opposes the direction of the z axis [hence the minus sign in the boundary condition (28.12)].

To solve the wave equation, let us employ the Laplace transform*. Then, instead of (28.10)-(28.13), we get

$$\frac{\partial^2 \bar{\varphi}}{\partial r^2} + \frac{1}{r} \frac{\partial \bar{\varphi}}{\partial r} + \frac{\partial^2 \bar{\varphi}}{\partial z^2} = \frac{v^2}{a_0^2} \bar{\varphi}, \quad (28.14)$$

$$\left. \frac{\partial \bar{\varphi}}{\partial z} \right|_{z=0} = \begin{cases} 0 & \text{where } r > a \\ -\bar{W}(v) \omega(r) & \text{where } r < a \end{cases} \quad (28.15)$$

$$\left. \bar{\varphi} \right|_{r=\infty} \rightarrow 0, \quad (28.16)$$

where

$$\bar{W}(v) = \int_0^\infty \dot{W}(t) e^{-vt} dt, \quad (28.17)$$

$$\bar{\varphi} = \int_0^\infty \varphi e^{-vt} dt, \quad (28.18)$$

v - a complex parameter having a positive real part.

As before, the solution of (28.14) will be sought by the Fourier method. Let us assume that

$$\bar{\varphi} = X(r) Y(z, v). \quad (28.19)$$

Then, substituting (28.19) into (28.14), we find that:

$$\frac{X''(r)}{X(r)} + \frac{1}{r} \frac{X'(r)}{X(r)} + \frac{Y''(z, v)}{Y(z, v)} - \frac{v^2}{a_0^2} = 0, \quad (28.20)$$

*This method was first used to solve the problem by Zamyshlyayev and Mironov for the motion of a rigid plate in terms of the first type of vibration.

whence

$$X''(r) + \frac{1}{r} X'(r) + \lambda^2 X(r) = 0, \quad (28.21)$$

$$Y''(z, v) - \left(\lambda^2 + \frac{v^2}{a_0^2} \right) Y(z, v) = 0. \quad (28.22)$$

Considering conditions of infinity and integrating (28.22), we find that

$$Y(z, v) = C_1(\lambda, v) e^{-z \sqrt{\lambda^2 + \frac{v^2}{a_0^2}}}. \quad (28.23)$$

The solution of equation (28.21), if we bear (28.16) in mind, will be

$$X(r) = C_2 J_0(\lambda r), \quad (28.24)$$

where $J_0(\lambda r)$ - a Bessel function of the zero order.

According to (28.19), (28.23), and (28.24), the general form of function $\bar{\phi}$ is

$$\bar{\phi} = \int_0^\infty J_0(\lambda r) C(\lambda, v) e^{-z \sqrt{\lambda^2 + \frac{v^2}{a_0^2}}} d\lambda. \quad (28.25)$$

To define $C(\lambda, v)$, let us employ the boundary condition (28.15), which we will write in the form of a Fourier-Bessel integral expansion

$$\left. \frac{\partial \bar{\phi}}{\partial z} \right|_{z=0} = - \int_0^\infty \lambda J_0(\lambda r) \int_0^a \mu \omega(\mu) \bar{W}(v) J_0(\mu \lambda) d\lambda d\mu; \quad (28.26)$$

however, according to (28.25)

$$\left. \frac{\partial \bar{\phi}}{\partial z} \right|_{z=0} = - \int_0^\infty J_0(\lambda r) C(\lambda, v) \sqrt{\lambda^2 + \frac{v^2}{a_0^2}} d\lambda. \quad (28.27)$$

whence

$$X''(r) + \frac{1}{r} X'(r) + \lambda^2 X(r) = 0, \quad (28.21)$$

$$Y''(z, v) - \left(\lambda^2 + \frac{v^2}{a_0^2} \right) Y(z, v) = 0. \quad (28.22)$$

Considering conditions of infinity and integrating (28.22), we find that

$$Y(z, v) = C_1(\lambda, v) e^{-z \sqrt{\lambda^2 + \frac{v^2}{a_0^2}}}. \quad (28.23)$$

The solution of equation (28.21), if we bear (28.16) in mind, will be

$$X(r) = C_2 J_0(\lambda r), \quad (28.24)$$

where $J_0(\lambda r)$ - a Bessel function of the zero order.

According to (28.19), (28.23), and (28.24), the general form of function $\bar{\phi}$ is

$$\bar{\phi} = \int_0^\infty J_0(\lambda r) C(\lambda, v) e^{-z \sqrt{\lambda^2 + \frac{v^2}{a_0^2}}} d\lambda. \quad (28.25)$$

To define $C(\lambda, v)$, let us employ the boundary condition (28.15), which we will write in the form of a Fourier-Bessel integral expansion

$$\left. \frac{\partial \bar{\phi}}{\partial z} \right|_{z=0} = - \int_0^\infty \lambda J_0(\lambda r) \int_0^a \mu \omega(\mu) \bar{W}(v) J_0(\mu \lambda) d\lambda d\mu; \quad (28.26)$$

however, according to (28.25)

$$\left. \frac{\partial \bar{\phi}}{\partial z} \right|_{z=0} = - \int_0^\infty J_0(\lambda r) C(\lambda, v) \sqrt{\lambda^2 + \frac{v^2}{a_0^2}} d\lambda. \quad (28.27)$$

consequently,

$$C(\lambda, \nu) = \frac{\lambda \bar{W}(\nu)}{\sqrt{\lambda^2 + \frac{\nu^2}{a_0^2}}} \int_0^a \mu w(\mu) J_0(\mu \lambda) d\mu. \quad (28.28)$$

Therefore,

$$\bar{\varphi} = \int_0^{\tilde{a}} \lambda J_0(\lambda r) \frac{a \bar{W}(\nu)}{\sqrt{\lambda^2 + \frac{\nu^2}{a_0^2}}} e^{-\nu \sqrt{\lambda^2 + \frac{\nu^2}{a_0^2}}} \int_0^a \mu w(\mu) J_0(\mu \lambda) d\mu. \quad (28.29)$$

To use the original instead of the transform, let us employ the Mellin integral

$$\begin{aligned} \varphi &= \int_0^{\tilde{a}} \lambda J_0(\lambda r) \int_0^a \mu w(\mu) J_0(\mu \lambda) \times \\ &\times \left[\frac{1}{2\pi i} \int_{i\delta_1} \frac{\bar{W}(\nu)}{\sqrt{\lambda^2 + \frac{\nu^2}{a_0^2}}} e^{\nu t - \nu \sqrt{\lambda^2 + \frac{\nu^2}{a_0^2}}} d\nu \right] d\lambda d\mu, \end{aligned} \quad (28.30)$$

or on the basis of the generalized Borel theorem

$$\begin{aligned} \varphi &= \int_0^{\tilde{a}} \lambda J_0(\lambda r) \int_0^a \mu w(\mu) J_0(\mu \lambda) \times \\ &\times \left[\int_0^t W(t-\tau) \left[\frac{1}{2\pi i} \int_{i\delta_1} \frac{e^{\nu \tau - \nu \sqrt{\lambda^2 + \frac{\nu^2}{a_0^2}}}}{\sqrt{\lambda^2 + \frac{\nu^2}{a_0^2}}} d\nu \right] d\tau \right] d\lambda d\mu. \end{aligned} \quad (28.31)$$

Because

$$\frac{1}{2\pi i} \int_{(L)} \frac{e^{v-\tau} \sqrt{\lambda^2 + \frac{v^2}{a_0^2}}}{\sqrt{\lambda^2 + \frac{v^2}{a_0^2}}} dv = a_0 J_0 \left(i a_0 \sqrt{\tau^2 - \frac{z^2}{a_0^2}} \right) J_0 \left(\tau - \frac{z}{a_0} \right). \quad (28.32)$$

we will get*

$$\begin{aligned} \varphi &= a_0 \int_0^{\infty} i J_0(i r) \int_0^a \mu \bar{w}(\mu) J_0(\mu \lambda) \int_{z/a_0}^t \ddot{W}(t-\tau) \times \\ &\quad \times J_0 \left(i a_0 \sqrt{\tau^2 - \frac{z^2}{a_0^2}} \right) d\tau d\lambda d\mu = \\ &= a_0 \int_0^{\infty} i J_0(i r) \bar{w}(\lambda) \int_{z/a_0}^t \ddot{W}(t-\tau) J_0 \left(i a_0 \sqrt{\tau^2 - \frac{z^2}{a_0^2}} \right) d\tau d\lambda, \end{aligned} \quad (28.33)$$

where

$$\bar{w}(\lambda) = \int_0^a \mu \bar{w}(\mu) J_0(\lambda \mu) d\mu. \quad (28.34)$$

Using pressure according to (28.33) instead of the potential function, we will find that

$$p_2(r, z, t) = -\rho_0 a_0 \int_{z/a_0}^t \ddot{W}(t-\tau) \int_0^{\infty} i J_0(i r) \bar{w}(\lambda) J_0 \left(i a_0 \sqrt{\tau^2 - \frac{z^2}{a_0^2}} \right) d\lambda d\tau. \quad (28.35)$$

Assuming that $z = 0$ in (28.35), let us derive an expression for pressure at points on the plate surface. To define second category hydrodynamic force, we must integrate this pressure with respect to plate surface, multiplied by the form of buckling,

$$F_z = \int_0^{2\pi} \int_0^a p_2(r, t) w(r) r dr d\alpha = 2\pi \int_0^a p_2(r, t) w(r) r dr \quad (28.36)$$

*The same result was obtained by Aleksandrin with the aid of a double integral transform (the Laplace transform with respect to t and the Hankel transform with respect to r).

We should bear in mind that (28.35) characterizes only the component of pressure forces conforming to the n -th main coordinate. Net pressure is

$$p_{21} = \sum_{n=0}^{\infty} p_{2n}. \quad (28.37)$$

The second category hydrodynamic force for the k -th form, in turn, is defined by integrating series (28.37), multiplied by the main type of vibration

$$F_{2k} = 2\pi \sum_{n=0}^{\infty} \int_0^a p_{2n} \omega_k r dr. \quad (28.38)$$

However, we can disregard all the terms of the series where $n \neq k$. Consequently, combining (28.35)-(28.38) we find that

$$F_{2k} = -2\pi \rho_0 a_0 \int_0^t \dot{W}_k(t-\tau) \int_0^{\infty} \bar{\omega}_k^{-2}(i) J_0(\lambda a_0 \tau) d\lambda d\tau. \quad (28.39)$$

It is convenient to write expression (28.39) in a somewhat different form

$$F_{2k} = -F_{0k} \int_0^t \dot{W}_k(t-\tau) \psi_k(\tau) d\tau, \quad (28.40)$$

where

$$F_{0k} = \rho_0 a_0 2\pi \int_0^a r \omega_k^2(r) dr = \rho_0 a_0 \gamma_{2k} S, \quad (28.41)$$

$$\gamma_k = \frac{1}{S} \int_S \omega_k^2 dS.$$

$$\psi_k(\tau) = \frac{2\pi}{\gamma_{2k} S_0} \int_0^{\infty} \bar{\omega}_k^{-2}(i) J_0(\lambda a_0 \tau) d\lambda, \quad (28.42)$$

$$\bar{\omega}_k(i) = \int_0^a r \omega_k(r) J_0(\lambda r) dr. \quad (28.43)$$

We can show that where $\tau > \frac{2a}{a_0}$, $\psi(\tau) \equiv 0$ and consequently, $\psi(\tau)$ changes during time $[0, \frac{2a}{a_0}]$ from one to zero during the motion of a plate in any type of vibration. Therefore where $t > \frac{2a}{a_0}$

$$F_{12} = -F_{00} \int_0^{\frac{2a}{a_0}} \ddot{W}_k(t-\tau) \dot{\varphi}_k(\tau) d\tau. \quad (28.44)$$

With the aid of (28.42) and (28.41), we can easily calculate the quantity of apparent mass of the fluid during vibration of the plate in a given form

$$M_{np} = F_0 \int_0^{\frac{2a}{a_0}} \ddot{\varphi}(t) dt = 2\pi \rho_0 a_0 \int_0^{\frac{2a}{a_0}} \lambda \bar{\omega}^2(\lambda) \int_0^{\frac{2a}{a_0}} J_0(\lambda a_0 \tau) d\tau d\lambda. \quad (28.45)$$

Calculation by this formula often leads to the goal more rapidly and in a simpler fashion than the classic scheme.

Let us now examine motion of a rectangular plate.

For a rectangular plate fastened to a rigid wall and deforming in a given main form of vibration, the problem of defining second category hydrodynamic force is reduced to finding the potential function ϕ which satisfies the wave equation

$$\frac{\partial^2 \varphi}{\partial x^2} + \frac{\partial^2 \varphi}{\partial y^2} + \frac{\partial^2 \varphi}{\partial z^2} = \frac{1}{a_0^2} \frac{\partial^2 \varphi}{\partial t^2} \quad (28.46)$$

with zero initial data

$$\varphi|_{t=0} = \frac{\partial \varphi}{\partial t}|_{t=0} = 0 \quad (28.47)$$

and boundary conditions

$$\frac{\partial \varphi}{\partial z}|_{z=0} = \begin{cases} 0 & \text{where } |x| > a \text{ or } |y| > b \\ -\ddot{W}(t) = (x, y) & \text{where } -a \leq x \leq a \text{ and } -b \leq y \leq b, \end{cases} \quad (28.48)$$

$$\varphi|_{r=\sqrt{x^2+y^2+z^2} \rightarrow \infty} \rightarrow 0. \quad (28.49)$$

A system of coordinates is selected as in the preceding section;

the origin of the coordinates is at the center of the plate.

After applying the Laplace integral transform, we will find that

$$\frac{\partial^2 \bar{\varphi}}{\partial x^2} + \frac{\partial^2 \bar{\varphi}}{\partial y^2} + \frac{\partial^2 \bar{\varphi}}{\partial z^2} = -\frac{v^2}{a_0^2} \bar{\varphi}, \quad (28.50)$$

$$\left. \frac{\partial \bar{\varphi}}{\partial z} \right|_{z=0} = \begin{cases} 0 & \text{where } |x| > a \\ & |y| > b \\ -\bar{W}(v) \omega(x, y) & \text{where } -a \leq x \leq a \\ & -b \leq y \leq b \end{cases} \quad (28.51)$$

$$\bar{\varphi} = \int_0^\infty \varphi e^{-vt} dt, \quad (28.52)$$

where

$$\bar{W}(v) = \int_0^\infty W(t) e^{-vt} dt. \quad (28.53)$$

Employing the Fourier method, we will find the solution in the form

$$\bar{\varphi} = X(x) Y(y) Z(z, v). \quad (28.54)$$

Then, after substituting (28.54) into (28.50) we will find that

$$\frac{X''}{X} + \frac{Y''}{Y} + \frac{Z''}{Z} = -\frac{v^2}{a_0^2}. \quad (28.55)$$

Equation (28.55) is equivalent to the system

$$\left. \begin{aligned} X'' + m^2 X &= 0, \\ Y'' + n^2 Y &= 0, \\ Z'' - \left(m^2 + n^2 + \frac{v^2}{a_0^2} \right) Z &= 0. \end{aligned} \right\} \quad (28.56)$$

Allowing for the boundary conditions

$$\left. \begin{aligned} X &= C_1 e^{imx}, \\ Y &= C_2 e^{iny}, \\ Z &= C_3 e^{-\sqrt{m^2 + n^2 + \frac{v^2}{a_0^2}} z} \end{aligned} \right\} \quad (28.57)$$

The solution of the wave equation in transforms is written in the following manner

$$\bar{\varphi} = \int_{-\infty}^{\infty} \int_{-\infty}^{\infty} C(m, n, v) e^{i(mx+ny)} e^{-z \sqrt{m^2 + n^2 + \frac{v^2}{a_0^2}}} dmdn. \quad (28.58)$$

To define the arbitrary function $C(m, n, v)$, let us employ the boundary condition (28.48), after first putting in the form of a Fourier integral

$$\left. \frac{\partial \bar{\varphi}}{\partial z} \right|_{z=0} = -\bar{W}(v) \int_{-\infty}^{\infty} \int_{-\infty}^{\infty} e^{i(mx+ny)} \bar{\omega}(m, n) dmdn, \quad (28.59)$$

where

$$\bar{\omega}(m, n) = \frac{1}{4\pi^2} \int_{-a}^a \int_{-b}^b e^{-i(m\lambda+n\mu)} \omega(\lambda, \mu) d\lambda d\mu. \quad (28.60)$$

Differentiating both parts of (28.58) with respect to z and assuming that $z = 0$, we will find that

$$\left. \frac{\partial \bar{\varphi}}{\partial z} \right|_{z=0} = - \int_{-\infty}^{\infty} \int_{-\infty}^{\infty} C(m, n, v) \sqrt{m^2 + n^2 + \frac{v^2}{a_0^2}} e^{i(mx+ny)} dmdn. \quad (28.61)$$

A comparison of (28.61) and (28.59) yields

$$C(m, n, v) = \frac{\bar{W}(v) \bar{\omega}(m, n)}{\sqrt{m^2 + n^2 + \frac{v^2}{a_0^2}}}. \quad (28.62)$$

Therefore, the solution of the initial wave equation in transforms appears as

$$\begin{aligned} \bar{\varphi} = & \int_{-\infty}^{\infty} \int_{-\infty}^{\infty} e^{i(mx+ny)} \bar{\omega}(m, n) \frac{\bar{W}(v)}{\sqrt{m^2 + n^2 + \frac{v^2}{a_0^2}}} \times \\ & \times e^{-z \sqrt{m^2 + n^2 + \frac{v^2}{a_0^2}}} dmdn. \end{aligned} \quad (28.63)$$

Using the original instead of the transform, and employing the Mellin integral, we find that

$$\varphi = \int_{-\infty}^{\infty} \int_{-\infty}^{\infty} e^{i(mx+ny)} \bar{\omega}(m, n) \times \\ \times \left[\frac{1}{2\pi i} \int_{(L)} \bar{W}(v) \frac{e^{vt-\tau} \sqrt{m^2 + n^2 + \frac{v^2}{a_0^2}}}{\sqrt{m^2 + n^2 + \frac{v^2}{a_0^2}}} dv \right] dmdn. \quad (28.64)$$

Because

$$\frac{e^{-\tau} \sqrt{m^2 + n^2 + \frac{v^2}{a_0^2}}}{\sqrt{m^2 + n^2 + \frac{v^2}{a_0^2}}} \rightarrow a_0 J_0 \left(a_0 \sqrt{m^2 + n^2} \sqrt{t^2 - \frac{z^2}{a_0^2}} \right) \times \\ \times \tau_0 \left(t - \frac{z}{a_0} \right). \quad (28.65)$$

then on the basis of the generalized Borel theorem we will find

$$\varphi = a_0 - \int_{-\infty}^{\infty} \int_{-\infty}^{\infty} e^{i(mx+ny)} \bar{\omega}(m, n) \int_{\frac{z}{a_0}}^t W(t-\tau) \times \\ \times J_0 \left(a_0 \sqrt{m^2 + n^2} \sqrt{\tau^2 - \frac{z^2}{a_0^2}} \right) d\tau dmdn. \quad (28.66)$$

Using pressure instead of the potential function, we get*

$$p_z = -\rho_0 a_0 \int_{\frac{z}{a_0}}^t W(t-\tau) \int_{-\infty}^{\infty} \int_{-\infty}^{\infty} e^{i(m\tau+ny)} \omega(m, n) \times \\ \times J_0 \left(a_0 \sqrt{m^2 + n^2} \sqrt{\tau^2 - \frac{z^2}{a_0^2}} \right) dmdnd\tau. \quad (28.67)$$

Assuming that $z = 0$ in (28.67), we derive an expression for pressure at points on the plate surface.

*A solution of the problem in this form was first derived by Zamyshlyayev and Mironov and Novoselov.

The appropriate component of second category generalized hydrodynamic force will be

$$F_z = \int_{-a}^a \int_{-b}^b p_z(x, y, z=0, t) \omega(x, y) dx dy. \quad (28.68)$$

The result of (28.67) relates only to the component of pressure forces satisfying the n-th main coordinate. By reiterating arguments from the first part of this section, which were developed for a round plate for the k-th main coordinate, we can write

$$F_{zk} = -F_{0k} \int_0^t W_k(t-\tau) \psi_k(\tau) d\tau, \quad (28.69)$$

where

$$F_{0k} = \rho_0 a_0 S x_{2k} = \rho_0 a_0 \int_{-a}^a \int_{-b}^b \omega_k^2(x, y) dx dy, \quad (28.70)$$

$$\psi_k(\tau) = 16\pi^2 \frac{1}{a_{2k} S} \int_0^\tau \int_0^\tau \bar{\omega}_k^2(m, n) J_0(a_0 \tau \sqrt{m^2 + n^2}) dm dn, \quad (28.71)$$

$$\bar{\omega}_k(m, n) = \frac{1}{4\pi^2} \int_{-a}^a \int_{-b}^b e^{i(mx + ny)} \omega(x, y) dx dy. \quad (28.72)$$

As before, where $t > t_0 = \frac{2a}{a_0} \sqrt{1 + \left(\frac{b}{a}\right)^2}$, $\psi_k(t) \equiv 0$. Consequently, for $t > t_0$

$$F_{zk} = -F_{0k} \int_0^{t_0} W_k(t-\tau) \psi_k(\tau) d\tau. \quad (28.73)$$

The expression derived for the function $\psi(t)$ permits us to rather simply define the quantity of apparent mass of a fluid for a rectangular plate attached to a rigid wall with its motion in a given form of buckling

$$\begin{aligned} M_{np} &= F_0 \int_0^{t_0} \psi(\tau) d\tau = 16\pi^2 \rho_0 a_0 \int_0^{t_0} d\tau \int_0^\tau \int_0^\tau \omega^2(m, n) \times \\ &\times J_0(a_0 \tau \sqrt{m^2 + n^2}) dm dn. \end{aligned} \quad (28.74)$$

As with round plates, calculations according to this formula are simpler than those using the customary method.

§29. The Practical Evaluation of the Parameters of Motion of an Elastic Plate Having Edges Attached to a Rigid Wall Under the Influence of an Underwater Shock-Wave

The methods of defining second category hydrodynamic forces which were developed in the preceding sections for a given main form of vibration, in conjunction with the approximate method for solving the integro-differential equation of motion, permit us to indicate a rather simple means for the dynamic calculation of a plate being deformed under the influence of an underwater shock-wave. This calculation is based on two assumptions:

1. the main forms of vibration are considered to be known a priori; as a rule, we are given a total of one form of vibration which roughly corresponds to the lower tone (reduction method).

2. the second category generalized hydrodynamic force is approximated by a linear relation; for this purpose we preliminarily calculate the apparent mass which corresponds to the assumed vibration type.

Upon fulfillment of these premises, the problem of motion of an elastic plate under the influence of an underwater shock-wave is reduced to the integration of an ordinary differential equation of the second order having constant coefficients. Let us consider a number of concrete examples.

A Round Plate Rigidly Fastened by its Edges

The type of buckling in this case may be roughly assumed as

$$w(r) = \left[1 - \left(\frac{r}{a} \right)^2 \right]^2. \quad (29.1)$$

According to (28.2) and (28.41), the values of the coefficients α_1 and α_2 are

$$\left. \begin{aligned} a_1 &= \frac{\int_S \cos^2 \varphi dS}{S} = \frac{\int_0^a \int_0^{2\pi} \left[1 - \left(\frac{r}{a}\right)^2\right]^2 r dr d\varphi}{\pi a^2} = \frac{1}{3}, \\ a_2 &= \frac{\int_S \sin^2 \varphi dS}{S} = \frac{\int_0^a \int_0^{2\pi} \left[1 - \left(\frac{r}{a}\right)^2\right]^2 r dr d\varphi}{\pi a^2} = 0.2. \end{aligned} \right\} \quad (29.2)$$

According to (28.43)

$$\bar{u}(\lambda) = \int_0^a r \left[1 - \left(\frac{r}{a}\right)^2\right]^2 J_3(\lambda r) dr = \frac{8}{a\lambda^3} J_3(a\lambda), \quad (29.3)$$

where $J_3(a\lambda)$ - a third-order Bessel function.

According to (28.42)

$$\begin{aligned} \psi(\tau) &= \frac{2\pi}{a\tau S} \int_0^a \lambda \bar{u}^2(\lambda) J_0(\lambda a_0 \tau) d\lambda = \frac{10}{a^3} \int_0^a \lambda \frac{64}{a^2 \lambda^6} J_3^2(a\lambda) J_0(\lambda a_0 \tau) d\lambda = \\ &= \frac{640}{a^5} \int_0^a \frac{J_3^2(a\lambda) J_0(\lambda a_0 \tau)}{\lambda^5} d\lambda. \end{aligned} \quad (29.4)$$

The integral (29.4) may be taken in the following manner. Let us employ the equation (cf., e.g., [1])

$$\int_0^{\frac{\pi}{2}} J_\nu(z \sin x) \sin^\nu x \cos^{2\nu} x dx = 2^{\nu-1} \sqrt{\pi} \Gamma\left(\nu + \frac{1}{2}\right) z^{-\nu} J_\nu^2\left(\frac{z}{2}\right). \quad (29.5)$$

Assuming that $\nu = 3$ and $z = 2a\lambda$ in it, let us calculate $J_3^2(a\lambda)$ and then, let us use the relationship

$$\int_0^{\frac{\pi}{2}} J_p(\alpha t) J_q(\beta t) t^{q-p} dt = \begin{cases} 0 & \text{where } \alpha < \beta \\ \frac{(a^2 - b^2)^{p-q} \beta^q}{2^{p-q} \Gamma(p+1) \Gamma(p-q+1)} & \text{where } \alpha > \beta \end{cases} \quad (29.6)$$

assuming that $p = 2$, $q = 0$; $\alpha = 2a \sin x$, $\beta = \tau a_0$, $t = \lambda$.

We will then find that

$$\int_0^{\pi} \frac{1}{\lambda^3} J_2^2(\lambda x) J_0^2(\lambda_0 \tau) dx =$$

$$= \begin{cases} 0 & 0 & \text{where } \tau > \frac{2a}{a_0} \sin x \\ \frac{1}{60\pi} \int_0^{\frac{\pi}{2}} [4a^2 \sin^2 x - (\tau a_0)^2]^2 \cos^2 x dx & \text{where } \tau < \frac{2a}{a_0} \sin x. \end{cases} \quad (29.7)$$

Substituting the values of the coefficients [$\Gamma(3 + \frac{1}{2}) = \frac{15}{8} \sqrt{\pi}$, $\Gamma(2 + 1) = 2$] and performing transformations, we get

$$\psi(\tau) = \frac{32 \cdot 16}{3 \cdot \pi} \int_{\arcsin \frac{\tau a_0}{2a}}^{\frac{\pi}{2}} \left[\sin^2 x - \left(\frac{\tau a_0}{2a} \right)^2 \right]^2 \cos^2 x dx =$$

$$= \frac{32 \cdot 16}{3 \cdot \pi} \left\{ \frac{\tau}{10} \left(\tau^2 + \frac{3}{8} \right) \sqrt{(1 - \tau^2)^3} - \frac{1}{160} \tau \sqrt{(1 - \tau^2)^5} + \right.$$

$$+ \frac{15\pi}{2560} - \frac{5}{160} \left[\frac{3}{8} \arcsin \tau + \frac{1}{2} \tau \sqrt{1 - \tau^2} + \right.$$

$$+ \frac{1}{8} \tau \sqrt{1 - \tau^2} (1 - 2\tau^2) \Big] - 2\tau^2 \left\{ \frac{1}{8} \tau \sqrt{(1 - \tau^2)^3} - \right.$$

$$- \frac{1}{48} \tau \sqrt{(1 - \tau^2)^5} + \frac{5\pi}{256} - \frac{5}{48} \left[\frac{3}{8} \arcsin \tau + \right.$$

$$+ \frac{1}{2} \tau \sqrt{1 - \tau^2} + \frac{1}{8} \tau \sqrt{1 - \tau^2} (1 - 2\tau^2) \Big] \Big\} +$$

$$+ \tau^4 \left\{ \frac{5\pi}{32} - \frac{1}{6} \tau \sqrt{(1 - \tau^2)^3} - \frac{5}{6} \left[\frac{3}{8} \arcsin \tau + \right.$$

$$+ \frac{1}{2} \tau \sqrt{1 - \tau^2} + \frac{1}{8} \tau \sqrt{1 - \tau^2} (1 - 2\tau^2) \Big] \Big\} \Big\}, \quad (29.8)$$

where

$$\tau = \frac{a_0 \tau}{2a}.$$

The function $\psi(\tau)$ may be approximated with sufficient precision by the relation

$$\psi(\tau) = (1 - \tau^2)^2 |v_0(\tau) - v_0(1)|, \quad (29.9)$$

and with a somewhat greater error by the formula

$$\psi(\tau) = e^{-2.2\tau} \cos \frac{\tau}{2} \tau. \quad (29.10)$$

The quality of approximations is shown in Fig. 122. Knowing the function $\psi(\bar{\tau})$, we can easily find the quantity of apparent mass. According to (28.45) and (28.41), we get

$$\begin{aligned} M_{app} &= F_0 \int_0^{\frac{2a}{\pi}} \psi(\tau) d\tau = \rho_0 a_0^2 S \cdot 0,34 \cdot \frac{2a}{a_0} = \\ &= \rho_0 a \cdot 0,2 \cdot 0,34 \cdot 2\pi a^2 = 0,43 \rho_0 a^3. \end{aligned} \quad (29.11)$$

A Round Plate Freely Resting On its Edges

The type of buckling may be assumed to be [25]

$$\omega(r) = 1 - \frac{6}{5} \left(\frac{r}{a} \right)^2 + \frac{1}{5} \left(\frac{r}{a} \right)^4. \quad (29.12)$$

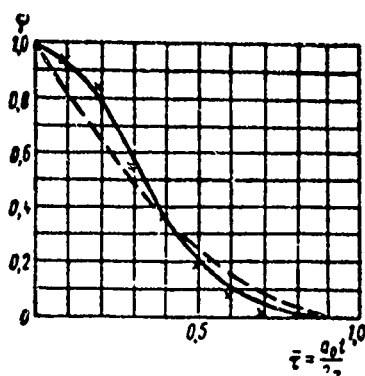


Fig. 122. The Function ψ for a Round Plate Rigidly Fastened by its Edges to a Rigid Wall.

——— precise solution;
----- approximation,

$$\begin{aligned} \psi(\tau) &= e^{-2.2\bar{\tau}} \cdot \cos(\pi/2)\bar{\tau}; \text{ x approximation of } \psi(\bar{\tau}) : \\ &= (1 - \tau^2)^6. \end{aligned}$$

This form corresponds to $\alpha_1 = 0.47$; $\alpha_2 = 0.30$.

Substituting (29.12) into (28.42) and performing calculations, we find:*

*For a freely resting plate being deformed by buckling type (29.12), the problem was solved by Mironov and Novoselov.

$$\psi(\bar{\tau}) = J_1 + 2J_2 + J_3, \quad (29.13)$$

where

$$\bar{\tau} = \frac{a_0 \tau}{2J_1},$$

$$J_1 = \begin{cases} \frac{1280 \cdot 4}{225 \cdot \pi} \int_{\arcsin \bar{\tau}}^{\frac{\pi}{2}} (\sin^2 x - \bar{\tau}^2) \cos^4 x dx & \text{where } 0 < \bar{\tau} < 1 \\ 0 & \text{where } \bar{\tau} > 1; \end{cases} \quad (29.14)$$

$$J_2 = \frac{80}{75\pi} \begin{cases} \begin{aligned} & - \arcsin(1-2\bar{\tau}) \\ & \pi \int_0^{\frac{\pi}{2}} |\cos^2 x - 4\bar{\tau}^2| \sin x \cos^5 x dx + \\ & + \int_{\arcsin(1-2\bar{\tau})}^{\frac{\pi}{2}} \left[(\cos^2 x - 4\bar{\tau}^2) \arccos \frac{4\bar{\tau}^2 - \cos^2 x}{4\bar{\tau} \sin x} + \right. \\ & \left. + 4\bar{\tau} \sin x \sqrt{1 - \left(\frac{4\bar{\tau}^2 - \cos^2 x}{4\bar{\tau} \sin x} \right)^2} \right] \sin x \cos^5 x dx \end{aligned} & \text{where } 0 < \bar{\tau} \leq \frac{1}{2}, \\ \begin{aligned} & \int_{\arcsin(2\bar{\tau}-1)}^{\frac{\pi}{2}} \left[(\cos^2 x - 4\bar{\tau}^2) \arccos \frac{4\bar{\tau}^2 - \cos^2 x}{4\bar{\tau} \sin x} + \right. \\ & \left. + 4\bar{\tau} \sin x \sqrt{1 - \left(\frac{4\bar{\tau}^2 - \cos^2 x}{4\bar{\tau} \sin x} \right)^2} \right] \sin x \cos^5 x dx \end{aligned} & \text{where } \frac{1}{2} < \bar{\tau} < 1, \\ 0 & \bar{\tau} > 1; \end{cases} \quad (29.15)$$

$$J_3 = \begin{cases} \frac{128 \cdot 8}{75 \cdot 3\pi} \int_{\arcsin \bar{\tau}}^{\frac{\pi}{2}} (\sin^2 x - \bar{\tau}^2)^2 \cos^5 x dx & \text{where } 0 < \bar{\tau} < 1, \\ 0 & \text{where } \bar{\tau} > 1. \end{cases} \quad (29.16)$$

In spite of the fact that all three integrals are written in finite form, it is simpler to employ integral representations directly in calculations.

The function $\psi(\bar{\tau})$ may be approximated by the expression

$$\psi(\bar{\tau}) = e^{-1.6\bar{\tau}} \cos \frac{\pi}{2} \bar{\tau}. \quad (29.17)$$

Error of approximation can be seen from Fig. 123.

The quantity of apparent mass, according to (28.45) and (28.41) is

$$M_{np} = 0.38 F_0 \cdot \frac{2a}{u_0} = 0.38 \gamma_0 2aS = 0.72 \gamma_0 a^3. \quad (29.18)$$

Rectangular Plates

The buckling type of rectangular plates rigidly attached by their edges is often described in dynamic problems by the relation

$$w(x, y) = \cos^2 \frac{\pi x}{2a} \cos^2 \frac{\pi y}{2b}. \quad (29.19)$$

Corresponding to this type is $\alpha_1 = \frac{1}{4}$, $\alpha_2 = \frac{9}{64}$.

The function $\bar{w}(m, n)$, according to (28.72) is

$$\bar{w}(m, n) = \frac{\pi^3}{4a^2b^2} \frac{\sin ma}{m \left(m^2 - \frac{\pi^2}{a^2} \right)} \frac{\sin nb}{n \left(n^2 - \frac{\pi^2}{b^2} \right)}. \quad (29.20)$$

Substituting this expression into (28.71) and bearing in mind that

$$\begin{aligned} J_0(a_0 \tau \sqrt{m^2 + n^2}) &= \frac{2}{\pi} \int_0^{\frac{\pi}{2}} \cos(ma_0 \tau \sin \lambda) \cos(na_0 \tau \cos \lambda) d\lambda = \\ &= \frac{2}{\pi} \int_0^{\frac{\pi}{2}} \cos ml \cos nL d\lambda, \end{aligned} \quad (29.21)$$

where

$$\left. \begin{aligned} l &= a_0 \tau \sin \lambda, \\ L &= a_0 \tau \cos \lambda, \end{aligned} \right\} \quad (29.22)$$

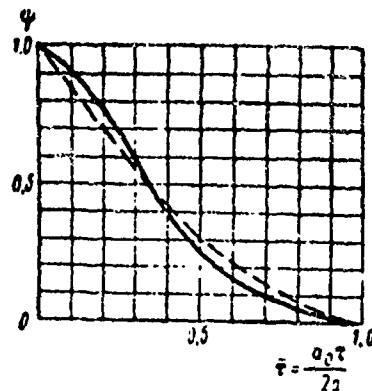


Fig. 123. Function ψ for a Round Plate Freely Resting on its Edges on a Rigid Wall.
 ——— precise solution;
 ----- approximation

$$\psi = e^{-1.6\tau} \cdot \cos \frac{\pi}{2}\tau.$$

for the function $\psi(\tau)$ we will find that

$$\begin{aligned} \psi(\tau) &= \frac{2\pi^3}{a^4 b^4 a_0 S} \int_0^{\frac{\pi}{2}} \int_0^{\frac{\pi}{2}} \int_0^{\frac{\pi}{2}} \frac{\sin^2 m a \cos m l}{m^3 \left(m^2 - \frac{\pi^2}{a^2}\right)^3} \frac{\sin^2 n a \cos n L}{n^3 \left(n^2 - \frac{\pi^2}{b^2}\right)^3} dmdndl = \\ &= \frac{128 \cdot \pi^6}{4a^4 b^4} \int_0^{\frac{\pi}{2}} I_m I_n dL, \end{aligned} \quad (29.23)$$

where

$$I_m = \int_0^{\frac{\pi}{2}} \frac{\sin^2 m a \cos m l}{m^3 \left(m^2 - \frac{\pi^2}{a^2}\right)^3} dm, \quad (29.24)$$

$$I_n = \int_0^{\frac{\pi}{2}} \frac{\sin^2 n b \cos n L}{n^3 \left(n^2 - \frac{\pi^2}{b^2}\right)^3} dn. \quad (29.25)$$

After performing the transformation

$$\sin^2 m a \cos m l = \frac{1}{2} \sin m a [\sin(a-l)m + \sin(a+l)m],$$

$$\sin^2 n b \cos n L = \frac{1}{2} \sin n b [\sin(b-L)n + \sin(b+L)n].$$

the integrals (29.24), (29.25) will be written in the form

$$I_m = -\frac{1}{2} I_{m_1} + \frac{1}{2} I_{m_2} = -\frac{1}{2} \int_0^{\infty} \frac{\sin ma \sin (l-a)m}{m^2 \left(m^2 - \frac{\pi^2}{a^2}\right)^2} dm +$$

$$+ \frac{1}{2} \int_0^{\infty} \frac{\sin ma \sin (l+a)m}{m^2 \left(m^2 - \frac{\pi^2}{a^2}\right)^2} dm, \quad (29.26)$$

$$I_n = -\frac{1}{2} I_{n_1} + \frac{1}{2} I_{n_2} = -\frac{1}{2} \int_0^{\infty} \frac{\sin nb \sin (l-b)n}{n^2 \left(n^2 - \frac{\pi^2}{b^2}\right)^2} dn +$$

$$+ \frac{1}{2} \int_0^{\infty} \frac{\sin nb \sin (l+b)n}{n^2 \left(n^2 - \frac{\pi^2}{b^2}\right)^2} dn. \quad (29.27)$$

Integration yields

$$I_m I_n = \frac{a^2 b^2}{64 \pi^2} f(\tau, l), \quad (29.28)$$

where

$$f(\tau, l) = \begin{cases} \left[\frac{3}{\pi} \sin \frac{\pi l}{a} + \left(2 - \frac{l}{a}\right) \left(2 + \cos \frac{\pi l}{a}\right) \right] \times \\ \times \left[\frac{3}{\pi} \sin \frac{\pi L}{b} + \left(2 - \frac{L}{b}\right) \left(2 + \cos \frac{\pi L}{b}\right) \right] & \text{where } 0 < l < 2a \\ & 0 < L < 2b, \\ 0 & \text{where } l > 2a \\ & L > 2b. \end{cases} \quad (29.29)$$

Let us examine the restrictions imposed by the inequalities $0 < l < 2a$ and $0 < L < 2b$ in the time interval $0 < t < \frac{2a}{a_0} \sqrt{1+k^2}$ ($k = b/a$, $b > a$). Let $0 < t < \frac{2a}{a_0}$. Then, for any λ from the interval $0 < \lambda < \frac{\pi}{2}$, both inequalities are fulfilled at the same time. The first inequality produces $0 < \lambda < \arcsin \frac{2a}{a_0 t}$. If $\frac{2b}{a_0} < t < \frac{2a}{a_0} \times \sqrt{1+k^2} = (2 \sqrt{a^2 + b^2})/a_0$, then it follows that $0 < \lambda < \arcsin$

$\frac{2a}{a_0 t}$ from the first inequality (as before), and $\arccos \frac{2b}{a_0 t} < \lambda < \frac{\pi}{2}$

from the second inequality.

Therefore, where $\frac{2b}{a_0} < t < \frac{2\sqrt{a^2 + b^2}}{a_0}$, we get

$$\arccos \frac{2b}{a_0 t} < \lambda < \arcsin \frac{2a}{a_0 t}.$$

Accordingly, and based on (29.23), (29.28) for the function $\psi(\tau)$ we will find that:

$$\psi(\tau) = \frac{2}{9\pi} \begin{cases} \int_0^{\frac{\tau}{2}} f(\tau, i) d\lambda & \text{where } 0 \leq \tau \leq \frac{2a}{a_0} \\ \int_{\arcsin \frac{2a}{a_0 t}}^{\arcsin \frac{2a}{a_0 t}} f(\tau, i) d\lambda & \text{where } \frac{2a}{a_0} \leq \tau \leq \frac{2b}{a_0} \\ \int_{\arcsin \frac{2a}{a_0 t}}^{\arccos \frac{2b}{a_0 t}} f(\tau, i) d\lambda & \text{where } \frac{2b}{a_0} \leq \tau \leq \frac{2\sqrt{a^2 + b^2}}{a_0} \\ 0 & \text{where } \tau > \frac{2\sqrt{a^2 + b^2}}{a_0} \end{cases} \quad (29.30)$$

Similar findings can be derived for a rectangular plate freely supported by its edges.* In this case,

$$w(x, y) = \cos \frac{\pi x}{2a} \cos \frac{\pi y}{2b}, \quad (29.31)$$

$$\psi(\tau) = \frac{1}{2\pi} \begin{cases} \int_0^{\frac{\tau}{2}} f(\tau, i) d\lambda & \text{where } 0 \leq \tau \leq \frac{2a}{a_0} \\ \int_{\arcsin \frac{2a}{a_0 t}}^{\arcsin \frac{2a}{a_0 t}} f(\tau, i) d\lambda & \text{where } \frac{2a}{a_0} \leq \tau \leq \frac{2b}{a_0} \\ \int_{\arcsin \frac{2a}{a_0 t}}^{\arccos \frac{2b}{a_0 t}} f(\tau, i) d\lambda & \text{where } \frac{2b}{a_0} \leq \tau \leq \frac{2\sqrt{a^2 + b^2}}{a_0} \\ 0 & \text{where } \tau > \frac{2\sqrt{a^2 + b^2}}{a_0} \end{cases}$$

$$f(\tau, l) = \left[\frac{2}{\pi} \sin \frac{\pi l}{2a} - \left(\frac{l}{a} - 1 \right) \cos \frac{\pi l}{2a} + \cos \frac{\pi l}{2a} \right] \cdot \\ \times \left[\frac{2}{\pi} \sin \frac{\pi L}{2b} - \left(\frac{L}{b} - 1 \right) \cos \frac{\pi L}{2b} + \cos \frac{\pi L}{2b} \right]. \quad (29.33)$$

With the aid of the functions $\psi(\tau)$, there are no theoretical problems in evaluating quantities of apparent mass corresponding to given types of buckling. As before, we get

$$M_{np} = F_0 \frac{2a}{a_0} \gamma, \quad (29.34)$$

where

$$F_0 = \rho_0 a_0 S \gamma_2, \quad (29.35)$$

$$\alpha_2 = \begin{cases} \frac{1}{4} & \text{for a freely supported plate moving in type} \\ & (29.31); \\ \frac{9}{64} & \text{for a rigidly fastened plate moving in type} \\ & (29.19); \end{cases}$$

The values of the coefficients γ as a function of the ratio of the sides $k = b/a$ are given in Fig. 124. It shows the findings calculated by N. V. Mattes* according to the approximate method.

Our attention is drawn to the common nature of relationships of $\gamma = \gamma(k)$ both for plates and for a rectangular piston (upper curve), which may be attributed to the similar physical picture of the effect's development in both cases. This is also illustrated by the nature of variation of the function $\psi(\tau)$ shown in Fig. 125 for plates having a ratio of sides $k = b/a = 3$.

Thus, the rough method of approximation which we earlier described earlier, using the linear relation $\psi(\tau)$ may be expanded to elastic plates with sufficient grounds. The best convergence of data

*N. V. Mattes, The Effect of General Buckling on Local Strength and Vibration of River Vessels, Izd. MRF SSSR, 1950.

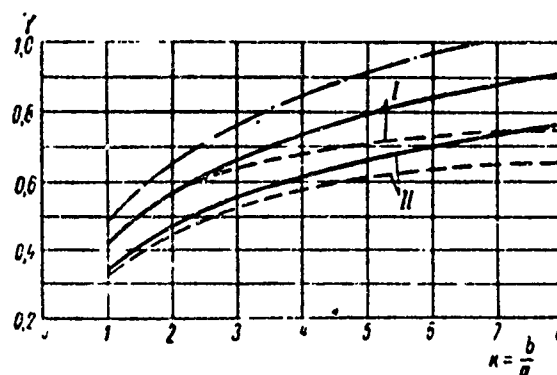


Fig. 124. Coefficient of Apparent Mass for Motion of Rectangular Plates Fastened Along Edges to Rigid Infinite Wall.

I - freely resting plate; II - rigidly fastened plate.
 ——— precise solution;
 ----- calculated with Mattes' data;
 -.-.-.- curve for rectangular rigid-walled piston.

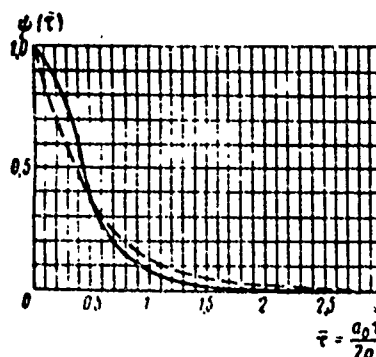


Fig. 125. The Function $\psi(\bar{\tau})$ for a Rectangular Plate Resting Freely on Its Edges Against a Rigid Wall.

———— precise solution;
 ----- approximation $= e^{-6\xi} \cos \frac{\pi}{2}\xi$,

where $\xi = (a_0 \tau) / 2 \sqrt{a^2 + b^2}$.

of three approximate and precise solutions will be achieved if we approximate the initial portion of the function $\psi(\tau)$ in the interval $0 < \tau < \frac{2a}{a_0}$. In this connection, second category generalized force, as before, can be expressed by the relation

$$F_z(t) = \begin{cases} -F_0 W + \frac{F_0}{T} W & \text{where } t < \frac{2a}{a_0}, \\ -M_{nr} W & \text{where } t > \frac{2a}{a_0}. \end{cases} \quad (29.36)$$

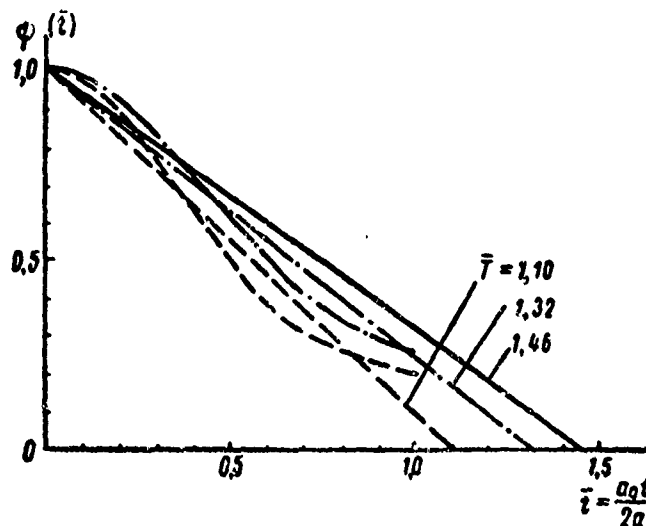


Fig. 126. The Function $\psi(\tau)$ for the Motion of a Piston and Plates Fastened Along Edges to Rigid Infinite Wall

($k = b/a = 8$)

————— for piston;
 for freely resting plate;
 ----- for rigidly-attached plate.

The quantity $\frac{2a}{a_0 T}$ is the tangent to the slope of the direct line approximating the initial portion of the curve of $\psi(\tau)$; it can be defined from the equality of corresponding areas (Fig. 126) and the area of its initial portion. Therefore, for practical evaluations we can recommend the relation

$$\frac{T_{nop}}{T_{na}} \approx \frac{\tau_{nop}}{\tau_{na}}. \quad (29.37)$$

Hence it follows that equations of motion of elastic plates under the influence of an underwater shock-wave are easy to write if we know the solution of the problem of pistons and we have calculated the apparent mass of the plate for a given type of vibration.

Equation (29.36) may be rewritten as

$$F_z(t) = \begin{cases} -F_0 \psi + \frac{F_0}{T_{na}} W & \text{where } t < \frac{2a}{a_0} \\ -M_{np} W & \text{where } t > \frac{2a}{a_0} \end{cases} \quad (29.38)$$

where

$$F_0 = \gamma_0 a_0 S a_2, \quad (29.39)$$

$$a_2 = \frac{1}{S} \iint_S \omega^2 dS, \quad (29.40)$$

$$T_{nn} \cong T_{nop} \frac{\gamma_{nn}}{\gamma_{nop}}, \quad (29.41)$$

$$M_{np} = F_0 \frac{2a}{a_0} \gamma_{nn}, \quad (29.42)$$

Specifically, for round plates

$$S = \pi a^2;$$

$$a_2 = \begin{cases} 0,3 & \text{for freely-resting} \\ 0,2 & \text{for rigidly-fastened plates,} \end{cases}$$

$$T_{nn} = \begin{cases} 0,8 \frac{2a}{a_0} & \text{for freely-resting} \\ 0,76 \frac{2a}{a_0} & \text{for rigidly-fastened plates,} \end{cases}$$

$$M_{np} = \begin{cases} 0,72 \gamma_0 a^3 = 0,38 F_0 \frac{2a}{a_0} & \text{for freely-fastened} \\ 0,13 \gamma_0 a^3 = 0,34 F_0 \frac{2a}{a_0} & \text{for rigidly-fastened plates.} \end{cases}$$

For rectangular plates

$$S = 4ab,$$

$$a_2 = \begin{cases} \frac{1}{4} & \text{for freely-resting} \\ \frac{9}{64} & \text{for rigidly-fastened plates;} \end{cases}$$

$$T_{nn} = \begin{cases} \frac{1}{1,15} \frac{2a}{a_0} \frac{3\pi}{2 \left(3 + 2 \frac{a}{b} \right)} & \text{for freely-resting} \\ \frac{1}{1,40} \frac{2a}{a_0} \frac{3\pi}{2 \left(3 + 2 \frac{a}{b} \right)} & \text{for rigidly-rastened plates,} \end{cases}$$

$$M_{np} = 8 \gamma_0 a^2 b \gamma_{nn},$$

where γ_{np} - the coefficient of apparent mass, whose magnitude is given in Fig. 124.

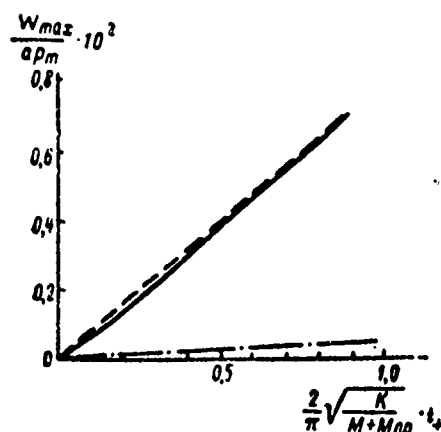


Fig. 127. Relationship of W_{\max} as a Function of t_+ for a Round Plate:

$$(\delta/a = 0.025; \frac{4a}{a_0\pi} \sqrt{(K)/(M + M_{np})} = 0.16)$$

The equations of motion of elastic plates under the influence of an underwater shock-wave, allowing for what we have stated, may be written in the following manner:

where $t < \frac{2a}{a_0}$

$$MW + F_0\dot{W} + \left(K - \frac{F_0}{T_{nn}}\right)W = F_1, \quad (29.43)$$

where $t > \frac{2a}{a_0}$

$$(M + M_{np})\ddot{W} + KW = F_1. \quad (29.44)$$

The solution of these equations, while ensuring the precision required for practical application, causes no difficulties.

Let us note in conclusion that if the time of acquisition of maximum buckling by the plate t_{\max} is considerably greater than the time of diffraction $t = (2a)/(a_0)$, we can calculate accurately using

the concept of fluid noncompressibility* (Fig. 127).

If the effect-time of the positive pressure phase t_+ is considerably less than t_{\max} , the evaluation of the maximum buckling can be made according to the pulse method

$$W_{\max} = a_1 \frac{2JS}{(M + M_{op})K} \quad (29.45)$$

For very rigid plates, where $K \gg \frac{F_0}{T_{\text{пл}}}$, the time of acquisition of maximum buckling may be less than the diffraction time $t = \frac{2a}{a_0}$. In this connection, evaluation of maximum buckling may be closely approximated on the basis of the hypothesis of plane reflection.

§30. Interaction of an Underwater Shock-Wave with a Rectangular Plate Forming Part of a Cover

Let us consider the incidence of a plane wave along the normal onto an infinite cover, resting on immobile equidistant supports which are mutually perpendicular. The cover divides water and air. Due to the infinite dimensions of the obstacle, there are basic difficulties involved in evaluating second category generalized force. As a result of symmetry, we only have to study the motion of a fluid in the area limited by planes which are perpendicular to the plate surface and passing through its rigidly-supported edges. The problem was first studied in this formulation by Aleksandrin, and later by Zamyshlyayev, Mironov, and Novoselov using other methods. In the mathematical sense, this reduces to a definition of the potential function ϕ which satisfies the wave equation

$$\frac{\partial^2 \phi}{\partial x^2} + \frac{\partial^2 \phi}{\partial y^2} + \frac{\partial^2 \phi}{\partial z^2} = \frac{1}{a_0^2} \frac{\partial^2 \phi}{\partial t^2} \quad (30.1)$$

with the following boundary and initial conditions

$$\left. \frac{\partial \phi}{\partial z} \right|_{z=0} = -W(t) \cos(\pi y) \quad \text{where} \quad -a \leq x \leq a \quad \text{and} \quad -b \leq y \leq b, \quad (30.2)$$

*This condition can be satisfied by many measuring devices.

$$\frac{\partial \varphi}{\partial x} \Big|_{x=\pm a} = \frac{\partial \varphi}{\partial y} \Big|_{y=\pm b} = 0, \quad (30.3)$$

$$\varphi \Big|_{z \rightarrow \infty} \rightarrow 0, \quad (30.4)$$

$$\varphi \Big|_{t=0} = \frac{\partial \varphi}{\partial t} \Big|_{t=0} = 0. \quad (30.5)$$

The system of coordinates is selected as in §28.

Applying the Laplace integral transform, we find that

$$\frac{\partial^2 \bar{\varphi}}{\partial x^2} + \frac{\partial^2 \bar{\varphi}}{\partial y^2} + \frac{\partial^2 \bar{\varphi}}{\partial z^2} = \frac{v^2}{a_0^2} \bar{\varphi}, \quad (30.6)$$

$$\frac{\partial \bar{\varphi}}{\partial z} \Big|_{z=0} = -\bar{W}(v) \omega(x, y) \text{ where } -a \leq x \leq a \text{ and } -b \leq y \leq b, \quad (30.7)$$

$$\frac{\partial \bar{\varphi}}{\partial x} \Big|_{x=\pm a} = \frac{\partial \bar{\varphi}}{\partial y} \Big|_{y=\pm b} = 0, \quad (30.8)$$

$$\bar{\varphi} \Big|_{z \rightarrow \infty} \rightarrow 0, \quad (30.9)$$

where

$$\bar{\varphi} = \int_0^\infty \varphi e^{-vt} dt, \quad (30.10)$$

$$\bar{W} = \int_0^\infty W e^{-vt} dt. \quad (30.11)$$

We will seek the solution of equation (30.6) in a form which satisfies the boundary condition (30.8):

$$\bar{\varphi} = \sum_{i,j=0}^\infty \cos \frac{j\pi x}{a} \cos \frac{i\pi y}{b} Z_{ij}(z, v). \quad (30.12)$$

After substituting (30.12) into (30.6) for the function Z_{ij} , we find that

$$\frac{\partial^2 Z_{ij}}{\partial z^2} - \left[\left(\frac{j\pi}{a} \right)^2 + \left(\frac{i\pi}{b} \right)^2 + \frac{v^2}{a_0^2} \right] Z_{ij} = 0, \quad (30.13)$$

whence, considering (30.9),

$$Z_{ij} = C_{ij} e^{-z \sqrt{\left(\frac{i\pi}{a}\right)^2 + \left(\frac{j\pi}{b}\right)^2 + \frac{v^2}{a_0^2}}} \quad (30.14)$$

The solution of a wave equation in transforms is written in the following manner

$$\bar{\varphi} = \sum_{i,j=0}^{\infty} C_{ij} \cos \frac{i\pi x}{a} \cos \frac{j\pi y}{b} e^{-z \sqrt{\left(\frac{i\pi}{a}\right)^2 + \left(\frac{j\pi}{b}\right)^2 + \frac{v^2}{a_0^2}}} \quad (30.15)$$

The coefficients C_{ij} may be defined from the boundary condition (30.7) which, for this purpose, should be written as a Fourier series

$$\left. \frac{\partial \bar{\varphi}}{\partial z} \right|_{z=0} = -\bar{W}(v) \sum_{i,j=0}^{\infty} A_{ij} \cos \frac{i\pi x}{a} \cos \frac{j\pi y}{b}, \quad (30.16)$$

where A_{ij} - coefficients of the Fourier function $\omega(x, y)$.

Differentiating (30.15) with respect to z and assuming the $z = 0$, we will find that

$$\begin{aligned} \left. \frac{\partial \bar{\varphi}}{\partial z} \right|_{z=0} &= - \sum_{i,j=0}^{\infty} C_{ij} \cos \frac{i\pi x}{a} \cos \frac{j\pi y}{b} \times \\ &\times \sqrt{\left(\frac{i\pi}{a}\right)^2 + \left(\frac{j\pi}{b}\right)^2 + \frac{v^2}{a_0^2}}. \end{aligned} \quad (30.17)$$

Comparison of (30.16) and (30.17) yields

$$C_{ij} = A_{ij} \frac{\bar{W}(v)}{\sqrt{\left(\frac{i\pi}{a}\right)^2 + \left(\frac{j\pi}{b}\right)^2 + \frac{v^2}{a_0^2}}}. \quad (30.18)$$

Therefore

$$\begin{aligned} \bar{\varphi} &= \sum_{i,j=0}^{\infty} A_{ij} \cos \frac{i\pi x}{a} \cos \frac{j\pi y}{b} \times \\ &\times \frac{\bar{W}(v) e^{-z \sqrt{\left(\frac{i\pi}{a}\right)^2 + \left(\frac{j\pi}{b}\right)^2 + \frac{v^2}{a_0^2}}}}{\sqrt{\left(\frac{i\pi}{a}\right)^2 + \left(\frac{j\pi}{b}\right)^2 + \frac{v^2}{a_0^2}}}. \end{aligned} \quad (30.19)$$

Because

$$\frac{-z \sqrt{\left(\frac{i\pi}{a}\right)^2 + \left(\frac{j\pi}{b}\right)^2 + \frac{z^2}{a_0^2}}}{\sqrt{\left(\frac{i\pi}{a}\right)^2 + \left(\frac{j\pi}{b}\right)^2 + \frac{z^2}{a_0^2}}} \rightarrow a_0 J_0 \left[\sqrt{\left(\frac{i\pi}{a}\right)^2 + \left(\frac{j\pi}{b}\right)^2} \times \right. \\ \left. \times a_0 \sqrt{\tau^2 - \frac{z^2}{a_0^2}} \right] J_0 \left(t - \frac{z}{a_0} \right). \quad (30.20)$$

then based on the generalized Borel theorem

$$\psi = a_0 \sum_{i,j=0}^{\infty} A_{ij} \cos \frac{i\pi x}{a} \cos \frac{j\pi y}{b} \int_{\frac{z}{a_0}}^t \ddot{W}(t-\tau) \times \\ \times J_0 \left[\sqrt{\left(\frac{i\pi}{a}\right)^2 + \left(\frac{j\pi}{b}\right)^2} a_0 \sqrt{\tau^2 - \frac{z^2}{a_0^2}} \right] d\tau. \quad (30.21)$$

Using pressure instead of the potential function, we find

$$p_z(x, y, z, t) = -\rho_0 a_0 \sum_{i,j=0}^{\infty} A_{ij} \cos \frac{i\pi x}{a} \cos \frac{j\pi y}{b} \times \\ \times \int_{\frac{z}{a_0}}^t \ddot{W}(t-\tau) J_0 \left(\sqrt{\left(\frac{i\pi}{a}\right)^2 + \left(\frac{j\pi}{b}\right)^2} a_0 \sqrt{\tau^2 - \frac{z^2}{a_0^2}} \right) d\tau. \quad (30.22)$$

Assuming that $z = 0$, we will derive an expression for pressure at points situated on the surface of the plate.

If we are limited, as is often done in practical problems, to the study of motion of a plate in the primary tone of vibration, the magnitude of second category generalized force can be found from the relationship*

$$F_z(t) = \int_{-a}^a \int_{-b}^b p_z(x, y, t) w(x, y) dx dy, \quad (30.23)$$

or after substituting (30.22)

*Consideration of other harmonics does not cause any theoretical problems. It is not examined at this point because it introduces no new parameters into either the mathematical or physical essence of the problem.

$$F_2(t) = -\rho_0 a_0 \int_0^t W(t-\tau) \int_{-a}^a \int_{-b}^b \omega(x, y) \sum_{i,j=0}^{\infty} A_{ij} \cos \frac{i\pi x}{a} \cos \frac{j\pi y}{b} \times \\ \times J_0 \left[\pi \tau a_0 \sqrt{\left(\frac{i}{a}\right)^2 + \left(\frac{j}{b}\right)^2} \right] dx dy d\tau. \quad (30.24)$$

Because where $\tau = 0$, $J_0(0) = 1$, and

$$\int_{-a}^a \int_{-b}^b \omega(x, y) \sum_{i,j=0}^{\infty} A_{ij} \cos \frac{i\pi x}{a} \cos \frac{j\pi y}{b} dx dy = \\ = \int_{-a}^a \int_{-b}^b \omega^2(x, y) dx dy = a_2 S, \quad (30.25)$$

the expression for second category generalized force can be written as

$$F_2(t) = -F_0 \int_0^t W(t-\tau) \psi(\tau) d\tau, \quad (30.26)$$

(where

$$F_0 = \rho_0 a_0^2 S, \quad (30.27)$$

$$\psi(\tau) = \frac{1}{a_2 S} \int_{-a}^a \int_{-b}^b \omega(x, y) \sum_{i,j=0}^{\infty} A_{ij} \cos \frac{i\pi x}{a} \cos \frac{j\pi y}{b} \times \\ \times J_0 \left[\pi \tau a_0 \sqrt{\left(\frac{i}{a}\right)^2 + \left(\frac{j}{b}\right)^2} \right] dx dy. \quad (30.28)$$

As our example, let us consider the motion of a plate in a type of vibration often employed for practical evaluations,

$$\omega = \frac{1}{4} \left(1 - \cos \frac{\pi x}{a} \right) \left(1 + \cos \frac{\pi y}{b} \right). \quad (30.29)$$

The Fourier coefficients A_{ij} for this type of buckling are

$$A_{00} = A_{01} = A_{10} = A_{11} = \frac{1}{4},$$

$$A_{ij} = 0$$

where $i > 1$ and $j > 1$.

According to (30.22) and (30.28), for the magnitudes of pressure and the function $\psi(\tau)$ we find that

$$\begin{aligned} p_2(x, y, t) = & -\frac{1}{4} \rho_0 a_0 \int_0^t \dot{W}(t-\tau) \left[1 + \cos \frac{\pi x}{a} J_0\left(\frac{\pi}{a} a_0 \tau\right) + \right. \\ & + \cos \frac{\pi y}{b} J_0\left(\frac{\pi}{b} a_0 \tau\right) + \cos \frac{\pi x}{a} \cos \frac{\pi y}{b} \times \\ & \left. \times J_0\left(\frac{\pi}{a} a_0 \tau \sqrt{1 + \frac{a^2}{b^2}}\right) \right] d\tau, \end{aligned} \quad (30.30)$$

$$\begin{aligned} \psi(\tau) = & \frac{4}{9} \left[1 + \frac{1}{2} J_0\left(\frac{\pi a_0 \tau}{a}\right) + \frac{1}{2} J_0\left(\frac{\pi a_0 \tau}{b}\right) + \right. \\ & \left. + \frac{1}{4} J_0\left(\frac{\pi a_0 \tau}{a} \sqrt{1 + \frac{a^2}{b^2}}\right) \right]. \end{aligned} \quad (30.31)$$

Where $b \rightarrow \infty$, for an infinitely-long plate we get

$$\psi(\tau) \Big|_{b \rightarrow \infty} \rightarrow \frac{2}{3} \left[1 + \frac{1}{2} J_0\left(\frac{\pi a_0 \tau}{a}\right) \right]. \quad (30.32)$$

As follows from (30.31) and (30.32), in this case for any τ the function $\psi(\tau)$ is not zero and where $\tau \rightarrow \infty$ it does not approach zero, but to some fixed limit. Consequently, the quantity of apparent mass has no finite value. This illustrates that within the framework of the noncompressibility hypothesis, no motion occurs.

The derived result differs in quality from previous results and can be attributed to the changed physical conditions of the problem. Indeed, symmetry of motion is equivalent to the absence of fluid flowing across the planing passing along the edges of a plate. Consequently, we cannot avoid an extreme deformation of the fluid flow.

This case is closest in nature to the motion of an infinite plate under the influence of a plane wave. Second category hydrodynamic force which satisfies the derived value of the function $\psi(\tau)$ may be written as

$$\begin{aligned}
F_2(t) = & -F_0 \int_0^t \dot{W}(t-\tau) \dot{\psi}(\tau) d\tau = -F_0 \frac{1}{9} \dot{W}(t) - \\
& -\frac{2}{9} F_0 \int_0^t \ddot{W}(t-\tau) \left[J_0\left(\frac{\pi a_0 \tau}{a}\right) + J_0\left(\frac{\pi a_0 \tau}{b}\right) + \right. \\
& \left. + \frac{1}{2} J_0\left(\frac{\pi a_0 \tau}{a} \sqrt{1 + \frac{a^2}{b^2}}\right) \right] d\tau.
\end{aligned}$$

(30.33)

The first term in (30.33) is a function of velocity during the entire period of motion, reflecting the effect of fluid resistance to extension and compression. The quantity of the second term can be defined by the kernel of a subintegral expression.

For small $\tau \left(0 \leq \tau < \frac{a}{\pi a_0 \sqrt{1 + \frac{a^2}{b^2}}} \right)$

$$J_0\left(\frac{\pi a_0 \tau}{a}\right) \approx J_0\left(\frac{\pi a_0 \tau}{b}\right) \approx J_0\left(\frac{\pi a_0 \tau}{a} \sqrt{1 + \frac{a^2}{b^2}}\right) \sim 1.$$

and consequently, second category generalized force is

$$F_2 = -F_0 \dot{W}. \quad (30.34)$$

For rather large τ the zero-order Bessel functions decrease in amplitude and fluctuate around zero. This fact permits us to derive another limiting idea of the second category generalized hydrodynamic force.

Let us employ linearization of the kernel of the subintegral function suggested by Yu. I. Kadashevich. Integrating (30.33) by parts, we find that:

$$F_2 = -\frac{1}{9} F_0 \dot{W} - \frac{2}{9} F_0 \dot{W}'(0) f(t) - \frac{2}{9} F_0 \int_0^t \ddot{W}(t-\tau) f(\tau) d\tau, \quad (30.35)$$

where

$$\begin{aligned}
f(t) &= \int_0^t \left[J_0\left(\frac{\pi a_0 \tau}{a}\right) + J_0\left(\frac{\pi a_0 \tau}{b}\right) + \frac{1}{2} J_0\left(\frac{\pi a_0 \tau}{a} \sqrt{1 + \frac{a^2}{b^2}}\right) \right] d\tau = \\
&= \frac{a}{a_0 \pi} \left\{ 1 + \frac{b}{a} + \frac{1}{2 \sqrt{1 + \frac{a^2}{b^2}}} - \left[\int_{\frac{\pi a_0 t}{a}}^{\frac{\pi a_0 t}{a}} \frac{J_1(\tau)}{\tau} d\tau - J_1\left(\frac{\pi a_0 t}{a}\right) \right] - \right. \\
&\quad \left. - \frac{b}{a} \left[\int_{\frac{\pi a_0 t}{b}}^{\frac{\pi a_0 t}{b}} \frac{J_1(\tau)}{\tau} d\tau - J_1\left(\frac{\pi a_0 t}{b}\right) \right] - \frac{1}{2 \sqrt{1 + \frac{a^2}{b^2}}} \times \right. \\
&\quad \left. \times \left[\int_{\frac{\pi a_0 t}{a} \sqrt{1 + \frac{a^2}{b^2}}}^{\frac{\pi a_0 t}{a} \sqrt{1 + \frac{a^2}{b^2}}} \frac{J_1(\tau)}{\tau} d\tau - J_1\left(\frac{\pi a_0 t}{a} \sqrt{1 + \frac{a^2}{b^2}}\right) \right] \right\}.
\end{aligned}
\tag{30.36}$$

Where $a/b > 0.3$ and $t \rightarrow \infty$

$$f(t) \rightarrow \frac{a}{a_0 \pi} \left(1 + \frac{b}{a} + \frac{1}{2 \sqrt{1 + \frac{a^2}{b^2}}} \right).
\tag{30.37}$$

The behavior of the function $f(t)$ for $a/b = 0.5$ is given in Fig. 128. Starting from time $t \geq \frac{a+b}{4a_0}$, the curve of $f(\tau)$ may be approximately replaced by a constant quantity. Consequently, according to (30.35) and (30.37), for second category hydrodynamic force where $t > \frac{a+b}{4a_0}$ and $\frac{a}{b} > 0.3$, we can write

$$\begin{aligned}
F_z(t) &\approx -\frac{4}{9} F_0 W - \\
&- \frac{1}{9} \left(1 + \frac{b}{a} + \frac{1}{2 \sqrt{1 + \frac{a^2}{b^2}}} \right) F_0 \frac{2a}{a_0} W.
\end{aligned}
\tag{30.38}$$

Where $\frac{a}{b} < 0.3$, the limiting value of the function $f(t)$ will be different. Thus, where $\frac{a}{b} \rightarrow 0$ & $t \rightarrow \infty$, we can easily derive

$$f(t) \Big|_{t \rightarrow \infty} \rightarrow 1 + \frac{3a}{2a_0 \pi}.
\tag{30.39}$$

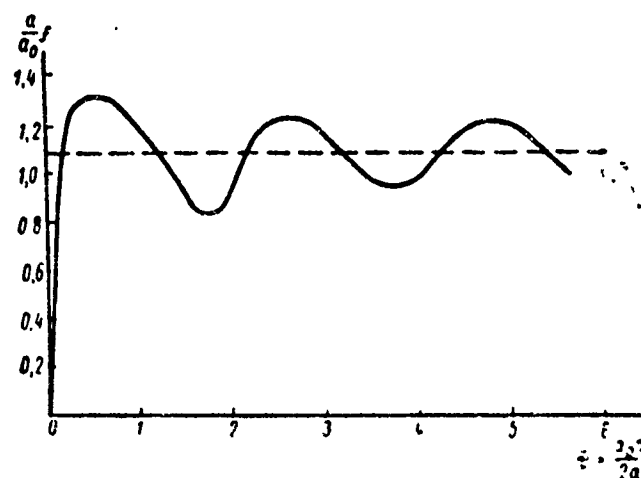


Fig. 128. The Function f for a Rectangular Plate Rigidly Fastened Along its Edges ($a/b = 0.5$).

$$\text{----- } \lim_{t \rightarrow \infty} \frac{a}{a_0} f = \frac{1}{\pi} \left(1 + \frac{1}{\frac{b}{a} + \sqrt{1 + \frac{a^2}{b^2}}} \right)$$

Second category hydrodynamic force conforms to this limiting value of $f(t)$ *

$$F_2(t) = -\frac{2}{3} F_0 \ddot{W} - \frac{1}{6\pi} F_0 \frac{2a}{a_0} W'. \quad (30.40)$$

Let us employ the method stated in §23. Limiting ourselves to three expansion terms of the function $W(t - \tau)$ into a Taylor series where $a/b > 0.3$, we can easily derive the change $F_2(t)$ for the entire time interval

$$F_2(t) = \begin{cases} -F_0 \ddot{W} + \frac{5}{9} \frac{F_0}{t^*} W & \text{where } t < t^* \\ -\frac{4}{9} F_0 \ddot{W} - \frac{1}{9\pi} \left(1 + \frac{b}{a} + \frac{1}{2\sqrt{1 + \frac{a^2}{b^2}}} \right) \times \\ \times F_0 \frac{1}{a_0} W & \text{where } t > t^*, \end{cases} \quad (30.41)$$

$$\text{where } t^* \simeq \frac{a+b}{4a_0}. \quad (30.42)$$

Similar relationships for $a/b \rightarrow 0$ (they may be used for approximation where $a/b < 0.3$) appear as

*Equation (30.40) is approximately valid where $t > \frac{2a}{\pi a_0}$

$$F_2(t) = \begin{cases} -F_0 \dot{W} + \frac{1}{3} \frac{F_0}{t^*} W & \text{where } t < t^* \\ -\frac{2}{3} F_0 \dot{W} - \frac{1}{6\pi} F_0 \frac{2a}{a_0} W & \text{where } t > t^*, \end{cases} \quad (30.43)$$

$$\text{where } t^* = \frac{1}{\pi} \frac{2a}{a_0}. \quad (30.44)$$

As we can see, the second equations in (30.41) and (30.43) coincide with the limiting expressions (30.38) and (30.40) for $F_2(t)$.

Therefore, the considered problem amounts to the integration of equations of the same type as were examined earlier. However, there is one principal difference in the results. This amounts to a considerable reduction in the initial interval t^* and the presence in the second period of motion of a considerable velocity effect W . This once again indicates the impossibility of interpreting this problem from the viewpoint of fluid noncompressibility.

Other types of buckling may be considered by analogy. Thus, if

$$w(x, y) = \cos \frac{\pi x}{2a} \cos \frac{\pi y}{2b}, \quad (30.45)$$

then from (30.28) we can easily derive¹:

$$\begin{aligned} \psi(\tau) = \frac{64}{\pi^3} & \left[1 + \frac{1}{8} \sum_{i=1}^{\infty} \frac{J_0\left(\frac{i\pi a_0 \tau}{a}\right)}{\left(\frac{1}{4} - i^2\right)^3} + \frac{1}{8} \sum_{j=1}^{\infty} \frac{J_0\left(\frac{j\pi a_0 \tau}{b}\right)}{\left(\frac{1}{4} - j^2\right)^3} + \right. \\ & \left. + \frac{1}{64} \sum_{i,j=1}^{\infty} \frac{J_0\left(\pi a_0 \tau \sqrt{\left(\frac{i}{a}\right)^2 + \left(\frac{j}{b}\right)^2}\right)}{\left(\frac{1}{4} - i^2\right)^3 \left(\frac{1}{4} - j^2\right)^3} \right]. \end{aligned} \quad (30.46)$$

or limited to only the first series terms,

¹ The function $\psi(\tau)$ for this type of buckling was calculated by Mironov and Novoselov.

$$\psi(\tau) = \frac{64}{\pi^4} \left[1 + \frac{2}{9} J_0 \left(\frac{\pi a_0 \tau}{a} \right) + \frac{2}{9} \left(\frac{\pi a_0 \tau}{b} \right) + \frac{4}{81} J_0 \left(\frac{\pi a_0 \tau}{a} \sqrt{1 + \frac{a^2}{b^2}} \right) \right]. \quad (30.47)$$

The structure of (30.47) is exactly the same as in (30.31). Consequently, omitting the argument and operations which are similar to previous arguments and operations, let us show only the final results.

Second category hydrodynamic force, in deformation of type (30.45) corresponds roughly to the primary tone of vibration of freely-resting plates, and can be defined by the expressions:

for $a/b > 0.3$

$$F_z(t) = \begin{cases} -F_0 \ddot{W} + 0.34 \frac{F_0}{t^*} \dot{W} & \text{where } t < t^* \\ -0.66 F_0 \ddot{W} - 0.023 \left(1 + \frac{b}{a} + \frac{2}{9 \sqrt{1 + \frac{a^2}{b^2}}} \right) \times \\ \times F_0 \frac{2a}{a_0} \dot{W} & \text{where } t > t^*, \end{cases} \quad (30.48)$$

$$(30.49)$$

$$\text{where } t^* \approx \frac{a+b}{3.5a_0};$$

for $a/b < 0.3$

$$F_z(t) = \begin{cases} -F_0 \ddot{W} + 0.20 \frac{F_0}{t^*} \dot{W} & \text{where } t < t^* \\ -0.80 F_0 \ddot{W} - 0.028 F_0 \frac{2a}{a_0} \dot{W} & \text{where } t > t^*, \end{cases} \quad (30.50)$$

$$(30.51)$$

$$\text{where } t^* = \frac{2a}{\pi a_0}.$$

Relations (30.48)-(30.50) indicate an even greater proximity than in the preceding case of the physical picture to the hypothesis of plane reflection. The differential equations of motion of a plate under the influence of an underwater shock-wave will be :

where $t < t^*$

$$M\ddot{W} + F_0\dot{W} + \left(K - \alpha \frac{F_0}{t^*}\right)W = F_1, \quad (30.52)$$

where $t > t^*$

$$(M + \bar{M})\ddot{W} + \beta F_0\dot{W} + KW = F_1, \quad (30.53)$$

where

$$\left. \begin{aligned} M &= \alpha_2 S m, \\ \bar{M} &= \gamma F_0 \frac{2a}{a_0}, \\ F_0 &= \alpha_2 S \rho_0 a_0, \\ F_1 &= \alpha_1 S \cdot 2p(t). \end{aligned} \right\} \quad (30.54)$$

The values of the coefficients and parameters entering into formulas (30.52)-(30.54) are given in Table 6.

To illustrate the material which we have given, Fig. 129 and Fig. 130 show a comparison of the findings of the approximate and precise solutions for an infinitely-long plate which is part of a cover, and is being deformed under the influence of an exponential-shape shock wave.* There is a completely satisfactory convergence of data in both velocities and in plate travel. The hypothesis of plane reflection (dashed and hatched curve) describes the quality of the effect; but for quantitative evaluations, it is only suitable for the initial period of motion.** Therefore, the theoretical approximate schemes may be recommended for practical applications.

To complete the statement of the problem, let us touch upon another problem which is close in formulation to the one we have already considered. Let us examine the hydrodynamic forces arising as a result of motion in various directions of contiguous plate sections making up a cover.

The first solution of this problem for a cover having unilateral supports was derived by Dimaggio [30], and slightly later by Aleksandr; for a cover having bilateral supports, this problem was solved

*The calculation of plate motion and its analysis was accomplished by D. A. Aleksandrin. **This is often enough, because cavitation occurs later and these notions are no longer valid. See §32-34 for calculations.

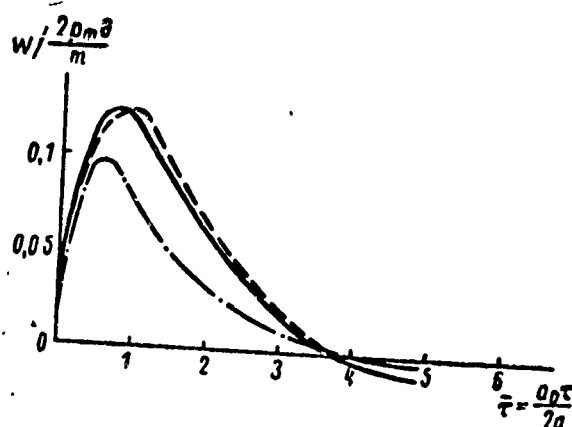


Fig. 129. Rate of Motion of a Plate on an Infinite Cover ($2a/\delta = 40$, $b/a = \infty$) Under the Influence on Said Plate of Exponential-Shape Shock-wave.

— precise solution;
 - - - approximate solution;
 - · - · - calculated according to hypothesis of plane reflection.

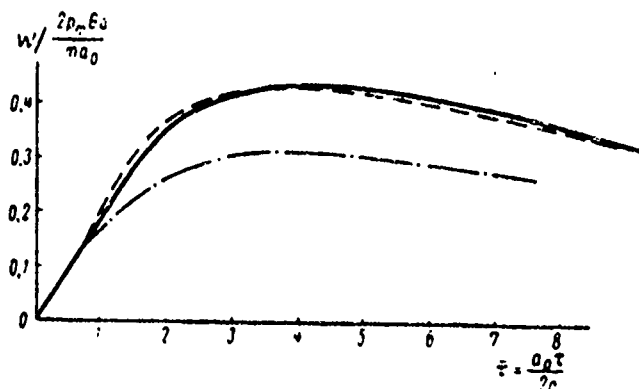


Fig. 130. Travel of a Central Point on a Plate of an Infinite Cover ($2a/\delta = 40$, $b/a = \infty$) Under the Influence on Said Plate of an Exponential Shock-wave.

— precise solution;
 - · - · - approximate solution;
 - - - calculated according to hypothesis of plane reflection.

Table 6

VALUES OF COEFFIC- IENTS			PLATE		VALUES OF COEFF- ICIENTS			PLATE	
			freely supp- orted	rig- idly made				freely sup- ported	rigid- ly made
a_1			$\frac{4}{\pi^2}$	$\frac{1}{4}$	$\bar{\gamma}$	$n > 0,3$		$\frac{2}{9} \sqrt{\frac{a^2}{1+b^2}}$	$\frac{1}{2} \sqrt{\frac{a^2}{1+b^2}}$
a_2			$\frac{1}{4}$	$\frac{9}{64}$				$\frac{b}{a} + \frac{1}{9}$	$\frac{b}{a} + \frac{1}{2}$
α	$\frac{a}{b} > 0,3$		0,34	$\frac{5}{9}$				$0,023 \left(1 + \frac{b}{a} \right)$	$\frac{1}{5}$
	$\frac{a}{b} < 0,3$		0,20	$\frac{1}{3}$	β	$n < 0,3$		0,028	$\frac{1}{6n}$
β	$\frac{a}{b} > 0,3$		0,66	$\frac{4}{9}$		$n > 0,3$		$\frac{a+b}{3,5a_0}$	$\frac{a+b}{4a_0}$
	$\frac{a}{b} < 0,3$		0,80	$\frac{2}{3}$		$n < 0,3$		$\frac{2a}{\pi a_0}$	$\frac{2a}{\pi a_0}$

by A. K. Pertsev and Yu. A. Kadashevich, as well as by Aleksandrin. Let us state the solution at this point, generalizing the arguments cited. We can do this easily if we consider the boundary conditions of integrating the initial wave equation. In this case, they may be written in the following manner

$$1) \quad \frac{\partial \varphi}{\partial z} \Big|_{z=0} = -W(t) |\varphi(x, y)| \quad (30.55)$$

$$mn > 0 \quad \text{and} \quad \begin{cases} 2n < \frac{x}{2a} < 2n+1 \\ 2m < \frac{y}{2b} < 2m+1, \end{cases}$$

$$mn > 0 \quad \text{and} \quad \begin{cases} 2n-1 < \frac{x}{2a} < 2n \\ 2m-1 < \frac{y}{2b} < 2m, \end{cases} \quad (30.56)$$

$$mn < 0 \quad \text{and} \quad \begin{cases} 2n < \frac{x}{2a} < 2n + 1 \\ 2m - 1 < \frac{y}{2b} < 2m, \end{cases}$$

$$mn < 0 \quad \text{and} \quad \begin{cases} 2n - 1 < \frac{x}{2a} < 2n \\ 2m < \frac{y}{2b} < 2m + 1; \end{cases} \quad (30.57)$$

$$2) \quad \left. \frac{\partial \varphi}{\partial z} \right|_{z=0} = W(t) |\omega(x, y)|$$

$$mn > 0 \quad \text{and} \quad \begin{cases} 2n < \frac{x}{2a} < 2n + 1 \\ 2m - 1 < \frac{y}{2b} < 2m, \end{cases}$$

$$mn > 0 \quad \text{and} \quad \begin{cases} 2n - 1 < \frac{x}{2a} < 2n \\ 2m < \frac{y}{2b} < 2m + 1, \end{cases} \quad (30.58)$$

$$mn < 0 \quad \text{and} \quad \begin{cases} 2n < \frac{x}{2a} < 2n + 1 \\ 2m < \frac{y}{2b} < 2m + 1, \end{cases}$$

$$mn < 0 \quad \text{and} \quad \begin{cases} 2n - 1 < \frac{x}{2a} < 2n \\ 2m - 1 < \frac{y}{2b} < 2m, \end{cases}$$

where $|\omega(x, y)|$ is the form of buckling of the section of plate between the supports.

The origin of the coordinates is assumed to be at the point of intersection of the supports.

Starting from those boundary conditions, we can specify the areas of the cover can be considered, in the hydrodynamic sense,

as independent of one another. At the same time, the basic condition must be the absence of fluid overflowing the boundary of these areas.

The boundaries in the assumed coordinate axes will be

$$\left. \begin{aligned} x &= (2n+1)a, \\ y &= (2m+1)b. \end{aligned} \right\} \quad (30.59)$$

The boundary conditions, therefore, can be written in a form which is close to (30.8), (30.7):

$$\left. \frac{\partial \varphi}{\partial z} \right|_{z=0} = -i\omega(x, y), \quad (30.60)$$

$$\left. \frac{\partial \varphi}{\partial x} \right|_{x=(2n+1)a} = \left. \frac{\partial \varphi}{\partial y} \right|_{y=(2m+1)b} = 0, \quad (30.61)$$

$$\varphi|_{z \rightarrow \infty} = 0. \quad (30.62)$$

After performing the Laplace integral transform, we can write a transformational solution which satisfies condition (30.61)

$$\bar{\varphi} = \sum_{i,j=0}^{\infty} \sin \frac{i\pi x}{2a} \sin \frac{j\pi y}{2b} Z_{ij}(z, v). \quad (30.63)$$

The function $Z_{ij}(z, v)$ can be defined by the equation

$$\frac{\partial^2 Z_{ij}}{\partial z^2} - \left[\left(\frac{i\pi}{2a} \right)^2 + \left(\frac{j\pi}{2b} \right)^2 + \frac{v^2}{a_0^2} \right] Z_{ij} = 0,$$

whence, considering (30.62),

$$Z_{ij} = C_{ij} e^{-z \sqrt{\left(\frac{i\pi}{2a} \right)^2 + \left(\frac{j\pi}{2b} \right)^2 + \frac{v^2}{a_0^2}}} \quad (30.64)$$

Therefore, for the potential $\bar{\varphi}$ we get

$$\bar{\varphi} = \sum_{i,j=0}^{\infty} C_{ij} \sin \frac{i\pi x}{2a} \sin \frac{j\pi y}{2b} e^{-z \sqrt{\left(\frac{i\pi}{2a} \right)^2 + \left(\frac{j\pi}{2b} \right)^2 + \frac{v^2}{a_0^2}}} \quad (30.65)$$

The arbitrary constants C_{ij} can be defined from boundary condition (30.60) by comparing the appropriate coefficients in expanding the function $\omega(x, y)$ into a Fourier series

$$C_{ij} = B_{ij} \frac{\bar{\psi}(y)}{\sqrt{\left(\frac{i\pi}{2a}\right)^2 + \left(\frac{j\pi}{2b}\right)^2 + \frac{z^2}{a_0^2}}}, \quad (30.66)$$

where B_{ij} - the Fourier coefficients of the function $\omega(x, y)$.

Using the original in place of the transform, we find that

$$\begin{aligned} \varphi = a_0 \sum_{i,j=0}^{\infty} B_{ij} \sin \frac{i\pi x}{2a} \sin \frac{j\pi y}{2b} \times \\ \times \int_{\frac{z}{a_0}}^t \bar{\psi}(t-\tau) J_0 \left[\sqrt{\left(\frac{i\pi}{2a}\right)^2 + \left(\frac{j\pi}{2b}\right)^2} a_0 \sqrt{\tau^2 - \frac{z^2}{a_0^2}} \right] d\tau. \end{aligned} \quad (30.67)$$

The magnitude of pressure at an arbitrary point in the fluid is

$$\begin{aligned} p_z = -\rho_0 a_0 \sum_{i,j=0}^{\infty} B_{ij} \sin \frac{i\pi x}{2a} \sin \frac{j\pi y}{2b} \times \\ \times \int_{\frac{z}{a_0}}^t \bar{\psi}(t-\tau) J_0 \left[\sqrt{\left(\frac{i\pi}{2a}\right)^2 + \left(\frac{j\pi}{2b}\right)^2} a_0 \sqrt{\tau^2 - \frac{z^2}{a_0^2}} \right] d\tau. \end{aligned} \quad (30.68)$$

Assuming that $z = 0$, we can derive pressure on the plate surface. We can accomplish the change to second category hydrodynamic force with the aid of (30.23): after substituting (30.68) into this relation, we find that

$$F_z = -F_0 \int_0^t \bar{\psi}(t-\tau) \psi(\tau) d\tau, \quad (30.69)$$

where

$$\begin{aligned} \psi(\tau) = \frac{1}{a_0 S} \int_0^{2a} \int_0^{2b} \omega(x, y) \sum_{i,j=1}^{\infty} B_{ij} \sin \frac{i\pi x}{2a} \times \\ \times \sin \frac{j\pi y}{2b} J_0 \left[\pi a_0 \tau \sqrt{\left(\frac{i}{2a}\right)^2 + \left(\frac{j}{2b}\right)^2} \right] dx dy. \end{aligned} \quad (30.70)$$

As an illustration, let us consider the motion of a plate in a form of buckling

$$w = \sin \frac{\pi x}{2a} \sin \frac{\pi y}{2b}.$$

For this form, only one of the Fourier coefficients is equal to zero - $B_{11} = 1$. Consequently, the expressions for p_2 and $\psi(t)$ acquire a particularly simple form:

$$p_2(x, y, t)|_{z=0} = -\rho_0 \gamma_0 \sin \frac{\pi x}{2a} \sin \frac{\pi y}{2b} \times \\ \times \int_0^t \ddot{w}(t-\tau) J_0\left(\frac{\pi a_0 \tau}{2a} \sqrt{1 + \frac{a^2}{b^2}}\right) d\tau, \quad (30.71)$$

$$\psi(\tau) = J_0\left(\frac{\pi a_0 \tau}{2a} \sqrt{1 + \frac{a^2}{b^2}}\right). \quad (30.72)$$

As we can see, the nature of variation in the function $\psi(\tau)$ differs in quality from that considered in the preceding case, and is similar to the motion of plates of finite dimensions. Here, the function $\psi(\tau)$ changes from one to zero. This permits us to calculate the quantity of apparent mass for such motion

$$M_{np} = F_0 \int_0^{\infty} \psi(\tau) d\tau = F_0 \int_0^{\infty} J_0\left(\frac{\pi a_0 \tau}{2a} \sqrt{1 + \frac{a^2}{b^2}}\right) d\tau = \\ = \frac{2a}{a_0 \pi \sqrt{1 + \frac{a^2}{b^2}}} F_0, \quad (30.73)$$

or

$$M_{np} = \gamma F_0 \frac{2a}{a_0} = \frac{1}{4} \gamma S_0 2a, \quad (30.74)$$

$$\gamma = \frac{1}{\pi \sqrt{1 + \frac{a^2}{b^2}}}. \quad (30.75)$$

For approximate evaluations of second category hydrodynamic force, the function $\psi(\tau)$ at the initial interval may be approximated by a

linear relation. Using the previous scheme, we get

$$\psi(\tau) = \left(1 - \frac{\tau}{t_*}\right) [\varphi_0(\tau) - \varphi_0(\tau - t_*)], \quad (30.76)$$

where

$$t_* = \frac{2M_{np}}{F_0} = 2 \frac{2a}{a_0} = \frac{2}{\pi \sqrt{1 + \frac{a^2}{b^2}}} \frac{2a}{a_0}. \quad (30.77)$$

According to (30.69) and (30.76)

$$F_z(t) = \begin{cases} -F_0 \dot{\psi} + \frac{F_0}{t_*} \psi & \text{where } t \leq t_* \\ -F_0 \dot{\psi} + \frac{F_0}{t_*} \psi - \frac{F_0}{t_*} \psi (t - t_*) & \text{where } t > t_* \end{cases} \quad (30.78)$$

or (where acceleration of plate motion in the interval $[t, t - t_*]$ undergoes little change)

$$F_z(t) = \begin{cases} -F_0 \dot{\psi} + \frac{F_0}{t_*} \psi & \text{where } t < t_* \\ -M_{np} \ddot{\psi} & \text{where } t > t_* \end{cases} \quad (30.79)$$

The derived expressions differ from similar expressions for plates fastened along their edges to a rigid wall by only the values of apparent mass (in this case, for plates in a rigid wall where $a/b = 1$, they are roughly 1.5 times less, while where $b/a = 8$, they are 2.3 times less). Consequently, the duration of the initial phase of unstable plate motion noticeably diminishes; in the course of this diminution fluid compressibility is of the greatest importance.

§31. The Interaction of an Underwater Shock-Wave with an Elastic Isolated Plate of Finite Dimensions

In the problems considered in this chapter, difficulties lay in defining second category hydrodynamic forces. The evaluation of first category hydrodynamic forces arising on an infinite obstacle

was reduced to integration with respect to the surface of the product of the type of buckling $w(x, y)$ multiplied by pressure on the direct wave $p(t)$.

The quantity $F_1(t)$ was defined by the relation

$$F_1(t) = 2p(t)S\gamma_1, \quad (31.1)$$

where

$$\gamma_1 = \frac{1}{S} \iint_S w(x, y) dS. \quad (31.2)$$

This simple method for calculating first category hydrodynamic force cannot be used in studying the interaction of a shock-wave with a plate of finite dimensions.

Let us illustrate the basic aspects of this problem using the incidence of a wave along the normal to the surface of an isolated rectangular plate, rigidly supported on lateral vertical walls. Let us assume that the plate divides water and air. As we mentioned in §15, the evaluation of diffraction and radiation on the end-faces of bodies boundary by rigid vertical walls can be closely approximated with the integral of radiation. The use of the integral of radiation is equivalent to the assumption of a rigid wall beyond the plate, whose plane coincides with the plate surface.

In this formulation, however, we established in §28 the relationships characterizing generalized second category hydrodynamic force. Accordingly, here we only have to consider first category force. This can be done in two ways: we can either employ the results of §14, which were derived for motion of a plate at a velocity which changes according to the unit discontinuity function, effecting the subsequent change to an arbitrarily-shaped wave using the Duhamel integral; or we can consider the corresponding boundary problem of the wave equation, employing the data in §28. Let us use the second method, because it produces simpler final relationships.

For the incidence of a shock-wave of arbitrary profile

$$p(t) = p_m f(t) a_0(t) \quad (31.3)$$

the boundary conditions will be satisfied if we assume that an additional field of velocities of the same magnitude arises on the plate surface as on the direct wave, but having the opposite sign, i.e.,

$$\left. \frac{\partial \varphi}{\partial z} \right|_{z=0} = \begin{cases} \frac{p_m}{\rho_0 a_0} f(t) & \text{where } -a \leq x \leq a \\ & -b \leq y \leq b \\ 0 & \text{where } -a > x > a \\ & -b > y > b. \end{cases} \quad (31.4)$$

If we assume

$$W(t - \tau) = \frac{p_m}{\rho_0 a_0} f(t - \tau) a_0(t - \tau), \quad (31.5)$$

$$\omega(x, y) = 1, \quad (31.6)$$

then the given boundary conditions coincide identically with (28.48). Consequently, we can immediately employ the result of (28.67).

For the diffraction component of pressure at an arbitrary point on a plate, we find that

$$\begin{aligned} p_2(x, y, t) = & p_m \int_{-\infty}^t \int_{-\infty}^{\infty} e^{i(m\lambda + ny)} \bar{\omega}(m, n) J_0(a_0 t \sqrt{m^2 + n^2}) dmdn + \\ & + p_m \int_0^t f'(t - \tau) \int_{-\infty}^{\infty} \int_{-\infty}^{\infty} e^{i(m\lambda + ny)} \bar{\omega}(m, n) \times \\ & \times J_0(a_0 \tau \sqrt{m^2 + n^2}) dmdnd\tau, \end{aligned} \quad (31.7)$$

where

$$\bar{\omega}(m, n) = \frac{1}{4\pi^2} \int_{-a}^a \int_{-b}^b e^{-i(m\lambda + ny)} d\lambda dy = \frac{1}{\pi^2} \frac{1}{mn} \sin ma \sin nb. \quad (31.8)$$

If velocity changed according to the unit discontinuity function law, then based on (31.7) we would get

$$p_2(x, y, t) = \frac{4}{\pi^2} \int_0^{\tilde{x}} \int_0^{\tilde{y}} J_0(a_0 t \sqrt{m^2 + n^2}) \frac{\sin ma}{m} \frac{\sin nb}{n} \times \\ \times \cos mx \cos ny dm dn. \quad (31.9)$$

To define the diffraction component of first category hydrodynamic force, the magnitude of pressure must be integrated with respect to the plate surface, considering the form of its buckling.

On the basis of (31.9), we will find that

$$F_2 = \frac{4}{\pi^2} \int_0^{\tilde{x}} \int_0^{\tilde{y}} J_0(a_0 t \sqrt{m^2 + n^2}) \frac{\sin ma}{m} \frac{\sin nb}{n} \times \\ \times \int_{-a}^a \int_{-b}^b \omega(x, y) \cos mx \cos ny dx dy dm dn; \quad (31.10)$$

specifically, for buckling

$$\omega(x, y) = \cos^2 \frac{\pi x}{2a} \cos^2 \frac{\pi y}{2b}, \quad (31.11)$$

which roughly corresponds to the basic tone of vibration of a rigidly made plate,

$$F_2 = \frac{16}{\pi^2} \int_0^{\tilde{x}} \int_0^{\tilde{y}} J_0(a_0 t \sqrt{m^2 + n^2}) \frac{\sin ma}{m} \frac{\sin nb}{n} \int_0^a \int_0^b \cos mx \cos ny \times \\ \times \cos^2 \frac{\pi x}{2a} \cos^2 \frac{\pi y}{2b} dx dy dm dn. \quad (31.12)$$

Let us integrate with respect to x and y

$$\int_0^a \cos mx \cos^2 \frac{\pi x}{2a} dx = \frac{\pi^2}{a^2} \frac{1}{2} \frac{\sin ma}{m \left(\frac{\pi^2}{a^2} - m^2 \right)}, \quad (31.13)$$

$$\int_0^b \cos ny \cos^2 \frac{\pi y}{2b} dy = \frac{\pi^2}{b^2} \frac{1}{2} \frac{\sin nb}{n \left(\frac{\pi^2}{b^2} - n^2 \right)}. \quad (31.14)$$

The zero-order Bessel function will be written as a fixed integral

$$\begin{aligned} J_0(a_0 t \sqrt{m^2 + n^2}) &= \frac{2}{\pi} \int_0^{\pi/2} \cos(a_0 m t \sin \lambda) \cos(a_0 n t \cos \lambda) d\lambda \\ &= \frac{2}{\pi} \int_0^{\pi/2} \cos ml \cos nL d\lambda, \end{aligned} \quad (31.15)$$

where

$$\begin{aligned} l &= a_0 t \sin \lambda, \\ L &= a_0 t \cos \lambda. \end{aligned}$$

Therefore, (31.12) is written as

$$F_{\lambda}^* = \frac{8\pi}{a^2 b^2} \int_0^{\pi/2} \int_0^{\infty} \int_0^{\infty} \frac{\cos ml \sin^2 ma}{m^2 \left(\frac{\pi^2}{a^2} - m^2 \right)} \frac{\cos nL \sin^2 nb}{n^2 \left(\frac{\pi^2}{b^2} - n^2 \right)} dmdnd\lambda. \quad (31.16)$$

Performing a transformation of the type

$$\sin^2 ma \cos ml = \frac{1}{2} \sin ma [-\sin(l-a)m + \sin(l+a)m] \quad (31.17)$$

we can write (31.16) in the following manner

$$F_{\lambda}^* = \frac{8\pi}{a^2 b^2} \int_0^{\pi/2} I_m I_n d\lambda, \quad (31.18)$$

where

$$\begin{aligned} I_m &= -\frac{1}{2} I_{m,1} + \frac{1}{2} I_{m,2} = -\frac{1}{2} \int_0^{\infty} \frac{\sin ma \sin(l-a)m}{m^2 \left(\frac{\pi^2}{a^2} - m^2 \right)} dm + \\ &\quad + \frac{1}{2} \int_0^{\infty} \frac{\sin ma \sin(l+a)m}{m^2 \left(\frac{\pi^2}{a^2} - m^2 \right)} dm. \end{aligned} \quad (31.19)$$

$$\begin{aligned} I_n &= -\frac{1}{2} I_{n,1} + \frac{1}{2} I_{n,2} = -\frac{1}{2} \int_0^{\infty} \frac{\sin nb \sin(L-b)n}{n^2 \left(\frac{\pi^2}{b^2} - n^2 \right)} dn + \\ &\quad + \frac{1}{2} \int_0^{\infty} \frac{\sin nb \sin(L+b)n}{n^2 \left(\frac{\pi^2}{b^2} - n^2 \right)} dn. \end{aligned} \quad (31.20)$$

Let us use the identity [1]

$$\int_0^{\pi} \frac{\sin px \sin rx}{x^2 (q^2 - x^2)} dx = \begin{cases} -\frac{\pi}{2q^3} \cos pq \sin qr + \frac{\pi}{2q^2} r & \text{where } p > r \\ -\frac{\pi}{2q^3} \sin pq \cos qr + \frac{\pi}{2q^2} p & \text{where } p < r. \end{cases} \quad (31.21)$$

Assuming that $p = a$, $r = l - a$, $q = \pi/a$, we get

$$I_{m_1} = \begin{cases} -\frac{a^3}{2\pi^3} \sin \frac{\pi l}{a} + \frac{a^2}{2\pi} (l - a) & \text{where } 2a > l \\ \frac{a^3}{2\pi} & \text{where } 2a < l, \end{cases} \quad (31.22)$$

$$I_{m_2} = \begin{cases} -\frac{a^3}{2\pi^3} \sin \frac{\pi l}{a} + \frac{a^2}{2\pi} (l + a) & \text{where } 0 > l \\ \frac{a^3}{2\pi} & \text{where } 0 < l, \end{cases} \quad (31.23)$$

consequently,

$$I_m = \begin{cases} \frac{a^3}{4\pi} \left(\frac{1}{\pi} \sin \frac{\pi l}{a} - \frac{l}{a} + 2 \right) & \text{where } 0 < l < 2a \\ 0 & \text{where } l > 2a. \end{cases} \quad (31.24)$$

By complete analogy

$$J_n = \begin{cases} \frac{b^3}{4\pi} \left(\frac{1}{\pi} \sin \frac{\pi L}{b} - \frac{L}{b} + 2 \right) & \text{where } 0 < L < 2b \\ 0 & \text{where } L > 2b. \end{cases} \quad (31.25)$$

Let us designate that

$$I_m J_n = \frac{a^3 b^3}{16\pi^3} \vartheta(l, l); \quad (31.26)$$

then

$$\vartheta(l, l) = \begin{cases} \left(\frac{1}{\pi} \sin \frac{\pi l}{a} - \frac{l}{a} + 2 \right) \times \\ \times \left(\frac{1}{\pi} \sin \frac{\pi L}{b} - \frac{L}{b} + 2 \right) & \text{where } 0 < l < 2a \\ 0 & \text{where } l > 2a \end{cases} \quad (31.27)$$

After analyzing the limitations imposed by the inequalities $0 < l < 2a$ and $0 < L < 2b$ (the analysis is completely analogous to that given in §29), we will find that*

$$F_x = a_1 S \psi_x(t) = ab \psi_x(t), \quad (31.28)$$

$$\psi_x(t) = \frac{1}{2\pi} \begin{cases} \int_0^{\pi/2} \vartheta(t, \lambda) d\lambda & \text{where } 0 < t < \frac{2a}{a_0} \\ \int_0^{\arcsin \frac{2a}{a_0 t}} \vartheta(t, \lambda) d\lambda & \text{where } \frac{2a}{a_0} < t < \frac{2b}{a_0} \\ \int_{\arccos \frac{2b}{a_0 t}}^{\arcsin \frac{2a}{a_0 t}} \vartheta(t, \lambda) d\lambda & \text{where } \frac{2b}{a_0} < t < \frac{2a}{a_0} \sqrt{1 + \frac{b^2}{a^2}} \\ 0 & \text{where } t > \frac{2a}{a_0} \sqrt{1 + \frac{b^2}{a^2}} \end{cases} \quad (31.29)$$

The same method can be used to derive a solution for the form of buckling

$$w(x, y) = \cos \frac{\pi x}{2a} \cos \frac{\pi y}{2b}, \quad (31.30)$$

which roughly corresponds to the basic tone of vibration of a freely resting plate.

The function $\phi_n(t)$ can be defined by an expression in finite form (for this type of buckling $\alpha_1 = 4/\pi^2$):

$$\begin{aligned} \psi_x(t) = \frac{1}{4} & \left[1 + J_0 \left(\pi \frac{a_0 t}{2a} \right) + \right. \\ & \left. + J_0 \left(\pi \frac{a_0 t}{2b} \right) + J_0 \left(\frac{\pi a_0 t}{2a} \sqrt{1 + \frac{a^2}{b^2}} \right) \right]. \end{aligned} \quad (31.31)$$

*The primary findings of this problem were derived by I. Novoselov.

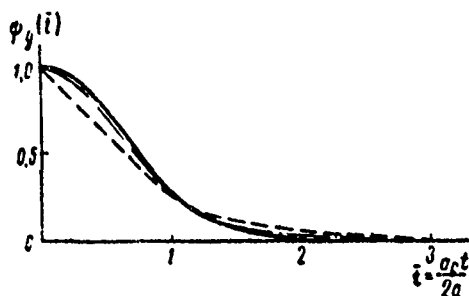


Fig. 131. The Function $\psi_D(\bar{t})$ for the Diffraction Component of Generalized Force Arising at End-Face Piston and Plates ($a/b = 0.3$) Under Influence of Unit Shock-Wave.

- for a rectangular piston;
- .-.-.- for a freely-resting plate;
- for a rigidly made plate.

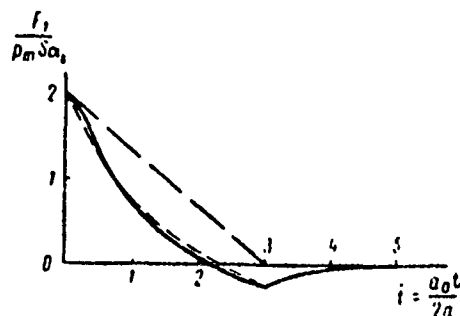


Fig. 132. First Component of Generalized Force During Interaction of Triangular Shock Wave with Rigidly-made End-Face Plate

($t_+ = 3$; $a/b = 0.3$)

- calculated, allowing for type of buckling;
- calculated without allowance for type of buckling;
- .-.-.-. calculated for a plate(piston) in a rigid infinite wall.

We can see from Fig. 131, where the function $\psi_{\Delta}(t)$ for a freely resting, a rigid-made elastic plate and a rectangular piston in a rigid wall are compared, how similar the three curves are. A similar finding also occurs at different wall ratios. Therefore, we may conclude that the form of buckling has little effect on the diffraction component of first category generalized hydrodynamic force.

The total quantity of this force is

$$F_1 = \alpha_1 S \{1 + \psi_{\Delta}(t)\}. \quad (31.32)$$

The values of $F_1(t)$ during the incidence of a triangular shock wave onto a rigidly-made plate having a ratio of sides $a/b = 0.3$ is shown in Fig. 132. Also plotted there is the curve of $F_1(t)$ for a piston. Comparison of Figs. 131 and 132 shows that calculation of the type of buckling of a plate in evaluating first category hydrodynamic force amounts to introducing the coefficient α_1 into the appropriate expression as a multiplier.

We can easily expand the solution to a wave of arbitrary profile $p_m f(t)$. Employing the Duhamel integral, according to (31.28), we get*

$$\frac{F_{\Delta}(t)}{\alpha_1 S \rho_m} = \dot{\psi}_{\Delta}(t) + \int_0^t f(t-\tau) \dot{\psi}_{\Delta}(\tau) d\tau, \quad (31.33)$$

or in another form of transcription

$$\frac{F_{\Delta}(t)}{\alpha_1 S \rho_m} = f(t) + \int_0^t f(t-\tau) \dot{\psi}_{\Delta}(\tau) d\tau. \quad (31.34)$$

The first term in (31.34) describes the reflected wave; the second describes the purely-diffraction pressure component.

Because the function $\psi_{\Delta}(t)$ can be adopted without considering the form of plate buckling, it would be most convenient to employ the result obtained in §14 for a rectangular piston. However, we established in §23 that the function $\psi_{\Delta}(t)$ can be roughly approximated

*In (31.33) and (31.34), we bear in mind that where $t = 0$, $f(0) = 1$ and $\psi_{\Delta}(0) = 1$.

by the linear approximation

$$\psi_A(t) \simeq \begin{cases} 1 - \frac{t}{T} & \text{where } 0 < t < \frac{2a}{a_0} \\ 0 & \text{where } t > \frac{2a}{a_0}, \end{cases} \quad (31.35)$$

where

$$T = \frac{2a}{a_0} \frac{3\pi}{2 \left(3 + 2 \frac{a}{b} \right)}. \quad (31.36)$$

Therefore,

$$\frac{F_A}{a_1 S \rho_m} = f(t) - \frac{1}{T} \int_0^t f(t - \tau) d\tau \quad (31.37)$$

and consequently, where $t < 2a/a_0$

$$F_A(t) = a_1 S \rho_m \left[2f(t) - \frac{1}{T} \int_0^t f(\tau) d\tau \right]. \quad (31.38)$$

To define $F_A(t)$ where $t > 2a/a_0$, let us expand function $f(t - \tau)$ in the neighborhood t into a Taylor series

$$f(t - \tau) = f(t) - \tau f'(t) + \frac{\tau^2}{2} f''(t) - \dots \quad (31.39)$$

Retaining the two first terms of series (31.39) and bearing in mind that $\psi_A(t) = 0$ where $t > t_0 = (2a/a_0) \sqrt{1 + b^2/a^2}$, substitution of (31.39) into (31.34) yields:

$$\begin{aligned} \frac{F_A(t)}{a_1 S \rho_m} &= f(t) + f'(t) \int_0^t \psi_A(\tau) d\tau - f'(t) \int_0^t \tau \psi_A(\tau) d\tau = \\ &= f(t) + f'(t) [\psi_A(t_0) - \psi_A(0)] - f'(t) \int_0^{t_0} \tau \psi_A(\tau) d\tau. \end{aligned}$$

Integrating by parts and bearing in mind that $\psi_A(t_0) = 0$, $\psi_A(0) = 1$, where $t > t_0$ we finally find that

$$\frac{F_A(t)}{a_1 S \rho_m} = f(t) \int_0^{t_0} \psi_A(\tau) d\tau = f(t) \gamma t_1, \quad (31.40)$$

where γ - the coefficient of apparent mass of a fluid during progressive motion of an end-face piston.

A completely analogous result where $t > t_1$ takes place for the entire first category generalized hydrodynamic force.

Therefore,

$$F_1(t) = z_1 S p_m \begin{cases} \left[2f(t) - \frac{1}{T} \int_0^t f(\tau) d\tau \right] & \text{where } t < t_1 \\ f(t) + f(t) \gamma t_1 & \text{where } t > t_1 \end{cases} \quad (31.41)$$

$$\left. \begin{aligned} T &= t_1 \frac{3\pi}{2 \left(3 + 2 \frac{a}{b} \right)} \\ t_1 &= \frac{2a}{a_0} \end{aligned} \right\} \quad (31.36a)$$

Formulas (31.41) permit us to simply derive the result for a shock-wave of arbitrary profile. So, for an exponential wave

$$f(t) = e^{-\frac{t}{\theta}}$$

$$F_1(t) = \begin{cases} z_1 S p_m \left[2e^{-\frac{t}{\theta}} - \frac{\theta}{T} \left(1 - e^{-\frac{t}{\theta}} \right) \right] & \text{where } t < t_1 \\ z_1 S p_m e^{-\frac{t}{\theta}} \left(1 - \frac{t_1}{\theta} \right) & \text{where } t > t_1 \end{cases} \quad (31.42)$$

and for a triangular wave

$$f(t) = \left(1 - \frac{t}{t_+} \right) [z_0(t) - z_0(t - t_+)]$$

where $t_+ > t_1$

$$F_1(t) = \begin{cases} z_1 S p_m \left[2 - \left(\frac{2}{t_+} + \frac{1}{T} \right) t + \frac{t^2}{2Tt_+} \right] & \text{where } 0 < t < t_1 \\ z_1 S p_m \left(1 - \frac{t}{t_+} - \frac{t_1}{t_+} \right) & \text{where } t_1 < t < t_+ \\ 0 & \text{where } t > t_+ \end{cases} \quad (31.43)$$

where $t_+ < t_1$

$$F_1(t) = \begin{cases} \alpha_1 S p_m \left[2 - \left(\frac{2}{t_+} + \frac{1}{T} \right) t + \frac{t^2}{2Tt_+} \right] & \text{where } 0 < t < t_+ \\ -\alpha_1 S p_m \frac{t_+}{2T} & \text{where } t_+ < t < t_1 \\ 0 & \text{where } t > t_1 \end{cases} \quad (31.44)$$

In spite of the fact that in the expansion $f(t - \tau)$ into a Taylor series a total of two terms are retained, relations (31.42)-(31.44) rather well describe the process. Considerable error can only take place in (31.44) where $t > t_1$. However, as a rule, during this period of time cavitation arises near the place and the developed scheme generally ceases being valid.

Employing results for first and second category hydrodynamic forces, the equations of motion of an isolated elastic plate under the influence of an underwater shock wave of arbitrary profile $p(t) = p_m f(t)$ can be written in the form:

where $t < t_1$

$$M\ddot{W} + F_p \dot{W} + \left(K - \frac{F_u}{T_{nn}} \right) W = \alpha_1 S p_m \left[2f(t) - \frac{1}{T_{nop}} \int_0^t f(\tau) d\tau \right], \quad (31.45)$$

where $t > t_1$

$$(M + F_{01} \gamma_{nn}) \ddot{W} + KW = \alpha_1 S p_m [f(t) + \dot{f}(t) \gamma_{nop} t_1]. \quad (31.46)$$

The quantities T_{nn} and γ_{nn} have been taken from §29 for a plate in a rigid wall; the values T_{nop} and γ_{nop} - according to formulas in §23 for a piston.

Some further specification of the values of T_{nn} and γ_{nn} is possible. The essence of these values lies in a stricter accounting of diffraction effects as was accomplished in §12. Omitting the arguments and operations, we will cite only the final results derived by B. V. Zamyshlyayev and I. G. Novoselov. Fig. 133 shows the curves of

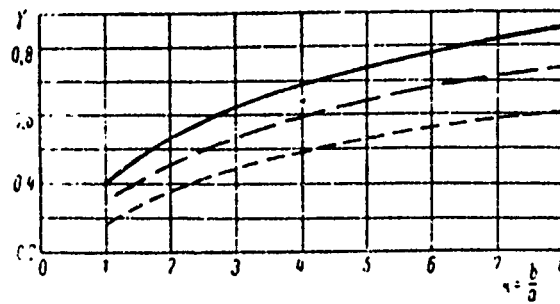


Fig. 133. Coefficient of Apparent Mass for the Motion of end-face Pistons and Plates.

————— for the piston;
 - - - - - for a freely resting plate;
 - · - · - for a rigidly made plate.

the coefficients of apparent mass for end-face elastic plates and a rectangular piston. These data should be employed for integrating (31.45) and (31.46).

The values of $T_{\text{пл}}$ and $T_{\text{ноп}}$ can be defined according to the formula

$$T_{\text{пл}} = \begin{cases} \frac{1}{1.15} \frac{1}{0.77 - 0.46 \frac{a}{b}} \frac{2a}{a_0} & \text{for a freely resting plate} \\ \frac{1}{1.16} \frac{1}{0.77 - 0.46 \frac{a}{b}} \frac{2a}{a_0} & \text{for a rigidly made plate} \end{cases} \quad (31.47)$$

$$T_{\text{ноп}} = \frac{1}{0.77 - 0.46 \frac{a}{b}} \frac{2a}{a_0} \quad (31.48)$$

§32. Formation and Development of Cavitation During Interaction of a Shock-Wave with a Plate

In studying the interaction of a shock wave with a pliable obstacle, we have more than once focused attention on the possible formation of tensile stresses in a fluid. If the absolute magnitude of these stresses exceeds hydrostatic pressure and cavitation pressure, discontinuities may arise in the fluid. All the previously stated theoretical schemes become invalid. Consequently, we must

consider the formation and development of cavitation during the interaction of a shock wave with a plate and perform an approximate evaluation of the generalized external forces involved in this process.

The physical picture of this effect does not differ greatly from the earlier considered situation of shock wave reflection on a free surface (cf. §8). The approximate theoretical scheme can be most simply illustrated with the example of motion of a free plate separating water and air. This problem was stated in §22, without consideration of cavitation effects. Specifically, we gave the results of calculating net pressure in a fluid during incidence onto a plate of an exponential wave (Fig. 95). Employing this graph and bearing in mind the conditions for formation of a cavitation discontinuity

$$p_{\text{pec}} = p_{\text{np}} + p_{\text{orp}} = -(p_k + p_0), \quad (32.1)$$

where p_{pec} - net pressure inducing fluid cavitation;
 p_0 - hydrostatic pressure at a given depth:

$$p_0 = p_{\text{atm}} + \rho_0 g h;$$

p_k - cavitation pressure,*

we can easily find the point of origin of this discontinuity in spatio-temporal coordinates.

The formation and development of cavitation during the interaction of an underwater shock-wave with a plate was first studied by Shauer [40] and Kirkwood [10]. Shauer's theory is based on the assumption that at the moment that net pressure is equal to the sum of hydrostatic pressure and cavitation pressure, the plate tears away from the fluid and travels in the air medium. We can easily

*As was shown by specially conducted tests, under real conditions, the quantity p_k lies within the range of 2-3.5 kg/cm².

find this moment in time with the aid of the relations established in §22.

For example, if we make a rough assumption that cavitation occurs when net pressure on the plate is equal to zero, then according to (22.46)

$$t_k = 0 \frac{\ln \beta}{\beta - 1}, \quad (32.2)$$

where t_k - the cavitation formation-time;

$$\beta = \frac{p_0 a_0}{m} 0.$$

The rate of speed of the plate at time $t = t_k$, according to (22.43) is

$$W' |_{t=t_k} = \frac{2p_m}{\rho_0 a_0} e^{-\frac{\ln \beta}{\beta-1}} = \frac{2p_m}{\rho_0 a_0} \beta^{-\frac{1}{\beta-1}}. \quad (32.3)$$

The kinetic energy of a free plate is canceled by the work of atmospheric counterpressure forces.

Aleksandrin developed Shauer's theory relative to problems of interaction of an underwater shock wave with marine structures.

In contrast to Shauer, Kirkwood suggested that the maximum travel of a plate can be defined not only by the quantity of kinetic energy transmitted to it by the shock wave when cavitation areas are formed, but likewise by the energy of the fluid layer in which this cavitation occurred.

Kirkwood's studies were continued by Zamyshlyayev. The picture of development of cavitation processes during the motion of a plate under the influence of a shock wave is very close to the one described above in §8. The difference lies in the fact that when studying the reflection of a wave on a free surface, it was possible to consider that the formation of a cavitation discontinuity coincides in time with the time at which the reflected wave front converges. At this

point, however, this point in time occurs later and more care is needed in studying the totality of wave interaction processes.

Let us consider the motion of a plate and cavitation layers of water for an arbitrary value of cavitation pressure p_K .

The time and place of origin of the first cavitation discontinuity can be defined by the equation

$$p_{\text{pes}}(t, z) = -(p_K + p_0),$$

while according to the problem conditions, the function $p_{\text{pes}}(t, z)$ at this point must have a minimum of

$$\frac{\partial p_{\text{pes}}(t, z)}{\partial z} = 0. \quad (32.4)$$

Equations (32.1) and (32.4) permit us to find the unknown quantities: t_K - the moment of onset of cavitation and h_K - the distance of the first cavitation discontinuity from the plate.

Specifically, for an exponential wave we get [cf. (22.52)]:

$$e^{-\frac{t_K - \frac{h_K}{a_0}}{\theta}} - \beta e^{-\frac{\beta(t_K - \frac{h_K}{a_0})}{\theta}} = \frac{\beta - 1}{\beta + 1} \frac{p_K + p_0}{2p_m}, \quad (32.5)$$

$$e^{-\frac{t_K - \frac{h_K}{a_0}}{\theta}} - e^{-\frac{t_K - \frac{h_K}{a_0}}{\theta}} = \frac{2\beta}{\beta + 1} \frac{p_K + p_0}{2p_m}. \quad (32.6)$$

For a triangular wave

$$h_K = \frac{a_0 t_+}{2} + \frac{p_K + p_0}{p_m}, \quad (32.7)$$

$$t_K = t_+ \left[\frac{p_K + p_0}{2p_m} + \frac{1}{\beta} \ln(1 + \beta) \right]. \quad (32.8)$$

With high pressure on the direct wave, the distance h_K will be small, and the difference between the rates of speed of water particles

and the plate at the moment of formation of the cavitation discontinuity can be disregarded:

$$\dot{W}|_{t_k} = \frac{p_{np}(t_k, -h_k) - p_{01p}(t_k, -h_k)}{\rho_0 a_0} = \frac{2p_{np}(t_k, -h_k)}{\rho_0 a_0} + \frac{p_k + p_0}{\rho_0 a_0}. \quad (32.9)$$

As time t_k approaches, plate travel can easily be found from the equations in §22. For an exponential wave

$$W(t_k) = \frac{2p_m}{\rho_0 a_0} \left[1 - \frac{1}{\beta - 1} \left(\beta e^{-\frac{t_k}{\theta}} - e^{-\frac{\beta t_k}{\theta}} \right) \right]; \quad (32.10)$$

for a triangular wave

$$W(t_k) = \frac{2p_m}{\rho_0 a_0} \left[-\frac{t_k^2}{2t_+} + \left(1 + \frac{1}{\beta} \right) \left[t_k - \frac{t_+}{\beta} \left(1 - e^{-\frac{\beta t_k}{t_+}} \right) \right] \right]. \quad (32.11)$$

The further propagation of net pressure exceeding water strength into the center of the fluid causes the formation of new cavitation layers. Each of these layers will move in a vacuum* at a constant velocity equal to the velocity at the time of its separation

$$\dot{W}_i(t_i) = \frac{2p_{np}(t_i, -h_i)}{\rho_0 a_0} + \frac{p_k + p_0}{\rho_0 a_0}. \quad (32.12)$$

The point in time t_i , when cavitation occurs at a given point $z = -h_i$ may be found from the equation

$$p_{res}(t = t_i, z = -h_i) = -(p_k + p_0). \quad (32.13)$$

In proportion to subsequent motion, the layers will gradually catch up to the plate. Let us find the time of collision of the i -th layer with the plate and its adjacent layers. It is apparently defined by the equality in the travel of the plate and the i -th layer. Prior to the time of separation, the surface of the i -th layer was traveling at a rate equal to

*The pressure of saturated water vapor may be disregarded.

$$W_i(t) = \int_{-\frac{h_i}{a}}^t v_{\text{pe3}} dt, \quad (32.14)$$

however,

$$v_{\text{pe3}} = \frac{p_{\text{np}}(t, -h_i) - p_{\text{отп}}(t, -h_i)}{\rho_0 a_0}, \quad (32.15)$$

and consequently,

$$\begin{aligned} W_i(t_i) &= \int_{-\frac{h_i}{a_0}}^{t_i} \frac{p_{\text{np}}(t, -h_i)}{\rho_0 a_0} dt - \int_{\frac{h_i}{a}}^{t_i} \frac{p_{\text{отп}}(t, -h_i)}{\rho_0 a_0} dt = \\ &= \frac{J_{\text{np}}(i) - J_{\text{отп}}(i)}{\rho_0 a_0}, \end{aligned} \quad (32.16)$$

where $J_{\text{np}}(i)$ and $J_{\text{отп}}(i)$ - magnitudes of pressure pulses in the direct and reflected waves, counted from the time of convergence of these waves with point $z = -h_i$ until the time of formation of the cavitation discontinuity:

$$J_{\text{np}}(i) = \int_0^{t_i + \frac{h_i}{a_0}} p_{\text{np}}(t) dt, \quad (32.17)$$

$$J_{\text{отп}}(i) = \int_0^{t_i - \frac{h_i}{a_0}} p_{\text{отп}}(t) dt. \quad (32.18)$$

Let us note that for an exponential shock wave

$$J_{\text{np}}(i) = p_m \theta \left(1 - e^{-\frac{t_i + \frac{h_i}{a_0}}{\theta}} \right), \quad (32.19)$$

$$J_{\text{отп}}(i) = p_m \theta \left[1 - e^{-\frac{t_i - \frac{h_i}{a_0}}{\theta}} - \frac{2}{\theta - 1} e^{-\frac{1}{\theta} \left(t_i - \frac{h_i}{a_0} \right)} - 1 \right]; \quad (32.20)$$

for a shock wave of triangular profile

$$J_{np}(i) = p_m t_+ \left[\frac{t_i + \frac{h_i}{a_0}}{t_+} - \frac{1}{2} \left(\frac{t_i + \frac{h_i}{a_0}}{t_+} \right)^2 \right], \quad (32.21)$$

$$J_{orp}(i) = p_m t_+ \left\{ \frac{2(1 + \frac{1}{3})}{3} \left[1 - e^{-\frac{3(t_i - \frac{h_i}{a_0})}{t_+}} \right] - \left(1 + \frac{2}{3} \right) \frac{t_i - \frac{h_i}{a_0}}{t_+} \right\}. \quad (32.22)$$

As we mentioned, after separation of the i -th layer, this layer moves at a constant velocity $W_i(t_i)$. According to (32.12) and (32.16), therefore, its travel for $t > t_i$ is

$$W_i(t) = W_i(t_i) + W_i(t_i)(t - t_i) = \frac{J_{np}(i) - J_{orp}(i)}{\rho_0 a_0} + \frac{2p_{np}(i) - p_m + p_0}{\rho_0 a_0} (t - t_i), \quad (32.23)$$

where $p_{np}(i) = p_{np}(t_i + h_i/a_0)$ - pressure on the direct wave at time $t = t_i + h_i/a_0$ where $z = 0$.

For an approximate evaluation of the motion characteristics of the cavitation layers and the plate, let us employ the law of conservation of energy and momentum. Let us consider a system consisting of a plate and its adjacent cavitation layers (thickness h_i).

Towards the separation time of the i -th layer*, this system acquires a momentum which is equal to the pulse of pressure forces acting on it as it converges with the plane $z = -h_i$ of the direct wave front ($t = -\frac{h_i}{a_0}$):

$$K_i(t_i) = \int_{-\frac{h_i}{a_0}}^{t_i} p_{np}(t) dt + \int_{\frac{h_i}{a_0}}^{t_i} p_{orp}(t) dt = J_{np}(i) + J_{orp}(i). \quad (32.24)$$

*We should once again stress that the formation time of the i -th cavitation layer, generally speaking, does not coincide with the time of convergence with plane h_i of the reflected wave front.

(pressure of saturated vapors on the part of the i -th layer can be disregarded). According to this principle, momentum of the system at some point in time $t > t_i$ will be

$$K_i(t) = K_i(t_i) - p_0(t - t_i). \quad (32.25)$$

On the other hand, after the i -th layer adjoins the plate, the momentum of the system can be expressed using some average velocity $\dot{W}_1(t)$

$$K_i(t) = (m + \rho_0 h_i) \cdot \dot{W}_1(t). \quad (32.26)$$

Comparison of (32.25) and (32.26) yields

$$\dot{W}_1(t) = \frac{K_i(t_i) - p_0(t - t_i)}{m + \rho_0 h_i} = \frac{J_{np}(t) + J_{orp}(t) - p_0(t - t_i)}{m + \rho_0 h_i}. \quad (32.27)$$

The kinetic energy of system motion is

$$T_i(t) = \frac{m + \rho_0 h_i}{2} \dot{W}_1^2(t). \quad (32.28)$$

Apparently, this quantity must be equal to the energy of the direct and reflected waves which is transmitted to the system, minus the work of atmospheric pressure forces*.

The energy of the direct wave is

$$E_{np}(t) = \int_0^{t_i + \frac{h_i}{a_0}} \frac{\rho_{np}^2(t)}{\rho_0 a_0} dt. \quad (32.29)$$

The energy of the reflected wave which is lost by the system toward the separation time of the i -th layer,

*We should bear in mind that if the direct wave introduces some energy to the system, the reflected wave removes it. Consequently, due to wave propagation, toward time t_i the system acquires energy $E_{np}(i) - E_{orp}(i)$.

$$E_{orp}(i) = \int_0^{t_i - \frac{h_i}{a_0}} \frac{p_{orp}^2(t)}{\rho_0 a_0} dt. \quad (32.30)$$

Specifically, for an exponential shock-wave

$$E_{np}(i) = \frac{p_m^2 h_i}{2\rho_0 a_0} \left[1 - e^{-\frac{2(t_i + \frac{h_i}{a_0})}{\beta}} \right], \quad (32.31)$$

$$E_{orp}(i) = \frac{p_m^2 h_i}{2\rho_0 a_0} \left\{ 1 - \frac{4\beta}{(\beta-1)^2} \left[e^{-\frac{2(t_i - \frac{h_i}{a_0})}{\beta}} - 2e^{-\frac{(\beta+1)(t_i - \frac{h_i}{a_0})}{\beta}} \right] - \left(\frac{\beta+1}{\beta-1} \right)^2 e^{-\frac{2(t_i - \frac{h_i}{a_0})}{\beta}} \right\}; \quad (32.32)$$

for a triangular shock-wave

$$E_{np}(i) = \frac{p_m^2 t_+}{3\rho_0 a_0} \left[3 \left(\frac{t_i - \frac{h_i}{a_0}}{t_+} \right) - 3 \left(\frac{t_i - \frac{h_i}{a_0}}{t_+} \right)^2 + \left(\frac{t_i - \frac{h_i}{a_0}}{t_+} \right)^3 \right], \quad (32.33)$$

$$E_{orp}(i) = \frac{p_m^2 t_+}{\rho_0 a_0} \left\{ \left[1 - \left(\frac{t_i - \frac{h_i}{a_0}}{t_+} \right) + \frac{1}{3} \left(\frac{t_i - \frac{h_i}{a_0}}{t_+} \right)^2 \right] \left(\frac{t_i - \frac{h_i}{a_0}}{t_+} \right) - \frac{2(1+\beta)^2}{\beta^3} \left[1 - \frac{3}{1+\beta} \left(\frac{t_i - \frac{h_i}{a_0}}{t_+} \right) - e^{-\frac{(t_i - \frac{h_i}{a_0})}{t_+}} \right] \right\}. \quad (32.34)$$

The work of atmospheric counterpressure forces is

$$A \approx \rho_0 [W_1(t) - W_1(t_i)]. \quad (32.35)$$

Gathering the derived evaluations, we arrive at the relationship

$$T_i(t) = E_{np}(i) - E_{orp}(i) - A, \quad (32.36)$$

or, likewise,

$$\frac{m \cdot \rho_0 h_i}{2} \dot{W}_1^2(t) = E_{np}(i) - E_{orp}(i) - \rho_0 [W_1(t) - W_1(t_i)]. \quad (32.37)$$

where $W_i(t_i)$ can be found according to formula (32.16).

Therefore, to define the quantity of plate travel $W_1(t)$, we get

$$W_1(t) = \frac{J_{np}(t) - J_{orp}(t)}{\rho_0 a_0} + \frac{F_{np}(t) - E_{orp}(t)}{\rho_0} - \frac{m \cdot \rho_0 h_i}{2\rho_0} W_1^2(t). \quad (32.38)$$

The motion of a plate described by expressions (32.38) and (32.27) will take place after the i -th layer adjoins the plate and before the $i + 1$ layer adjoins it.

Let us define the point in time t_i^* where the i -th layer adjoins the plate. We can easily write a quadratic equation relative to t_i^* from the condition of equality in travel of the plate and the i -th layer, according to (32.38). After solving this quadratic equation, we find that

$$t_i = t_i + b_i + \sqrt{b_i^2 + c_i}. \quad (32.39)$$

where

$$b_i = \frac{J_{np}(t) + J_{orp}(t)}{\rho_0} - \frac{m \cdot \rho_0 h_i}{\rho_0 a_0 \rho_0} (2\rho_{np}(i) + \rho_\kappa + \rho_0). \quad (32.40)$$

$$c_i = \frac{2(m \cdot \rho_0 h_i)}{\rho_0^2} [E_{np}(i) - E_{orp}(i)] - \frac{[J_{np}(t) + J_{orp}(t)]^2}{\rho_0^2}. \quad (32.41)$$

The quantity t_i for a given h_i can be defined by (32.13).

The maximum plate travel is attained at the point in time t_m for which

$$\dot{W}_1(t_m) = 0. \quad (32.42)$$

From (32.27) and (32.42), we get

$$t_m = t_N + \frac{J_{np}(N) + J_{orp}(N)}{\rho_0}, \quad (32.43)$$

where N - the number of layers adjoined to the plate toward time $t = t_m$.

Employing (32.39) and (32.43) to evaluate h_N and t_N , after performing some simple transformations we find the transcendental equation

$$\begin{aligned} E_{np}(N) - E_{otp}(N) = \\ = \frac{1}{\rho_0 a_0} [2\rho_{np}(N) + \rho_k + \rho_0] [J_{np}(N) + J_{otp}(N)]. \end{aligned} \quad (32.44)$$

Moreover, we previously had

$$\rho_{pc} = \rho_{np}(N) + \rho_{otp}(N) = -(\rho_k + \rho_0). \quad (32.45)$$

These two equations include two unknown quantities h_N and t_N . After defining these quantities, we can easily calculate the quantities of the pulses and energy in the direct and reflected waves, and likewise define all the parameters of motion.

According to (32.38), maximum plate travel is

$$W''_{\max} = -\frac{J_{np}(N) - J_{otp}(N)}{\rho_0 a_0} + \frac{E_{np}(N) - E_{otp}(N)}{\rho_0}. \quad (32.46)$$

The plate subsequently (where $t > t_m$) in the reverse direction. New cavitation layers adjoin it. At a certain moment, the entire system collides with the main bulk of fluid: a shock wave is formed which defines the secondary effect of cavitation.

Let us make an approximate evaluation of these effects. The last cavitation layer will be formed at time t_n , where pressure on the direct wave is close to zero. This assumption made be made with conviction for a triangular or parabolic wave. Consequently,

$$\left. \begin{aligned} \rho_{np}(t = t_n, z = -h_n) &= 0, \\ \rho_{otp}(t = t_n, z = -h_n) &= -(\rho_k + \rho_0). \end{aligned} \right\} \quad (32.47)$$

For the exponent, pressure becomes equal to zero in infinity. We thus usually consider that where $t = t_n$, $\rho_{np} = 0.2\rho_m$.

Consequently,

$$\left. \begin{aligned} \rho_{np}(t=t_n, z=-h_n) &\simeq 0,2\rho_m, \\ \rho_{orp}(t=t_n, z=-h_n) &\simeq -(0,2\rho_m + \rho_k + \rho_0). \end{aligned} \right\} \quad (32.48)$$

The cavitation layer will reach the plate where $t = t_n^*$, where the value of t_n^* can be found with the aid of (32.39): $h = h_n$ and $t = t_n$, as calculated according to formulas (32.47) or (32.48).

Where $t > t_n^*$, the plate will move according to the law (32.38), (32.27). The moment of collision, which defines the end of this motion, is found as before from the condition of equality in travel of the boundary of the main bulk of water (of the last cavitation discontinuity) and the system of the plate-and-adjoining-cavitation layers. Travel of the surface of the last cavitation discontinuity at the time of its formation can be defined by (32.16). Subsequently, this motion is similar to the motion of a free surface where $p_0 = 0$, i.e.,

$$\begin{aligned} W_{non}(t) &= W_n(t_n) + \int_{t_n}^t \frac{2\rho_{np}(t, z=-h_n) \rho_0}{\rho_0 a_0} dt : : \\ &= \frac{1}{\rho_0 a_0} \left[\rho_0(t-t_n) + 2J_{np}\left(t + \frac{h_n}{a_n}\right) - J_{np}(n) - J_{orp}(n) \right]. \end{aligned} \quad (32.49)$$

Employing (32.39), (32.38), and (32.49), and performing some simple calculations similar to those shown above, we find that

$$\begin{aligned} t_{oy,n} &= t_n + \frac{J_{np}(n)}{\rho_0} \frac{J_{orp}(n)}{\rho_0} + \\ &+ \sqrt{\frac{2(m - \rho_0 h_n)}{\rho_0^2} [E_{np}(n) - E_{orp}(n)]}. \end{aligned} \quad (32.50)$$

The velocity of the plate at the moment of collision can be defined according to formula (32.27).

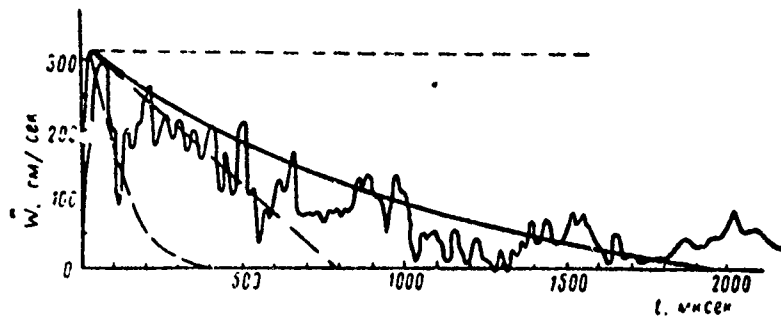


Fig. 134. Rate of Speed of Plate 3 mm Thick Under Influence of Shock Wave $p_m = 37 \text{ kg/cm}^2$;

$\theta = 71 \text{ } \mu\text{s}$.

- calculated by proposed method;
- ~~~~~ experimental data;
- Shauer theory, no atm. counterpressure;
- .-.-.-.- Shauer theory, allowing for atm.
- calculated without cavitation.

The pressure of collision which corresponds to this velocity (cf. §8)

$$p_{0,y,z} \approx \rho_0 W_0 \left[\frac{L_{1,p}(n) - L_{0,p}(n)}{2(m - \frac{1}{2}h_n)} \right] \quad (32.51)$$

The secondary shock wave formed as a result of the collision will propagate in two directions from the collision plane. After reaching the plate surface, it will induce the formation of a reflected wave. The parameters of this wave may be defined from the equality of pressure and velocity on the plate.

Considering that the coefficient of reflection is equal to 1, for $t > t_{\text{coyA}} + h_n/a_0$, we get

$$mW = p_{\text{coyA}} + p_{\text{отр. coyA}} - p_0 \quad (32.52)$$

$$W = \frac{p_{\text{coyA}} - p_{\text{отр. coyA}}}{\rho_0 a_0} + W_1(t_{\text{coyA}}) \quad (32.53)$$

Combining (32.52) and (32.53) yields

$$mW + \rho_0 a_0 W = 2p_{\text{coyA}} - p_0 + \rho_0 a_0 W_1(t_{\text{coyA}}) \quad (32.54)$$

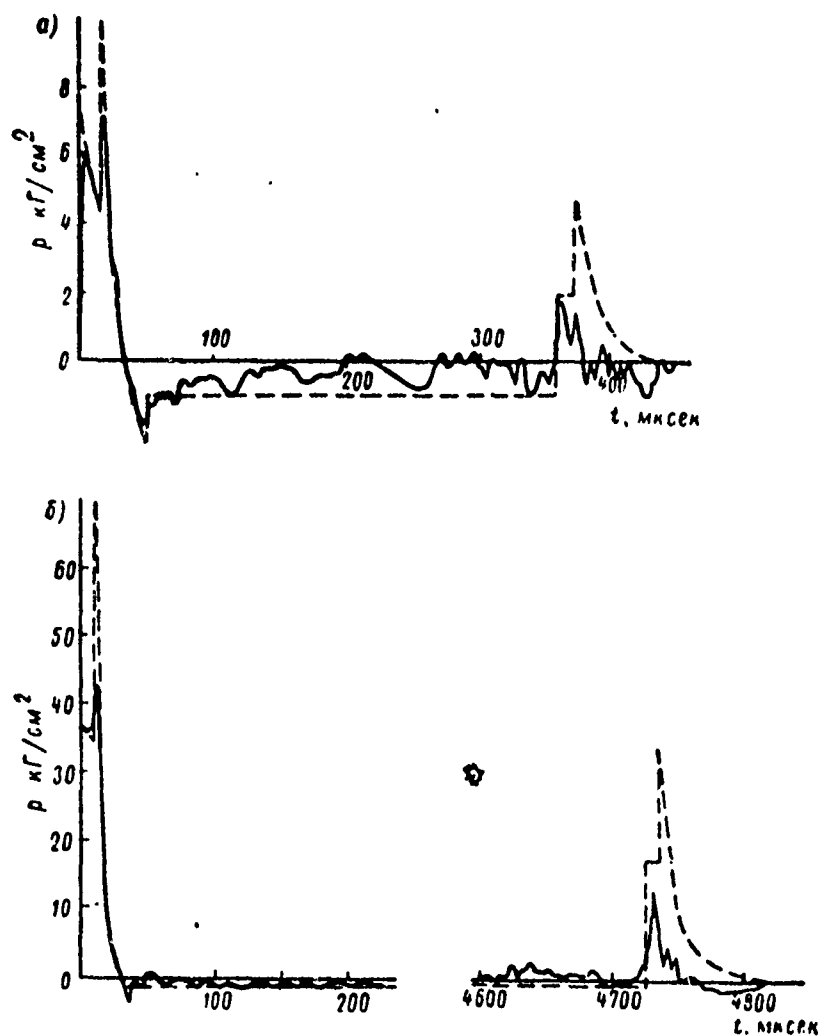


Fig. 135. Net Pressure in front of a Plate 3 mm Thick: (a) in front of the plate at a distance of 1.1 cm from it, during underwater explosion $G = 0.6$ g ($p_m = 7225$ kg/cm², $\theta = 26$ μ s); (b) in front of the plate at a distance of 0.7 cm from it, during underwater explosion $G = 53$ g ($p_m = 37$ kg/cm², $\theta = 71$ μ s).

————— experimental data;
 ----- theoretical data.

At time $t = t_{\text{coyA}} + h_n/a_0$ with initial data

$$\Psi = \Psi_1(t_{\text{coyA}}),$$

$$\Psi = \Psi_1(t_{\text{coyA}})$$

the solution of equation (32.54) appears as

$$W = W_1(t_{\text{coyA}}) + \left[\frac{2p_{\text{coyA}} - p_0}{\rho_0 a_0} + W_1(t_{\text{coyA}}) \right] \left(t - t_{\text{coyA}} - \frac{h_n}{a_0} \right) - \frac{(2p_{\text{coyA}} - p_0) m}{\rho_0^2 a_0^2} \left[1 - e^{-\frac{\rho_0 a_0}{m} \left(t - t_{\text{coyA}} - \frac{h_n}{a_0} \right)} \right], \quad (32.55)$$

whence

$$W(t) = W_1(t_{\text{coyA}}) + \frac{(2p_{\text{coyA}} - p_0)}{\rho_0 a_0} \left[1 - e^{-\frac{\rho_0 a_0}{m} \left(t - t_{\text{coyA}} - \frac{h_n}{a_0} \right)} \right], \quad (32.56)$$

$$p_{\text{orp. coyA}} = (2p_{\text{coyA}} - p_0) e^{-\frac{\rho_0 a_0}{m} \left(t - t_{\text{coyA}} - \frac{h_n}{a_0} \right)} - p_{\text{coyA}} + p_0. \quad (32.57)$$

Fig. 134 gives a comparison of the theoretical rates of speed of a plate at the experimentally obtained velocity. We can see that our proposed scheme is in good agreement with the experimental result. The Shauer theory produces much greater error.

An additional support for the validity of the ideas developed in this section can be found in oscillograms shown in Fig. 135. A certain amount of discrepancy in the nature of variation of pressure seems to be associated with the absence, under actual conditions, of clear-cut cavitation discontinuity surfaces.

In summary, we should note that consideration of cavitation effects must be considered as an obligatory condition of dynamic structure calculation. Serious errors which may tend to be dangerous are possible in evaluating the maximum velocities and travel of plates. Analysis of foreign experimental data [29] leads to the same conclusion.

The subject of the last two sections of this book are devoted to the simple tasks of dynamic calculation of plates, allowing for cavitation.

§33. Dynamic Calculation of an Infinite Plate on a Solid Elastic Foundation, Allowing for Cavitation

The results derived in the preceding section may easily be expanded to a plating lying on a solid elastic foundation.

The equation of motion of such a plate, not allowing for cavitation effects, will be

$$m\ddot{W} + \rho_0 a_0 \dot{W} + KW = 2\rho_m f(t). \quad (33.1)$$

Equation (33.1) differs from the equation of motion of a free plate by only the term which takes into account the rigidity of the elastic foundation K . In problems which are of the greatest importance from a practical standpoint, this rigidity is not great and does not exert any noticeable effect on the initial period of motion. Consequently, the formation and development of cavitation in this case will occur just as in the interaction of an underwater shock-wave with a free plate.

Limiting ourselves to the consideration of plates having low rigidity of their elastic foundation, let us note that the forces of rigidity in this case will only be revealed in the nature of subsequent motion of the plate, and in the temporal picture of cavitation layers of water adjoining it. The easiest way to consider the effect of rigidity is to employ the law of conservation of energy and momentum. We must calculate the pulse of rigidity and the potential deformation energy of the elastic foundation.

The pulse of rigidity is

$$J_m = \int_0^t KW dt = K \int_0^t W dt. \quad (33.2)$$

Because we did not know the function $W(t)$, let us use the approximate method to define the quantity J_m . Let us assume that in a rather small time interval $t_j^* - t_j^{*-1}$, the quantity of rigidity

is equal to $K \frac{W(t_j^*) + W(t_{j-1}^*)}{2}$.

Then,

$$J_{\kappa}(t_i^*) \simeq K \sum_{j=1}^i (t_j^* - t_{j-1}^*) \frac{W(t_j^*) + W(t_{j-1}^*)}{2}, \quad (33.3)$$

where t_j^* - the time that the j -th cavitation layer, formed at time t_j at a distance of h_j , adjoins the plate (where $j = 0$, $t_j^* = t_{\kappa}$, $t_{j-1}^* = 0$; $W(t_j^*) = W_1(t_{\kappa})$; $W(t_j^* - \kappa) = 0$);

$W(t_j^*)$ - plate travel at the time that a layer of water h_j thick adjoins to it;

t_i^* - the time that a layer of water h_i thick adjoins the plate, for which we define travel and plate velocity.

The law of conservation of momentum, allowing for (33.3) and (32.25), can be written as

$$J_{\kappa}(t_i^*) + p_0(t_i^* - t_i) = K_i(t_i) - K_i(t_i^*), \quad (33.4)$$

whence, by total analogy with (32.27)

$$\dot{W}(t_i^*) = \frac{1}{m + p_0 h_i} [J_{np}(i) + J_{orp}(i) - (t_i^* - t_i) p_0 - J_{\kappa}(t_i^*)]. \quad (33.5)$$

Let us now evaluate the potential deformation energy of the elastic foundation. Apparently,

$$V = \int_0^{W^*} K W dW = \frac{K W^2}{2}. \quad (33.6)$$

Consequently, for the moment in time $t = t_i^*$, by analogy with (32.37), we can write the law of conservation of energy in the following manner

$$\frac{K}{2} W^2(t_i) + \frac{m \cdot \rho_0 h_i}{2} \dot{W}^2(t_i^*) = E_{np}(i) - E_{orp}(i) - \rho_0 [W(t_i^*) - W_i(t_i)], \quad (33.7)$$

whence

$$W(t_i^*) = \frac{\rho_0}{K} \left\{ -1 + \sqrt{1 + \frac{2K}{\rho_0^2} \left[\rho_0 W_i(t_i) + E_{np}(i) - E_{orp}(i) - \frac{m \cdot \rho_0 h_i}{2} \dot{W}^2(t_i^*) \right]} \right\}, \quad (33.8)$$

where $W_i(t_i)$ can be defined according to formula (32.16).

The moment t_i of adjunction of cavitation layers h_i thick to the plate can be found from the condition of equality in travel of the plate and the i -th layer. Reiterating the arguments from §32 [cf. (32.39)], we find that

$$t_i^* = t_i + b_i + \sqrt{\bar{b}_i^2 + \bar{c}_i}, \quad (33.9)$$

where

$$\bar{b}_i = \frac{J_{np}(i) + J_{orp}(i) - J_{\kappa}(t_i^*)}{\rho_0} - \frac{m \cdot \rho_0 h_i}{2 \rho_0 \rho_0^2} (2\rho_{np}(i) + \rho_{\kappa} + \rho_0) [KW_i(t_i) + \rho_0], \quad (33.10)$$

$$\bar{c}_i = \frac{2(m \cdot \rho_0 h_i)}{\rho_0^2} \left[E_{np}(i) - E_{orp}(i) - \frac{KW_i^2(t_i)}{2} - \frac{\rho_0^2}{2K} \right] - \frac{1}{\rho_0^2} [J_{np}(i) + J_{orp}(i) - J_{\kappa}(t_i^*)]^2. \quad (33.11)$$

Maximum plate travel is attained at time $t = t_m$. At the same time $W(t_m) = 0$. According to (33.5), we get

$$t_m = t_N + \frac{J_{np}(N) + J_{otp}(N) - J_m(t_m)}{p_0}, \quad (33.12)$$

where N - the number of layers adjoined to the plate at time $t = t_m$.

The thickness of the layer h_N adjoined to the plate at time $t = t_m$ can easily be found from the condition $t_m = t_N^*$ [cf. formula (33.9), (33.12), and (32.13)]. After performing the given calculations, we can derive the quantity of maximum buckling with the aid of (33.8), assuming that $W(t_m) = 0$,

$$W_{max} = \frac{p_0}{K} \left\{ -1 + \sqrt{1 + \frac{2K}{p_0^2} \left[p_0 \frac{J_{np}(N) - J_{otp}(N)}{t_N u_0} + E_{np}(N) - E_{otp}(N) \right]} \right\}. \quad (33.13)$$

Upon subsequent motion of the plate in the opposite direction, the remaining incipient layers will adjoin it. The last of these layers will adjoin at time t_n^* , which can be defined by formula (33.9). Then, motion will occur at a constant mass under the influence of the forces of rigidity and atmospheric counterpressure. Motion can be described by the differential equation

$$(m + \rho_0 h_n) \ddot{W} + KW = -p_0. \quad (33.14)$$

Integrating (33.14) at time $t = t_n^*$ with the initial data

$$W = W_1(t_n^*),$$

$$\dot{W} = \dot{W}_1(t_n^*),$$

we will find that

$$W = W_1(t_n^*) \cos \lambda(t - t_n^*) + \frac{\dot{W}_1(t_n^*)}{\lambda} \sin \lambda(t - t_n^*) - \frac{p_0}{m + \rho_0 h_n} \frac{1}{\lambda^2} [1 - \cos \lambda(t - t_n^*)],$$

$$\dot{W} = \dot{W}_1(t_n^*) \cos \lambda(t - t_n^*) - \left[\lambda \dot{W}_1(t_n^*) + \frac{p_0}{\lambda(m + \rho_0 h_n)} \right] \sin \lambda(t - t_n^*), \quad (33.16)$$

where

$$\lambda^2 = \frac{K}{m + \rho_0 h_n}.$$

Equations (33.15) and (33.16) are valid up to the moment of collision of the plate-layer system with the main bulk of water. As before, this moment can be found from the condition of equality in travel of the plate and the boundary of the cavitation area [comparing (32.49) and (33.15)]. The velocity of the plate and its adjoining layers can be defined both with the aid of (33.16) and (33.7).

Employing the law of the conservation of energy [in the form of formula (33.7)], we find that

$$\dot{W}(t_{\text{coyA}}) = - \sqrt{\frac{2}{m + \rho_0 h_n} \left\{ E_{\text{np}}(n) - E_{\text{orp}}(n) - \frac{K}{2} W^2(t_{\text{coyA}}) - \right.} \\ \left. - p_0 [W(t_{\text{coyA}}) - W_n(t_n)] \right\}}. \quad (33.17)$$

Where $p_m \gg p_H + p_0$ and small K , eliminating small second-power terms, we find

$$\dot{W}(t_{\text{coyA}}) = - \sqrt{\frac{2}{m + \rho_0 h_n} [E_{\text{np}}(n) - E_{\text{orp}}(n)]}. \quad (33.18)$$

The collision pressure which corresponds to this quantity is

$$p_{\text{coyA}} = p_0 a_0 \sqrt{\frac{E_{\text{np}}(n) - E_{\text{orp}}(n)}{2(m + \rho_0 h_n)}}. \quad (33.19)$$

After collision, the motion of the plate occurs in almost the same way as the motion of a free plate, and can be defined by formulas

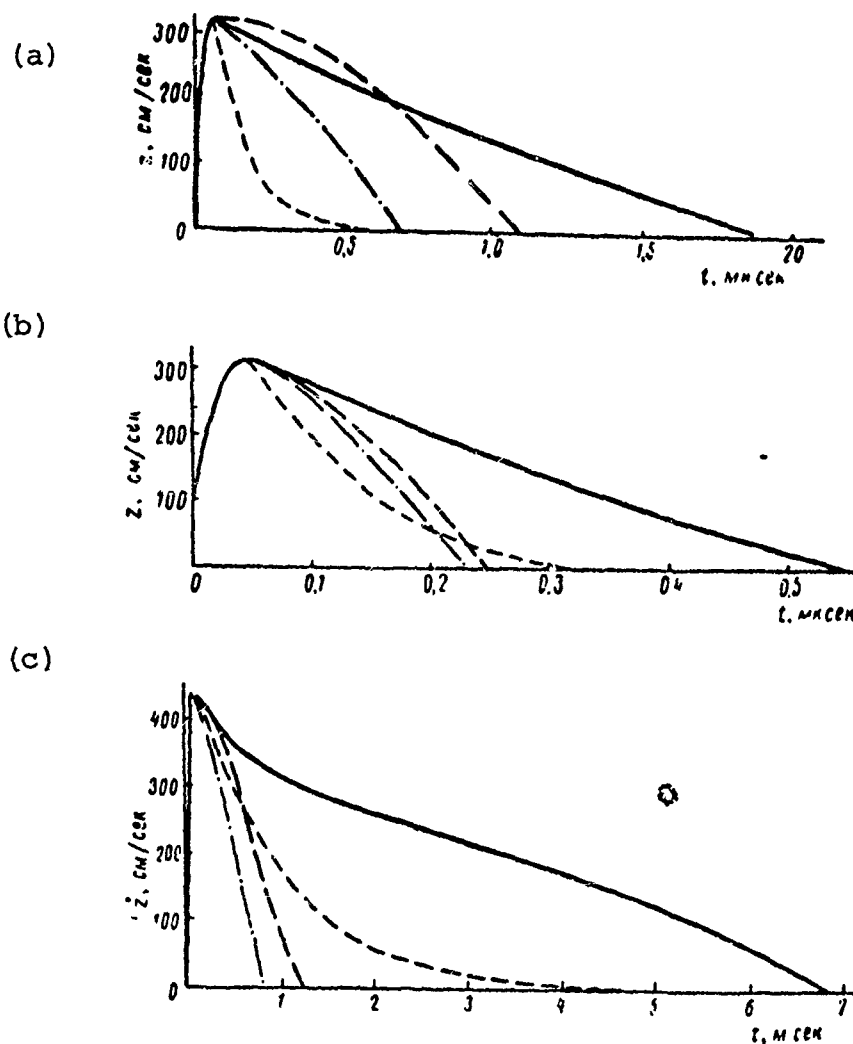


Fig. 136. Rate of Speed of a Plate 4 mm Thick, Lying on a Solid Elastic Foundation, Under the Influence of Pressure of an Underwater Shock-Wave $p_m = 37 \text{ kg/cm}^2$: (a) - $k = 6.85 \text{ kg/cm}^2$; $\theta = 110 \mu\text{s}$; (b) - $K = 137.5 \text{ kg/cm}^2$, $\theta = 110 \mu\text{s}$; (c) - $K = 6.85 \text{ kg/cm}^2$; $\theta = 1000 \mu\text{s}$.

- calculated acc. to stated method;
- calculated according to Shauer, without allowing for atmospheric counter-pressure;
- .-.-.- calculated according to Shauer, allowing for the effect of atmospheric counterpressure;
- - - - - calculated without considering cavitation.

(32.52) - (32.57).

In most cases, we are interested in the interval $[0, t_{\max}]$ and in evaluating maximum plate travel W_{\max} . Fig. 136 shows the curves for the rate of plate speed, calculated with the aid of different methods. As we can see, at small values of K and θ , calculation of the parameters of motion not allowing for cavitation produces the greatest error.

The action of the adjoining cavitation layers is partially neutralized by the action of atmospheric counterpressure. Consequently, calculation of maximum plate travel according to Shauer's theory, without allowing for atmospheric counterpressure, produces a result which is close to the true value. If we employ the Shauer theory allowing for atmospheric counterpressure, both the rate of plate travel and the travel itself come out to be too low.

An increase in the rigidity of the elastic foundation K (Fig. 136b) or in the time constant θ (Fig. 136c) yields a much greater error in calculating the parameters of plate motion using the Shauer theory. Under these conditions, the action of atmospheric counterpressure is small in comparison with the effect of the motion of cavitation layers.

There is often no need to calculate all the parameters of motion in evaluating the effect of an underwater explosion. It suffices to find the maximum buckling W_{\max} . In this case, since the difference between times t_n^* and t_m is small, it is possible to assume, without making serious errors, that at time t_m all the cavitation layers have succeeded in adjoining the plate.* Then, formula (33.13) acquires the form

$$W_{\max} = \frac{p_0}{K} \left\{ -1 + \sqrt{1 + \frac{2K}{\rho_0^2} \left[\rho_0 \frac{J_{np}(n) - J_{crp}(n)}{\mu_0 a_0} + E_{np}(n) - \dot{E}_{orp}(n) \right]} \right\}. \quad (33.2_0)$$

*Moreover, the energy of the last incipient cavitation layers is also small.

Where $p_m \gg p_0$, the role of the term $p_0 \frac{J_{np}(n) - J_{orp}(n)}{\rho_0 a_0} = p_0 W_n(t_n)$ is small in comparison with initial kinetic energy $T_0 = T_n(t_n) = E_{np}(n) - E_{orp}(n)$ which is transmitted by the shock-wave to the plate and cavitation layers. We can therefore write

$$W_{max} = \frac{p_0}{K} \left\{ -1 + \sqrt{1 + \frac{2K}{p_0^2} [E_{np}(n) - E_{orp}(n)]} \right\} =$$

$$= \frac{p_0}{K} \left(-1 + \sqrt{1 + \frac{2K}{p_0^2} T_0} \right).$$

(33.21)

Let us consider the relationship of the quantity of initial kinetic energy T_0 as a function of inertial properties of the plate for an exponential shock-wave having a limited effect-time of positive pressure phase (τ_{ak}). Because the cavitation discontinuity in a fluid cannot arise after pressure on the direct wave becomes equal to zero (in this case where $t_n + h_n/a_0 > \tau_{ak}$), the parameters t_n and h_n , which define the quantity T_0 , can be found from the relationships

$$p_{np} \left(t_n + \frac{h_n}{a_0} \right) = 2p_m, \quad (33.22)$$

$$p_{orp} \left(t_n - \frac{h_n}{a_0} \right) = -(2p_m + p_k + p_0), \quad (33.23)$$

where

$$\alpha = e^{-\frac{t_n + \frac{h_n}{a_0}}{\tau_{ak}}} = e^{-\frac{\tau_{ak}}{\tau_{ak}}}, \quad (33.24) *$$

*Relation (32.24) is valid where $\tau_{ak} < 1.80$. For $\tau > 1.80$, the form of the underwater shock-wave differs greatly from the exponential. Where $\tau_{ak} > 1.80$, we can roughly assume that $\alpha \approx -0.17$.

after transformations

$$h_n = \frac{a_0 \theta}{2} \ln \frac{x}{a}, \quad (33.25)$$

$$t_n = \frac{\theta}{2} \ln \frac{1}{ax}, \quad (33.26)$$

where $x = e^{-\frac{t_n - \frac{h_n}{a_0}}{\theta}}$ can be defined by the equation

$$\left. \begin{aligned} x - \frac{2\beta}{1+\beta} x^3 &= \frac{\beta-1}{\beta+1} \left(\alpha + \frac{p_k + p_0}{p_m} \right), \\ \beta &= \frac{p_0 a_0 \theta}{m}. \end{aligned} \right\} \quad (33.27)$$

Considering (32.31) and (32.32), and performing the appropriate calculations, we will find that

$$\begin{aligned} T_0 &= E_{np}(n) - E_{orp}(n) = \\ &= \frac{p_m^2 \theta}{2\rho_0 a_0} \left[x^2 + \frac{1}{\beta} \left(x + \alpha + \frac{p_k + p_0}{p_m} \right)^2 - \alpha^2 \right]. \end{aligned} \quad (33.28)$$

With the aid of these same relations, we can easily calculate kinetic energy of the plate at the beginning of cavitation (with an adjoining layer of water h_H thick):

$$\begin{aligned} T_{nn} = E_{np}(k) - E_{orp}(k) &= \frac{p_m^2 \theta}{2\rho_0 a_0} \left\{ -e^{-\frac{2(t_k + \frac{h_k}{a_0})}{\theta}} + \right. \\ &+ \frac{4\beta}{(1+\beta)^2} \left[e^{-\frac{2(t_k - \frac{h_k}{a_0})}{\theta}} - 2e^{-\frac{(1+\beta)(t_k - \frac{h_k}{a_0})}{\theta}} + \right. \\ &\left. \left. + \frac{(1+\beta)^2}{4\beta} e^{-\frac{2(t_k - \frac{h_k}{a_0})}{\theta}} \right] \right\}. \end{aligned} \quad (33.29)$$

Where $p_m \gg p_H + p_0$, we can roughly assume that $p = p_0 = 0$, $h_H = 0$, $t_H = t_0 = (\theta/\beta - 1)\ln\beta$. In this case, the expression of kinetic energy of the plate becomes simplified

$$T_{na} = \frac{p_m^2 \theta}{2 p_0 a_0} 4 \beta^{\frac{1+\beta}{1-\beta}} \quad (33.30)$$

and coincides with the expression established in study [10].

We can achieve considerable simplifications for the expression of T_0 if we assume that the quantities $p_H + p_0/p_m$ and α are small. Then, according to (33.27)

$$x \approx \left(\frac{2\beta}{1+\beta} \right)^{\frac{1}{1-\beta}}. \quad (33.31)$$

Hence, on the basis of (33.28)

$$T_0 = \frac{p_m^2 \theta}{p_0 a_0} \left(\frac{2\beta}{1+\beta} \right)^{\frac{1+\beta}{1-\beta}} = \frac{p_m^2 \theta}{2 p_0 a_0} 4 \beta^{\frac{1+\beta}{1-\beta}} \left[\frac{1}{2} \left(\frac{2}{1+\beta} \right)^{\frac{1+\beta}{1-\beta}} \right], \quad (33.32)$$

or because

$$E_{np} \approx \frac{p_m^2 \theta}{2 p_0 a_0}, \quad (5.56)$$

$$T_{na} \approx \frac{p_m^2 \theta}{2 p_0 a_0} 4 \beta^{\frac{1+\beta}{1-\beta}}, \quad (33.30)$$

$$T_0 = E_{np} \cdot 2 \cdot \left(\frac{2\beta}{1+\beta} \right)^{\frac{1+\beta}{1-\beta}} = T_{na} \frac{1}{2} \left(\frac{2}{1+\beta} \right)^{\frac{1+\beta}{1-\beta}}. \quad (33.33)$$

The ratios of T_0/T_{na} and T_0/E_{np} for several values of the parameter are given in Table 7.

Table 7

β	5	10	15	20	25
$\frac{T_0}{T_{na}}$	2.59	4.02	5.36	6.75	7.75
$\frac{T_0}{E_{np}}$	0.93	0.96	0.98	0.98	0.99

We can easily see that kinetic energy acquired by the plate and the cavitation layers is roughly equal to the energy of the direct wave, and exceeds by several times the kinetic energy of the plate alone.

We can arrive at the same result on the basis of stricter evaluations. Thus, Table 8 shows the calculated results of T_0/E_{np} for $p_m = 30 \text{ kg/cm}^2$ according to precise relations (33.27), (33.28), and (33.29).

Table 8

β	5	10	15	20	25
$\frac{T_0}{E_{np}}$	0.90	0.94	0.95	0.95	0.96

We can see that again $T_0 \approx E_{np}$.

Because the range $\beta = 5-25$ encompasses almost all important cases of the effect of an underwater explosion on a ship's plates, we can conclude that the basic parameter which characterises the deformation of structures in the formation of cavitation is the energy flux density of the direct wave.

We will arrive at the same conclusion by considering a shock-wave of arbitrary profile. Therefore, according to (33.21), the theoretical relation for maximum buckling will be

$$W_{max} \approx \frac{p_0}{K} \left(-1 + \sqrt{1 + \frac{2K}{p_0^2} E_{np}} \right). \quad (33.34)$$

At small values of KE_{np}

$$W_{max} \approx \frac{E_{np}}{p_0} \approx \frac{p_m}{p_0} - \frac{p_m}{2\rho_0 a_0} \eta. \quad (33.35)$$

If KE_{np} is large ($KE > 50 \text{ kg}^2/\text{cm}^4$), then

$$W_{\max} \approx \sqrt{\frac{2E_{np}}{K}}. \quad (33.36)$$

§34. Dynamic Calculation of Plates Attached by their Edges,
Allowing for Cavitation Effects

The conditions of deformation of the exterior clad sheets in a ship's body are considerably different from those considered in the preceding section. The distinction mainly amounts to the displacement of all points on an infinite plate lying on a solid elastic foundation being identical, whereas the presence of a set determines a non-uniform distribution of mass; consequently, there is a heterogeneous field by the sheath covering. Pressure near the support contour becomes greater than at the middle of span. There is a fluid return flow and the diffraction processes associated with it. The pliancy of supports exerts a considerable effect on the nature of the hydrodynamic field.

All these facts are also reflected in the development of cavitation effects. We can no longer speak of plane surfaces of the cavitation discontinuities. A mathematical description of the process of interaction of the shock wave with the ship's body becomes extremely unwieldy.* We must design a simplified model which is suited for practical evaluations. Let us consider such a model.

As the object of our study, let us select a rectangular plate on a rigid support contour forming an infinite casing. We can indicate the areas which are hydrodynamically independent of each other (due to symmetry) for this type of plate (cf. §30).

*Because cavitation occurs rather rapidly when the plate travels almost parallel to itself, and its form at this time is quite different from the form of the main vibrations of the basic tone, we can no longer limit ourselves to considering the motion of a body in form alone, as we did in preceding section.

The analysis of numerous experimental materials has indicated the extremely diverse nature of plate deformation in the initial period of motion. The moment of incidence of the shock wave is accompanied by the progressive motion of the plate along almost its entire surface. Henceforth, a portion of the progressive motion gradually decreases and ultimately, its area becomes equal to zero. The mean rate of propagation of the portion boundary, as a rule, is less than the rate of propagation of longitudinal and transverse waves of the plate material.

These facts can be explained in view of the ideas stated in §26. Indeed, during the incidence of a shock wave onto a plate, a reflected and refracted wave is formed. In propagating through the metal, the refracted wave reaches the lee surface (the steel-air interface). All points on the plate are drawn into motion, acquiring identical velocity. The process of multiple reflection and refraction of waves induces an abrupt change in the rates of motion of the plate sides. The nature of this change totally corresponds to the similar process in an infinite plate until the flexural wave propagating from the support contour reaches the point in question. After the flexural wave arrives, the presence of the supports will retard the motion at the given point. Vibration begins which roughly corresponds to the basic tone.

Therefore, in order to evaluate how the formation conditions of cavitation by plates of finite dimensions differ from those for infinite plates, we must know the distance x which is traveled by the flexural wave from the edges to the point in the center of the plate where negative net pressure is established. A semi-empirical relation may be used for this purpose. This relation is established as a result of analyzing materials of specially conducted tests*,

$$x = A \sqrt{gt}, \quad (34.1)$$

*Tests conducted by Novoselov and Basov under guidance of Zamyshlyayev.

where δ - plate thickness, cm; t - propagation time of the flexural wave, sec., A - dimensional coefficient (for rigidly fastened steel plate $A \approx 830 \text{ cm}^{1/2}/\text{sec}^{1/2}$).

For the plates which are most frequently encountered in practice, where a relatively rapid formation of negative net pressure in the central portion is capable of inducing fluid cavitation, the flexural wave propagates from the edges at a comparatively small distance. Cavitation encompasses almost the entire plate plane, except for the immediate proximity of the support contour. The ship's covering seems to tear away from the water along almost its entire surface. It would seem that under these conditions, we can fully employ the previously developed scheme for dynamic calculation of a plate lying on a solid elastic foundation. However, this is not completely so.

In the motion of a plate, three basic periods can be noted:

1. From the moment of incidence of the direct wave front to the moment of formation of cavitation ($0 < t < t_H$). During this period, the central plane of the plate which is not subject to the effect of the edges, travels progressively like a plate of infinite dimensions. Where $t = t_H$, a cavitation discontinuity arises along almost the entire surface of the fluid, directed parallel to the plane of the plate.

2. From the moment of the inception of cavitation t_H until the flexural waves arrive at the center ($t_H < t < t_H$). During this period, the central portion continues its progressive motion. Its motion is affected by air counterpressure as well as that resulting from the cavitation layers adjoining the plate.

3. From the moment the flexural waves arrive at the central point on the plate ($t > t_H$). Motion occurs in roughly the main tone of vibration. For our generalized coordinate, we can adopt the buckling of the central point on the plate with respect to the

immobile supports $W_1(t)$. In addition to the adjoined cavitation layers and atmospheric counterpressure, the forces of rigidity exert a considerable influence on plate motion.

In the first period ($0 < t < t_H$), the motion of the central point on the plate can be described by the differential equation

$$mW''(t) + \rho_0 a_0 W'(t) = 2p(t) \quad (34.2)$$

with initial conditions $W(0) = \dot{W}(0) = 0$. The velocity and travel of the central plate point at time $t = t_H$ have been defined according to the formulas in §22. The formation time of the first cavitation discontinuity in the fluid t_H and its distance from the plate h_H can be found from relations (32.5)-(32.8).

Motion in the second period ($t_H < t < t_H$) can be described by the relations of §32 and are not very different from the motion of a free infinite plate, allowing for the effect of atmospheric counterpressure and the adjoining cavitation layers of water. The evaluation of subsequent cavitation-layer formation during the motion of a plate in a given form of buckling is not easy matter. It generally requires the examination of nonlinear effects. However, as our calculations have shown, this fact can be considered in approximation, considering that at time $t = t_H$, only one layer has adjoined the plate, whose thickness is equal to the total thickness of all actually formed fluid cavitation layers.

Under this assumption, travel and velocity of the central plate point can be found with the aid of the laws of the conservation of energy and momentum for the plate-fluid system.

According to (32.38) and (32.27), we get

$$W'(t_H) = \frac{J_{np}(n) - J_{orp}(n)}{\rho_0 a_0} - \frac{E_{np}(n) - E_{orp}(n)}{\rho_0} - \frac{m + \rho_0 h_n}{2\rho_0} W'^2(t_H). \quad (34.3)$$

$$\dot{W}(t_n) = \frac{J_{np}(n) + J_{отр}(n) - \rho_n(t_n - t_n)}{m + \rho_0 h_n}, \quad (34.4)$$

where t_n, h_n - the moment of formation and the distance from the plate of the last cavitation discontinuity.

The quantities t_n and h_n can be defined by equations (32.47) and (32.48);

$J_{np}(n), E_{np}(n), J_{отр}(n)$ and $E_{отр}(n)$ - the momentum and energy of the direct and reflected waves, calculated with the aid of relations (32.19)-(32.22), (32.31)-(32.34);

t_H - the arrival time of the flexural waves at the center of the plate [cf. (34.1)].

where $t > t_H$, the differential equation of motion of the central point on the plate will be

$$W(t) + \bar{\omega}^2 W(t) = -Q \quad (34.5)$$

(with initial conditions (at time $t = t_H$)

$$W = W(t_H), \quad \dot{W} = \dot{W}(t_H).$$

where $\bar{\omega}$ - the frequency of vibration of the plate in the basic tone:

$$\bar{\omega}^2 = \frac{\omega^2}{1 + \frac{\rho_0 h_n}{m}} = \frac{K_{np}}{u_2(m + \rho_0 h_n) S}, \quad (34.6)$$

K_{np} - the reduced coefficient of rigidity, defined according to formulae: for a plate rigidly fastened along its edges

$$K_{np} = \frac{E h^3}{12(1-\mu^2)} \frac{\pi^4}{16} \frac{1}{a^2} \left(3k + \frac{3}{k^3} + \frac{2}{k} \right), \quad (34.7)$$

for a freely resting plate

$$K_{np} = \frac{E h^3}{12(1-\mu^2)} \frac{\pi^4}{16} \frac{1}{a^2} k \left(1 + \frac{1}{k^2} \right); \quad (34.8)$$

E - the Young modulus (for steel, $E = 2.1 \cdot 10^6$ kg/cm²);

μ - Poisson factor (for steel $\mu = 0.3$);
 $k = b/a$ - the ratio of plate sides ($2b$ - the long side);
 Q - the generalized force of atmospheric counterpressure:

$$Q = \frac{p_0 a^2}{(m - \gamma_0 A_0) a^2}; \quad (34.9)$$

α_1, α_2 - coefficients of evenly-distributed load and reduced mass (for a rigidly fastened plate $\alpha_1 = 0.25$; $\alpha_2 = 0.141$ and for a freely resting plate $\alpha_1 = 0.405$; $\alpha_2 = 0.25$);
 $S = 4ab$ - the area of the plate surface.

The travel and the rate of speed where $t > t_H$ can be defined by the relations

$$W(t) = -\frac{Q}{\omega^2} + \frac{\dot{W}(t_H)}{\omega} \sin \omega(t - t_H) + \left[W(t_H) + \frac{Q}{\omega^2} \right] \cos \omega(t - t_H); \quad (34.10)$$

$$\dot{W}(t) = \dot{W}(t_H) \cos \omega(t - t_H) - \left[W(t_H) \omega + \frac{Q}{\omega} \right] \sin \omega(t - t_H). \quad (34.11)$$

The quantity of maximum buckling W_{\max} and its time of acquisition t_m can be found from the formulas

$$W_{\max} = -\frac{Q}{\omega^2} + \frac{\dot{W}(t_H)}{\omega} \sin \omega(t_m - t_H) + \left[W(t_H) + \frac{Q}{\omega^2} \right] \cos \omega(t_m - t_H). \quad (34.12)$$

$$t_m = t_H + \frac{1}{\omega} \operatorname{arctg} \frac{\dot{W}(t_H)}{W(t_H) \omega + \frac{Q}{\omega}}. \quad (34.13)$$

For the approximate evaluation of maximum buckling, we can also employ relation (33.20)

$$W_{\max} = \frac{p_0 S}{K_{np}} \times \left\{ \sqrt{1 + \frac{2K_{np}}{p_0 S} \left[\frac{E_{np}(n) - E_{orp}(n)}{p_0} + \frac{J_{np}(n) - J_{orp}(n)}{I_0 a_0} \right]} - 1 \right\}. \quad (34.14)$$

Where $p_m > 30 \text{ kg/cm}^2$ and $\beta = 5-25$ (which is most often encountered in practice), with a precision of up to 10%, it follows from (34.14) that

$$W_{\max} = \frac{p_0 S}{K_{np}} \left[\sqrt{1 + \frac{2K_{np}}{r_{np}^2 S} E_{np}(n)} - 1 \right]. \quad (34.15)$$

If

then $Ec_{\text{all}} \frac{K_{np} E_{np}(n)}{S} > 50 \text{ кг}^2/\text{см}^4.$

$$W_{\max} \approx \sqrt{\frac{2E_{np}(n) S}{K_{np}}} [\text{cm}]. \quad (34.16)$$

This scheme is valid for plates making up casings and coverings where the counterflow of fluid is encumbered, due to the symmetry of the process. For plates which are fastened to a rigid wall, or end plates, the diffraction phenomena become quite substantial. Diffraction waves, propagating at the speed of sound, rapidly overtake the flexural waves, changing the hydrodynamic field and the form of plate buckling. It follows from (34.1) that the rate of propagation of flexural waves even when $x/\delta = 2.3$ is less than the speed of sound in water. Until diffraction waves from the support contour reach the central point on the plate, a central portion will exist whose motion is similar to the travel of an infinite plate. Then, this portion ceases to exist, and conditions are created where cavitation is either not formed or if it forms, it exerts not substantial effect on the nature and magnitude of the external load.

There is much interest in comparing the diffraction time $t_d = a/a_0$ and the cavitation occurrence time t_k .

Kirkwood suggested the following condition [10] as a criterion for the formation of cavitation:

$$t_k < t_d.$$

where $t_d = \frac{a}{a_0}$

- diffraction time (short side of plate = $2a$);

t_K - the moment of formation of cavitation in the center of the plate, if we consider it in our assumption of infinity of dimensions.

The analysis of experimental materials confirmed the validity of the Kirkwood criterion and permitted him to slightly refined it. It was found that for individual plates fastened to a rigid wall and for end plates, three typical cases of motion can be indicated: $t_K < 0.5t_d$; $0.5t_d < t_K < t_d$ and $t_d < t_K$.

Where $t_K < 0.5t_d$, when cavitation is formed much earlier than the arrival time of the diffraction wave at the plate center, it too defines the nature of motion. Diffraction effects do not exert any substantial effect on the external load. In this case, the end plate and the plate fastened to a rigid wall move just like a casing plate. To evaluate the parameters of this motion, we can employ the preceding formulas. If, however, the time of cavitation is greater than the time of diffraction ($t_K > t_d$), then cavitation has little effect or has no effect on the net load during interaction of a shock wave with a plate.

The hydrodynamic fields and the first and second category generalized forces can be calculated on the basis of the hypothesis of continuity, as was done in the main sections of this book. Motion of the central portion of a plate prior to time $t = t_d = a/a_0$ can be accurately described by the formulas in §22. After the convergence of the diffraction wave with the center, vibrations begin in the basic tone. First and second category generalized forces F_1 and F_2 can be defined according to the formulas in §27 and §31. At the same time, in the time interval $t_d < t < 2a/a_0 = 2t_d$, the function $F_1(t)$ can be written as the sum of the terms which are linear functions of velocity and travel. Where $t > 2t_d$ second category generalized force is proportional to acceleration (hypothesis of noncompressibility of a fluid).

The case $0.5t_d < t < t_d$ represents the greatest difficulties. Both diffraction and cavitation processes are substantial at this point. Based on our previously developed ideas, we could design a theoretical plane for it. However, in practice, such temporal relationships are not that frequently encountered. Consequently, we can simply recommend the use of linear interpolation of the two solutions we have given ($t_H < 0.5t_d$; $t_H > t_d$).

In conclusion, let us note that the enormous amount of work which was recently been published in the field of envelope dynamics compels us to consider the problem of underwater shock-wave interaction with an envelope as an independent, highly important, and interesting problem. Even a brief statement of the primary aspects of this problem would require a separate monograph.

REFERENCES

1. Gradshteyn, I. S., Ryzhik, I. M., Tables of Integrals, Sums, Series, and Derivations (GIFML, 1962).
2. Grib, A. A., Ryzhov, O. S., Khristianovich, S. A., Short Wave Theory, ZhPMTF, 1960, No. 1.
3. Grib, A. A., Ryabinin, A. G., Khristianovich, S. A., On Reflection of a Plane Shock Wave in Water on a Free Surface, PMM, 1956, v. XX, issue 4.
4. Zvolinskiy, N. V., Multiple reflection of elastic waves in a layer, Trudy of the Geophysics Institute, 1954, No. 22(149).
5. Zel'dovich, Ya. B. The Theory of Shock Waves and Introduction to Gas Dynamics (AS USSR, 1946).
6. Zel'dovich, Ya. B. On pressure and velocity distribution in detonation products, specifically in spherical propagation of a detonation wave, Journal of Experimental Theoretical Physics, 1942, v. 12, No. 9, pp. 389-406.
7. Kol'skiy, G. K. Stress Waves in Solid Bodies (IL, 1955).
8. Kornfel'd, M. Elasticity and Strength of Fluids (GITTL, 1951).
9. Korotkov, P. F. On shock waves at considerable distances from the locus of explosion, AS USSR, Tech. Sci. Div., 1958, #3.
10. Cowle, R. Underwater Explosions. (IL, 1950).
11. Landau, L. D. On shock waves at great distances from their point of origin, PMM, 1945, v. IX, issue 4.
12. Logovtsev, V. A. Propagation of a shock wave in a flat basin at a great distance from the locus of explosion, PMTF, 1962, No. 3.
13. Novozhilov, V. V. On the travel of an absolutely solid body under the influence of an acoustic pressure wave, PMM, 1959, v. XXIII, issue 4.
14. Petrashen', G. I., Marchuk, G. I., Ogurtsov, K. I. On the Lamb problem for a half-space, Scholarly Notes of Leningrad Univ., 1950, No. 135, iss. 21.
15. Petrashen', G. I., Makarov, G. I. Nonstationary diffraction of acoustic and electromagnetic waves from spheres, Scholarly Notes of Leningrad Univ., 1953, No. 170, iss. 27.
16. Riemann, I. S., Krebs, R. A., Apparent Masses of Bodies of Various Shapes, Trudy TsAGI, 1947, No. 635.
17. Slepyan, L. I. On travel of a deformable body in an acoustic medium, PMM, 1963, v. XXVII.
18. Smirnov, V. I., Sobolev, S. L. On the application of new methods in studying elastic vibration, Trudy of the Seismology Institute, 1934, No. 41.
19. Sobolev, S. L. The theory of Plane Wave Diffraction, Trudy of the Seismology Institute, 1934, No. 41.
20. Frenkel', Ya. I. The Kinetic Theory of Fluids (AS USSR, 1945).
21. Kharkevich, A. A. Unstable Wave Effects, (Gostekhteorizdat, 1945).
22. Khristianovich, S. A. A shock wave at a considerable distance from the point of explosion, PMM, 1956, v. XX, iss. 5.
23. Shal', R. The equation of state of water under high pressures from data of x-ray photographs of intensive explosive waves, "Mekhanika", 1952, No.3.

24. Shemyakin, Ye. I., Markova, K. N. The propagation of unstable disturbances in a fluid contacting with an elastic half-space, PMM, 1957, v. XXI, iss. 1.
25. Shimanskiy, Yu. A. Dynamic Calculation of Marine Structures, (Sudpromgiz, 1963)
26. Yakovlev, Yu. S. The Hydrodynamics of Explosion, (Sudpromgiz, 1961)

in English (as in original text)

27. Arons, A. B. Underwater Explosion Wave Parameters at Large Distances from the Charge, JASA, 1954, vol. 26, no.3.
28. Briggs, I. J. Limiting Negative Pressure of Water. J. of Appl. Phys., 1950, vol. 21, no. 7, July, pp. 721-722.
29. Davies, R. M., Trevena, D. H., Rees, N. J. M., Lewis, G. M. Cavitation in Hydrodynamics, Proceedings of a Symposium held at the National Physical Laboratory on September 1955. London, 1956.
30. Dimaggio, F. L. Effect of an Acoustic Medium on the Dynamic Buckling of Plates. J. of Appl. Mech., 1956, vol. 23, no.2, June, pp. 201-206.
31. Fisher, J. C. The Fracture of Liquids, J. of Appl. Phys., 1948, vol. 10, No. 11, pp. 1062-1067.
32. Fox, E. N. The Diffraction of Sound Pulses by an Infinitely Long Strip. Philosophical Transactions of the Royal Society of London, 1948, vol. 241, no. 828, June, Ser. A, pp. 71-103.
33. Gilmore. Pulsation of Spherical Bubble in Viscous Compressible Fluid. California Institute of Technology Reports, No. 26-4, 1952.
34. Irvin Kay. The Diffraction of an Arbitrary Pulse by a Wedge. Communications on Pure and Applied Mathematics, 1953, vol. VI, no. 3, August, pp. 419-434.
35. Klinger, J. B., Blank, A. Diffraction and reflection of pulses by wedges and corners. Comm. on Pure and Appl. Math. 1951, vol. IV, no. 1, June, pp. 75-94.
36. Lamb, H. The Early Stages of a Submarine Explosion. Phil. Magazine and Journal of Science, 1923, vol. 45, No. 266, February, Ser. VI, pp. 257-265.
37. Lindh, G. The Transmission and Reflection of an Exponential Shock Wave Impinging on a Homogeneous Elastic Plate Immersed in a Liquid. Acoustica, 1955, vol. 5, no. 5, pp. 257-262.
38. Lu Ting. The Diffraction of Disturbances around a convex right corner with application right corner and wing-body interference. J. Aeronaut. Sci., 1951, 24, no. 1.
39. Osborne, M. F. M., Taylor, A. N. Non-Linear Propagation of Underwater Shock Waves. The Physical Review, 1946, 70, 5-6, Ser. 2, pp. 322-328.
40. Shauer. The Afterflow Theory of the Relating of Airbaked Plates at Underwater Explosions. Proc. of 1st U. S. Nat'l Congress of Appl. Mechanics, 1953.